



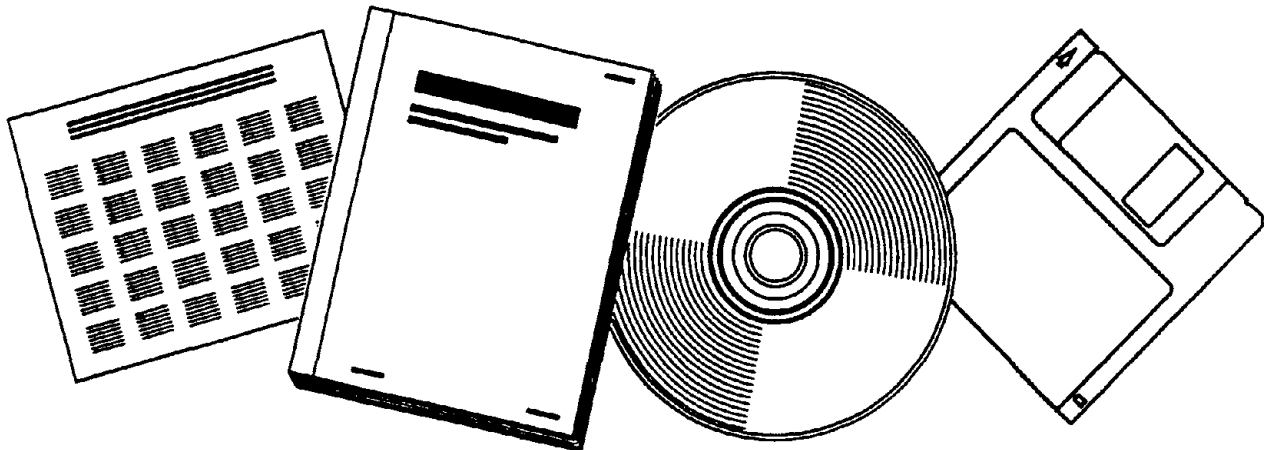
PB97-184196

NTIS[®]
Information is our business.

**MEETING OF THE UJNR PANEL ON FIRE
RESEARCH AND SAFETY (13TH). HELD IN
GAITHERSBURG, MARYLAND ON
MARCH 13-20, 1996. VOLUME 1**

(U.S.) NATIONAL INST. OF STANDARDS AND TECHNOLOGY (BFRL)
GAITHERSBURG, MD

JUN 97



U.S. DEPARTMENT OF COMMERCE
National Technical Information Service

NISTIR 6030



PB97-184196

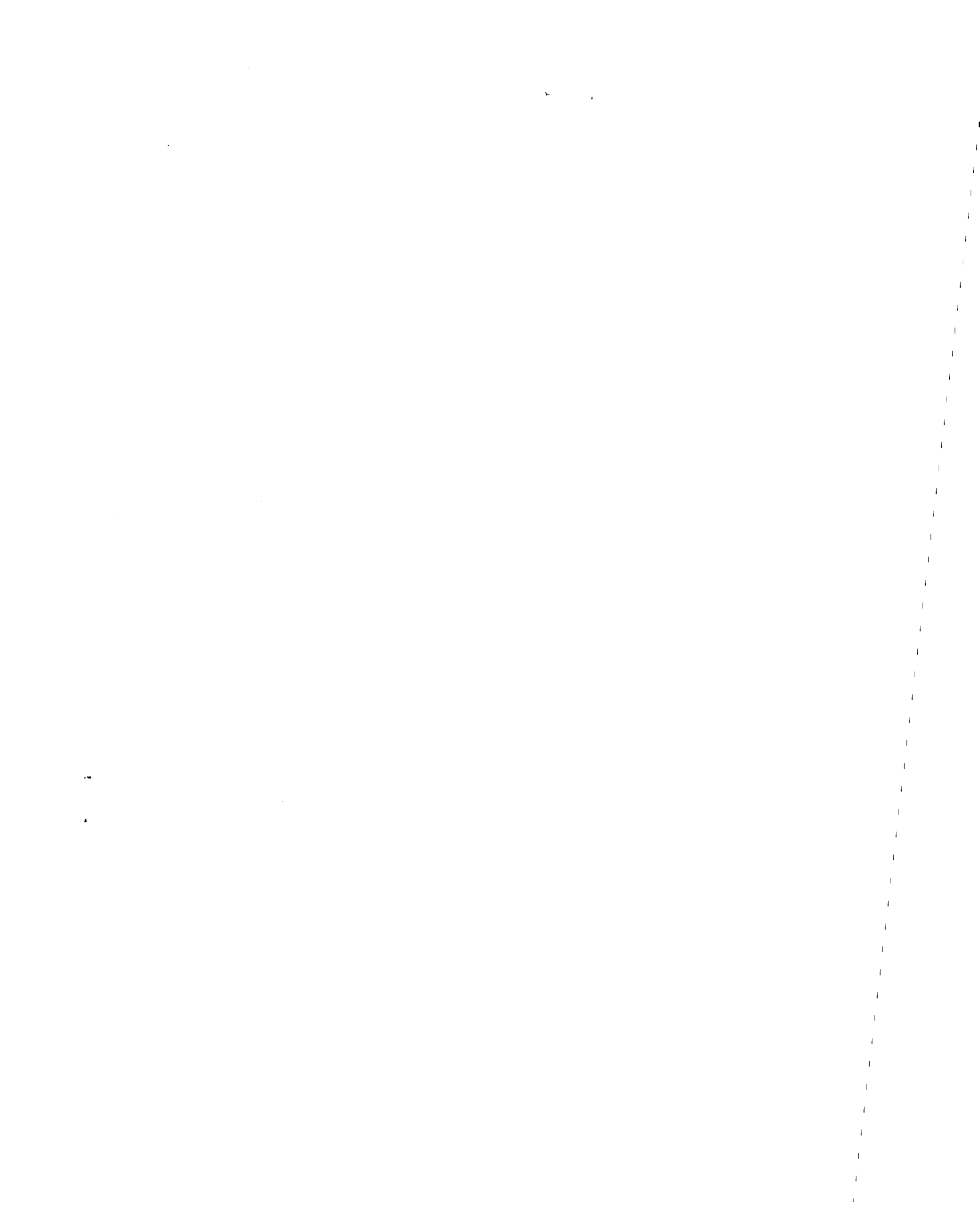
**THIRTEENTH MEETING OF THE UJNR
PANEL ON FIRE RESEARCH AND SAFETY,
MARCH 13-20, 1996**

VOLUME 1

Kellie Ann Beall, Editor

NIST

**United States Department of Commerce
Technology Administration
National Institute of Standards and Technology**



NISTIR 6030

**THIRTEENTH MEETING OF THE UJNR
PANEL ON FIRE RESEARCH AND SAFETY,
MARCH 13-20, 1996**

VOLUME 1

Kellie Ann Beall, Editor

June 1997
Building and Fire Research Laboratory
National Institute of Standards and Technology
Gaithersburg, MD 20899



U.S. Department of Commerce
William M. Daley, *Secretary*
Technology Administration
Gary R. Bachula, *Acting Under Secretary for Technology*
National Institute of Standards and Technology
Robert E. Hebner, *Acting Director*

NIST-114 (REV. 11-94) ADMAN 4.09	U.S. DEPARTMENT OF COMMERCE NATIONAL INSTITUTE OF STANDARDS AND TECHNOLOGY	(ERB USE ONLY)	
		ERB CONTROL NUMBER W97-1207	DIVISION 865

MANUSCRIPT REVIEW AND APPROVAL

PP97-184196



CATEGORY CODE

240

PRINTED PAGES

INSTRUCTIONS: ATTACH ORIGINAL OF THIS FORM TO ONE (1) COPY OF MANUSCRIPT AND SEND TO THE SECRETARY, APPROPRIATE EDITORIAL REVIEW BOARD.

TITLE AND SUBTITLE (CITE IN FULL)

Thirteenth Meeting of the UJNR Panel on fire Research and Safety, March 13-20, 1996

CONTRACT OR GRANT NUMBER

TYPE OF REPORT AND/OR PERIOD COVERED

AUTHOR(S) (LAST NAME, FIRST INITIAL, SECOND INITIAL)

EDITOR: Beall, Kellie A.

PERFORMING ORGANIZATION (CHECK (X) ONE BLOCK)

- NIST/GAITHERSBURG
 NIST/BOULDER
 JILA/BOULDER

LABORATORY AND DIVISION NAMES (FIRST NIST AUTHOR ONLY)

Building and Fire Research Laboratory, Fire Science Division (865)

SPONSORING ORGANIZATION NAME AND COMPLETE ADDRESS (STREET, CITY, STATE, ZIP)

NIST Category No.

NIST- 240

PROPOSED FOR NIST PUBLICATION

- | | | |
|---|---|--|
| <input type="checkbox"/> JOURNAL OF RESEARCH (NIST JRES) | <input type="checkbox"/> MONOGRAPH (NIST MN) | <input type="checkbox"/> LETTER CIRCULAR |
| <input type="checkbox"/> J. PHYS. & CHEM. REF. DATA (JPCRD) | <input type="checkbox"/> NATL. STD. REF. DATA SERIES (NIST NSRDS) | <input type="checkbox"/> BUILDING SCIENCE SERIES |
| <input type="checkbox"/> HANDBOOK (NIST HB) | <input type="checkbox"/> FEDERAL INF. PROCESS. STDS. (NIST FIPS) | <input type="checkbox"/> PRODUCT STANDARDS |
| <input type="checkbox"/> SPECIAL PUBLICATION (NIST SP) | <input type="checkbox"/> LIST OF PUBLICATIONS (NIST LP) | <input type="checkbox"/> OTHER |
| <input type="checkbox"/> TECHNICAL NOTE (NIST TN) | <input checked="" type="checkbox"/> NIST INTERAGENCY/INTERNAL REPORT (NISTIR) | |

PROPOSED FOR NON-NIST PUBLICATION (CITE FULLY)

U.S. FOREIGN

NISTIR 6030

PUBLISHING MEDIUM

- PAPER CD-ROM
 DISKETTE (SPECIFY) _____
 OTHER (SPECIFY) _____

SUPPLEMENTARY NOTES

ABSTRACT (A 2000-CHARACTER OR LESS FACTUAL SUMMARY OF MOST SIGNIFICANT INFORMATION. IF DOCUMENT INCLUDES A SIGNIFICANT BIBLIOGRAPHY OR LITERATURE SURVEY, CITE IT HERE. SPELL OUT ACRONYMS ON FIRST REFERENCE.) (CONTINUE ON SEPARATE PAGE, IF NECESSARY.)

The 13th meeting of the U.S.-Japan Panel on Fire Research and Safety was held at the National Institute of Standards and Technology March 13-20, 1996. The core of the meeting consisted of technical sessions on design/risk/hazard/performance standards, burning of real objects, experimental refinement and validation of fire models, suppression, materials testing, detection, and fires after earthquakes. The last of these topics took on special meaning in the wake of two disasters since the 12th meeting: a major earthquake in Northridge, California and the Great Hanshin-Awaji Earthquake on the largest Japanese island of Honshu. In addition, the meeting hosted two one-day Symposia honoring two long-time principals of fire research in general and this UJNR Panel in particular. The first was in honor of Professor Edward Zukoski on the occasion of his retirement from the California Institute of Technology. The second was in memory of Professor Kunio Kawagoe of the Building Research Institute and Tokyo Science University.

KEY WORDS (MAXIMUM OF 9; 28 CHARACTERS AND SPACES EACH; SEPARATE WITH SEMICOLONS; ALPHABETIC ORDER; CAPITALIZE ONLY PROPER NAMES)

AVAILABILITY

- UNLIMITED FOR OFFICIAL DISTRIBUTION - DO NOT RELEASE TO NTIS
 ORDER FROM SUPERINTENDENT OF DOCUMENTS, U.S. GPO, WASHINGTON, DC 20402
 ORDER FROM NTIS, SPRINGFIELD, VA 22161

NOTE TO AUTHOR(S): IF YOU DO NOT WISH THIS MANUSCRIPT ANNOUNCED BEFORE PUBLICATION, PLEASE CHECK HERE.

ELECTRONIC INFORMS

**VOLUME 1
CONTENTS**

Introduction v
Agenda vii
List of Members (Japan) xvii
List of Members (U.S.) xxi
Group Photograph xxvii

Opening Remarks 1

DESIGN/RISK/HAZARD/PERFORMANCE STANDARDS SESSION

Progress Report on Design, Risk, Hazard, and Performance-Based Codes 7
Progress Report on Performance-based Fire Safety Design Method 15
Society of Fire Protection Engineers (SFPE) Perspectives of Performance-Based Fire Safety Design . 19
Life Safety Evaluation of Large Populations with Mixed Abilities 27
High Rise Evacuation Modeling--Data and Applications 35
Assessment of Clarity of Egress Route in Buildings 43
A Consideration on Required Number of Exits in a Room -- A Study on the Safety Performance of Exit Provisions -- Part 1 53
A Consideration on Common Path Length and Single Stairway -- A Study on the Safety Performance of Exit Provisions -- Part 2 65
Risk and Performance Standards 79
Using Fire Models to Establish Performance Requirements for the Design of Buildings 89
Cost-effective Compliance with the Life Safety Code for Health Care Occupancies 97

BURNING OF REAL OBJECTS SESSION

Flammability of Real Objects: A Progress Report 107
Progress Report on Full Scale Fire Test in Japan 115
Upward Flame Spread on Vertical Surfaces 121
Wall Flame Correlations and Upward Flame Spread a Vertical Channel and Its Relevance to Fire Safety 129
Assessment of Material Flammability with the FSG Propagation Model and Laboratory Test Methods 154
Concurrent Flame Spread in Fires--State of the Art of Modeling and Future Problems for Engineering Application 165
Input Data for Fire Modeling 187
Measurement and Predictions of the Velocity Field Induced by Pool Fires 201
Corrosion from Combustion Products--An Overview 209

ZUKOSKI SYMPOSIUM

Symposium in Honor of Prof. Edward Zukoski

Opening Remarks 227
A Universal Orifice Flow Formula 229

Modeling of Heating Mechanism and Thermal Response of Structural Components Exposed to Localized Fires: A New Application of Diffusion Flame Modeling to Fire Safety Engineering	237
Large Eddy Simulations of Smoke Movement in Three Dimensions	249
Experimental Study of Smoke Movement with Scale Model	259
Radiation Transfer and Temperature Distribution in a Few Small Pool Flames	265
Self-preserving Buoyant Turbulent Plumes	275
Characteristics of Oscillating Buoyant Plumes	285
On Q^* and the Dynamics of Diffusion Flames	295
Zukoski's Intellectual Progeny	305

KAWAGOE MEMORIAM

Symposium in Memory of Kunio Kawagoe

Opening Remarks	317
Memory of Professor Kawagoe	319
Recollection of Meetings with Kunio Kawagoe	321
Behavior of Wind Blown Crib Fires	323
Fire Investigation	331
Simple Formula for Ventilation Controlled Fire Temperatures	341
Zone Model Plume Algorithm Performance	357
Mathematical Modeling for Building Fire	375
Performance Based Fire Safety	389
Flame Length and Width Produced by Ejected Propane Gas Fuel from a Pipe	401
The Effect of Pool Diameter on the Properties of Smoke Produced by Crude Oil Fires	413
Heat and Mass Transfer in the Walls Subjected to Fire	423
Full-Scale Burn Test of Wooden Three-Story Apartment Building	437
Author Index	453

INTRODUCTION

The 13th meeting of the U.S.-Japan Panel on Fire Research and Safety was held at the National Institute of Standards and Technology March 13-20, 1996. It had been scheduled for October 25 - November 1, 1995 but was postponed due to uncertainties regarding the U.S. Federal budget and the eventual temporary shutdowns of the Government.

The core of the meeting consisted of technical sessions on design/risk/hazard/performance standards, burning of real objects, experimental refinement and validation of fire models, suppression, materials testing, detection, and fires after earthquakes. The last of these topics took on special meaning in the wake of two disasters since the 12th meeting: a major earthquake in Northridge, California (January 17, 1994) and the Great Hanshin-Awaji Earthquake on the largest Japanese island of Honshu (January 17, 1995). The participants intend that the losses from these momentous events will galvanize the development of solutions to mitigate future life loss and destruction.

In addition, the meeting hosted two one-day Symposia honoring two long-time principals of fire research in general and this UJNR Panel in particular. The first was in honor of Professor Edward Zukoski on the occasion of his retirement from the California Institute of Technology. We regret to report that Prof. Zukoski passed away on May 26, 1997, just prior to the publication of these Proceedings. The second symposium was in memory of Professor Kunio Kawagoe of the Building Research Institute and Tokyo Science University. Each was a celebratory event, with excellent technical papers, fond memories, and renewed friendships. Both men were outstanding contributors to fire science, and both will be deeply missed by their colleagues and friends.

Among the technical sessions, the participants found time to visit the NIST fire research laboratories, with demonstrations of CFD modeling, "Fire on the Web," research on halon alternatives and fire-safe materials, and flame measurements. The Saturday between sessions included tours of the lovely Luray Caverns and the Old Town Section of Alexandria, Virginia. These provided further opportunity for the new participants in this venerable bi-national conference to spend time with those with extensive experience, and for the veterans to strengthen the fellowship of the international fire research community. Even as these memories transition to recollection by manuscript and photograph, the plans are underway for the 14th Meeting, to be held in Japan in the spring of 1998.

**Thirteenth Joint Panel Meeting of the
UJNR Panel on Fire Research and Safety**

March 13 - 20, 1996
Gaithersburg Hilton Hotel
Gaithersburg, Maryland

Wednesday, March 13, 1996 (opening ceremony and single technical session)

- 8:45 Opening
- 9:45 Leave for NIST for Group Photo
- 10:30 Return to Hotel, Break

Design/Risk/Hazard/Performance Standards

- 10:45 John R. Hall, Jr. (NFPA): **“Progress Report on Design, Risk, Hazard, and Performance-Based Codes”**
- 11:00 Takeyoshi Tanaka (BRI): **“Progress Report on Performance-based Fire Safety Design Method”**
- 11:15 Brian Meacham (SFPE): **“Society of Fire Protection Engineers (SFPE) Perspectives of Performance-Based Fire Safety Design”**
- 11:45 Shuji Kakegawa (Shimizu Corp.): **“Life Safety Evaluation of Large Populations with Mixed Abilities”**
- 12:15 Lunch
- 13:15 Rita Fahy (NFPA): **“High Rise Evacuation Modeling--Data and Applications”**
- 13:45 Manabu Ebihara (Shimizu Corp.): **“Assessment of Clarity of Egress Route in Buildings”**
- 14:15 Takeyoshi Tanaka (BRI): **“A Consideration on Required Number of Exits in a Room -- A Study on the Safety Performance of Exit Provisions -- Part 1”**
- 14:45 Ichiro Hagiwara (BRI): **“A Consideration on Common Path Length and Single Stairway -- A Study on the Safety Performance of Exit Provisions -- Part 2”**
- 15:15 Break

- 15:45 Dick Bukowski (BFRL): **“Risk and Performance Standards”**
- 16:15 David Stroup (BFRL): **“Using Fire Models to Establish Performance Requirements for the Design of Buildings”**
- 16:45 Barbara Lippiatt (BFRL): **“Cost-effective Compliance with the Life Safety Code for Health Care Occupancies”**
- 17:15 Adjourn

Thursday, March 14, 1996 (single technical session)

Burning of Real Objects

- 8:30 Tom Ohlemiller (BFRL): **“Flammability of Real Objects: A Progress Report”**
- 8:45 Osami Sugawa (Science University of Tokyo): **“Progress Report on Full Scale Fire Test in Japan”**
- 9:00 Craig Beyler (Hughes Assoc.): **“Upward Flame Spread on Vertical Surfaces”**
- 9:30 Yuji Hasemi (BRI): **“Wall Flame Correlations and Upward Flame Spread a Vertical Channel and Its Relevance to Fire Safety”**
- 10:00 Ronald Alpert (Factory Mutual Research Corp.): **“Assessment of Material Flammability with the FSG Propagation Model and Laboratory Test Methods”**
- 10:30 Break
- 11:00 Yuji Hasemi (BRI): **“Concurrent Flame Spread in Fires--State of the Art of Modeling and Future Problems for Engineering Application”**
- 11:30 Henri Mitler (BFRL): **“Input Data for Fire Modeling”**
- 12:00 Lunch
- 13:00 Jayavant Gore (Purdue Univ.): **“Measurement and Predictions of the Velocity Field Induced by Pool Fires”**
- 13:30 Pravinray Gandhi (Underwriters Laboratories): **“Corrosion from Combustion Products--An Overview”**
- 14:00 End of Session
- 14:15 Bus to NIST
- 14:30 Lab Tour
- 16:30 Adjourn, Bus to Hotel
- 17:30 Leave Hotel for Shopping and Dinner

Friday, March 15, 1996

Zukoski Symposium

- 9:00 Howard Emmons (Harvard University): **“A Universal Orifice Flow Formula”**
- 9:40 Yuji Hasemi (BRI): **“Modeling of Heating Mechanism and Thermal Response of Structural Components Exposed to Localized Fires: A New Application of Diffusion Flame Modeling to Fire Safety Engineering”**
- 10:20 Break
- 10:40 Howard Baum (BFRL): **“Large Eddy Simulations of Smoke Movement in Three Dimensions”**
- 11:20 Makoto Tsujimoto (Nagoya University): **“Experimental Study of Smoke Movement with Scale Model”**
- 12:00 Lunch
- 1:30 Hiroshi Hayasaka (Hokkaido University): **“Radiation Transfer and Temperature Distribution in a Few Small Pool Flames”**
- 2:10 Gerard M. Faeth (University of Michigan): **“Self-preserving Buoyant Turbulent Plumes”**
- 2:50 Baki M. Cetegen (University of Connecticut): **“Characteristics of Oscillating Buoyant Plumes”**
- 3:30 Break
- 3:50 Gunnar Heskestad (Factory Mutual Research Corp.): **“On Q^* and the Dynamics of Diffusion Flames”**
- 4:30 Patrick Pagni (University of California, Berkeley): **“Zukoski’s Intellectual Progeny”**
- 5:30 Reception
- 7:00 Banquet

Monday, March 18, 1996 (Kawagoe Memoriam)

~Sponsored by the Japanese Delegates ~

Kawagoe Memoriam

- 9:00 Yoshio Mimura (BRI): **“Opening Remarks”**
- 9:20 Jack Snell (BFRL): **“Memory of Professor Kawagoe”**
- 9:40 Alex Robertson (former NBS): **“Recollection of Meetings with Kunio Kawagoe”**
- 10:00 Takashi Sekine (Former Co-worker of Prof. Kawagoe, possible presented by Hayashi):
“Behavior of Wind Blown Crib Fires”
- 10:30 Break
- 11:00 Jim Quintiere (U. Maryland): **“Fire Investigation”**
- 11:30 Takeyoshi Tanaka (BRI): **“Simple Formula for Ventilation Controlled Fire
Temperatures”**
- 12:00 Lunch
- 13:00 John Rockett (former NBS): **“Zone Model Plume Algorithm Performance”**
- 13:30 Masahiro Morita (Sci. Univ. of Tokyo): **“Mathematical Modeling for Building Fire”**
- 14:00 Bud Nelson (Hughes Associates): **“Performance Based Fire Safety”**
- 14:30 Osami Sugawa (Sci. Univ. of Tokyo): **“Flame Length and Width Produced by
Ejected Propane Gas Fuel from a Pipe”**
- 15:00 Break
- 15:30 George Mulholland (BFRL): **“ The Effect of Pool Diameter on the Properties of
Smoke Produced by Crude Oil Fires”**
- 16:00 Kazunori Harada (Kyoto Univ.): **“Heat and Mass Transfer in the Walls Subjected to
Fire”**
- 16:30 Yuji Hasemi (BRI): **“Full-Scale Burn Test of Wooden Three-Story Apartment
Building”**
- 17:00 Adjourn
- 18:00 Cocktail Hour
- 19:00 Dinner Reception

Tuesday, March 19, 1996 (double technical session)

Session One

Experimental Refinement and Validation of Fire Models

- 8:30 Yoshihiko Hayashi (BRI): **“Progress Report on Fire Modeling -- Numerical Simulation of Variable Density Flow with High Buoyancy”**
- 8:45 Walter Jones (BFRL): **“Progress Report on Fire Modeling and Validation”**
- 9:00 Kermit Smyth (BFRL): **“Computations of Enhanced Soot Production in Flickering Diffusion Flames”**
- 9:30 Tokiyoshi Yamada (FRI): **“Experimental Study of the Exchange Flow through a Horizontal Ceiling Vent in Atrium Fires”**
- 10:00 Osami Sugawa (Sci. Univ. Of Tokyo): **“Modeling on Temperature and Ventilation Induced by a Model Fire in a Tall and Narrow Atrium Space”**
- 10:30 Break
- 10:45 Hiroshi Koseki (FRI): **“Radiation Properties and Flame Structure of Large Hydrocarbon Pool Fires”**
- 11:15 Bill Pitts (BFRL): **“Carbon Monoxide Formation Algorithm”**
- 11:45 Lunch
- 12:45 Walter Jones (BFRL): **“The Fire Hazard Assessment Methodology”**
- 13:15 Yoshifumi Ohmiya(Sci. Univ. of Tokyo) **“A Room Fire Model in View of Predicting Fire Spread by External Flames”**
- 13:45 Rick Peacock (BFRL): **“Evaluation of Complex Fire Models”**
- 14:15 Takeyoshi Tanaka (BRI): **“Experiments on Smoke Behavior in Cavity Spaces”**
- 14:45 Walter Jones/Rebecca Portier (BFRL): **“A Prototype FDMS Database for Model Verification”**
- 15:15 Adjourn

Tuesday, March 19, 1996 (double technical session)

Session Two

Suppression

- 8:30 Richard G. Gann (BFRL): **“Progress Report on Fire Suppression Research in the U.S.”**
- 8:45 Naoshi Saito (FRI): **“Progress Report on Suppression in Japan”**
- 9:00 Anthony Hamins (BFRL): **“Flame Suppression by Halon Alternatives”**
- 9:30 Naoshi Saito (FRI): **“Evaluation of Fire Suppression Efficiency of Halon Replacements in Japan”**
- 10:00 Jack Mawhinney (Hughes Assoc.): **“Status Report on Water Mist Fire Suppression Systems -- 1996”**
- 10:30 Break
- 10:45 Ai Sekizawa (FRI): **“Experimental Study on Fire Hazard of Residential Fires Before and After Sprinklers Activation”**

Materials and Testing

- 11:15 Yuji Hasemi (BRI): **“Progress Report on Materials and Test Methods”**
- 11:30 Takashi Kashiwagi (BFRL): **“Progress Report on U.S. Research on Test Methods and Materials”**
- 11:45 Lunch
- 12:45 Yuji Hasemi (BRI): **“Asia-Oceania ISO5660 Cone Calorimeter Inter-Laboratory Trials”**
- 13:15 Tom Ohlemiller (BFRL): **“Flammability of Upholstered Furniture”**
- 13:45 Yuji Hasemi (BRI): **“Heat Release Rates Measured by Cone Calorimeter and Intermediate Scale Electrical Radiant Panels”**
- 14:15 Eiji Yanai (FRI): **“A Flammability Test for Granular Synthetic Resins Using a Modified Oxygen Index Method”**
- 14:45 Richard Lyon (FAA Technical Center): **“Advanced Fire safe Materials for Aircraft Interiors”**
- 15:15 Jeff Gilman (BFRL): **“Fire Retardant Additives for Polymeric Materials - I. Char Formation from Silica Gel--Potassium Carbonate”**
- 15:45 Adjourn

Wednesday, March 20, 1996 (double technical session and closing ceremony)

Session One

Fires After Earthquakes

- 8:30 David Evans (BFRL): **“Progress Report on Fires Following the Northridge Earthquake”**
- 8:45 Akihiko Hokugo (BRI): **“Progress Report on Fires Following the 1995 Great Hanshin-Awaji Earthquake”**
- 9:00 Ai Sekizawa (FRI): **“Post-Earthquake Fires and Firefighting Activities in the Early Stage in the 1995 Great Hanshin Earthquake”**
- 9:30 Frank Borden (City of Los Angeles Fire Dept.): **“The 1994 Northridge Earthquake and the Fires That Followed”**
- 10:00 Break
- 10:30 Akihiko Hokugo (BRI): **“The Performance of Fire Protection of Buildings Against the Fires Following the Great Hanshin-Awaji Earthquake”**
- 11:00 Charles Scawthorn (EQE Engineering): **“Fires Following the Northridge and Kobe Earthquakes”**
- 11:30 Kazuyoshi Ohnishi (Kobe Univ.): **“Causes of the Seismic Fires Following the Great Hanshin-Awaji Earthquake-Survey”**
- 12:00 Lunch
- 13:00 Daniel Madrzykowski (BFRL): **“Durable Agents for Exposure Protection in Wildland/Urban Interface Conflagrations”**
- 13:30 Kevin McGrattan (BFRL): **“Smoke Plumes from Large Fires”**
- 14:00 Closing
- 15:00 Adjourn

Wednesday March 20, 1996 at the Hilton

Session Two

Detection

- 8:30 Bill Grosshandler (BFRL): **“Progress Report on Fire Detection Research in the U.S.”**
- 8:45 Hiroaki Tamura (FRI): **“Progress Report on Detection Research in Japan”**
- 9:00 Bill Grosshandler (BFRL): **“Test Fire Signatures and the Fire-Emulator/Detector-Evaluator”**
- 9:30 Ron Mengel (System Sensor): **“Industry Advances in Fire Detection Technology”**
- 10:00 Break
- 10:30 Joji Kawada (Nohmi Bosai Ltd): **“Fire Detection in Atrium Buildings”**
- 11:00 James A. Milke (Dept. of Fire Protection): **“Multivariate Methods for Fire Detection”**
- 11:30 Bill Davis (BFRL): **“NASA Fire Detection Study”**
- 12:00 Lunch
- 14:00 Closing
- 15:00 Adjourn

LIST OF MEMBERS (JAPAN)

Panel Members

Dr. Yoshio Mimura (Japan Chairman)
Director General
Building Research Institute

Mr. Nobuo Jiromaru (Japan Vice-Chairman)
Director General
National Research Institute of Fire and Disaster

Dr. Takeyoshi Tanaka (BRI Coordinator)
Head, Smoke Control Division
Building Research Institute

Dr. Ai Sekizawa (NRIFD Coordinator)
Head, Information Analysis Section
National Research Institute of Fire and Disaster

Dr. Yuji Hasemi
Head, Fire Safety Division
Building Research Institute

Dr. Akihiko Hokugo
Smoke Control Division
Building Research Institute

Dr. Naoshi Saito
Head, Second Extinguishing Section
National Research Institute of Fire and Disaster

Dr. Hiroshi Koseki
Head, Hazardous Material Section
National Research Institute of Fire and Disaster

Dr. Tokiyoshi Yamada
Head, Special Fire Section
National Research Institute of Fire and Disaster

Associate Members

Dr. Ichiro Hagiwara
Research Staff, Fire Safety Division
Building Research Institute

Dr. Yoshihiko Hayashi
Research Staff, Fire Safety Division
Building Research Institute

Dr. Kazunori Harada
Research Staff, Smoke Control Division
Building Research Institute

Mr. Eiji Yanai
Head, Combustion Section
National Research Institute of Fire and Disaster

Mr. Hiroyuki Tamura
Research Staff, Alarm and Communication Section
National Research Institute of Fire and Disaster

Ms. Yuko Saso
Research Staff, Second Extinguishing Section
National Research Institute of Fire and Disaster

Dr. Makoto Tsujimoto
Professor
Nagoya University

Dr. Hiroshi Hayasaka
Associate Professor
Hokkaido University

Dr. Masahiro Morita
Associate Professor
Science University of Tokyo

Dr. Osami Sugawa
Associate Professor
Science University of Tokyo

Dr. Yoshifumi Ohmiya
Assistant Professor
Science University of Tokyo

Dr. Kazuyoshi Ohnishi
Assistant Professor
Kobe University

Mr. Shuji Kakegawa
Technical Research Institute
Shimizu Corporation

Mr. Manabu Ebihara
Izumi Office
Shimizu Corporation

Mr. Joji Kawada
Senior Assistant Manager
System Engineering Section 1st, Technical Department
Nohmi Bosai Ltd.

LIST OF MEMBERS (U.S.)

Panel Members

Dr. Jack E. Snell (U.S. Chairman)
Deputy Director, Building and Fire Research Laboratory
National Institute of Standards and Technology

Dr. Richard G. Gann (BFRL Coordinator)
Chief, Fire Science Division
Building and Fire Research Laboratory
National Institute of Standards and Technology

Dr. Takashi Kashiwagi (Secretary)
Leader, Materials Fire Research Group
Fire Science Division
Building and Fire Research Laboratory
National Institute of Standards and Technology

Dr. Ronald Alpert
Assistant Manager
Research Division
Factory Mutual Research Corporation

Dr. Howard Baum
Large Fire Research Group
Fire Safety Engineering Division
Building and Fire Research Laboratory
National Institute of Standards and Technology

Dr. David D. Evans
Chief, Fire Safety Engineering Division
Building and Fire Research Laboratory
National Institute of Standards and Technology

Dr. John R. Hall, Jr.
Assistant Vice President
Fire Analysis and Research
National Fire Protection Association

Mr. Harold Nelson
Consultant
Hughes Associates

Prof. Patrick Pagni
Department of Mechanical Engineering
University of California-Berkeley

Prof. James Quintiere
Department of Fire Protection Engineering
University of Maryland

Honorary Members

Prof. Howard Emmons (retired)
Harvard University

Prof. Edward Zukoski (retired)
Director of Engineering and Applied Sciences
California Institute of Technology

Associate Members

Mr. Donald Bathurst
Deputy Administrator
U.S. Fire Administration

Dr. Craig Beyler
Technical Director
Hughes Associates, Inc.

Mr. Frank Borden (retired)
Chief
Los Angeles City Fire Department

Mr. Richard W. Bukowski
Large Fire Research Group
Fire Safety Engineering Division
Building and Fire Research Laboratory
National Institute of Standards and Technology

Prof. Baki M. Cetegen
Mechanical Engineer
University of Connecticut

Mr. William Davis
Fire Modeling and Applications Group
Fire Safety Engineering Division
Building and Fire Research Laboratory
National Institute of Standards and Technology

Prof. Gerald M. Faeth
Aerospace Engineering
University of Michigan

Ms. Rita Fahy
Fire Analysis and Research
National Fire Protection Association

Dr. Pravinray D. Gandhi
Senior Staff Engineer
Underwriters Laboratories

Dr. Jeffrey W. Gilman
Materials Fire Research Group
Fire Science Division
Building and Fire Research Laboratory
National Institute of Standards and Technology

Prof. Jayavant Gore
School of Mechanical Engineering
Purdue University

Dr. William Grosshandler
Fire Sensing and Extinguishment Group
Fire Science Division
Building and Fire Research Laboratory
National Institute of Standards and Technology

Dr. Anthony Hamins
Materials Fire Research Group
Fire Science Division
Building and Fire Research Laboratory
National Institute of Standards and Technology

Dr. Gunnar Heskestad
Principal Research Scientist
Factory Mutual Research Corporation

Mr. James Hoebel
Program Manger, Fire
Consumer Product Safety Commission

Dr. Walter Jones
Fire Modeling and Applications Group
Fire Safety Engineering Division
Building and Fire Research Laboratory
National Institute of Standards and Technology

Ms. Barbara Lippiatt
Office of Applied Economics
Building and Fire Research Laboratory
National Institute of Standards and Technology

Dr. Richard Lyon
Fire Safety Branch
FAA Technical Center

Mr. Daniel Madrzykowski
Large Fire Research Group
Fire Safety Engineering Division
Building and Fire Research Laboratory
National Institute of Standards and Technology

Mr. Jack Mawhinney
Senior Engineer
Hughes Associates, Inc.

Mr. Kevin McGrattan
Large Fire Research Group
Fire Safety Engineering Division
Building and Fire Research Laboratory
National Institute of Standards and Technology

Mr. Brian Meacheam
Technical Director
Society of Fire Protection Engineers

Mr. Ron Mengel
Director of Industry Affairs
System Sensor

Dr. James A. Milke
Department of Fire Protection Engineering
University of Maryland

Dr. Henri Mitler
Fire Modeling and Applications Group
Fire Safety Engineering Division
Building and Fire Research Laboratory
National Institute of Standards and Technology

Dr. George Mulholland
Advanced Fire Measurements Group
Fire Science Division
Building and Fire Research Laboratory
National Institute of Standards and Technology

Dr. Thomas J. Ohlemiller
Materials Fire Research Group
Fire Science Division
Building and Fire Research Laboratory
National Institute of Standards and Technology

Mr. William Page
Senior Product Market Specialist
Dow Corning Corporation

Mr. Richard Peacock
Fire Modeling and Applications Group
Fire Safety Engineering Division
Building and Fire Research Laboratory
National Institute of Standards and Technology

Dr. William Pitts
Advanced Fire Measurements Group
Fire Science Division
Building and Fire Research Laboratory
National Institute of Standards and Technology

Dr. Alexander Robertson
Consultant

Dr. John A. Rockett
Consultant

Dr. Charles Scawthorn
Senior Vice President
EQE Engineering

Dr. Kermit Smyth
Advanced Fire Measurements Group
Fire Science Division
Building and Fire Research Laboratory
National Institute of Standards and Technology

Mr. Usman Soriathia
Fire Materials Engineer
Naval Surface Warfare Center

Mr. David Stroup
Large Fire Research Group
Fire Safety Engineering Division
Building and Fire Research Laboratory
National Institute of Standards and Technology

Dr. King-mon Tu
Principal Research Engineer
AKZO Nobel Chemicals, Inc.

Mr. William D. Walton
Large Fire Research Group
Fire Safety Engineering Division
Building and Fire Research Laboratory
National Institute of Standards and Technology



13th Joint Panel Meeting
 UJNR Panel on
 Fire Research and Safety
NIST
 National Institute of Standards and Technology
 Building and Fire Research Laboratory
 March 13-20, 1995



OPENING REMARKS

Dr. Richard N. Wright
Building and Fire Research Laboratory

Dr. Mimura, Dr. Snell, it gives me great pleasure to welcome the Thirteenth Joint Meeting of the UJNR Panel on Fire Research and Safety. Our increasing urbanization and growing fire losses show that your work is of increasing importance to our nations and the world. The tragic fires following the Hyogo ken Nanbu earthquake on January 17, 1995 specifically illustrate the need for your work.

Your program describes advances in fire science and fire safety engineering that confirm that resolute efforts in research and development and implementation of fire safety practices can address our two nations' needs for risk reduction.

Among my responsibilities are to chair the U.S.-side of the UJNR Panel on Wind and Seismic Effects and to represent NIST in the U.S. National Earthquake Risk Reduction Program. We are planning in further collaborations with Japan that will involve the UJNR Fire Research and Safety and Wind and Seismic Effects Panels. We are working with the Japanese Science and Technology agency to formulate a U.S.-Japan Earthquake R&D Initiative tentatively entitled "Mitigating Urban Earthquake Disasters." A major component would be mitigation and control of post-earthquake fires. The expertise and collaborations of this Panel on Fire Research and Safety should provide strong bases for enhanced collaborations.

As a result of the agreement of our President and Japan's Prime Minister last June, we jointly are planning Earthquake Policy Symposia for the U.S. in September 1996 and Japan in May or June 1997. We expect that the inputs of our panels to these symposia will inform our policy makers of opportunities to substantially reduce U.S. and Japanese vulnerability to conflagrations following earthquakes.

We have benefitted from the many accomplishments of the UJNR Panel on Fire Research and Safety in its twenty-some years of effective collaborations. We are gratified that our Japanese and U.S. colleagues have endured the inconvenience of the postponement of this important meeting and are ready to continue and strengthen our joint efforts to reduce human and economic fire losses. Best wishes for a fruitful meeting.

OPENING REMARKS

Dr. Yoshio Mimura
Building Research Institute, Japan

Ladies and Gentlemen,

It is a great pleasure to have visited this country again to join the 13th UJNR Panel on Fire Research and Safety.

This meeting was planned to be held last autumn, but because of the U.S. budget problems, it has been postponed until today. Since the Japanese fiscal year is from April to March the next year, if this meeting would have been postponed over April this year, it would have been quite difficult for us to join the meeting. Therefore, we requested the U.S. panel to try to hold the meeting this time here. But I can imagine how much hard work the U.S. panel did to hold the meeting this time. On behalf of the Japanese panel, I would like to extend our deep gratitude and appreciation to Dr. Snell and the U.S. Panel.

Well, as you have known, Japan was shaken and shocked by the Kobe Earthquake last year, and the importance of disaster prevention was recognized. On the other hand, the demands of rationalization of standards and the moderation of restrictions have increased corresponding to the aim of international harmonization.

To meet the needs of an age, it is inevitable to establish the concept of safety as the one which can be evaluated more scientifically and substantially on the basis of internationally common understanding.

In the field of fire research as well as earthquake resistance research, U.S. and Japan are the leading countries in the world. So UJNR should play a more important role from now on.

I certainly wish the fire research of both the U.S. and Japan will be developed much more in the future and the experts in the field of both countries will enhance the mutual understanding as usual and will tighten their collaborative spirit much more to do their mission through the UJNR Panel on Fire Research and Safety of this time.

Thank you very much.

DESIGN/RISK/HAZARD/PERFORMANCE STANDARDS

Progress Report on Design, Risk, Hazard, and Performance-Based Codes

John R. Hall, Jr.
National Fire Protection Association
1 Batterymarch Park, P.O. Box 9101
Quincy, Massachusetts 02269-9101

Abstract

Recent activity in the US regarding fire risk and hazard analysis has included validation and data development but has primarily emphasized the steps required to refine such calculation methods for use in performance-based design and codes, including the development of appropriate organizational arrangements and procedures.

Institutionalization of Fire Hazard and Risk Analysis

Since the last UJNR meeting, there has been an unprecedented level of activity in the area of fire risk and hazard analysis methods, particularly as applied to performance-based design, codes and standards. Much of this activity has focused on organizational arrangements and innovative procedures to make engineered fire safety routine, as opposed to new approaches to the calculation methods themselves. Also, this work is increasingly multi-national, even global, which makes it increasingly difficult to isolate progress in the US. Accordingly, this progress report includes reference to work by some non-US researchers where that work has proved particularly influential in the US.

Several important papers were delivered or published on the subject of general approaches to fire risk or hazard analysis suitable for use in a performance-based code [5, 17, 40]. Most were general, but one addressed trade-offs of several major components of fire protection (detection, suppression, construction) without addressing all components (e.g., omitting prevention and evacuation) [6]. The US-based American Society for Testing and Materials (ASTM) published a standard which contains the format to be used in ASTM to write standards (typically standards for products that could burn) using a fire hazard assessment format [41]. A second standard, based on the first, will provide guidance in writing fire risk assessment standards and is now being voted on.

Other papers focused specifically on the steps required to reshape existing code-writing procedures to accommodate performance-based approaches [8, 20, 24, 37, 38]. Several of these papers were intended to acquaint important US fire safety organizations, such as the National Fire Protection Association [36] and the Society of Fire Protection Engineers [28], with the status of performance-based code design around the world.

Still other work has served to assemble known methods of fire risk or hazard assessment in one place so as to facilitate application of the methods

and education of prospective users. Examples include the publication of basic documentation on CFAST [32] and FPEtool [9], two multi-part methods capable of modeling many aspects of fire and serving as the fire effects core of fire hazard or risk assessment models. Others include compilations of available methods applicable to fire risk analysis for products [18], buildings [45], industrial settings [2], and rail transportation properties [33].

Within the US, much attention has been given to emerging national performance-based code approaches in Australia [3], Canada [7, 16, 19, 23, 35, 46], and New Zealand [4]. Each has been used as a basis for design choices in the US, but with the major difference that fire codes in the US are not operated through an agency of the national government. Changes must be implemented through several private groups that develop model codes.

Components of Fire Hazard and Risk Analysis for Performance-Based Designs or Codes

There is now general agreement on the major elements required to support the institutionalized use of fire risk or hazard analysis methods within a performance-based code: (a) identification and documentation of suitable fire models whose valid uses and limitations are known and whose capabilities have been validated; (b) identification and development of data appropriate to those models and the intended applications of them; (c) fire safety goals, objectives, criteria, acceptable levels, and safety factors that translate the national consensus of values into a form suitable to guide analysis to evaluate designs; (d) identification of fire scenarios that can be analyzed using the models and the data and thereby used to define the conditions under which the fire safety goals must be met; and (e) provisions for education, certification, or accountability of fire safety engineers or others who may be asked to show that goals will be met.

Since the last UJNR meeting, there have been a number of papers published on validation of models relevant to the construction of fire hazard and risk assessment methods [14, 19, 25, 34].

Other papers have addressed data. Some have provided specific data addressed to particular issues, including factors in the propensity of different cigarettes to cause fires [21]; human behavior when confronted with a major incident in a high-rise building [12]; behavior changes induced by changes in cigarette lighter design, which may affect the impact of the design on fire risk [43]; factors leading to high vs. low fire risk in residential settings [39]; fire conditions associated with most fire deaths due to toxic effects [15]; and new probabilistic measures of the effects of sprinklers [29]. More general reviews of data needs or data usage procedures also appeared [30], some specific to special environments, such as spacecraft [1]. One article provided a compilation of the implied cost per year of life saved for each of 500 US government regulations, including

many related to fire [42]. Yet another article addressed the issue of safety factors in general terms [26].

A number of articles appeared providing material on fire risk or hazard analysis in industrial settings [22], including spacecraft [1], chemical process industries [2], offshore oil platforms [13, 31, 44], and nuclear power plants [27].

Finally, miscellaneous papers addressed fire-related issues of risk perception [11] and the application to fire safety engineering of some less-recognized methods developed in the field of operations research, such as the analytical hierarchy procedure for addressing multiple objectives [10].

References

1. G.E. Apostolakis et al., "Experimental needs for spacecraft risk assessment," *Proceedings of the Fourth Symposium of the International Association for Fire Safety Science*, 1994, pp. 949-960.
2. Thomas F. Barry, "An introduction to quantitative risk assessment in chemical process industries," Chapter 5-12, *SFPE Handbook of Fire Protection Engineering*, 1995, pp. 5-102-5-127.
3. V.R. Beck, "Fire research lecture 1993: Performance based fire safety design -- Recent developments in Australia," *Fire Safety Journal*, 1994, pp. 133-158.
4. A.H. Buchanan, "Fire engineering for a performance based fire code," *Fire Safety Journal*, 1994, pp. 1-16.
5. R. Bukowski, "A review of international fire risk prediction methods," *Proceedings of the Sixth International Fire Conference, Interflam '93*, London: Interscience Communications, Ltd., 1993, pp. 437-446.
6. R.W. Bukowski, *Balanced design concepts workshop, June 30, July 1-2, 1993*, Gaithersburg, Maryland: National Institute of Standards and Technology, NISTIR 5264, September 1993.
7. A. Cornelissen, "Risk-cost assessment for non-residential buildings," *Proceedings of the Sixth International Fire Conference, Interflam '93*, London: Interscience Communications, Ltd., 1993, pp. 331-342.
8. G. Deakin and G. Cooke, "Future codes for fire safety design," *Fire Safety Journal*, 1994, pp. 193-218.
9. S. Deal, *Technical reference guide for FPEtool version 3.2*, Gaithersburg, Maryland: National Institute of Standards and Technology, NISTIR 5486, August 1994.

10. F.J. Dodd and H.A. Donegan, "Prioritisation methodologies in fire safety evaluation," *Fire Technology*, Second quarter, 1994, pp. 232-249.
11. John Eyles et al., "The social construction of risk in a rural community: Responses of local residents to the 1990 Hagersville (Ontario) tire fire," *Risk Analysis*, June 1993, pp. 281-290.
12. Rita F. Fahy and Guylene Proulx, "Collective common sense: A study of human behavior during the World Trade Center evacuation," *NFPA Journal*, March/April 1995, pp. 59-67.
13. M. Finucane, "The adoption of performance standards in offshore fire and explosion hazard management," *Fire Safety Journal*, 1994, pp. 171-184.
14. P. Gandhi, "Validation of FAST for room corner fire tests," *Proceedings of the Sixth International Fire Conference, Interflam '93*, London: Interscience Communications, Ltd., 1993, pp. 331-342.
15. R.G. Gann et al., "Fire conditions for smoke toxicity measurement," *Fire and Materials*, May/June 1994, pp. 193-199.
16. George V. Hadjisophocleous and David Yung, "Parametric study of the NRCC fire risk-cost assessment model for apartment and office buildings," *Proceedings of the Fourth Symposium of the International Association for Fire Safety Science*, 1994, pp. 829-840.
17. J. Hall, "Practical rules for selecting fire science tools appropriate to the decision to be made," *Proceedings of the Sixth International Fire Conference, Interflam '93*, London: Interscience Communications, Ltd., 1993, pp. 75-82.
18. John R. Hall, Jr., "Product fire risk," Chapter 5-10, *SFPE Handbook of Fire Protection Engineering*, 1995, pp. 5-87-5-94.
19. Akihiko Hokugo, David Yung, and George V. Hadjisophocleous, "Experiments to validate the NRCC smoke movement model for fire risk-cost assessment," *Proceedings of the Fourth Symposium of the International Association for Fire Safety Science*, 1994, pp. 805-816.
20. Peter F. Johnson, "International implications of performance based fire engineering design codes," *Journal of Fire Protection Engineering*, 1993, pp. 141-146.
21. Michael J. Karter, Jr. et al., "Cigarette characteristics, smoker characteristics, and the relationship to cigarette fires," *Fire Technology*, Fourth quarter, 1994, pp. 400-431.
22. D. Karydas, "A probabilistic methodology for the fire and smoke hazard analysis of electronic equipment," *Proceedings of the Sixth International*

Fire Conference, Interflam '93, London: Interscience Communications, Ltd., 1993, pp. 509-518.

23. H. Katzin and M. Khoury, "Fire risk analysis and assessment for the Canadian building code assessment framework," *Proceedings of the Sixth International Fire Conference, Interflam '93*, London: Interscience Communications, Ltd., 1993, pp. 699-708.

24. David A. Lucht, Charles H. Kime, and Jon S. Traw, "International developments in building code concepts," *Journal of Fire Protection Engineering*, 1993, pp. 125-133.

25. M. Luo and V. Beck, "The fire environment in a multi-room building -- comparison of predicted and experimental results," *Fire Safety Journal*, 1994, pp. 413-438.

26. S.E. Magnusson et al., "Determination of safety factors in design based on performance," *Proceedings of the Fourth Symposium of the International Association for Fire Safety Science*, 1994, pp. 937-948.

27. F.D. Mawby and A.P. Haighton, "The approach adopted in England and Wales in defining the level of fire safety at nuclear power stations," *Fire Safety Journal*, 1994, pp. 185-192.

28. Brian J. Meacham, "International development and use of performance-based building codes and fire safety design methods," *SFPE Bulletin*, March/April 1995, pp. 7-16.

29. S.J. Melinek, "Effectiveness of sprinklers in reducing fire severity," *Fire Safety Journal*, 1993, pp. 299-312.

30. Harold E. Nelson and Eric W. Forssell, "Use of small-scale test data in hazard analysis," *Proceedings of the Fourth Symposium of the International Association for Fire Safety Science*, 1994, pp. 971-982.

31. Elisabeth Pate-Cornell, "Managing fire risk onboard offshore platforms: lessons from piper alpha and probabilistic assessment of risk reduction measures," *Fire Technology*, May 1995, pp. 99-119.

32. R.D. Peacock et al., *CFAST, the consolidated model of fire growth and smoke transport*, Gaithersburg, Maryland: National Institute of Standards and Technology, NIST TN 1299, February 1993.

33. R.D. Peacock et al., "New concepts for fire protection of passenger rail transportation vehicles," *Second International Fire and Materials Conference*, London: Interscience Communications, Ltd., 1993, pp. 171-180.

34. R.D. Peacock, W.W. Jones, and R.W. Bukowski, *Verification of a model of fire and smoke transport*, *Fire Safety Journal*, 1993, pp. 89-129.

35. Guylene Proulx and George Hadjisophocleous, "Occupant response model: A sub-model for the NRCC risk-cost assessment model," *Proceedings of the Fourth Symposium of the International Association for Fire Safety Science*, 1994, pp. 841-852.
36. Milosh Puchovsky et al., "NFPA's future in performance-based codes," Quincy, MA: National Fire Protection Association, July 1995.
37. J.K. Richardson, "Moving toward performance-based codes," *NFPA Journal*, May/June 1994, pp. 70-78.
38. J. Kenneth Richardson, "Changing the regulatory system to accept fire safety engineering methods," *Journal of Fire Protection Engineering*, 1993, pp. 135-140.
39. Carol W. Runyan et al., "Risk factors for fatal residential fires," *Fire Technology*, Second quarter, 1993, pp. 183-193.
40. J. Snell, A. Fowell, and V. Babrauskas, "Elements of a framework for fire safety engineering," *Proceedings of the Sixth International Fire Conference, Interflam '93*, London: Interscience Communications, Ltd., 1993, pp. 447-456.
41. *Standard Guide for Development of Fire-Hazard-Assessment Standards*, ASTM E 1546, Philadelphia: ASTM, 1993.
42. Tammy O. Tengs et al., "Five-hundred life-saving interventions and their cost-effectiveness," *Risk Analysis*, June 1995, pp. 369-390.
43. W. Kip Viscusi and Gerald O. Cavallo, "The effect of product safety regulation on safety precautions," *Risk Analysis*, December 1994, pp. 917-930.
44. R. Brady Williamson, W. Gale, Jr., and R. Bea, "Fire safety assessment for offshore platforms," *Proceedings of the Sixth International Fire Conference, Interflam '93*, London: Interscience Communications, Ltd., 1993, pp. 797-807.
45. David Yung and Vaughan R. Beck, "Building fire safety risk analysis," Chapter 5-11, *SFPE Handbook of Fire Protection Engineering*, 1995, pp. 5-95-5-101.
46. D. Yung, G. Hadjisophocleous, and H. Takeda, "Comparative risk assessments of 3-storey wood-frame and masonry construction apartment buildings," *Proceedings of the Sixth International Fire Conference, Interflam '93*, London: Interscience Communications, Ltd., 1993, pp. 499-508.

Discussion

Henry Mitler: Could you give us some numbers about the value of lives saved?

John Hall: The study I referred to examined 500 different U.S. Government-related programs and analyzed their cost and of the number of lives that they saved. Their calculated ratios found, as one might expect, a tremendous variation: multiple orders of magnitude in the value of life that those agencies had achieved.

Professor Pagni: I too was very interested in the study of life evaluation. Can you tell us which of your references gives that information in detail and can you tell us anything more about it?

John Hall: Look for reference 42 in the written paper.

PROGRESS REPORT ON PERFORMANCE-BASED FIRE SAFETY DESIGN METHOD

Takeyoshi TANAKA

Building Research Institute, Ministry of Construction

1 Tatehara, Tsukuba-shi, Ibaraki-ken 305, JAPAN

1. FIRE SAFETY DESIGN METHOD

A subcommittee of MOC's 5 year project: "Development of Evaluation Method of Fire Performance of Building Elements (1993 - 1997)" is undertaking the development and refinement of the performance-based design method of buildings jointly with the AIJ (Architectural Institute of Japan) Fire safety design method committee.

The current stage of the development is about as follows:

(1) It is the first step for developing performance based fire safety design method to identify and define the fundamental requirements (Objectives) for fire safety of buildings. These have been completed. The requirements for prevention of urban fire is included as well as the requirements for fire safety of individual buildings.

(2) The technical standards for verification of compliance have been developed for most of the requirements, but the standards for some objectives remains to be undeveloped. Currently stress is placed on the development of performance oriented criteria for means of escape alternative to the prescriptive requirements in the existing building codes:

(a) The requirement of "two or more exits" from a room was considered from the viewpoint of expected number of occupants unable to escape due to the onset of fire in front of exits, and the criterion alternative to the existing requirement was established.[1]

(b) The requirements on "common path length" and "single stairway (exemption of two or more stairways)" were also considered from the viewpoint of expected number of occupants unable to escape due to the obstruction of corridor and stairway by fire, and the criterion alternative to the existing requirement was established.[2]

(c) The method for assessing the degree of legibility of escape route is explored using computer simulations from the viewpoint of the expected distance that evacuees who are unfamiliar with the building cover before they arrive at one of the exits. The practical criterion for use in actual design practice is still under consideration. [3]

(3) Design Fire

The effect of the consumption of oxygen on the design fire for compartment fire was studied, and the previous design fire, which consists of the initially growing and the threshold heat release rates were revised. A sudden decrease of the transient heat release rate may appear in the new design fire depending on the conditions of initial air capacity and ventilation of fire room.

2. FIRE SAFETY ENGINEERING TOOLS

For the verification of compliance with requirements based on the performance standards, which are usually prescribed in terms of safety criteria and design fire, fire safety engineering tools for estimating the effect of fire behaviors are indispensable. Considering the difficulty in validating computer fire models, analytical or hand calculation methods should be developed as many as possible. Such calculation method, even though limited to simple conditions, will be useful in many practical applications.

The recent activities addressing the development of the simple calculation methods are as follows:

(1) Simple formula for ventilation controlled room fire temperature

McCaffrey-Quintiere correlation was extended to predict the temperatures of the room of origin under ventilation controlled fire and the connected corridor.[4]

(2) Heat of combustion of excess fuel in widow flames

The experimental investigations were carried out for the validity of empirical correlation on the mass burning rate of fully developed fire for different fuel conditions in order to estimate the total heat of window flames, which is important for assessing the hazards of upper floor fire spread.[5]

(3) Temperature of smoke and pressure in cavity fire

Behavior of smoke ejected into cavity like spaces in buildings cannot be predicted by zone fire models and using field model takes painful time. The experimental correlation of temperature of plume and the pressure difference induced in the space with heat release rate, dimensions of cavity space and bottom opening size has been developed.[6]

(4) Time of initial ascent of plume front

The time that the rising plume front arrives at a given height right after the ignition of the source was experimentally investigated in the open air and in the shafts and the correlation of the time and the heat release rate and height has been developed.[7]

(5) Practical method for predicting evacuation

Computer models for predicting evacuation of occupants in fire exist but practical methods for assessing the evacuation time and the magnitude of queue in front of exits are necessary. The development of such methods is still under stage of consideration.

REFERENCES

- [1]Tanaka, Hagiwara & Mimura: A Consideration on Required Number of Exits in a Room
- [2]Hagiwara, Tanaka & Mimura: A Consideration on Common Path Length and Single Stairway
- [3]Ebihara: Assessment of Clarity of Egress Route in Buildings
- [4]Tanaka, Sato & Wakamatsu: Simple Formula for Predicting Ventilation Controlled Room Fires
- [5]Ohmiya, Tanaka & Wakamatsu: A Compartment Fire Model in view of Predicting Fire Spread by External Flames
- [6]Tanaka, Fukuda & Wakamatsu: Experiments on Smoke Movement in Cavity Space
- [7]Fujita, Tanaka & Wakamatsu: Time of Ascent of Fire Plume Front, under preparation for AIJ Buletin.

(Note: References[1] - [6] will be presented in this UJNR joint meetings)

Discussion

James Quintiere: I will be interested in your paper using our simple method because the method was used for controlled records and support data. My question is one on clarification. What do you mean by cavity space?

Takeyoshi Tanaka: What we call cavity space is the space integrated into buildings which have no roof.

James Quintiere: One of the things you mentioned is that you need to define performance. I wanted to ask whether this task group is going to look at specific installations, for example, and suggest how one can arrive at what performance would provide safety?

SFPE PERSPECTIVES ON PERFORMANCE-BASED FIRE SAFETY DESIGN

Brian J. Meacham, P.E.
Society of Fire Protection Engineers
One Liberty Square
Boston, MA 02109, USA

ABSTRACT

Performance-based codes* and fire safety engineering** methods are the focus of significant discussion, research, and development activities worldwide. In many respects, this is a result of the large increase in knowledge in the areas of fire science and engineering over the past twenty years and of the societal and economic pressures to provide an acceptable level of fire and life safety in buildings at a reasonable cost. While several countries have begun to use, or are developing, performance-based codes, many people have concerns about the availability of proven engineering and design methods for use within a performance-based code framework. Although many of the countries that are developing performance-based codes are also developing performance-based engineering and design methods, the codes are preceding the engineering methods, and the engineering methods have gone essentially unvalidated. There is also concern about the availability of qualified fire safety engineers to undertake performance-based designs, the availability of qualified authorities to review performance-based design, and the issue of liability related to performance-based design. The Society of Fire Protection Engineers supports the development of performance-based codes and fire safety engineering methods. However, the SFPE also recognizes that practical barriers to the widespread acceptance of performance-based fire safety codes and engineering methods exist in the United States, and in other countries of the world, and is working in several areas to address the needs of the fire safety engineering community in this regard.

INTRODUCTION

There are a number of interest groups that comprise the global fire and building community. These include building owners and managers, architects, engineers, construction contractors, building officials, fire officials, product manufacturers, the insurance industry, and more. The Society of Fire Protection Engineers represents one segment of this community: fire protection engineers. As such, the SFPE represents the body of knowledge of fire protection engineering, and is an advocate for the profession and its technology within the greater community. In this role, the SFPE advocates the proper use of fire safety engineering principles and supports the implementation into practice of emerging fire safety engineering tools and methodologies that can benefit the greater fire and building community.

* The term 'codes' will be used to cover the broad areas of codes, standards and regulations.

** The terms fire safety engineering, fire protection engineering and fire engineering are used interchangeably throughout.

Given this position, the SFPE finds itself becoming increasingly involved in discussions and projects related to performance-based codes and fire safety design methods in the United States and around the world. The reasons for this are clear: for a performance-based system to be effective, there must be acceptable engineering practices available to support performance-based codes, and there must also be acceptable engineering tools and methods available to support the engineering practices.

THE INTERACTION OF PERFORMANCE-BASED CODES AND DESIGN METHODS

The interaction between performance-based codes and design methods can be viewed as a single, *performance-based system* with three major components:

- The Code, which reflects society's expectations of the level of health and safety provided in buildings (e.g., requirements for acceptable access, egress, ventilation, fire protection, electrical services, sanitary services, etc.);
- Engineering Practices, which describe acceptable processes and procedures for complying with the requirements of the Code (e.g., acceptable design approaches); and,
- Tools and Methodologies, which provide the means for undertaking designs in accordance with Engineering Practices (e.g., equations, correlations, models).

If any one of the three components is missing, the system is considerably weakened, and in some cases, may not function (e.g., the availability of an engineering tool without guidance on its applications and limitations limits the effectiveness of the tool).

To support the development of the overall performance-based system, the SFPE is focusing on the two fire safety engineering areas: development of engineering practices (engineering practice documents) for use in fire safety design, and identification and evaluation of engineering tools and methodologies, developed by research and academia, that are intended for use in fire safety engineering practice.

To help place the engineering aspects of the performance-based system into perspective, the SFPE is also looking at how a performance-based system might be structured if implemented in the United States. This is important: the system may not work if the components are improperly aligned or out of balance (e.g., a performance-based code without engineering practices available to meet code requirements).

The SFPE is convening a focus group of leaders from the fire and building communities in the United States, supplemented with experts from around the world who have been active in the development and implementation of performance-based systems in their countries. The group will be given working concepts and definitions to use as bases, and will be asked to comment on items of interest and concern to them regarding the implementation of a performance-based system in the United States. Some of the working concepts and definitions that will form the basis for discussion are as follows.

PRESCRIPTIVE CODES AND PERFORMANCE-BASED CODES

In general, building codes describe how a building should perform under normal and adverse conditions (e.g., fire) in meeting the health and safety needs of the community.

Prescriptive codes describe the desired level of performance for health and safety through a set of minimum requirements that are generic by occupancy. Examples include occupancy-based spacing requirements for detectors or sprinklers, a specified fire resistance rating for an interior wall, or the maximum travel distance to an exit. While these may be appropriate for a general minimum, the true objective of a stated requirement in a specific design situation can be lost.

For example, one may know the maximum permitted travel distance to the exterior of the building, but not know the extent of smoke spread within a building before the last occupant is expected to have escaped. Thus, if the intended objective of the travel distance restriction is life safety, it would be easy to state that the requirement has been met, but difficult to state that the objective has been met. By contrast, performance-based codes describe requirements for health and safety through a set of flexibly defined performance objectives and functional requirements. Examples include broad-based statements such as:

- the objective of this requirement is to safeguard people from injury from the effects of fire while evacuating a building, and,
- installation of an automatic suppression system intended to control the development and spread of fire shall be appropriate to the building use and characteristics, the fire hazard, the height of the building and the size of the fire compartment.

In this case, the solution is not prescribed in the regulations. Rather, it is the responsibility of the designer to demonstrate that the proposed design meets the health and safety needs of the community by meeting the performance objectives and functional requirements of the code. This demonstration of compliance can be accomplished through the application of either deemed-to-satisfy (prescriptive) solutions or performance-based design solutions based on accepted engineering practice (with prescriptive-type requirements for test, installation and maintenance).

ENGINEERING PRACTICES AND PERFORMANCE-BASED DESIGN

Engineering practices (or engineering practice documents) are generally considered framework or guidance documents that establish appropriate process and procedure for the undertaking of an engineered approach to a problem. Where only a small number of analytical procedures exist, they may be incorporated into the document, otherwise they will likely be referenced. One example of an engineering practice might be an engineering practice for the calculation of structural fire resistance. One might expect such a document to identify the analysis process and include material properties, dimensions and orientation, failure temperatures, effects of protective coverings, and possibly analytical procedures as well. If properly developed, this document should provide all of the necessary information to undertake a calculation of structural fire resistance.

To promote the development and use of engineering practice documents for fire safety engineering, the SFPE has formed a task group to develop engineering practice documents. The goal for the Engineering Task Group (ETG) on Engineering Practices is to begin developing a range of engineering practices for the fire protection engineering community. These documents will help fire protection engineers and regulatory officials understand the process to be followed, the engineering tools and methodologies available for use within the process and how to apply the engineering tools and methodologies with confidence. The first task of this group is to develop an engineering practice document on thermal radiation hazard calculations. A number of other fire safety engineering topics will be addressed in the future.

A document that outlines a performance-based approach to fire safety design can also be considered an engineering practice. A performance-based approach to fire safety design is an engineering approach to fire safety design based on (1) agreed upon fire safety goals, loss objectives and performance objectives, (2) deterministic and probabilistic evaluation of fire initiation, growth and development, (3) the physical and chemical properties of fire and fire effluents, and (4) a quantitative assessment of design alternatives against the loss and performance objectives.

Although a performance-based approach can be undertaken with or without the presence of a performance-based code, a performance-based code must reference at least one performance-based design approach, or engineering practice, to outline the process and procedure for complying with the requirements of the code. This is necessary because a performance-based code may contain only functional objectives and performance criteria, and likely does not contain detailed requirements as are present in a prescriptive code. Therefore, without the requirements of a prescriptive code to follow, an engineering practice document will assist the designer in identifying critical components of the design process which should be considered. The SFPE is currently attempting to identify the fundamental components of such an engineering practice, or framework for performance-based fire safety design, for application within the United States.

ENGINEERING TOOLS AND METHODOLOGIES

Fire safety engineering tools and methodologies encompass those equations, correlations, models and procedures used for engineering analysis and prediction of fire and fire related phenomena. Computer models used in fire and life safety analysis and design, for example, are considered fire protection engineering tools. So too are many of the equations and correlations found in the SFPE Handbook of Fire Protection Engineering. The difference between an engineering practice and engineering tools and methodologies is that an engineering practice provides the process and procedure to solve a global problem, and tools and methodologies are used to solve components of the global problem in accordance with the engineering practice.

For example, to estimate the available time for safe egress from a particular building, one might well undertake a process that includes determining building characteristics and features, fuel loading and arrangement (contents, interior finish, etc.), determining occupant characteristics, developing performance criteria (e.g., what renders the egress path unsafe), developing potential

fire scenarios, evaluating protection alternatives and evaluating evacuation factors. A process such as this would be well-suited to an engineering practice for evaluation of safe egress times.

Within this process, it will be necessary to perform a number of specific analyses, such as estimation of fire growth and spread, estimation of smoke production and propagation and estimation of fire detector activation. For these analyses, specific tools, such as computer fire models, and methodologies, such as those outlined in the SFPE Handbook for estimation of fire detector response to a growing fire, may be applied.

The first step that the SFPE has taken towards evaluating engineering tools and methodologies is the formation of an Engineering Task Group on Computer Model Evaluation. The goal for the ETG on Computer Model Evaluation is to evaluate computer models, intended for use in fire safety engineering, on their applicability, use and limitations within the evaluation and design processes. It will do this by stating the intended use of the model (from the model documentation) and evaluating the model and its documentation against its intended function. (It is not the intent to compare different models to each other.)

To minimize duplication of efforts in the area of developing evaluation methods for computer models, the ETG on Computer Fire Model Evaluation will apply various ASTM guides, i.e., ASTM E 1355, Standard Guide for Evaluating the Predictive Capability of Fire Models, ASTM E 1472, Standard Guide for Documenting Computer Software for Fire Models, and ASTM E 1591, Standard Guide for Data for Fire Models. Additional evaluation criteria and procedures will be used and/or developed as necessary. Sub-groups have been established within this ETG to look at procedures and protocol, documentation, test data for model evaluation, and algorithm evaluation. A framework for the evaluation reports is under discussion.

FIRE PROTECTION ENGINEERS AND FIRE PROTECTION ENGINEERING

Given that a performance-based system will be new to the United States, and that such a system will ultimately be more fire safety engineering intensive than a prescriptive-based system, the role of fire protection engineers in the performance-based system will likely increase. To help better clarify the role of fire protection engineers in the performance-based system, and why their role may be increasing, the following principles are currently being discussed within the SFPE:

- A performance-based system is based on the ability to engineer solutions to meet objectives.
- The use of engineering tools and methodologies in the analysis or design of fire safety measures to meet fire safety objectives constitutes the practice of fire safety engineering.
- The identification, evaluation and selection of fire scenarios, for use in an engineering tool, methodology or practice, that are based on fuel characteristics, loading and arrangement, compartment characteristics (e.g., volume), environmental characteristics (e.g., ventilation), occupant characteristics and situation related information, constitutes the practice of fire safety engineering.

- Fire safety engineering tools and methodologies should be utilized in the engineering of fire safety measures (performance-based or prescriptive) and reconstruction of fire incidents only where deemed acceptable by the fire safety engineering community.
- To attain “acceptable” status, fire safety engineering tools and methodologies should have been widely challenged in a peer-review process, or have been developed in or received positive evaluations in a consensus process among qualified engineers, educators and researchers, and have been validated in their ability to generate outcomes consistent with those claimed by the developer when used in accordance with the appropriate documentation. Safety and reliability factors that are included, or are required to be added, should be explicitly stated and based on accepted engineering theory, practice or statistics.

These are just a few of the concepts currently being discussed. Although the wording may change with additional discussion, the basic principles will likely remain in place: a performance-based system, in some form, is coming to the United States. A complete performance-based system requires a performance-based code, engineering practices, and acceptable engineering tools and methodologies, and a performance-based system requires qualified people to undertake performance-based designs. It will be interesting to see how these concepts evolve over the next few years.

SUMMARY

As in many other parts of the world, code development organizations in the United States are beginning to discuss the use of performance wording in their codes and standards. For such wording to become a reality in building and fire regulations, and for a performance-based system to see wide-spread acceptance in the United States, a number of practical fire protection engineering issues need to be addressed. The Society of Fire Protection Engineers recognizes this and is taking significant steps towards attaining their goal of identifying, evaluating and implementing into practice those engineering tools and methods necessary for fire safety design within a performance-based code framework in the United States. This includes helping to identify a performance-based system for the United States, outlining the needed components of a framework for performance-based fire safety design, developing engineering practice documents to support a performance-based system, identifying and evaluating engineering tools and methodologies for use in a performance-based system, and continuing to transfer knowledge and provide educational services in the area of performance-based fire safety engineering.

ACKNOWLEDGMENTS

The SFPE would like to thank the National Institute for Standards and Technology for their support of the focus group on performance-based codes and fire safety design methods, and associated research, under grant number 60NANB5DO138: Assessment of the Technological Requirements for the Realization of Performance-Based Fire Safety Design in the United States. This paper is an excerpt of the paper “Performance-Based Codes and Fire Safety Engineering Methods: Perspectives & Projects of the Society of Fire Protection Engineers” which can be found in the proceedings of Interflam ‘96, Interscience Communications Ltd, London, 1996.

Discussion

Ronald Alpert: I was curious as to where the financial resources are coming from for this very ambitious effort that you have outlined. I'm betting on a Swiss bank account.

Brian Meacham: As I have mentioned earlier, NIST has been very supportive of SFPE in these efforts. In particular, with this focus group, the SFPE has a grant from NIST to study the technology requirements for implementation of a performance-based system in the U.S., and much of our support now comes from NIST. We would welcome future support from Factory Mutual Research.

Life Safety Evaluation of Large Populations with Mixed-Abilities

Shuji Kakegawa and Yoshiro Yashiro
Institute of Technology, Shimizu Corporation
3-4-17 Etchujima Koto-ku, Tokyo 135, Japan

Manabu Ebihara
Izumi Research Institute, Shimizu Corporation
2-2-2 Uchisaiwai-cho Chiyoda-ku, Tokyo 100, Japan

Abstract

The authors had developed an evacuation model which can predict evacuation of large populations with mixed abilities. The advantages of the model are: 1) to handle the evacuation of persons with mixed abilities, 2) to change egress routes in accordance with local environmental conditions, 3) to handle contra-flows and overtaking which occur between evacuees, 4) to handle interactions between individuals in a crowd and 5) to handle total evacuation of a multi-story building. In this study, we describe the outline of the model and its application. In order to clarify the influence of variation of egress capabilities on evacuation time, some case studies are carried out. After that, we clarify the problems in planning life safety for large populations with mixed-abilities against a fire.

1. Introduction

In recent years, large-scale buildings have increased especially in urban areas in Japan. In Tokyo, there are 68 high-rise buildings which are over 100 meters tall in 1994[1]. Large-scale buildings have some problems in total evacuation from a fire, because they have a large population with mixed-abilities. Some important aspects of the evacuation from large-scale buildings are summarized as follows; 1) a long period of total evacuation time via staircases, 2) congestion of mixed-ability population and 3) rapid smoke spread to the upper floors via vertical compartments.

In Japan, high-rises and other specified occupancies must meet requirements according to *The Guide for Building Fire Safety Planning*[2]. It requests life safety evaluation by calculating some egress times on the fire floor at assigned limits[3]. However, in planning buildings for large populations with mixed-abilities, more detailed information will be needed to clarify problems in planning to improve. If a building designer or an engineer supposes to evaluate evacuation safety for those building, detailed simulation of evacuation behavior will play important roles.

In predicting evacuation behavior of mixed abilities, interactions between individual evacuees is one of the most important factors. Recently, some attempts have been made to predict individual egress behavior, for example, EXIT89[5], SIMULEX[6], EvacSim[7]. These models are intended to handle individual egress movement and it enables us to examine the influence of egress capabilities of evacuees on life safety.

To evaluate life safety of the disabled in health care facilities, the authors had developed an evacuation model which can predict mixed population evacuation[4]. We have modified the model in order to handle larger number of individual people with mixed-abilities. In this study, we describe the evacuation model which is modified for large populations with mixed-abilities and clarify the problems in planning life safety for them against a fire.

2. Model Description

2.1 Characteristics and Assumptions

The evacuation model is a deterministic simulation program implemented by the object-oriented computer language, C++. The model is an advanced version of the previous one, which was developed for health care facilities[4]. The model comprises three sub-models; the space model, the human model and the smoke model. The simulation process corresponds to information exchange between the sub-models. Figure 1 shows the evaluation process for evacuation safety using the evacuation model. These sub-models play roles as follows:

- 1) Space Model; for modeling all rooms of a building and connection between rooms,
- 2) Human Model; for modeling evacuees and their decision making process to determine positions of them and their evacuation routes,
- 3) Smoke Model; for modeling the spread of smoke in a building.

The advantages of the evacuation model are: 1) to handle the evacuation of persons with mixed abilities, 2) to change egress routes in accordance with local environmental conditions, 3) to handle contra-flows and overtaking which occur between evacuees, 4) to handle interactions between individuals in a crowd and 5) to handle total evacuation of a multi-story building. The advantages which are expanded in this version correspond to items 4) and 5) as mentioned above. However the previous version can handle the rescuers' behavior, the current version abbreviates them for simplicity of calculation. Psychological factors influencing evacuation behavior are not considered in the model.

2.2 Egress Behavior Modeling

In choosing egress routes, occupants select two types of targets; a short term target and a long term target. The short term target indicates a place which people should pass through, for example, a door. The long term target indicates a place where people finally escape. People continue evacuation until they reach a long term target. Rules for choosing a target and determining the position at the next step are described in the previous paper[4]. In the Human Model, evacuees are modeled according to the following parameters: spatial requirement of a person, travel walking speed and type of egress route finding.

(1) Spatial Requirement of a Person

In the model, all people are modeled in circles individually to consider human spatial requirement. The diameter of a circle is determined as 0.4 meter with consideration of the size of body. Using the distance between evacuees and spatial requirements, interactions between people are assessed. It is an important factor in predicting congestion or contra-flows of a crowd.

(2) Travel Walking Speed

In this model, fluctuations in individual walking speed is defined due to the crowd density. Relationship between the walking speed and density is defined as following equation with reference to the previous studies, for example, by Predtechenskii & Milinskii[8]:

$$\begin{aligned} V_h &= V_{max} / p & (p \geq 1.0 \text{ person/m}^2) & (1) \\ V_h &= V_{max} & (p < 1.0 \text{ person/m}^2) & (1)' \end{aligned}$$

where V_h is horizontal walking speed, V_{max} is maximum horizontal walking speed and p is crowd density. V_{max} varies from 0.5 to 1.5 meter per second according to the egress capabilities of occupants. p is calculated for the area of half circle having a radius of 3.0 meters around an evacuee as illustrated in Figure 2(a). If p is below 1.0 in person per square meter, V_h is constant at V_{max} .

If crowd density of the adjacent room around a door is high, people can not merge and have to queue in front of the door. To model merging of crowd flows at a door, queuing is assumed to be caused when crowd density is over six person per square meter in the area of half circle having a radius of 1.0 meters around him/her (see Figure 2(b)).

(3) Type of Egress Route Finding

Egress route finding is modeled according to the results of a survey to occupants of a sixty story complex high-rise building in Tokyo[1]. The survey was carried out by asking questionnaire about the egress route finding to 757 respondents. They include 193 office workers, 464 visitors of a department store or a hall and 100 visitors of a hotel. From the survey, occupants are categorized as three types in egress route finding;

- 1) occupants who evacuate according to the self-judgment (Type I),
- 2) occupants who evacuate following the instruction (Type II),
- 3) occupants who move depending on the other people (Type III).

In the model, Type I occupants always choose the nearest door or exit. Type II occupants determine egress direction according to the guide light which is modeled in the Space Model. Type III occupants follow the neighbors.

2.3 Multi-Story Evacuation Modeling

The model of this version can take into account total evacuation of a multi-story building. Staircases are modeled as one room like a corridor which has the same width of the stair. Steps on a staircase are not considered. Travel walking speed in a staircase is reduced in comparison with the horizontal walking speed as shown in the following equation:

$$V_s = C V_h \quad (2)$$

where V_s is horizontal component of walking speed in staircases, V_h is horizontal walking speed on a floor and C is a speed reduction factor (=0.8).

2.4 Smoke Spread Modeling

To predict the spread of smoke, the two-layer zone model, BRI2, is employed[9]. Using the results of smoke simulation, physiological impact of smoke at time t , $S(t)$, is calculated for each room. $S(t)$ is given by the following equation:

$$S(t) = \sum_{ts}^t (\Delta T)^2 \delta t \quad (3)$$

where δt is time interval for simulation (in this study, $\delta t=1.0$ second), ts is the smoke-exposure starting time, and ΔT is the temperature rise in the smoke layer. If $S(t)$ in a room i becomes over 4,000, the room i is assumed to reach the critical egress time[9], te , when any persons in the room i are assumed to become victims. After falling under te , the room is blocked due to smoke and anyone cannot enter there. In this model, the influence of people's movement on smoke movement cannot be considered because the two-layer zone model is separated from the evacuation model.

3. Model Validation

To validate the evacuation model, the predicted results of total evacuation are compared in part with a previous evacuation drill in a high-rise building[9]. A hypothetical building for model validation consists of seventy floors of office space. Initial occupant load is 0.125 persons per square meter at the average, which is derived from *The Guide for Building Fire Safety Planning*[2].

Figure 3 illustrates a typical floor plan of the building. There are 272 occupants on each floor. The ground floor is used for a lobby and there are no occupants initially.

The building where the evacuation drill were carried out consists of seventeen floors of office space. There were 1,242 occupants in the building.

The flow rate at an exit door on the first floor, crowd density and walking speed in a staircase are chosen as the indexes to compare the results with the one of the observed evacuation drill. Smoke spread and variation of egress capabilities are not considered. Horizontal walking speed of an evacuee is set at 1.0 meter per second.

Table 1 shows the comparison of the predicted and the observed evacuation. The predicted flow rate at the exit door of the staircase agreed approximately with the observed one. Modeling individuals influences a good agreement of the results. Although the horizontal component of walking speed of the predicted evacuation is lower than the observed one, it does not so much influence the predicted total evacuation time. This is because flow rate at the exit door much influences the total evacuation time in these cases. From the results, it is considered that the model can be used to predict the total evacuation in a multi-story building.

4. Application of the Model

In order to clarify the influence of egress capability profiles of occupants, some case studies were carried out. In the case studies, types of egress route finding and travel walking speed are chosen for the parameters of egress capabilities. A building for application has the same floor plan as the one for model validation. It consists of five floors of office space. In these cases, all occupants in the building are assumed to start evacuation at the same time. For simplicity, smoke movement is not considered in the case studies.

4.1 Case 1: Influence of Variation of Walking Speed

For the first example, influence of egress capability profiles in walking speed are examined. Table 2 shows a number of occupants on one floor for three different cases.

Figure 4(a) shows relationship between time and a total number of evacuated occupants. If rates of occupants at slow speed are higher, total evacuation time becomes longer remarkably. It takes about 1.8 times in total evacuation of Case 1-1 in comparison with the one of Case 2-3. In general, population profiles in Case 1-1, 1-2, 1-3 almost correspond to an office, a department store and a hospital, relatively. If the disabled have to evacuate from large-scale building, it possibly takes a long time in total evacuation and they may be in more dangerous situation.

Figure 5(a) shows an average crowd density in a staircase. The average crowd density represents a number of people in unit area of staircase where people are evacuating. The highest density becomes about 3.0 persons per square meter in Case 1-1 and 1-2. It is approximately equal to 1.3 persons per one stair step. Contrary to these cases, peak crowd density in Case 1-3 becomes about 5.8 persons per square meter. It is over twice as the results of the previous experiment carried out by Paul[10]. In the case where rates of occupants at fast speed are high, no consideration of stair steps in modeling staircases seems to influence the crowd density in the staircase. In real evacuation, stair steps restrict the evacuation flow.

4.2 Case 2: Influence of Type of Egress Route Finding

For the second example, influence of egress capability profiles in types of egress route findings are examined. Table 3 shows a number of occupants on one floor for three different cases. In the case studies, occupant Type I and II are supposed to be the same, because evacuation instruction was not considered in these cases.

Figure 4(b) shows relationship between time and a total number of evacuated occupants. Although profiles of occupants in type of egress route finding are different, total evacuation times were almost the same. In the case study, congestion around the door of the staircase offset their delay due to the relatively simple egress route. Occupants who depend on the other people delayed to start evacuation, because their egress targets were uncertain in the beginning of the evacuation. In more geometrically complex building, for example, a department store, types of egress route finding will much influence total evacuation time.

5. Conclusions

The proposed evacuation model of the advanced version can handle the total evacuation of large population with mixed-abilities. By comparison between the predicted and the observed evacuation, it is considered that the model is validated for the observed drill evacuation.

From the results of applications, it is concluded that variation in walking speed much influences on total evacuation time than types of egress route finding in a building which has simple egress routes. Large-scale buildings have much difficulty in total evacuation as shown in the case of World Trade Center Bombing in 1993, especially for the disabled[11]. The strategies of total evacuation, for example, partial evacuation, will be one of the important factors to ensure life safety of mixed-ability large population.

The evacuation simulation provides a quantitative evaluation method of life safety to aid building designer. It can possibly be applied to the performance based design of a building to compare the effects of fire safety provisions. To use the evacuation model in planning buildings, valid fire and evacuation scenarios for evaluating life safety should be determined in reference to previous fire accidents.

Acknowledgements

This research was supported in part by the Tokyo Fire Department. We would like to express our appreciation for their helpful corporation.

References

- [1] The Tokyo Fire Department: "Report on the appropriate fire safety measures in large-scale buildings," 1995 (in Japanese)
- [2] The Building Center of Japan: The Guide for Building Fire Safety Planning, 1985 (in Japanese)
- [3] Yoshida, Y.: "Evaluating building fire safety through egress prediction: a standard application in Japan," Fire Technology, No.2, Vol.31, 1995
- [4] Kakegawa, S., Y.Yashiro, M.Ebihara and A.Otsuki: "Evaluation of fire safety measures in care facilities for the elderly by simulating evacuation behavior," Fire Safety Science- Proceedings of the Fourth International Symposium, 1994
- [5] Fahy, R.F.: "Exit 89- An evacuation model for high-rise buildings- model description and example applications," Fire Safety Science- Proceedings of the Fourth International Symposium, 1994
- [6] Thompson, P.A. and E.W.Marchant: "A computer model for the evacuation of large building populations," Fire Safety Journal, Vol.24, 1995
- [7] Poon, L.S.: "EvacSim: a simulation model of occupants with behavioural attributes in emergency evacuation of high-rise building fires," Fire Safety Science- Proceedings of the Fourth International Symposium, 1994
- [8] Predtechenskii, V.M. and A.I. Milinskii: "Planning for foot traffic flow in buildings," Amerind Publishing Company Inc., New Delhi, 1978
- [9] Ministry of Construction in Japan: Report in fire safety design methods for buildings (in Japanese), 1988
- [10] Paul, J.L.: "Building evacuation: research findings and recommendations," Fires and Human Behavior, John Wiley & Sons Ltd., 1980
- [11] Juliet, E.: "Evacuating people with disabilities," Fire Engineering, No.12, Vol.146, 1993

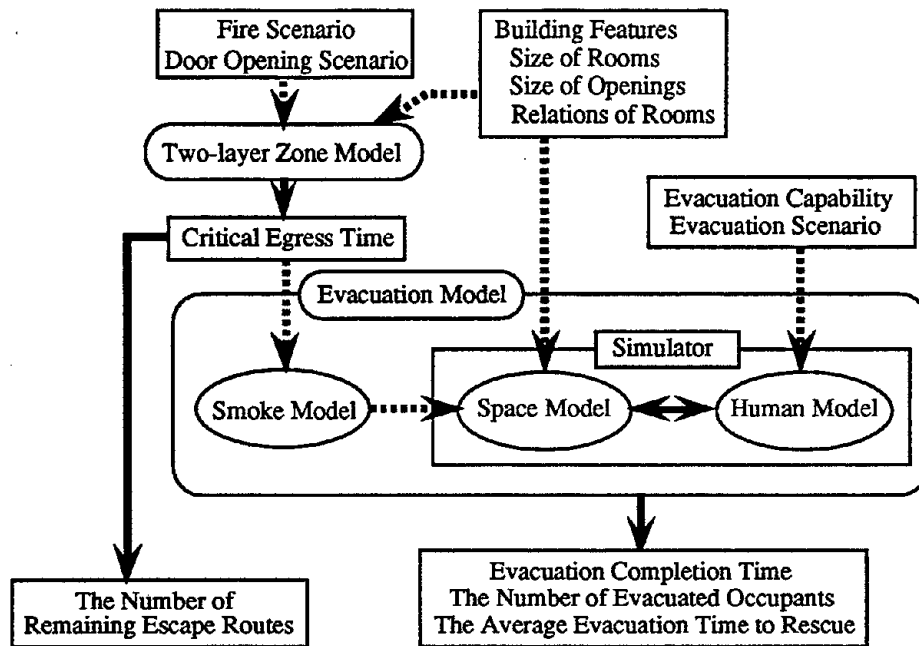
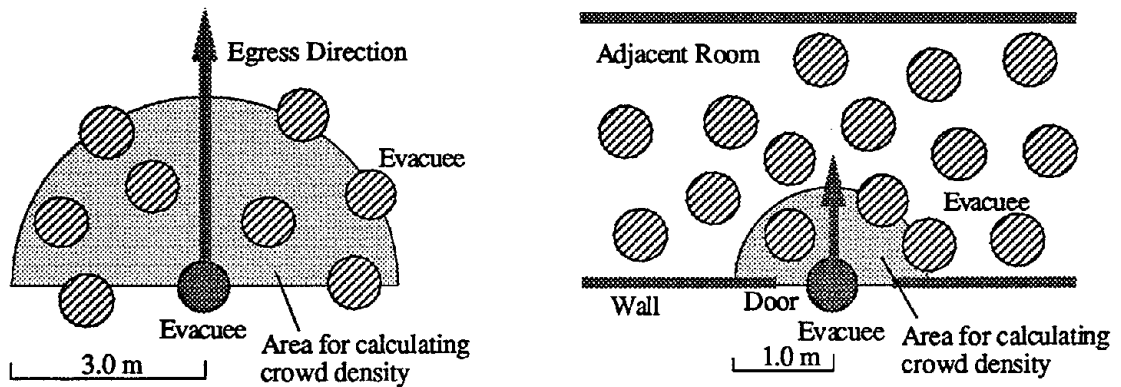


Figure 1. Life Safety Evaluation Process Using the Evacuation Model



(a) Speed Reduction Assessment in a Crowd

(b) Flow Mergence Assessment at a Door

Figure 2. Obstruction Zone for Egress Behavior

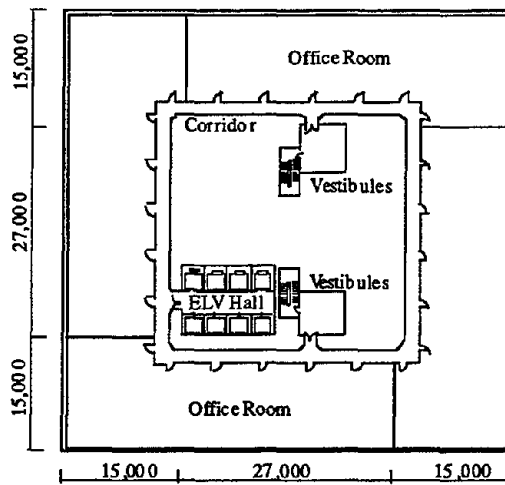
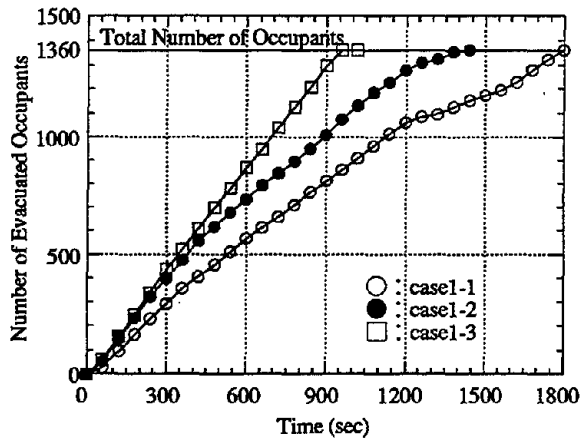
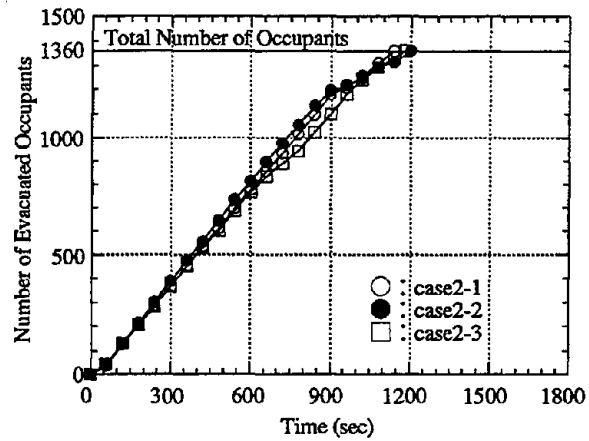


Figure 3. Typical Floor Plan for Applications of the Evacuation Model

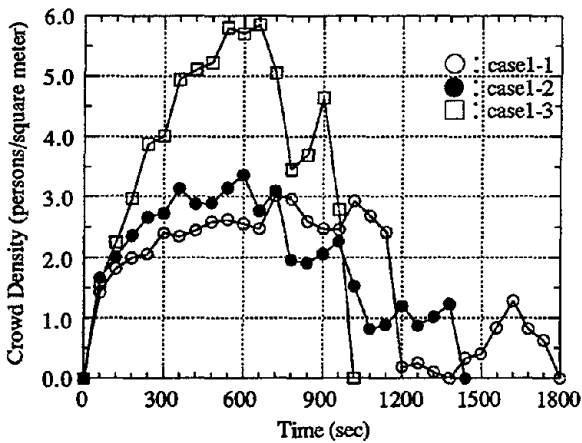


(a) Case 1: influence of walking speed

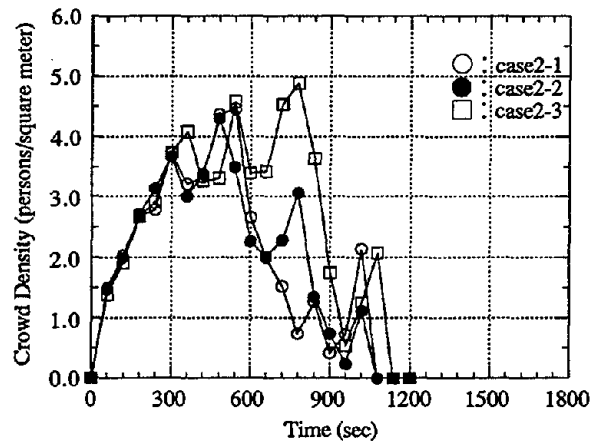


(b) Case 2: influence of type of route finding

Figure 4. Relationship between Time and Number of Evacuated Occupants



(a) Case 1: influence of walking speed



(b) Case 2: influence of type of route finding

Figure 5. Relationship between Time and Average Crowd Density in a Staircase

Table 1. Comparison between Observed and Predicted Evacuation

	The Observed Evacuation [9]	The Predicted Evacuation
Stories of the building	17	70
Populations per one staircase (persons)	621	9520
Stair width (meter)	1.2	1.4
Exit door width of the staircase (meter)	0.88	0.9
Flow rate at a door on the first floor (persons/meter/second)	0.80~0.89	0.83
Maximum crowd density (persons/square meter)	4	3.5
Horizontal component of walking speed in a staircase (meter/sec)	0.35~0.5	0.15~0.3

Table 2. Egress Capability Profiles in the Case Studies (Case 1)

Maximum Travel Walking Speed : Vmax	Number of Occupants on each Floor		
	Case 1-1	Case 1-2	Case 1-3
0.5 (meter/sec)	177 (65%)	91 (33%)	— (—)
1.0 (meter/sec)	95 (35%)	90 (33%)	95 (35%)
1.5 (meter/sec)	— (—)	91 (33%)	177 (65%)

Table 3. Egress Capability Profiles in the Case Studies (Case 2)

Type of Egress Route Finding	Number of Occupants on each Floor		
	Case 2-1	Case 2-2	Case 2-3
Self-Judgment (Type I & II)	245 (90%)	190 (70%)	136 (50%)
Dependants (Type III)	27 (10%)	82 (30%)	136 (50%)

Discussion

John Hall: Have you compared the modeling approach that you've used to other evacuation models that have been developed and reported?

Shuji Kakegawa: No, not yet.

HIGH-RISE EVACUATION MODELING - DATA AND APPLICATIONS

Rita F. Fahy
Fire Analysis and Research Division
National Fire Protection Association
Quincy, Massachusetts 02269-9101 U.S.A.

ABSTRACT

A model called EXIT89 has been developed at NFPA to simulate the evacuation of a large building, with the capability of tracking each occupant individually. The output of this model, in combination with a fire and smoke movement model using the same building layout, can be used to predict the effects of cumulative exposure to the toxic environment present in a structure fire. The capability of modeling the presence of disabled occupants has recently been added to the model. Data to test and enhance the model was obtained from fire drills conducted in office buildings in the U.S. and U.K., as well as evacuations involving able-bodied and disabled subjects in a hotel.

1. MODEL DESCRIPTION

EXIT89 requires as input a network description of the building, geometrical data for each room and for openings between rooms, the number of occupants located at each node throughout the building, and smoke data if the effect of smoke blockages is to be considered. The user is allowed to select among several options, including whether the occupants of the building will follow shortest paths out of the building or will use familiar routes; whether smoke data, if any, comes from a fire and smoke model or will be input as blockages by the user; whether there are any delays in evacuation throughout the building; whether there are any additional delays in evacuation among the occupants of the building and, if so, what percentage of the occupants will delay and what are the minimum and maximum delay times; and whether any of the occupants are disabled and if so, at what percentage of "normal" speed each disabled person will travel.

The following is a brief overview of the model. It either calculates the shortest route from each building location to a location of safety (usually outside) or sets user-defined routes through the building. It moves people along the calculated or defined routes until a location is blocked by smoke. Affected exit routes are recalculated and people movement continues until the next blockage occurs or until everyone who can escape has reached the outside.

Evacuation can begin for all occupants at time 0 or can be delayed. Additional delays over a specified range of time can be randomly assigned to occupants. Smoke data can be used to predict when the activation of a smoke detector would occur and evacuation will begin then or after some user-defined delay beyond that time. The program is written in FORTRAN and currently runs in mainframe and PC versions.

2. USER OPTIONS

There are six options set by the user at the beginning of the input file. The first indicates whether metric or standard measurements will be used in input and output. Internally, all calculations are done in metric scale but this option allows the simple use of evacuation data and floor plans from a variety of sources. The second option specifies the body size used as the basis of density calculations that are used to calculate velocities. These choices are described in more detail in a later section. The third option allows the user to specify whether occupants will be moving at emergency or normal (slower) speeds. This also is described more fully later.

The fourth option allows the user to determine whether the program should calculate the shortest paths between nodes or whether the user will be specifying the node to which occupants will move from each node. If the user selects specified routes, the node to which occupants of a node will move is included as part of the node description in the input. User-specified paths will be used until a node on a floor becomes blocked by smoke. In that case, the routes for the floor will be recalculated using the shortest-route routine.

The fifth option indicates whether or not the user is reading in smoke data from CFAST or whether there will be user-defined blockages or no blockages. And finally, the user selects full output, which prints information every time someone moves from one space to another, or summary output showing floor and stairway clearing times and usage of exits.

On the next two lines, the user indicates whether or not additional delay times should be randomly distributed among the occupants. If yes, the user then specifies for what percentage of the occupants there will be additional delays and over what range of time (in seconds) those delays should be chosen.

3. CALCULATING WALKING SPEEDS

EXIT89 uses walking speeds calculated as a function of density based on formulas from Predtechenskii and Milinskii. [1] Their formula for density of a stream of people, D , is:

$$D = Nf/wL \quad (\text{m}^2/\text{m}^2) \quad (1)$$

where N = number of people in the stream
 f = the area of horizontal projection of a person
 w = width of the stream
 L = length of the stream.

Their model established an optimal density of 0.92. Although a higher density can be observed in real situations, 0.92 is the maximum they used in empirical expressions for walking speeds. Based on their observations, they developed the following equations for normal circumstances. For the mean values of velocity as a function of density for horizontal paths:

$$V = 112 D^4 - 380 D^3 + 434 D^2 - 217 D + 57 \quad (\text{m}/\text{min}) \quad (2)$$

for $0 < D \leq 0.92$.

For movement through doors

$$V_o = Vm_o \quad (\text{m/min}) \quad (3)$$

$$\text{where } m_o = 1.17 + 0.13 \sin(6.03D_o - 0.12)$$

For movement down stairs

$$V_{\emptyset} = Vm_{\emptyset} \quad (\text{m/min}) \quad (4)$$

$$\text{where } m_{\emptyset} = 0.775 + 0.44 e^{-0.39D_{\emptyset}} \cdot \sin(5.16 D_{\emptyset} - 0.224)$$

Since the model does not yet move people up stairs, the values for travel up stairs are not shown.

In emergencies, such as earthquakes or fire, the fear that makes people try to flee danger raises the speed of movement at the same densities.

Predtechenskii and Milinskii found the following relationship between the two velocities:

$$V_e = \mu_e \cdot v \quad (5)$$

$$\begin{array}{ll} \text{where } \mu_e = 1.49 - 0.36 D & \text{for horizontal paths and through openings} \\ \mu_e = 1.21 & \text{for descending stairs.} \end{array}$$

Tables of velocities by density were given for normal, emergency and comfortable movement along horizontal paths, through openings and on stairs. EXIT89 currently incorporates the velocities for normal and emergency movement.

Queueing is handled by the decreased walking speeds that result from increased densities as more occupants move into a room or stairway. The program does not currently allow occupants to select less crowded routes; they simply join the queue at nodes along the shortest route.

4. BODY SIZE DATA

Predtechenskii and Milinskii's work used body sizes calculated from the measurements of Soviet subjects. The area of horizontal projection of a person used in these calculations is 0.113 m^2 (1.22 ft^2) -- the mean dimensions of an adult in mid-season street dress. Subsequent work by Ezel Kendik using Austrian subjects found significant differences in the results. [2] The value of 0.113 m^2 described above compares to the Austrian result for subjects between the ages of 10 and 15 years without coats. The value for Austrian subjects between ages 15 and 30 wearing coats was 0.1862 m^2 and without coats was 0.1458 m^2 . The value for adults over age 30 without coats was 0.1740 m^2 .

A table of mean body dimensions representative of U.S. male and female workers between 18 and 45 years of age was obtained from *Occupational Safety and Health in Business and Industry*. Based on this data, an "American"

value for horizontal projection of a person of 0.0906 m² was calculated, far smaller than that calculated for Soviet or Austrian subjects. The choice among the three sets of data is an input option set by the user.

5. MODELING PRESENCE OF DISABLED OCCUPANTS

The presence of disabled people during an evacuation is a feature recently added to EXIT89. The strategy chosen at this time assumes, as demonstrated in work by the University of Ulster, that the presence of disabled occupants does not impede able-bodied occupants. [3]

The user specifies how many of the occupants at a node are "disabled." This can mean not only how many will evacuate slower than the average occupant, but also any able-bodied people who will evacuate with someone who is disabled. People with disabilities include those whose travel speed is slowed by the use of a walker, wheelchair or age, as well as small children and those who will accompany them.

If a node has any disabled occupants, the user enters on the next line the proportion of "normal" speed at which that person will move. For example, if a disabled person moves at three-quarters of the speed of an able-bodied person, the user enters 0.75 as the speed factor for that person.

This method of handling disabled occupants assumes that their presence does not impede the able-bodied occupants. The densities used to calculate travel speeds for able-bodied occupants count all occupants of a node and treat them as if they were all of the same body size. This does not account for the size of wheelchairs or the space taken up by walkers and strollers, for instance. The justification for this assumption is based on the evacuations studied by the University of Ulster that showed that the presence of people in wheelchairs or with walkers did not affect the travel speed of other occupants.

By using this feature, people moving at more rapid than normal speeds can also be modeled by identifying them as "disabled" but setting their speed factors at some value greater than 1.0.

6. EXAMPLE 1 - RANDOMLY DISTRIBUTED DELAY TIMES

A series of evacuations were conducted by the University of Ulster to test the effect of disabled persons on occupant flow in mixed ability populations. Three of these evacuations took place in a hotel with two daytime scenarios and one nighttime scenario. The night and one of the day scenarios used the same fire location and these were the two evacuations for which EXIT89 was run.

The hotel wing used for the evacuation was a two-story structure with exit stairs at both ends and another stairwell in the center. One of the end stairs was made unavailable for the evacuation. Several of the occupants taking part in the evacuation were disabled. They included users of wheelchairs, canes and walkers. Disabled occupants were not included in this first set of example runs.

In the course of the actual evacuations, alarm bells did not consistently ring

throughout the bedroom section of the hotel. In the first example, the alarm was inaudible for many of the occupants, significantly delaying their evacuation. In the second example, the alarm was at least slightly audible for all occupants.

The initial locations of the occupants for each of the evacuation exercises were provided on floor plans. Also available were the length of time it took occupants to leave their rooms and their time to leave the building. The location of cameras through the building allowed researchers to determine the duration and causes of additional delays during evacuation.

In the first daytime scenario, estimated delays in evacuating bedrooms ranged from one to 30 seconds. In addition, 14 out of 27 occupants observed by cameras delayed at some point in the corridors during their evacuation. The duration and reasons for these delays were detailed in the report. The reasons included, among others, stopping to read a notice on the foyer door (one to two second delay), holding doors open for wheelchair users (nine to 13 second delay), calling on friends (up to 30 second delay) and traveling in the opposite direction of designated escape route (up to nine second delay).

Among the 22 non-disabled occupants observed by cameras in this evacuation, the times to reach the exit ranged from 16.6 to 60.0 seconds with a mean time of 37.1 seconds. The first run of this evacuation used reported and estimated delay times in the rooms for these occupants and resulted in evacuation times that ranged from 23.1 to 60.1 seconds with a mean time of 39.5 seconds. A second run of this evacuation added random delays of one to 30 seconds to half of the occupants. In this case, the predicted evacuation times ranged from 23.1 to 79.1 seconds with a mean time of 45.8 seconds. A closer look at the movement of the occupants showed that many of the occupants actually reached the exit sooner because the delays reduced congestion in the corridors and allowed them freer and more rapid movement. Since most of the reported delays during evacuation actually lasted less than 10 seconds, the example was run a third time with random delays of one to 10 seconds distributed among half the occupants. This resulted in predicted evacuation times that ranged from 23.1 to 65.8 seconds with a mean time of 41.8 seconds.

In the nighttime scenario, observations were provided for 55 non-disabled occupants. For these people, estimated delays in evacuating bedrooms ranged from five to 78 seconds. In addition, 33 of these 55 occupants were observed to delay in the corridors during their evacuation. These delays ranged from one to 15 seconds and were due to making decisions, queueing, and assimilating information.

Among these 55 occupants, the times to reach the exit ranged from 17.3 to 90.0 seconds with a mean time of 42.6 seconds. The first run of this evacuation used reported and estimated delay times in the rooms for these occupants and resulted in evacuation times that ranged from 24.9 to 107.8 seconds with a mean time of 50.1 seconds. A second run of this evacuation added random delays of one to 15 seconds to 60 percent of the occupants. In this case, the predicted evacuation times ranged from 27.1 to 116.3 seconds with a mean time of 56.0 seconds. Since most of the reported delays during evacuation actually lasted less than five seconds, the example was run a third time with random

delays of one to five seconds distributed among 60 percent of the occupants. This resulted in predicted evacuation times that ranged from 27.7 to 110.9 seconds with a mean time of 52.3 seconds.

In both of the actual evacuations, disabled occupants were present; however, it was found that they did not adversely impact the movement of the non-disabled evacuees.

7. EXAMPLE 2 - ADDING DISABLED OCCUPANTS

Building on the final results of Example 1, four disabled occupants were added to the modeled population. There were actually five disabled occupants in the real evacuation, but travel speed was not available for one of the wheelchair occupants. Two wheelchair occupants traveled at speeds close to the average for able-bodied occupants (1.15 m/s vs. 1.52 m/s). The other two disabled occupants were a wheelchair user who traveled at about one-eighth of the average speed of the able-bodied occupants, as a result of impedance from a walker user who traveled at about one-fifteenth of the average speed of the able-bodied occupants.

The model was rerun with these four disabled occupants added. As was observed in the actual evacuation, there was no effect on the travel times of the able-bodied evacuees. The travel times observed in the actual evacuation for these four people were 51.0 seconds, 56.9 seconds, 174.0 seconds and 222.0 seconds. The times estimated for them in the model were 58.0 seconds, 61.7 seconds, 182.3 seconds and 295.4 seconds, respectively.

8. CONCLUSION

The model in its current form does not include any explicit behavioral considerations but it does allow behavioral considerations to be handled implicitly by incorporating time to perform investigation activities or to alert others before evacuating in the delay times that the user specifies for the occupants of each node. In addition to specifying delay times for each location, the user now can also have the computer randomly assign additional delays to some percentage of the individuals throughout the building. In this same way, another behavior that can be dealt with implicitly is the tendency of able-bodied adults in the presence of other able-bodied adults to ignore early warnings of the presence of a fire.

EXIT89 now allows the user to model the frequently observed tendency of occupants to follow the route out of the building that they are most familiar with, not the shortest paths out of building which often would involve the use of emergency exits. These familiar paths defined by the user will remain in place until a location on that floor becomes blocked by smoke and the routes on that floor need to be recalculated using the shortest route algorithm. The model now also allows the simulation of disabled people, who can be incorporated using slower walking speeds.

Walking speeds in the model are calculated as a function of densities and are based on tables of values from Predtechenskii and Milinskii. The model does not yet simulate crawling through smoky rooms by reducing walking speeds,

or reversing direction where possible to use a less smoky, though longer escape route.

One of the program's inputs is the capacity of nodes. The reason for including this value was to allow evacuees to avoid nodes that were already crowded if alternate routes are available. This would prevent occupants from queueing at one stairway while the other section or sections of the floor emptied out into less busy stairways. Refinements of the program to define and possibly limit the range of a smoke detector also need to be added to the model.

Future plans for the model include documenting observed travel speeds and the delay times that can be used for occupants to begin evacuation and for delays during evacuation. These travel speeds and delay times may be occupancy-specific. Testing of the model using data from actual emergency and non-emergency evacuations will also continue. A PC-version of the model will be tested during the Fall of 1995.

ACKNOWLEDGMENTS

This work has been funded in part by the National Institute of Standards and Technology Building and Fire Research Laboratory, grant No. 60NANB2D1286.

REFERENCES

1. Predtechenskii, V.M. and Milinskii, A.I., Planning for Foot Traffic Flow in Buildings, Amerind Publishing Company, Inc., New Delhi, 1978.
2. Kendik, E., "Assessment of Escape Routes in Buildings and a Design Method for Calculating Pedestrian Movement," SFPE Technology Report 85-4, Society of Fire Protection Engineers, Boston, Massachusetts, 1985.
3. Shields, T.J., "Fire and Disabled People in Buildings," Building Research Establishment Report BR 231, Building Research Establishment, Garston, 1993.

Discussion

Edward Zukoski: How does a person in a wheelchair get down from the second floor to the ground floor?

Rita Fahy: They don't, and that's one of things that I hadn't put in. They should be heading to areas of refuge (safety). Which means that every floor should have a location that functions like the outside. The people in the examples were all on the first floor.

Masahiro Morita: When the fire is expanding and if you are in the hallway and there's no smoke, it's hard to know in which direction that people would go. Then, as the fire progresses, chances are that the path would vary. How did you take care of that when you input the data?

Discussion cont.

Rita Fahy: First, everyone in one room will travel to the next room, but if the user decides to set the routes themselves, those would be the expected travel routes. We would probably all leave this building that way because that's the way we came in. Even if the user determines the routes, once blockage occurs and the routes are recalculated, they're recalculated using the shortest route algorithm.

Howard Baum: How much of the building or the room geometry is actually used in calculating these delay times? If the room has an unusual shape or if there's a major chunk of furniture in the room or if there's a zigzag in a hall, does that enter into the calculations?

Rita Fahy: There are two things going on there, the delay time is set by the user, and that's reaction time if you were doing an office evaluation. For instance, there may be some shut down procedure that people would have to do. The accounting department can't just get up and leave, so that's delay time, and that's set by the user. The evacuation distance is measured from the center of the space. The speed is calculated using the densities based on the usable floor area. So if there's a complicated geometry within the room, that's not addressed directly.

Howard Emmons: The real problem seems to be what you talked about plus the fact that the fire is growing at the same time and maybe even faster than the people are going out. Have you coupled this with a fire model to take this into account? And if not, do you have plans to do so?

Rita Fahy: The only way the model deals with the fire is when it's coupled with the smoke model. If rooms are blocked as people are evacuating, they are trapped. It's up to the next model to "kill" them. It also doesn't take into consideration the actions of the people and what they can do to affect smoke and fire spread by opening and closing doors, things like that.

Pravinray Gandhi: It looks like a lot of the data that you have may be interpreted in a probabilistic manner. Are you thinking of adding that complexity in your model to make it more probabilistic by introducing distribution functions for people movement and so forth?

Rita Fahy: There are some types of real behavior that it would be really hard to model, like back and forth sorts of things. I would like to have it be more probabilistic, but I would want there to be some data from real life, otherwise, it would add complexity without being defensible.

Assessment of Clarity of Egress Route in Buildings

MANABU EBIHARA and HIROAKI NOTAKE
Izumi Research Institute, Shimizu Corporation
2-2-2 Uchisaiwaicho, Chiyoda-ku, Tokyo, 100 Japan

YOSHIRO YASHIRO
Institute of Technology, Shimizu Corporation
3-4-17 Etchujima, Koto-ku, Tokyo, 135 Japan

ABSTRACT

A framework of a new fire safety design method based on a concept of performance-based design is now in preparation in Japan[1]. In this paper, the authors turned their attention to the clarity of the egress route as an important performance for assuring the life safety of occupants in buildings, and intensively discussed its assessment. The relevant previous work on the evaluation of the clarity of the egress route was reviewed and studied. The clarity of the egress route was considered dependent upon the physical measure which could quantitatively evaluate how quickly occupants could escape from buildings or how easily they could find exits or safety zones in floors. In this point of view, the travel distance during the emergency evacuation was one of the effective and quantitative measures of the clarity of the egress route. The assessment of the travel distance based on some probabilistic assumptions of the occupant's evacuation behavior was introduced. The network modeling technique was utilized to represent the configuration of the egress route and to calculate the expected value of the travel distance. Through numerical computations, an effective configuration was discussed in such a way that the average of expected travel distance in a floor was minimized among possible layouts of the egress route. Finally, it was concluded that the proposed procedure with an emphasis on the clarity of the egress route was based on the minimization of the travel distance and it could provide a practical basis for the new fire safety design of buildings.

1. INTRODUCTION

Buildings in Japan tend to become large and complex according mainly to the variety of usage. Most of the existing regulations of the fire safety design in Japan were established by means of empirical judgments, which were not always solidly based on any engineering or scientific basis[2]. Under these circumstances, it is necessary to grope for new and effective strategy in the fire safety design or the evacuation planning for the new type of large-scale and complex buildings. A performance-based design system of buildings was proposed to the Building Community of Japan as a new fire safety design system. Ministry of Construction launched the five year research project to make clear the detail of the building design regulations based on the concept of the performance-based design system.

In this paper, one of the ideas how to establish a regulation concerning the egress route design in the performance-based design is introduced. The authors turn their attention to the assessment of the clarity or the complexity of the egress route in buildings. It is considered that

the clarity of the egress route have to be evaluated from the two points of view. One is the effectiveness of evacuation that means the assessment with regard to the occupant's evacuation behavior. Another is the simplicity of the structure which is constructed by routes in a floor that means the assessment of the geometrical relation or the configuration of routes (Figure 1). In other words, the state, that the clarity of the egress route is maintained in way-finding or decision-making during an emergency evacuation, may be the one that the travel distance will be in the appropriate level for assuring the life safety, according to the scale of buildings. In this point of view, the relation between the travel distance and the clarity of the egress route is discussed. At first, two existing works on the evaluation of the clarity or the complexity of the route[3,4,5] is reviewed and discussed from the viewpoint of their applicability to the measure of clarity of the egress route in the performance-based design system. After that, some calculation result of the travel distance is introduced, under a probabilistic assumption on the choice of egress route at a T-junction or a crossroads in the occupant's evacuation behavior. The calculation results are provided by applying the network modeling technique to modeling of the egress route in the floor. Through the calculation results, the effective factors to minimize the expected travel distance in the layout of egress route with the emphasis on the assessment of the clarity of the egress route can be measured by the assessment of the expected travel distance. Finally, we mention about the future subjects in this field.

2. NETWORK MODELING OF EGRESS ROUTE

The network modeling technique is applied to representing the configuration of the egress route in buildings. The network model consists of nodes and links. The node represents a point at which some judgment is required to the occupant during the emergency evacuation along the route in the floor. The link, which has the length as a variable, represents a relation between the points represented by the nodes with regard to the connection of the routes. The node is constructed based on the several rules, as follows:

- i) the point of parting of routes (for example a crossroads or a T-junction)
- ii) the point of making a right angle or a blind curved corner
- iii) the end point of a route
- iv) the indoor temporary safety zone (this means a kind of exit in a floor)
- v) the point in front of the door which connects the room and the corridor.

Figure 2 shows an example of the network model of an existing office floor in Japan.

3. REVIEW OF EXISTING MEASURES OF CLARITY OF EGRESS ROUTE

Two existing measures which are used to evaluate the clarity of the egress route using the network model are introduced. One was proposed by Yoshimura[3,4], the other was by Donegan[5]. Figure 3 shows the concept of these measures. Yoshimura's measure indicates that if the value is close to 1.0, the clarity of the egress route is maintained. In the case of Donegan's measure, if the value is close to 0.0, it is maintained. These measures were applied to existing office floors in Japan. Figure 4 shows the relation between two measures, and the relation between each measure and the index which is assumed to represent the characteristics of the network model. Each measure is discussed by using the average value of the measures of all the origin and the destination pairs in the floors. The clear correlation is found in the relation between Yoshimura's measure and the total number of degrees of nodes, and in the relation between the Donegan's measure and the total number of links. Each measure is basically proposed as the value of evaluating the relation between the nodes, in short, the relation between the origin and the

destination, in consideration of the shortest route between them. Thus, it is convenient to compare the clarity of the route among various relations between nodes. But it is unclear that what level is sufficient to assure the clarity of the egress route. In this point of view, these measures are not so applicable to assess the clarity of the whole structure of route.

4. ASSESSMENT OF CLARITY OF EGRESS ROUTE USING TRAVEL DISTANCE

The applicability to assess the clarity of egress route using the travel distance is discussed. The reason why the travel distance is proposed as the measure of the clarity of the egress route is that it is supposed to be easy to handle in the fire safety design of buildings by the designers or the planners. In this section, we make clear the effect of the number of exits or safety zones and the layout of them on the travel distance. In the numerical calculations of the travel distance, basically it is assumed that the each direction on the corner, the T-junction and the crossroads has the same probability on the choice of egress route, including a backward motion. In the calculation steps, first the expected travel distances of all origin and destination pairs of nodes in the network model are determined, and then the average of expected travel distance is determined by averaging all expected travel distances.

4.1 EFFECT OF NUMBER OF EXIT ON TRAVEL DISTANCE

Figure 5 shows examples of the network models for studying the effect of the number of the exits on the travel distance. Each link in the network model has unit length, and all links in the network model are assumed to have the same length. Figure 6 represents the results of the relation between the number of exits and the average of expected travel distance. The average of expected travel distance and the value of the total length of the route divided by the total degree of exits are correlated. A similar tendency toward the correlation is shown between the network models constructed by the existing floor plans and the assumed network models. This result means that it is possible to control the travel distance by the number of exits which are arranged in a floor corresponding to the total length of routes.

Figure 7 shows the change of the expected travel distance between the node and the exit due to the change of the probability of the backward motion. The x-axis indicates the probability ratio of the occurrence of the backward motion to the probability of the choice of other directions. Here, the value of 0.0 indicates the case that the backward motion is not considered with the exception of the node which corresponds to the end of the route. The dashed line indicates the minimum travel distance to the exit from the node. Through the calculation results, it is pointed out that the probability of the backward motion has the effect on the expected travel distance. However, this effect is different from the characteristics found in the relation between nodes and the structure of the network model. In the case of the network model without loop structures, the expected travel distance is larger than the case of the network model with loops. This result indicates that the number of the end points has some effect on the expected travel distance, and it is supposed to be important to control the number and the layout of the end points of the routes in the floor.

4.2 EFFECT OF LAYOUT OF EXIT ON TRAVEL DISTANCE

In this section, the effect of the layout of exits on the travel distance is studied from the two kinds of viewpoints. One is the centralized layout of exits, the other is the distributed layout. Figure 8 shows the examples of the network models used in this study. The same assumption on the length of the link in the network model, which is described in the previous section, is applied.

Figure 9 shows the relation between the number of exits and the average of expected travel distance. It is understood that the distributed layout of exits is effective for minimizing the average of expected travel distance compared with the centralized layout. It is also understood that the effective number of exits for minimizing the average of expected travel distance exists, depends on the structure of the network model.

Figure 10 shows the example of the distribution chart of the travel distance used in the assessment of the expected travel distance between the nodes. The expected travel distance between nodes is close to the distance which has the high probability of occurrence. In the case of the centralized layout, the distribution of the travel distance has a tendency to become wide. This effect appears that the expected travel distance becomes larger compared with the case of the distributed layout. Therefore, it is important to control the distribution of the travel distance for minimizing the expected travel distance.

5. CONCLUSIONS

The assessment of the clarity of the egress route using the travel distance is discussed. In the evacuation planning, the existing regulation of the maximum travel distance during emergency evacuation plays an important role for assuring the safe egress routes or the life safety of occupants. So, it is supposed that the assessment of the clarity of the egress route based on the travel distance is easy to accept, and also easy to understand as a quantitative measure by designers. The average of expected travel distance, which is directly calculated from the network model of routes based on a probabilistic assumption of the occupant's evacuation behavior, is studied in two ways. The first is to regulate the number of safety zones or exits in a floor. The second is to regulate their layout in the floor. It is confirmed that the appropriate number of exits in the floor exists corresponding to the scale of the floor or the total length of the routes, and it is better to distribute the exits in the floor for minimizing of the average of expected travel distance. It is also confirmed that the travel distance is applicable to assess the clarity or the complexity of the egress route in the floor. Figure 11 proposes a flow chart to regulate the egress route in which the clarity is considered. The first step is set up with the aim of minimizing the average of expected travel distance corresponding to the scale of the floor. In this point of view, it is considered that the important factor is to control the number and the layout of exits, safety zones, and end points in the floor. On the other hand, even if two networks have similar characteristics in the total length of the route, this does not necessarily mean two models are identical, for example the distribution of the length of links in the network model. It is considered that these characteristics between the network models have to be taken into account in discussing from an equal point of view about the assessment of the clarity of the egress route using the travel distance. In this point of view, the assessment of the simplicity of the structure of the network model will be required, and it is necessary to assess the simplicity by using parameters which characterize the network model, for example the number of nodes or links, and the average length of the links. The second step is established for the purpose of an improvement of reliability in applying the average of expected travel distance to the measure of clarity of the egress route.

The calculation result of the expected travel distance is affected by how to construct the network model based on the floor plan. Therefore, it is necessary to make clear the rules for the constructing the network model based on the floor plan. At the same time, in the case of applying the travel distance as the quantitative measure of the clarity of the egress route, it is necessary to collect the data which is used for determining the probability on the choice of route during the emergency evacuation, including the choice of a straight or a wide egress route and so on. If the

data, which have high reliability, are obtained from the survey of occupant's evacuation behavior, it is possible to confidently treat the travel distance as the assessment measure of clarity of the egress route.

REFERENCES

- 1) Tanaka, T: State of the Art - Development of a Performance-based Fire Safety Design Method of Building in Japan, Proceedings of Mini-Symposium Fire Safety Design of Buildings and Fire Safety Engineering, Building Research Institute, 1995. 12
- 2) Hagiwara, I. and Tanaka, T: International Comparison of Fire Safety Provisions for Means of Escape, Fire Safety Science - Proceedings of the Fourth International Symposium, 1994
- 3) Yoshimura, H: On Measuring Escapability from a Maze, A study on Arrangement of Fire Escape in a Buildings Part 1, Journal of Architecture, Planning and Environmental Engineering, Transaction of AIJ (in Japanese), No. 375, 1987. 5
- 4) Yoshimura, H: A Metrical Evaluation of the Arrangement of Fire Escapes by Goal Programming, A Study on Arrangement of Fire Escape in a Buildings Part 2, Journal of Architecture, Planning and Environmental Engineering, Transaction of AIJ (in Japanese), No. 403, 1989. 9
- 5) Donegan, H. A., Pollock, A. J. and Taylor, I. R.: Egress Complexity of a Building, Fire Safety Science - Proceedings of the Fourth International Symposium, 1994

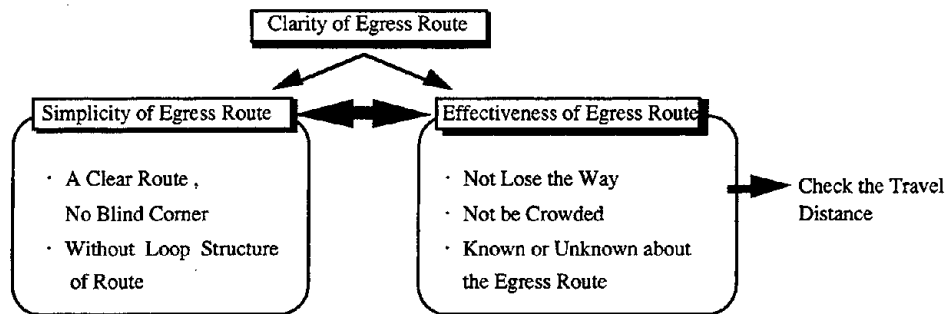


Figure 1 Concept of Assesment of Clarity of Egress Route

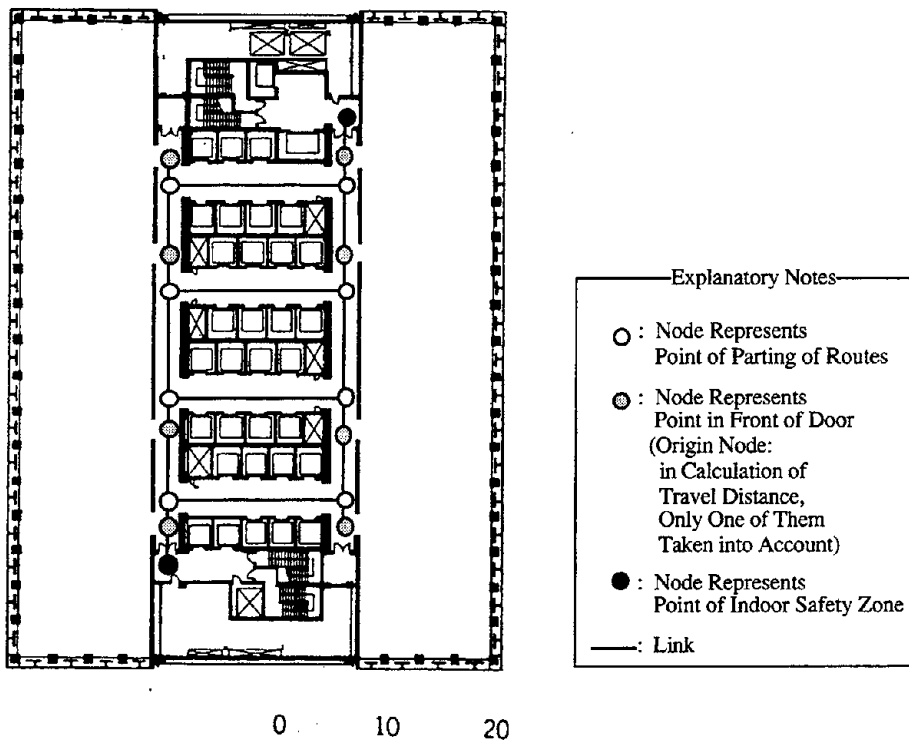
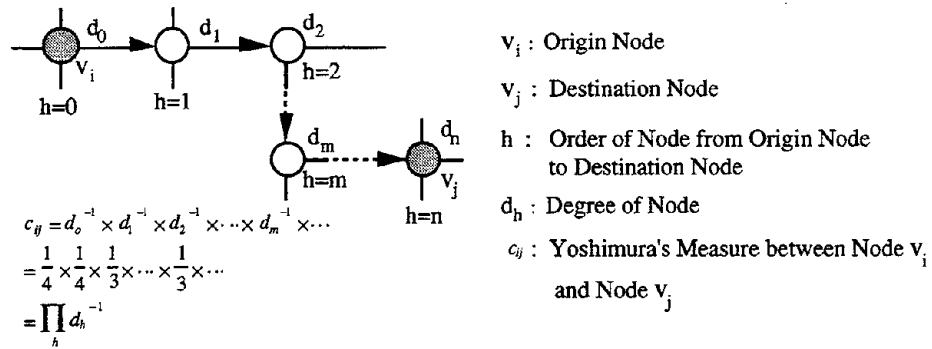
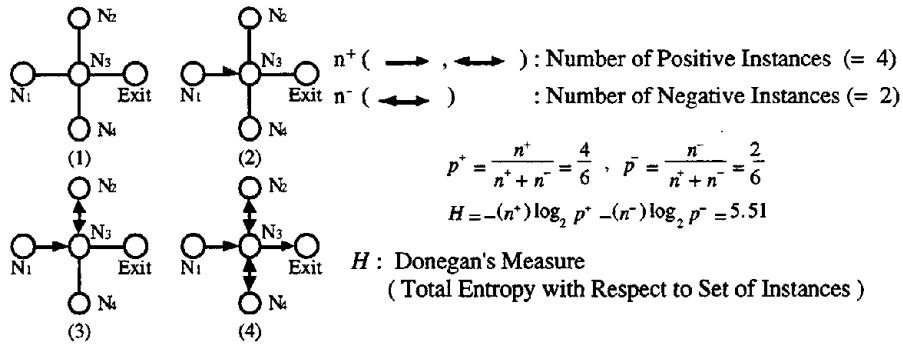


Figure 2 Example of Network Model of Office Floor

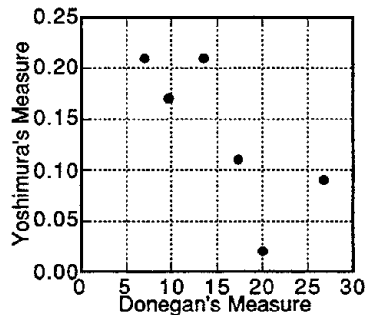


(a) Yoshimura's Measure

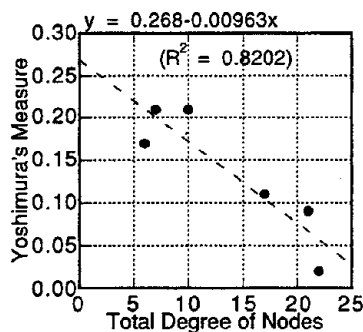


(b) Donegan's Measure

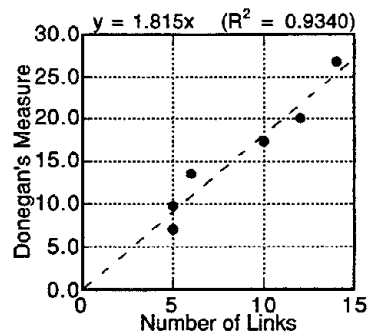
Figure 3 Existing Measures of Clarity of Egress Route



(a) Relation between Two Measures

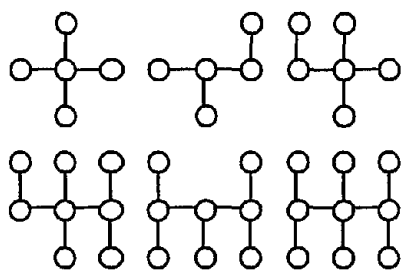


(b) Relation between Yoshimura's Measure and Total Degree of Nodes

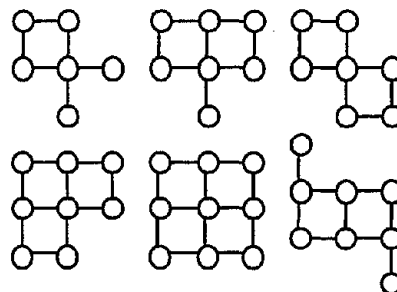


(c) Relation between Donegan's Measure and Number of Links

Figure 4 Calculation Results of Two Measures

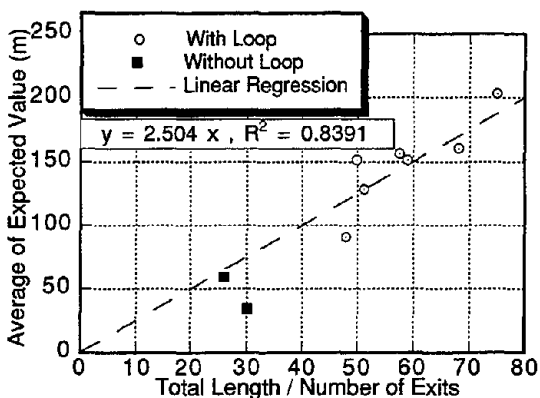


(a) Network Models Without Loop Structure

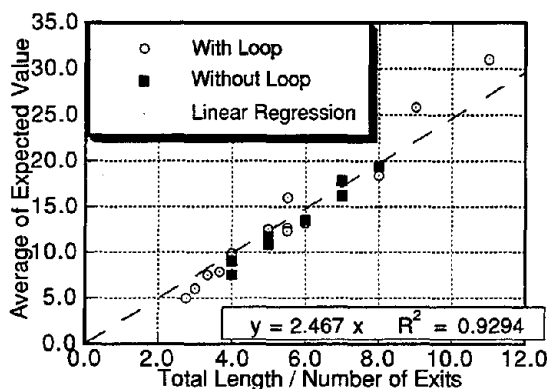


(b) Network Models With Loop Structure

Figure 5 Examples of Network Models

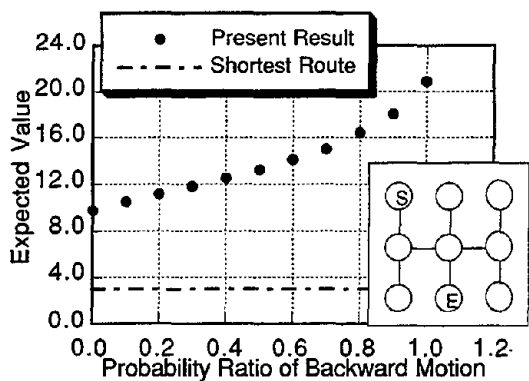


(a) Network Models of Existing Floors

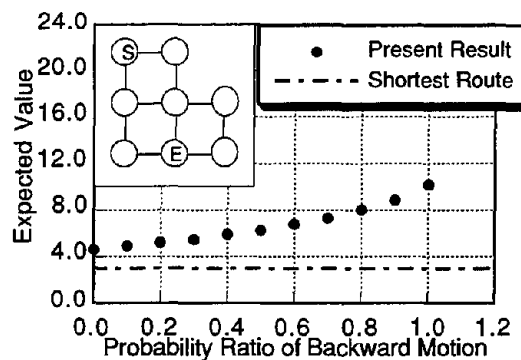


(b) Assumed Network Models

Figure 6 Calculation Results of Average of Expected Travel Distance



(a) Without Loop Structure



(b) With Loop Structure

Figure 7 Change of Expected Travel Distance Due to Change of Probability of Backward Motion

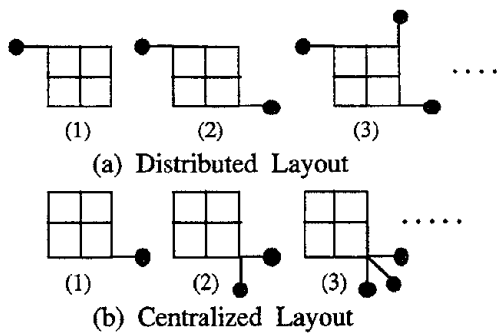


Figure 8 Examples of Exits Layout

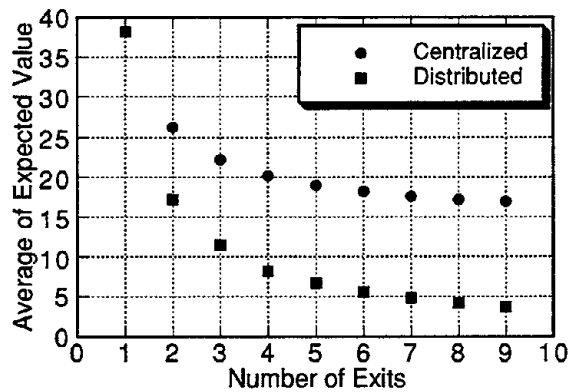


Figure 9 Relation between Number of Exits and Average of Expected Travel Distance

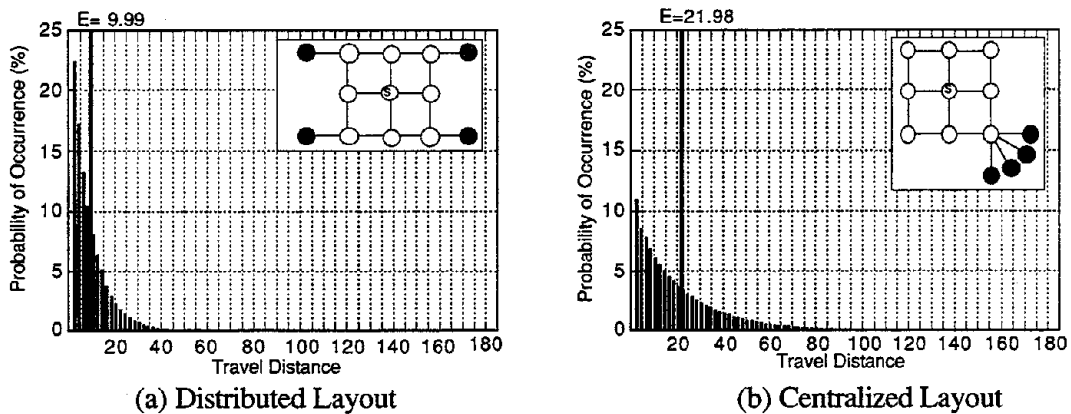


Figure 10 Examples of Distribution Chart of Travel Distance

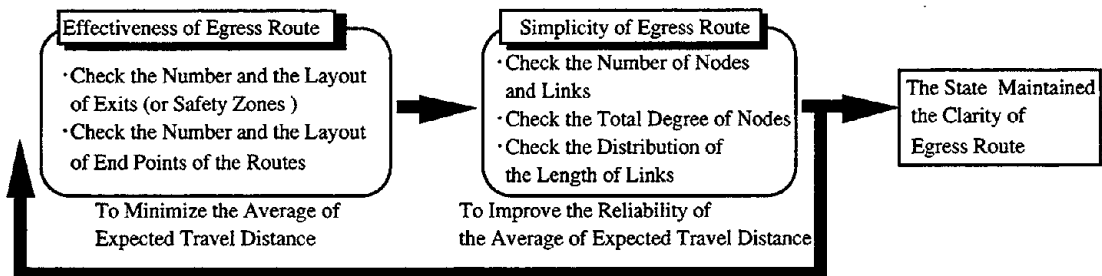


Figure 11 Flow Chart to Regulate Egress Route in Consideration of Clarity

Discussion

Tokiyoshi Yamada: Is it possible to add in smoke movement in the near future?

Manabu Ebihara: At this moment, we are not considering taking of smoke movement into consideration because smoke movement itself is probabilistic. So that it is very difficult to take that factor into consideration.

Brian Meacham: It seems to me that both the smoke movement issue and the number of people in a room are variables and the question would be how do you handle the weighting of the variables? Do you have a statistical background?

Manabu Ebihara: At this moment, we do not have any data with respect to route selection, and we do not have data on smoke movement either. So in order to weight the various different variables, first of all, we have to collect the necessary data so that we can weigh them properly.

Takeyoshi Tanaka: I'm afraid there is some misunderstanding here. This particular model is not an evacuation model. This is a model to determine whether the evacuation route is simple or complicated in terms of distance and speed and so forth. So this does not take into consideration smoke movement or other variables which can be used in an evacuation model.

Masahiro Morita: So if that was the case, it is not the shortest range, rather it has to be shortest time using maximum flow.

Manabu Ebihara: This does not deal with the shortest distance, rather, this model is to get an expected value for different nodes. Then if this value is small, the evacuation time would be shorter. Of course, we can assess the walking speed at certain levels when we make calculations. So for that reason, as Mr. Tanaka mentioned earlier, we are not taking into consideration, at this time, density and smoke movement.

John Rockett: Perhaps my question is more directed at the assembly of the papers rather than yours in particular. When you have high population densities, and particularly if the evacuation routes are limited, you would expect queuing to occur. When queuing occurs with a large population density, a signal should propagate up the line that a particular route is being successful. Do any of these models take that kind of effect into account?

Manabu Ebihara: No, those things are not taken into consideration. In this model we only took into consideration the horizontal data. And just by using such data, we try to give some kind of indicator for the degree of clarity of the routes. And that was the purpose of this paper so that we did not take into consideration factors such as density.

A CONSIDERATION ON REQUIRED NUMBER OF EXITS IN A ROOM
A Study on the Safety Performance of Exit Provisions Part 1

Takeyosi TANAKA, Ichiro HAGIWARA, Yoshio MIMURA

Building Research Institute, Ministry of Construction
1 Tatehara, Tsukuba-shi, Ibaraki-ken 305, JAPAN

ABSTRACT

It is commonly believed that it is important for safe evacuation in building fire to arrange two or more escape routes in different directions. The various provisions are prescribed in building and fire codes of many countries to realize this concept in buildings. The requirement of two or more exits from a room is one of such provisions. However, the way for requiring two or more exits is significantly different from one country to another, and the level of safety assured by the provisions is not clear. In this paper, the meaning of the requirement of two or more exits is considered from the view point of the expected number of occupants unable to escape and a criterion for required exits is proposed as an alternative to the existing provisions. The proposed criterion is basically the same as the existing provisions in terms of the average level of safety assured, but allows to assess the effect of the number of exits on safety more explicitly.

1. INTRODUCTION

It is commonly believed that it is important for safe evacuation in building fire to arrange two or more escape routes in different directions. The requirement of two or more exits for a space having floor area or number of occupants exceeding certain limits, which is found in building or fire codes in many countries, is one of the evidences of the belief. This, needless to say, intends to assure alternative exits should one of the exits be blocked by the influence of fire.

It would be absolutely desirable from the viewpoint of pure safety to provide two or more exits in every space. In reality, however, it is not always easy to achieve the ideal arrangement of exits because of the constraints raised by building economy, everyday convenience and so forth. Fire is a relatively rare danger. Even though safety is undeniably the first priority for building planning, it is understandable that reluctance exists in sacrificing the benefit or the convenience in time of normal use. It is by such consideration that only one exit is allowed for relatively small space.

In this study, the meaning of the concept and the provisions of two or more exits are reviewed from the viewpoint of safety performance. The final goal is to contribute to the establishment of more rational design of means of escape in buildings.

2. REQUIREMENTS OF TWO OR MORE EXITS IN THE EXISTING REGULATIONS

The provisions concerning the requirements of two or more means of escape in the building codes of several countries are summarized in Table 1¹. Usually, two or more means of escape are required when story or height of a building, or area or number of occupants of a room exceeds a certain limit. Incidentally, the legal principle in the U.S. and the U.K. codes seem to

TABLE 1 Minimum Number of Means of Escape

	Australia	France	Japan	U.K.	U.S.
General	2 exits for story a) >6 stories or >25 m height <u>Hospital, Assembly, School</u> b) >6 stories or >25 m height c) ward floor d) preschool e) primary or secondary school & >=2 stories f) any story >50 Ps.	for story or part of story 1) =<19Ps. 1 2) =<50 Ps. 1+sub 3) =<100 Ps. 2 or 1+sub 4) =<500 Ps. 2 5) >500 Ps. +1 per 500 Ps. sub: sub-exit	2 exits for story a) >5th floor b) on 3-5th floor & S >200 m ² c) on 2nd floor & S >400 m ² d) story for Assembly or Shop e) ward floor & S >100 m ² f) Hotel : floor with sleeping rooms & S >200 m ² g) Apartment & S >200 m ²	for story or part of story 1) =< 500 Ps. 2 2) =<1000 Ps. 3 3) =<2000 Ps. 4 4) =<4000 Ps. 5 5) =<7000 Ps. 6 6) =<11000 Ps. 7 7) =<16000 Ps. 8 8) >16000 Ps. +1 per 5000 Ps.	for story or part of story 1) =< 500 Ps. 2 2) =<1000 Ps. 3 3) >1000 Ps. 4 2 exit access doors for a room <u>School</u> a) >50Ps. or S >93m ² <u>Hospital</u> b) sleeping room S >93 m ² c) others S >230 m ² <u>Hotel</u> d) S >185 m ²
Single Means of Escape		<u>Apartment</u> single stairs a) combinations of stairs and corridors opened to the air or with smoke control b) stairs with smoke control	<u>Assembly</u> exits door for auditorium 1) =<250 Ps. 2 2) =<500 Ps. 3 3) =<1000 Ps. 4 4) =<2000 Ps. 5 5) >2000 Ps. 6	<u>Apartment</u> a) top floor <11m, =<4 stories, door-exit < 4.5m <u>Others</u> c) top floor <11m, =<50 Ps. d) room =< 50 Ps. e) story =<50 Ps.	<u>Assembly</u> a) balcony =<50 Ps. <u>Hotel, Apartment</u> b) =< 4 stories, =<4 living units per story, sprinklered <u>Office</u> c) room/area <100Ps. - outside < 30m d) =<3 stories, each story < 30Ps., - outside <30 m

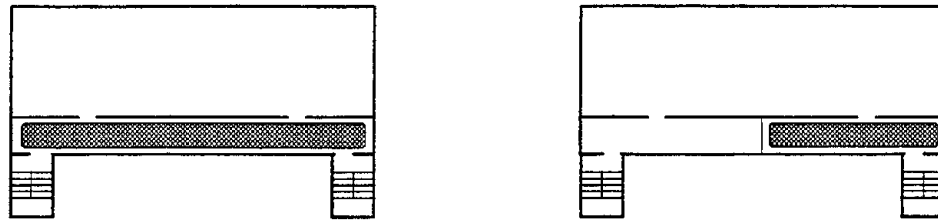
Ps.: persons, S: room area

require two or more for every space. But since this requirement is exempted for small rooms, the practical effects on the building planning is the same as the other codes. In average, 50 seems to be the threshold number of the occupants allowed in the rooms having only one exit.

In many countries, providing only two exits is not sufficient but the number of required exits must increase with the number of occupants. As can be seen in Table 1, the required number of exits for a large number of occupants significantly differs in different countries. Which provision is the most rational from the viewpoint of safety? Is it enough to provide only two exits whatever the number of occupants may be or is it necessary to increase the number of exits with the increase of occupants? Should it be necessary, how many exits for how many occupants? A clear account has not been given to these crucial questions.

3. THE OBJECTIVE OF REQUIREMENT OF TWO OR MORE EXITS

The objective of the requirement of two or more exits for rooms is considered to assure alternative exit/exits even when an exit happens to be blocked by fire.² Two possibilities are conceivable as the scenarios that an exit is made impassable by fire: one is that a hazardous fire occurs at an area adjacent to a door way inside the room as illustrated by Figure 1a; and the other is that a fire occurs somewhere outside the room and an exit is made impassable by the effect of the fire such as the smoke propagating to the corridor connected to the room.



a. two or more exits are blocked by smoke b. smoke partitioning of a corridor

FIGURE 1 A fire occurs somewhere outside the room and an exit is made impassable by the effect of the fire

The scenario that is assumed in the requirement of two or more exits for rooms is considered to be the former, i.e. an inside fire adjacent to a door way. In case of the latter scenario, the other exits along the corridor will be made impassable too when an exit is blocked by smoke, so if the intent of the requirement is to prevent this scenario some additional provisions such as smoke partitioning of the corridor, as illustrated in Figure 1b, have to go along with. Such codes are not found, however.

4. THE EXPECTED NUMBER OF OCCUPANTS UNABLE TO ESCAPE FROM A ROOM

4.1 Probability that an Exit is Blocked by Fire

It is when a fire breaks out in a room, grows to be a hazardous size and the fire happens to be in the area adjacent to the exit that occupants are unable to escape through a doorway. The probability of such an event to take place is expressed as:

$$P = p1 \cdot p2 \cdot p3 \tag{1}$$

where $p1$: probability of fire occurrence in the room
 $p2$: probability that the fire develops to be a hazardous fire
 $p3$: probability that the fire is located in the area that impede the escape through an exit

Let's call the probability P as Exit obstruction probability. The probabilities $p1$ and $p2$ may be evaluated if detailed fire incidents data are available. These probabilities must be very small for the rooms accommodating many occupants such as theaters and offices since it is hard to believe that the ignition and growth of fire are overlooked in front of many awake people. But some concern may remain in the rooms used for sales, exhibition and special amusement etc.

It is not easy to estimate probability $p3$. Normally, little combustible is expected in the vicinity of a doorway since it is usually used as a passage area. From this point of view the probability of fire occurrence is suspected to be lower than other place in the room. But it might be higher if arsons have to be taken into account. Since no means is available for estimating the probability distribution of fire occurrence in a room, it is assumed here that the probability $p3$ is uniform within a room.

4.2 Rooms Having Only One Exit

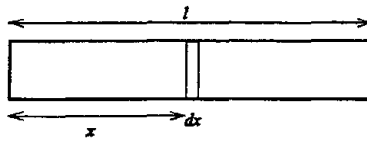


FIGURE 2 Long and narrow rooms having only one exit

(1) Long and narrow rooms

For the first step, let's imagine a very narrow room as shown in Figure 2. In such a room, if a fire occurs at a point, the escape of the occupants located at the inner part of the room will be blocked. The expected number of occupants unable to escape E is calculated as

$$E = \int_0^l \left(\frac{Qx}{l} \right) p_1 \cdot p_2 \left(\frac{dx}{l} \right) = \frac{Q}{2} p_1 \cdot p_2 \quad (2)$$

where Q : number of occupants in the room
 l : length of the room (m)
 x : distance of fire from exit (m)

(2) Ordinary rooms

In ordinary rooms, the occupants are able to make a round the fire to make a way to the exit as shown in Figure 3a. It is only when the fire occurs in the vicinity of the exit that the escape is impeded. Let a be the area that a fire therein impedes the escape through the exit. From the assumption of uniform probability distribution of fire occurrence within the room,

$$p_3 = \frac{a}{A} \quad (3)$$

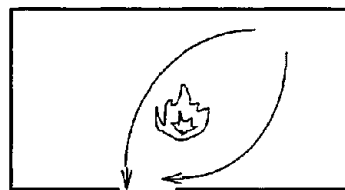
where A : floor area of the room

Not only the source of physical danger such as flames and heat radiation, but also psychological fear may need be taken into account in assessing area a . If such is the case, area a may not necessarily be small but involves somewhat large area around the exit.

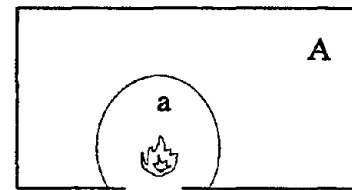
The expected number of occupants unable to escape E in this case is given as

$$E = Q \cdot P = Q \cdot p_1 \cdot p_2 \cdot \frac{a}{A} \quad (4)$$

Although the absolute value cannot be known, area a is considered to be determined by the



a. occupants are able to make a round the fire to make a way to the exit



b. area that a fire therein impedes the escape through the exit.

FIGURE 3 Ordinary rooms having only one exit

definition of the size of hazardous fire and independent from room floor area A , so $p3 \propto A^{-1}$. On the other hand, usually $Q \propto A$. Hence $E \propto p1 \cdot p2$, that is, if $p1$ and $p2$ are the same regardless the floor area A , the expected number of occupants unable to escape E becomes independent from A .

If the expected number E is independent from the area, it follows that there is no reason to require more than one exit for sizable room. Therefore, it is suspected that $p1 \propto A$ is implicitly assumed in the existing regulations, in which case $E \propto A$.

4.3 Rooms Having Two or More Exits

Two exits are supposed to be sufficient if all the occupants are able to escape through the other exit when one exit is blocked by a fire, as long as the two exits is adequately separated so that the two exits are not simultaneously involved in the influence of a fire. However, in many countries, more than two exits are required for the rooms accommodating a large number of occupants, as shown in Table 1. This is partly because care has been paid to prevent the danger due to excessive queuing in front of a doorway. But it may be taken into consideration to mitigate the direct hazard from smoke or fire. This possibility is investigated in the following.

(1) When "available escape time" = "escape time"

If a fire occurs in a room, a smoke layer which develops under the ceiling gradually descends to make the room untenable after a while. Available escape time t_A is defined here as the time from the start of escape to when such untenable condition reaches. Engineering methods usable to predict t_A are now available, although we do not refer to them here.

On the other hand, escape time t_E is defined as the time from the start to the completion of the escape. When the escape time t_E is controlled by the width of doorway, it is calculated by

$$t_E = \frac{Q}{NB} \quad (5)$$

where B : total width of the exits(m)
 N : doorway egress flow rate(person/m sec)

Now, suppose there are n exits in a room, and let the width of each exits be $B_1, B_2, \dots, B_k, \dots, B_n$, respectively, and that the total width of the exits be exactly enough to evacuate the room within the available escape time t_A .

When a fire occurs in the vicinity of door k , the number of occupants unable to escape within the available escape time t_A is $(B_k/B)Q$. Hence, if the probability $p3 (= a/A)$ is the same for any door, the expected number of occupants unable to escape E is given as

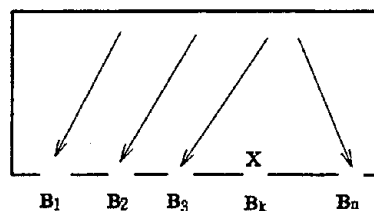


FIGURE 4 A fire occurs in the vicinity of door k

$$E = \sum_{k=1}^n \left(\frac{B_k}{B} \right) QP = \frac{\sum_{k=1}^n (B_k)}{B} QP = QP \quad (6)$$

that is, when the total width of exits B is exactly enough to evacuate the room the available escape time, the expected number of occupants unable to escape E is constant regardless the number of the exits. Hence, it follows that increase of number of exits does not increase the safety of the escape, although it may increase the conditional safety when a fire has occurred at an exit.

(2) When "available escape time" > "escape time"

Usually, the total width of exits is determined more to prevent excessive queuing at the exits than to evacuate the room within the available escape time. As a result, escape time t_E is more or less shorter than available escape time t_A . In other words,

$$Q = NBt_E < NBt_A \quad (7)$$

Let B_A be the width that is necessary for evacuating the room exactly within the available escape time, that is

$$Q = NB_A t_A \quad (8)$$

Then the width given as follows

$$B_\alpha = B - B_A \quad (9)$$

can be considered as the surplus of the width.

The number of the occupants manage to escape Q' when exit k is blocked by fire is given as

$$Q'_k = N(B - B_k)t_A \quad (10)$$

provided that Q' cannot be larger than Q .

From Eqns.(9) and (10), the number of the occupants unable to escape is

$$\begin{aligned} Q - Q'_k &= NB_A t_A - N(B - B_k)t_A = N\{B_A - (B - B_k)\}t_A \\ &= N(B_k - B_\alpha)t_A \end{aligned} \quad (11)$$

provided that $Q - Q' = 0$ when $B_k - B_\alpha < 0$, since the number of the occupants unable to escape cannot be negative.

Hence, the total expected number of occupants unable to escape E is calculated by taking the summation of Eqn.(11) multiplied by P for all the exits of the room, that is,

$$E = \sum_{k=1}^n (Q - Q'_k)P = \sum_{k=1}^{n(B_k - B_\alpha > 0)} N(B_k - B_\alpha)t_A P \quad (12)$$

provided that the summation is only taken for $B_k - B_\alpha > 0$.

Needless to say, $E=0$ when $B_k - B_\alpha > 0$ for any k , in other words, whichever exit may be blocked by a fire, all the occupants are expected to be able to escape when extra width of the exits is larger than the width of any exit.

5. AN ALTERNATIVE RULE TO EXISTING TWO OR MORE EXITS REQUIREMENTS

5.1 Proposed Criterion

Applying Eqn.(12) for $n=1$, a room with a single exit, we obtain

$$E = N(B - B_{ex}) \gamma_A P = N B_A t_A P = QP \quad (13)$$

Therefore, Eqn.(12) can be applied consistently for any number of exits.

The absolute value of P in Eqn.(12) is not known, although suspected to be trivial, so there is no way to calculate the absolute value of the expected value E . However, because the exit codes in many countries require two or more exits for a room accommodating more than 50 occupants and having no sleeping facilities, as shown in Table 1, the requirement of the codes is interpreted as

$$E = QP < 50P^* \quad (14)$$

where P^* is the exit obstruction probability for the typical space the character of which is such that one exit is deemed to be acceptable up to 50 occupants by many of the exit codes.

This limit on the expected value for the reference room having one exit may be extended to more generic rooms with arbitrary number of exits and various character, namely,

$$E = \sum_{k=1}^{n(B_k - B_{ex} \neq 0)} N(B_k - B_{ex}) \gamma_A \bar{P} \leq Q_{ref} \quad (15)$$

where $\bar{P} = P/P^*$ and $Q_{ref} = 50$

Eqn.(15) can be used as the criterion equitable to any room in terms of the acceptable level of safety. The character of a specific room associated with fire risk can be taken into account by \bar{P} , which is the relative exit obstruction probability reference to P^* . For example, if probability of fire occurrence $p1$ of the room is twice larger than the reference room, it follows that $\bar{P} = 2$ through Eqn.(1) provided that the other conditions are the same; if the initial fire growth rate of the combustible contents in the room is likely to be larger than the contents in the reference room, P will become somewhat large through the increase of the value of $p2$.

Note, however, that for such a space that the probability of fire occurrence is in proportion to the floor area, $P \propto A^0$ since $p3 \propto A^{-1}$ while $p1 \propto A$. In other words, floor area is not the factor which affects \bar{P} .

5.2 Sample Applications

The following examples illustrate how the arrangement of exits from a room is assessed based on the above criterion can be used for the assessment. Let the number of occupant $Q=1,000$, the available egress time $t_A = 120$ sec, and the relative exit obstruction probability $\bar{P}=1$. Note that the exit width that is necessary for evacuating the room exactly within the available escape time B_A is calculated as

$$B_A = \frac{Q}{Nt_A} = \frac{1000}{15 \times 120} = 5.56(m)$$

(1) In case the widths of exits are the same

Suppose that the room has four exits and the width of each exit is 1.9m. The total width of the exits is $4 \times 1.9m = 7.6m$. The surplus of the exit width B_{ex} is

$$B_{ex} = B - B_A = 7.6 - 5.56 = 2.04(m) > 1.9(m)$$

Hence, the expected number of occupants unable to escape $E=0$, so needless to say the criterion of Eqn.(15) is satisfied, in the case of this room.

(2) In case the widths of exits are different

Suppose that the room has four exits with different widths: two with 2.4m width each and the other two with 1.4m width each. The total width is $2 \times 2.4 + 2 \times 1.4 = 7.6$, that is, the same as (1). In this case, the expected value becomes as

$$E = \sum_{k=1}^{n(B_k - B_{ex} > 0)} N (B_k - B_{ex}) \bar{P} = 2 \times 15 \times (2.4 - 2.04) \times 120 \times 1 = 129.6 > 50$$

that is, the criterion of Eqn.(15) is not satisfied by such unbalanced arrangement of exits.

(3) In case the number of exits is increased

Let's consider the case that the room has five exits and the width of each exit is 1.4m. The total width of the exits is $5 \times 1.4m = 7.0m$. The surplus of the exit width B_{ex} in this case is

$$B_{ex} = B - B_A = 7.0 - 5.56 = 1.44(m) > 1.4(m)$$

Hence, again $E=0$. This implies that in some cases the criterion may be met by less total width if number of exits is increased.

5.3 Consideration on Required Number of Exits

As we have seen before, the required number of exits increases with number of occupants in the exit codes of many countries. Now let's study how many exits are required to satisfy the criterion given by Eqn.(15). Here we assume that every exit has the same width for simplicity, i.e.

$$B_k = \frac{B}{n} \tag{16}$$

Let the surplus rate of exit α be

$$\alpha = \frac{B_{ex}}{B_A} \tag{17}$$

then total exit width can be expressed as

$$B = B_A + B_{ex} = (1 + \alpha) B_A \tag{18}$$

Firstly, using Eqns.(16) - (19) to the condition that $E=0$ when $B_k - B_{ex} < 0$ yields the number of exits which never generates the occupants unable to escape as

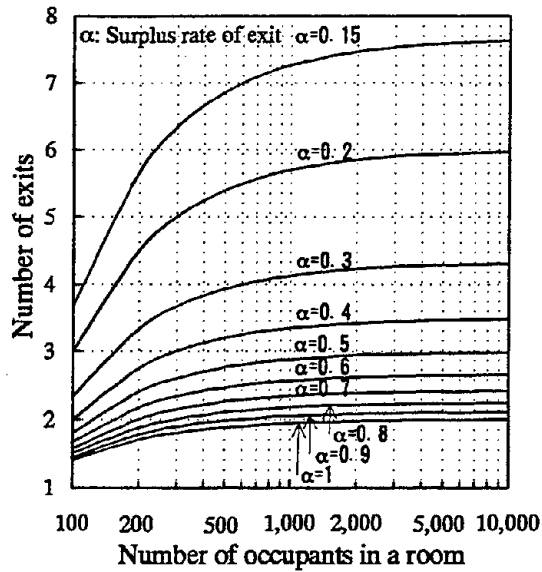


FIGURE 5 Required number of exits based on number of occupants in a room and exit surplus rate

$$n \geq \frac{1+\alpha}{\alpha} \tag{19}$$

Next, substituting Eqns.(16) –(19) into Eqn.(15) gives

$$n \geq \frac{(1+\alpha) - \frac{Q_{ref}}{QP}}{\alpha} \tag{20}$$

Eqn.(20) indicate that required number of exits is governed by number of occupants and exit surplus rate. This relationship is shown in Figure 5. The smaller the exit surplus rate, the larger the required number of exits and vice versa. Specifically, when the surplus rate equal 1, namely, when the exit width is twice as large as B_A , number of the exit can be only two.

When the surplus rate is the same, the number of required exits increases with the number of occupants, but the rate of increase is relatively small for the increase of number of occupants, and furthermore asymptotically approaches to the value given by Eqn.(19). Note, however, that the total width of exits has to increase in order to get the occupants escape within the available escape time. Hence, it is considered that the required number of exits for large occupant load tends to be satisfied without difficulty if the width of each exit is only normal.

6. CONCLUSIONS

The requirement of two or more exits of a room was discussed from the view point of the expected number of occupants unable to escape and a criterion for required exits is proposed as an alternative to the existing provisions. The proposed criterion is basically the same as the existing provisions in terms of the average level of safety assured, but allows to assess the effect of the number of exits on evacuation safety more explicitly.

Also, the relationship between number of occupants and the required number of exits was discussed based on the criterion. The required number of exits depend not only on the number of occupants but also on surplus width of exits.

NOMENCLATURE

A	Room floor area (m^2)
B	Total exit width (m)
B_k	Width of exit k (m)
B_{ex}	The surplus of exit width (m)
B_A	The exit width that is necessary for evacuating the room exactly within the available escape time (m)
E	Expected number of occupants unable to escape
N	Doorway egress flow rate (person/m sec)
$p1$	Probability of fire occurrence in the room
$p2$	Probability that the fire develops to be a hazardous fire
$p3$	Probability that the fire is located in the area that impede the escape through an exit
P	Exit obstruction probability
P^*	Reference exit obstruction probability
\bar{P}	Relative exit obstruction probability reference to P^*
Q	Number of occupant of a room
Q'_k	The number of the occupants manage to escape when exit k is blocked by fire
t_E	Egress time (s)
t_A	Available egress time (s)
α	Surplus rate of exit

REFERENCE

- ¹ Hagiwara, I and Tanaka, T: International Comparison of Fire Safety Performance for Means of Escape, in Proceedings of the 4th International Symposium for Fire Safety Science, p.633-644, 1994
- ² Post-War Building Studies No.29, FIRE GRADING OF BUILDINGS, Part III. Personal Safety, Her Majesty's Stationery Office, pp.49-54, 1952.

Discussion

Akihiko Hokugo: Fifty people is the figure set forth by the regulation. Could you please elaborate on that. Do you think that is the appropriate level?

Ichiro Hagiwara: The requirements for an evacuation route vary depending on the country. In Australia, it is determined by the number of floors and the height of the building. However, in buildings for special use, there are special requirements, such as if there are people working and one floor exceeds more than fifty, then a minimum of two evacuation exits are required. And not only in Australia, but on France and England, fifty is the minimum required for two evacuation exits. In the United States, as is shown here, in case of an assembly hall, if the building has a balcony, if the number of people there is less than fifty, then only one exit is required. In other words, if the number exceeds fifty, they are required to have two exits. So it seems that in a lot of major countries, it seems that this number fifty is used as the standard to divide one versus two exits. However, there is no clear cut explanation as to why fifty is used for that purpose. Nonetheless, in order to have consistency with the current existing codes, we used fifty in our study.

A CONSIDERATION ON COMMON PATH LENGTH AND SINGLE STAIRWAY
Study on the Safety Performance of Exit Provisions Part 2

Ichiro HAGIWARA, Takeyoshi TANAKA and Yoshio MIMURA

Building Research Institute, Ministry of Construction
1 Tatehara, Tsukuba-shi, Ibaraki-ken 305, JAPAN

ABSTRACT

Usually, it is required by building codes that two or more escape routes be available from every point in a building for the purpose of assuring at least one available egress route should the other happen to be blocked by fire. The limitation of common path length and the requirement of two or more stairways for buildings exceeding certain size are typical examples of such requirements. Despite of their vital influence on building design, lucid explanation has not been given to the adequacy of the provisions. In this paper, the meaning of the code requirements on common path length and number of stairway are discussed, and the criterion that may be used as an alternative to such prescribed standards is derived based on the consideration of the expected number of occupants unable to escape.

1. INTRODUCTION

It is commonly deemed to be important for safe evacuation in building fire that two or more escape routes are arranged in different directions. Usually, it is required by building codes that two or more escape routes be available from every point in a building. This intends to assure at least one available egress route should the other happen to be blocked by fire.

The limitation of common path length and the requirement of two or more stairways for buildings exceeding certain size are typical examples of such requirements. Purely from the viewpoint of safe escape, it is desirable that the common path is as short as possible, and that two or more stairways are provided for every building. But such ideal plans are not always realized in real buildings because of the constraints of economy and convenience in normal use. However ideal they may be from the fire safety point of view, it is difficult to oblige to sacrifice everyday benefits excessively since fires are no longer so frequent threats in developed countries.

In building codes, a certain length of common path and single stairway are accepted under some conditions as a result of compromise between the safety and the building economy in broad sense. Still, building plans are significantly affected by such requirements. Despite of the vital influence on building design, lucid explanation has not been given to the adequacy of the provisions.

In this paper, the meaning of the code requirements on common path length and number of stairway are discussed, and the criterion that may be used as an alternative to such prescribed standards is derived based on the consideration of the expected number of occupants unable to escape.

2. PROVISIONS OF COMMON PATH LENGTH IN THE EXISTING REGULATIONS

2.1 Provisions for the Arrangement of Exits

The provisions for the arrangement of escape routes in the existing codes dealing with fire safety include maximum travel distance to stairway, minimum distance between exits or stairway, maximum length of dead end corridor etc. as well as the limitation of common path length.

The provisions on maximum travel distance and common path length in several countries are compared in Table 1¹. The values of maximum travel distance in the countries differ significantly depending on various features of buildings such as occupancy, number of stories, sprinkler installation and so forth. Common path length is likely to be determined in connection with , at roughly one half of, the maximum travel distance.

2.2 Maximum Travel Distance

Maximum travel distance is the limit of distance to cover from a point on a floor to an exit to outdoor or a protected escape path such as a smokeproof tower. There are two ways of measurement for the maximum travel distance depending on code, that is, one which measure from the remotest point including the interior of a room and the other which measure from the doorway of a room.

TABLE 1 Arrangement of Means of Escape

	Australia	France	Japan	U.K.	U.S.
Maximum Travel Distance	a) Apartment, Hotel N.R. b) Assembly 60 m in room 40 m door-exit 20 m c) Hospital(ward) 30 m d) others 40 m	a) General 40 m b) from unprotected stairs 30 m c) from dead-end 30 m d) Hotel door-exit 40 m e) Apartment smoke controlled door-exit 15 m open-air corridor door-exit N.R.	a) Shop, Office =<14th stories 30m >=15th stories 20m b) others =<14th stories 50m >=15th stories 40m * interior finished with non-combustible material +10 m	number of direction <1>/<2> a) Assembly, School 15 m/ 32 m b) Hospital 9 m/ 18 m c) Hotel bedroom 9m/18m elsewhere 18m/35m d) Apartment in room 9 m unit door-exit	a) Assembly 45m (60m) b) School 45m (60m) c) Hospital (60m) in room 23m (38m) door- 30m (60m) d) Hotel, Apartment in room 23m (38m) door- 30m (60m) e) Shop 30m (60m) f) Office 60m(91m)
Common Path of Travel	a) Apartment, Hotel door-exit 6 m others 20 m b) Hospital(ward) 12 m c) Shop, Office 30 m d) single stairs 30 m e) others 20 m	from door at dead-end 10 m	1/2 of maximum travel distance	7.5 m/ 30 m e) Shop, Office 18 m/ 45 m	a) Assembly 6.1m (6.1m) area =< 50 Ps. 23m (23m) b) School 23m (23m) c) Hospital N.R. d) Hotel, Apartment except in room 10.7m (15m) e) Shop 23m (30m) f) Office 23m(30m) one tenant =< 30Ps. 30m

Ps.: persons, (): sprinklered

The meaning of maximum travel distance in the context of escape in fire is interpreted as either of the followings:

- (1) The limit of the distance which evacuees can manage to reach a stair running through a smoke clogged space such as a corridor etc.
- (2) The limit of the distance which evacuees can manage to reach a stair before the escape routes such as a corridor has been smoke clogged.

In any case, the essential meaning of the maximum travel distance is nothing but the limitation of travel time to a protected stair in view of safety from smoke. In this sense, it may be allowed to relax the limitation of maximum travel distance if the danger by smoke is considered to be low. In fact, the distance is relaxed according to the degree of fire retardation of interior linings in Japan, and by sprinkler installation in the U.S.A. In France, there is no limitation on the distance for open-air corridors of apartment buildings.

2.3. The Objective of the Limitation of Common Path Length

Common path length is the distance from where egress start to where two or more escape directions are available. Typical concept of common path is illustrated in Figure 1a. Common path length is usually measured from the remotest point in a room, but may be measured from doorway in some cases, such as collective dwellings and lodging facilities.

In actual buildings, common path appears in such plans as shown in Figure 1b more frequently than the plan in Figure 1a. In such a case, evacuees only have to cover the distance of the common path length to reach a stair as long as they do not fail to find the stair, so practically the limitation of common path length induces the reinforcement of maximum travel distance.

The role of the limitation of common path length is different from that of maximum travel distance: The basic concept of common path length is shown by Figure 1a. Obviously, it is not enough to cover the common path to get to a safe place such as a stair case. It is not common path length but maximum travel distance that has to be limited if the objective is to avoid or mitigate hazards due to smoke.

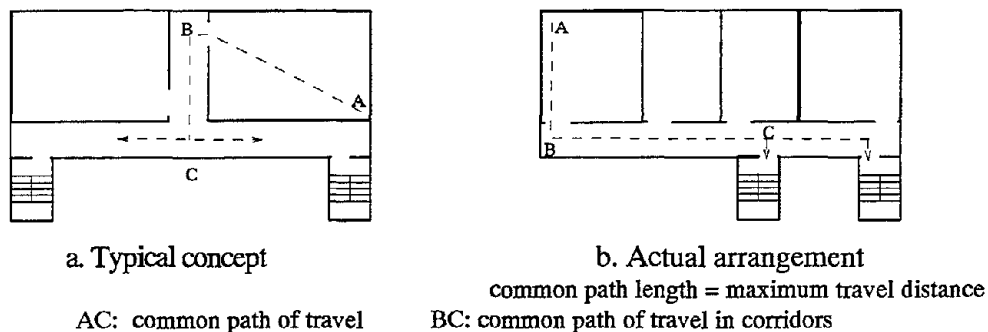


FIGURE 1 Examples of Common Path of Travel

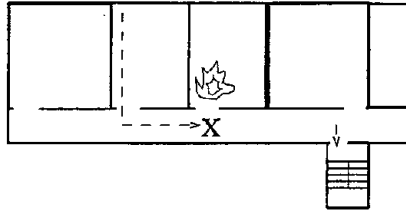


FIGURE 2 A fire blocks only one escape route to a stairway

The objective of the limitation of common path length is considered to reduce the risk that escape is blocked by the fire which happens to occur on the egress path to a stair or other places of final safety. The typical scenario will be, as shown in Figure 2, that a fire breaks out in a room along one way corridor and the flames or hot gases ejecting out from the doorway impedes the passage of the occupants in the rooms located at the opposite side of a stairway. The meaning of the limitation of common path length is to limit the number of the occupants who may lose the only escape means.

3. CONDITIONS ALLOWED IN CASE OF SINGLE STAIRWAY

In principle, building codes require two or more stairways as the vertical escape routes in multiple story buildings. However, it is allowed to have only one stairways under certain conditions since it is not practical to require two or more stairways to all buildings. Table 2 summarizes the conditions associated with the relaxation of the requirements of two or more exits¹.

From Table 2, it can be recognized that basically three main factors are involved when a single stairway is accepted, i.e., number of occupants on a floor, number of floors and characteristic of occupants, but other different factors are also taken into account in different codes. In average, the maximum number of occupants are limited to 50, but the number is limited to a smaller value for buildings of residential or medical care uses. With this restriction, goes the limitation of number of floors, or building height, which differs somewhat in different codes. This limitation is considered

TABLE 2 Condition allowed in case of single stairway

	Australia	France	Japan	U.K.	U.S.
Single Stairs	a) =<6 stories or =<25 m height <u>Hospital, Assembly, School</u> b) =<6 stories or =<25 m height & any story >50 Ps. * ward floor * preschool * primary or secondary school	for story or part of story 1) =<19Ps. 1 2) =<50 Ps. 1+sub <u>Apartment</u> a) combinations of stairs and corridors opened to the air or with smoke control b) stairs with smoke control	=<5th floor & a) on 3-5th floor & S =<200 m ² c) on 2nd floor & S =<400 m ² d) ward floor & S =<100 m ² e) Hotel : floor with sleeping rooms & S =<200 m ² f) Apartment & S =<200 m ² except * Assembly, * Shop	<u>Apartment</u> a) top floor <11m, =<4 stories, travel to exit <4.5 m <u>others</u> c) top floor <11m, =<50 Ps. d) room =< 50 Ps. e) story =<50 Ps.	<u>Assembly</u> a) balcony <50 Ps. <u>Hotel, Apartment</u> b) =< 4 stories, =<4 living units per story, sprinkled <u>Office</u> c) room/area <100Ps. travel to outside <30m d) =<3 stories, each story < 30Ps., travel to outside <30m

Ps.: persons, S: room area

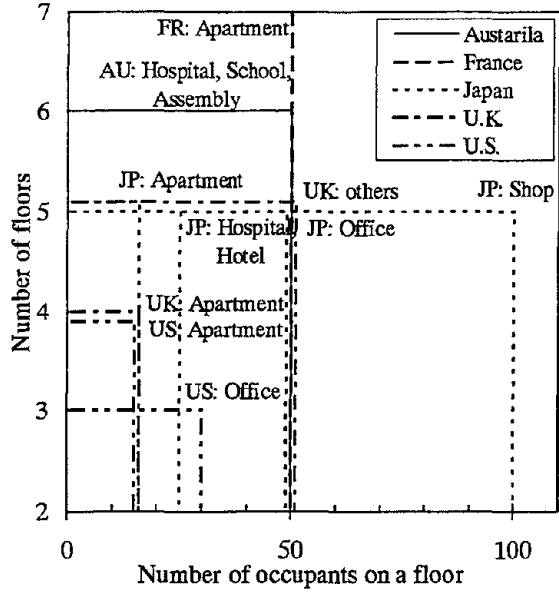


FIGURE 3 Relation between number of occupants on a floor and number of floors for buildings having a single stairway

to be associated with the chance of rescue by fire brigades.

Such concurrent limitations on number of occupants on a floor and number of floors are followed by the limitation of the total number of occupants in a building. Total number of occupants allowed to be accommodated on the second and upper floors in a building ranges from 50 to 400 depending on use of buildings and different codes. The type of buildings in which a large number of occupants are allowed are likely to be those which have no sleeping facility.

4. EXPECTED NUMBER OF OCCUPANTS UNABLE TO ESCAPE ASSOCIATED WITH SINGLE MEANS OF ESCAPE

4.1 Theoretical Consideration

Common path in a corridor and a single stairway have the same issue from the viewpoint of evacuation safety, that is, the occupants are trapped by fire when the fire breaks out in a space on the way to the exit.

(1) Expected number of occupants unable to escape due to common path

The typical plan of the part of buildings to which the limitation of common path applies is shown in Figure 4. Our interest is how the risk on evacuation is related with the common path length. Let n be the number of the rooms along the corridor having only one escape direction to the stairway. The escape from a room is impeded when a fire breaks out between the room and the stair, grows to a hazardous fire and ejects flames or hot gases to the corridor through open doorway. Probability of such an event to occur for an arbitrary room k , which we call here "Escape route obstruction

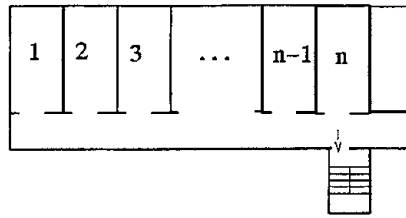


FIGURE 4 n rooms along a corridor having only one escape route to a stairway

probability" can be given as

$$P(k) = p1(k) \cdot p2(k) \cdot p3(k) \quad (1)$$

where $p1(k)$: probability of fire occurrence in the room
 $p2(k)$: probability that the fire grows to a hazardous fire
 $p3(k)$: probability that the door is left open in fire

Next, letting $Q(i)$ be the number of occupants in room i , the expected number of occupants who are unable to escape to the stair e for each potential room of origin k is calculated as

$$\begin{aligned} e(k) &= \{Q(1) + Q(2) + \dots + Q(k-1)\} P(k) \\ &= \left\{ \sum_{i=1}^{k-1} Q(i) \right\} P(k) \end{aligned} \quad (2)$$

respectively.

Hence, the total expected number E which takes into account the possibility of fire occurrence in every room is given as

$$E = \sum_{k=1}^n \left\{ \sum_{i=1}^{k-1} Q(i) \right\} P(k) \quad (3)$$

At the stage of planning of a building, it will be likely that the conditions of such rooms as above is practically regarded as uniform, that is, $P(k) = P$ and $Q(i) = Q$ in Eqn.(2), then the total expected number E is calculated simply as

$$E = \frac{n(n-1)}{2} PQ \quad (4)$$

The value of n is only dependent on the specific plan, and Q may be evaluated from the use and the area of the room. It would be desirable that the probability P be obtained based on fire statistics, but currently not ample statistical data is available for the probabilities included in the right hand side of Eqn.(1), although $p1$ and $p2$ could be roughly estimated. As it is expected to be difficult to determine the absolute value of P , some other way must be sought for handling this factor.

(2) Expected number of occupants unable to escape due to single stairway

Next, let's consider the building consisting of a single stairways and multiple floors as shown in Figure 5. Although the problem in this case may involve some difference from common path, for

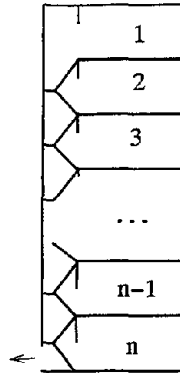


FIGURE 5 n stories high building having a single stairways

instance, the primary threat to evacuation in stairway is more smoke filling than hot gases ejection from door, the issues associated with a single stairway and common path of corridors are considered to be much similar. Hence the same consideration and the equations (1) – (3) may be extended to use for the problem of a single stairway.

4.2 Some Consideration on Effect of Factors

(1) Number of occupants

The provisions of common path length in any country does not explicitly take into account the variables such as n and Q . However, in case of the assemblies and offices in the U.S.A., the limitation of common path length is relaxed when the number of occupants is low. This is considered to be rational because, as can be readily recognized from Eqn.(3), the expected number of occupants unable to escape decreases proportionally to the reduction of the number of occupants.

The expected number E increases drastically with number of rooms n if the number of occupants in a room Q is the same. For instance, E increases by 6 fold if n is doubled from 2 to 4. If the total number of occupants nQ is the same, the expected number E increases proportionally to the number of rooms $n-1$.

(2) Fire suppression system

In the building codes of the U.S. the limitation of common path length is relaxed when the building is sprinklered. This provision may be justified by considering that sprinklers have the effect to reduce the probability that a fire develops to a hazardous level, that is, p_2 in Eqn.(1).

According to the statistics in the U.S. and Canada, the probability of flashover occurrence is reduced to about $1/4 - 1/5$ by the installation of sprinkler system². Because the expected number of occupants should be the same between with and without sprinkler system,

$$\frac{n(n-1)}{2}QP = \frac{n_{sp}(n_{sp}-1)}{2}QP_{sp} \quad (5)$$

that is,

$$\frac{P_{sp}}{P} = \frac{n(n-1)}{n_{sp}(n_{sp}-1)} \approx \frac{1}{4} \quad (6)$$

where n_{sp} : number of rooms in sprinklered condition
 P_{sp} : fire probability in sprinklered condition

For $n > 2$, the value of n_{sp}/n lies between 1.7–2.0. The number of rooms along the corridor forming the common path is considered to be about in proportion to the common path length. Hence, it follows that common path length can be approximately doubled without lowering the safety level of evacuation if the relevant part is sprinklered. In this sense, the U.S. standard for common path length, which relax the length by the equipment of sprinkler system, is thought to be reasonable.

5. CRITERION ALTERNATIVE TO EXISTING STANDARDS ON SINGLE MEANS OF ESCAPE

5.1 Consideration on Some Other Factors

As we have seen in the above, Eqn.(3) can take into account some of the factors which have been incorporated in the existing standards associated with common path length, such as number of occupants, sprinkler system and so forth, by fairly logical manners. But as can be seen in Table 2, some other factors have been taken into account in the existing codes. Hence, we should pay due respect on such factors. They are particularly as follows:

(1) Rescue by fire brigade

Single stairway is basically allowed for relatively low-rise buildings. This implies that the possibly of rescue by fire brigade using fire ladder or some other means of escape are taken into account in case the built-in means of escape, such as stairway and corridor, are made unavailable by fire.

On the other hand, rescue by fire brigade seem to be disregarded in the provisions for common path length in most building codes. The building standards law of Japan is the only code that prescribes different length of common path depending on height of floor, perhaps for some other reason. However, it will be logical that the factor of rescue is considered in common path.

(2) Degree of fire protection of escape route

In France, single stairway is allowed if the stair is protected properly from fire and smoke including being opened to outdoor air. In principle, a single stairway should be sufficient if it is perfectly free from the hazards due to fire. However, perfectly protected stairways are seldom found in real buildings so the level of safety varies depending on the degree of protection. More generally, the degree of protection of staircases and corridors should be added to the assessment by Eqn.(3). In most cases, corridor is closer than stairway to the room of origin, so direct impact of fire is stronger in corridors than in stairway. However, a high degree of protection is conceivable for corridor in some cases. For instance, if a corridor is wide enough, it will be possible to pass in front of the doorway ejecting hot gases from the room of origin.

5.2 Proposed Criterion

Considering the factors mentioned in the above, Eqn.(3) should be slightly modified as

$$E = \left\{ \sum_{k=1}^n \left\{ \sum_{i=1}^{k-1} Q(i)\varphi \right\} P(k) \right\} \delta \quad (7)$$

where φ and δ are the efficiencies of the rescue by fire brigade and degree of protection of escape route on the reduction of occupants unable to escape, respectively.

It is virtually hopeless to obtain the absolute value of $P(k)$, φ and δ , however, if we consider the reference conditions of building space having only one escape route to which maximum number of occupants is allowed by building codes, the critical value of E has to be

$$E \leq Q_{ref} P^* \varphi^* \delta^* \quad (8)$$

where Q_{ref} is the maximum number of occupants, and P^* , φ^* and δ^* are the value of P , φ and δ implicitly assumed for such a space by the codes.

Using Eqns.(7) and (8) yields the expression of the criterion as

$$\left\{ \sum_{k=1}^n \left\{ \sum_{i=1}^{k-1} Q(i)\bar{\varphi} \right\} \bar{P}(k) \right\} \bar{\delta} \leq Q_{ref} \quad (9)$$

where $P(k)$, φ and δ are relative probability and efficiencies defined as

$$\bar{P}(k) = P(k)/P^*, \quad \bar{\varphi} = \varphi/\varphi^*, \quad \bar{\delta} = \delta/\delta^* \quad (10)$$

5.3 Values of Parameters

From Table 2, it can be recognized that in average sense 50 seems to be the maximum number of occupants allowed for a space without sleeping facilities which has only one escape route, and since no particularly important measure is required on allowing the 50 occupants we may be able to assume such condition that the rescue by fire brigade is not expected nor the escape route is protected. Therefore, for such conditions, let the values of the parameters be as

$$\bar{P}(k) = 1, \quad \bar{\varphi} = 1, \quad \bar{\delta} = 1 \quad \text{and} \quad Q_{ref} = 50 \quad (11)$$

(1) Common path in corridor

Next, let's consider on the issue of common path length. Applying Eqn.(9) and (11) to a corridor having only one direction to stairway and n rooms of the same conditions on each side as shown in Figure 4, we have

$$2n(n-1)P_c \bar{\varphi} \bar{\delta} Q \leq 50 \quad (12)$$

where P_c is the relative escape route obstruction probability of corridor.

From Table 1, it is fairly evident that the common path length measured from the doorway of a room to staircase is restricted within 10 m in average. Four single bed rooms may be arranged on each side of the corridor of this length in the business hotel in Japan. Also, considering that the limit of the common path length apply unconditionally, we may be able to let $\varphi=1$ and $\delta=1$. Hence, from Eqn.(12)

$$2 \times 4 \times 3 P_c \overline{\varphi \delta} \times 1 = 24 P_c \leq 50$$

that is $P_c = 2$.

Noting that 50 occupants are allowed for the condition without sleeping facilities, applying Eqn.(12) to the same configuration but non sleeping condition yields

$$2 \times 4 \times 3 P_c \overline{\varphi \delta} \times \frac{50}{8} = 150 P_c \leq 50$$

that is $P_c = 1/3$.

In summary, the relative escape route obstruction probability of corridor turns out to be

$$P_c = \begin{cases} 2 & \text{(for sleeping use)} \\ 1/3 & \text{(for non-sleeping use)} \end{cases} \quad (13)$$

(2) Single stairway

Now, let's apply Eqn.(9) and (11) to a building having n floors and only one stairway, then we have

$$\frac{n(n-1)}{2} P_s \overline{\varphi \delta} Q \leq 50 \quad (14)$$

where P_s is the relative escape route obstruction probability of stairway.

From Table 2, it can be recognized that single stairway is allowed for buildings having four or less floors and four or less dwelling units on each floor. Because the number of floor is four or less it is considered the rescue by fire brigade is normally taken in to account, but a high level of stairway protection is not required. Average number of occupants in a dwelling unit may be estimated as four. Hence, substituting $n=4$, $\delta=1$ and $Q=4$ into Eqn.(14), we have

$$\frac{4 \times 3}{2} P_s \overline{\varphi \delta} \times 16 = 96 P_s \overline{\varphi} \leq 50 \quad (15)$$

that is, $P_s \overline{\varphi} = 1/2$.

Noting that 50 occupants are allowed for the condition without sleeping facilities, applying Eqn.(14) to the same configuration but non sleeping condition yields

$$\frac{4 \times 3}{2} P_s \overline{\varphi \delta} \times 50 = 300 P_s \overline{\varphi} \leq 50 \quad (16)$$

that is, $P_s \overline{\varphi} = 1/6$.

Fires usually breaks out in a room on a floor. Let's imagine a fire occurred in a building for

sleeping use having an unprotected single stairway. It may be reasonable to assume that the stairway will be involved in the hazard of the fire at the same time. Accordingly,

$$P_s \approx P_c = 2 \quad (17)$$

Using this value in Eqn.(14) yields

$$\bar{\varphi} = \frac{1/2}{P_s} = \frac{1/2}{P_c} = \frac{1}{4} \quad (18)$$

The efficiencies of the rescue by fire brigade $\bar{\varphi}$ should be independent of building use, so the same value as Eqn.(18) is invoked to Eqn.(15) to yield the relative stairway obstruction probability for non sleeping use as

$$P_s = \frac{1/6}{\bar{\varphi}} = \frac{2}{3}$$

Therefore, in summary

$$P_s = \begin{cases} 2 & \text{(for sleeping use)} \\ 2/3 & \text{(for non-sleeping use)} \end{cases} \quad (19)$$

Compared with Eqn.(12) for corridor, the difference between sleeping and non-sleeping uses is small. The interpretation may be such that a fire on a different floor is perceived by the occupants of the other floor less easily than a fire on the same floor even when the occupants are awake.

6. CONCLUSION

The criterion which may be used as an alternative to the existing provisions on common path length and the conditions allowed for a building having only one stairway is proposed. The criterion is summarized as follows:

$$\left\{ \sum_{k=1}^n \left\{ \sum_{i=1}^{k-1} Q(i) \bar{\varphi} \right\} \bar{P}(k) \right\} \bar{\delta} \leq Q_{ref} \quad (20)$$

and the values of the associated parameters are

$$\bar{\varphi} = \begin{cases} 1 & \text{(for no possibility of rescue)} \\ 1/4 & \text{(for possibility of rescue by fire brigade)} \end{cases}, \quad \bar{\delta} = 1,$$

$$\bar{P}(k) = \begin{cases} 2 & \text{(for sleeping use)} \\ 1/2 & \text{(for sleeping use and sprinklered)} \\ 1/3 & \text{(corridors, for non-sleeping use)} \\ 2/3 & \text{(stairways, for non-sleeping use)} \end{cases}, \quad Q_{ref} = 50$$

However, further consideration is needed for $\bar{\delta}$ for the various degree of stairway protection.

The average level of evacuation safety will be basically the same between the proposed standard and the existing provisions. However, the advantage of the proposed standard is that it is able to

take into account more factors affecting the safety of unidirectional escape within a logical context. This method will allow much more flexibility in building plans without deteriorating the current level of safety.

NOMENCLATURE

E	Expected number of occupants unable to escape
$p1$	Probability of fire occurrence in the room
$p2$	Probability that the fire develops to be a hazardous fire
$p3$	probability that the door is left open in fire
P	Exit obstruction probability
P^*	Reference exit obstruction probability
\bar{P}	Relative exit obstruction probability reference to P^*
P_c	Relative escape route obstruction probability of corridor
P_s	Relative escape route obstruction probability of stairway
Q	Number of occupant of a room or in a floor
φ	Efficiencies of the rescue by fire brigade
δ	Degree of protection of escape route

REFERENCE

- ¹ Hagiwara, I and Tanaka, T: International Comparison of Fire Safety Performance for Means of Escape , in Proceedings of the 4th International Symposium for Fire Safety Science, p.633-644, 1994
- ² Gaskin, J. and Yung, D. :Canadian and U.S.A. Fire Statics for Use in the Risk-Cost Assessment Model, Internal Report No.637, pp.4-6, 1993.1

Discussion

Brian Meacham: It seems to me in both this presentation and the past one, that you looked at finding a way to determining an equivalent level of safety to the existing codes. Did you put any effort into determining whether or not the current level of safety is really what you want to have in the new approach?

Ichiro Hagiwara: These two papers are consistent with the current level of safety provided by existing codes. However, in the various countries the codes vary. For example, in some countries, if there are sprinklers, then the length of the common path can be half. So those things could be taken into consideration as probabilities if the evacuation routes are blocked. And that's the purpose of this study. With this study, we will be able to discuss the various different types of codes in various countries on a common ground. I think that is the advantage of the formula. When we consider the performance-based fire design, it is necessary for us to establish standards for requirements for the purpose of compliance.

Howard Emmons: I'm a bit confused over one item, your capital "P" symbols are defined in your notations as probabilities. Probabilities must be between zero and one. Yet, your probabilities seem to be able to be two. What am I missing?

Ichiro Hagiwara: Well, yes, the "P" has to be between zero and one. In order to get the expected value, we should be able to know the absolute probability, but sometimes it is difficult to this. For example, under the existing code, if there are more than 50 occupants in the room, there should be more than two exits. However, it is not known how much of a risk is involved in this particular situation, in terms of absolute probability. The reason we have such regulations under the existing code is because that they consider there is a risk of the occurrence of such dangerous events as the probability of fifty multiplied by a certain probability value. So, in relation to the existing codes, this "P" refers to relative probability. If the probability of risk is twice as much, then "P" becomes two.

King-Mon Tu: I noticed in equation 10 you have $P(\text{bar})$ equals P divided by P^* . I would like to know if you could give me some example of how in equation 1, you have $P=(P1)(P2)(P3)$. Can you give me an example?

Ichiro Hagiwara: This is something I explained in the previous paper. $P1$ is the probability of fire occurrence in the room, $P2$ is the probability of fire expanding, and $P3$ is the probability of the fire expanding to the other area of the building, that is, fire or smoke extending to other parts of the building because the door is open, that probability. P^* means the probability of fire occurrence when an evacuation route is determined into one direction. And given that situation, $P(\text{bar})$ means the relative degree of danger.

Richard W. Bukowski, P.E.

NIST Building and Fire Research Laboratory
Gaithersburg, MD 20899-0001 USA

Abstract

Performance codes are replacing prescriptive codes in much of the world. As the form of the codes change, the form of standards which support those codes needs to evolve in concert. Thus, performance standards need to be explicit about the purpose(s) served by the standardized systems and to provide quantitative means to assess the degree to which they serve that purpose. Most of the engineering methods evolving to support performance based codes assess risk to life of building occupants relative to the risk to occupants in buildings which comply with the prescriptive code. Such *relative* risk assessment is cumbersome and unreliable, and should be replaced by absolute risk limits to enjoy all of the efficiencies of performance codes. Financial risk is easy to understand but is inappropriate to codes that exist to protect life. Risk to life is difficult to understand and communicate to the public. These risk analysis methods utilize scenarios as a bridge to experience and the means to quantify likelihoods. In the absence of incident data some systematic methods of identifying scenarios is needed. This paper deals with each of these issues in an attempt to stimulate research needed to find the answers.

1. BACKGROUND

The worldwide migration to performance-based fire and building codes has placed new demands on the engineering profession. One of the most challenging is for meaningful ways of assessing the degree to which specific designs meet the requirements which society places on its constructed facilities.

With regard to fire safety, it can be argued that society expects the risk of death or injury from fire to be held to some acceptable level that varies with occupancy. For example in residential occupancies, people are generally willing to accept higher risks in their own homes as compared to hotels. The general risk literature suggests that society expects the risk of multiple deaths or injuries per incident to be decreased, roughly in inverse proportion to the numbers (i.e., the risk of 10 deaths in an incident should be 1/10 that of a single fatality). What is not clear is how to communicate risk implications to policy makers and the public, and how to arrive at risk targets that society considers acceptable.

The fact that every draft performance evaluation system is risk based makes it clear that risk is the metric of choice for the performance-based safety regulations of the future. This fact raises certain issues which need to be addressed early so that this beneficial process is not unnecessarily delayed. Some such issues include:

1. The regulatory system is made up of codes and standards -- the former dictate *what* is required and the latter *how* to implement something that is required or provided voluntarily. When adopted, both have the force of law, but codes establish the fundamental requirements and standards expand on the details. In the debate over performance-based codes and standards, they are lumped together. How should standards change (if at all) to support the evolving performance-based codes?

2. Insurance has long used financial loss as the metric for risk decisions, as this can be compared against rates charged, and the customer can choose to lower the risk and reduce the premium. However, fire codes are concerned with life loss, raising the specter of the “value of a human life” problem. Use of the risk of death directly is no better since this is a difficult concept to understand, and people are willing to accept much higher risk of the death of strangers as compared to themselves or their family. Thus, what is the most appropriate unit for fire risk?
3. There are (at least) two ways of performing a fire risk analysis. One is to identify a small number of scenarios that are representative of a class of scenarios and do detailed (and time consuming) predictions with a complex set of models. The other is to identify a range of values for a number of independent variables which define the scenarios and do a Monte Carlo simulation of a large number of variations using simple (and very fast) calculations. Which provides a more reliable picture of the risk?
4. Risk analysis requires the likelihood and consequences of events, some of which may not be known in advance. Fire safety engineering analysis can address the consequences, given the event. This leaves us to determine the scenarios of concern and their likelihoods. Fire incident data can yield both, but these are uncommon in the world, and those that exist are not always reliable or don’t provide all the needed data. Can scenarios and their likelihoods be generated by models of initiating events?

2. PERFORMANCE CODES

Much of the discussion to date has focused on performance-based codes. From those codes in place or under development around the world there is a clear consensus on their general characteristics¹. These include first, a set of clear, quantitative objectives and second, a means to establish whether those objectives have been met. A performance code will usually also include “deemed to satisfy” provisions which codify approaches which experience has shown to provide acceptable solutions, such as the dimensions of egress stairs. These performance codes further include “Approved Documents” which are intended to catalog acceptable solutions for use in cases where a performance analysis is not needed. The first such approved document is generally the old prescriptive code.

In this way, the role of the code is to make clear the objectives which society desire for its constructed facilities. Examples from the fire regulations in the New Zealand Building Regulations of 1992² (which are typical of those being developed in other countries) include:

“Clause C2 - MEANS OF ESCAPE

OBJECTIVE

C.2.1 The objective of this provision is to:

- (a) Safeguard people from injury or illness from a fire while escaping to a safe place, and
- (b) Facilitate fire rescue operations.”

Nearly everyone would agree that this is the fundamental intent of fire regulations -- to allow for safe egress. With prescriptive codes it was implied that buildings which provided all of the

features and arrangements required would be “safe,” and in a performance code this is an explicit objective. It can be argued, however, that this is still not sufficiently clear. For example, does society intend that *everyone* be able to exit without injury? Does this include those with physical limitations, infants, persons intimate with the ignition, and under all conditions and at all times of the day or night? Are even minor injuries which do not result in lasting deficits prohibited? Is society willing to accept the cost implications of fully protecting everyone all of the time? We certainly need to do a better job of understanding what society expects and at what cost.

3.0 PERFORMANCE STANDARDS

As the world transitions to performance codes, standards will still be needed to provide the detail of how to meet the intent of the code. However, since the form of the code has changed, the form of the standard should be re-thought so as to best complement the performance oriented nature of the system. Specifically, what form should a standard take relative to that generally agreed for a performance code?

Since the code is built around explicit objectives, the standard needs to clearly state its intent regarding the purpose of the system or feature covered. For example, alarm systems are intended to provide early detection of an unwanted fire, notification to the occupants of the need to evacuate or relocate, and notification of the fire service of the need for their assistance and, in large buildings, direct them to where they need to go. Further, an alarm system should **not** respond to conditions not associated with an unwanted fire and should **not** direct the fire service to areas other than where the fire is to be extinguished. Finally, alarm systems should be reliable and able to meet their stated objectives (or some subset thereof) during any single fault condition from a specified set.

Thus, the form of a performance standard is first, to explicitly state its purposes and second, to provide a means to establish quantitatively what constitutes meeting those purposes. In addition, any quantitative measure of the ability of the system to fulfil its purpose needs to include the reliability of systems. This refers to the likelihood that such protective systems will perform as intended when called upon to do so. Like the code, the performance standard will have “deemed to satisfy” provisions which describe arrangements which are known to meet the intent. Current prescriptive standards are likely to comprise early “Approved Documents” for standards as well.

3.1 Purposes of Standards

Fire safety standards cover a myriad of topics, but can be considered to fall into several, broad categories. Standards on fire protection systems and components such as fire alarm, sprinkler systems, fire pumps, emergency power systems, etc., are all intended to assure the reliable operation of critical equipment in the event of a fire. They detail the proper installation, maintenance, and use of the equipment or systems covered which are deemed necessary to assure reliable operation. Here, the purpose statement would include the function provided by the system, such as notification of occupants and emergency services for an alarm system, extinguishment of the fire for a sprinkler system, provision of sufficient pressure and flow for a fire pump or voltage, current, and frequency for an emergency power system.

Another category of fire standards covers the safe installation and operation of equipment and systems needed to prevent fires from starting or to limit their size or impact. Examples would include standards on ovens and furnaces, chimneys and fireplaces, power plants (nuclear or fossil fueled), and various standards on the safe storage and handling of combustible or hazardous

materials. In this case, the statement of purpose needs to include quantitative performance measures such as the maximum heat release rate which would be allowed from the maximum quantity of material which can be stored in a given fire area, or the maximum temperature which is allowed on a surface under the most severe conditions of operation.

A third category of fire standards relate to test or measurement methods or standard guides on methods for the collection of information or to define a process such as the investigation of fires or the conduct of fire hazard or fire risk assessments. These standards attempt to provide reliable and consistent information on which decisions can be made with confidence.

3.2 Quantitative Measures of Performance

The first category of standards might talk of detection of fires before they constitute a threat to occupants and while there is sufficient time for safe egress, or of sprinkler activation and fire extinguishment before tenability limits are exceeded in the room of fire origin. In these cases, the quantitative measures of performance are the fire size at detection or activation and the “worst case” exposure to occupants before extinguishment. In addition, an estimate of the system reliability in terms of the likelihood that the system will perform its function when called upon if the provisions of the standard are followed, must be included.

For those standards intended to prevent fires or limit their impact or size, the measure of performance is the assumed rate of ignitions or the limiting conditions that can be assumed if the standard is followed. Where standards are intended to provide uniform procedures for making measurements or testing performance, techniques of assessing repeatability and reproducibility exist and should be used as both the measure for performance and reliability.

4. ASSESSING RISK

Once the Performance Codes and Performance Standards are in this format, the use of risk assessment as the method to determine compliance becomes possible. The Codes will express for any occupancy, the consequences of fire which society is willing to accept as its objectives, and the types of analysis or “acceptable solutions” which demonstrate compliance.

From these, an engineering analysis will identify what approaches can satisfy the list of acceptable consequences. Each approach requires that certain functions are performed, and these are associated with Standards that explain how the equipment, systems, or procedures are to be implemented and maintained in order to assure the function, and an associated reliability by which the function must be discounted.

This method identifies the complementary aspects of systems such that if one fails to provide its function, another will provide it, perhaps at a reduced level (in the absence of common failure modes). This allows redundancy without unnecessary duplication, allowing cost optimization without sacrificing safety.

However, what has been described so far (avoidance of specified consequences) is not risk, but rather hazard assessment. Design fires may be specified in the codes by occupancy along with the ability of the engineer to suggest alternatives for specific applications, based on an analysis of the fuels and ignition sources present. If probability distributions for these as well as some other parameters such as occupant loadings and characteristics (e.g., age, sex, physical and mental capabilities) are provided, a risk assessment can then be performed.

4.1 Relative Risk

In all but one of the engineering methods proposed in support of performance codes the risk assessment is for *relative* risk. This requires that the risk of the subject building be assessed and that the risk for a similar building (same occupancy and general characteristics) but designed in accordance with the prescriptive code also be calculated so the two can be compared. This doubles the computational burden and discourages the calculated solution in all but those few cases where no alternative exists.

Justification of the relative risk approach usually takes a form similar to statements made by Australia's Building Regulatory Review Task Force (BRRTF) which said,³

“... with a few exceptions the Australian community appears to be reasonably satisfied with the safety levels achieved by our current regulations.”

This leads to their conclusion that,

“... the risk levels achieved by buildings designed to the current regulations can be used for the time being, as convenient benchmarks of the risk levels which must be achieved by any alternative fire safety system arrangements.”

But relative risk poses some potential pitfalls which need to be considered. For example, Brannigan argues,⁴

“The statement that the public is satisfied with the level of fire safety is debatable, but even if true it does not necessarily support the statement of equivalence (to buildings built to current regulations) for at least four reasons:”

Paraphrasing Brannigan's points: First, the equivalence statement assumes that the public is satisfied with an expected risk to life rather than a safety level. Fire, especially disastrous fires are rare events. When dealing with rare events the public may believe that the risk to life is actually zero.

Second, the claim that society is “satisfied with the level of safety achieved by our current regulations” assumes that the current regulations are the sole cause of this socially acceptable level of safety. Codes specify minimum requirements which are often exceeded in the recognition of liability or public image (e.g., significant improvements in fire safety were implemented by the lodging industry following the fires of the 1980's, well in advance of changes to the codes). If the performance level is set as equivalent to the minimum code, the result may be an increase in losses when compared to the code compliant building.

Third, they assume that the engineering methods accurately reflect the expected risk to life in different buildings. It may not be possible to predict accurately loss rates in the future due to the fact that stochastic elements are based on past materials and lifestyles which may change (e.g., smoking materials are among the most commonly cited ignition sources in fatal fires, and the rate of smoking is rapidly declining in many countries).

Fourth, they assume that both the buildings and society's views of risk are static. Fire disasters often point out flaws in the code which are subsequently corrected. If such a flaw were uncovered, the performance method would allow buildings to continue to be built with that aspect of risk uncorrected as long as that hazard goes unrecognized by the prescriptive code. Most societies would not accept such a practice.

4.2 Absolute Risk

The draft Code of Practice from the British Standards Institution (BSI)⁵ is the only method which has attempted to set acceptable levels of risk. The proposed values are based on current fire losses in the UK. The authors suggest

“... that the public broadly tolerates the average risk of death from fire provided that the number of deaths in any one incident is small.”

They suggest a value for the risk of death per individual per year at home (1.5×10^{-5}) or elsewhere (1.5×10^{-6}), and for the risk of multiple deaths per building per year (>10 deaths, 5×10^{-7} ; and >100 deaths, 5×10^{-8}). Of course, the comments made in the previous section concerning any assumption that society is satisfied with current losses apply here as well. Thus, some better method of making public policy decisions about acceptable levels of risk is needed.

As discovered by the nuclear power industry, the problem is that risk to life is too abstract to be understood by the public. Risk acceptance is highly variable, depending on to whom the risk applies (individual vs. society), the perceived value of the activity, whether the risk is assumed voluntarily, and whether the people at risk are considered especially deserving of protection (e.g., children, elderly, handicapped, or involuntarily confined). Perhaps if the risk were expressed in a way which had meaning to the public it would be easier to obtain policy decisions on what is acceptable.

5. EXPRESSING RISK

5.1 Risk to life

Expressing risk to life in a way which can be understood by the public is a problem which has been addressed for years by the nuclear power and air transport industries with limited success. At the most basic level risk to life is a small number generally expressed in scientific notation, which itself is not understood by most people. The risk is normally compared to events or activities such as the risk of being struck by lightning or the risk of death during skydiving. While the public impression is that these are rare events, they really have no good feel for how rare.

5.2 Risk of financial loss

This leads to the consideration of other metrics for risk. The general unit of value in society is money, and the insurance industry has expressed risk in monetary terms for most of its history. Risk of financial loss is easy to understand and allows direct evaluation of offsetting benefits of investment in reducing risk or in the costs of insurance against the loss.

Financial loss is thus the perfect metric for risk but for one problem. The primary focus of fire codes is life safety, requiring that risk to life must then include a measure of the value of human life. Numerous (at least partially) objective measures of such value have been proposed -- earning potential over the remaining expected life, potential contributions to society, costs of insurance or legal settlements, costs associated with regulation intended to reduce accidental fatalities, to name just a few. In each case the concept that some people have less “value” to society than others is met with great objection, especially by those whose value is deemed lower.

6. ESTIMATING RISK

Traditional risk analysis has involved probabilistic techniques for both the likelihood estimates and the consequences of the events. These techniques may use experience (generally the case in most fire analysis) or may involve expert judgement and failure analysis methods where there is

little or no experience (such as in the nuclear power industry). Regardless of how it is approached, one of the strengths of risk analysis is its ability to deal with distributions of outcomes based on variations in conditions which affect these outcomes. For example, doors may be open or closed, systems may be out of service, people may be present or not, and so forth. When major fire incidents are examined, it is generally recognized that a number of unfavorable conditions needed to be present for the accident to proceed to the observed condition.

In recent years the evolution of deterministic fire models and other predictive techniques has led to the desire to assess the consequences of events in a more objective manner. An early attempt to develop methods to quantify the fire risk of products met with limited success^{6,7}. Since then, other risk assessment methods have been developed which have followed a different philosophy. The early method cited identified a limited number of scenarios, each representing a larger number of scenarios in a class, and used detailed physical models to estimate consequences. A more recent risk model⁸ limits the level of detail included in the physical models to minimize execution time, and identifies much larger numbers of scenarios (by establishing distributions for most input variables). It then uses a Monte Carlo technique to determine distributions of outcomes.

This difference raises an interesting question. Is the fire risk affected more by the distribution of possible conditions of the scenarios or by the physical and chemical processes present in the fire itself? Or more directly, how important is it that the simplified models may predict the wrong consequences because of their simplicity, or that the Monte Carlo approach may miss a dominant case? The former can be addressed by validation studies and the latter by parametric studies. Some of both have been done, but more work is needed.

7. SCENARIO GENERATORS

Most of the research effort in the development of risk assessment methods has been in the estimation of the consequences of events. But the quantification of risk is equally dependant on the ability to describe detailed scenarios and their likelihood of occurrence. In a few countries fire incident data are collected that can be used for this purpose, but often we find that not all the needed information is collected⁶. The most recent national fire incident data system was initiated in Australia to provide such data for risk assessment in support of their new performance codes.

But these are the exception. Most countries do not collect incident data in any comprehensive way. Instead, risk methods use scenario descriptions and frequency estimates obtained from experts such as the fire service or insurance interests. This approach suffers from numerous shortcomings not the least of which are data skewed by the perception of the expert and lack of representativeness in sampling.

In 1989 NIST sponsored some work at UCLA on the feasibility of modeling initiating events for the purpose of making improved scenario descriptions and ignition frequencies, based on techniques developed for use in nuclear power plants⁹. While the techniques show some promise, limited resources has resulted in a halt to this line of research.

8. CONCLUDING REMARKS

The world community is clearly moving toward performance codes as replacements for both building and fire codes of a more prescriptive nature. Standards support codes in the building regulatory process and the format of performance standards needs to change in a way which is

consistent with their need to support performance codes. Since the codes specify objectives it would seem that the standards need to specify the functions to be performed and the reliability with which these functions are provided.

For public safety related objectives, risk seems to be the method of choice on which to base judgements of acceptable performance. Most fire safety engineering methods currently under development use relative risk based on the hypothesis that society is satisfied with the current fire risk in buildings. Some, such as in New Zealand, Japan, and Australia do so implicitly by accepting relative risk assessment against buildings which comply with the prescriptive code. One, developed for England and Wales, has established explicit risk targets equal to current loss experience. However, arguments have been raised which may mean that either approach might not withstand legal challenges. Further, no regulatory bodies other than in Japan have accepted either approach in practice. Hazard based approaches that measure performance in a prescribed set of scenarios avoid these problems, but these generally do not consider the most rare events which still may incur public outrage. Deterministic models have a seminal role in fire safety engineering analysis to support this process, but the engineering community has yet to sort out the best approaches to estimating risk and communicating the results.

9. REFERENCES

1. Bukowski, R. W. and Babrauskas, V., Developing Rational, Performance-based Fire Safety Requirements in Model Building Codes, *Fire and Materials*, **18**, pp 173-191, 1994.
2. Anon., BIA 1992, New Zealand Building Code Handbook and Approved Documents, Building Industry Authority, Wellington, NZ, 1992.
3. Anon., Building Regulatory Review Task Force, Micro Economic Reform: Fire Regulation, Building Regulation Review, May 1991.
4. Brannigan, V. and Meeks, C., Computerized Fire Risk Assessment Models: A Regulatory Effectiveness Analysis, *J Fire Sciences*, **13**, 177-196, 1995.
5. Barnfield, J., Cooke, G., Deakin, G., Hannah, M., Jones, T., Law, M., and Malhotra, B., Draft British Code of Practice for The Application of Fire Safety Engineering Principles to Fire Safety in Buildings, British Standards Institution, London, 1995.
6. Clarke, F. B., III, Bukowski, R. W., Stiefel, S. W., Hall, J. R., Jr., and Steele, S. A., The National Fire Protection Research Foundation Fire Risk Assessment Project: Final Report, NFPRF, Quincy, MA 02269 (1990).
7. Bukowski, R. W., Stiefel, S. W., Clarke, F. B., III, and Hall, J. R., Jr., Predicting Product Fire Risk: A Review of Four Case Studies. National Institute of Standards and Technology, Gaithersburg, MD, Benjamin/Clarke Associates, Inc., Kensington, MD National Fire Protection Association, Quincy, MA, ASTM STP 1150; American Society for Testing and Materials. Fire Hazard and Fire Risk Assessment. Sponsored by ASTM Committee E-5 on Fire Standards. ASTM STP 1150. December 3, 1990, ASTM STP 1150, San Antonio, TX, ASTM, Philadelphia, PA, Hirschler, M. M., Editor, 136-160 pp, 1990.

8. Beck, V.R. and Yung, D., The Development of a Risk-Cost Assessment Model for the Evaluation of Fire Safety in Buildings, Fire Safety Science Proceedings of the Fourth International Symposium, T. Kashiwagi, ed., Society of Fire Protection Eng. Boston, MA, 817-828 pp, 1994.
9. Brandyberry, M.D. and Apostolakis, G.E., Fire Risk in Buildings: Scenario Definition and Ignition Frequency Calculations, *Fire Safety Journal*, 17, No. 5, 363-386 pp, 1991.

Discussion

Patrick Pagni: Dick, I've got a real problem with that idea of minimizing the physics. It's crucial, I think, when we start making these performance-based analyses, that we get it right. If we get it wrong, people are going to throw us away with the bath water and we won't have a chance to come back and do it right later. So, while it may be important to have a fairly broad range of scenarios and while picking those is a key problem, being willing to throw away the physics in order to broaden the range of scenarios is a path down in which we ought not go.

Richard Bukowski: I certainly agree with that. That's why I said we have to find the right balance. We can't throw away all the physics, but at the same time, I think we want to look, for example, to see if there is some easy way to make an estimate. There's parts of it, I think, we can finesse and save a certain amount of time. The approach that David Young took was to go to a simple reactor model instead of two.

Howard Emmons: I was interested in Pat's remark because I have always thought, as you might expect, in terms of the ultimate future, when we have a program that is so complete that we can compute any fire with any accuracy we please. But when we look at the big building, there are at least dozens of places a fire might start. There are probably thousands of combinations of open doors and closed doors and windows, and goodness knows what. I have never thought in terms of your present statement in which by reducing the physics, we might examine these thousands of possibilities quickly, but not very accurately. However, by looking at the results, we could pick out the four or five combinations that are essential because they are the worst possible ones. Then we could run those with the ultimate model, if and when we get one, so that we really can say this building is safe.

Discussion cont.

Edward Zukoski: I sort of agree with Howard. There are so many physical combinations of the building, and there are so many different-sized fires, and the thing your worried about most, as far as life safety, is often what happens a long way from the fire. But it seems to me what you suggest is a very reasonable way to approach it, particularly given the wide range of fuel types and everything else you have to worry with.

Takeyoshi Tanaka: I also agree with the comments made by the two previous speakers. If we can come up with simpler models, then that would be better. And if it takes the form of an equation, it will be even better because by doing so, we can see the effect of changing the parameters or changing the size of the fire. We would know how much the size of fire would impact the results. I think that would be a very convenient thing for designers to use. So, I believe such simple model would be very useful to get an estimate of the risk at the first stage, and I think we should do more work in developing such simple models.

John Hall: In statistics, we're accustomed to stratifying random samples to put our power where the leverage is greatest. In computational fluid dynamics, we're accustomed to making the grid sizes smaller in areas where we want more leverage. I take your presentation, whether it's talking about the public's checkered view of risk or the balance between physics and scenarios, as a call for a more comprehensive approach to managing and minimizing the overall error in our analysis and our decision making procedures, and I think it's great.

Makoto Tsujimoto: When risk evaluation was discussed about ten years ago, there was not much interest expressed. However, this time there is a lot of interest in risk evaluation and I welcome this trend. I would like to make a few comments because I have been involved in risk assessment in a very serious way in Japan for a long time. In this kind of research, we have to find out where acceptable risk is. We conducted a survey using a questionnaire to compare the level of acceptable risk and what people perceive as absolute risk. Of course, there are not many methods to correctly calculate absolute risk, but with the use of many methods, we compared absolute risk verses the perceived risk, and we didn't find any correlations. So when we conduct such risk assessment, I think it's important for us to pay attention to what kind of risk environment we are in.

John Rockett: This pertains to Howard Emmons's comment. The model that I published in 1968, which was a horrible model, had somewhat the idea in mind that was just expressed. However, after I had been doing that for a while, I began to be very sensitive to what is now referred to as chaos theory in the highly non-linear nature of fire and the fact that even though you have surveyed a lot of cases with a simple model and you think you have identified some extreme cases for further detailed analysis, you may have completely missed the point.

USING FIRE MODELS TO ESTABLISH PERFORMANCE REQUIREMENTS FOR THE DESIGN OF BUILDINGS

David W. Stroup, P.E.*
National Institute of Standards and Technology
Building and Fire Research Laboratory
Gaithersburg, MD 20899

ABSTRACT

Based on continuing research into fire phenomena, the General Services Administration (GSA) has developed a methodology for assessing building fire safety. Fire modeling together with product test data is used to identify fire safety risks and develop corrective actions. This methodology gives GSA the ability to develop performance-based fire protection requirements for each of its buildings. This paper describes recent cooperative work between GSA and the National Institute of Standards and Technology to enhance the GSA Fire Risk Assessment methodology. Efforts to develop a procedure for using small scale test data in place of full or medium scale tests are discussed. In addition, an actual fire experience is used to illustrate the successful application of the methodology.

INTRODUCTION

The General Services Administration (GSA) is the business agent for the United States Government. It is responsible for the acquisition and management of everything from pencils to buildings. Within GSA, the Public Buildings Service (PBS) operates as the federal government's real property manager. In this capacity, PBS is responsible for the acquisition, design, construction, and operation and management of various types of space for federal agencies

Currently, the inventory of space includes 1700 Government owned buildings and 5100 leased locations. This represents approximately 28 million square meters of space. A number of historic buildings are included in the multitude of buildings controlled by GSA. GSA real estate leasing policy gives preferential treatment to historic buildings. A recent survey of buildings indicated the oldest building in the inventory was 180 years old.

GSA is responsible for ensuring the fire and life safety of the employees and visitors occupying the space under its control. In addition, GSA must protect federal real and personal property assets, assure continuity in the mission of occupant agencies, and provide safeguards for emergency forces if an incident occurs. Within PBS, the Office of Property Management develops the methodologies and procedures used for evaluating the safety of government occupied buildings and coordinating implementation by the GSA regional offices throughout the nation.

* formerly with the Public Buildings Service, U.S. General Services Administration

EQUIVALENCY CONCEPTS

Traditionally, the design of building fire safety in the United States has relied on building or fire safety code compliance. Conformance of individual building elements to specific code requirements is assumed to yield an adequate level of safety. While prescriptive-based codes are easier to enforce, design flexibility and innovation are limited severely. Typically, new code requirements are added after a disaster to prevent recurrence. Since only individual components of the total building fire safety system are addressed, the entire system never is evaluated to determine the need for previously instituted code requirements. This means that building fire protection features require an ever increasing portion of the construction budget with possibly little or no increase in safety.

In partial recognition of this, most building and fire safety codes contain equivalency clauses. These clauses permit the use of alternative methods and materials when their equivalency can be proven to the *authority having jurisdiction*. In the past, subjective judgement formed the basis for determining equivalency. Continuing research into fire phenomena has made it possible to perform an engineering analysis of the fire safety performance of a building. This building could differ widely from current perceptions of a code conforming building. Using analytical engineering tools, the development and impact of fire in a building can be assessed. Recommended improvements can be prioritized based on their predicted impact on the risks associated with potential fire exposure.

The United States Congress included an equivalency option in the Federal Fire Safety Act. This Act, passed by Congress and signed by President George Bush in 1992, is part of the Fire Administration Authorization Act (Public Law 102-522). The Federal Fire Safety Act requires sprinklers or an *equivalent level of safety* in all new six story or higher Federal Employee Office Buildings, and during renovations of such buildings if they are six stories or higher and the renovation is more than 50 percent of the value of the structure. In addition, when the Government leases 3,250 total aggregate square meters or more of space and any portion is on or above the sixth floor, the entire building must be protected with sprinklers or an *equivalent level of safety*. A "Federal Employee Office Building" is defined as any building, owned or leased by the Federal Government, that can be expected to house at least 25 Federal employees during the course of their employment.

The General Services Administration was required by the Act to issue regulations further defining the term *equivalent level of safety*. In developing the regulations, GSA held meetings with a working group composed of representatives from the United States Fire Administration, the National Institute of Standards and Technology, and the Department of Defense as well as a number of other affected federal agencies, trade associations, state fire marshals, fire chiefs, consulting engineering firms, building owners, academia, and research institutions. The final regulation was established in the form of a performance requirement¹. A fire protection engineering analysis is used to measure hazard and the amount of protection provided by the building. The concept for the final rule was derived from GSA fire protection program philosophy and built upon the equivalency concept contained in building and fire safety codes.

RISK MANAGEMENT

Typically, government agencies in the United States do not have insurance like private sector building owners or occupants. Any loss that occurs must be paid out of an agency's operating budget. A single loss could severely impact an agency's ability to conduct nationwide operations. Building and fire codes are intended to protect against loss of life and limit fire impact on the community. These codes do not necessarily protect the assets of the building owner or occupant. Simple code compliance does not ensure a level of safety acceptable to the building owner or occupant. The continual search for code compliance is not sufficient justification for resource allocation.

With cost effectiveness in mind, the GSA fire protection program addresses all aspects of fire safety important to a building owner or occupant (life safety, property protection, and mission continuity). To ensure adequate levels of safety, the relationship between expenditures on fire safety and the actual impact of these expenditures is examined through technical analysis. Each building in the GSA inventory is subjected to a fire safety analysis every five years. These building surveys are conducted by fire protection engineering professionals.

A critical step in the evaluation of a building's fire safety performance is identification of a set of design fires. These fires are ones that could produce severe effects on the building and its occupants. Full scale testing of fuel packages, analysis of fire loss statistics, and professional judgment are used to establish the set of design fires. Using the design fires and building characteristics, potential fire scenarios are modeled to determine the effects on life safety, property, and mission. Based on this professional analysis, actual risk conditions in each building are identified and corrective actions recommended. As necessary, building owners allocate resources to abate significant risks.

RESEARCH ACTIVITIES

In support of its risk management philosophy, GSA has sought to look beyond the codes and standards for methods that would allow technical assessment of building fire safety risks and development of necessary solutions. GSA professional staff have been involved in the development of various alternative methods of analyzing life safety such as system concepts² and National Fire Protection Association Standard 101A, *Alternative Approaches to Life Safety*³.

In addition, significant resources have been devoted to the development of life safety alternatives through scientific research. GSA has focused its research activities in three major areas: model development and verification, suppression system effectiveness, and protection of mobility impaired persons. The development of *FPETool*^{4,5} was a significant result of these research activities.

GSA initiated development of a Fire Protection, Facility Assessment and Risk Analysis Methodology (*FPETool*) at the Center for Fire Research at the National Bureau of Standards, now the Building and Fire Research Laboratory at the National Institute of Standards and

Technology, in the late 1980's. The first official release of *FPETool* occurred in early 1991. Using this package of analytical engineering tools, the development and impact of fire in a building can be assessed. GSA has integrated the use of *FPETool* into its design review and facility assessment processes for evaluation of fire risk in GSA controlled space and appropriate resource allocation.

GSA is continuing to fund efforts to enhance and validate *FPETool*. Recently, the National Institute of Standards and Technology developed a sprinkler fire suppression algorithm⁶ for *FPETool*. As part of this effort, fuel packages consisting of office furnishings and equipment were selected and burned to determine their heat release rate characteristics with and without fire suppression. All of the furniture fuel packages were ignited with a 50 kW natural gas burner which simulated a small trash can fire.

The primary fuel packages used in the tests fell into four categories: 1) reception area furnishings, 2) office furnishings, 3) workstations and 4) maintenance carts. These "typical" fuel packages had been identified during a physical survey of furnishings at the GSA Central Office in Washington DC. Of the four fuel package categories, the workstation fuel package category produced the widest range of heat release rates and the highest peak heat release rates. The workstations were composed of partitions and laminated wood composite work surfaces with metal support structures. A plastic "tub chair", a computer terminal, and a paper product load of 98 kg completed each of the workstation fuel packages.

For a workstation composed of 2 partitions, forming a corner around the work surface, a peak heat release rate of 1,700 kilowatts (kW) or 1.7 megawatts (MW) was attained at approximately 300 seconds after ignition. A workstation enclosed by partitions on three sides, produced a peak heat release rate of 6.7 MW at approximately 9 minutes after ignition. The fire in the three sided workstation developed slowly until it reached a plateau at approximately 1 MW. Shortly thereafter, the fire rapidly filled the confines of the workstation in a manner similar to that of a flashover.

As a result of this work, additional full scale testing is being conducted to evaluate whether materials or geometry is the dominate phenomena in the observed behavior. A representative cross section of commercially available workstations was selected and is being tested in two, three, and four sided configurations under a large calorimeter. Cone calorimeter⁷ and LIFT⁸ tests are also being conducted on appropriate size samples of the partition and furnishing materials. Finally, a single type of workstation is being used for a set of three multiple workstation fire tests using no suppression, quick response pendant sprinklers, and quick response sidewall sprinklers, respectively. For each test, three workstations are placed in a large compartment (6 m x 6 m x 3 m) which has one wall open to simulate the effects of a typical open plan office space.

In addition to enhancing the understanding of fire growth, this study is intended to evaluate alternatives to the tunnel test (ASTM E 84) and current GSA flame spread requirements. GSA specifies workstation fire performance characteristics based on results obtained from the tunnel test. The data obtained from the full scale test series will be used to expand the GSA

catalog of product heat release rate data. This data is vital in applying fire modeling techniques to the assessment of fire hazard. In addition, the sprinklered heat release rate data will be useful in demonstrating the effectiveness of sprinkler systems in mitigating potential fire and smoke hazards and verifying the sprinkler fire suppression algorithm in *FPETool*.

GSA research activities have resulted in a number of additions to the *FPETool* suite of programs. The *FPETool* Version 3.2 includes a sprinkler suppression module, a routine to calculate smoke flow down a corridor⁹, and a model of smoke and toxic gas intrusion into a room. In addition, significant efforts have been directed at developing data for verification and validation of the model and its components^{10,11}.

Several projects have been completed or are underway to examine the impact of sprinkler response characteristics and sprinkler head placement on activation time. GSA is participating in the National Fire Protection Research Foundation study to analyze sprinkler and heat detector placement under obstructed and sloped ceilings¹². This study utilizes computational fluid dynamics models to calculate three dimensional flow fields near detector sensing elements. Other projects include analysis of quick response sprinklers in open plan office space¹³, assessment of the impact of recessed sprinkler installation on activation time, investigation into sidewall sprinklers in open plan office space, and development of methods for installation of sprinklers in buildings with asbestos fireproofing¹⁴.

Finally, a number of issues associated with developing and assessing the effectiveness of various strategies for protecting disabled persons have been addressed. Some specific topic areas include evaluation of staging areas for the disabled¹⁵, analysis of fire evacuation by elevators¹⁶, and investigation into post flashover fire gas exposure to corridors and adjoining refuge areas^{17,18}. The latter project included assessment of both sprinklered and unsprinklered scenarios.

APPLICATION

Currently, research efforts are being used in GSA construction standards to supplement the national codes. Legally, buildings built on federal property are exempt from local building codes. However, buildings developed on private land for lease by the federal government are subject to applicable local codes. Through active involvement in various national consensus standards making bodies, information obtained through research is being translated into practical applications. As a developer, owner, and operator of buildings, GSA's unique position enables it to rapidly implement new technologies providing equivalent or better protection at reduced cost.

GSA developed its Fire Risk Assessment methodology as part of an effort to provide engineers with the tools necessary to scientifically evaluate fire safety risks. The methodology has been used to evaluate a number of buildings including several historic buildings: the Danville Post Office-Courthouse¹⁹, the Klinge Mansion²⁰, the Department of Commerce headquarters building, and the Department of Interior headquarters building. Recently, the

effectiveness of the methodology was demonstrated through an actual fire incident in the Department of Interior building.

The Department of Interior building, constructed in the late 1920's, is an eight story granite and limestone structure occupying two square blocks in northwest Washington, DC (see Figure 1). Floor slabs and columns supporting the structure are made of reinforced concrete. Typical office space, measuring 5.8 m x 3.9 m x 3.3 m, is constructed of 0.1 m thick terra cotta walls and finished with plaster and metal partitions. The offices have fuel loads typical of business occupancies including desks, tables, chairs, paper, and electronic office equipment. Offices are located in twelve wings which join a main corridor at one common end. Six wings extend from each of the long sides of the main corridor. A typical wing is at least 41 m long, 2 m wide, and 3 m high. The means of egress from each of these wings is stairs located in the central corridor. The building contains decorative asbestos acoustical ceiling material and original wiring, installed in 1934.

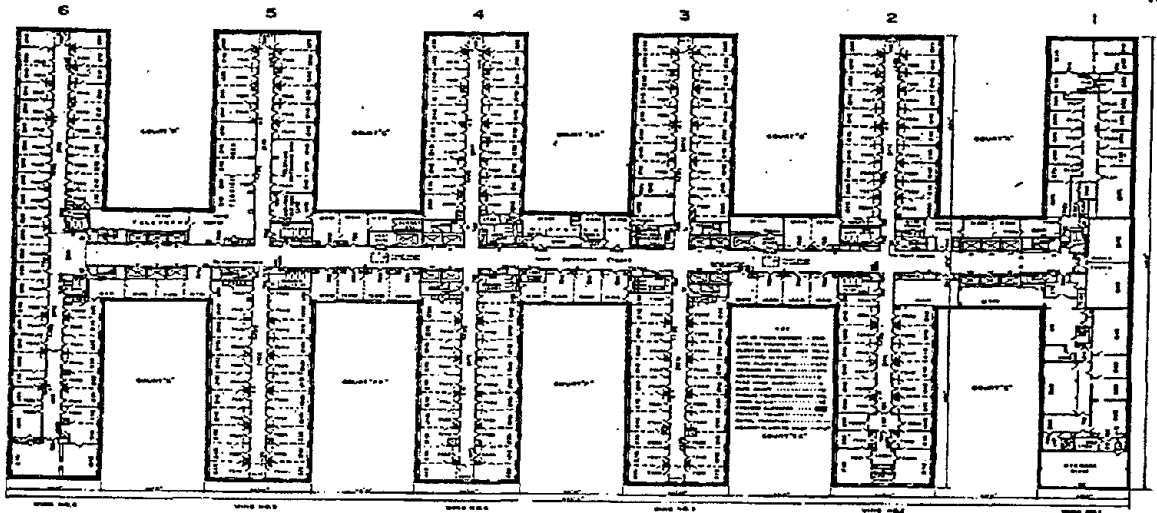


Fig. 1. Department of Interior Building - Typical Floor Plan

The potential impact of a fire in the Department of Interior building was analyzed using *FPETool* and the GSA Fire Risk Assessment methodology. Based on the results of this analysis, a recommendation was made and implemented to install a temporary sprinkler system in the building. This system was installed exposed, under the ceiling using mostly quick response, extended coverage sidewall sprinklers. The system covered approximately 85 percent of the floor area in the building. On December 26, 1993, as installation of the temporary system was being completed, a fire occurred in the building. The sprinkler system activated, controlling the fire and limiting fire damage to the workstation of origin. If the sprinkler system had not been in place, significant fire damage would have occurred in at least one wing of the building. Smoke damage would have extended throughout the floor on which the fire occurred, and some smoke would have spread to the upper floors of the involved wing. It would probably have been necessary to close parts of the building for several days while cleanup and restoration efforts were underway.

INNOVATION INCREASES SAFETY

Through the use of the Fire Risk Assessment Methodology and *FPETool*, GSA is implementing a performance-based system of building design and assessment. This methodology enables GSA to rapidly apply the knowledge gained from its research activities in practical applications.

The National Institute of Standards and Technology and GSA continue to work together to expand the science of fire protection. Optimal utilization of sprinklers is a key component in most fire protection strategies. Efforts are underway to further evaluate sprinkler response and improve their application.

In order to use most fire models like *FPETool*, heat release rate data must be available. A catalog of heat release rates for typical office furnishings is being developed. In addition to the data required by the models, this catalog will include video footage of the fire tests and still pictures of the tested items. Finally, validation of the *FPETool* fire model and its subcomponents is an on-going effort.

Significant advances in the scientific understanding of fire have occurred over the last several years. These advances have resulted in the development of a number of engineering tools for measuring building fire performance. However, the application of these tools remains limited because there is no widely accepted framework in which to apply these tools. Building and fire codes simply state that equivalency based on performance is possible without giving any guidance on how it is to be judged.

Currently, work is underway to develop a framework in which to utilize performance-based equivalency. The results of this effort will foster the application and acceptance of fire protection engineering analysis tools. By designing to meet the expected fire challenge and not the specific code book requirements, the overall level of fire safety in buildings can be increased.

REFERENCE LIST

- ¹ 41 CFR Subpart 101-6.6 Fire Protection (Firesafety) Engineering, Federal Register, Vol 59, No. 210, November 1, 1994, pp. 54524-54532.
- ² Nelson, H. E., *The Application of Systems Analysis to Building Firesafety Design*, Canadian Structural Engineering Conference, 1974.
- ³ *Alternative Approaches to Life Safety*, National Fire Protection Association Standard 101A, National Fire Protection Association, Quincy, MA.
- ⁴ Nelson, H. E., *FPETool: Fire Protection Engineering Tools for Hazard Estimation*, NISTIR 4380, National Institute of Standards and Technology, October 1990.
- ⁵ Nelson, H. E., *FPETool Users Guide*, NISTIR 4439, National Institute of Standards and Technology, October 1990.

- 6 Madrzykowski, D. and Vettori, R. L., *A Sprinkler Fire Suppression Algorithm*, Journal of Fire Protection Engineering, Vol. 4, No. 4, Society of Fire Protection Engineers.
- 7 Babrauskas, V., *Development of the Cone Calorimeter - A Bench Scale Heat Release Rate Apparatus Based on Oxygen Consumption*, Fire and Materials, 8, 81-95, 1984.
- 8 Quintiere, J. G., and Harkleroad, M. T., *New Concepts for Measuring Flame Spread Properties*, pp. 239-267 in Fire Safety Science and Engineering (ASTM STP 822), American Society for Testing and Materials, Philadelphia, PA, 1985.
- 9 Nelson, H.E. and Deal, S., *A Routine for Estimating the Initial Wave Front Resulting from High Temperature Fire Exposure to a Corridor*, NISTIR 4869, National Institute of Standards and Technology, July 1992.
- 10 Walton, W.D. and Notarianni, K.A., *A Comparison of Ceiling Jet Temperatures Measured in an Aircraft Hanger Test Fire with Temperatures Predicted by DETACT-QS and LAVENT Computer Models*, NISTIR 4947, National Institute of Standards and Technology, January 1993.
- 11 Notarianni, K.A. and Davis, W.D., *The Use of Computer Models to Predict Temperatures and Smoke Movement in High Bay Spaces*, NISTIR 5304, National Institute of Standards and Technology, December 1993.
- 12 Forney, G.P., Bukowski, R.W., and Davis, W.D., *Field Modeling: Effects of Flat Beamed Ceilings on Detector and Sprinkler Response*, Technical Report - Year 1, National Fire Protection Research Foundation, October 1993.
- 13 Walton, W.D. and Budnick, E.K., *Quick Response Sprinklers in Office Configurations: Fire Test Results*, NBSIR 88-3695, National Institute of Standards and Technology, September 1988.
- 14 Mathey, R.G., et. al., *Procedures for Sprinkler Anchor Installation on Surfaces with Fireproofing Materials*, NBSIR 87-3676, National Institute of Standards and Technology, February 1988.
- 15 Klote, J., et. al., *Staging Areas for Persons with Mobility Limitations*, NISTIR 4770, National Institute of Standards and Technology, October 1990.
- 16 Klote, J., et. al., *Feasibility and Design Considerations of Emergency Evacuation by Elevators*, NISTIR 4870, National Institute of Standards and Technology, September 1992.
- 17 Stroup, D. W. and Madrzykowski, D., *Conditions in Corridors and Adjoining Areas Exposed to Post-Flashover Room Fires*, NISTIR 4678, National Institute of Standards and Technology, September 1991.
- 18 Madrzykowski, D., *The Reduction in Fire Hazard in Corridors Provided by Sprinklers*, NISTIR 4631, National Institute of Standards and Technology, July 1991.
- 19 Frale, D. W., *Fire Protection Engineering Assessment Report - Dan Daniels Federal Building, Danville, Virginia*, U. S. General Services Administration, July 1991.
- 20 Stroup, D. W. and Levy, S. J., *Fire Safety Report - Klinge Mansion, Washington, DC*, U. S. General Services Administration, January 1991.

Discussion

Ronald Alpert: Did you characterize the heat release rate from these workstations? The peak heat release rate that resulted when you had a successful suppression?

David Stoup: Yes. Typically, the heat release rate was well under 500 kW. We had a shield of fire underneath the work space.

Cost-Effective Compliance with the Life Safety Code for Health Care Occupancies

Stephen F. Weber
Barbara C. Lippiatt
Office of Applied Economics
Building and Fire Research Laboratory
National Institute of Standards and Technology
Gaithersburg MD 20899

ABSTRACT

ALARM, Alternative Life Safety Analysis for Retrofit Cost Minimization, is a personal computer software tool that helps building managers and fire safety officers achieve cost-effective compliance with the widely-used *Life Safety Code*. This first version of *ALARM* supports analysis of health care occupancies. An equivalency provision of the code, called the Fire Safety Evaluation System, establishes a scoring system that permits trade-offs among safety features. *ALARM* exploits this flexible provision by helping users find cost-effective solutions to compliance. *ALARM* generates a set of near least cost alternative code compliance strategies and their estimated costs. These strategies offer decision support by providing a set of alternatives from which to select the most appropriate code compliance strategy based on both cost and design considerations. The software offers a code compliance optimizer, a comprehensive file manager, and a full-screen data editor. The optimization method used in *ALARM* has been field tested in nearly 100 hospitals since 1981. Cost savings have averaged between 30 and 35 percent of the cost of prescriptive compliance strategies. Future versions of *ALARM* could address other building occupancies.

1. Introduction

This paper describes new software designed to help fire safety officers and building managers at health care facilities achieve cost-effective compliance with fire codes. The software is called *ALARM*, which stands for Alternative Life Safety Analysis for Retrofit Cost Minimization, and was developed at the National Institute of Standards and Technology's Building and Fire Research

Laboratory in cooperation with the U.S. Public Health Service (USPHS).¹ The software generates a set of alternative compliance strategies, and their estimated costs, for meeting the *Life Safety Code (LSC)*² of the National Fire Protection Association (NFPA). The LSC is a widely used, voluntary code for identifying the minimum level of fire safety in buildings. Compliance with the LSC is a condition for accreditation by the Joint Commission on Accreditation of Health Care Organizations.

The primary code of the LSC is prescriptive, since it requires specific solutions for fire safety. For example, it might require a minimum flame spread rating for interior finishes and the presence of manual fire alarms. However, a special provision allows for **alternative code compliance** through a goal-oriented, equivalency approach. This approach permits **combinations** of fire safety parameters to achieve a level of fire safety equivalent to that required by the prescriptive code.

2.0 Background

Health care is the first building occupancy to be covered by a formal equivalency system. The system was originally developed in the late 1970's at NIST (then the National Bureau of Standards).³ The NFPA subsequently adopted this equivalency system into the Life Safety Code in 1981.⁴ This equivalency method, known as the Fire Safety Evaluation System (FSES), has been modified and updated several times since then. The current (1995) version is published as NFPA 101A and includes FSESs for business, board and care, and correctional occupancies.⁵ *ALARM* currently supports only the FSES for health care occupancies.

The health care occupancy FSES of NFPA 101A requires analysis and scoring of each zone in the facility. A zone is building space that is separated from all other spaces by floors, horizontal exits, or smoke barriers. The analysis looks at 13 fire safety parameters with up to seven levels of safety for each parameter, for a total of 56 safety levels. Zones earn points for each safety parameter

¹Stephen F. Weber and Barbara C. Lippiatt, *ALARM 1.0: Decision Support Software for Cost-Effective Compliance with Fire Safety Codes*, National Institute of Standards and Technology, NISTIR 5554, Gaithersburg MD 20899, December 1994. The software and manual are available for \$9.95 from NFPA, One-Stop Data Shop, 1 Batterymarch Park, P.O. Box 9101 Quincy, MA 02269-9101 (Phone: 617-984-7450).

²National Fire Protection Association, NFPA 101, *Life Safety Code*, 1994 edition, Quincy, MA, 1994.

³H. E. Nelson and A. J. Shibe, *A System for Fire Safety Evaluation of Health Care Facilities*, National Bureau of Standards, NBSIR 78-1555, Washington, DC, 1980.

⁴National Fire Protection Association, *Code for Safety to Life from Fire in Buildings and Structures*, NFPA 101-1981, Appendix C, Quincy, MA, 1981.

⁵National Fire Protection Association, "Fire Safety Evaluation System for Health Care Occupancies," Chapter 3 of NFPA 101A, *Guide on Alternative Approaches to Life Safety*, 1995 edition, Quincy, MA, 1995.

based on its impact on each of four categories of fire safety. Point totals earned across the 13 parameters in a zone are then compared with the mandatory point requirements for the four fire safety categories: (1) containment, (2) extinguishment, (3) people movement, and (4) general safety. If the point totals meet or exceed all four requirements, the zone achieves equivalency. Every zone must make the grade for the building as a whole to be in conformance.

3.0 Cost Minimization Method

Since the mandatory point requirements are established only for total scores across all fire safety parameters, tradeoffs among the 13 fire safety parameters are possible. For example, in exchange for more widespread automatic sprinklering, less smoke control may be permitted. These potential tradeoffs generate the opportunity for savings in complying with fire codes. Less expensive fire safety parameters may be substituted for more expensive ones, all the while maintaining an acceptable level of fire safety. With four independent mandatory point requirements, 13 fire safety parameters each with up to seven levels of fire safety, and many zones to analyze, the problem quickly becomes unwieldy and difficult to solve by manual computation and comparison. A cost minimization method, implemented in a software tool, is needed.

A cost minimization method for this kind of problem was originally developed by Chapman and Hall and applied to the 1981 edition of the FSES for health care occupancies through the software, *Fire Safety Evaluation System Cost Minimizer (FSESCM)*.⁶ The method is an application of the mathematical technique known as linear programming. This approach efficiently evaluates all possible code compliance solutions. The general idea is to balance improvements in fire safety scores with the costs necessary to achieve them. In this way, the least-cost means of achieving code compliance can be identified.

Since the 1981 edition of the FSES for health care occupancies was adopted, the *FSESCM* software has been extensively field tested. Important changes have occurred in fire safety technology for buildings, in construction costs, and in the FSES itself. Moreover, the improved performance of computer hardware and software development tools now support user-friendly, interactive software. In response, the optimization software, the cost estimating algorithms, and the supporting data have all been updated. In addition, an interactive environment for the updated optimization software has been developed and integrated into *ALARM*. All of the cost algorithms and supporting data are thoroughly documented.

⁶For an extended discussion of FSESCM and the underlying optimization method, see R. E. Chapman and W. G. Hall, *User's Manual for the Fire Safety Evaluation System Cost Minimizer Computer Program*, National Bureau of Standards, NBSIR 83-2797, Washington, DC, 1983; R. E. Chapman and W. G. Hall, *Programmer's Manual for the Fire Safety Evaluation System Cost Minimizer Computer Program*, National Bureau of Standards, NBSIR 83-2749, Washington, DC, 1983; and R. E. Chapman, "Assessing the Costs of Fire Protection in Health Care Facilities," *Fire Safety Journal*, Vol. 9, No. 2, 1985, pp. 221-231.

4.0 Data Requirements

ALARM allows easy, quick, and reliable data entry through an integrated file manager and full-screen data editor. The file manager lists all building data files in the current directory. These are files created with the data editor and containing all data necessary for running the optimizer for an entire building. The software even includes a sample building file. The file manager is the command center from which the user can perform typical data file operations, such as copying, renaming, deleting, and printing, as well as the primary operations of entering building and zone data and running the optimizer.

The data editor is used to enter data on the hospital building under study. The editor displays on-screen prompts and complete data validation routines to facilitate the creating and editing of error-free data files. To facilitate the data entry process, the manual offers a data collection form that mirrors the layout of the data editor.

Data must be entered on the building as a whole, on each zone, and on each fire safety parameter within each zone. Building information consists of general information, a building qualifier, construction cost modifiers, and a zone listing. General information includes the name and address of the building. The building qualifier indicates whether the building has sprinklers and whether it is new, in order to determine in part the four mandatory point requirements. The construction cost modifiers are used to adjust by the same percentage the automatic cost estimates for all retrofits. These modifiers permit time- and location- specific cost adjustments to all default unit costs.

Data needed for each zone include its name, identification number, floor number, and occupancy risk factors. The risk factors are used to determine the mandatory point score for general safety. They cover patient mobility, patient density, zone location, ratio of patients to attendants, and average patient age.

For each of the 13 fire safety parameters, users must enter the current fire safety state of the zone and all the retrofit quantities needed to achieve each state that is safer than the current state. For some fire safety parameters special design specifications may be entered to further define a zone's fire safety status or potential retrofits. For example, a specification for the Automatic Sprinklers parameter covers whether asbestos must be removed as part of the sprinkler installation. Users may rule out any state to force the optimization procedure to ignore it. The cost estimation algorithms use the retrofit quantities and special design specifications to compute the cost of moving from the current state to each of the safer states available. A cost adjustment (positive or negative) may also be entered for each state to include costs for a retrofit not on the retrofit list or to reduce the automatic cost estimate.

5.0 Reports

Once the data on all the zones has been entered and saved in the file, the user selects the optimizer feature from the file manager. The optimizer generates a report file with alternative code compliance options and their estimated costs. Users can select the most appropriate compliance option based on both cost and design considerations. For benchmarking purposes, the optimizer also reports the prescriptive solution cost for each zone and for the building as a whole.

The report file consists of key FSES tables, zone reports, and building summary reports, as shown in exhibit 1. The FSES tables are included for informational purposes. There are three zone reports. The first report gives occupancy risk factors and the current fire safety state, the prescriptive compliance state, and the retrofit quantities entered for each fire safety feature. The second zone report shows the total retrofit costs for each fire safety state and the prescriptive compliance cost for the zone as a whole. The third report lists all code compliance strategies generated by the optimizer for the zone. Each strategy is identified by its solution states for the 13 fire safety parameters. The total compliance cost for each strategy is also reported. Finally, this report gives the number of surplus points earned by each strategy in excess of the four mandatory point requirements.

Exhibit 1. Optimization Reports

1. FSES Tables
 - 1.1 Occupancy Risk Factors
 - 1.2 Mandatory Safety Requirements
 - 1.3 Fire Safety Parameter Values
2. Zone Reports
 - 2.1 Data Inputs
 - 2.2 Estimated Retrofit Costs
 - 2.3 Code Compliance Strategies
3. Building Summary Reports
 - 3.1 Design Class Reports (20)
 - 3.2 Prescriptive Solution Report

The Building Summary Reports match common compliance strategies across all zones in the building. Twenty default design classes are built into the software. A design class defines specific safety levels for some of the fire safety parameters. For example, one default design class calls for automatic sprinklers throughout the entire building, a single deficiency in hazardous areas, no

horizontal exits, and no changes in construction type, zone dimensions, or smoke detection. The Design Class Reports identify the least-cost compliance strategy that satisfies the design class specifications. The reports are sorted in order of total compliance costs. If a zone cannot achieve code compliance under a given design class, that class is not reported. Each report provides a set of alternatives from which to select the most appropriate compliance strategy based on both cost and design considerations. If the default design classes do not satisfy design requirements for a facility, the user may select a customized set of solutions from the individual Zone Reports. The Prescriptive Solution Report gives the cost of prescriptive compliance for the total building.

6.0 Conclusions and Future Directions

Since 1981, the approach used in *ALARM* has been field tested by the USPHS in a large number of military, public, and private hospitals. The cost savings have been substantial; *ALARM*'s economical, equivalency solutions are typically saving hospitals between 30 and 35 percent of the cost of implementing prescriptive codes. Over 250 copies of *ALARM* have been sold to date. In 1993, the software was applied to the largest hospital yet, the 60-zone, 62,710 square meter (675,000 square foot) Wright-Patterson Air Force Base hospital in Ohio. *ALARM* estimated that the cost savings from using the alternative FSES solution was over \$500,000. In the same year the forty-bed hospital at Yokota Air Force Base in Fussa, Japan was also surveyed, resulting in an estimated cost savings of \$136,000 compared with the prescriptive code approach. The results of the surveys on 86 military hospital facilities representing about 16,000 beds show estimated cost savings of over \$35 million, an average savings of \$2,200 per bed.

This first version of *ALARM* is designed with built-in flexibility for efficiently making changes for future versions of the software. The software will need to be revised when the FSES for health care occupancies is significantly modified or when retrofit cost estimates become so outdated that across-the-board inflation adjustments are no longer realistic. A network version would permit many users to edit the same building data file simultaneously. On-site data entry could be enabled through a laptop and ultimately a pen-based version of the software. On-site data entry would improve productivity because building data is currently developed in two stages: notes are made on building blueprints on site, then they are later translated into data for entry into *ALARM*. A pen-based computing application could load digitized blueprints into a hand-held computer. Notes made on these digitized blueprints could automatically be converted into the necessary building data.

With the success of the FSES for health care occupancies, equivalency systems were developed for business, board and care, and detention and correctional occupancies. The *ALARM* methodology for reducing code compliance costs is equally applicable to these and even other occupancies as more FSES systems are developed. Software tools tailored to these occupancies could be developed in the future.

Discussion

Brian Meacham: I think that's probably a wonderful tool for doing cost benefit analyses for prescriptive code options. NFPA 101A is not a performance-based code, and it doesn't say that it is anywhere in the document to my knowledge. The options that you're giving on the output of 101A are the same prescriptive requirements that are in NFPA documents that are just lessening of some requirements over another one. There is no measurement of performance of how the building operates. I think there is a fundamental difference between looking at the performance of the building in its entirety against the effects of fire verses the cost benefit of one system over another. And so I see a good benefit for this tool in reducing costs in the current system. I hope that it will be applicable to performance codes when we have them in the future.

Barbara Lippiatt: I think 101A is the first step towards what Brian refers to as a true performance-based code and that a tool such as ALARM can be used to make the trade-offs necessary, whether it's applied on a more restrictive basis like 101A, or a true trade-off basis such as would be provided by a true performance-based code.

James Quintiere: I have two questions. First, do you know if there's been any retrospective analysis on the equivalency criteria used in this evaluation system since it was developed in the 70s? And maybe there is different thinking now with some new knowledge.

Barbara Lippiatt: Well, the code has been updated a number of times. But, Dick Bukowski tells me that, no, there has not been any retrospective analysis done.

James Quintiere: Just another question out of curiosity. Since we are talking about performance codes and if we were to apply that to fire, do you know of any examples where performance codes have been used in other safety areas? When they reach the appropriate level of safety, do they cost more? See, I don't know if it's clear that it will cost more or less if we go to performance-based codes.

Barbara Lippiatt: Unfortunately, I usually use the fire example in my other work to illustrate the performance concept. So the answer is: not to my knowledge on the first part of your question. And the second part, I believe that the ALARM software points in the direction that there can be cost savings in the performance-based approach.

Takeyoshi Tanaka: Construction costs vary every year, depending on what materials you use and what equipment you use. And there is also some regional variance. So how often do you update data? And do you take into consideration yearly changes of construction costs in you system? That's the first question. And the second question: you said that this system was used in Japan. How did you obtain cost-related data?

Barbara Lippiatt: The system is now based on 1991 U.S. average costs. We used a cost adjustment for Japan of a factor between 3 or 4 times those costs. We provide cost adjustments to take account of the regional and time-sensitive cost differences, and we hope to have further funding to update the costs in the future.

Discussion cont.

John Hall: I have three brief comments related to previous questioners. First, I think prescriptive and performance-based codes are better thought of not as strict alternatives, but as two ends of a spectrum. Our current codes are not purely prescriptive, but they are more prescriptive than NFPA 101A, and so I think your characterization of ALARM is correct. My second point is that in answer to Dr. Quintiere, if you would do performance based codes, as most people do, as either an alternative or a framework in which the prescriptive codes are an accepted solution, it is impossible for performance-based codes to cost more because if they do, you don't use them. And finally, because your analysis compares low cost solutions to the prescriptive solution, it is not as dependent on up to date cost data, it is looking at relative comparisons and they are not as likely to change over time or between regions.

Yuji Hasemi: I was involved in the safety evaluation of a hospital building construction in Japan, and I found that a lot of times we ran into the situation where safety and convenience or use of the building equipment just did not go along with each other. For example, fire safety can be satisfied by building a wall, however, it is very inconvenient to have a wall in a practical sense. I assume that you also run into problems of this kind, particularly, when you consider retrofitting effects in existing buildings. Do you take this kind of thing into consideration?

Barbara Lippiatt: That's where the engineering judgement comes in. The engineer that surveys the building has the option of selecting from the identified list of retrofitting effects or entering any other retrofitting effect that he or she deems appropriate.

END: March 13, 1996

BURNING OF REAL OBJECTS

Flammability of Real Objects: A Progress Report

T. J. Ohlemiller
Building and Fire Research Laboratory
National Institute of Standards and Technology

Abstract

With United States residential fire statistics as a guideline, this report briefly focuses on the status of research in a few select areas. These include floor coverings, interior wall coverings, and mattresses/bedding. Only in the case of wall coverings are there models which come close to adequately describing real world fire behavior.

1) Which Objects.

There are two relevant questions here: 1) Which objects should fire researchers be concerned with? and 2) Which objects are we able to deal with? It will be evident that there is a disparity between the two classes of objects defined in the context of residential fires in the U. S.

The answer to the first question is suggested by the fire statistics on home fires reported by Miller [1]. The top five objects first ignited in residential fires, in terms of yielding the greatest number of fatalities, are: upholstered furniture, mattresses and bedding, a structural or framing member of a building, interior wall coverings and floor coverings. These account for 55% of U. S. residential fire deaths. On this basis, these would seem to be a natural focus for fire research.

2) Summary of Status

In answering the second question above, the highly varied state of affairs with regard to each is briefly summarized. First, however, it is worthwhile to summarize what it is that fire researchers seek to achieve in addressing the flammability of real objects.

Real objects are, of course, the real problem, as the above summary of fire statistics indicates. Thus the ultimate goal of fire research is the development of means to make each of these classes of objects less hazardous. As a practical matter, this means providing to manufacturers quantitative technical guidelines regarding the relationships between product composition plus configuration and flammability performance in a test relevant to the actual hazard. In general, this requires a balance of empirical testing and modeling as the only realistic way with which to cope with the extreme materials diversity of real products.

With some classes of objects, such as furniture and bedding, the scenario leading to uncontrolled burning is fairly well defined. This makes it possible to significantly reduce such fire occurrences by working to suppress ignitability by the most common sources. In the case of furniture and bedding, this mainly means cigarette ignition; work along these lines has had some success in the past. This is only a first line of defense, however, and real improvements in flammability behavior must come from control of the potential for fire growth on real objects. This fire growth is measured by the rate of heat release from the object in response to some

arbitrary but plausible ignition source. Understanding and, ultimately, controlling this rate of heat release response, in turn, requires a quantitative knowledge of the relation between material composition, configuration and fire growth rate. One way to obtain this knowledge is to burn the full-scale object. All too often, this is the only feasible option but it is obviously expensive and the results are scenario dependent. Models are the preferred route around this costly process.

A general modeling approach, adopted with increasing frequency, is one of viewing any burning object as consisting of a large number of area elements, each igniting and releasing heat in response to the incident heat flux imposed by the entire ensemble of burning area elements at any given time. This is in accord with the widespread use of the Cone Calorimeter to characterize heat release rate per unit area as a function of incident heat flux. This device makes it possible to characterize a material (or composite) on a small scale, hopefully obviating the need to build and test each new variant of an object such as a chair covered in a new fabric blend.

This approach is highly attractive and, ultimately, should be quite effective. It will be evident, however, that it has not yet been adequately developed for most real objects.

In turning to the several classes of real objects mentioned above, we begin by dismissing one of these categories as ill-defined, i.e., that of structural or framing member. True structural framing members are normally covered and thus subject to a very limited variety of ignition sources such as electrical shorts or overheated flue pipes. We note that significant work on the safe use of wood heating appliances, including proper practice for passing flue pipes through walls so as to prevent ignition of wooden structural elements, was done some years ago at NIST [2]. This category will not be pursued further here, in the absence of a clearly defined hazard scenario.

Upholstered furniture. Upholstered furniture is the subject of a separate report in this conference [3]. Here we note only that it is both the number one cause of residential fire fatalities and perhaps the most difficult common object for which to predict the fire response because of its geometric complexity and the poorly understood behavior of the thermoplastic materials typical of furniture construction. The goal of a model which can predict the time-dependent heat release rate behavior of real furniture remains elusive, in spite of significant progress in some aspects of the problem in the recent European CBUF study [4].

Flooring materials. According to Hirschler [5], the high level of fatalities in the category in which flooring materials are listed as the first item ignited is misleading. True floor coverings actually account for only one third of the fatalities; accelerants and other items on the floor account for the bulk of the fatalities. Thus flooring materials *per se* are not such a serious threat.

All carpeting sold in the U. S. is subject to a methenamine pill test for flammability which mandates that flame can spread no more than 7.6 cm from this flaming ignition source. Carpeting to be used in corridors of public buildings is usually subject to the Flooring Radiant Panel Test (ASTM E 648) which specifies that the minimum external radiant (as if from a hot gas layer overhead) for flamespread be at least a certain level (e.g., 4.5 kW/m²). There is some indication that this test is not always an adequate indication of full-scale performance in corridor fire situations [6]. However, recent full-scale tests in rooms also show that burning carpets do

not yield a very high rate of heat release ($< 75 \text{ kW}$) [7]. Thus the relatively minor activity level in this category of fire hazard seems justified.

Another possible role for carpeting as a fire safety hazard derives from its frequent presence beneath upholstered chairs. Some chairs reach their heat release peak as a result of the interaction between the burning surfaces of the chair and a pool fire which forms on the floor, initiated by flaming drips of molten polyurethane. A carpet is a potentially significant contributor to this type of behavior but no studies of this effect are available.

Interior wall coverings. The flat, vertical surface of a wall has been the logical starting point for most attempts to model fire growth. In recent years a number of models have been proposed, based on a variety of assumptions [8-12]. Their degree of validation against upward spread experiments varies, but all have been applied successfully by their authors to some limited set of circumstances.

A significant aspect of any such attempt to model upward fire spread is the input parameter values. Thus it is not sufficient to pose a model of fire growth *per se* without also specifying the set of experiments and/or procedures which will provide the necessary inputs. This aspect has not received sufficient attention, except perhaps from Delichatsios [13], although his subsidiary measurements include surface temperature, which is difficult to obtain. Furthermore, there has been insufficient attention to the issue of how sensitive the models are to these inputs, and thus how accurately they need to be measured.

Another significant problem for models which use Cone Calorimeter data as a primary input is a procedure for transforming the data from the few constant external heat flux values at which it is obtained to other constant or transient flux values. Mitler [14] proposed a simple procedure which appears to be acceptable for non-charring materials but, in general, it appears that one needs a model of the transient burning process, especially to deal with time-dependent heat input such as would result from interactions with a closed compartment. Delichatsios [11, 13] has proposed such a model.

Another problem which Cone Calorimeter data pose as an input is the choice of the proper external flux for which data are to be used. In general the actual external flux under which the flames are spreading is below that for ignition of the fuel so that special procedures must be used to obtain such data [15,16]. There has been a tendency to choose data from a flux which makes the model agree with experiments rather than to choose a credible value.

Many of these same concerns and difficulties carry over to the case of upward flame spread in a corner wall configuration. Here, Saito [17] has shown that the flow patterns are potentially quite complex and certainly not one dimensional. Hasemi [18] and Kokkala [19] have provided empirical heat flux correlations which can become an integral part of attempts to model this spread configuration. The most prominent attempts thus far [8,20] have been focused on a specific corner test method (ISO 9705) and have not really given much attention to the details of growth in the corner so much as they followed subsequent growth on the ceiling of the room used in this test.

In spite of all the caveats above, it is worth noting that a recent test of three of the above models [8, 9, 10] for flat wall upward flame spread, coupled with a set of procedures for inferring the input data from Cone Calorimeter tests, gave reasonably encouraging results [16, 21]. The materials tested were fiber/resin composites subjected to uniform external radiative heating and a small gas flame igniter at the base. None of the models predicted the results with quantitative accuracy but all were adequate to indicate that the test material was unacceptably flammable. Thus these models may soon be ready to serve the fire safety function of assessing potential fire hazards of interior finish materials.

Mattresses and bedding. The flat, horizontal surface of a bare mattress would also seem to be a logical starting point for fire growth modeling. Rather surprisingly, this has not been the case. An early Federal test requirement (FF 4-72) for cigarette ignition resistance, in effect since 1974 for all mattresses sold in the U. S., may have deflected the attention of fire researchers. The fire statistics above indicate that it did not eliminate the problem.

Atreya [22] developed a model of radial fire growth on a horizontal fuel surface; however, it was applied to wood and required an experimental measure of time-dependent surface temperature as an input. Only recently in the European CBUF study [4] has a model been proposed for growth of a fire on the top surface of a mattress. The CBUF model assumes radial symmetry and a flame spread model essentially the same as that used by Quintiere [8] for upward flame spread. Radiation from the fire plume preheats the remote surface of the mattress. Actual implementation of the model is greatly simplified with extensive empirical fitting to experimental heat release data. There is room for substantial improvement in this type of model.

It must be noted that, as with furniture, the real behavior of a burning mattress is considerably more complex than any model has ever attempted to describe. The most current test methods for mattress flammability testing, California Technical Bulletins 121 and 129, involve strong flaming ignition sources applied to the bottom and the side of the mattress, respectively. Either mode of ignition tends to yield a flame front that involves the full depth of the mattress, not simple surface burning. Furthermore, mattresses can incorporate a complex, layered structure that may include metal springs; these details can, in some cases, make a large difference in the fire behavior [23]. An implication of this is that models cannot be expected to become quantitative prediction tools for designing fire-safe mattresses (or furniture, for that matter). They are tools for clarifying the relative importance of various variables, including those which they may omit. They might become semi-quantitative predictors for limited classes of soft furnishings designs when "calibrated" against full-scale data or they might become a basis for practical correlations between bench-scale and full-scale fire behavior.

Other real objects. If one moves beyond the most common objects implicated by residential fire statistics, one finds examples of much greater complexity with regard to fire behavior. For example, television sets or automobiles. Such objects involve large fractions of thermoplastic materials of arbitrarily complex shape. The specifics of these shapes may play a substantial role in the ease of ignition. Their thermoplastic nature means that they cannot be expected to retain their shape during any fire growth process. A pool fire of polymer melt may interact strongly with the burning mass. There are no models or guidelines for estimating fire growth on such objects. There clearly is a need for systematic study of the burning of at least simple classes of

thermoplastic objects. In the meantime testing is likely to be on a very *ad hoc* basis yielding useful data such as total heat release rate which, however, cannot be generalized beyond the specific test configuration.

3) Conclusions

While fire statistics point out a strong need for practical means to make many common objects less flammable, our ability to deal with these in anything other than a very empirical manner is very limited. Only for the simplest geometry (flat, vertical wall) has there been substantial progress in developing models with the potential to generalize the test results from practical, economical small-scale tests on constituent materials. Yet this general approach, the combination of models with empirical inputs which characterize the local response of an element of material to a heat input, still appears to be very promising. Considerable further effort is needed to apply it successfully to most real objects.

4) References

- 1) Miller, A., "U. S. Home Product Report; Forms and Types of Materials First Ignited in Fires," National Fire Protection Association, Quincy, Mass., February, 1995
- 2) Peacock, R., "Wood Heating Safety Research: An Update," Fire Technology, Vol. 23, No. 4, pp 292-312, November, 1987
- 3) Ohlemiller, T., "Flammability of Upholstered Furniture," Proceedings of the Thirteenth Panel Meeting of the UJNR Panel on Fire Research and Safety, March, 1996
- 4) Sundstrom, B. (ed.), "Fire Safety of Upholstered Furniture - the full report of the European Commission research programme CBUF," June, 1995
- 5) Hirschler, M., "Fire Tests and Interior Furnishings," in Fire and Flammability of Furnishings and Contents of Buildings, ASTM STP 1233, ASTM , Philadelphia, PA, 1994, pp 7-31
- 6) Briggs, P., "Full Scale Testing of Floor-Coverings in Room/Corridor Scenarios and Comparisons with Small-Scale Test Procedures," Proceedings of the Fire Retardant Chemicals Association Conference on Fire Safety, New Orleans, March, 1993
- 7) Rogers, S., Murray, C. and Ames, S., "Small and Full-Scale Studies of Heat Release from Building Contents," Interflam '93, Interscience Communications Ltd, London, UK, 1993, p 213
- 8) Cleary, T. and Quintiere, J., "A Framework for Utilizing Fire Property Tests," Fire Safety Science - Proceedings of the Third International Symposium, Elsevier, London, 1991, pp 647-656

- 9) Kulkarni, A., Kim, C. and Kuo, C., "Turbulent Upward Flame Spread for Burning Vertical Walls Made of Finite Thickness," NIST-GCR-91-597, National Institute of Standards and Technology, May, 1991
- 10) Mitler, H. and Steckler, K., "SPREAD - A Model for Flame Spread on Vertical Surfaces," NISTIR 5619, National Institute of Standards and Technology, Feb., 1993
- 11) Delichatsios, M, Mathews, M., and Delichatsios, M., "An Upward Fire Spread and Growth Simulation," Fire Safety Science - Proceedings of the Third International Symposium, Elsevier, London, 1991, p. 207
- 12) Hasemi, Y., "Thermal Modeling of Upward Wall Fire Spread," Fire Safety Science - Proceedings of the First International Symposium, Hemisphere Publishing Corp., New York, 1986, p. 87
- 13) Chen, Y., Delichatsios, M. and Motevalli, V., "Material Pyrolysis Properties. Part II: Methodology for the Derivation of Pyrolysis Properties for Charring Materials," Combustion Science and Technology, Feb. 1993
- 14) Mitler, H., "Predicting the Spread Rates of Fires on Vertical Surfaces," Twenty-Third Symposium (International) on Combustion, The Combustion Institute, Pittsburgh, PA, 1990, pp. 1715- 1721
- 15) Brehob, E. and Kulkarni, A., "Time-Dependent Mass Loss Rate Behavior of Wall Materials Under External Radiation," Fire and Materials, Vol. 17, 1993, pp. 249-254
- 16) Ohlemiller, T. and Cleary, T., "Upward Flame Spread on Composite Materials," in Fire and Polymers II, Nelson, G. (ed.), American Chemical Society Symposium Series 599, 1995, pp 422-435
- 17) Qian, C. and Saito, K., "Fire Induced Flow Along the Vertical Corner Wall", in Fire Science and Technology, Proceedings of the First Asian Conference, International Academic Publishers, 1992, pp 257-262
- 18) Hasemi, Y. and Tokunaga, T., Combustion Science and Technology, Vol. 40, 1984, pp1-17
- 19) Kokkala, M., "Characteristics of a Flame in an Open Corner of Walls," Interflam '93, Interscience Communications, Ltd, London, 1993, pp. 13-24
- 20) Karlsson, B., "Mathematical Models for Calculating Heat Release Rate in a Corner Test," in Fire and Flammability of Furnishings and Contents of Buildings, ASTM STP 1233, ASTM, Philadelphia, PA, 1994, pp 216-236
- 21) Ohlemiller, T. Cleary, T., Brown, J. and Shields, J., "Assessing the Flammability of Composite Materials," Journal of Fire Sciences, Vol. 11, No. 4, 1995, p. 308

- 22) Atreya. A., "Fire Growth on Horizontal Surfaces of Wood," Combustion Science and Technology, Vol. 39, 1984
- 23) Damant, G. and Nurbakhsh, S., "Heat Release Rate Tests of Mattresses and Bedding Systems," Journal of the Fire Sciences, Vol. 10, Sept. - Oct., 1992, pp 386-410

Discussion

James Hoebel: Tom, on the issue of wall coverings: the incident data you showed at the beginning is based on products that are the first item ignited in residential fires and then get the wall covering involved. Are you aware of work going on having to do with the ignition resistance of wall coverings?

Thomas Ohlemiller: Actually, no, I'm not.

Pravinray Gandhi: You mentioned that you are looking into the development of better fire resistant objects. Would that include pillows, bedclothes and fire barriers?

Thomas Ohlemiller: The answer is yes. That's definitely an interesting part of the problem. The bed covers can be used as a very large ignition source to the mattress, for example, and that has to be dealt with. So we'll be looking for that, yes.

John Hall: A couple of observations, Tom. Building on your presentation, in the flooring area, you went directly from flooring to carpeting. And there are a number of other important kinds of flooring and I would particularly cite area rugs as an area worthy of interest. My other observation is that on the interior wall coverings, there is a problem similar to the fuel spill of accelerants for floor coverings and that is a grease build-up.

King-Mon Tu: Among your transparencies, you mentioned that Cone Calorimeter data is very important for this application and you also said that the flux level is very important. Do you have any recommendations on what kind of heat flux level we should use? For example, 25, 25,, 50, 75 or 100 kW/m²? Is there any justification for this?

Thomas Ohlemiller: The answer is that you have to look at your real problem. You have to put some flux gages into a full-scale test and find out what kind of fluxes are measured. Then you have to realize that some of that is coming from the flame itself and doesn't count as being part of the external flux. You then have to look at the growth problem. The appropriate flux may change, so you may need quite a bit of Cone Calorimeter data, quite a bit of characterization of your material.

Progress Report on Full Scale Fire Test in Japan

Osami Sugawa
Center for Fire Science and Technology
Science University of Tokyo

Many full scale fire tests have been carried out as Prof. K Kawagoe had encouraged the fire researchers to pursue the fire behavior through fire tests which simulate a real fire. On 5th March 1996, about one week ago of this meeting, a full scale fire test was done in BRI using a wooden 3 story building with two 2 story wooden houses which were set in downwind of fire spreading course. Many researchers and students joined and supported to the full scale fire test. This experimental research was planned by Dr. Y. Hasemi, his colleagues, and members of BRI to observe whether this building can suppress the fire spreading velocity in case of such building locates in a city fire. Kobe City fire, occurred after the earthquake of 17th January 1995, was uppermost in everyone's mind.

Followings are the titles and author(s) who carried out full scale and semi-full scale fire test(s) which includes full scale test pieces.



1995

An Experimental Study of Early Warning Fire Detector System in Telecommunications Equipment Rooms, Part I - Conventional Smoke Sensors Characteristics in a Testing Chamber, and Part II - Smoke Movement in a Full Scale Testing Room, by Noda et. al , [JAFSE Annual Meeting,

pp62-69]

They carried out two series of the tests; chamber test to characterize the conventional smoke sensors, and full scale test to observe smoke movement in a model room for a telecommunications equipment. In the first test, they used PVC cables, fire retarded polyethylene cables, epoxy boards with electric parts, paper, and wood for fuel. High precision smoke detector (ASSD) connected with air sampling tube lines, HC ℓ sensor, smoke detectors (light scattering and ionization type) were set in the return space of the chamber (2.4m x 2.4m x 2.4m(H)) with upwind air conditioned at the 45 times/h air exchange rate. In the detectors and sensors, ASSD showed earliest detection with and without air ventilation, and the little difference in detecting times between these ventilation conditions. Smoke detectors (light scattering and ionization type) showed delay in detecting time but HC ℓ sensor showed earlier when ventilation was given to the chamber. The second test was carried out using a full scale equipment room of 14.4m x 36m x 2.8m(H) with 1.75m of the return ceiling chamber and 0.45m air supply floor chamber (free access floor type). Ten sets of ASSDs were used to monitor the early smoke detection system for a smoldering fire changing the ventilation rates.

A System for the Evaluation of the Intelligibility of Outdoor Speaker System, [JAFSE Annual Meeting, pp.116-119] by Y. Matsubara, and M. Inagaki (Fire Research Institute)

A Study on toward light, when human select a evacuation passage - Verification of evacuation drill at office building, [JAFSE Annual Meeting, pp.132-135] by K. Kubota (Fujita Corporation), and Y. Murosaki (Kobe Univ.)

Walking Speeds of People in Refuge, Part II, [JAFSE Annual Meeting, pp.140-143] by Y. Ohshima, M. Watanabe (Bunka Shutter), M. Nara (Sci. Univ. of Tokyo)

Study on People Movement under High Density - Doorway and Stair - Part II, [JAFSE Annual Meeting, pp.144-147] by T. Uetake, M. Watanabe (Bunka Shutter), M. Nara (Sci. Univ. of Tokyo)

Study on Refugee Density in case of Escape in a Building, Part II, [JAFSE Annual Meeting, pp.148-151] by T. Kumagai, M. Watanabe (Bunka Shutter), M. Nara (Sci. Univ. of Tokyo)

Evaluation on Smoke and Gases Using Full Scale Fire Test, , [JAFSE Annual Meeting, pp.172-175] by K. Yoshida, and S. Nagasawa (Research Institute of Marine Engineering)

Experimental Study on Full Scale Fire Tests in Atrium Space, , [JAFSE Annual Meeting, pp.176-179] by H. Kuwana, H. Satoh, H. Kurioka (Kajima Technical Research Institute), and O. Sugawa(Sci. Univ. of Tokyo)

Ignition Mechanism of Fuel leaked in Vehicles, , [JAFSE Annual Meeting, pp.220-223] by T. Takahashi, M. Sugisaki, T. Sada, and T. Tsurumi

Ignition Process of Intermittent Short-circuit on the Modeled Automobile Wires, , [JAFSE Annual Meeting, pp.224-227] by Y. Tamura and J. Suzuki (Japan Automobile Research Institute)



1994

Flow Characterization of Smoke and CO gas, [JAFSE Annual Meeting, pp.248-251] by D. Kouzeki, et. al (Fire Research Institute), and S. Kusanagi et. al (Matsushita Electric Works, Ltd.),

Flow and diffusion behavior of smoke and CO gas was measured using a model step shaft (19m high, 4.5m x 4 steps with 1.3m wide) connected with a corridor at the ground level. Smoke detectors, heat detectors, and CO gas sensors were mounted under each ceiling. Cotton wick, beech wood, polyurethane foam, news paper were used as fuel simulating smoldering and flaming fire.

Analysis of Heat of Fire by Color TV Camera, [JAFSE Annual Meeting, pp.20-21] by Y. Fujiwara, T. Ono, and H. Ishii (Nihon University)

Study of Fire Detection in Air Conditioned Rooms, [JAFSE Annual Meeting, pp.30-33] by K. Satoh (Fire Research Institute)

Heat Release Characteristics of Combustible Loads/Linings in Train Vehicles, [JAFSE Annual Meeting, pp.104-107] by Y. Hasemi (Building Research Institute), R. Kikuchi (Sci. Univ. of Tokyo), and M. Yoshida (Building Research Institute)

Grasping the Actual Condition of Occupant in a Building and Defining Standard Figures, [JAFSE Annual Meeting, pp.220-223] by Y. Murosaki (Kobe University), and M. Nakano (Konoike Construction Co., Ltd.)

In Site Tests of a Air Sampling Smoke Detection in Telecommunications, [AIJ Annual Meeting, No. 3003, 3004] by S. Noda and M. Ichimura (NTT Power and Build. Facilities Inc.)

Survey and Analysis on Surface Area of Fire Load, [AIJ Annual Meeting, No. 3016] by K. Aburano et. al. (Sci. Univ. of Tokyo)

A Study on Fire Resistance for the Partitioning Wall and so on by Wood Frame Construction, [AIJ Annual Meeting, No. 3046] by M. Takada et. al (Japan Housing & Wood Tech Center, Foundation)

Experimental Study on Fire Wall with Fire-Resistant Glass, [AIJ Annual Meeting, No. 3048] by K. Kubota and I. Takahashi

Fire Safety Design of Tall and Narrow Atrium, [AIJ Annual Meeting, No. 3064, 3065, 3066] Part 4, Plume Behavior and Analytical Model by O. Sugawa et. al (Sci. Univ. of Tokyo) Part 5, Full Scale Test of Atrium Space by H. Kuwana et. al (Kajima Tech. Res. Inst.) Part 6, Propriety of Simplified Model to Full Scale Test by H. Kurioka et. al (Kajima Tech. Res. Inst.)

A Demonstration Test of the Pressurizing Smoke Control System via an Atrium and Shaft, [AIJ Annual Meeting, No. 3070] by M. Hirota (Inst. of Tech., Shimizu Corporation)

Pressurization Smoke Control System, [AIJ Annual Meeting, No. 3072, 3073] Part I- Full Scale Test of Exterior Wall-through Type Pressurization System by A. Nohara et. al (Res. and Devlp. Inst., Takenaka Corp.) Part II - Smoke Movement in Office Space at Initial Fire Stage by T. Nagaoka et. al (Res. and Dev. Inst., Takenaka Corp.)

Experiments on Stair Lobbies Pressurization for Smoke Control with Air Supply Duct, [AIJ Annual Meeting, No.3074] by I. Takahashi, T. Hara, S. Yamamoto, and I. Kasahara (Mech. Elect. Eng. Design Div., Taisei Corp.)

Effect of Architectural Factors on Wayfinding in an Emergency, [AIJ Annual Meeting, No.3085] by H. Hayashi, Y. Murosaki, and T. Nishigaki (Kobe University)

A Verification on the Presumption of Evacuation, Fire and Smoke Behavior using Survivors' Evidence at the Time of Fire, [AIJ Annual Meeting, No.3087] by K. Kawamura, S. Nemoto and S. Okishio (Sci. Univ. of Tokyo)



1993

Reverse Stratified Flow of smoke and Gases in Tunnel-like Underground Fires, [JAFSE Annual Meeting, pp.58-61] by T. Komai, N. Shikada, M. Tanaka, and Y. Nakagawa (Natl. Inst. of Resource and Environment)

Experimental Study on Smoke Control Method Considering the Influence of Opening Condition for Smoke Movement, [JAFSE Annual Meeting, pp.90-93] by K. Kojima and S. Hashimoto and K. Okajima (Hazama Research Institute)

A Study on Smoke Flow in a Galleried Large Scale Void, [JAFSE Annual Meeting, pp.94-101] Part I - An Experimental Study of the Smoke Flow in a Full Scale Gallery, by T. Nagaoka, A. Kodaira, and S. Uehara (Takenaka Komuten Res. Inst.) Part II - Consideration on Smoke Behavior by Simulation and Test by S. Uehara, A. Kodaira, and T. Nagaoka (Takenaka Komuten Res. Inst.)

Full scale test was carried out on smoke movement in a galleried Void of 41m high, 16m wide, and 193m long. Triangular roof of polycarbonate was put on the top and of which base periphery had 2m high opening (540m² in total opening area) for natural ventilation. Model fire source of methanol (16 pans of 50cmx50cm square) was set at the center of the void gave 1.54MW for 5min. Flow visualization was carried out using smoke candles. Temperatures distribution for vertical and horizontal directions, and smoke depth were measured. Some of the detailed results including 3D simulation was presented in 12th UJNR Mini-Symposium.

Study of Behavior of Fire Gas in Air Conditioned Flow [JAFSE Annual Meeting, pp.102-105] by K. Satoh (Fire Research Institute) He made a model compartment fire with air conditioned using a compartment of 4.45m x 4.45m x 2.45m(H) and 3D computer simulation was done using UNDFRI code. Calculated results for smoldering fire of cotton wicks were compared with measured ones .

Measurements of the Shaft Pressure Variation caused by the Movements of Elevator Cars by K. Harada, T. Terai, and Y. Zhi Jun (Kyoto University) [JAFSE, Annual Meeting, pp106-109]

In order to establish the pressurized smoke control, Harada et. al carried out the measurements of differential pressure between shaft and floor changing the elevator velocity (150m/min, 120m/min, and 80m/min), number of elevator cars, and operation schedule of 6 cars. They estimate the pressure difference shaft and floor based on ventilation network. Models proposed by Matsushita and Klote were used and good agreement was obtained between the estimation and measured ones.

Experimental Study on Elevator Evacuation in a Fire Emergency by K.Muraoka and Y. Miyagawa (Res. Ins. Ohbayashi Corp.) [AIJ, Annual Meeting, pp106-109]

A Study on the Limitation of Building Height to apply a Pressurizing Smoke Control System Based on Pressure Difference between Escape Route on a Fire-Floor and Shaft, [AIJ Annual Meeting, No. 3025] by M. Hirota (Inst. of Tech., Shimizu Corp.)

An Experimental Study on Direction Judgment of Travelers in Emergency in Urban Underground Environment, [AIJ Annual Meeting, No. 3043, 3044] Part I - by M. Ohkura (Seikei Univ.) et. al Part II - by M. Oiri (Labor Sci. Inst.) et. al

Fundamental Study on Pedestrian Crowd Flow for a Simulation Method for Fire Escape Planning, [AIJ Annual Meeting, No. 3045, 3046] Part I - Outline of Simulation Model Regarding Pedestrian Crowd Flow by T. Higashiguchi (Toda Corp.), et. al Part II - Comparison with Actual Measurement by H. Nigorikawa (Nagano Corp.) et. al

They measured the human movement velocity at the door ways when the meeting was held in Matsumoto Theater of which has three different capacity of 608, 1311, and 1352 seats. Effluent velocity of persons measured at door was 0.52 - 1.28 persons/msec and which was smaller than 1.5 persons/msec used for fire safety design. They also simulated the time needed for escape based on human density and path width as Dr. Togawa had proposed.

Development of Hybrid Robot System to assist Firefighting in a High Building, [AIJ Annual Meeting, No. 3089, 3090, 3091, 3092] Part I - Basic Specifications by H. Hoshino et. al (Takenaka Corp.) Part II - Basic Design by Y. Takada et. al (Komatsu Corp.) Part III - Demonstration by O.Hukutomi (Nippon Biso Corp.), Part IV - Evaluation by T. Hayakawa (Takenaka Corp.)

They designed a robot based on a gondola which is lifted by a crane mounted on a roof of a high-rise building. This robot can move along a wall vertically and horizontally to find a fire compartment utilizing TV camera eyes, and IR detector. The robot has extinguishing chemical agent, and drill unit. In the case of the robot find and detect a hot zone (fire zone) in a compartment through a window, it makes a hole by a drill unit to inject the extinguishing chemical agent. It can move 30m/min for horizontal direction and climb up 40m/min having an operator. They demonstrated an evacuation using a full size robot but no model fire was given to the test.

JAFSE: Japanese Association on Fire Safety Engineering

AIJH: Architectural Institute of Japan

UPWARD FLAME SPREAD ON VERTICAL SURFACES

Craig L. Beyler, Sean P. Hunt, and Naeem Iqbal
Hughes Associates Inc.
3610 Commerce Drive, Suite 817
Baltimore, Maryland, 21227, USA

Frederick W. Williams
Naval Research Laboratory
Washington, DC 20375, USA

ABSTRACT

A model which describes the physical processes of upward flame spread and fire growth on wall materials has been developed and implemented as a computer program. The computer based flame spread model simulates the fire growth along a vertical combustible wall. The vertical wall material may be heated by an imposed external heat flux and is ignited at its bottom edge with a flame from a line burner of user specified strength. The model predicts the flame spread rate, the heat release rate of the fire, the flame height, the net heat flux to the wall surface and the time varying surface temperature. The model uses inputs developed from cone calorimeter data. The results from the model compare favorably to upward flame spread experimental results for PMMA and plywood found in the literature.

1.0 INTRODUCTION

In this paper a vertical flame spread model is developed and validated against literature data. This work is a part of U.S. Navy Passive Fire Protection (PFP) Program and designed to provide a technique for specifying the performance required for the U.S. Navy material applications in terms of small-scale tests. The PFP program will result in known fire performance of material applications and will allow manufacturers/developers to provide cost-effective materials with the required performance, leading to cost saving and known performance.

The upward flame spread model on vertical surfaces is the first part of the modeling effort designed to develop a general modeling framework which will assess performance of materials in Navy fire scenarios from small-scale test data. This model is formulated on the basis of a review of the fire dynamics literature relevant to fire growth presented by Williams and Beyler (1994).

A computer model has been developed which calculates the flame spread on a vertical wall subject to a line ignition source. Flame spread is calculated using sub-models derived from the literature from inputs determined from cone calorimeter tests. The model is formulated based on existing sub-models of (1) ignition, (2) material heating, pyrolysis, and burning rate, (3) flame spread, and (4) flame and surface heat transfer. The details for each component of the analysis will be described in the following sections.

2.0 THEORY AND DESCRIPTION OF THE MODEL

The computer model calculates the flame spread on a vertical surface by breaking up the surface into a large number of elements. The conditions of each element are independently computed. The centroid of an element is assumed to be representative of the entire element. There are a

number of global conditions that are calculated by summing the contributions from each element: the heat release rate, the height of the pyrolysis, the flame height along the wall and, the height of burnout front along the wall.

Each element is in one of four states: (1) preheat (above the flame), (2) preheat (exposed to the flame), (3) burning, and (4) consumed. The model keeps track of these conditions for each element, and the model stops when either the user entered simulation time is reached, the fuel is entirely consumed, or the flame propagation ceases.

In the present model, the wall can be heated by three sources: (1) an imposed external heat flux, (2) a line fire placed against the base of the wall (the ignitor), and (3) the wall flame itself. It has been shown that the heat flux to the wall from line fires against the wall and the wall itself can be correlated in the same manner. Heat fluxes distributions are prescribed based on prior work available in the literature which summarized by Quintiere (1988).

Prior to ignition, the wall surface is assumed to be a semi-infinite one-dimensional slab with a time dependent surface heat flux determined from the wall flame and external sources as described above. The conduction model used in this computer model is an approximate solution to the semi-infinite slab problem using an assumed cubic temperature profile and an integral solution [Eckert and Drake (1972)]. This method was selected based on its excellent predictive performance and computational efficiency.

Once an element has reached the ignition temperature, it is allowed to pyrolyze, burn and contribute energy to the wall fire. The heat release rate of the wall is determined by summing up the heat release rates of each burning element.

The material properties required by the model are determined using the cone calorimeter ASTM standard test method E-1354. These properties are as follows:

- (1) Ignition temperature, T_{ig} (K)
- (2) Thermal inertia, $k\rho c$, $(kW/m^2-K)^2 \text{ sec}$
- (3) Effective heat of gasification, Δh_g (kJ/kg); and
- (4) Heat of combustion, ΔH_c (kJ/kg).

The detailed method for determining these properties is described in a Naval Research Laboratory (NRL) forthcoming report.

3.0 RESULTS OF THE MODEL

The model results were compared with full-scale tests to evaluate the capabilities of the computer program in predicting vertical spread. Heat release rates, surface temperatures, and flame heights were compared with data available in the literature. No tests were found that described in adequate detail all of the potential characteristics for comparison. In addition, the test conditions were not adequately described in terms of the ignition temperature, material properties, and heat flux conditions. Comparisons were made using values or data from other literature sources.

Validation of the numerical solution for upward flame spread was made by comparing with full-scale experimental results using material properties from bench-scale data available in the literature. Full-scale data was available for vertical flame spread on Polymethylmethacrylate (PMMA) and plywood. The present numerical solution was compared to the experimental measurement of flame spread over a vertical PMMA surface by Wu, Delichatsios, and de Ris (1993), the experimental measurements of flame spread over a vertical surface of plywood with externally applied radiation flux by Delichatsios et al., (1994).

The ignition and flame spread properties and dimensions (input for model) are based on the bench-scale test data available in the literature.

3.1 Comparison of Predicted Results with Experimental Results for Non-charring Polymethylmethacrylate (PMMA)

Wu, Delichatsios, and de Ris (1993) conducted experiments to measure heat release rate for bench-scale and full-scale PMMA wall fires. In the bench-scale tests, a vertical PMMA slab measuring 0.90 m high, 0.2 m wide and 25 mm thick was ignited at the bottom of the panel by 20 ml of methanol and cotton balls in an aluminum dish (0.025 m x 0.20 m x 0.01 m high). The full-scale flame spread experiments were carried out with a 25 mm thick PMMA slab, 0.58 m wide x 5 m high. The ignition source was 35 ml of heptane in a copper dish (0.025 m x 0.6 m x 0.025 m high) at the bottom of the wall. This was simulated in the model as a 1 kW/m line fire source.

Figure 1 shows a comparison of heat release rate during upward flame spread over 0.90 m x 0.20 m vertical PMMA surface. The solid line is the model prediction while dash line is the experimental data of Wu, Delichatsios, and de Ris (1993). Due to the sensitivity of the computer model to the heat flux and flame height correlations, several simulations of the test were performed in order to determine the optimum combination. The flame heat flux in the burning region used was 21 kW/m². Since exact value of flame heat flux after ignition were not described in the test conducted by Wu, Delichatsios, and de Ris (1993), after several runs of the model a value of 21 kW/m² heat flux after ignition was found to yield the most adequate results.

3.2 Comparison of Predicted Results with Experimental Results for Plywood

Delichatsios et al., (1994) have conducted theoretical and experimental analysis of upward fire spread along 2.4 m high, 0.61 m wide and 12.7 mm thick vertical wall made of plywood. Five full-scale flame spread experiments were conducted. The samples were exposed to a specified heat flux from a large-scale radiant panel. The following measurements were made:

- (1) Rate of heat release,
- (2) Total heat flux to the specimen surface,
- (3) Surface temperature, and
- (4) Propagation of the pyrolysis front.

The full-scale test results demonstrated the sensitivity of the flame rate to the external heat flux. The samples of plywood in the experiments were ignited by a red-hot nichrome wire. The wire was preheated using a welder power supply set to provide a 40 Amp current through the wire. After preheating, the wire was brought into direct contact with the specimen at a location approximately 25 mm above the base of the specimen. A thin spacer located between specimen holder and the center of the specimen was used to make the specimen slightly convex at the base and ensure good contact for the ignition wire over the entire width of the specimen.

Comparison of PFP upward flame spread model predictions to the full-scale experimental results [Delichatsios et al. (1994)] is shown in Figure 2. The predictions and experimental propagation of pyrolysis front (determined using surface thermocouples) are shown in Figure 2. In general, there is a reasonable agreement between predicted and measured propagation of the pyrolysis zone.

4.0 CONCLUSIONS

A computer model has been developed that successfully addressed upward fire growth on vertical surfaces. The agreement with experimental results is good. Assumptions have been made based on the limited information for flame heat transfer rates to cause burning and spread, and more complete experimental results are needed.

It is the intent of this work to present a simple flame spread model that integrates many of the features and capabilities of those described and that requires a minimum of input data and accurately predicts the fire growth along vertical walls subject to ignition sources. Ultimately, the model will be generalized so that two and three dimensional geometries may be modelled. The ultimate goal of these modeling efforts is to predict and evaluate the fire performance of U.S. Navy materials, products, and assemblies and to provide a link between small-scale ignition and heat release rate measurements in the cone calorimeter with the full-scale fire performance to ensure an environment safe from destructive fires.

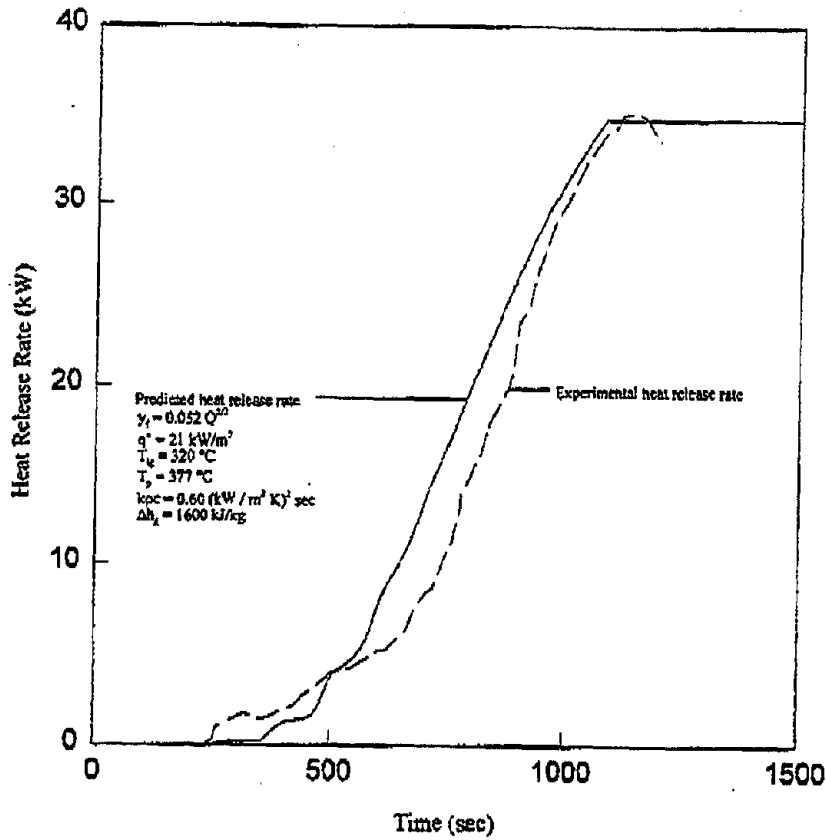


Figure 1 Comparison of heat release rate predictions for a 0.90 m x 0.20 m vertical PMMA surface with Wu, Delichatsios, and de Ris, 1993 data

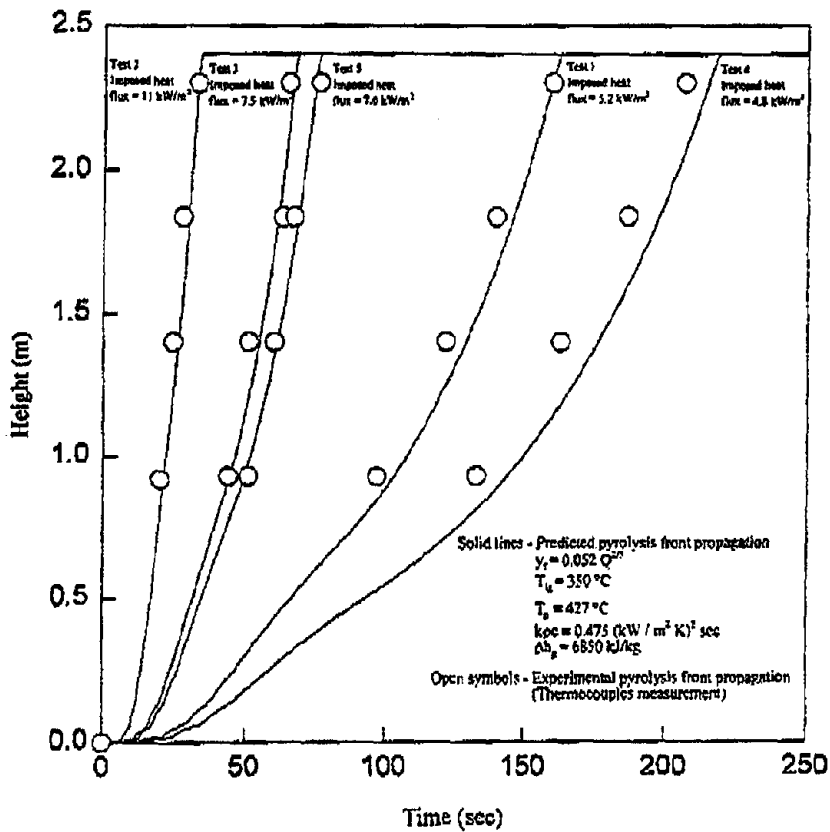


Figure 2 Comparison of pyrolysis front propagation predictions for a 2.4 m x 0.61 m vertical plywood surface with Delichatsios et al. 1994 data

REFERENCES

- Delichatsios, M. M., Wu, P-K., Delichatsios, M. A., Loughheed, G. H., Crampton, G. P., Qian, C., Ishida, H., and Satio, K., 1994, "Effects of External Radiant Heat Flux on Upward Fire Spread: Measurements on Plywood and Numerical Predications", *Fire Safety Science-Proceeding of the Fourth International Symposium*, International Association of Fire Safety Science, Kashiwagi, Editor, 1994, pp. 421-432.
- Eckert, E. R., and Drake, R. M., 1972, "*Analysis of Heat and Mass Transfer*", Chapter 4 - Unsteady Heat Conduction, McGraw-Hill Book Company, 1972, pp. 138-221.
- Quintiere, J. G., 1988, "The Application of Flame Spread Theory to Predict Material Performance", *Journal of Research of the National Bureau of Standards*, 93 (1), January/February 1988, pp. 61-70.
- Williams, F. W., and Beyler, C. L., 1994, "Passive Fire Protection (PFP) Modeling Literature Review", NRL Letter Report Serial 6180/0221A, 13 July 1994.
- Williams, F. W., Beyler, C. L., Hunt, S. P., and Iqbal, N., 1995, "Upward Flame Spread on Vertical Surfaces", NRL Memorandum Report 1995 in publication.
- Wu, P-K, Delichatsios, M. M., and de Ris, J., 1993, "Upward Fire Spread Over PMMA Walls-A Model/Experiment Comparison", *1993 Annual Conference on Fire Research: Book of Abstract*, NISTIR - 5280, U.S. National Institute of Standard and Technology, Gaithersburg, Maryland, 1993, pp. 7-10.

Discussion

Richard Gann: Craig, for what types of walls are you intending to model to be used?

Craig Beyler: The most immediate interest with the Navy is for thin covering type of materials. Not paint, as much as coverings over insulating materials, just a couple millimeters thick type coatings as opposed to a coat of paint.

Richard Gann: For those kinds of layered materials, will your heat and flame spread model, which is appropriate for simple materials, work?

Craig Beyler: On a good day, yes. I think the thermal underlying material tends to dominate the behavior there. And of course, things like ignition temperatures and pyrolysis are dominated by the coating material. I think there are undoubtedly situations where that won't be true, but I think there are non-trivial cases where I think that will work.

Henri Mitler: First, where did you obtain your $\kappa\rho c$ data?

Craig Beyler: Basically, we deduced the properties from the Cone Calorimeter data, and I should have addressed that more. We did ignition experiments and used known ignition temperatures from direct measurement to fit the ignition temperature. We then took the ignition time as a function of flux and determined the $\kappa\rho c$ which would reproduce that ignition behavior.

Henri Mitler: My second question is more philosophical. There are at least four existing upward spread models available, and you obviously decided that another attack was worth doing. I'm curious as to what inadequacies you found in the earlier models that led you to that.

Craig Beyler: I wouldn't say it was the inadequacies of the existing models that motivated us to start over. Certainly, we were standing on the shoulders of the existing models. We could well have done this part of the work by taking your model or other models and using them and adjusting them if necessary. Our ultimate goal here was to do something that was going to be able to do walls, corners, lateral spread, a more generalized kind of prediction than the ones that were available. The infrastructure we think we created in the code is one that can grow into these other applications.

Yuji Hasemi: When you observe fire spread, if radiation is very high, the flame velocity becomes very fast, and that would make measurement difficult. When the heating is weak, then the heat release rate is difficult to measure. There is some difficulty in getting reproducible results. I would like to hear your opinion as to at what level we should try to start.

Craig Beyler: If I understand your question, it relates to levels of the heat fluxes in the Cone Calorimeter vs. Full scale and that at high fluxes, ignition times are very quick and at low fluxes, it's difficult to get good burning rate data. It certainly is. With regard to ignition, I haven't seen much problem inasmuch as the heat fluxes in a wall flame are something on the order of zero to fifty kW/m² and the Cone Calorimeter has no particular difficulty in resolving ignition behavior.

Discussion cont.

So in that regard, I haven't seen a problem. Clearly in the Cone Calorimeter, low heat release rates are less accurately measured than very vigorous burning items. We often find it necessary to not use standard Cone Calorimeter methods for thin materials and low heat release to improve the resolution of the data.

Mark Janssens: Your model relies on experimental correlations for the heat flux, which is based on incident heat flux measurements, using the heat of gasification concept. How does your model account for losses?

Craig Beyler: You've almost given the answer yourself. Basically, the model, as we use it, has a constant heat gasification and a specified surface temperature. So the losses are simply due to black-body radiation and the net flux is a constant. We did assume a constant temperature and that is the weakness.

WALL FLAME CORRELATIONS AND UPWARD FLAME SPREAD IN A VERTICAL CHANNEL AND ITS RELEVANCE TO FIRE SAFETY

Y. HASEMI and M. YOSHIDA

Building Research Institute, Ministry of Construction
Tatehara 1, Tsukuba-City, Ibaraki-Pref., 305, Japan

S. TAKASHIMA and S. YOKOBAYASHI

Graduate School of Science and Engineering, Science University of Tokyo
Yamazaki, Noda-City, Chiba-Pref., 278, Japan

ABSTRACT

Experimental results on wall flame behavior and upward flame spread within vertical channels of different width/depth ratios without external radiation are shown. It has been found that flame height and wall flame heat transfer become significantly higher in a channel with the width/depth ratio not larger than unity. Significant acceleration of flame spread has also been observed in a channel covered with Douglas Fir Particleboards for the similar range of the width/depth ratio. This shift of wall flame and flame spread to risky side in a channel is believed to be due to the restriction of air entrainment, radiation feedback among surfaces within the channel and increase of effective pyrolysis area.

Key Words: flame height, heat flux, upward flame spread, vertical channel.

INTRODUCTION

Upward turbulent flame spread is one of the fire problems in which the progress of scientific understanding during the last decade has been the most evident. Recent comparisons between theories and experiments suggest a considerable capability that thermal models can predict upward flame spread using bench-scale test data with reasonable accuracy for engineering purposes[1,2]. However, all these achievements are still limited to the application to a flat vertical surface, although lining materials are very often grooved or uneven in end-use conditions for acoustic performance or for other architectural-design purposes. Theoretical modeling of upward flame spread for uneven vertical surface may not be easy; however, practice through fire experiences and large full-scale fire tests suggests possible significant augmentation of fire hazard in grooved or channeled vertical, or, inclined surfaces[3,4,5]. Also recent experimental works on inclined surfaces suggest notable influence of sidewalls on the flame and flame spread[6,7]. Theories of upward flame spread for flat walls suggest the primary importance of the preheating of unburnt surface beyond the pyrolysis front by wall flame and external radiation sources[2,8,9,10,11,12], and any effect enhancing this preheating is believed to accelerate flame spread. Possible increase of fire hazard on a grooved or channeled surface may result from:

- (1) greater flame length in a vertical groove or channel than over an even wall due to the restriction of entrainment of air to the flame
- (2) decreased loss of radiation from the wall surface to ambiance due to the radiation feedback between the surfaces within the groove or the channel
- (3) increase of effective pyrolyzing surface area

Although it is not the central problem discussed in this particular study, it is important to note that the mechanisms (1) and (2) can be a cause for raising fire hazard even along an incombustible dented surface as typically seen in the flame projection from a window on a facade with sidewalls[5]. Also acceleration of upward flame spread and heat release rate on parallel vertical PMMA slabs due to the similar mechanism has been demonstrated experimentally[13]. The restriction of air entrainment may further increase the wall heat transfer by the induction of the flame flow onto the wall surface(Coanda effect). The mechanism(3) may increase flame height, since the height of a wall flame is controlled essentially by the heat release rate per unit width of the projected vertical plane of the pyrolysis zone. Previous analysis already suggests the significant sensitivity of flame spreading velocity to the heat release rate per unit width[12]. This study intends to correlate

such measures as flame height, wall flame heat transfer and flame spreading velocity against W/D ratio, the aspect ratio of the cross-sectional groove or channel space using experimental facilities available in the "laboratory-attic" as a first quantitative approach to evaluating the configuration effects in wall fires along a dented wall.

EXPERIMENTAL ARRANGEMENTS

Two series of tests, steady flame measurements and flame spread tests, have been conducted using almost identical experimental arrangements. A 0.2m x 1.0m rectangular propane burner consisting of five 0.2m square porous burner-elements has been used as the heat/ignition source for both series of the experiments. The burner was originally built for a study of fuel-shape effects on turbulent diffusion flames[14], and was designed such that fuel supply rate of each square burner-element can be controlled independently. The burner was placed against a 12mm thick, 2.4m tall vertical mineral fibre reinforced cement board surface, and sidewalls of the same material were attached to the wall above the sides of the burner to make a favorable aspect ratio(Figure 1). Fuel gas was supplied only to the burner elements surrounded by the backwall and the sidewalls. This arrangement makes it possible to produce varieties of W/D ratios within the range of $W/D=1/5\sim 5$. No external radiation source has been used. In the previous upward flame experiments with flat Douglas Fir Particleboards, it has been already established that upward flame spread on this material never develop much if only the surface is flat and external radiation is not applied on the specimen[1].

Steady Flame Tests

The steady flame tests were conducted to see the influence of the channel geometry on the flame height and wall flame heat transfer quantitatively. This measurement is believed to provide basic informations on the first two possible mechanisms which may increase fire hazard in a vertical channel. Flame height and incident heat flux measurement were made using Video camera and 12.5mm diameter Schmidt-Boelter heat flux gages after the surface heat flux had reached steady state at each steady flame test. Reported values of flame height are average of the maximum flametips height for three minutes observed by eyes with the interval of one second on the Videotape records. Flame height was correlated against the modified dimensionless heat release rate, which is defined as[14]

$$Q^*_{mod}=Q/\rho_0 C_p T_{og}^{1/2} W D^{3/2} \quad (1)$$

where Q is the heat release rate estimated assuming the complete combustion. Heat flux and flame height were measured along the vertical centerline of the backwall and along the corner between the backwall and one sidewall, since during preliminary tests it had been already observed that flame tends to become taller at the corner than at the center of the backwall. This local flame development is attributed to the mechanism that characterizes room corner fires, and is believed to be important from the firesafety point of view. Each heat flux gage at the corner was installed on the sidewall, with its center 15mm apart from the real corner. In order to compare the flame in a vertical channel with that over an unconfined flat wall, measurement of wall heat flux and flame height was also made using the same instrumentation without the sidewalls.

Flame Spread Tests

The flame spread tests were conducted using 12.5mm thick Douglas Fir Particleboard("Versaboard") covering the incombustible backwall and sidewalls. The propane burner used as the heat source was kept on until the end of each test. Measurements were made on surface heat flux, flame height and heat release rate. Heat release measurement was made by the oxygen consumption method using O₂, CO and CO₂ monitoring. Heat flux and flame height measurements were made using the identical sensors with the steady flame tests; however, measurements were started at the ignition to the propane burner elements. Flame spread tests with Particleboard only on the backwall and with water-cooled copper sidewalls were

conducted to compare the flame spread in vertical combustible channels with that on an unconfined combustible surface. The Particleboard specimens were conditioned for at least one week before test. Water content of the specimens just before test varied from 8.1% to 9.0%.

STEADY-FLAME CORRELATIONS IN A VERTICAL CHANNEL

Flame Height

Flame height measured on a flat wall, at the backwall in a channel, and at its corner are summarized against Q_{mod}^* for different aspect ratios of the burner in Figure 2. The experimental parameters, γ and n , for the flame height represented as

$$L_f/D = \gamma \cdot Q_{\text{mod}}^{*n} \quad (2)$$

are summarized in Table 1. It is noteworthy, in Figure 2, that influence of the aspect ratio of the heat source becomes much less significant in a channel than on a flat wall, although it is natural since sidewalls are generally believed to make the flame closer to a two-dimensional flow, especially in the large Q_{mod}^* domain. Figures 2(b) and (c) suggest merging of the L_f/D - Q_{mod}^* relation into the line-fire correlation at Q_{mod}^* greater than the present test conditions for a channel fire. Flame flow closer to a two-dimensional one in a channel than on a flat wall may be endorsed by the n value close to $2/3$, the theoretical value for a line fire, in a channel irrespective of the W/D ratio as seen in Table 1, whilst n value for relatively small W/D ratio without sidewalls for a flat wall is between $2/3$ and $2/5$, the theoretical value for a point source fire. As a result of this fluiddynamic effect, flame height in a narrow channel becomes significantly taller than on an unconfined wall; flame height in a channel for $W/D=0.5$ is found to be approximately 1.8 times the unconfined wall flame height for Q_{mod}^* less than unity. Flame height in a channel is always larger at the corner than at the center of the backwall. The difference was the most pronounced for the W/D ratio between 2.0 and 3.0. The difference is found to be ignorable for $W/D \leq 1.0$, and is less significant for W/D greater than 3.0. The difference is believed to merge into the difference between the flame height on a purely flat wall and that in a wall corner[10,16,17] as W/D ratio is further increased. It is also noteworthy that flame height in a channel for $W/D=3.0$ and 5.0 is smaller than on a flat unconfined wall. This unexpected shortening of a flame in a wide-channel configuration is probably due to the raise of flame height at the edges of a flame by sidewalls, which is always lower than the flame height at the center only if the sidewalls are not provided.

Heat Flux to the Wall Surface

Wall surface heat fluxes measured on a flat wall, at the backwall in a channel, and at its corner have been correlated against height above the burner surface normalized by the flame height as shown in Figure 3~5. The correlation for a flat wall shown in Figure 3 is nearly consistent with the line fire correlation[10,15] except for the low Q_{mod}^* regime. The characteristic decay of heat flux between around $x/L_f=0.5$ and $x/L_f=1.0$ at the backwall in a channel, shown in Figure 4, is nearly consistent with the flat wall correlation. However, heat flux observed in $x/L_f < 0.5$, solid flame, shows evident increase as the location of the measurement becomes closer to the heat source, whilst heat flux without sidewalls is nearly constant in that domain. This augmentation of surface heat flux on the backwall for low W/D ratios is attributed to the additional radiation from the sidewalls and induction of the wall flame onto the backwall due to the Coanda effect characteristic to narrow channels. Although the surface heat flux in such configuration is believed to depend partly on the temperatures of the surfaces within the channel which is further influenced by the conduction loss through each wall, it should be still noteworthy that the maximum heat flux observed for $W/D=0.5$, the smallest W/D ratio during this series of experiments, reached approximately 90 kW/m^2 , nearly twice to three times the typical value caused by a wall fire on a flat wall[10,15]. Dependence of heat flux on x/L_f at the corner, Figure 5, is found to be nearly consistent with that at the center of the backwall.

Increase of heat flux generally seen in narrow vertical channels should accelerate the generation of fuel gas once the channel is covered with combustible lining; this can be another cause for higher fire hazard in a vertical channel. Also, the combination of longer flame and stronger wall flame heat transfer in a narrow vertical channel suggests that preheating of the unburnt surface beyond the pyrolysis front in such configuration should be more efficient than on a flat wall of the same material. All these suggest faster flame spread in a narrow vertical channel than on a flat wall.

UPWARD FLAME SPREAD OVER COMBUSTIBLE LINING IN A VERTICAL CHANNEL

Result of the steady-flame tests suggests potential significant increase of fire hazard for $W/D \leq 1.0$. Flame spread tests were conducted on Douglas Fir Particleboard for $W/D = 0.5, 1.0$ and 2.0 to verify the significance of the channel effects on wind-aided flame spread. Two-dimensional upward flame spread tests using the identical material without external radiation had already demonstrated that flame spread stop at approximately $x_{\text{poff}} = 0.025 \sim 0.036 Q_t$. In order to make measurement of the maximum pyrolysis front height as far as possible, Q_{mod}^* of the heat source had to be chosen within the range of $0.35 \sim 0.5$, close to the minimum heat release rate with which a stable turbulent flame can be established above the burner.

Figure 6 shows summary of the records of observation for several W/D ratios and for the flat wall. The heat release rate is summarized as heat release rate per unit width of the whole combustible specimen, $Q/(W+2D)$. The gradient that \bigcirc and \triangle data demonstrate indicates the flame spreading velocity. Flame spread for $W/D=0.5$ and 1 was rather fast; pyrolysis front height became almost $6 \sim 7$ times within a few seconds once the pyrolysis front height had exceeded approximately 20 cm. Stop of flame spread never occurred under these particular conditions, while both burnout and flame spread die-out took place for $W/D=2$. Figure 7 is a summary of the ultimate burn pattern for $W/D=2$ and for the flat wall. The result for $W/D=2$ demonstrates significant local development of fire in the corners. Figure 8~10 show summary of heat flux time history obtained at the center of the backwall and at the corner from each test. It is important to note that, for $W/D=2.0$, heat flux higher than 40kW/m^2 was observed only on the gages near the ignition source, whilst such strong heat flux was observed even at higher part of the specimen for $W/D=0.5$ and 1.0 . It is probably this strong heat flux that prevented fast burnout for W/D not larger than unity. Especially for $W/D=0.5$, fire lasted until the whole specimen was burnt through. Figure 11 is a summary of the heat release rate for ignition source heat output 10kW per burner-element. Heat release rate from the ignition burner, Q_b , was eliminated from this summary. The heat release time history for $W/D=0.5$ demonstrates dual peak typical to the sustained burning of charring materials. Heat release rate per unit effective width, Q_t , can be obtained by dividing this heat release rate by the width of the whole working burner elements (0.2m for $W/D=0.5$ and 1 , 0.4m for $W/D=2$, and 0.6m for $W/D=3$ and for the flat wall). The first peak heat release rate per unit effective width thus calculated is approximately $2,150\text{kW/m}$ for $W/D=0.5$, and 900kW/m for $W/D=1$. These are remarkably larger than the peak heat release for the wider channels such as 238kW/m for $W/D=2$, 97kW/m for $W/D=3$ and 93kW/m for the flat wall.

IMPLICATION TO FIRE SAFETY

The present experiments suggest that difference in wall flame and flame spread in a vertical channel compared with those on a flat wall becomes noticeable at around $W/D=2.0$, and the significant augmentation of fire hazard may occur in a vertical channel with W/D ratio around 1 or less. It had taken relatively long time until the rapid flame spread started at each tests. However, this delay is partly because of the weak ignition source used for the present tests. Growth of heat release by over 10 times during approximately a minute as observed at $W/D=0.5$ should be enough risky for lifesafety in the ignition room of a fire. Fire problem with combustible lining in a channel may relate not only with flame spread, since wall burning in an compartment may rise smoke layer temperature which can cause different types of fire

hazard. Of course, there should be a variety of size and configuration for such vertical, or inclined, channels in the end-use conditions of building materials; grooved wooden wall of auditoria, escalators and building facade with sidewalls are only practical examples that occur to the authors. However, conclusion of previous large scale tests[3,4,5] some of which did not intend to focus this problem are still somewhat consistent with the present work; the W/D ratio of the grooves on a Oak vertical slab which caused significant upward flame spread compared with an even Oak slab was 0.6[3]. The W/D ratio for the combustible escalator trench whose fire is considered the main cause for the large number of deaths at the Kings' Cross underground fire is between 1.2 and 1.5[4]; however, existence of treads and surface grooves on the escalator are believed to increase the pyrolyzing surface and have made the flame spread faster than in a simple channel. The sidewalls which caused notable increase in heat flux to the external wall surface during a facade test[5] made a W/D=1.0 vertical channel above the window of a fire room. Recent work in construction industry suggests other design example for facade which may cause similar problem for $W/D \leq 2.0$ [18]. Significance of the configuration effects to fire behavior and its relevance to fire safety should probably depend on such end-use conditions, although scale effects and other problems resulting from end-use conditions are not considered enough in the present work partly because of the limitation of the available facility and specimens. However, it is important that such effects that may arise from end-use conditions of building materials are not yet considered in most of the present fire safety regulations and there is not yet any clear prospect that reasonable fire safety evaluation can be achieved on such problem on the basis of bench-scale tests.

ACKNOWLEDGMENTS

The authors wish to thank Messrs.T.Miyamura and T.Hara, former students of School of Science and Engineering, Science University of Tokyo, and Mr. R.Kikuchi, graduate student of the same School for their assistance in the experiments. The present address of S.Takashima is Technical Institute, Daiwa House Inc., Nara-City.

TERMINOLOGY

C_p : specific heat of air, D: channel depth, H: L_f/D , L_f : flame height, Q: heat release rate, Q_b : heat release rate from the ignition burner, Q_l : heat release rate per unit width, Q_{mod}^* : dimensionless heat release rate for rectangular fire source($Q/\rho C_p T_o g^{1/2} W D^{3/2}$), T_o : ambient temperature, W: channel width, g: gravitational acceleration, x: height from fire source, x_{poff} : maximum pyrolysis front height, γ : constant, ρ : density of ambient air.

REFERENCES

1. Hasemi, Y., Yoshida, M., Yasui, N., and Parker, W.J.: Upward Flame Spread along a Vertical Solid for Transient Local Heat Release Rate, Fourth International Symposium on Fire Safety Science, Ottawa, 1994.
2. Delichatsios, M.M., Wu, P., Delichatsios, M.A., Loughheed, G.D., Crampton, G.P., Qian, C., Ishida, H., and Saito, K.: Effect of External Radiant Heat Flux on Upward Fire Spread: Measurements on Plywood and Numerical Predictions, Fourth International Symposium on Fire Safety Science, Ottawa, 1994.
3. Building Center of Japan: Technical Report for the Fire Safety Design of New National Theater Project, 1988(*in Japanese*).
4. Fire Safety Journal, Special Issue: The Kings' Cross Fire, Vol.18, No.1, 1992.
5. Oleszkiewicz, I.: Heat Transfer from a Window Fire Plume to a Building Facade, ASME Winter Annual Meeting, San Francisco, 1989.
6. Smith, D.A.: Measurements of Flame Length and Flame Angle in an Inclined Trench, Fire Safety Journal, 18, p.231, 1992.
7. Drysdale, D.D., and Macmillan, A.J.R.: Flame Spread on Inclined Surfaces, Fire Safety Journal, 18, p.245, 1992.
8. Orloff, L., de Ris, J., and Markstein, G.H.: Upward Turbulent Fire Spread and Burning of Fuel Surface, Fifteenth Symposium(International) on Combustion, p.183, 1974.

9. Fernandez-Pello,A.C.: Upward Laminar Flame Spread under the Influence of Externally Applied Thermal Radiation, Combustion and Flame, Vol.17, p.87, 1977.
10. Hasemi,Y.: Experimental Wall Flame Heat Transfer Correlations for the Analysis of Upward Flame Spread, Fire Science and Technology, Vol.4, No.2, p75-90, 1984.
11. Saito,K., Quintiere,J.G., and Williams,F.A.: Turbulent Upward Flame Spread, Proceedings of the First International Symposium on Fire Safety Science, Gaithersburg, Md, 1985.
12. Hasemi,Y., Yoshida,M., Nohara,A., and Nakabayashi,T.: Unsteady-state Upward Flame Spreading Velocity along Vertical Combustible Solid and Influence of External Radiation on the Flame Spread, Proceedings of the Third International Symposium on Fire Safety Science, Edinburgh, 1991.
13. Bellin,B.: Upward Turbulent Fire Spread and Burning of Fuel Surface in the Configuration of Two PMMA Surfaces Facing Each Other, STA Fellow Interim Report, Fire Research Institute, 1991.
14. Hasemi,Y., and Nishihata,M.: Fuel Shape Effect on the Deterministic Properties of Turbulent Diffusion Flames, Proceedings of the Second International Symposium on Fire Safety Science, Tokyo, 1988.
15. Quintiere,J.G., Harkleroad,M., and Hasemi,Y.: Wall Flames and Implications for Upward Flame Spread, Combustion Science and Technology, Vol.48, p.191, 1986.
16. Hasemi,Y., and Tokunaga,T.: Some Experimental Aspects of Turbulent Diffusion Flames and Buoyant Plumes from Fire Sources against a Wall and in a Corner of Walls, Combustion Science and Technology, Vol.40, p.1, 1984.
17. Kokkala,M.: Characteristics of a Flame in an Open Corner of Walls, INTERFLAM '93.
18. Sato,H., Kurioka,H., Sugawa,O., and Takahashi,W.: Opening Jet in Semi-Confined Space, Annual Meeting, Japan Association for Fire Science and Engineering, 1994(*in Japanese*).

Table 1(a) Wall Flame Height Parameters(no Sidewalls), $L/D = \gamma \cdot Q_{mod}^{*n}$

W/D	n
0.5	0.535
1	0.566
2	0.660
3	0.613
5	0.641

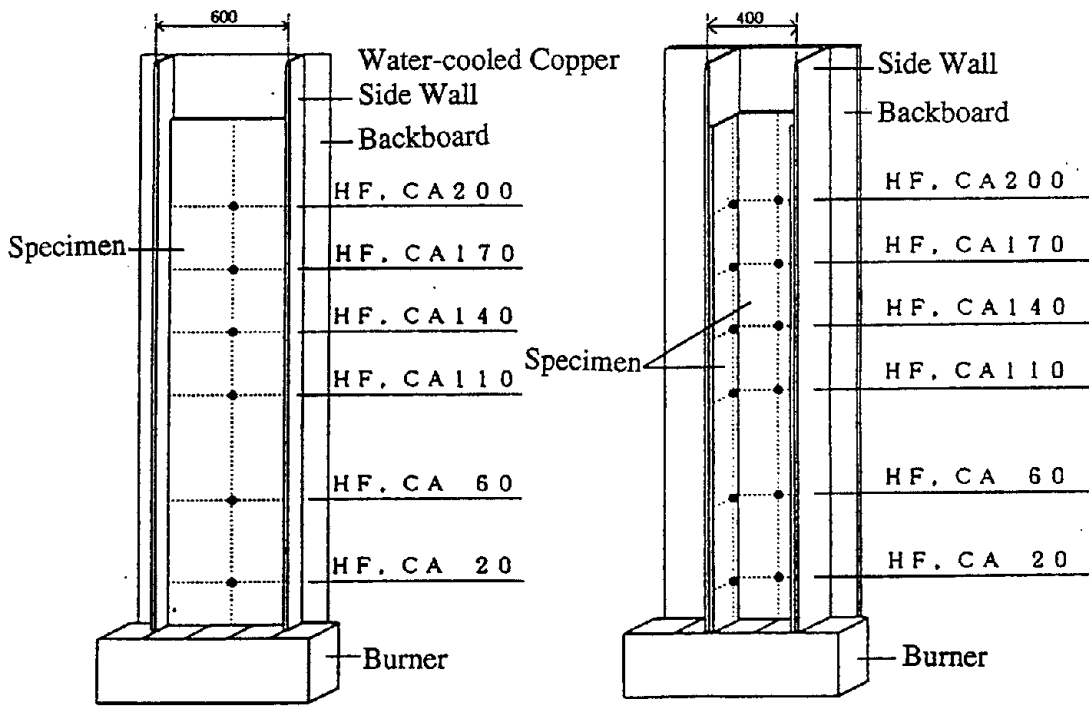
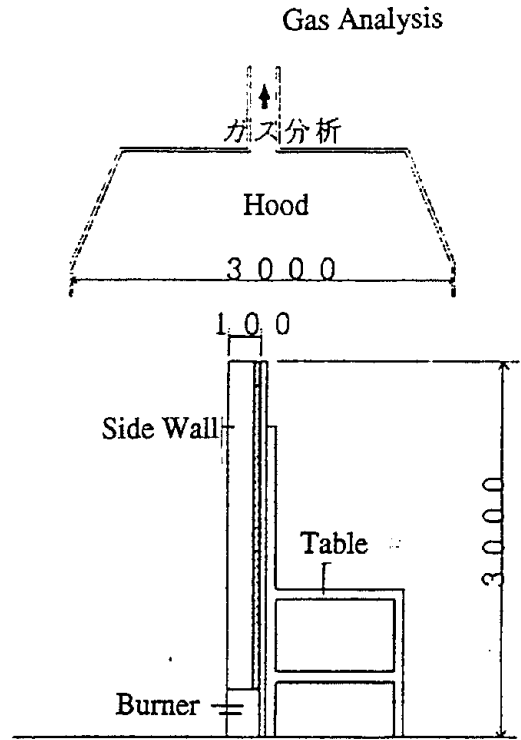
		γ				
Q^*	W/D	0.5	1	2	3	5
0.3		2.856	3.953	5.534	6.275	7.572
0.4		2.857	—	5.492	7.014	7.197
0.5		2.898	4.441	4.740	6.118	7.797
0.6		2.957	—	4.903	6.155	6.937
0.7		2.723	3.671	5.062	7.466	6.284
0.8		2.817	4.538	5.214	6.306	7.500
1.0		2.750	4.000	5.000	5.500	7.500
1.2		2.948	4.059	5.320	6.260	7.562
1.5		2.817	3.975	5.356	7.409	7.711
2.0		2.933	4.391	5.063	5.884	7.054
2.5		2.756	4.167	5.462	6.558	—
3.0		2.917	4.027	5.327	6.629	—
4.0		—	4.107	5.007	—	—
5.0		—	4.021	—	—	—
average		2.852	4.113	5.191	6.465	7.311

Table 1(b) Wall Flame Height Parameters(Channels), $L_i/D = \gamma \cdot Q_{mod}^{*n}$

W/D	n	
	Backwall	Corner
0.5	0.734	0.702
1	0.714	0.719
2	0.656	0.639
3	0.513	0.649
5	0.706	0.667

		γ Backwall				
Q^*	W/D	0.5	1	2	3	5
	0.3		4.074	4.725	5.507	5.564
0.4		4.757	—	5.472	5.600	6.684
0.5		4.474	4.921	5.515	6.422	6.525
0.6		5.010	—	5.592	5.848	6.454
0.7		4.817	4.515	5.504	5.404	6.432
0.8		4.678	5.277	5.209	5.606	6.438
1.0		4.500	5.500	5.000	5.000	6.000
1.2		4.179	5.267	5.767	5.009	6.594
1.5		4.702	4.866	5.365	4.873	6.384
2.0		4.764	4.572	5.077	5.606	6.346
2.5		4.599	4.938	5.482	5.937	—
3.0		4.278	5.248	5.351	6.261	—
4.0		—	4.831	5.639	—	—
5.0		—	4.754	—	—	—
average		4.486	4.951	5.422	5.594	6.371

		γ Corner				
Q^*	W/D	0.5	1	2	3	5
	0.3		4.234	4.753	6.475	6.553
0.4		4.408	—	6.286	7.250	6.449
0.5		4.158	4.115	6.229	7.056	6.351
0.6		4.728	—	5.544	6.269	6.327
0.7		4.872	5.169	6.280	6.302	6.977
0.8		4.712	5.870	6.343	6.357	6.383
1.0		4.500	6.000	6.000	6.000	6.000
1.2		4.155	5.263	6.230	5.775	7.084
1.5		4.641	5.230	6.560	6.149	6.867
2.0		4.660	4.860	6.422	6.377	7.243
2.5		4.466	4.916	6.403	6.345	—
3.0		4.130	5.220	6.195	6.372	—
4.0		—	4.798	5.979	—	—
5.0		—	4.716	—	—	—
average		4.472	5.076	6.227	6.400	6.749



(a) Flat Wall Flame Spread Test

(b) Vertical Channel

Figure 1 Vertical Channel Specimen and Experimental Set Up

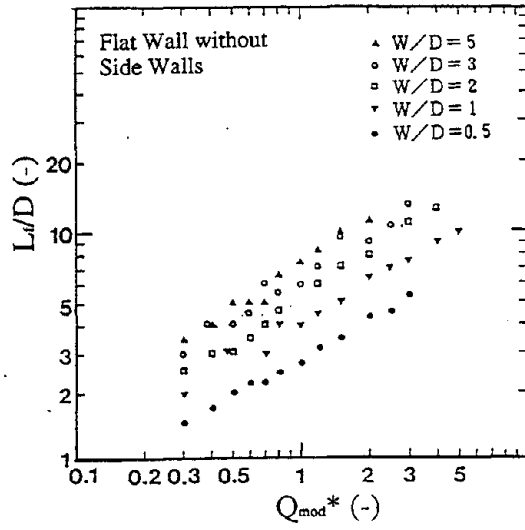


Figure 2(a) Flat Wall

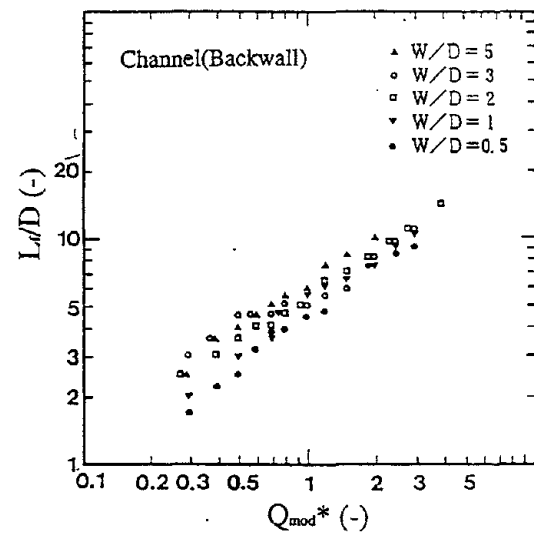


Figure 2(b) Flame Height Measured at the Center of the Backwall of a Channel

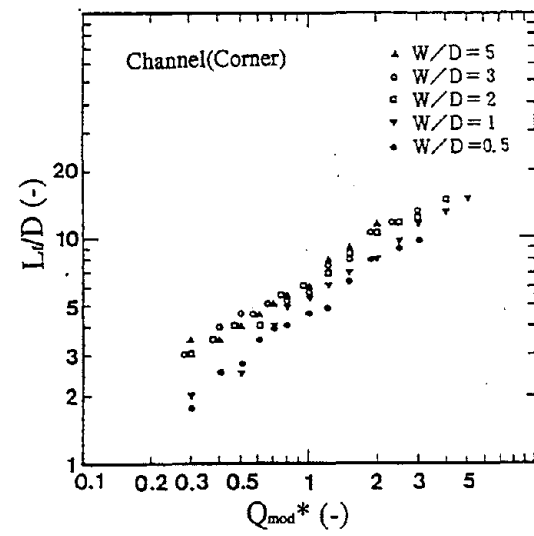


Figure 2(c) Flame Height Measured at the Corner between the Backwall and a Sidewall of a Channel

Figure 2 Flame Height vs Dimensionless Heat Release Rate, Q_{mod}^*

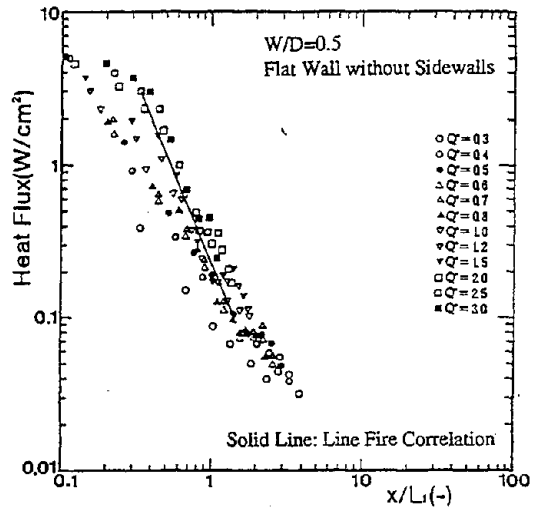


Figure 3(a) W/D=0.5

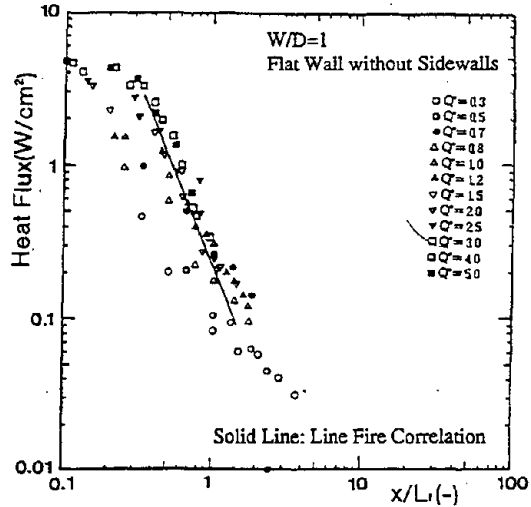


Figure 3(b) W/D=1.0

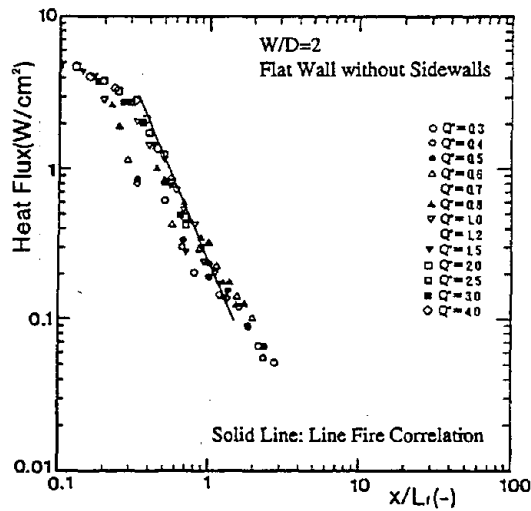


Figure 3(c) W/D=2.0

Figure 3 Heat Flux to Wall Surface vs Height Normalized by Flame Height, Flat Wall

Figure 3 Heat Flux to Wall Surface vs Height Normalized by Flame Height, Flat Wall(cont.)

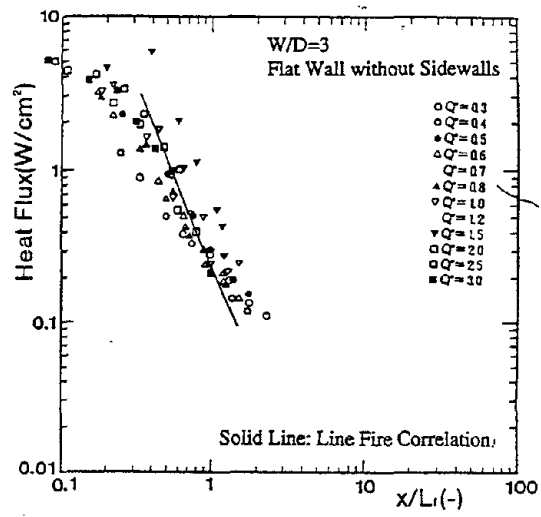


Figure 3(d) W/D=3.0

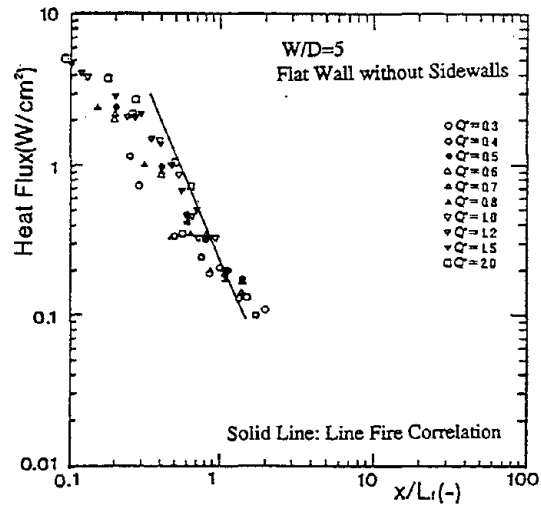


Figure 3(e) W/D=5.0

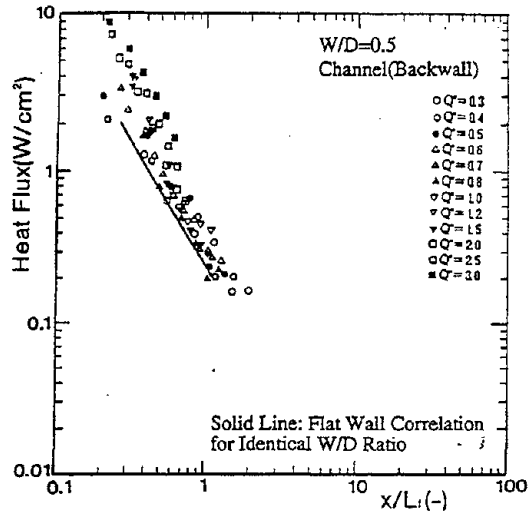


Figure 4(a) W/D=0.5

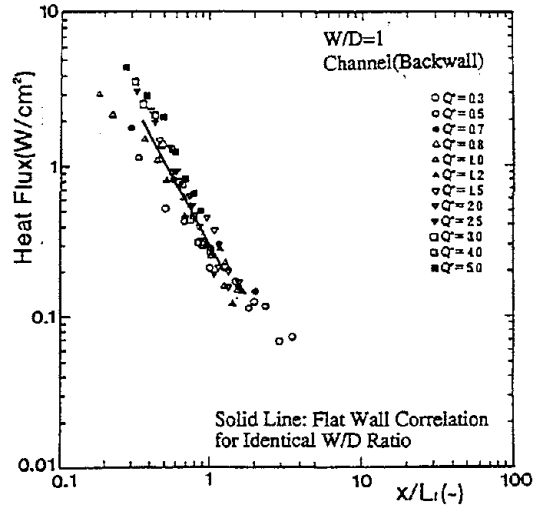


Figure 4(b) W/D=1.0

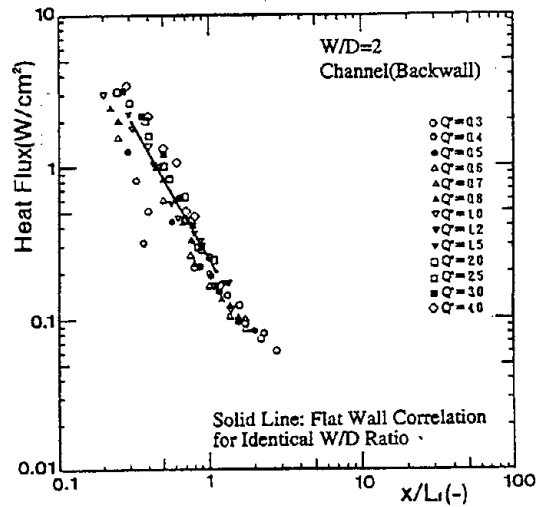


Figure 4(c) W/D=2.0

Figure 4 Wall Heat Flux vs Normalized Height in Channel, Center of the Backwall

Figure 4 Wall Heat Flux vs Normalized Height in Channel, Center of the Backwall(Cont.)

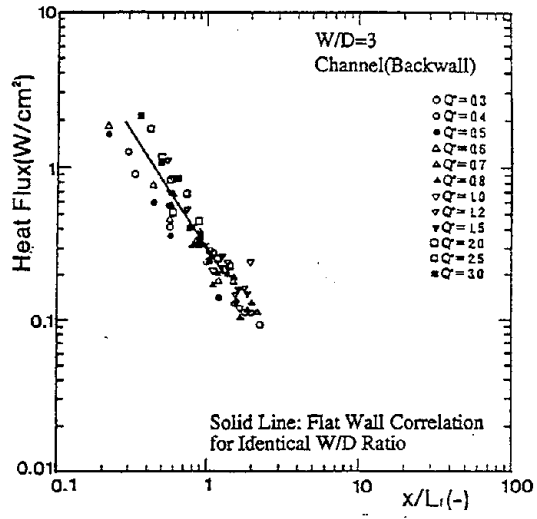


Figure 4(d) W/D=3.0

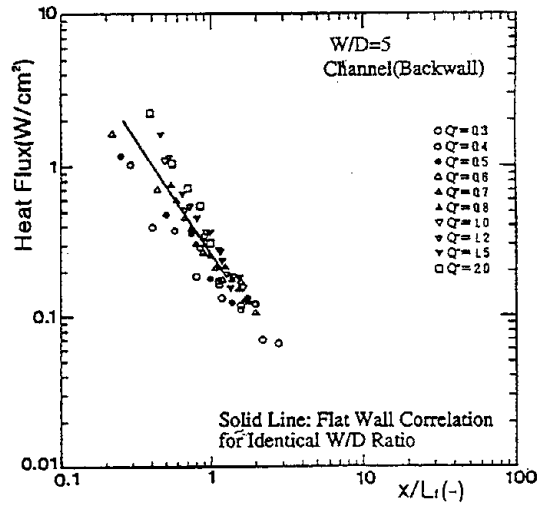


Figure 4(e) W/D=5.0

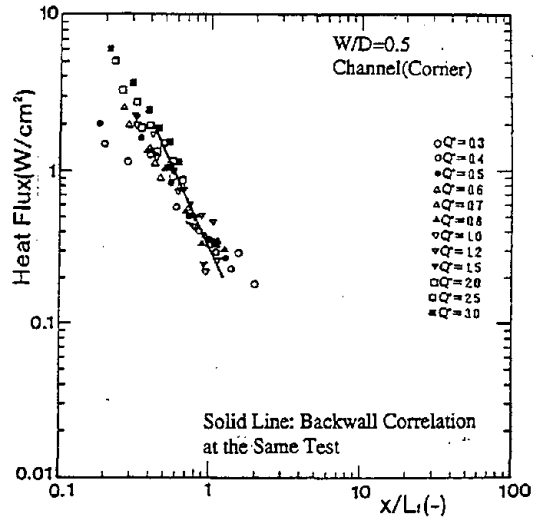


Figure 5(a) W/D=0.5

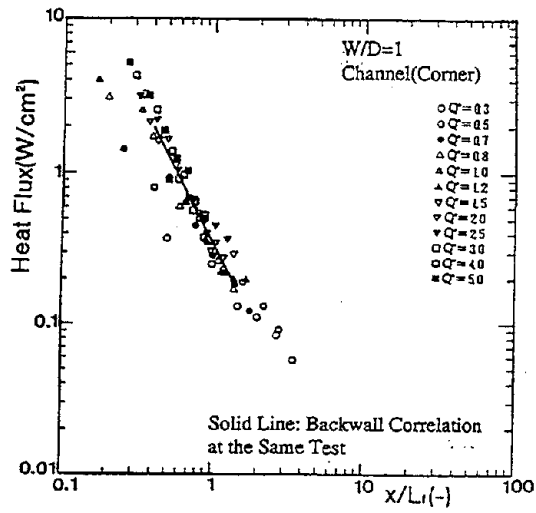


Figure 5(b) W/D=1.0

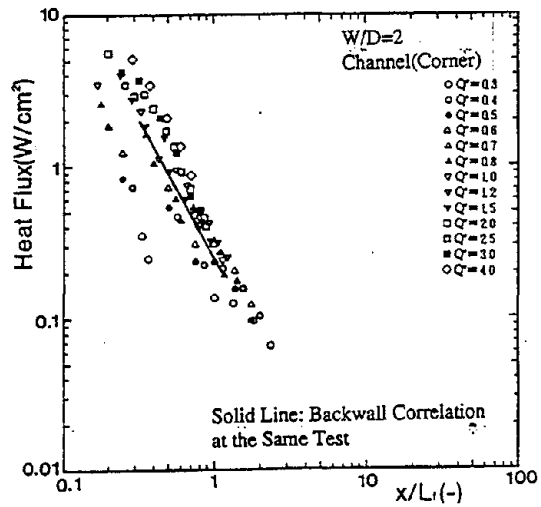


Figure 5(c) W/D=2.0

Figure 5 Wall Heat Flux vs Normalized Height in Channel, Backwall/Sidewall Corner

Figure 5 Wall Heat Flux vs Normalized Height in Channel, Backwall/Sidewall Corner(cont.)

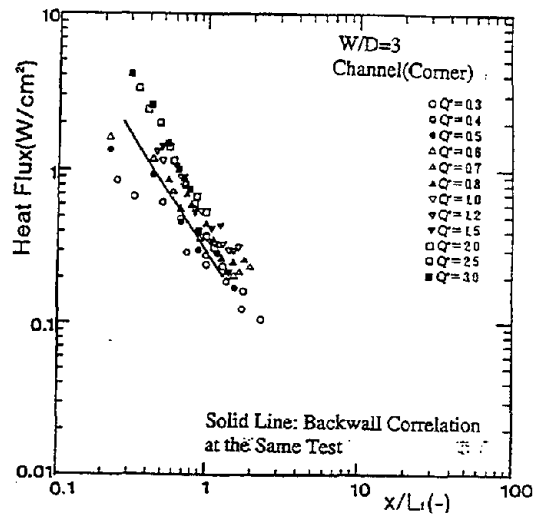


Figure 5(d) W/D=3.0

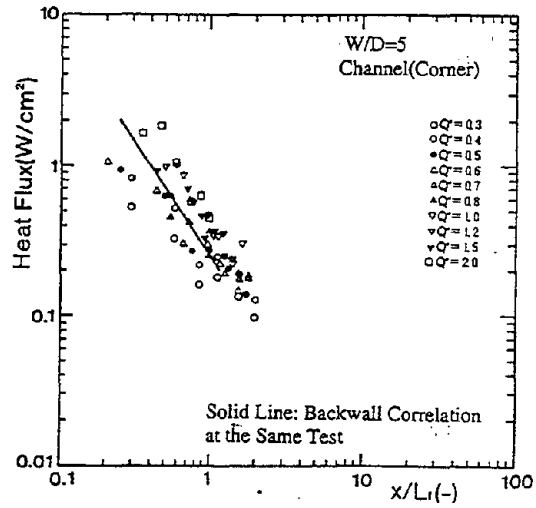


Figure 5(e) W/D=5.0

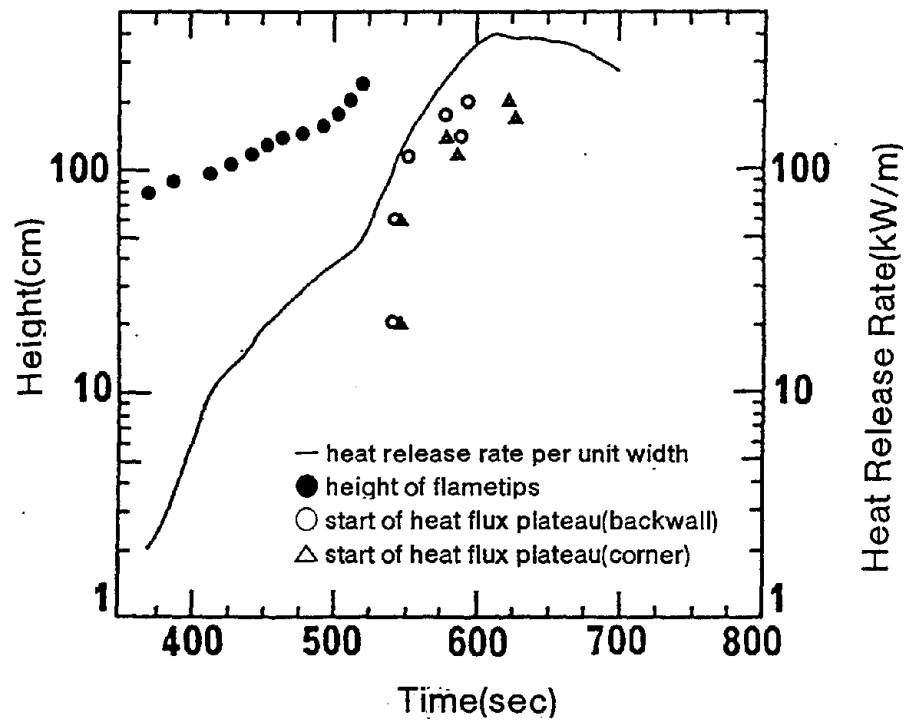


Figure 6(a) $W/D=0.5$, $Q_b=20\text{kW}$

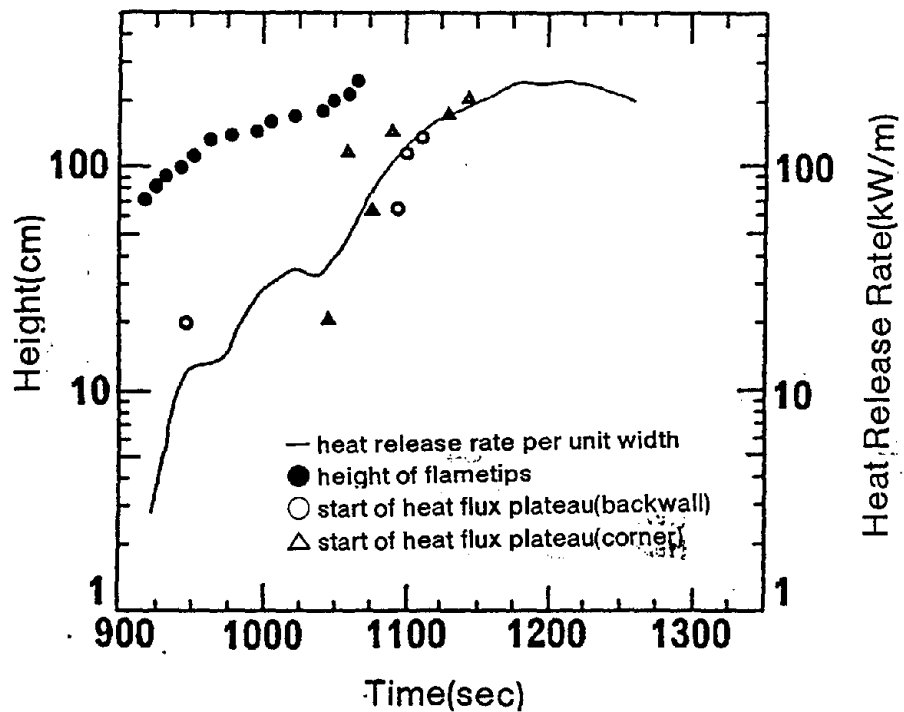
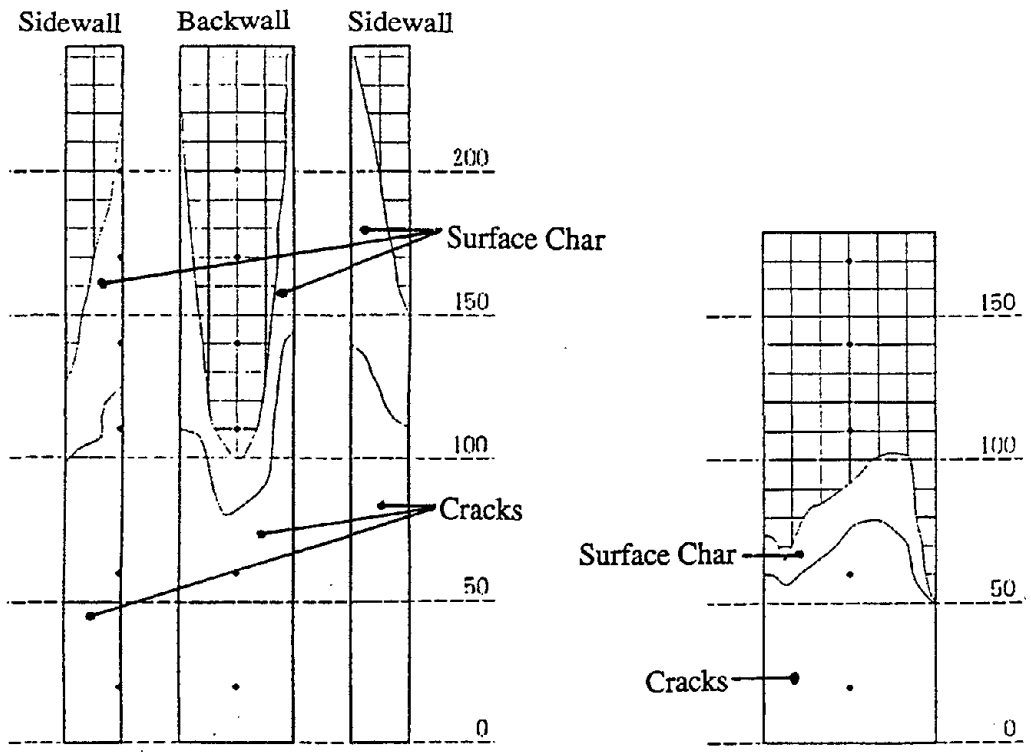


Figure 6(b) $W/D=1$, $Q_b=10\text{KW}$

Figure 6 Summary Observation Records during Flame Spread Test



(a) $W/D=2$

(b) Flat Wall

Figure 7 Ultimate Burn Patterns(Particleboard), $Q_b=10\text{kW}/\text{burner element}$

Figure 6 Summary Observation Records during Flame Spread Test(Cont.)

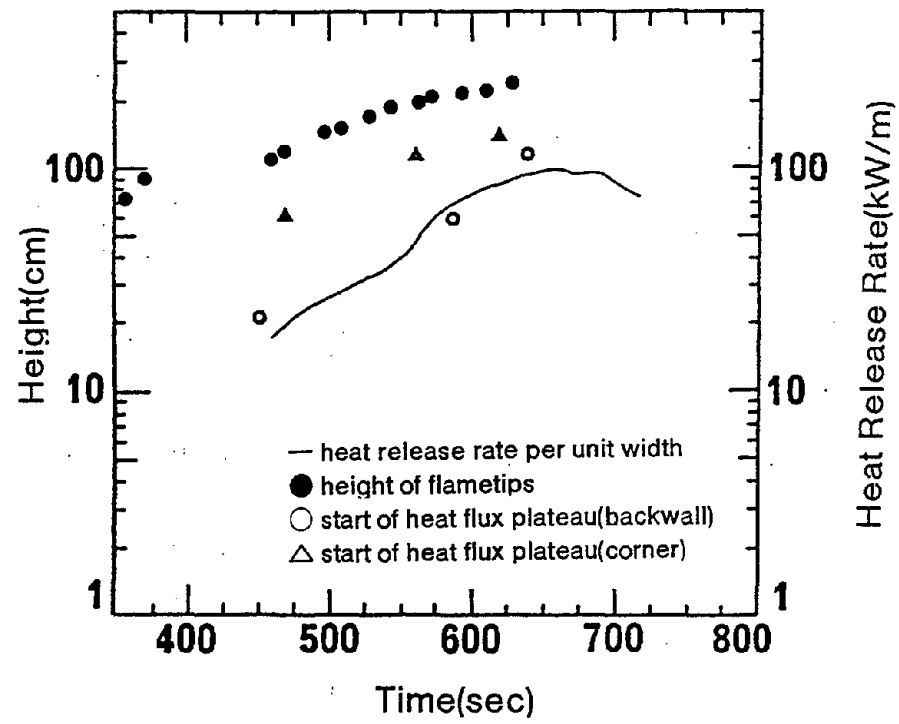


Figure 6(c) $W/D=2$, $Q_b=20\text{kW}$

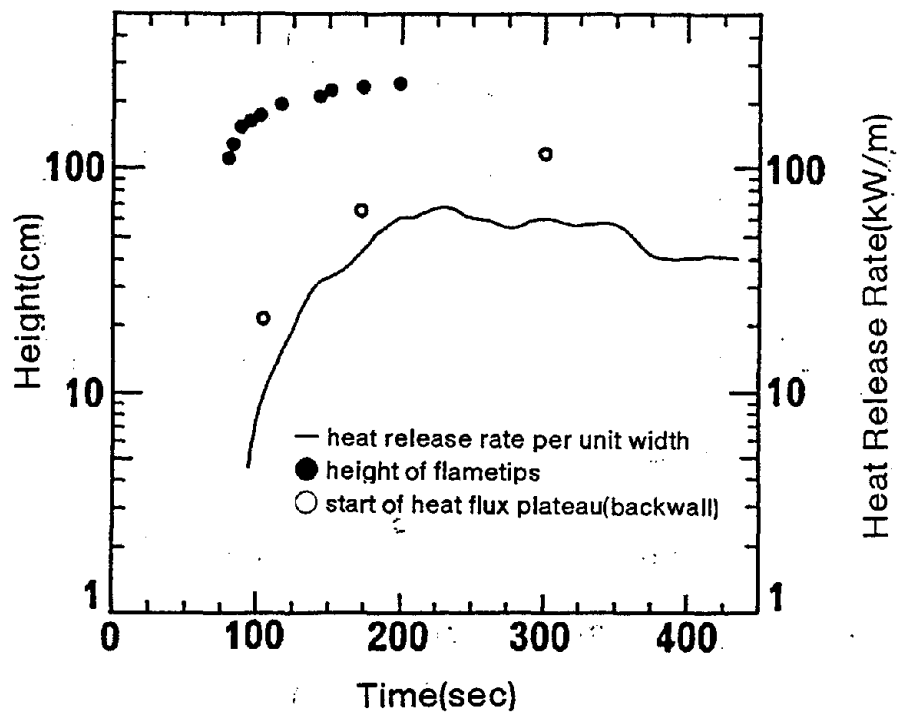


Figure 6(d) Flat Wall, $Q_b=60\text{kW}$

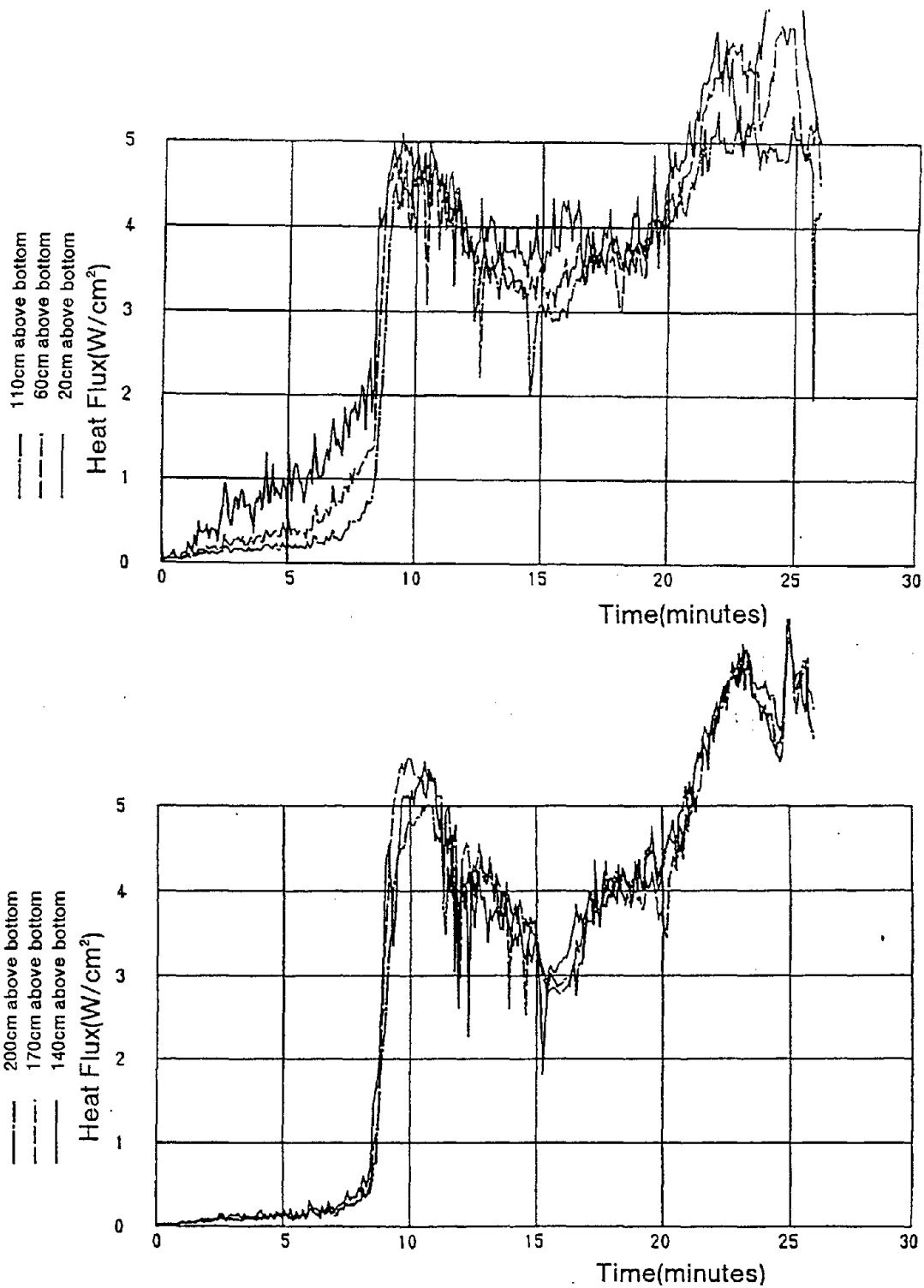


Figure 8 Time History of Heat Flux in Channel, $W/D=0.5$, $Q_b=20kW$, Center of Backwall

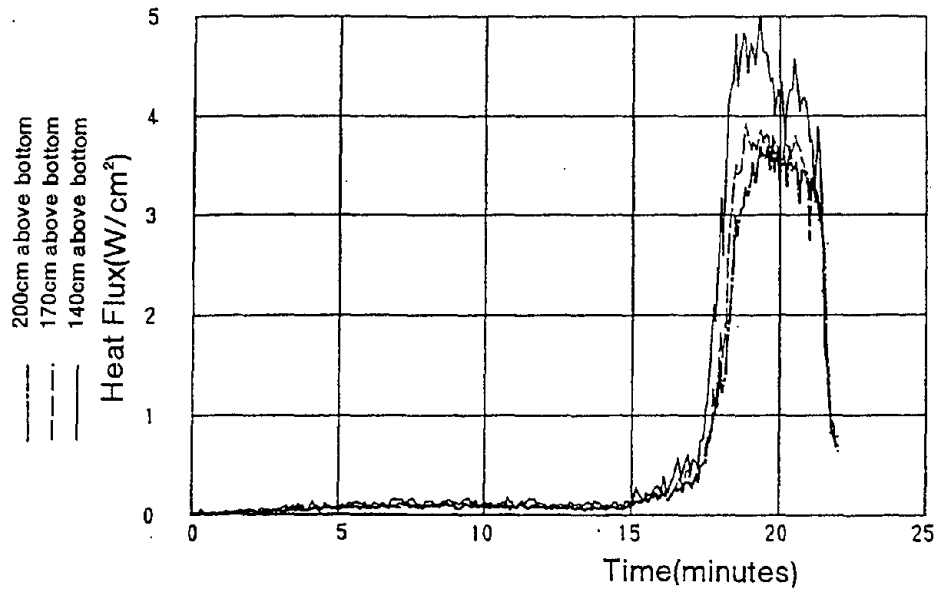
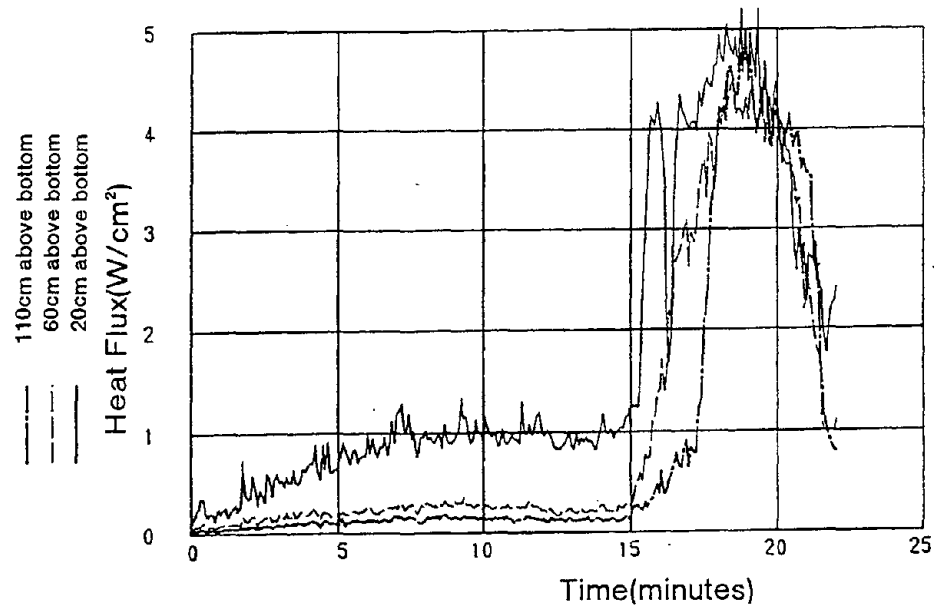


Figure 9 Time History of Heat Flux in Channel, W/D=1.0, , Q_b=10kW, Center of Backwall

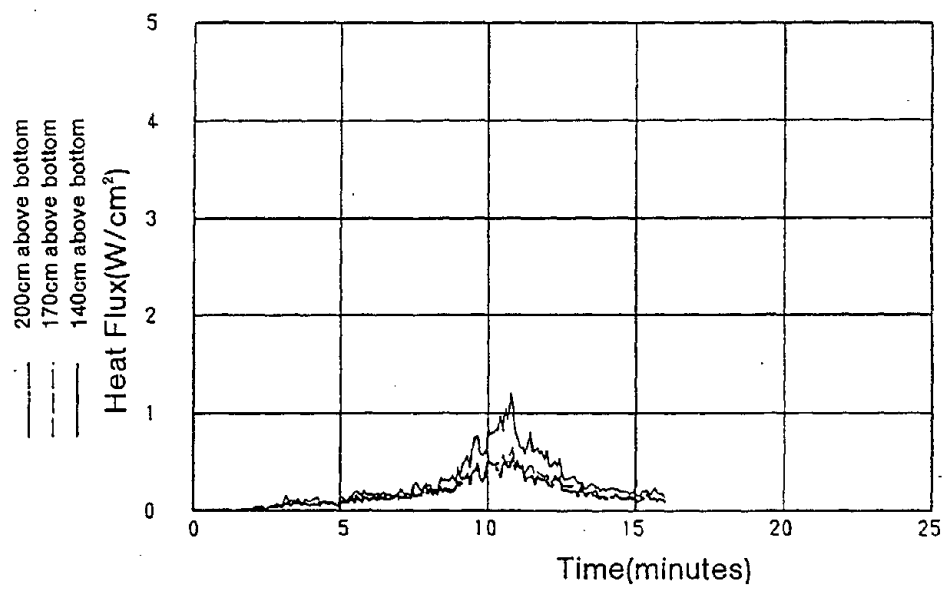
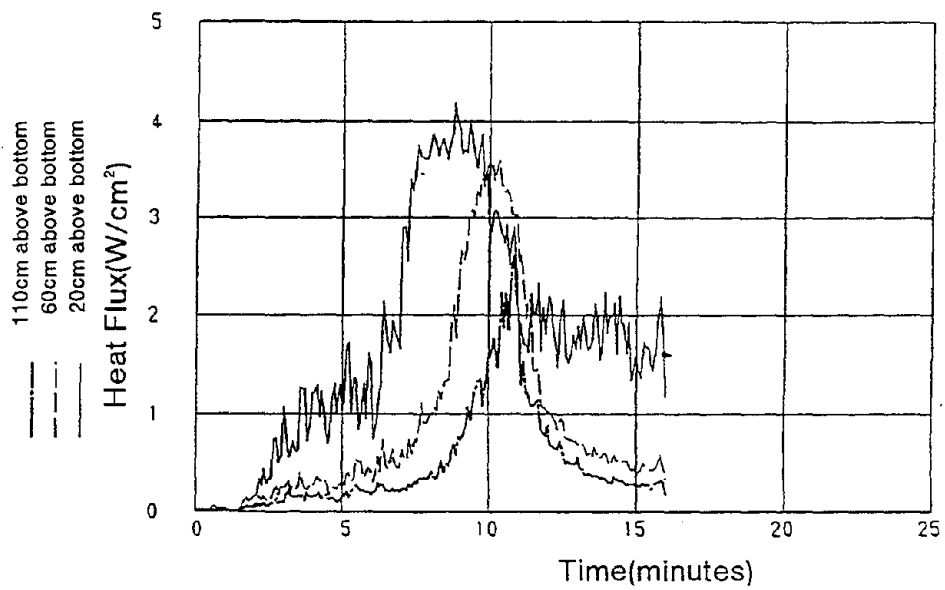


Figure 10 Time History of Heat Flux in Channel, W/D=2.0, Q_b=20kW, Center of Backwall

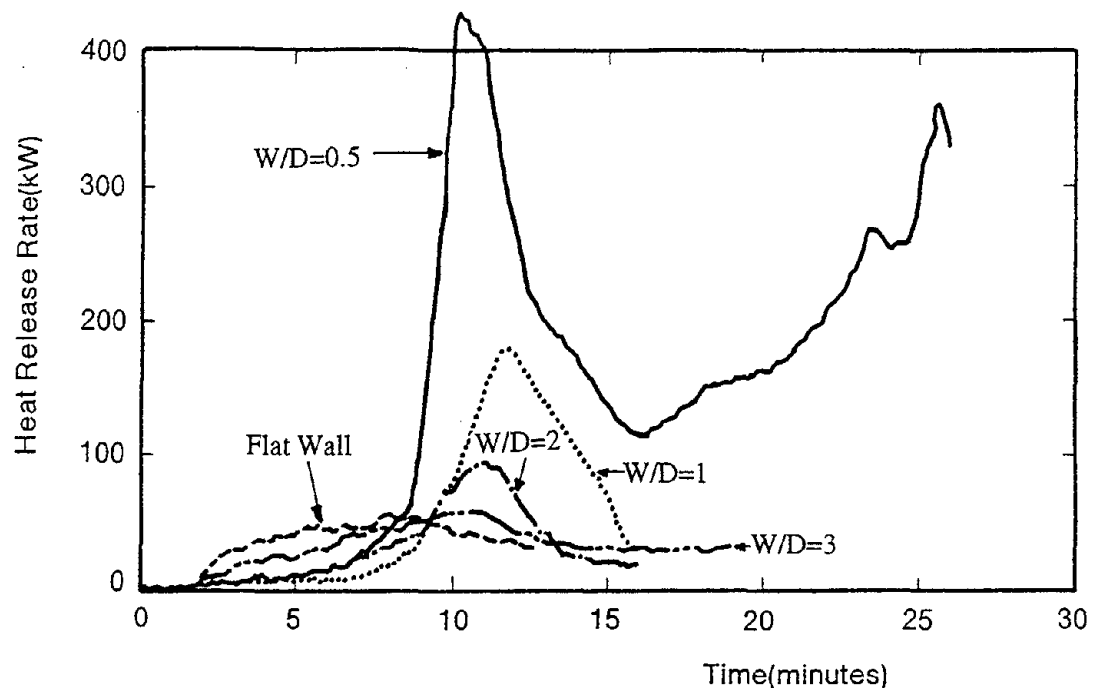


Figure 11 Time History of Heat Release Rate at Flame Spread Tests ($Q_b = 10\text{kW/burner element}$)

Discussion

James Quintiere: May I ask two quick questions? First, would you agree that the different models are really based on the same physics, but they just have some different approximations?

Yuji Hasemi: Yes.

James Quintiere: My experience in some work we are doing now suggests that there are some other aspects to this problem. One is the effect of the ignition source which influences the flame height and the heat flux. And the second is transient burning. Particularly, the influence of thin materials and burnout. Just as an anecdote, there were some serious fires in New York City in stairways in which there were something like sixteen coats of paint. Had the paint coats been fewer, there would probably have been no fire spread. Do you agree that these are two significant effects? What is your experience?

Yuji Hasemi: We are currently studying that.

Ronald Alpert: I just want to call you attention to reference 3 in your concurrent flame spread paper. In that reference, Orloff and Markstein, in the Fifteenth International Symposium on Combustion, conducted a study with a gas burner in which they rotated the burner for different angles and discovered that effect back in 1974.

Yuji Hasemi: Yes, indeed I am aware of the experiment. However, they are not utilized in the practice of fire separation. We hope that as researchers, we should promote taking the results into practice so they would be used in actual situations.

**ASSESSMENT OF MATERIAL FLAMMABILITY WITH THE FSG
PROPAGATION MODEL AND LABORATORY TEST METHODS**

by

**P.K. Wu, L. Orloff and A. Tewarson
Factory Mutual Research Corporation
Norwood, Massachusetts, USA**

March 1996

For presentation at the Thirteenth Joint Panel Meeting of the UJNR Panel on
Fire Research and Safety, March 13 - 20, 1996, Gaithersburg Hilton Hotel,
Gaithersburg, Maryland, USA

Assessment of Material Flammability with the FSG Propagation Model and Laboratory Test Methods

ABSTRACT

Full-scale tests to determine the flammability of new types of materials for various applications are expensive and time consuming. We have developed a technique, based on the combination of a small-scale flammability apparatus and a fire spread model, that has the potential to determine material flammability more efficiently. This technique involves the use of a numerical simulation of upward fire spread, the FSG model, and the FMRC Flammability Apparatus. The FSG model was constructed to be able to accept property inputs in terms of measurements from Flammability Apparatus experiments and was validated by a full-scale PMMA upward fire spread test. The measurements from small-scale Flammability Apparatus (e.g., time to ignition, heat of combustion and material response to heat flux in an inert environment) provide an effective first generation pyrolysis correlation to predict pyrolysis rates in fires. The combination of the model and the measurements eliminates the need to know the detailed components and configuration of the material. Hence, this technique is suitable for fire hazard assessment of complex fire retardant materials with unknown properties. The technique has been applied to various polymers and composite materials and the results are consistent with earlier evaluations performed using correlation techniques (e.g., by evaluating the Fire Propagation Index, or, FPI, from Flammability Apparatus measurements). The present method has the potential to provide a description of fire propagation for a wide range of configurations, as opposed to an index that correlates with only certain specific full-scale scenarios.

INTRODUCTION

The FMRC 50/500 kW Flammability Apparatus has been developed for many years (Ref.1) and effectively used for various applications (i.e., the influence of oxygen concentration on fire propagation, Ref. 2; the flame propagation for polymers, Ref. 3; and flame spread over Polymethylmethacrylate (PMMA) Ref. 4.). An upward fire spread simulation code (The FSG Model) was being developed. The FSG model was constructed with the physical understandings from small-scale laboratory experiments. Full-scale tests are needed for model validation. In validating the FSG model as well as providing badly needed full-scale heat flux data, an upward fire spread experiment was carried-out under the Fire Products Collector at the FMRC Test Center, West Glocester, Rhode Island with a 0.025 m thick PMMA wall, 0.58 m x 5 m high. The results from the full-scale test have been incorporated into the FSG model which provide excellent agreements with data.

The FSG Model assumes that the material is homogeneous and requires various chemical properties (i.e., density, thermal conductivity, heat of gasification, ...) of the material. However, materials of interest are usually composite with complex geometries and many components. A technique has been devised to test an unknown composite and provide some meaningful flammability assessment of the sample. The FMRC Flammability Apparatus is first used to carry-out the time-to-ignition and the mass loss measurements and the results then provide the needed inputs for the calculations with the FSG Mode. The FSG Model/FMRC Flammability Apparatus package was applied to various polymers and composites, and the results are not only consistent with the earlier Fire Propagation Index (FPI) evaluation but also providing a more comprehensive fire spread description than the FPI index alone.

In this paper, the FMRC 50/500 kW Flammability Apparatus is first reviewed for its main features. The essential characteristics of the FSG Model are then discussed with its' validation against a 5 m PMMA wall Fire Test. The technique is then applied to the flammability assessment of three complex composites (i.e., the E-701 Baseline Composite, S-2 Glass/Epoxy, and Graphite / Cyanate). The results clearly show the usefulness of the technique.

THE FMRC 50 kW FLAMMABILITY APPARATUS

The FMRC Flammability Apparatus (50 kW-scale) is shown in Fig. 1 and the 500 kW-scale Apparatus has similar features. Both Apparatus have a lower section and an upper section. The lower section is used for the measurements of time to ignition, mass loss rate during pyrolysis and combustion and other quantities (Ref.4). The upper section is used for the measurements of total mass and volumetric flow rates of chemical compounds - air mixture, temperature, concentrations of CO, CO₂, O₂ total gaseous hydrocarbons and others. From the species concentrations and volume flow rate, one calculates the chemical heat release rate and hence the heat of combustion. The Apparatus can provide the needed thermal properties and the mass loss (i.e., pyrolysis rate) history for the FSG model to carry-out the flammability assessments of a composite material.

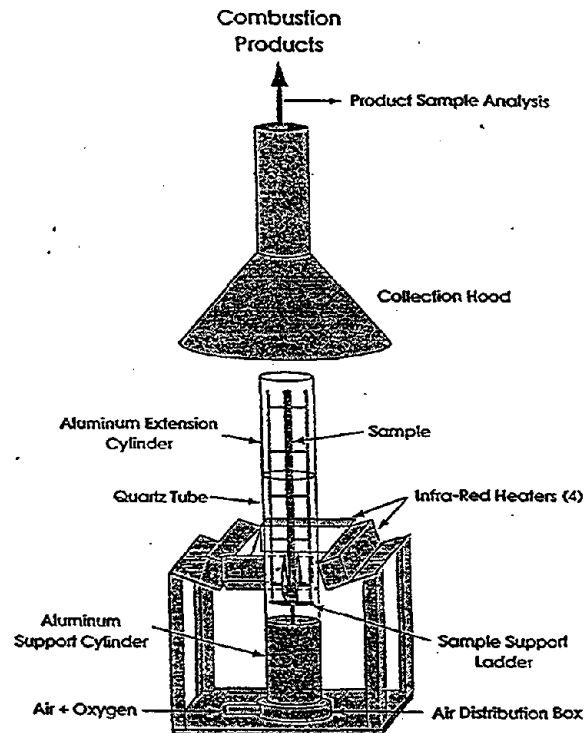


Figure 1. The FMRC 50 kW Flammability Apparatus

THE VALIDATION OF THE FSG MODEL

The FSG Model is clearly described in Ref. 5 and the details will not be repeated here. The model was constructed with the physical understandings of small-scale fires. When the model is extrapolated to full-scale fires, there are uncertainties in three areas of the model, i.e., the flame height correlation, the radiant fraction and the radiant (or total) heat flux distributions. The flame height Z_f was taken to be the 2/3 power of chemical heat release rate \dot{Q}''_{ch} ($Z_f \sim \dot{Q}''_{ch}{}^{2/3}$). The radiant fraction was assumed to be a constant ($X_r \sim 0.3$) and the radiant heat flux distributions were taken to be triangular (Ref. 5).

A FULL-SCALE FIRE TEST

To validate the model with a full-scale test, an upward fire spread experiment was carried out under the Fire Products Collector at the FMRC Test Center, West Glocester, Rhode Island with a 0.025 m thick PMMA wall, 0.58 m wide x 5 m high. As shown in Fig.2, the PMMA wall was extended another 0.3 m on each side by Marinite panels. At the outer edge of the Marinite

panels, a perpendicular 0.6 m flow barrier (24 gauge steel) is used to minimize the effects of room drafts. On top of the wall, a 3 m extension provided a background for measuring the flame heights. Among many data acquisition instruments, seven total heat flux gauges and thermocouples were placed at various locations on the PMMA wall.

The measured total heat flux histories at various locations on the PMMA wall provide an important insight into the heat flux distributions in a upward propagating flame. As shown in Fig.3, the total heat flux histories at six locations were given. One gauge was destroyed in the test. Now, one can obtain the total heat flux distributions by cross plotting Figure 3. The results are given in Fig.4. The total heat flux is plotted as a function of vertical distance. The symbols are the data points and the lines are put in to aid visual interpretation of the trend. The pyrolysis height reached the top of the PMMA wall at about 1200 seconds and the steady state distribution from Orloff's study (Ref.6) was presented for comparison. When the measured total heat flux was plotted as a function of normalized vertical distance, Z/Z_f , the profiles are similar for Z/Z_f greater than about 0.8.

The heat flux distributions are clearly going through three phases. Initially, the flame starts with a triangle-like profile. As the flame races up the PMMA wall, the profiles have a top-hat distribution with peak values between about 30-40 kW/m². Finally, after the pyrolysis zone reached the top of the PMMA wall, the profile evolves toward the steady state shape. The flame height result provides a flame height correlation, $Z_f = 0.048 * Q_{ch}^{2/3}$. Summing up the total energy gives a radiant fraction of about 0.26. After incorporating the new understandings into the FSG model, we repeated the calculations. The theory / data comparison was reasonable. The pyrolysis height history is given in Fig.5, while the chemical heat release rate history is plotted in Fig.6.

AN EXERCISE WITH THE FSG MODEL

After the validation, an upward fire spread calculation was carried out with the FSG model for a 5 meters PMMA wall. The mass loss and the net heat flux were traced at four locations, i.e., at heights of 1, 2, 3 and 4 meter. The results were plotted as a function of time modified by \dot{Q}_{net}^2 , Fig. 7 and 8. The mass loss and the net heat flux increase with height. However, when we differentiated the mass loss and normalized with the corresponding net heat flux, the results at four heights collapsed into a universal curve, Fig.9. This suggested that if we measured the distribution, it can be used everywhere at the surface.

APPLICATION OF THE FMRC APPARATUS / FSG MODEL TECHNIQUE

The technique of combining the small-scale test and the FSG model to carry out flammability assessments for complex materials have been applied to polymers and composites. The small-scale flammability measurements (i.e., time to ignition, heat of combustion and pyrolysis measurements in an inert environment) provide an effective pyrolysis correlation to predict mass loss rates in fires (i.e., the universal curve in Fig. 9). Sample results from the application of the technique to three widely different composites can demonstrate its usefulness. The composites are given in Table 1.

TABLE 1

	E-701 Baseline	S-2 Glass/Epoxy	Graphite/Cyanate
Critical Heat Flux (kW/m ²)	10	15	20
TRP (kW-s ^{1/2} /m ²)	382	400	1000
FPI	13	9	4

The pyrolysis measurements for these three composites are shown in Fig.10. The external heat flux for these measurements was 50 kW/m². The unified mass loss rate curve does not depend on the external heat flux used in the pyrolysis measurement. As shown in Fig.10, the mass loss rate is highest for S-2 Glass/Epoxy. The FSG model used the pyrolysis rate to carry out an upward flame spread calculation for two parallel walls. The flame radiation flux to the surface and the re-radiation loss from the hot surface depend on the aspect ratio of D/W, where D is the separation distance and W is the width of the wall. When the two walls are far apart, the view factor for the radiation transport is zero. When the walls are close, the view factor is essentially one. When D and W are of the same order, the view factor is approximately 1/3. Calculations were carried out for all three composites with three view factors, i.e., 0, 1/3 and 1. The results of flame height and heat release rate histories are shown in Fig.11 and 12. The flame was ignited at about 100 seconds. For view factors of 0 and 1/3, the flame moves slow with heat release rate less than about 100 kW. However, the flame rapidly accelerates up the wall for view factor of 1. This implies that E-701 composite can not be used in confined space structure such as in vehicles. For comparison of the three composites, we choose the view factor of 1/3. As shown in Fig.13 and 14, S-2 Glass/Epoxy and E-701 composites are ignited at about 100 seconds while Graphite/Cyanate delays ignition to 600 seconds. Clearly E-701 composite is the worst one.

SUMMARY

The FMRC FSG Model has been validated for PMMA panels with height of up to 5 m. Full-scale data for other materials are needed to broaden our capability to carry-out confidently flammability assessment of various types of complex materials. The viability of combining the FSG Model and the FMRC Flammability Apparatus to test the fire hazard of a complex material has been shown by applying the technique to the PE/PVC cable tray, conveyer belts and composites. The results are encouraging. The FSG Model/FMRC Flammability Apparatus package offers the advantages of: (1) extrapolating the bench-scale flammability measurements to full-scale events with complex configuration (significantly reducing the testing cost) and (2) economically testing the effectiveness of fire retardants as passive fire protection agents to reduce thermal and nonthermal damages.

References

1. Tewarson, A., "Generation of Heat and Chemical Compounds in Fires," Section 1, Chapter 13, pp.1-179, The SFPE Handbook of Fire Protection Engineering (P.J. DiNenno, Ed.), National Fire Protection Association Press, Quincy, MA (1988).
2. Tewarson, A., Lee, J.L. and Pion, R.F., "The Influence of Oxygen Concentration on Fuel Parameters For Fire Modeling," Eighteenth Symposium (International) on Combustion, The Combustion Institute, Pittsburgh, PA. pp.563-570 (1981).
3. Tewarson, A. and Khan, M.M., "Flame Propagation For Polymers in Cylindrical Configuration and Vertical Orientation," Twenty-Second Symposium (International) on Combustion, p.1231, The Combustion Institute, Pittsburgh, PA (1988)
4. Tewarson, A. and Ogden, S.D., "Fire Behavior of Polymethylmethacrylate," Combustion And Flame, NO. 89, pp.237-259 (1992)
5. Delichatsios, M.M., Mathews, M.K. and Delichatsios, M.A., "Upward Fire Spread Simulation Code: Version I - Noncharring Fuels," Factory Mutual Research Corporation, Norwood, MA. Tech. Report FMRC J.I. 0R0J2.BU (1990).
6. Orloff, L., de Ris J. and Markstein, G.H., "Upward Turbulent Fire Spread And Burning of Fuel Surface," Presented at the 15th International Symposium On Combustion, Tokyo, Japan (1974)

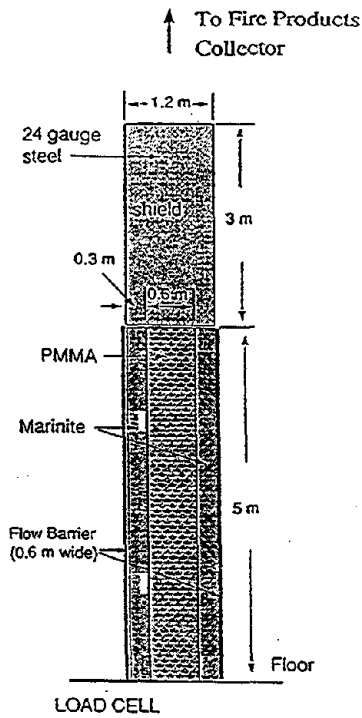


Figure 2. Full-Scale PMMA Wall Fire Test

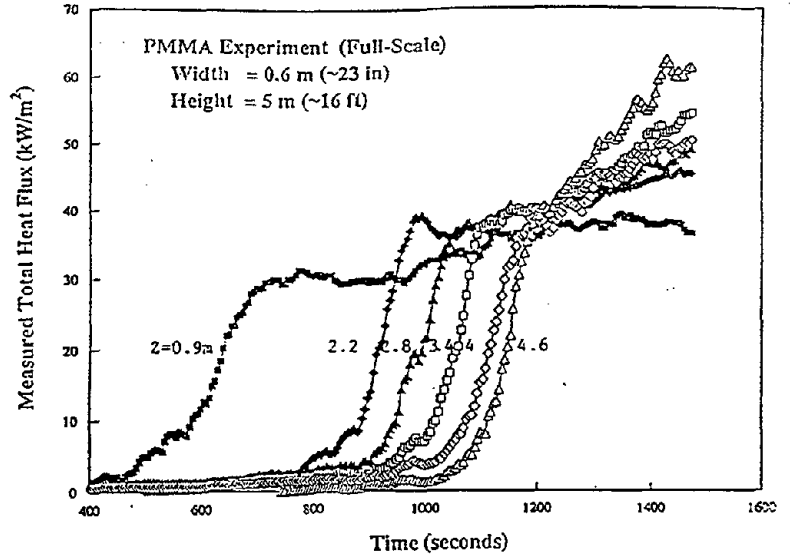


Figure 3. Total Heat Flux Histories At Various Heights

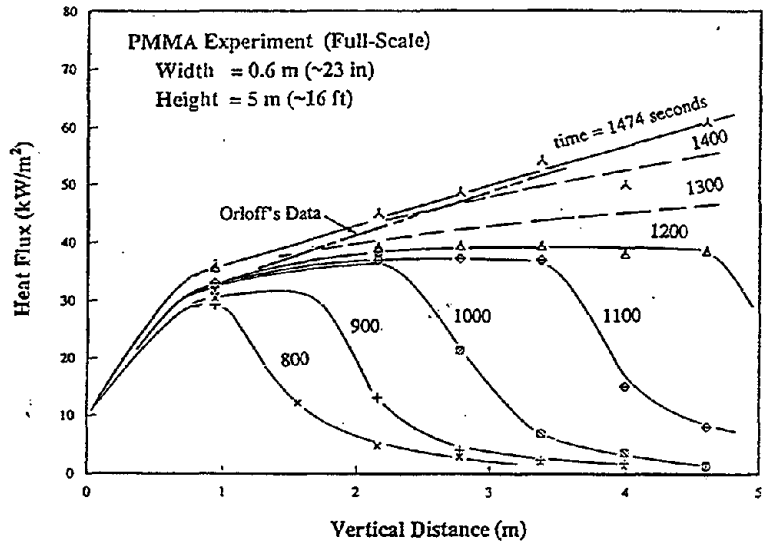


Figure 4. Heat Flux Distributions At Various Times

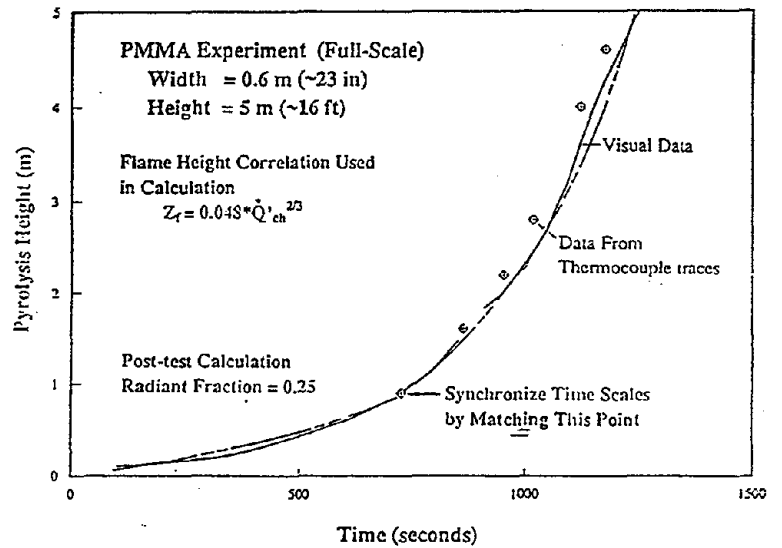


Figure 5. Model / Data Comparison On Pyrolysis Height History

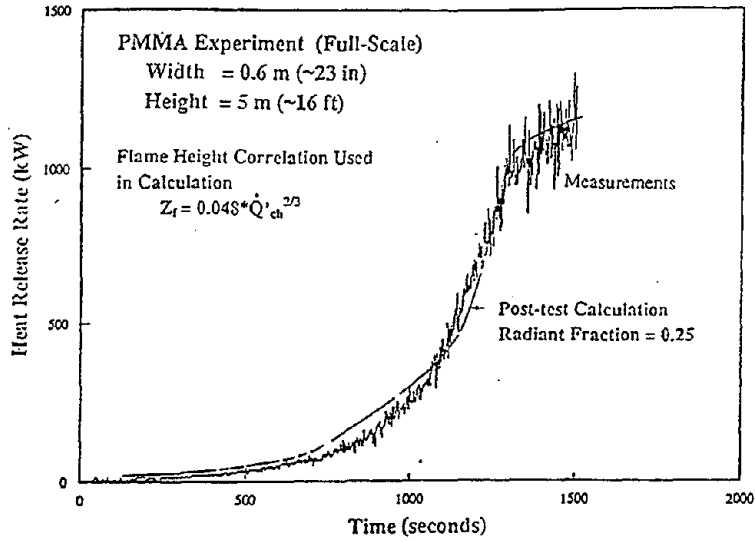


Figure 6. Model / Data Comparison On Heat Release Rate History

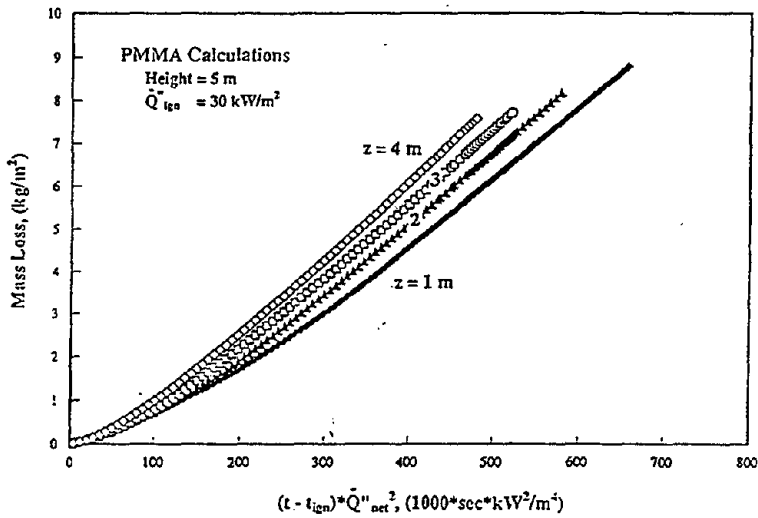


Figure 7. Mass Loss Rate Histories At Various Heights

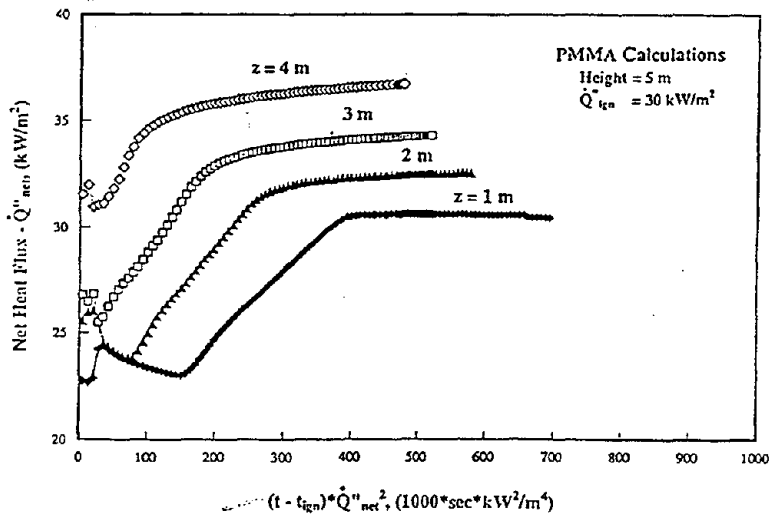


Figure 8. Net Heat Flux Histories At Various Heights

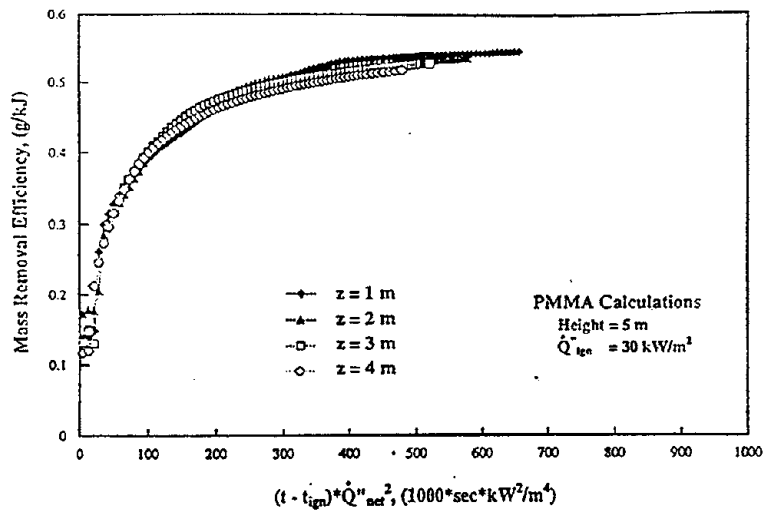


Figure 9. Mass Removal Efficiency Histories At Various Heights

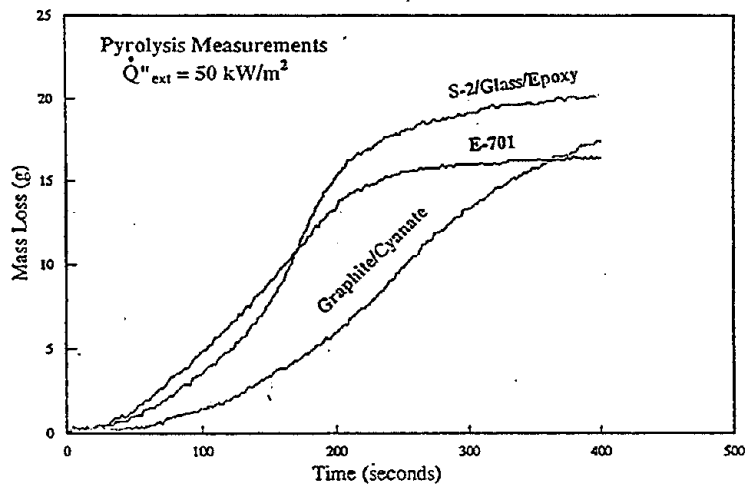


Figure 10. Pyrolysis Measurements For Three Composites

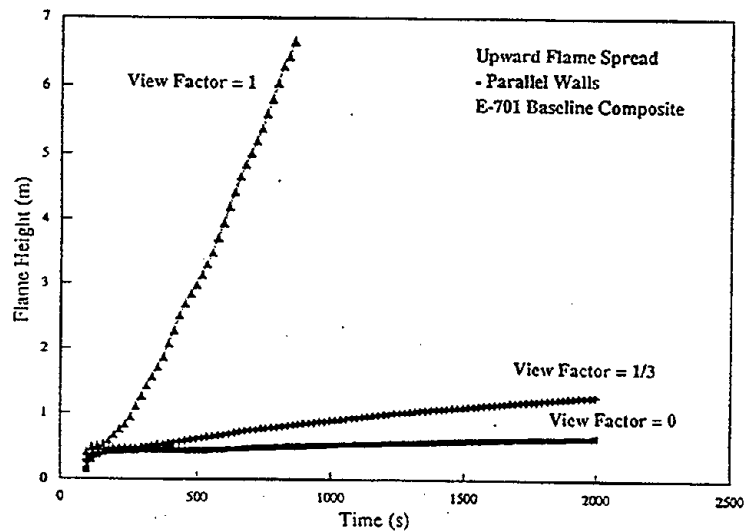


Figure 11. Flame Height Histories For Parallel Wall Fire

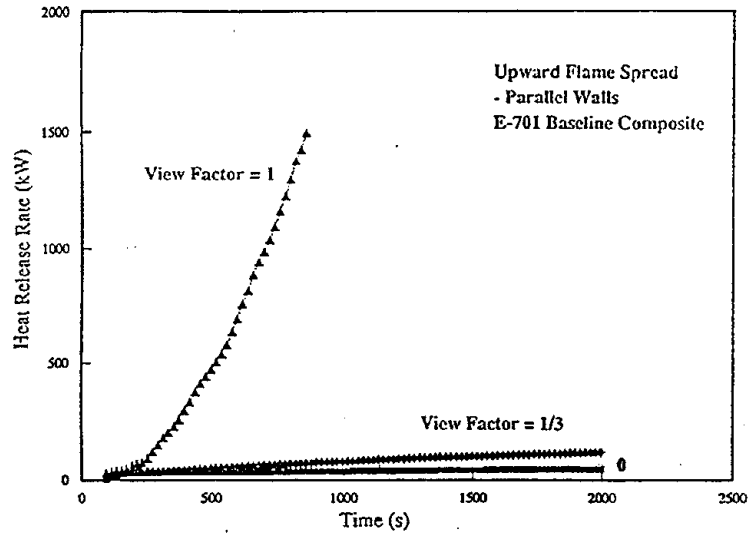


Figure 12. Heat Release Rate Histories For Parallel Wall Fire

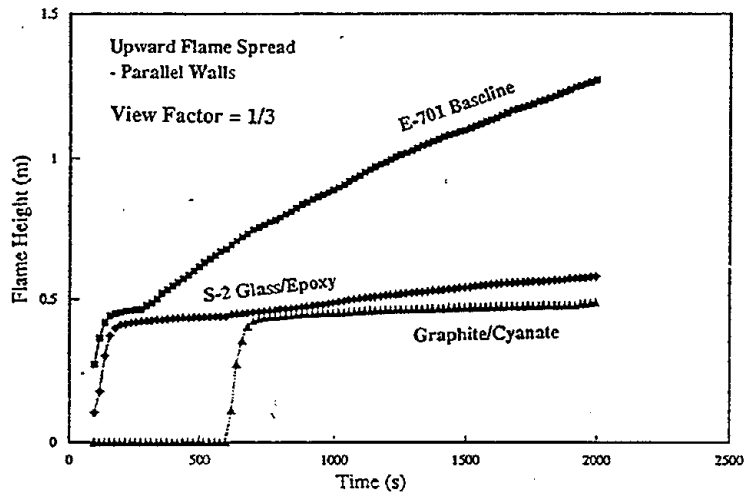


Figure 13. Comparison For Three Composites - Flame Height

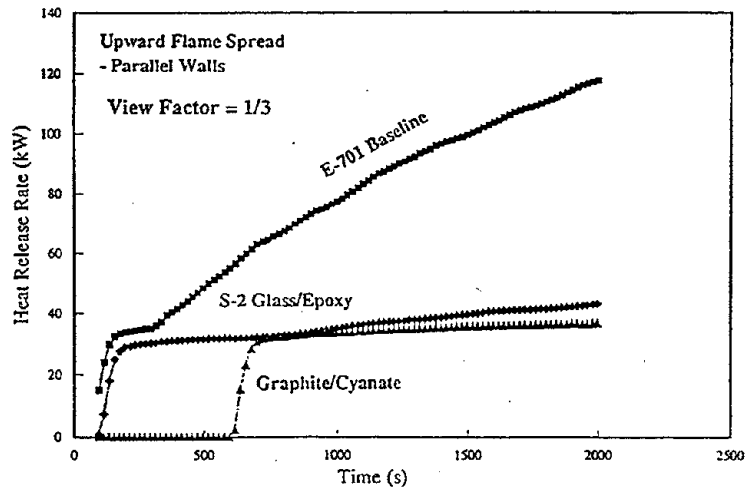


Figure 14. Comparison For Three Composites - Heat Release Rate

Discussion

Henri Mitler: The chronicled radiation fraction from PMMA was about 30%. Your colleagues have found 25% fitted better. I wonder if that could be explained by just noting that there is a substantial amount of radiation blockage?

Ronald Alpert: The answer is yes. Orloff and Markstein determined that there is roughly a 30% blockage factor of flame radiation back to the fuel surface. And I'm sure that has an effect.

William Grosshandler: I'm not an expert in this area, but I've observed for over a number of years, that so much is put on the results from either the FM flammability apparatus or the Cone Calorimeter results. Is there anything to be gained by doing a thorough analysis of those apparatus? That is, we have very sophisticated modeling methods, experimental measurement techniques. Is it useful to go back now and try to model what happens in these very fundamental laboratory apparatus to extract more information about pyrolysis and surface combustion?

Ronald Alpert: There are several organizations that are thinking about not necessary looking in more detail at these flammability apparatus, but in trying to determine more fundamental flammability properties going back to thermogravimetric analysis and differential scanning calorimeter. I know in particular, the FAA Technical Center is following this track.

Takashi Kashiwagi: Actually, when you look at a real sample, a lot of complicated things are happening, and these might be very important. The important questions is, can you include these phenomena? So far, the models are one-dimensional. Surfaces are flat, there is no swelling or bubbling, no cracking. These things actually happen. To model these requires a very basic scientific understanding. So my opinion is that, for now, if you want to model actual materials, we need to stay global. Meanwhile, we should look at the phenomena as deeply as we can.

Ronald Alpert: I agree. I prefer the global approach and that's what we are currently working with now with the University of Lund. We're trying to develop a global pyrolysis model that can be applied to real materials and develop parameters, equivalent flammability parameters, for real materials that can be used in these models.

Pravinray Gandhi: As you already mentioned, the problem arises when real materials are installed on real substrates. Many times, the burning behavior depends upon the distortion of the substrate. It may accelerate the burning because now the real surface gets exposed to fire. Would the model that FM is working on tackle the structure of fire problem together?

Ronald Alpert: Yes, I believe the global pyrolysis approach will, to some extent, take into account whatever the total material is as long as the total thickness is the sample is less than about 10 cm. Whatever happens will come out in the pyrolysis model. It will be reflected in the equivalent flammability parameter. I just want to emphasize the type of the variety of real materials that we see every day or week or month in our practice is truly amazing. There are different types of materials sent in from all over the world, and we have to deal with them, and it's a real challenge. You learn to appreciate the people that can deal with those materials when you see what they have to contend with.

CONCURRENT FLAME SPREAD IN FIRES -- STATE OF THE ART OF MODELING AND FUTURE PROBLEMS FOR ENGINEERING APPLICATION

Yuji Hasemi
Building Research Institute, Ministry of Construction
Tatehara 1, Tsukuba-City, Ibaraki-Pref. 305, Japan

ABSTRACT

Significance of concurrent flame spread for fire safety is summarized from experiences of unwanted fires and fire tests. State of the art of theoretical modeling and experimental findings on concurrent flame spread in fires is reviewed. Problems left unsolved for the rational assessment and design of fire safety are discussed. Similarity in the theoretical formulations of flame spread in different scales, configurations and fire scenarios and general complexity of the phenomena suggest needs of cooperation in different subfields of fire safety science which tend to deal with fires in specific environments.

Key Words: flame spread, heat flux, heat release, flame length, configuration effect.

INTRODUCTION

Concurrent flame spread is an important driving force of fire at any phase of its development. Upward flame spread along a combustible wall lining is very often a trigger for the occurrence of flashover. Horizontal flame spread along the ceiling surface or along the ceiling-wall boundary is another significant example of concurrent flame spread in room fire, and is believed to be a direct cause of flashover. The investigations on the King's Cross Underground fire disaster in 1987[1] have revealed the significance of fire growth in such an inclined trench with combustible lining as the escalators lined with wood at the London subway stations; this can be another example of concurrent flame spread which can cause tremendous fire hazard. City fires and forest fires are also typical examples of flame spread assisted by wind. It is important to note that fire spreading velocity in such mass fires very often reaches several to over-ten km per hour[2]. Such acceleration of the development of mass fires can take place only by the assistance of strong wind; however, still mathematical models of wind-aided mass fires tend to use similar concept and formulation with other types of concurrent flame spread[3]. In spite of the primary importance of concurrent flame spread in fire, there was considerable delay in its modeling in comparison with such other areas as smoke control and structural firesafety. However, there has been considerable progress in the modeling of concurrent flame spread in fires since 1980's. This paper intends to review present status of the scientific understanding of this phenomenon, and discuss strategies to develop engineering methodology to assess fire safety in view of concurrent flame spread.

EMPIRICAL AND EXPERIMENTAL EVIDENCES FOR THE IMPORTANCE TO MODEL CONCURRENT FLAME SPREAD IN FIRE

Modeling of concurrent flame spread in fires is not yet matured engineering. Although there are many mathematical models for idealized conditions, it is recognized experimentally that even slight change of configurations, or initial/boundary conditions can very often lead to extreme difference in experimental results. Also there are many empirical and experimental evidences demonstrating extreme fire hazard that can be hardly anticipated from conventional knowledge on fires. It should be useful to summarize evidences showing importance of concurrent flame spread in fires from previous experiments and fire investigations, before starting review of the theoretical framework for this process.

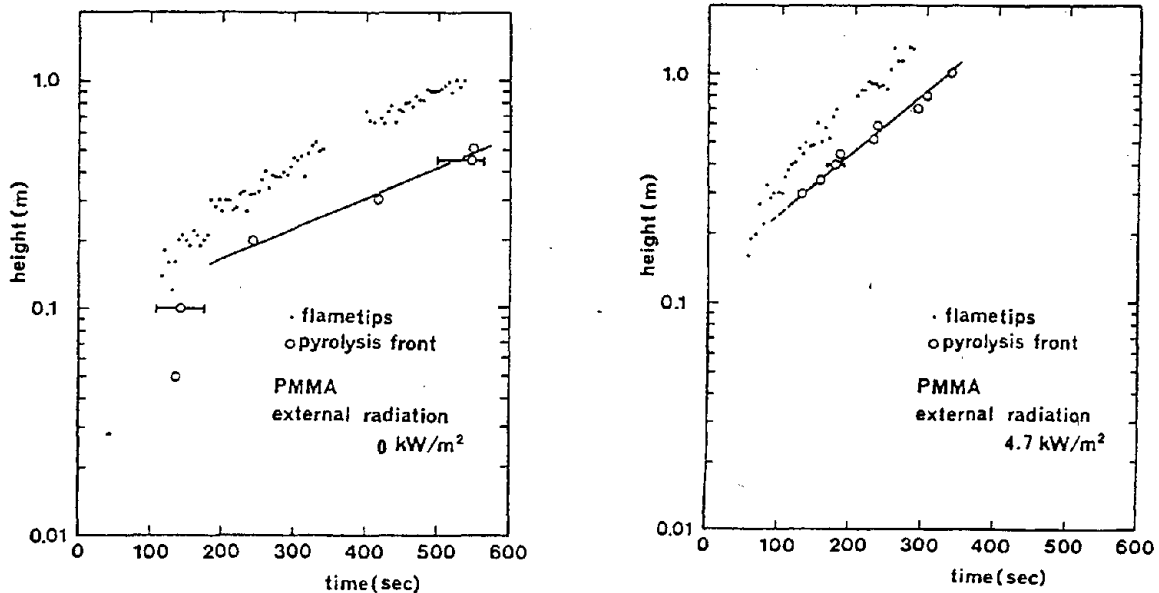
Flame Spread along an Inclined Combustible Solid

Upward flame spread along a vertical solid is a typical concurrent flame spread process in

quiescent environment. Many flame spread experiments suggest several to several-ten times faster flame spread on a wall than on an upward horizontal surface. Flame spread on an upward horizontal surface is essentially an opposed-flow flame spread; therefore it is an interesting and practically important problem at what angle the mode of flame spread changes from opposed flow to concurrent one on an inclined combustible surface. This problem was first dealt with by Hirano et al[4] through measurement of flame spreading velocity along inclined computer cards. According to their result, flame spreading velocity starts to become noticeably higher at an angle of approximately 30° . The King's Cross fire in 1987 drew strong international attention to the importance of flame spread on inclined surfaces for fire safety, and computational and experimental works have been carried out in relation to this problem[1]. Experiments by Drysdale and Macmillan on inclined PMMA slabs in relation with this fire disaster[5] demonstrate significant increase of flame spread velocity with respect to the angle of inclination beyond 15° while flame spread velocity was nearly independent of the angle of inclination from 0° (horizontal) to 15° . Especially their experiments with inert sidewalls show almost a jump of flame spreading velocity between 15° and 25° . Experimental work on a slightly different inclined trench[6] showed that the flame will attach to the trench base at an angle of 27° . These suggest a sudden transition from the opposed-flow flame spread mode to the concurrent one in an inclined trench although the transition is rather gradual on an inclined surface without sidewalls.

Acceleration by External Radiation

From experiences of real fires, it is widely recognized that flame spread can be accelerated significantly by external radiation from fire sources. Figure 1 compares development of flame tips and pyrolysis front during turbulent upward flame spread over vertical flat PMMA slabs without external radiation and with $q_e''=4.7 \text{ kW/m}^2$ [7]. Although the level of the external radiation is considerably weaker than typical flame radiation, the slope representing the flame spread velocity with external radiation was still notably steeper than that without external radiation. Flame spreading velocity divided by the length of pyrolysis front, V_p/x_p , is approximately twice greater for $q_e''=4.7 \text{ kW/m}^2$ than for $q_e''=0$.



(a) without external radiation

(b) $q_e''=4.7 \text{ kW/m}^2$

Figure 1 Movement of flame front and pyrolysis front (vertical PMMA slabs, Ref.7)

Fernandez-Pello[8] first pointed out possible significant acceleration of laminar flame spread by external radiation through enhancement of preheating of the unburnt surface and the activation of pyrolysis. The significant influence of external radiation shown in Figure 1 can be explained from the similarity solution of the thermal modeling[7] as discussed later. It is also important to note that, under stronger external radiation enough to ignite the surface by itself, external radiation may become a problem of surface ignition rather than that of flame spread.

Configuration Effects

The significant difference in the transition from opposed-flow flame spread to concurrent one between flat inclined open surfaces and inclined trenches suggests importance of configuration in the dynamics of flame spread. Such enhancement of flame spread in an inclined trench due to fluiddynamic effect has become widely known as the "trench effect" since the Kings Cross fire disaster, which is essentially a combination of the Coanda effect and the flame extension due to the restriction of entrainment. Air velocity measurements within open and closed parallel heated walls [9] suggest that stack effect can be another fluiddynamic effect to accelerate flame spread. Also the significant acceleration of concurrent flame spread over a flat wall by external radiation suggests potential importance of configuration effect on flame spread in a channel, wall corner and other 3-dimensional surface configurations through radiation feedbacks. Complexity in the cross-section of the combustible surface normal to the flow field, e.g. trench, groove and roughness, should generally increase effective surface area to feed fuel to the flame. This effect is believed to increase heat release rate, a driving force of flame spread. Configuration effects on flame spread in a real fire should be interpreted as a result of the combination of these three different mechanisms, i.e. the fluiddynamic effects, increase of heat transfer and increase of effective pyrolyzing surface.

There are also experimental evidences for the significance of configuration effects on concurrent flame spread. Acceleration of flame spread in parallel combustible-wall configuration with decreasing separation has been demonstrated experimentally on laminar flow[10] and on turbulent flow[11]. There are also many experimental evidences for the acceleration of flame spread in combustible wall-corner and in combustible corner-wall-ceiling configurations, and fire source in a wall-corner is already widely considered the worst scenario for a room fire. Notable acceleration of flame spread has been reported experimentally on grooved vertical wood panels[12], and vertical channels with combustible lining(Figure 2)[13].

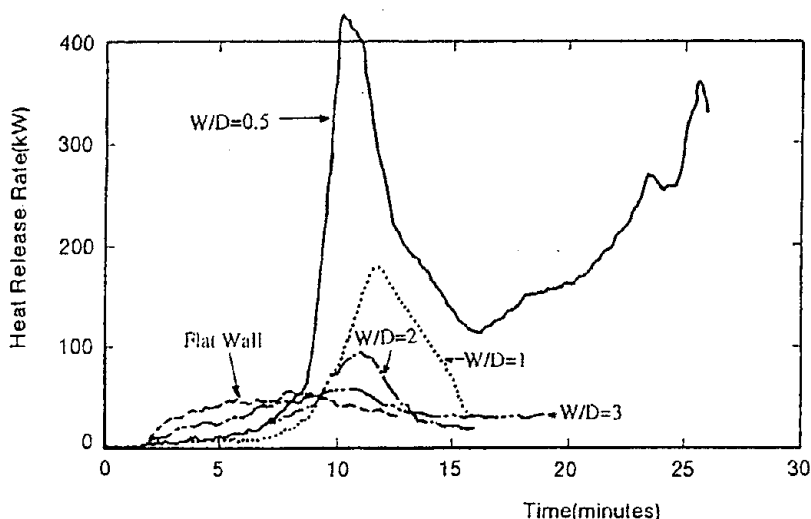


Figure 2 Time history of heat release rate by fires in vertical channels lined with particleboard ($D=0.20\text{m}$ for $W/D \geq 1$ and $D=0.40\text{m}$ for $W/D=0.5$, Fire source (surface area= WD) intensity in channel= 250kW/m^2 , Ref.13)

THERMAL MODELING OF CONCURRENT TURBULENT FLAME SPREAD

Concept

Main focus of flame spread for fire safety is the description of the movement of pyrolysis front. Location of flame front is often more important for practical purposes; however, in a concurrent flame spread, flame length is believed to be a function of length of pyrolysis zone and heat release rate, calculation of which essentially needs information on the location of pyrolysis front. Pyrolysis front is normally identified as the location where the surface temperature has reached an ignition temperature. Modeling approach of flame spread assuming primary importance of the heating mechanism in the vicinity of the pyrolysis front is called "thermal modeling". This approach describes ignition and flame spread as a result of inert heating of the solid to an ignition temperature, Fig. Mathematical modeling of flame spread over a combustible solid based on this concept was first applied to laminar flame spread by de Ris[14], and there was significant progress in quantitative understanding of various modes of laminar flame spread over a solid and liquid fuels during 1970's[4,8,10,15-20]. However, modeling of turbulent flame spread should be much more important for fire safety since turbulence is a principal feature characterizing flames in unwanted fires. Main difference between laminar and turbulent concurrent flame spreads is the mode of heat transfer from the flame to the surface; flame radiation dominates the surface preheating in turbulent flame spread, whereas gas phase thermal conduction is the main mode of the heat transfer in laminar one. Modeling of turbulent concurrent flame spread also needs formulation of flame length for the determination of the preheat distance. In spite of these notable differences between turbulent and laminar flame spreads, many of knowledges and modeling concepts obtained for laminar flame spread are probably useful for the understanding and the modeling of turbulent flame spread. Figure 3 shows a conception of the thermal modeling of turbulent concurrent flame spread (applied to a combustible wall). This model assumes a flame spread in the x-direction and a one-dimensional thermal conduction in the solid normal to the surface. Insignificance of the thermal conduction in the parallel direction to the surface has been established for vertical PMMA slabs by Ito and Kashiwagi[21]. If the char formation near the fuel surface is negligible, the surface temperature at x, $T_w(x,0)$ can be represented by the convolution as

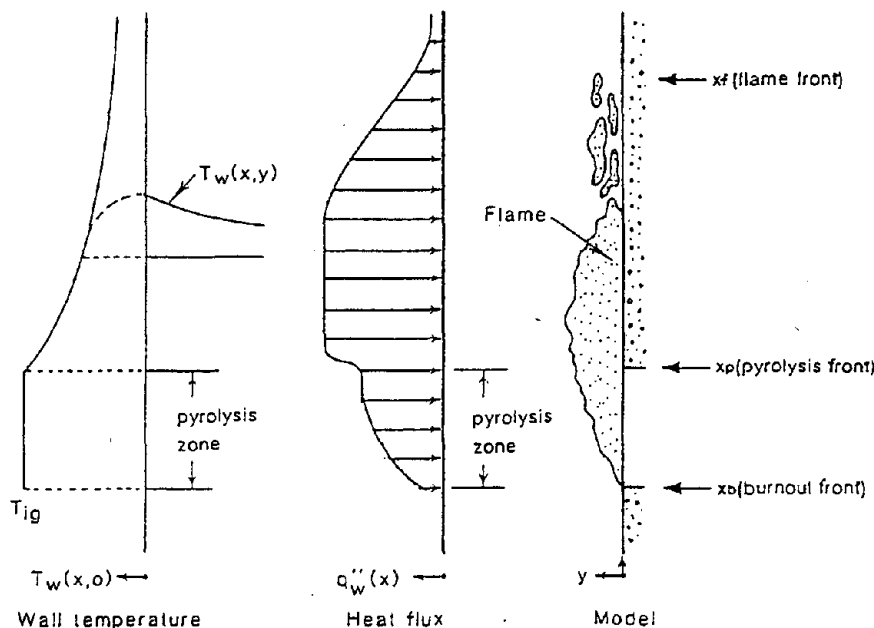


Figure 3 Schematic diagram of upward flame spread(Ref.30)

$$T_w(x,0) - T_o = \int q_w''(x,t-s) \cdot \phi(s) ds \quad (1)$$

where $q_w''(x, t-s)$ is the heat flux applied to the surface at $(t-s)$ after the beginning of experiment. $\phi(s)$ is an impulse response of the surface temperature to heat application, and is a function of such thermal properties as thermal conductivity, density and specific heat. Functional form of $\phi(s)$ depends on the boundary conditions; $\phi(s) = (\pi k \rho c s)^{-1/2}$ for a semi-infinite slab is a simplest example. The location of the pyrolysis front is given as a function of time by solving

$$T_{ig} - T_o = \int q_w''(x_p,t-s) \cdot \phi(s) ds \quad (2)$$

for x_p . Thermal properties and ignition temperature in equation (2) are believed to be obtained from bench-scale material tests. It has been confirmed that both $h(T_{ig}-T_o)$ and $h^2/k \rho c$ can be estimated through practical analysis of the ISO5657 Ignitability test results. Use of only parameters which can be obtained in engineering manner is an important benefit of this approach. Other approaches, field model for example, cannot draw an overall picture to assess fire hazard using such engineering properties. Surface heat flux is an important part of the model, and has been represented as a function of distance normalized by flame length, x/L_f , for most of practical situations. As discussed later, flame length can be further correlated against dimensionless heat release rate, $Q^* \equiv Q/\rho C_p T_{og}^{1/2} A D^{1/2}$ [22]. Formulation of flame length is also important for the prediction of flame front height, and is represented as $L_f = \gamma \cdot Q^* D$ for a flat wall with length of the pyrolysis zone to be substituted into the characteristic length scale D . Assuming the sole dependence of local heat release rate on local heat flux condition, contribution of the burning surface to total heat release can be formulated as

$$Q(t) = A_o \cdot q(t) + \iint q(x,t-s) V_p(s) \cdot \ell(s) ds \quad (3)$$

where A_o is the surface area of the first ignited part, and $\ell(t)$ is the width of pyrolysis front at t .

Local burnout is often observed during surface burning especially of charring material and thin linings. Burn out itself does not have a direct relevance with fire safety; however, modeling of the movement of the burnout front is necessary for the prediction of the length of pyrolysis zone, an important element determining the flame length. Except for thin linings, there is not yet clear engineering criterion determining the occurrence of local burnout.

Prediction of flame spread can be essentially made through calculating the surface temperature of a burning solid surface. However, since equation(1) or (2) generally cannot be solved in analytical manner for realistic heat flux conditions, several approaches of the formulation as follows have been attempted.

(a) Numerical calculation

(b) Analytical solution based on similarity assumption

(c) Analytical solution based on linearized flame length approximation

Effectiveness and limitation of each model depends on the level of adopted assumptions and analytical capabilities.

Numerical Calculation

Numerical calculation using finite difference grids along the burning surface and calculating the temperature of each grid is perhaps the most elaborate but simple formulation. Delichatsios et al[23], Kulkarni et al[24], and Mitler and Steckler[25] have developed numerical models, slightly different to each other. Either assumption of the functional form for temperature profile within the

slab normal to the surface or convolution-type formulation for the surface temperature of each grid could be adopted for simplification. Finite difference approximation for the heat transfer in the normal direction to the surface generally needs data of conductivity, density and specific heat of the material independently, whereas semi-infinite or thin-bed approximation needs such combination of the properties as $k \rho c$ that makes the engineering estimation of the input data much simpler. Numerical calculation of the pyrolysis and degradation of the burning surface can be complicated especially for charring materials. Treatment of the heat release from the pyrolysis zone can be simplified by using the time history of heat release rate exposed to the identical level of heat flux into the local heat release rate per unit area.

Benefit of the numerical approach is the relatively large capability to deal with realistic heat flux distributions and other conditions without introducing any simplification. Numerical models have been developed not only for flat walls[23-26] but also for vertical group cables[27]. Similar approach has been adopted in the modeling of forest fires, e.g.[28]. However, effect of embers in the spread of mass fires is seldom modeled although embers generally dominate flame spread velocity in mass fires[3,29].

Similarity Solution

Analytical solution of equation(1) for $x=x_p$ as a function of t can be obtained in a relatively simple form either if

- a) $dx_p/dt = \text{constant}$
- b) $x_p(t)/x_p(s) = f(t-s)$

The condition a) represents obviously the steady state, and $f(t) = \exp(\alpha t)$ is the only function satisfying small fire on the wall, and grows exponentially with time. Analytical solution for both assumptions for a semi-infinite combustible wall with realistic heat flux distribution have been reported by Hasemi[30] and Hasemi et al[7]. using the wall flame heat transfer represented as a function of $x_p/L_f \propto x_p/Q_f^{2/3} \xi$ and $\phi(s) = (\pi k \rho c s)^{-1/2}$, equation(2) are solved for the two conditions as

$$a) V_{pa} = \left[\int Q_f^{2/3} q_w'' (\lambda + 1/Q_f^{2/3}) / \lambda^{1/2} d\lambda \right]^2 \cdot x_p / \pi k \rho c (T_{ig} - T_o)^2 \quad (4)$$

$$b) V_{pb} = \left[\int q_w'' \{ \exp(\lambda) / Q_f^{2/3} \} / \lambda^{1/2} d\lambda \right]^2 \cdot x_p / \pi k \rho c (T_{ig} - T_o)^2 \quad (5)$$

Constant Q_f is assumed in the derivation of equations (4) and (5) from equation(2). It is important that the functional forms of equation(4) and (5) are very close; the integral part in the parenthesis [] is the only difference. With flame spreading velocity represented as a function of x_p , it is important that the preheating of unburnt surface by wall flame is the most significant for the steady flame spread and is the weakest for the case b) as the preheat length is essentially an increasing function of x_p . In the sense that any growing flame spread starting with a finite ignition source must fall in between the steady fire and the exponential fire, conditions a) and b) should be considered to give the upper and lower bound of the possible growing flame spread respectively. Figure 4 is a summary of the calculated $V_p / \{ x_p / \pi k \rho c (T_{ig} - T_o)^2 \}$ for a) and b) using the experimental q_w'' correlation summarized in Figure 6. $\Psi = V_{pa}(x_p) / V_{pb}(x_p)$ can be a measure of the predictability of flame spreading velocity in the sense that, if Ψ value is close to unity, flame spreading velocity starting with arbitrary initial condition must fall within a narrow range between the two solutions.

In Figure 4, it is noteworthy that $\psi = \pi k \rho c (T_{ig} - T_o)^2 \cdot V_p / x_p$ is very sensitive to Q_f especially in the low Q_f region. Since Q_f of a wall fire during an early stage of a building fire is generally lower than 0.5[7], this high sensitivity means that even a small change in the heat release rate from

the burning wall can result in dramatic change in the flame spreading velocity. Equations(4) and (5) also suggest a strong sensitivity of flame spreading velocity on $(T_{ig}-T_0)$. Surface temperature before the start of preheating by plume, T_0 , can be raised by external heating, e.g. radiation from fire source or convective/radiative heat transfer from smoke layer. Equations(4) and (5) suggest general importance of the evaluation of such external heating to the combustible surface for fire safety assessment.

Equation(4) is a generalization of the earlier steady flame spread velocity formulations assuming specific heat flux distributions, e.g. de Ris[14], Orloff, de Ris and Markstein[31], and Sibulkin and Kim[32]. Especially Orloff, de Ris and Markstein[31] derived a flame spread velocity formula using their experimental finding, $x_f(t) = x_p(t + \tau)$, which was found to be effective for transient growing fires on vertical PMMA. This relation may lead to another type of formulation of flame spreading velocity by taking the Taylor expansion of this relation with regard to τ as $x_f(t) - x_p(t) = x_p(t + \tau) - x_p(t) = dx_p(t)/dt \cdot \tau + d^2x_p(t)/dt^2 \cdot \tau^2/2 + \dots$;

$$V_p(t) = dx_p(t)/dt = \{x_f(t) - x_p(t)\} / \tau - d^2x_p(t)/dt^2 \cdot \tau / 2 - \dots \quad (6)$$

Equation(6) demonstrates equivalency of steady-state flame spread velocity to $\{x_f(t) - x_p(t)\} / \tau$. As discussed later, this relation is used as a main assumption for the modeling of concurrent flame spread based on the linearized flame length approximation. Equation(6) also suggests $\{x_f(t) - x_p(t)\} / \tau$ greater than $V_p(t)$ for an accelerated flame spread ($d^2x_p(t)/dt^2 > 0$) and $\{x_f(t) - x_p(t)\} / \tau$ smaller than $V_p(t)$ for a decelerated flame spread. However, it is also important that effectiveness of the empirical relation $x_f(t) = x_p(t + \tau)$ has been established only for growing flame spread[7,31, 33]. This relation should perhaps fail for decelerated flame spread.

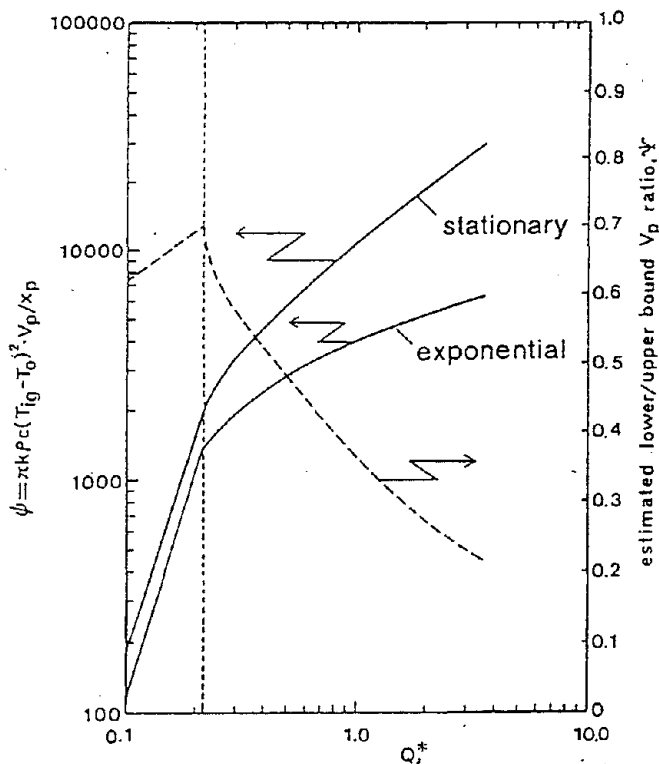


Figure 4 $\phi = \pi k \rho c (T_{ig}-T_0)^2 \cdot V_p/x_p$ for stationary and exponential flame spread modes and estimated lower/upper bound V_p ratio(Ref.7)

Comparing equation(4) and (6), τ can be formulated as

$$\tau = K \{ Q_0^{2/3} - 1 \} \pi k \rho c (T_{ig} - T_0)^2 / [\int Q_0^{2/3} q_w'' (\lambda + 1/Q_0^{2/3}) / \lambda^{1/2} d\lambda]^2 \quad (7)$$

Benefit of the similarity solution is the simplicity of the solution. Influence of any conditions on flame spreading velocity could be estimated easily in analytical manner. Nevertheless, this approach is believed to have limitation in the practical application, since equation(4) nor (5) cannot be applied to any situation where flame die out is anticipated.

Linearized Flame Length Approximation

A Volterra type integral equation has been developed for upward flame spread by Saito, Quintiere and Williams[33] assuming the following two proportionalities:

a) proportionality of V_p to the distance between the flame front, x_f , and the pyrolysis front, x_p , i.e.

$$V_p(t) = dx_p(t)/dt = \{ x_f(t) - x_p(t) \} / \tau \quad (8)$$

b) proportionality of flame length to heat release rate per unit width, i.e.

$$x_f = KQ_l \quad (9)$$

where Q_l is the total of heat release from the pilot flame, Q_0 and that due to the combustion of the wall, $Q_w(t)$. $Q_w(t)$ can be formulated as

$$Q_w(t) = \int q(t-s) V_p(s) ds + x_{p0} \cdot q(t) \quad (10)$$

where x_{p0} is the initial condition of the pyrolysis front height. Saito et al assumes equivalency of x_{p0} with the pilot flame height, KQ_0 [33]. Although flame length measurements support dependence of flame height on the 2/3 power of heat release rate[30,55], some measurements suggest apparent proportionality of flame height to the length of the pyrolysis zone[7,33]; it may reflect increase of surface heat flux in accordance with increasing the heat release rate[42]. Substitution of these relations into equation(8) makes a linear integral equation for $V_p(t)$ as

$$V_p(t) = [K \{ Q_0 + Q_w(t) \} - x_p] / \tau = [K \{ Q_0 + \int q(t-s) V_p(s) ds + x_{p0} \cdot q(t) \} - \{ x_{p0} + \int V_p(s) ds \}] / \tau \quad (11)$$

Equation(11) is often referred to as the SQW equation. SQW equation has been analyzed in detail[33,34,35,36], and its analytical solution has been obtained for several functional forms of heat release rate, $q(t)$ by Laplace transform. These analyses have revealed that the asymptotic behavior of flame spread can be classified into three different categories, divergence, vibration, and convergence, according to the combination of the peak heat release rate, $a = KQ_0$, characteristic decay time of heat release, t_c , and τ (Figure 5). Flame spread is expected to stop at certain height if the solution is categorized in the convergence or vibration regimes, and the maximum pyrolysis front height, x_{poff} , divided by x_{p0} becomes a function of only q_{max} , t_c and τ . Modification of SQW equation to incorporate the effect of local burnout has been proposed recently[36,37]. Substituting $x_f = KQ_l + x_b = KQ_l + x_{p0} + \int V_p(s) ds$ into equation(8) and ignoring the pilot flame after x_b has reached the pilot flame height x_{p0} , equation(8) yields

$$V_p(t) = [K \{ Q_0 \{ 1 - U(t-t_b) \} + \int q(t-s) V_p(s) ds + x_{p0} \cdot q(t) \}] + \{ x_{p0} + \int V_p(s) ds \} U(t-t_b) - \{ x_{p0} + \int V_p(s) ds \} / \tau \quad (12)$$

which will be referred to as the generalized SQW equation. As reported in many burn tests, local burnout is rather common for charring materials and thin combustible linings. Consideration of the

development of burnout front is important since it raises the bottom of the pyrolysis zone and can lead to higher flame front height and faster flame spreading velocity. Laplace transform of equation(12) can be summarized as

$$V_p(s)/x_{po} = [(KQ_0(s)/x_{po} - 1) \{1 - \exp(-tbs)\} + sKq(s)] / [s\tau - sKq(s) + \{1 - \exp(-tbs)\}] \quad (13)$$

Change of the sign of the roots of the characteristic equation for equation(13) for a step-like heat release function, $q(t) = q_0 \{1 - U(tb)\}$,

$$s\tau + \{1 - \exp(-tbs)\}(1-a) = 0 \quad (14)$$

occurs at $\tau/tb = a - 1$; for $\tau/tb > a - 1$, the real root of equation(14) is negative and flame spread is expected to stop at certain height. Flame spreading velocity is expected to diverge for $\tau/tb < a - 1$. Similar criticality has been derived for thin linings by Mowrer and Williamson[38] through different definition of the local burnout time, t_b .

A model of a room corner fire assuming a two-dimensional development of pentagonal pyrolysis zone has been developed by Cleary and Quintiere[39]. This model formulates the growth of the pyrolysis zone according to the rule represented by equation(8), and is considered an extension of this approach from a one-dimensional wall fire to room fires. The model uses similar treatment of the local burnout time with the one-dimensional wall fire model for thin linings[38].

Linearized flame length approximation is useful to see what parameters are the most dominant for flame spread, and to obtain overall picture of the flame spread. One important practical relation that this approach can offer is the similarity of flame spread velocity and pyrolysis front height with regard to the pilot flame height, x_{po} . Figure 5 also summarizes solution of equation(12) for x_{poff}/x_{po} with $q(t) = q_0 \cdot \exp(-t/t_c)$ without consideration of the movement of burnout front for the location of the maximum pyrolysis front height, x_{poff} .

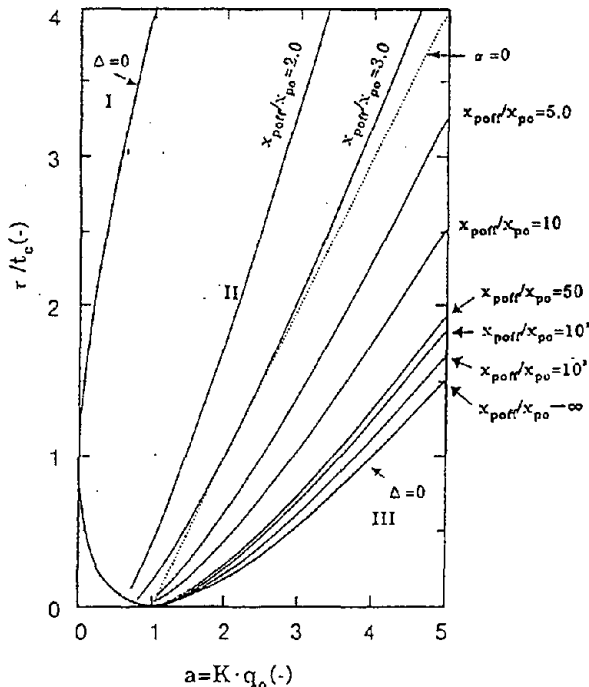


Figure 5 Division of the $Kq_0 - \tau/t_c$ plane for $q(t) = q_0 \cdot \exp(-t/t_c)$ (sustained pilot flame). The solution is diverged in the region III.

In spite of the extensive analytical capability of this approach, this approach seems to have still unsolved difficulties in the basic assumptions and the treatment of local heat release rate. Equation(6) demonstrates that equation(8) can hold in general only for steady state flame spread, although this approach uses equation(8) as a basic assumption even for transient flame spread. In the interpretation of experimental results, use of measured time between the arrivals of pyrolysis front and flame front into τ should lead to greater $\{x_f(t) - x_p(t)\}/\tau$ than $V_p(t)$ for accelerated flame spreads, and that for decelerated flame spread should result in smaller $\{x_f(t) - x_p(t)\}/\tau$ than measured $V_p(t)$. Another condition in which the form $V_p = \{x_f(t) - x_p(t)\}/\tau$ can be effective is a wall fire developing exponentially with time. Solution of equation(12) for $q(t) = q_0$ and $Q_0(t) = 0$, $x_p(t) = x_{p0} \cdot \exp\{(a-1)t/\tau\}$, relation between and the time interval between the arrivals of pyrolysis front and flame front, t^* , can be obtained from $x_f(t) = x_p(t+t^*) = a \cdot x_p(t)$ as $t^*/\tau = \ln(a)/(a-1)$, and τ can be quantified as

$$\tau = K \{Q_0^{2/3} - 1\} \pi k \rho c (T_{ig} - T_0)^2 / \left[\int q_w'' \{ \exp(\lambda) / Q_0^{2/3} \} / \lambda^{1/2} d\lambda \right]^2 \quad (15)$$

from comparison between equation(5) and equation(8). Application of this approach to transient fires needs such redefinition of τ . The linearized flame length approximation may also cause unignorable discrepancy especially for an accelerated flame spread. Proportionality of flame length on a wall to 2/3 power of heat release rate has been established experimentally; this suggests gradual approach of the pyrolysis front to the flame front on a thick combustible wall with development of the pyrolysis front as far as heat release rate per unit area is kept constant and local burnout is ignorable[40]. However, effectiveness of this anticipation is critical since dependence of surface heat flux on scale and fire intensity has been reported experimentally[41]. Difficulty related to the local heat release rate comes from the limitation of the functional form of $q(t)$ for analytical solution of equation(12). Complicated time history of heat release rate common for thick charring materials is perhaps difficult to describe with any function which fits Laplace transform.

Recent extension of this approach to a nonlinear flame length formulation by Kokkala and Baroudi[42] may resolve at least the heat release rate part and the flame length approximation part of the difficulties. They derived the following finite difference approximation for equation(8).

$$x_p(t_{i+1}) = (1 - \Delta t_{i+1}/\tau) x_p(t_i) + x_f(t_i) \Delta t_{i+1}/\tau \quad (16)$$

where t_i and t_{i+1} represent " i "th and " $i+1$ "th time steps respectively. Flame front height is formulated in the front $x_f(t_i) = KQ(t_i)^{2/3}$, and the contribution of the wall flame to total heat release rate is calculated by using $V_p(t) = \{x_f(t) - x_p(t)\}/\tau$ in equation(3). This quasi-numerical model does not need linearized flame approximation any longer, and has been applied to the wall burning of thick charring materials. Comparison of this model with full scale tests shows considerable capability to deal with the dual peaks of local heat release characteristic to thick wood slabs.

FLAME LENGTH AND FLAME HEAT TRANSFER CORRELATIONS

Distribution of surface heat flux especially from the flame is an important input for the prediction of upward flame spread. Since flame heat transfer is believed to be controlled by flame length, it is important to summarize flame length and surface heat flux as a function of properties available from fire source and building conditions. Previous experimental works on flame length and flame heat flux are summarized on different configurations in this section. However, heat flux measurement became common in fire research only in 1980's probably because of the only recent popularization of the use of heat flux gages in fire research; in spite of the importance of heat flux for fire growth, only few works have been done on ceiling fire, and inclined upward surfaces.

Flat Wall

Measurement of surface heat flux due to a wall fire was pioneered by Faeth et al[43,44] in 1970's, and practical correlations were obtained during 1980's[30,45]. Summary of wall flame heat flux distributions from line burners, vertical wicks and burning walls demonstrates nearly sole-dependence of heat flux on the height normalized by flame length, x/L_f . Since wall flame height from a line fire is represented as $L_f = \gamma Q_f^{2/3} \cdot D$ with $n \approx 2/3$, q_w'' could further be correlated against $x/Q_f^{2/3} \cdot D$ as seen in Figure 6. Heat flux within the solid flame ($x < 1.2x/Q_f^{2/3} \cdot x_p$) was nearly constant with height, and, for $Q_f < 100 \text{ kW/m}$, q_w'' was found to be approximately $25\text{-}35 \text{ kW/m}^2$ irrespective of fuel or heat release rate. However, recent measurement on larger heat release rate from a square burner against a inert wall by Back et al[41] demonstrates gradual increase of heat flux in solid flame with increasing source heat release rate, and q_w'' in the solid flame for approximately $Q > 500 \text{ kW}$ was found to exceed 100 kW/m^2 . The decay of heat flux characteristic in the intermittent flame and in the plume was still consistent with previous experimental correlations[30]. The very high heat flux in the solid flame observed for large source heat release rate is probably enough high to maintain pyrolysis from common charring materials, whereas it is common that forest products be self-extinguished if the surface is not exposed to external radiation. Height of wall flames from rectangular or square burning surfaces has been correlated against $Q_{\text{mod}}^* = Q / \rho C_p T_{\text{og}}^{1/2} (DW) W^{1/2}$ [13]; flame height becomes larger as the aspect ratio of the burning source, W/D , is increased until it reaches the line fire limit (Figure 7(a)).

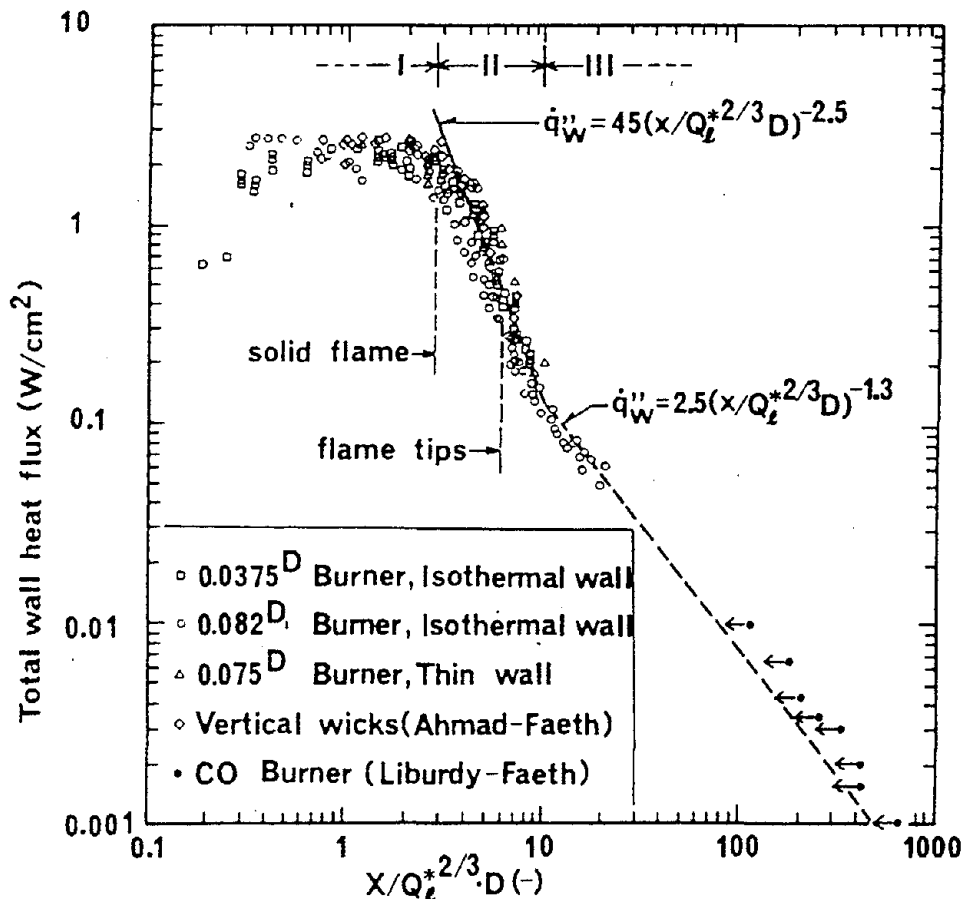
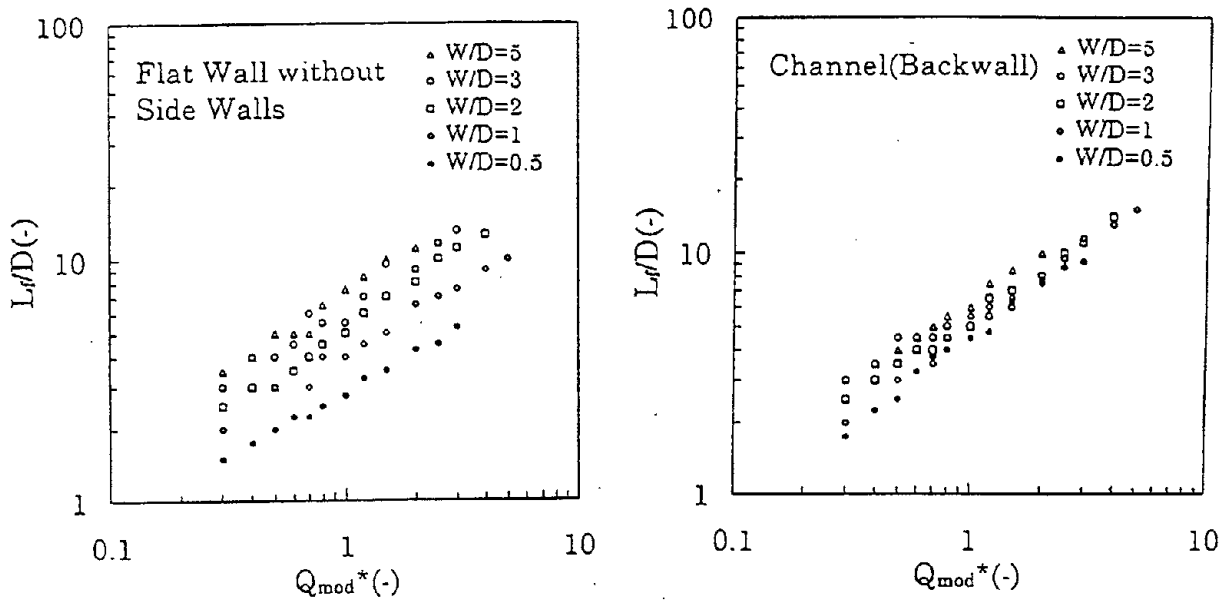


Figure 6 Total wall heat flux vs. height normalized by $Q_f^{2/3} \cdot D$ (data from various resources, Ref.30)



(a) Flat Wall

(b) Flame height measured at the center of the backwall of a channel

Figure 7 Flame height vs. Dimensionless heat release rate, Q_{mod}^* (Ref.13)

Wall Corner

It is widely recognized that flame height from a fire source can become considerably higher in a wall corner than on a flat wall due to the restriction of entrainment [46,47]. Height of flame from a pool fire in a corner of walls without ceiling has been correlated against $Q^* = Q / \rho C_p T_{og}^{1/2} D^{3/2}$ with D as the characteristic scale length of the fire source. More recent experiments on surface burning in a wall-corner [48] show approximately 40% larger flame height for wall burning than for a pool fire in the corner if $Q_{DH}^* = Q / \rho C_p T_{og}^{1/2} (DH) H^{1/2}$ with H as the burner height is used for the dimensionless heat release rate. However, it is also important that, in a wall-corner configuration, heat flux to the wall surface within and above the flame can also become higher than on a flat wall due to the radiation between the two adjacent heated wall surfaces. According to the two-dimensional measurements of heat flux in open wall-corner configurations, this extra heating effect is particularly pronounced within the solid flame [47,48]. These measurements show sole dependence of heat flux along the corner edge on the height divided by the flame length.

Corner-Wall-Ceiling

Although horizontal flame spread along the ceiling and the upper part of the walls exposed to flame or smoke layer is an important part of fire growth in room fires, most of compartment fire models [49,50] seem to use unverified empirical estimates for the flame heat transfer or flame spread velocity for these horizontal concurrent flame spread. However, this only reflects the lack of experimental data and analysis for such configurations.

Flame length from a fire source in the open room corner configuration, with ceiling, has been reported by Gross [51]. His data showed failure of flame length correlation against Q^* in this configuration; replacement of burner size by ceiling height in the expression of Q^* has resulted in a remarkable concentration of his data along one curve [52]. However, physical implication of this redefinition is unclear since $D^{3/2}$ part of the definition of Q^* is essentially the product of the area

normal to the forced-flow direction and the square root of the length representing buoyancy. Some heat flux data have been published on a 7.6m tall open corner-wall ceiling configuration with and without combustible linings[53]. More recent experiments using a reduced-scale open corner-wall-ceiling rig[48] have correlated flame length from pool fires in the corner and from corner-wall fire against Q_{DH}^* and have described the distribution of surface heat transfer to the ceiling surface and to the ceiling-wall boundary as a function of the horizontal distance normalized by horizontal flame length measured from the corner. According to this flame length correlation, horizontal flame length depends only very weakly on heat release rate; this suggests easier involvement of ceiling by flame with decreasing the size of enclosure. Gross' data of flame length have been found to be consistent with this correlation. Decay of heat flux with respect to relative distance to flame length has been found to be steeper in the wall-corner surface burning than in the pool fires.

Vertical Channel

Flame height and surface heat flux have been measured on inert vertical channels of different aspect ratios with porous rectangular propane burners settled at the bottom of the channels[13]. The measurements demonstrate notable augmentation of flame height for the aspect ratio, W/D , not larger than 1, compared with flames over a flat wall. The L/D vs Q_{mod}^* curve for each aspect ratio becomes closer to the line-fire limit probably because of the restriction of entrainment in the horizontal direction to the wall surface(Figure 7). Surface heat flux to the backwall within the solid flame reached almost 90kW/m^2 , twice to three times larger than that on a flat wall. Surface heat transfer correlations against height divided by flame height in a channel beyond the solid flame have been found to be nearly consistent with the flat-wall correlations. A full-scale burn test of flame projection due to fully-developed room fires[54] has also reported significantly higher heat flux to the facade in vertical channel configuration of the facade than on a flat facade. The reported facade heat flux value exposed to a solid flame in a channel of the aspect ratio approximately 1.0, 130kW/m^2 , is higher than the laboratory tests[13], and is believed to endorse the fire-source dependence of heat flux reported more systematically by Back et al[41]. 130kW/m^2 is equivalent to $1,000^\circ\text{C}$ black body radiation, and is believed to be close to the upper bound for possible heat flux in fire.

Other Configurations and External Heating from Smoke Layer

Other configurations in which concurrent flame spread can be accelerated include parallel walls and shafts. Foley and Drysdale[55] measured heat flux to the surfaces of parallel vertical walls from line fires against one wall and between the two walls and represented its vertical distribution as functions of Q^* and δ/D , the separation distance between walls divided by the burner length.

In the flame spread over a combustible lining surface exposed to smoke layer, heating of the surface by the smoke layer can influence the flame spreading velocity. Heat transfer from the smoke layer to the wall or ceiling surface should depend at least on the emissivity of the smoke and the surface, roughness of the surface, and the orientation; fire experiments using a porous burner with heat output $100 \sim 300\text{kW}$ as the heat source and approximately $3\text{m} \times 12\text{m} \times 2.4\text{m}$ (tall) enclosure with a continuous opening along the longer side reported $0.03 \sim 0.04\text{kW/m}^2\text{K}$ for the total heat transfer coefficient[56]. This heat transfer coefficient range suggests 6kW/m^2 gage output for $150 \sim 200\text{K}$ excess temperature which is believed to be rather typical in a preflashover fire. This heat flux is enough to cause considerable acceleration of flame spread as shown in Figure 7. Janssens[57] has reported consistent h values for the ISO5657 ignitability test apparatus.

FIRESAFETY ASSESSMENT AND ENGINEERING APPLICATION OF THERMAL MODELS OF CONCURRENT FLAME SPREAD

Some of the flame spread models discussed in previous sections have been validated against

relatively large scale burn tests[e.g. 7,24,26,37]. However, the tests were conducted on ideal materials from the experimental point of view to reproduce ideal conditions that the models try to simulate. It is believed that application of these models to firesafety assessment needs special consideration of the conditions of building occupancies, availability of practical test methods fitting the modeling methodology and other conditions which may have influence on fire behavior in the real world. In this section, research and technical informations concerned with the application of the concept of flame spread models are reviewed, although perhaps many of these studies may not have direct relevance with flame spread modeling.

Practical Evaluation of Flame Spread Hazard

Strong sensitivity of flame spread behavior to environmental conditions and configurations suggests necessity of the consideration of detailed design informations for the firesafety assessment with regard to flame spread. Direct application of the thermal models with such consideration could be made for the design of standardized mass products such as aircraft and other transportation vehicles or for the design of a big construction project. However, firesafsty assessment of buildings generally has to deal with small projects designed and built by amateurs on fire safety engineering. Application of mathematical models to small construction projects is believed to be difficult also in the sense that, although fire growth is believed to sensitive to furnishings in small enclosures, it is generally difficult to predict or identify what furnishings be used after the completion of the building.

Dimensional analysis and the use of the key parameters controlling the growth of fire are generally considered effective and robust approaches to evaluate rationally the fire hazard in any conditions characterized by such uncertainty. Quintiere[58] has shown clear bifurcation of the qualitative results of the ISO9705 Room Corner Test according to a dimensionless parameter which is essentially equivalent to the acceleration/deceleration criticality for upward flame spread derived from equation(14). The room fire behavior dominated by wall fires[58] may possibly be a result of the use of a small room; validation of this correlation against larger rooms should be interesting problem for the generalization of such approach. Dimensional analysis by Karlsson and Magnusson[59] using the thermal inertia, peak heat release rate and its decay parameter of material exposed to certain heat flux level and lateral flame spread parameter and that by Kokkala, Thomas and Karlsson[60] using time-to-ignition and integrated heat release rate at certain heat flux level reproduce results of numerical calculations of fire growth in the ISO9705 Room Corner Test. The analysis of Quintiere[58], and Kokkala, Thomas and Karlsson[60] use essentially data only from ignitability and dynamic heat release measurements.

Material Properties for the Flame Spread Assessment

Material properties necessary for the input for the thermal models are k , ρ , c , T_{ig} , and the time history of heat release rate under anticipated heat flux from flame and fire environment. For the engineering application of the thermal modeling, it is important to develop practical methodology to estimate these properties. The current activity at ISO/TC92/SC1(Reaction to fire) tries to develop bench-scale tests conforming to this approach and summarize the methodologies for the application of the test results to the prediction of fires[61,62].

Among the parameters listed above, k , ρ , c and T_{ig} are believed to represent the ignitability. Thermally-thick solid assumption is very often used to reduce the number of unknowns from k , ρ , c and T_{ig} to $k \rho c$ and T_{ig} . These properties can be estimated from time-to-ignition, t_{ig} , data for different levels of external radiation, q_e generated from such radiation exposure test as ISO5657 Ignitability test. The methodology was first demonstrated in 1960's[61], and numbers of modification have been reported since then. Using an approximation of the equation(2) for a semi-infinite inert solid, Janssens[57] has obtained

$$q_e'' = q_{cr}'' \{ 1 + 0.73(k \rho c / h^2 t_{ig})^{0.547} \} \quad (17)$$

where q_{cr}'' is the critical heat flux for ignition defined as $q_{cr}'' = h(T_{ig} - T_0)$, and h is the total heat transfer coefficient. An apparent $k \rho c$ value can be estimated from the linear fit according to equation(17) whilst q_{cr}'' follows from the intercept with the abscissa. Simplicity of the procedure and testing method is an important benefit of this estimation method. However, estimated $k \rho c$ value is so sensitive to the slope of $t_{ig}^{-0.547}$ against q_e'' that data-scattering or failure of semi-infinite inert solid approximation should result in considerable uncertainty of the material properties.

Advancement of the measurement of combustion heat release based on the oxygen consumption method since late 1970's has made it possible to measure dynamic combustion heat release in an open environment within the accuracy acceptable for engineering purposes[64]. These have been numbers of applications of the oxygen consumption principle from bench scale tests to such full scale tests as Room Corner Test. Cone Calorimeter is the most popularized bench scale testing apparatus for the measurement of dynamic heat release under external radiation[64].

The state of the art of bench scale ignitability and heat release test methods suggests considerable possibility that concurrent flame spread be assessed through bench scale tests. Application of these tests to the prediction of flame spread has been reported already[25,26,37,39,40,49,50,58,61,63]. However, it is important that the capability of bench scale test apparatus to reproduce end-use conditions of tested materials and the correspondence of test conditions with fire environment are not yet very clear. Originally heat release rate from common combustible building and furniture materials is believed to be sensitive to the heating condition[37,58]. In spite of the primary importance of flame spread for firesafety at relatively weak external heating, say less than 10kW/m^2 , there is still general technical difficulty in running Cone Calorimeter at such weak level of irradiance. Heat release rate obtained from Cone Calorimeter at a level of external heat flux of 25kW/m^2 or lower was considerably lower than that obtained for identical heating condition from full scale or intermediate scale heat release measurement[65], whereas only a slight difference has been observed at an external radiation of 30kW/m^2 or higher[66]. This lower heat release rate obtained from Cone Calorimeter(vertical orientation) especially at low external heat flux is attributed to the lower combustion efficiency[63]. Intermediate scale heat release measurement[66] may lead to heat release rate value closer to that in fire. Determination of the ignitability parameters through time-to-ignition measurement may not need strict consideration of the reproduction of fire environment. However, it is generally recognized that ignition temperature can be affected by the orientation and configuration of the surface of the material[67].

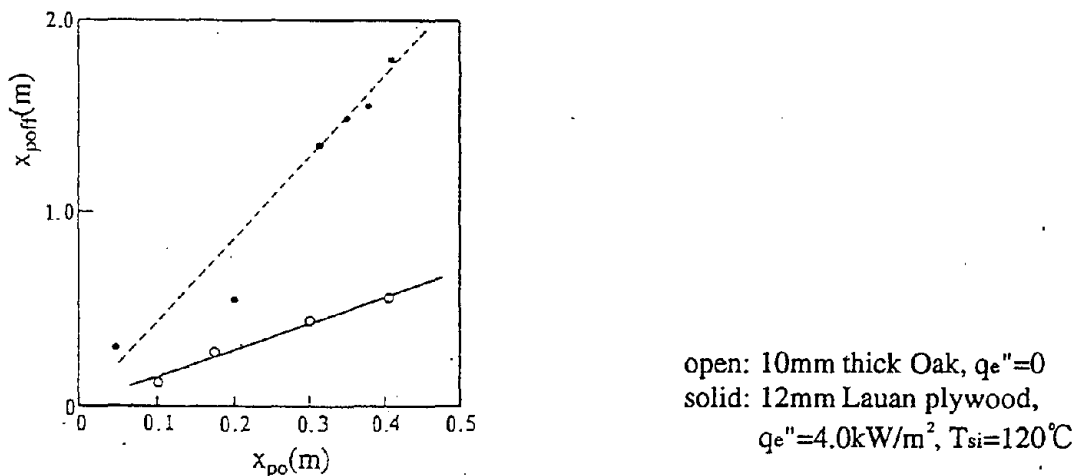


Figure 8 Relation between pilot flame height and maximum pyrolysis front height(Ref.37)

Intermediate-Scale Flame Spread Test

Independence of x_{poff}/x_{po} on x_{po} for upward flame spread is an important relation derived from the linearized flame length approximation. This relation suggests the possibility that x_{poff} for a full scale fire can be estimated from a small scale test using a small pilot flame even if solution of equation(12) cannot be obtained either due to the complexity of the functional form of $q(t)$ or even the lack of the data of material properties[36]. Figure 8 is a summary of the measured maximum pyrolysis front heights for different pilot flame heights, and show general support of the conservation of x_{poff}/x_{po} value against the change of pilot flame height. Although reduced scale flame spread test is only a sort of ad-hoc test, this approach does not need any mathematical treatment of the test data nor sophisticated apparatuses.

Evaluation of Ignition Source Intensity

The conservation of x_{poff}/x_{po} for x_{po} suggests general importance of the evaluation of ignition source intensity for fire safety assessment of wall fires. Combustion of furniture is a typical ignition source to wall lining. Identification of possible fire sources for the ignition and external heating of lining surface and control of the combustion heat release from furnitures should be useful for rationalizing the evaluation procedure. The oxygen consumption principle has been applied to the measurement of heat release rate from possible fire sources in buildings[68], and has been implemented into furniture combustibility regulations[e.g. 69]. Methodologies to reduce heat release rate from furnishings without causing significant influence on other furniture performances have been developed[70].

Another important condition of ignition source which may have significant influence on wall fires is the relative location of the ignition source to the wall. Measurements of heat flux at the corner wall from fire sources at different distances in the room corner fire configuration[71] have demonstrated relatively large change of surface heat flux by only the differences of 5cm in ignition source location. The measurements also showed relatively large heat flux value, 60kW/m^2 , to the wall corner exposed to the solid flame from the burner attached to the corner. This strong heat flux is attributed partly to the radiation feedback between the two adjacent corner walls.

CONCLUDING REMARKS

It was perhaps in ancient times or even prehistoric age that concurrent flame spread was first recognized as the primary cause for significant fire disaster. Ideas to prevent this phenomenon in built environment or in wildland can be seen in the tradition of any culture all over the world. However, until recently, it seems that significance of concurrent flame spread was excessively connected with its extreme sensitivity to environment and configurations. The state of the art of the understanding of concurrent flame spread in fire, especially upward turbulent flame spread, and advancement and popularization of measurement technology seem to show fairly good achievement in the establishment of the framework to deal with this important process of fire growth in sound scientific manner, although there are still unsolved problems and progress of its scientific understanding has revealed new uncertainty of this phenomenon.

There is considerable delay in the application of engineering concept in the control of fire growth in comparison with smoke control and structural fire safety. Although the present stream of mathematical models to predict structural behavior and smoke movement in fire started already in 1960's and the framework for engineering evaluation of these were nearly established in 1970's, only pioneering works were available on turbulent flame spread in fire until around the beginning of 1980's. As introduced in this review, there are already many trails to develop testing and evaluation method on concurrent flame spread especially in buildings. These efforts will probably develop engineering firesafety design method of interior and exterior linings and classification of materials based on firesafety engineering. However, another potential important subject which may

result from the establishment of engineering approach to this phenomenon is the design of the material properties for firesafety. Of course control of material combustibility has a long history; however, it seems that conventional fire retardant technologies lack in the guidelines to demonstrate quantitatively what change in the structure or composition of materials can lead to the improvement of firesafety. Engineering modeling of pyrolysis, solid phase heat and mass transfer and heat release in conjunction with surface burning should be encouraged to develop strategies for the engineering design of materials from the firesafety viewpoint. Mathematical models to predict concurrent flame spread from material properties should be useful to develop techniques to control likelihood for fire development at various stages from chemical composition of the materials to the construction and finish of the materials. Effectiveness of other firesafety measures such as smoke exhaustion for the prevention of the acceleration of flame spread by the heating from smoke layer would also be worth studying.

There are fewer engineering modeling works on mass fires, inclined surfaces, vertical combustible shaft and other special configurations than on vertical surface and room fires. Comparison with upward flame spread may resolve some of the unsolved problems in these areas. Interactions in experts dealing with different modes or configurations of concurrent flame spread and related combustion and pyrolysis processes should be encouraged.

Only the diagrams from the publications by the author are used in this report only because of the anticipation of possible copyright limitation, and it does not imply any superiority of the work of the author to others. The readers are invited to consult with relevant papers in the list of reference. Also turbulent concurrent flame spread may relate with varieties of fire problems. Perhaps the list still misses many valuable works in this area worth studying for deeper understanding of the problems discussed in this report.

TERMINOLOGY

A: surface area of burning surface, C_p : specific heat of air, D: characteristic fuel size or channel depth, H: ceiling height or height of burning surface of wall, K: constant representing the proportionality of flame length to heat release rate based on the linearized flame length approximation, L_f: flame length, Q: heat release rate, Q*: dimensionless heat release rate ($Q / \rho C_p T_o g^{1/2} D^{5/2}$), $Q_{DH}^* : Q / \rho C_p T_o g^{1/2} (DH) H^{1/2}$, $Q_H^* : Q \rho / C_p T_o g^{1/2} H^{5/2}$, Q_l : heat release rate per unit width, $Q_l^* : Q_l / \rho C_p T_o g^{1/2} D^{3/2}$, $Q_{mod}^* : Q_l / \rho C_p T_o g^{1/2} (DW) W^{1/2}$, Q_o : heat release rate from ignition source, Q_w : heat release rate due to surface burning, T_{ig} : ignition temperature, T_o : ambient temperature, T_{si} : initial surface temperature, T_w : wall surface temperature, U(t): Heaviside's Unit function, V_p : flame spreading velocity, W: width of burning surface or channel, a: Kq_o , c: specific heat of material, g: gravitational acceleration, h: surface heat transfer coefficient (total), k: thermal conductivity, q: local heat release rate, q_e'' : heat flux due to external radiation, q_o : peak heat release rate, q_w'' : heat flux from flame, τ_c : characteristic decay time of heat release rate, t_{ig} : time to ignition, t^* : time from the arrival of flame front to that of pyrolysis front, x_b : location of burnout front, x_f : location of flame front, x_p : location of pyrolysis front, x_{po} : height of pilot flame, x_{poff} : maximum pyrolysis front height, δ : separation distance between parallel walls, ρ : density, τ : characteristic ignition time, $\phi(t)$: impulse response of surface temperature to surface heat flux. A *Symbol in italics* is the Laplace transform of the variable represented by that symbol.

REFERENCES

1. Fire Safety Journal, Special Issue: The Kings' Cross Fire, Vol.18, No.1, 1992.
2. Han, S., Han, Y., Jin, J. and Zhou, W.: The Method for Calculating Forest Behavior Index, Proceedings of the First Asian Conference on Fire Science and Technology, p.77, 1992.

3. Telitsin, H.P.: Flame Radiation as a Mechanism of Fire Spread in Forests, Afgan, N.H. and Beer, J. M. ed: Heat Transfer in Flames, Wiley, 1974.
4. Hirano, T., Noreikis, S.E., and Waterman, T.E.: "Postulations of Flame Spread Mechanisms", Combustion and Flame, 22, p.353, 1974.
5. Drysdale, D.D., and Macmillan, A.J.R.: Flame Spread on Inclined Surfaces, Fire Safety Journal, 18, p.245, 1992.
6. Smith, D.A.: Measurements of Flame Length and Flame Angle in an Inclined Trench, Fire Safety Journal, 18, p.231, 1992.
7. Hasemi, Y., Yoshida, M., Nohara, A., and Nakabayashi, T.: Unsteady-state Upward Flame Spreading Velocity along Vertical Combustible Solid and Influence of External Radiation on the Flame Spread, Proceedings of the Third International Symposium on Fire Safety Science, Edinburgh, 1991.
8. Fernandez-Pello, A.C.: Upward Laminar Flame Spread under the Influence of Externally Applied Thermal Radiation, Combustion and Flame, 17, p.87, 1977.
9. Bellin, B., Most, J.M., Joulain, P. and Sztal, B.: Interaction between Two Burning Vertical Parallel Walls, Proceedings of the Second International Symposium on Fire Safety Science, Tokyo, 1988.
10. Kim, J.S., de Ris, J. and Kroesser, F.W.: Laminar Burning between Parallel Fuel Surfaces, International Journal of Heat and Mass Transfer, 17, p.439, 1974.
11. Bellin, B.: Upward Turbulent Fire Spread and Burning of Fuel Surface in the Configuration of Two PMMA Surfaces Facing Each Other, STA Fellow Interim Report, Fire Research Institute, 1991.
12. Anon.: Technical Report for the Fire Safety Design of the New National Theater Project, Building Center of Japan, 1988(in Japanese).
13. Hasemi, Y., Yoshida, M., Takashima, S. and Yokobayashi, S.: Wall Flame Correlations and Upward Flame Spread in a Vertical Channel and Its Relevance to Fire Safety, CIB W14 Workshop on Fire Growth Modeling for Engineering Applications, Espoo, 1995.
14. de Ris, J.: Spread of a Laminar Diffusion Flame, Proceedings of the Twelfth Symposium (International) on Combustion, 1968.
15. Fernandez-Pello, A.C.: A Theoretical Model for the Upward Laminar Spread of Flames over Vertical Fuel Surfaces, Combustion and Flame, 31, p.135, 1978.
16. Fernandez-Pello, A.C.: Downward Flame Spread in an Opposed Forced Flow, Combustion Science and Technology, 19, p.19, 1978.
17. Fernandez-Pello, A.C.: Flame Spread in a Forward Forced Flow, Combustion and Flame, 36, p.63, 1979.
18. Annamalai, K. and Sibulkin, M.: Flame Spread over Combustible Surfaces for Laminar Flow Systems, Part I: Excess Fuel and Heat Flux, Combustion Science and Technology, 19, p.167, 1979.
19. Fernandez-Pello, A.C. and Mao, C.P.: A Unified Analysis of Concurrent Modes of Flame Spread, Combustion Science and Technology, 26, p.147, 1981.
20. Fernandez-Pello, A.C. and Hirano, T.: Controlling Mechanisms of Flame Spread, Combustion Science and Technology, 32, p.1, 1983.
21. Ito, A. and Kashiwagi, T.: Characterization of Flame Spread over PMMA Using Holographic Interferometry Sample Orientation Effects, Combustion and Flame, 71, p.189, 1988.
22. Cetegen, B., Zukoski, E.E., and Kubota, T.: Entrainment and Flame Geometry of Fire Plumes, NBS-GCR-82-402, 1982.
23. Delichatsios, M.M., Mathews, M.K., and Delichatsios, M.A.: An Upward Fire spread and Growth Simulation, Proceedings of the Third International Symposium on Fire Safety Science, Edinburgh, 1991.
24. Brehob, E.G. and Kulkarni, A.K.: A Numerical Model for Upward Flame spread under External Radiation, Annual Conference on Fire Research, Rockville, Md., 1993.

25. Mitler, H.E. and Steckler, K.D.: SPREAD- A Model of Flame Spread on Vertical Surfaces, NISTIR 5619, 1995.
26. Delichatsios, M.M., Wu, P., Delichatsios, M.A., Lougheed, G.D., Crampton, G.P., Qian, C., Ishida, H., and Saito, K.: Effect of External Radiant Heat Flux on Upward Fire Spread: Measurements on Plywood and Numerical Predictions, Proceedings of the Fourth International Symposium on Fire Safety Science, Ottawa, 1994.
27. Delichatsios, M.A. and Delichatsios, M.M.: Upward Flame Spread and Critical Conditions for PE/PVC Cables in a Tray Configuration, Proceedings of the Fourth International Symposium on Fire Safety Science, Ottawa, 1994.
28. Andersen, C.K.: Development of a Dynamic Forest Fire Propagation Model, Proceedings of ASIAFLAM95, p.255, Hong Kong, 1995.
29. Anon., Investigation Report on 1976 Sakata Fire, Fire Research Institute, Japan, 1977 (*in Japanese*).
30. Hasemi, Y.: Thermal Modeling of Upward Flame Spread, Proceedings of the First International Symposium on Fire Safety Science, Gaithersburg, Md, 1985.
31. Orloff, L., de Ris, J., and Markstein, G.H.: Upward Turbulent Fire Spread and Burning of Fuel Surface, Proceedings of the 15th Symposium (International) on Combustion, 1974.
32. Sibulkin, M., and Kim, J.: The Dependence of Flame Propagation on Surface Heat Transfer II. Upward Burning, Combustion Science and Technology, 17, p.39, 1977.
33. Saito, K., Quintiere, J.G., and Williams, F.A.: Upward Turbulent Flame Spread, Proceedings of the First International Symposium on Fire Safety Science, Gaithersburg, Md, 1985.
34. Thomas, P.H., and Karlsson, B.: On Upward Flame Spread, Department of Fire Safety Engineering, Lund University, 1991.
35. Baroudi, D. and Kokkala, M.: Analysis of Upward Flame Spread, VTT Publications 89, 1992.
36. Hasemi, Y. and Yasui, N.: A Strategy to Develop Engineering Upward Flame-Spread Evaluation Methodology Based on the Linearized Flame Height Approximation, accepted by Fire Science and Technology, 1995.
37. Hasemi, Y., Yoshida, M., Yasui, N., and Parker, W.J.: Upward Flame Spread along a Vertical Solid for Transient Local Heat Release Rate, Proceedings of the Fourth International Symposium on Fire Safety Science, Ottawa, 1994.
38. Mowrer, F. and Williamson, R.B.: Flame Spread Evaluation for Thin Interior Finish Materials, Proceedings of the Third International Symposium on Fire Safety Science, Edinburgh, 1991.
39. Cleary, T.G. and Quintiere, J.G.: A Framework for Utilizing Fire Property Tests, Proceedings of the Third International Symposium on Fire Safety Science, Edinburgh, 1991.
40. Kokkala, M., and Baroudi, D.: A Thermal Model to Predict Fire Growth on a Wall, CIB W14 Workshop on Fire Growth Modeling for Engineering Applications, Espoo, 1995.
41. Thomas, P.H.: On Concurrent Upward Surface Spread of Flame, Fire Safety Journal, 22, p.89, 1993.
42. Back, G., Beyler, C., DiNenno, P. and Tatem, P.: Wall Incident Heat Flux Distributions Resulting from an Adjacent Fire, Proceedings of the Fourth International Symposium on Fire Safety Science, Ottawa, 1994.
43. Liburdy, J.A. and Faeth, G.M.: Fire Induced Plume along a Vertical Wall: Part I. The Turbulent Weakly Buoyant Region, NBS Grant No.5- 9020, 1977.
44. Ahmad, T. and Faeth, G.M.: Fire Induced Plume along a Vertical Wall: Part III. The Turbulent Combusting Plume, NBS Grant No.5- 9020, 1978.
45. Quintiere, J.G., Harkleroad, M.M., and Hasemi, Y.: Wall Flames and Implications for Upward Flame Spread, Combustion Science and Technology, Vol.40, p.191, 1986.
46. Hasemi, Y. and Tokunaga, T.: Some Experimental Aspects of Turbulent Diffusion Flames and Buoyant Plumes from Fire Sources against a Wall and in a Corner of Walls, Combustion Science and Technology, Vol.40, p.1, 1984.
47. Kokkala, M.A.: Characteristics of a Flame in an Open Corner of Walls, INTERFLAM'93, 1993.

48. Hasemi, Y., Yoshida, M., Takashima, S., Kikuchi, R., and Yokobayashi, S.: Flame Length and Flame Heat Transfer Correlations in Corner-Wall and Corner-Wall-Ceiling Configurations, submitted to Interflam'96, 1995.
49. Karlsson, B.: Modeling Fire Growth on Combustible Lining Materials in Enclosures, Lund University, 1992.
50. Wickström, U., and Goransson, U.: Full-scale/Bench-scale Correlations of Wall and Ceiling Linings, Fire and Materials, 16, p.15, 1992.
51. Gross, D.: Measurements of Flame Lengths under Ceilings, Fire Safety Journal, 15, p.31, 1989.
52. Thomas, P.H.: Fire, Flames and Dimensional Analysis, Proceedings of the Third International Symposium on Fire Safety Science, Edinburgh, 1991.
53. Newman, J.S. and Tewarson, A.: Flame Spread Behavior Char-Forming Wall/Ceiling Insulating Materials, Proceedings of the Third International Symposium on Fire Safety Science, Edinburgh, 1991.
54. Oleszkiewicz, I.: Heat Transfer from a Window Fire Plume to a Building Facade, ASME Winter Annual Meeting, San Francisco, 1989.
55. Foley, M. and Drysdale, D.D.: Heat Transfer from Flames between vertical Parallel Walls, Fire Safety Journal, 24, p.53, 1995.
56. Hasemi, Y., Yoshida, M., Nakabayashi, T., and Yasui, N.: Transition from Room Corner Fire to Flashover in a Compartment with Combustible Walls and Noncombustible Ceiling, Proceedings of the First Asian Conference on Fire Science and Technology, p.77, 1992.
57. Janssens, M.L.: A Thermal Model for Piloted Ignition of Wood Including Variable Thermophysical Properties, Proceedings of the Third International Symposium on Fire Safety Science, Edinburgh, 1991.
58. Quintiere, J.G.: Fire Tests and Hazard Evaluation, UNCRD Proceedings Series No. 7, Improved Firesafety Systems in Developing Countries, Tokyo, 1994.
59. Karlsson, B., and Magnusson, S.E.: Combustible Wall Lining Materials: Numerical Simulation of Room Fire Growth and the Outline of a Reliability Based Classification Procedure, Proceedings of the Third International Symposium on Fire Safety Science, Edinburgh, 1991.
60. Kokkala, M.A., Thomas, P.H., and Karlsson, B.: Rate of Heat Release and Ignitability Indices for Surface Linings, Fire and Materials, 171 p.209, 1993.
61. Anon., ISO TR 11696(7th draft) Fire tests - Reaction to fire - Application of test results to predict fire performance of building products, 1994.
62. Kokkala, M.A.: Use of Modern Reaction-to-Fire Test Methods for Fire Safety Assessment of Products, UNCRD Proceedings Series No. 7, Improved Firesafety Systems in Developing Countries, Tokyo, 1994.
63. Simms, D.: On the Piloted Ignition of Wood by Radiation, Combustion and Flame, 7, p.253, 1963.
64. Babrauskas, V. and Grayson, S.J. ed: Heat Release in Fires, Elsevier Applied Science, 1992.
65. Hasemi, Y., Yoshida, M., Goto, T., Kikuchi, R., Hosomi, M., and Yamamoto, E.: On the Predictability of Turbulent Upward Flame Spread Based on Material Fire Tests, Proceedings of the Annual Meeting, Japan Association for Fire Science and Engineering, Kobe, 1995(*in Japanese*).
66. Urbas, J.: Analysis of Intermediate Scale Calorimeter(ICAL) Data Generated in the Weyerhaeuser Fire Technology Laboratory, Western Fire Center, 1994.
67. Atreya, A. and Abu-Zaid, M.: Effect of Environmental Variables on Piloted Ignition, Proceedings of the Third International Symposium on Fire Safety Science, Edinburgh, 1991.
68. Babrauskas, V.: Full-Scale Heat Release Rate Measurements, in Babrauskas, V. and Grayson, S.J. ed., Heat Release in Fires, Elsevier Applied Science, 1992.
69. Anon.: California Technical Bulletin 133 "Flammability Test Procedure for Seating Furniture for Use in Public Occupancies", California State Bureau of Home Furnishings and Thermal Insulation, 1984.

70. Fowell,A.J. ed.: Fire and Flammability of Furnishings and Contents of Buildings, ASTM STP 1233, 1994.
71. Williamson,R.B., Revenaugh,A. and Mowrer,F.W.: Ignition Sources in Room Fire Tests and Some Implications for Flame Spread Evaluation, Proceedings of the Third International Symposium on Fire Safety Science, Edinburgh, 1991.

Discussion

Edward Zukoski: I was confused about the nomenclature. W is the width of the burner and D is the depth. What was the width of the depth of the sidewalls?

Yuji Hasemi: They are the same.

Edward Zukoski: So the burner filled up the space between the side walls and the back wall?

Yuji Hasemi: Yes.

Input Data for Fire Modeling

Henri E. Mitler

Building and Fire Research Laboratory
National Institute of Standards and Technology

February 1996

ABSTRACT

Reliable burn data are needed as inputs for fire models, for use as well as for model validation. To this end, a set of five merchandise kiosks have been burned, and the results carefully analyzed. A number of conclusions emerge, many of them of a cautionary nature. Perhaps the most important ones are that (a) The results of apparently identical fires can differ substantially; it follows that a number of runs must be made to get statistically significant results. (b) the "raw" data must be analyzed and rationalized. (c) the time delay for the O₂ analyzer is variable, not constant. Suggestions are made for further work.

INTRODUCTION

In order to get information and insight as to how a fire spreads on furniture or other items, many test burns have been carried out (refs. [1]-[4]). These have yielded the history of the rate of heat release, the production of CO, CO₂, soot and smoke, and other interesting data. The rate of heat release (RHR) is the most useful indicator of the impact of a fire [1]. These data are important for fire protection engineers in order to make rational decisions on risk, for manufacturers to know what materials to use, and in order to get data for verification of room-fire models and/or as input to such models (see [5]-[10]). The present study adds to that data base. These data are to be included in a large data base in FDMS format [11].

It was decided to examine merchandise kiosks (booths); they are now found everywhere, indoors as well as outdoors; in malls, cinemas, etc. No one has, at present, any quantitative knowledge of how these burn. Five burns were carried out: three ostensibly identical open-air burns with the kiosk opened up (these serve as a baseline), one burn with the kiosk closed up, and one with the kiosk open, but in a large enclosure.

Description of kiosk.

Fig.1 is a photograph of the kiosk we used, with the shelves down and merchandise placed on it. With the hinged shelves up (that is, the kiosk closed, as for the evening), it is 1.2 m square, and 2.1 m high. The bottom part is essentially a box, with two hinged doors in front to permit access to the interior. The doors in the underside of the kiosk were kept slightly open. The top surface of the box serves as the counter-top. There are columns at each corner,

which support a light superstructure. The interior of the box principally serves for storage of inventory; it also contains electric cables for lights, heat, etc. We have assumed that cotton Tee shirts are on display. Three cardboard boxes which contain excess inventory are placed under the counter (inside the box).

Ignition

It is assumed that ignition would occur only through a concatenation of two accidents: first, some defect in the electric lines produces sparking or arcing. Second, the shipping/storage boxes under the counter (inside the box) are not pushed all the way in, preventing the door(s) from closing completely; this provides for the ventilation, which is essential. The short in the cable is simulated with a modified electric heat tape. The tip of the tape is placed between the two rear boxes; it reliably produces a flame 7 to 8 cm high at the tip whenever power is applied.

The series of photographs of test 2 shown in the talk help to visualize and understand the progress of the fires in the open. The kiosk collapsed at $t = 1500$ s. The weight measurements are useless after the collapse, and the test was discontinued at $t \approx 1660$.

EXPERIMENTAL RESULTS

The heat release rate of kiosk 2, burning in the open, is shown in figure 2. Note that \dot{Q} is limited to about 40 kW for the first 10 minutes. As we will show later, this is because the burn is ventilation-limited. There are several abrupt drops in the remaining mass, the last quasi-discontinuity being the largest (about 43 kg). These occur when pieces of the structure, such as the cabinet doors and the superstructure, fall, either on or off the weigh platform.

The mass-loss rate $\dot{m}(t)$ is found by making a running five-point polynomial fit to smooth the $m(t)$ data, then taking the derivative at consecutive points. The places where there were sudden displacements of material are seen as sharp spikes, both positive and negative. These are irrelevant to the pyrolysis rate, and have been removed; the resulting mass loss rate curve is displayed in Figure 3.

The effective values of the heat of combustion, H_c , are obtained by dividing the values of the rate of heat release (RHR) by the pyrolysis rate (as represented by the mass loss rate \dot{m}):

$$H_c(t) \equiv \frac{\dot{Q}(t)}{-\dot{m}(t)} \quad (1)$$

This is shown in Figure 4. The raw data, however, cannot be naively accepted as is: even though the spurious spikes in \dot{m} were removed, spikes still appear in $H_c(t)$. The reason is inadequate time phasing between \dot{m} and \dot{Q} . The correct phasing is found by associating real spikes in \dot{m} and \dot{Q} ; thus, the doors fall in at $t \approx 1600$ s, producing a spike. There is an associated spike in $\dot{m}(t)$, but it occurs at $t \approx 1650$. The resulting (spurious) spikes in H_c were removed, as were the remaining spikes, which were also spurious. The remaining curve has been fitted with a non-linear least-squares fit, as shown. The results for kiosks 3 and 4 are similar.

The fact that H_c starts at low values is intriguing -- it probably reflects very incomplete combustion in the early stages. This is consistent with the large amount of white smoke which was apparent early on. The radiative heat fluxes from the flames from kiosk 2 are shown in Figure 5.

To summarize: as time goes on, the fire becomes stronger, in the three "standard" tests. This is in part due to the overhanging shelf beginning to burn on the underside; partly, too, the fuel pyrolyzed from within the box, which does not get to burn on the inside, can burn outside. It does not do so at first, so that white smoke is visible, instead. Later, when there is flame outside the box, that flame pilots the fuel, so that the power output increases even more. When the doors fall off, internal flashover takes place in the box, and the power output goes much higher.

Comparisons

Runs 2 to 4 were ostensibly identical; figure 6 shows the three resulting HRR curves. The heat release rates are similar for the first 600 seconds or so. Moreover, it is clear that the peak outputs were about 1.8 MW. The greatest single *difference* among these curves lies in the time delays to the onset of serious burning -- a nine-minute difference. When the curves are shifted so that the first peaks overlap, the similarities are much more striking; see figure 7.

The effective heat of combustion curves should be more nearly a property of the kiosk, and hence more nearly identical to each other (except, possibly, for the scaling along the time axis). The comparison is best made with smoothed values (see figure 8). The results are similar in terms of the peaks and valleys and the general upward trend; indeed, the curves nearly overlap for the first 600 seconds. The difference between them beyond 600 s is, however, surprising.

Note that the mass-loss rate depends on the pyrolysis rate of the solids, whereas the rate of heat release depends on the **combustion rate**, which depends on other factors besides the fuel supply rate. Hence what we have identified as H_c is in fact a function which depends on the (instantaneous) combustion efficiency as well as the effective heat of combustion, so that the curves labeled "effective heat of combustion" really are of $\chi_A(t)H_c(t)$.

Attempts to correlate the peaks and valleys of $\chi_A(t)H_c(t)$ with easily recognizable events, such as the falling-off of the doors, was not successful. A possible alternative explanation is that perhaps the ignition and burning of different items, such as the boxes, the shirts, etc. produces these variations. It would be interesting to test out this hypothesis.

Finally, just as the rates of heat release all have similar peak values, so do the fluxes -- about 30 kW/m² for the lower gauge and about 35 kW/m² for the eye-level gauge.

Burning in different configurations

Test 5 was for the kiosk all closed up, as it would be for the night: the shelves are folded up, and all the shirts which are otherwise displayed during the day are stored in the three boxes underneath. In burns 2 to 4, the shelf just above the doors was the first "external" item to

ignite; with this shelf folded up out of the way, there was some question as to whether the fire would ever grow beyond the ventilation-limited fire underneath. If it did, however, it would be expected that during a fire, these interior "walls" (consisting of folded-up shelves) would radiate to each other, as in a furnace, resulting in much faster evolution of pyrolysis products.

The results of this burn are shown in the following figures. Figure 9 shows the rate of heat release; the fire is seen to "take off" after $t = 600$ s, about the same time as the open-kiosk fires did; surprisingly, the shelf being out of the way made no difference. The expectation of a higher peak output, on the other hand, is borne out: the peak is 3.2 MW. The $\dot{m}(t)$ curve is similar, as would be expected.

Finally, we consider test 1, the kiosk burning in an enclosure; the enclosure that was built for these tests was 18'x18' and 12' high. The doorway height was 8' and its width 2 m. For this case, two thermocouple trees were included, one in the doorway and one in the back.

As expected, the fire initially progresses the same way as in tests 2-5. At $t \approx 26$ min., the superstructure collapses; within 15 seconds, the fuel in the enclosure -- including the paper on the gypsum-board walls and ceiling -- is burning, and flashover begins; one can see flames emerging from the compartment. The fire was extinguished at this point, before it grew any greater.

The HRR curve is plotted on semi-logarithmic paper, to give equal weight to comparable fractional increases in power output; see figure 10. The curve shows several asymptotes, indicating several "stages" of burning. The first asymptote, at about 45 kW, corresponds to ventilation-limited burning inside the box. At $t \approx 750$ s, there is renewed growth, apparently connected with ignition of material outside the box, to about 400 kW. At $t \approx 1100$ s, there is another growth spurt, connected with the doors to the box falling out. The output then rapidly reaches a peak of 1.2 ± 0.2 MW, until the last stage, which is flashover.

The radiation flux to the eye-level gauge and that registered by the floor-level gauge follow very similar patterns. The peak values before flashover are about 20 and 5 kW/m², while at flashover, 185 and 36 kW/m², respectively.

ANALYSIS.

General observations. The fire is ventilation-limited so long as the box retains its integrity. The counter-top protects the shirts above it; indeed, the shirts which were hung in the center of the kiosk did not burn until 20 minutes into the burn, in test 2.

The **intrinsic replicability** of the basic test is of interest. The first peaks for the RHR curves are 1440 kW, 1519 kW, and 1757 kW for kiosks 2 to 4, respectively. These are insufficient data from which to draw statistical conclusions; however, if we merely average the highest and lowest values, then the first peak is 1600 ± 160 kW; the second peak is 1407 ± 22 kW, and the third peak is 1645 ± 200 kW. The highest peak for a test was 1645 ± 200 kW. The differences (or uncertainties) are of the order of 10%, a not uncommon value for large-scale tests. The *times of occurrence* of the peaks, however, vary by considerably more: the first peaks occur at

$t = 1086$ s, 1218 s, and 1620 s, respectively. These differences are, most likely, attributable to slightly different vent openings in the three cases; as in hydrodynamics, a small cause has a large effect.

When the time axis for the RHR curve for kiosk 3 was shifted so that the peaks at 1200 s coincide, the spurious peak in H_c at 1200 was removed; however, another one at 1700 was then increased. This result appears to show that the delay time for the oxygen measurement is not constant. This effect has not heretofore been considered in the data analysis, but it is obvious if one thinks of it: the delay time between the probe and the oxygen analyzer is independent of the heat release rate; but when the HRR increases by an order of magnitude, even at a constant gas temperature, the gas velocity is ten times greater and therefore the time delay between flame and probe is cut by a factor of ten, decreasing the overall delay time. In the future, it should be straightforward to incorporate this correction into the data analysis.

Flashover

An expression for the minimum steady-state power output theoretically required to provide flashover in an enclosure with a given fire was given by Heskestad [12]:

$$\dot{Q} \approx 7.8 A_T + 378 A \sqrt{H} \quad (2)$$

where A is the vent area (assuming a single vent), H the enclosure height, and A_T its total area. For the enclosure under consideration, Eq.(2) yields $\dot{Q}_{\min} = 4.0$ MW.

As we have seen, however, the peak power output in the open is 1.7 to 1.8 MW, nowhere near this minimum. Thus the fact that there was flashover in the compartment is a puzzle. Assuming 4 MW was achieved, it must have been because of:

- (a) burning rate enhancement due to the radiative feedback from the room, plus
- (b) the effect of paper burning off the gypsum-board walls and ceiling.

In order to estimate the feedback effect quantitatively, a dynamical room-fire model must be used, where the heat-flux feedback from the room to the burning object is explicitly taken into account. FIRST (see [13], [14]) is such a model. FIRST was run for a growing fire on a slab of material inside of a very large "room," to simulate the burning of the kiosk in the open. The dimensions and properties of the slab were so chosen that the power output peaks at 1700 kW, and runs out of fuel shortly afterwards. This same slab was then made to "burn" in an enclosure of the same size and venting as used in the test. The difference in output was surprisingly small: an increase, at the peak, of only 43 kW. This is certainly insufficient to trigger flashover.

On the other hand, suppose that the paper had ignited first. We can estimate its contribution to the RHR from work done by Nelson and Tu [15]. Careful measurement of the excess heat output due to the paper in an ASTM room lined by gypsum-board yielded about 68 MJ. This was released over a period of 75 seconds, yielding an average of 900 kW; if distributed as a triangle (a single peak), the peak would be 1.8 MW. The enclosure was considerably larger,

and presumably would yield a higher peak. Conservatively, suppose that the paper in the present enclosure provided the same output; then, together with the 1.7 MW from the kiosk itself, this would result in a peak output of 3.5 MW -- still insufficient to trigger flashover.

Now reconsider the acceleration due to feedback. FIRST was run again, this time with an "equivalent" slab which yields a peak burning rate of 3.5 MW in the open. This time, the peak output changes from 3515 kW to 4374 kW, indeed enough to trigger flashover. Finally, FIRST was run with a slab of the same size but larger mass, so that burning could continue past 4374 kW. The calculation indicates that 10 seconds later, the heat output would be 7595 kW. The model indicates that the peak lies substantially above 8 MW.

Radiation Fluxes

We can estimate a relationship between the radiation flux and the flame height as follows: The burning kiosk can be considered a kind of pool fire. For pool fires, Heskestad has shown that the flame height z_f is well correlated with the convective power output \dot{Q}_c according to

$$z_f \approx 0.23 \dot{Q}_c^{2/5} - 1.02 D \quad (3)$$

where $D = 2R$ is the diameter of the pool fire. To a first approximation, we may take z_f to be proportional to D . Then Eq.(3) implies that

$$\dot{Q} \approx B z_f^{5/2}. \quad (4)$$

The mean flux seen by a flux gauge at the distance r from the fire is

$$\phi = \frac{\dot{Q}_{rad}}{4\pi r^2} \approx \left(\frac{\chi_R B}{4\pi r^2} \right) z_f^{5/2} \quad (5)$$

We tried to verify this by correlating the radiative fluxes with the flame heights. Consider the flux data for kiosk 3. The correlation is shown in figure 11. The radiometer is at a height $z = 1.8$ m above the floor, while the top of the door, from which the flames first emerge, was about 0.66 m above the floor. Hence $z_o = 1.8 - 0.66 = 1.14$ m. For $z_f < 1.14$, the flux is expected to be negligible; we see that this is indeed the case.

It is apparent from figure 11 that the largest concentration of readings were in the region $2.5 < z_f < 3.1$ m, $3 < \phi < 7$ kW/m². As the flame height increases, the flux increases, as we would expect. However, there is a puzzling distribution of points in the lower right-hand corner of the figure, corresponding to flame heights of 3.5 to 4.4 m, but where the flux reading was as low as 2 kW/m². Examination of the data shows that at $t = 1604$ s, the flux reading falls abruptly from over 20 kW/m² to 4.4 kW/m², unaccompanied by any similar drop in the RHR. The lower radiometer shows the same behavior, so that this reading was not spurious. However, that was the moment at which the superstructure collapsed -- hence the fire became several fires, spread out on the floor. This completely explains the behavior, and shows that we must ignore these outlying points as not relevant to a correlation.

When these outlying points, and some analogous ones at $t \approx 1340$, were removed, the correlation improved, but not startlingly so. On the other hand, we have already noted, in examining the heat of combustion curve, that there is a phase difference between the mass-loss rate and the rate of heat release curves. By shifting the \dot{Q} curve forward in time, the points are shifted into a much more nearly coherent pattern; a shift of 48 seconds raises the correlation coefficient r^2 from 0.7808 to 0.9444 (figure 12).

Another way to obtain a correlation is to assume that it is a power law. The flux was plotted logarithmically *versus* the flame height, for all five tests. When this was done, the correlation for kiosk 3 was even better: $r^2 = 0.9791$. The correlations for the other tests are equally good; however, the slopes vary, from a low of 2.3 for kiosk 5, to a high of 5.2 for kiosk 1. Why these various powers differ among themselves, as well as with the theoretically expected 5/2 power, is not clear. On the other hand, it is quite remarkable that the correlations are as good as they are, considering the complexity of the geometry and of the fires. This warrants further study.

CONCLUSIONS

1. The reason(s) for much (though not all) of the detailed burning behavior becomes clear *after* the fact -- but could not have been readily predicted, other than in a very crude way.
2. The results of apparently identical fires can differ substantially. Since the results are not "chaotic," they must be highly sensitive to initial conditions; that is, very small initial differences (in the experimental setup, initial conditions, ignition, etc). can lead to quite large differences in results. The equations describing the dynamics must be highly nonlinear and/or stiff. The most obvious probable initial difference is in the size of the opening of the kiosk doors.
3. In light of the variability of the results from the three nominally identical tests, it is essential to have a number of replicate tests; three is a minimum, and more are required in order to achieve statistically useful results.
4. As has been stated elsewhere (see, for example, [13]), this also implies that if the results of a computer run lie within the experimental limits, this must be considered to be "perfect" agreement, in the sense that agreement cannot be better.
5. Without the boxes below and the lower doors being opened a bit, the fire would never have "taken off."
6. As was confirmed by the runs with FIRST, the first ten minutes of burning was ventilation-limited burning in the lower box. When the doors fall off, internal flashover results, in the box.
7. In obtaining $\dot{Q}(t)$, the sum of the various time delays prior to measurement shift with the power output, and this should be taken into account in the analysis.

8. It would be naive and misleading to use the raw data; time-shifts and other adjustments must be carried out, and in such a fashion that the results are internally consistent, as well as reasonable. Thus, the mass loss rate is best found by first adjusting \dot{m} to remove spurious peaks and valleys, then smoothing the "adjusted" data.
9. When the HRR curve is plotted on semi-logarithmic paper, this gives equal weight to comparable fractional increases in power output, it is easier to interpret; the curve shows several asymptotes, indicating several "stages" of burning.
10. The mass-loss rate depends on the pyrolysis rate of the solids, whereas the rate of heat release depends on the combustion rate, which depends on other factors besides the fuel supply rate. Hence what we have identified as H_c is in fact a function which depends on the (instantaneous) combustion efficiency as well as the effective heat of combustion, and the curves labeled "effective heat of combustion" really are curves of $\chi_A(t)H_c(t)$.
11. Although a 1.8 MW fire is quite fierce, it will generally not pose the risk of a flashover in a mall, since the enclosure is much larger than the one used in this experiment.

FURTHER WORK

There are a number of interesting lines of inquiry which should be pursued in the future:

1. Correlate the full-scale results with Cone Calorimeter and ICAL tests of the kiosk materials.
2. Show and analyze the results for the production of CO, CO₂, soot and smoke.
3. Discuss the temperature distribution in the enclosure, and its relation to the burn.
4. Understand why the flame-height/RHR correlations sometimes deviate from the theoretical expression.
5. Investigate any possible effects of the hood (e.g., puffing modes) in producing the peaks and valleys observed in the effective heat of combustion curve.
6. The most obvious probable initial difference in the three replicate tests is in the size of the opening of the kiosk doors. Therefore, if the experiment were to be done again, it would be advisable to drill holes in the closed doors, to get more precisely identical ventilation openings.

REFERENCES

1. Babrauskas, V., and Peacock, R.D. (1992) "Heat Release Rate: The Single Most Important Variable in Fire Hazard," *Fire Safety J.* 18, p.255-272
2. Tewarson, A. (1988) "Generation of Heat and Chemical Compounds in Fires," Section 1, Chapter 13 in *SFPE Handbook of Fire Protection Engineering*; DiNenno, P., Beyler, C.L., Custer, R.L.P., Walton, W.D., and Watts, J.M., Jr., editors; published jointly by the National Fire Protection Association, Quincy, MA, and the Society of Fire Protection Engineers, Boston, MA

3. Babrauskas, V. and Krasny, J. (1985) "Fire Behavior of Upholstered Furniture," NBS Monograph 173, National Bureau of Standards, Gaithersburg, MD 20899
4. Tewarson, A., and Khan, M.M. (1990) "A New Standard Test Method for Fire Propagation Behavior of Electrical Cables in Industrial and Commercial Occupancies," Proceedings of Interflam '90, Proceedings of the 5th International Fire Conference on Fire Safety; C.A. Franks, Editor; Interscience Communications Ltd, London England. p.101
5. Rockett, J.A., "Modeling of NBS Mattress Tests With the Harvard Mark V Fire Simulator," NBSIR 81-2440, National Bureau of Standards, Gaithersburg, MD 20899, 1982
6. Tran, H.C. (1990) "Experimental Aspects of Validating a Compartment Wall Fire Model," Proceedings of Interflam '90, Proceedings of the 5th International Fire Conference on Fire Safety; C.A. Franks, Editor; Interscience Communications Ltd, London, England. p.13.
7. Peacock, R.D., Davis, S., and Lee, B.T., "An Experimental Data Set for the Accuracy Assessment of Room Fire Models," Nat. Bur. of Standards (U.S.), NBSIR 88-3752, April 1988
8. Peacock, R.D., and Babrauskas, V. (1991) "Analysis of Large-Scale Fire Test Data," Fire Safety Journal 17, p.387
9. Peacock, R.D., Davis, S., and Babrauskas, V. (1991) "Data for Room Fire Model Comparisons," J. Res. Natl. Inst. Stand. Technol. 96, p.411
10. Peacock, R.D., Jones, W.W., and Bukowski, R.W. (1993) "Verification of a Model of Fire and Smoke Transport," Fire Safety Journal 21, p.89
11. Portier, R.W. (1994) "Fire Data Management System, FDMS 2.0, Technical Documentation," NIST Technical Report 1407, National Institute of Standards and Technology, Gaithersburg, MD, 20899
12. Heskestad, G. (1983) "Luminous Heights of Turbulent Diffusion Flames," Fire Safety Journal 5, p.103
13. Mitler, H.E., and Rockett, J.A. (1987) "Users' Guide to FIRST, a Comprehensive Single-Room Fire Model", NBSIR 87-3595; National Bureau of Standards, Gaithersburg, MD 20089
14. Mitler, H.E. (1985) "The Harvard Fire Model", Fire Safety Journal 9, No.1-2, p.7
15. Nelson, H.E., and Tu, K-M. (1991) "Engineering Analysis of the Fire Development in the Hillhaven Nursing Home Fire, October 5, 1989," - NISTIR 4665, National Institute of Standards and Technology, Gaithersburg, MD, 20899

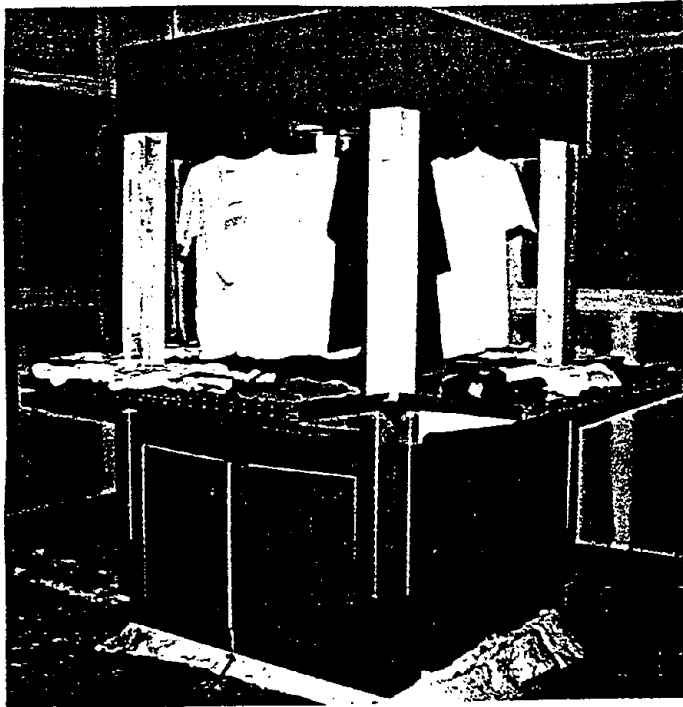


Figure 1. Photograph of the kiosk that was used, with the shelves down.

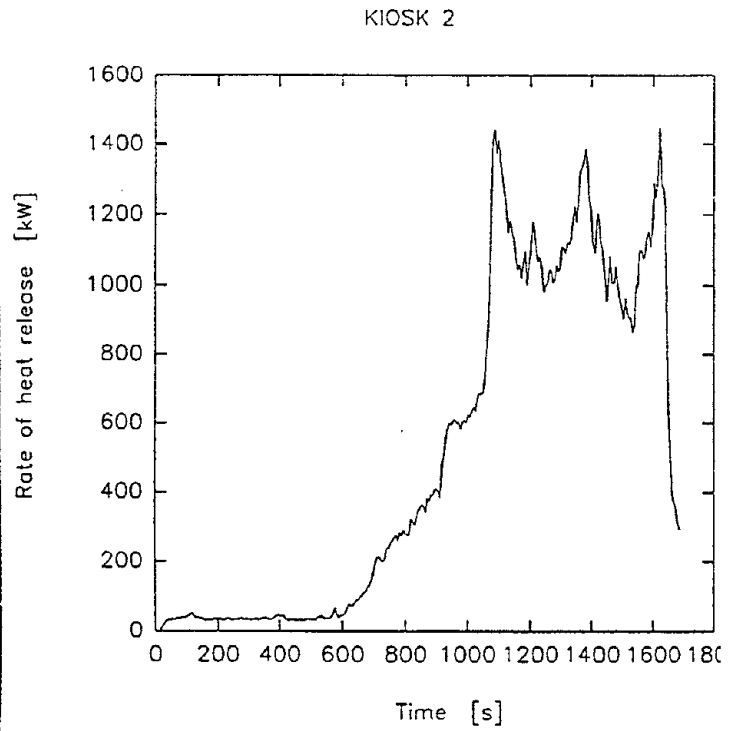


Figure 2. The heat release rate of kiosk 2, burning in the open

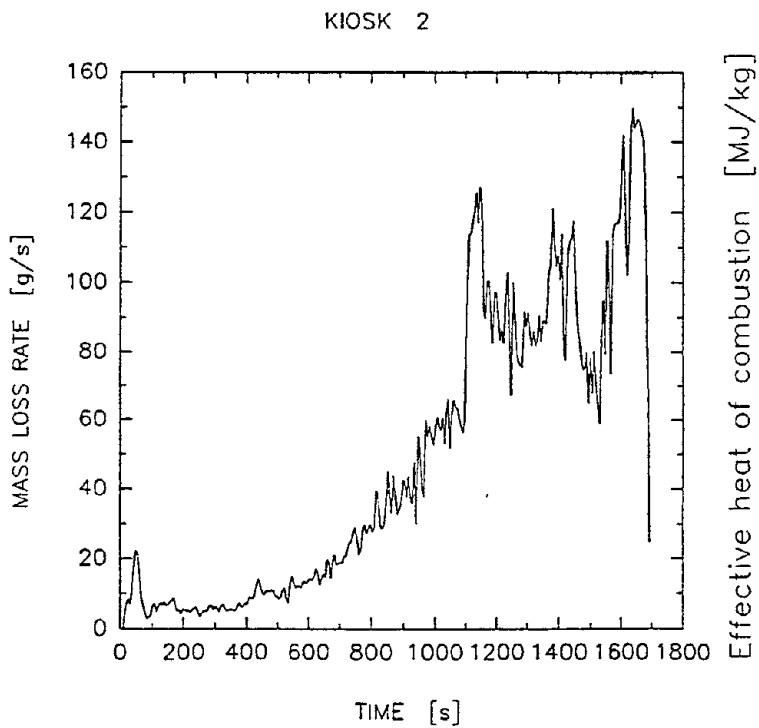


Figure 3. Mass-loss rate of kiosk 2.

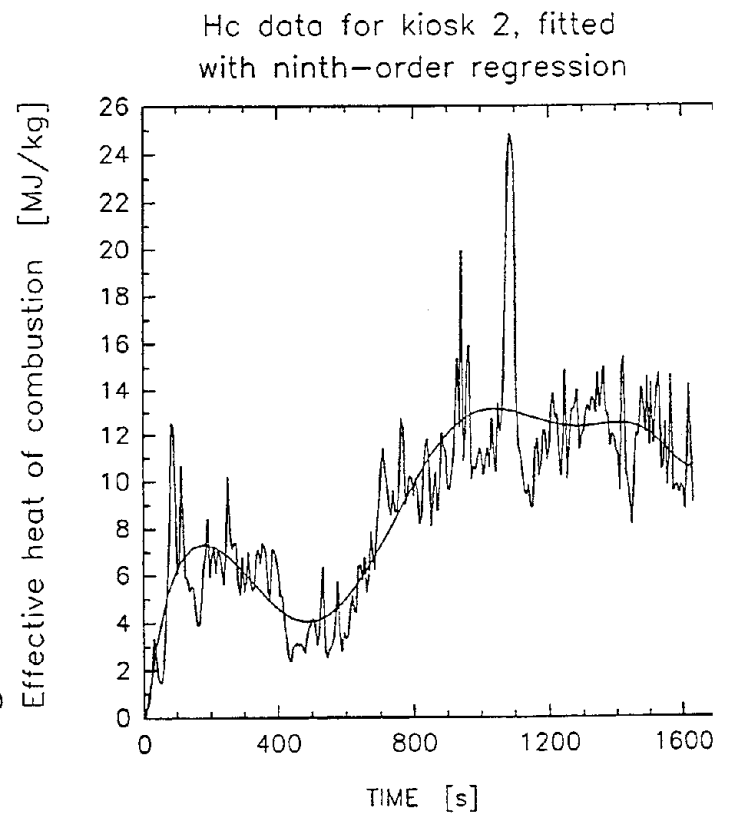


Figure 4. Effective heat of combustion of kiosk 1.

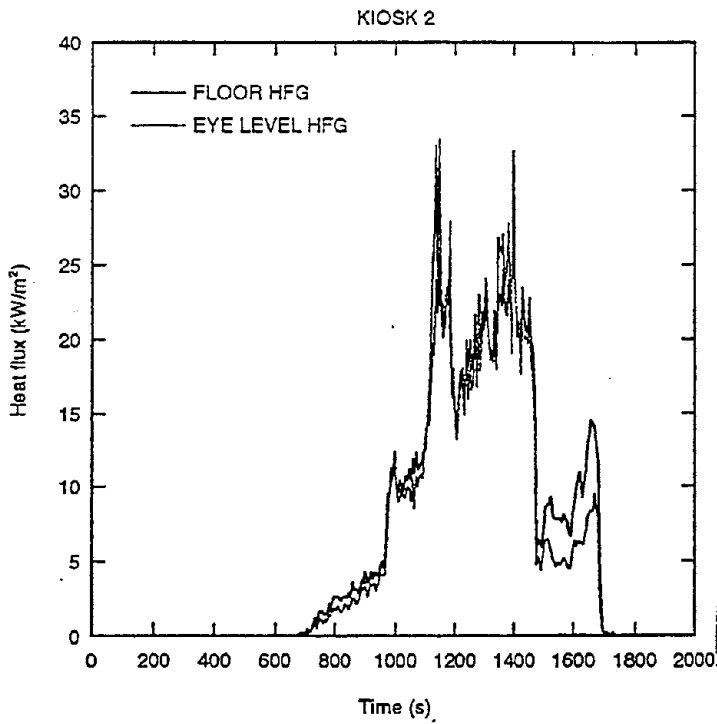


Figure 5. Radiative heat fluxes from the flames from kiosk 2.

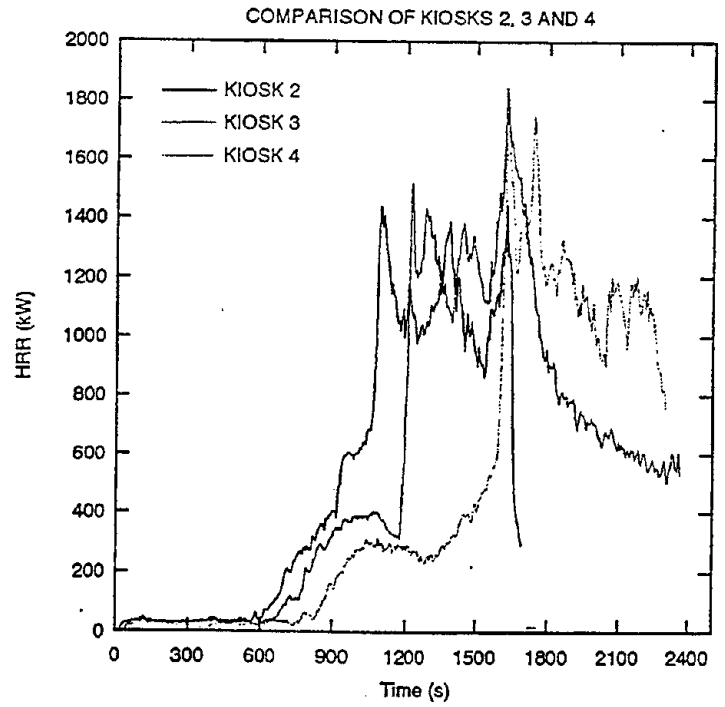


Figure 6. Simultaneous plot of the three rate of heat release curves.

The curves for kiosks 2 and 3 have been shifted 535 s and 415 s, respectively, so that all the first peaks coincide.

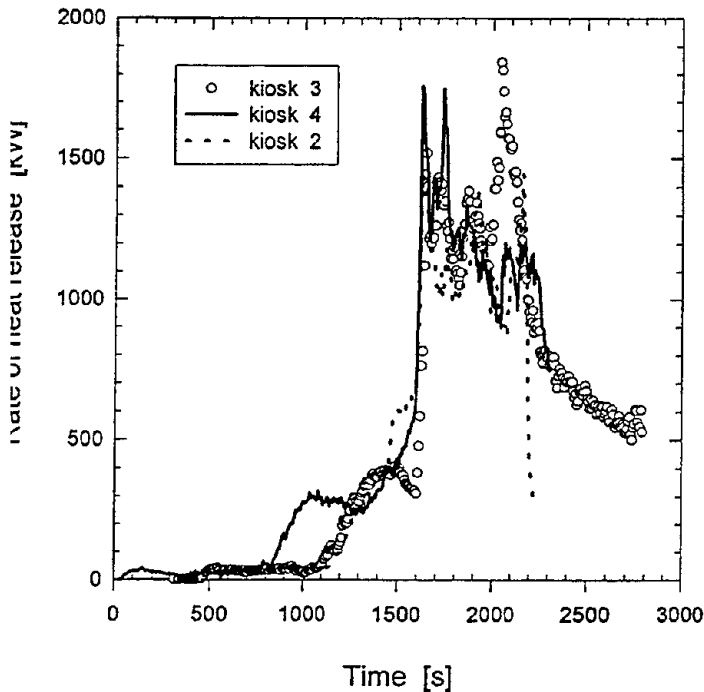


Figure 7. All three outputs, made to agree as closely as possible.

Smoothed $H_c(t)$ for kiosks 2, 3, and 4

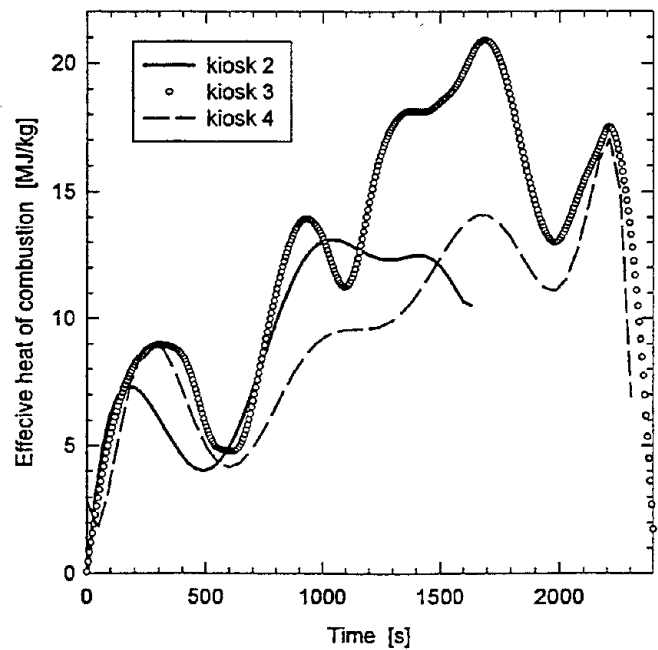


Figure 8. Effective heat of combustion for the three kiosks; the comparison is best made with smoothed values.

Kiosk 5; closed position

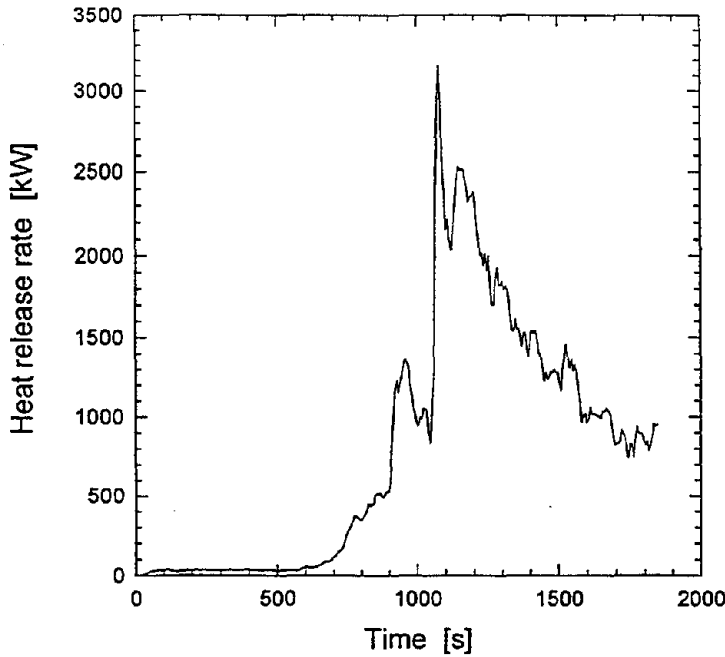


Figure 9. Rate of heat release of kiosk 5.

Semi-log plot of the rate of heat release of kiosk 1 (in the enclosure)

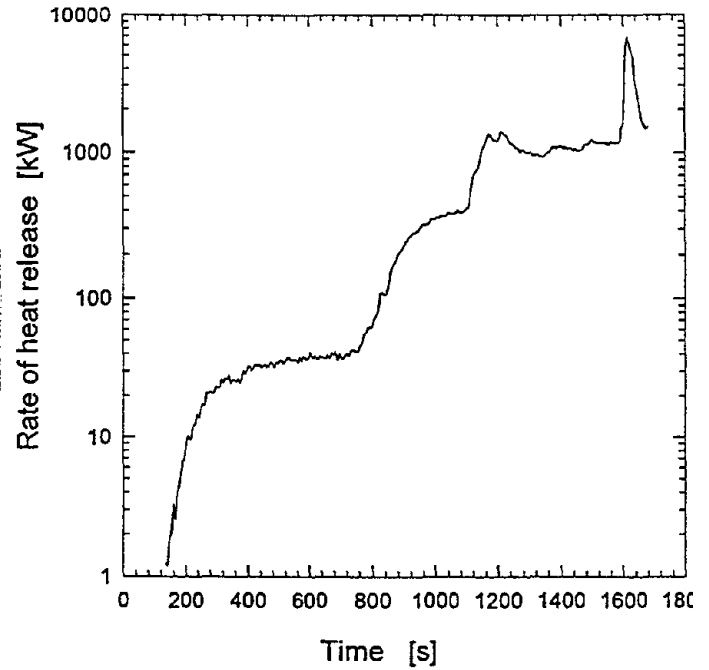


Figure 10. Semi-logarithmic plot of the rate of heat release of kiosk 1.

Correlation of eye-level flux with flame height for kiosk 3. Quadratic fit yields $r^2 = 0.656$

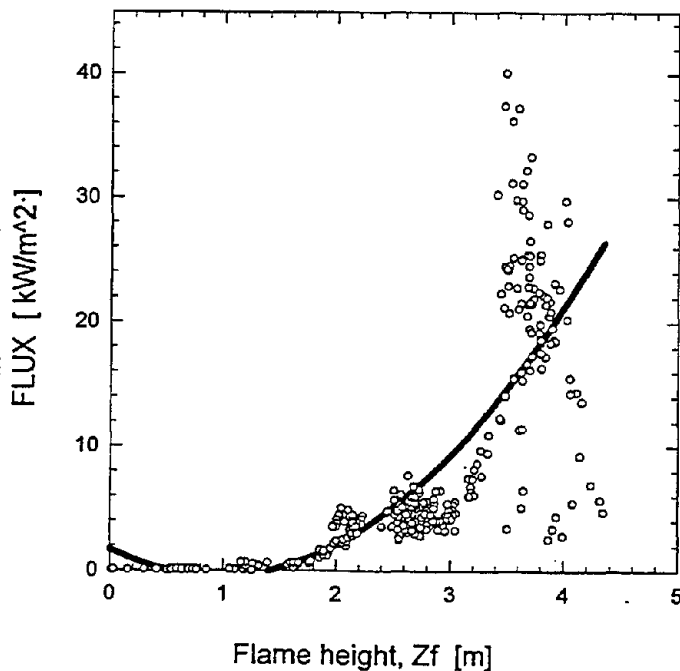


Figure 11. Flux versus flame height, raw data.

Correlation of eye-level flux with calculated flame height, for kiosk 3. Data for heights < 1.15 m has been suppressed, time shifted by 48 seconds. Quadratic regression.

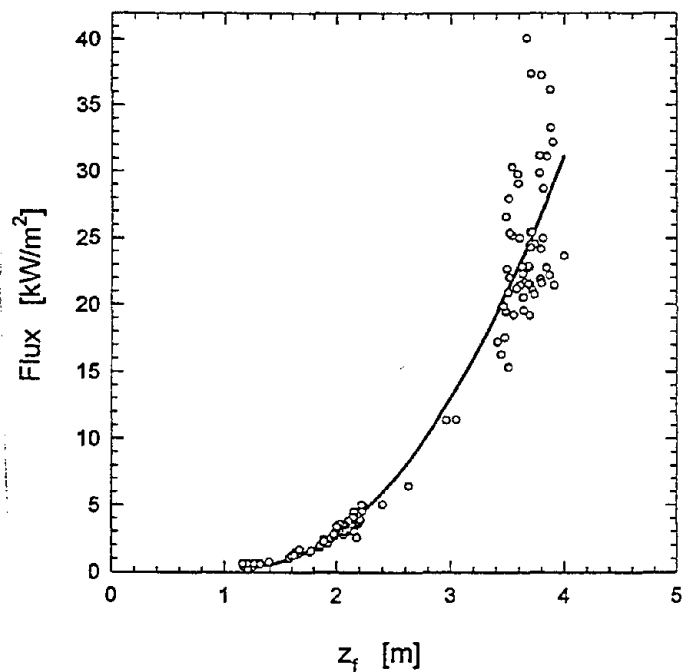


Figure 12. Flux versus flame height, adjusted data.

Discussion

Ronald Alpert: You implied that if those small doors at the bottom had been fully closed, there would have been no flaming. Did you verify that?

Henri Mitler: No.

Walter Jones: These experiments were done last summer. Subsequent to that, NIST had its Annual Fire Conference in Orlando in conjunction with SFPE. During that conference, such a fire occurred in a shopping center about two miles from where we were holding the conference. It was not done for our benefit, so we did not have any instruments to make measurements. But indeed, the case in point was a kiosk for selling cotton t-shirts that had been closed up for the night. The ignition was from an electrical fixture on high as opposed to low, but it's equivalent to the electrical tape. Since we did not have any measurements, we don't know the size of the fire, but it was sufficient to turn on sprinklers that were between 20 and 40 feet above the kiosk, thus indicating that the fire was on order of megawatts and that they do happen in real life. Our intention with these experiments is to try to have sets of fuel packages that occur in real situations.

Measurements and Predictions of the Velocity Field Induced by Pool Fires

X. C. Zhou and J. P. Gore
Thermal Sciences and Propulsion Center
School of Mechanical Engineering
Purdue University
West Lafayette, IN 47907

Howard R. Baum
Center for Fire Research, Building and Fire Research Laboratory
National Institute of Standards and Technology
Gaithersburg, MD 20899

Introduction

Due to the importance of the air entrainment rate in determining fire size, radiation properties, and soot production, various techniques have been applied to its measurement. The measurement techniques can be roughly classified into four categories. The first category involves monitoring of the air flow rate needed to meet the entrainment requirement of the fire while maintaining ambient pressure [1, 2]. The second category is to sample combustion products and solve a set of global mass balance equations to obtain equivalence ratio and hence the entrainment rate [3-5]. The third category involves measurement of the velocity and the temperature profiles inside the flame and subsequent calculation of the axial flow rate by either direct radial integration or integration of resulting curve fits [6-8]. One common disadvantage of the above three experimental methods is that information about the details of the entrainment flow field itself is not obtained. The fourth measurement category addresses the problem by obtaining detailed measurements of the flow induced by the fire [9, 10]. In Ref.[10], the mean and the fluctuating velocity field around a 7.1 cm toluene pool fire was mapped with a Laser Doppler Velocimeter (LDV). It was found that the value of the entrainment rate depends strongly on its definition implied by the first three measurement categories. In addition to the experimental work, a few studies involving analyses and computations of the entrainment flow field have also been reported [11, 12]. Taylor [11] calculated the air flow outside a thermal jet originating from a point source with the assumption that the entrainment rate is proportional to the jet velocity. Utilizing published experimental data, Baum and McCaffrey [12] applied a kinematic approach to predict the flow pattern induced by unconfined fires. The present paper reports application and extension of their methodology to the prediction of the entrainment flow field around 7.1 cm and 15 cm pool fires burning heptane and toluene.

The flow field is first decomposed into an irrotational flow and an incompressible flow component. The nonhomogeneous source terms in the partial differential equations governing these two flows, namely the volumetric heat release rate distribution and the vorticity distribution, are calculated from correlations given by McCaffrey [13]. The boundary conditions for the irrotational flow equation are approximated by an asymptotic solution to the potential flow generated by a point heat source, while the boundary conditions for the solenoidal flow are obtained by transforming the original equation into spherical coordinates and solving the resulting ordinary differential equation. In the present work, the analysis was extended to the case of a pool fire without a floor. The results show that the presence of a floor around the fire changes the entrainment flow field dramatically. Comparison of the predictions with velocity data obtained in the laboratory using a Particle Imaging Velocimetry (PIV) system are made and possible reasons for the discrepancies are discussed.

Theoretical Analysis

The entrainment flow velocity \vec{V}^* is first decomposed into two components, namely the irrotational velocity \bar{V}^* and the incompressible velocity \tilde{V}^* . The irrotational velocity field and the incompressible velocity field can be expressed in terms of a potential function ϕ^* and a stream function ψ^* as:

$$\bar{V}^* = \frac{\partial \phi^*}{\partial z^*} \hat{e}_z + \frac{\partial \phi^*}{\partial r^*} \hat{e}_r, \quad \tilde{V}^* = \frac{1}{r^*} \frac{\partial \psi^*}{\partial r^*} \hat{e}_z - \frac{1}{r^*} \frac{\partial \psi^*}{\partial z^*} \hat{e}_r, \quad (1)$$

where the superscript * indicates a dimensional quantity. Following the nondimensionalization of Ref. [12] and representing the resulting nondimensional quantities with identical symbol without the asterisk, the governing equations in a nondimensional axisymmetric cylindrical coordinate system can be written as

$$\frac{\partial^2 \phi}{\partial z^2} + \frac{1}{r} \frac{\partial}{\partial r} \left(r \frac{\partial \phi}{\partial r} \right) = Q(\bar{r}) \quad (2)$$

$$\frac{\partial^2 \psi}{\partial z^2} + \frac{\partial^2 \psi}{\partial r^2} - \frac{1}{r} \frac{\partial \psi}{\partial r} = r \omega_\theta(\bar{r}) \quad (3)$$

As in Ref. [12], the nondimensional source terms in the two equations, $Q(\bar{r})$ and $\omega_\theta(\bar{r})$, are estimated using the correlations of buoyant diffusion flame structure given by McCaffrey [13]. Gaussian distributions are assumed for radial profiles of both velocity and excess temperature. Flame radius at different heights is calculated in closed analytical form following the procedure of Ref. [12]. The boundary conditions along the floor (as in [12]) are:

$$\frac{\partial \phi}{\partial z} = 0, \quad \psi = 0 \quad \text{at } z=0 \quad \text{for all } r \quad (4)$$

$$\frac{\partial \phi}{\partial r} = 0, \quad \psi = 0 \quad \text{at } r=0 \quad \text{for all } z \quad (5)$$

The boundary conditions for the velocity potential at the outer edge of computational domain are taken to be equal to those of a potential flow caused by an equivalent normalized point heat source $(1-\eta)$, where η is the radiative loss fraction:

$$\phi = \frac{1-\eta}{2\pi\sqrt{r^2+z^2}} \quad (6)$$

The boundary values of the stream function are obtained by transforming the elliptical partial differential eq. (3) into an ordinary differential equation in the spherical coordinate system. Substituting $\psi = \rho^{5/3} F(\mu)$, where $\rho = \sqrt{r^2+z^2}$, $\mu = \cos \theta$, and θ is the polar angle, into eq. (3) yields:

$$\frac{d^2 F}{d\mu^2} + \frac{10F}{9(1-\mu^2)} = \Omega(\mu) \quad (7)$$

where $\Omega(\mu)$ is the normalized vorticity in the far field. At the floor, μ is equal to zero and along the centerline, μ is equal to unity, while the stream function is zero at both locations, thus the boundary conditions for eq. (7) are:

$$F(0) = F(1) = 0 \quad (8)$$

Equation (7) with boundary conditions (8) is solved numerically to obtain a value of $F(\mu)$.

For the case of a buoyant fire without a floor, at the centerline eq. (6) still holds. However, along the outer edge, the velocity potential is half of that given by eq. (6). The F for a fire without a floor is calculated by solving eq. (7) with the boundary conditions:

$$F(-1) = F(1) = 0 \quad (9)$$

Equations (2) and (3) are solved using a finite difference method subject to the boundary conditions discussed above and the volumetric heat release rate field and the distribution of the azimuthal vorticity field given in [12]. The stream function yields the solenoidal velocity field \tilde{V} , which is induced by the vorticity generated by the buoyancy in the flame, and the velocity potential yields \bar{V} , the irrotational expansion of hot gases in the flame. The entrainment velocity field is the sum of these two components.

Experimental Methods

A fire burning heptane or toluene is stabilized on a 15 cm pool in a 1.5m×1.5m×4m enclosure. The top 1 m of the enclosure is made of glass in order to establish an upper layer as the downstream boundary condition for the fire. The remaining 3 m of the enclosure is constructed using a fine wire cloth to protect the fire from ambient disturbances. The lip height (the distance from the fuel surface to the burner edge) is 0.8 cm in the case with no floor. With a 51cm sheet metal floor placed around the pool, the lip height had to be increased to 1.5 cm to avoid the establishment of flames at much larger radius on the floor. The burning rate dropped from 385 mg/s to 360 mg/s with the increased lip height, probably due to the decrease in the area of heat transfer to the fuel. The enclosure is seeded with Al₂O₃ particles of 0.5 μm mean diameter using a bank of specially developed seeders.

The configuration of the PIV system (FFD Inc.) is shown schematically in Fig. 1. A CW Argon-ion laser with a multiline power of 12 W is used to generate a train of dual pulses by passing through a two-slot chopper plate rotating at a frequency of 100 Hz. A cylindrical lens is used to illuminate a section of the flow field for two closely spaced short time intervals. A 1.4 MB CCD camera and a frame grabber are used to capture the light scattered from the seeding particles in the view region during the two laser pulses. To eliminate the ambiguity in the direction of motion, a shift in the direction of the mean velocity is introduced by a scanning mirror, which is synchronized to the chopper with a digital delay. The shift is larger in magnitude than the maximum reverse flow velocity to ensure a correct ordering of the two exposures. The images are processed with a resolution box of the size 32 × 32 pixels (corresponding to 2.5 × 2.5 mm in the flow field). The shift is subtracted from the resolved vector field in the analysis stage. The mean velocity field is obtained by averaging 100 instantaneous vector plots.

Results and Discussion

Predictions of the velocity field around the pool fire have been obtained using the model discussed above. Figure 2 shows the predicted entrainment flow pattern around a 15 cm heptane pool fire at a heat release rate of 17.4 KW and $\eta=0.3$. Near the floor, the flow is almost horizontal and without significant change in magnitude with radial distance. This is the mechanism by which a fire can cause strong inward wind. Near the fire, the velocity turns upwards, due to an intense source of vorticity caused by the density gradient. The magnitude of the velocity increases significantly in the near flame region, due to a combination of reduced flow area and an increase in the temperature. At greater distances from the floor, the flow is predominantly vertical. Figure 3 depicts the entrainment flow induced by the same fire as in Fig. 2 except for the absence of a floor and a small change in the lip height and the heat release rate. The flow becomes predominantly vertical everywhere in complete contrast to the fire with a floor. These differences need to be taken into account when using a method belonging to the first three categories discussed above. The predictions show that the velocity increases with height in the region close to the flame, as a result of the increase in temperature with height, while in the region away from the fire, the velocity remains largely unchanged.

- NBS-GCR-87-538, California Institute of Technology, 1987.
5. Beyler, C.L., Ph. D. Thesis, Harvard University. 1983.
 6. McCaffrey, B. J. and Cox, G., *National Bureau of Standards*, NBSIR 82- 2473, 1983.
 7. Koseki, H. and Yumoto, T., *Fire Technology*, Feb., 33 - 47 (1988).
 8. Weckman, E. J., *National Heat Transfer Conference, HTD-Vol. 106, Heat Transfer Phenomena in Radiation, Combustion and Fires*, 399 - 406 (1989).
 9. Thomas, P. H., Baldwin, R., and Hesselden, A. J., *Tenth Symposium (International) on Combustion*, 983 - 996 (1983).
 10. Zhou, X. C. and Gore, J. P., *Combustion and Flame*, 100, 52 - 60 (1995).
 11. Taylor, G. I. *J. Aerospace Sciences* 25, 464 (1958).
 12. Baum, H. R. and McCaffrey, B. J., *Fire Safety Science Proceedings, 2nd Intl. Symposium*, 129-148 (1989).
 13. McCaffrey, B. J., *Combustion and Flame*, 52, 149 (1983).

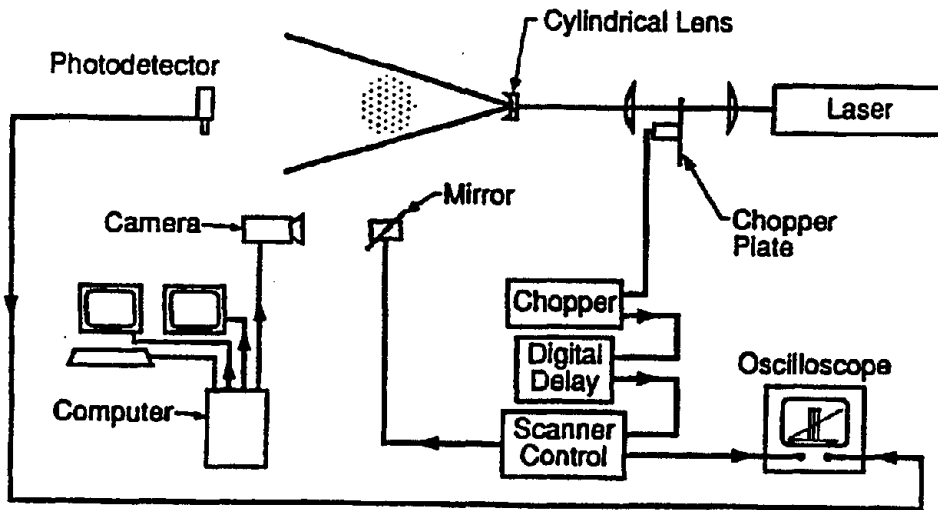


Figure 1. Schematic configuration of the PIV system.

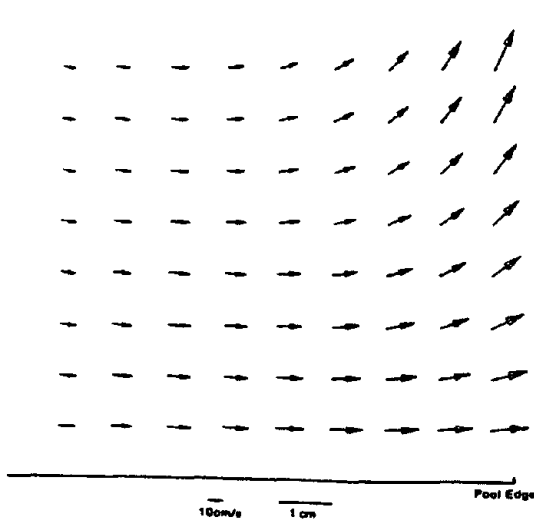


Figure 2. The predicted velocity field induced by a 15 cm pool fire with a floor.

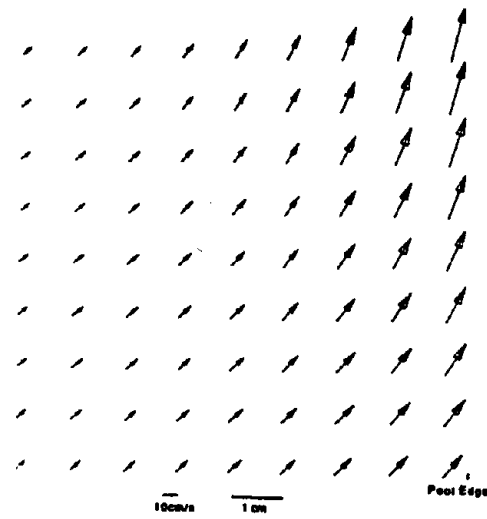


Figure 3. The predicted velocity field induced by a 15 cm pool fire without a floor.

Figure 4 shows the measurements of the mean velocity induced by a 15 cm heptane pool fire with a metal floor, obtained in our laboratory using the PIV system. The predictions in Fig. 2 agree well with the experimentally observed characteristics of the flow field in Fig. 4. The velocity is horizontally inward until the flame boundary is approached, where the vertical velocity component increases. Figure 5 shows the measurements of the mean entrainment flow field for a fire without a floor. The measured radial velocity is much smaller than the axial velocity in this case. These results support the predictions of Fig. 3.

Quantitative comparison of the predicted nondimensional axial velocity U_z^* and the measurements for both cases (with and without floor) at a dimensionless height of $Z^* = 0.1$ as a function of R^* are shown in Fig. 6. The radial distance R , the axial distance Z , the radial velocity U_r and the axial velocity U_z are nondimensionalized using the same parameters as in Refs. [12] and [13]. For the case with a floor, the predicted axial velocity is almost zero in very good agreement with the measurements. However, the difference between the predictions and the measurements is relatively large for the fire without a floor. Figure 7 shows the comparison between measurements and predictions for the nondimensional radial velocities U_r^* . The discrepancy is larger although the predictions capture the fact that the radial velocity component of the flow induced by a fire with the floor is much larger than that induced by the same fire but without the floor. The discrepancies are most likely a result of the differences in the size and type of the present fires and those used in Ref. [13] in generating the velocity and temperature data used in the specification of $Q(\bar{r})$ and $\omega_\theta(\bar{r})$. McCaffrey [13] also had a floor at some distance below the pool surface. In view of the sensitivity of the velocity field to the presence of a floor, this difference in experimental conditions may be crucial. Indeed, the strongly elliptic nature of the flow makes it extremely difficult to isolate the fire plume from its surroundings.

Conclusions

A kinematic model utilizing existing flame data shows that the flow patterns of the entrainment flow field are dramatically different depending upon whether a floor is present. These differences are in complete agreement with experimental observations. Quantitative predictions of the vertical velocities are satisfactory. However, the radial velocities are overpredicted. Improved correlations for heat release and vorticity distribution in liquid fueled pool fires with appropriate boundary and floor conditions are needed since the data used currently [13] were obtained in 30 cm x 30cm square gas-fired burners and appear to be unsatisfactory for liquid fires.

Acknowledgement

The work at Purdue University is supported by the Center for Fire Research, Building and Fire Research Laboratory, National Institute of Standards and Technology under Grant No. 60NANB2D1291 with Dr. Anthony Hamins and Dr. Takashi Kashiwagi serving as NIST Scientific Officers.

References

1. Ricou, F. P. and Spalding, D. B., *J. Fluid Mech.* 11 : 21-32 (1961).
2. Hill, B. J., *J. Fluid Mech.* 51: 773-779(1972).
3. Cetegen, B. M., Zukoski, E. E. and Kubota, T., *Combust. Sci. Tech.*, 39: 305 - 331 (1984).
4. Toner, S. J., Zukoski, E. E. and Kubota, T., *National Bureau of Standards*,

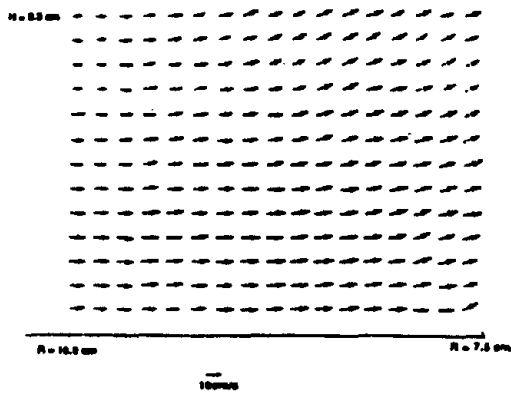


Figure 4. The measured velocity field induced by a 15 cm heptane pool fire with a floor.

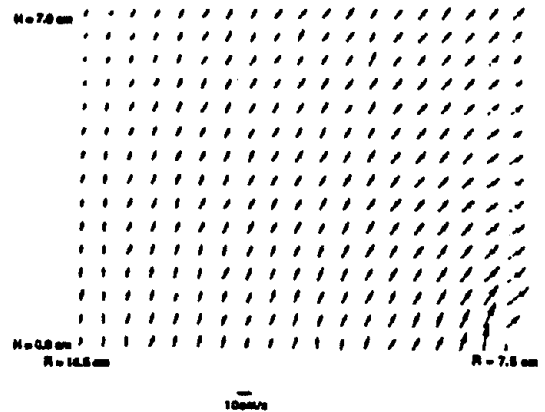


Figure 5. The measured velocity field induced by a 15 cm heptane pool fire without a floor.

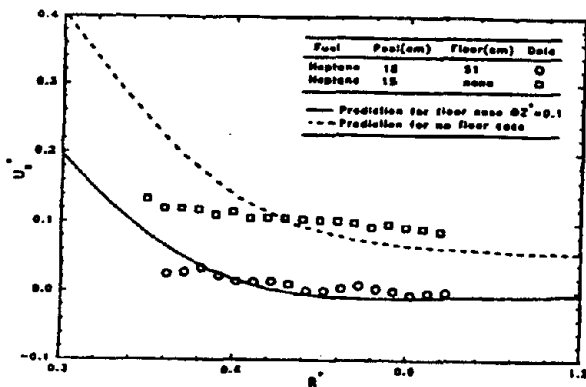


Figure 6. Comparison between predicted and measured nondimensional axial velocity for the fire with and without a floor.

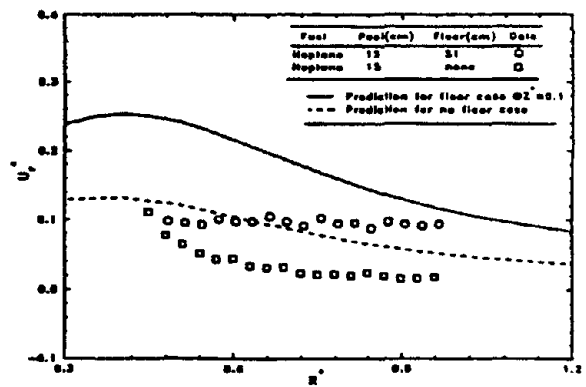


Figure 7. Comparison between predicted and measured nondimensional radial velocity for the fire with and without a floor.

Discussion

Hiroshi Koseki: You made some reference to the data I created. You made some comments about a scale effect. Could you repeat that part again?

Jayavant Gore: Yes. I made it in the context of many other people's work also. In some papers, if they changed R then the intended rate changed and therefore, it's a function of burner size, while some others will say it's not a function of burner size. So I did not want to single out any one. There is room for more work and I know you are doing more work.

Edward Zukoski: It would be very interesting if you could look at what happens near the interface because we use an old Japanese trick of using an incense stick, and the flow is always inward. There was no sign of a big circulation, and you wonder where this air that's coming from the flame goes as it gets to the interface. It did not go out, it always went in towards the fire.

Jayavant Gore: We have not looked at the flow field right here and certainly, we would like to look at it in the future. It becomes very challenging when you go there. It would be very interesting to see what happens to that air. Just the question you pose is very important because if you measure down here, you see a lot of air being set in motion. And if it's traveling up here and it's not going out and it's not going into the plume as indicated in some measurements, where is it going? We'd like to find out. My hypothesis would be that it's going out horizontally this way.

Corrosion from Combustion Products - An Overview

Pravinray D. Gandhi
Senior Staff Engineer

Underwriters Laboratories Inc.
333 Pfingsten Road, Northbrook, IL 66062
(847) 272-8800 (Ext. 43354)

Corrosion from Combustion Products - An Overview

Abstract

There has been a keen focus to understand corrosion from combustion products as it is related to potential damage from their deposition on equipment. Several test methods are available to assess the potential for corrosion damage from combustion products. These include indirect methods using the pH and conductivity measurements, and also direct methods that measure loss of metal on a target. These are discussed in this presentation. A recent development of determining the reliability of electronic equipment when exposed to combustion products uses an interdigitated target and measures leakage current after the exposure. Data developed using this technique is presented and discussed.

Introduction

There has been a keen focus to understand corrosion from combustion products as it is related to potential damage from their deposition on equipment. Of specific interest is the impact on the reliability of electrical and electronic equipment. Since the effluents can be carried away by the buoyancy of the gases, the potential for damage exists remotely from the fire. For this reason, this phenomenon is also termed "non-thermal fire damage". Another feature of this phenomenon is that in many instances, the damage may become evident after significant passage of time. The time delay for the impact of corrosive deposits to become evident on equipment performance depend upon the rate of chemical reactions taking place, and the availability of the appropriate conditions of temperature and relative humidity.

Three forms of corrosion have been identified. These may be defined as follows:

1. Metal loss due to electrolytic and chemical attack on metal;
2. Leakage current due to increased surface conductance; and
3. Increased contact resistance due to deposition of combustion product and subsequent chemical reactions.

The loss of metal results in reduction in the strength of structural members, and increase in electrical resistance of exposed metal parts. However, the exposed metal components on electronic circuit boards is limited to contacts. The second form of corrosion from the deposition of combustion products on electronic circuit boards, may lead to increased leakage currents to cause malfunction of circuitry. The third form of corrosion influences the electrical resistance between contacts for equipment such as relays and switches. Corrosion between contacts may lead to increased electrical resistance and thus cause a malfunction.

In this paper, the methods currently used to assess corrosion of combustion products, and a new approach to determine the impact of combustion products to the reliability of electronics are presented.

Methods

Several techniques have been devised to determine the corrosiveness of combustion products. These techniques may be divided into indirect measurement, and direct measurement methods.

Indirect Methods of Measurement

The indirect methods of measurement consist of measuring the either halogen acid gases, or the change in pH or electrical conductivity of a solution through which combustion products have been bubbled. Some of the methods have been standardized as shown in Table 1.

Table 1 - Indirect Methods of Measuring Corrosion

Standard	Title	Test Method
IEC 754-1 ¹	Test on gases evolved during combustion of materials from cables - Part 1: Determination of amount of halogen acid gases	Sample: 0.5 - 1 g Furnace: Static Temperature: 800° C Air flow: 0.4 - 0.7 l/min. Test duration: 20 min.
IEC 754-2 ²	Test on gases evolved during combustion of materials from cables - Part 2: Determination of degree of acidity of gases evolved during the combustion of materials taken from electric cables by measuring pH and conductivity.	Sample: 1 g Furnace: Static Temperature: 950 °C Air flow: 0.4 - 0.7 l/min Test duration: 30 min.
VDE 0472 ³ Part 813	Testing of cables, wires, and flexible cords; corrosivity of combustion gases	Sample: 1 g Furnace: Dynamic (10mm/min.) Temperature: 750-800° C Air flow: 10 l/hr Test duration: 30 min.

¹ IEC 754 -1, Test on gases evolved during combustion of materials from cables - Part 1: Determination of amount of halogen acid gases, International Electrotechnical Commission, Geneva, Switzerland.

² IEC 754-2, Test on gases evolved during combustion of materials from cables - Part 2: Determination of degree of acidity of gases evolved during the combustion of materials taken from electric cables by measuring pH and conductivity, International Electrotechnical Commission, Geneva, Switzerland.

³ VDE 0472, Part 813, Testing of cables, wires, and flexible cords; corrosivity of combustion gases, Deutsche Institut für Normung e.V., Postfach, 1107, D-1000 Berlin 30, Germany.

Standard	Title	Test Method
MIL-C-24643, section 4.7.25 ⁴	Acid gas generation	Sample: 0.25 - 0.5 g Furnace: Static Temperature: Ramped to 800° C in 20 min. Air flow: 60 l/hr Test duration: 60 min.

A typical test arrangement for the pH and conductivity based methods is shown in Figure 1.

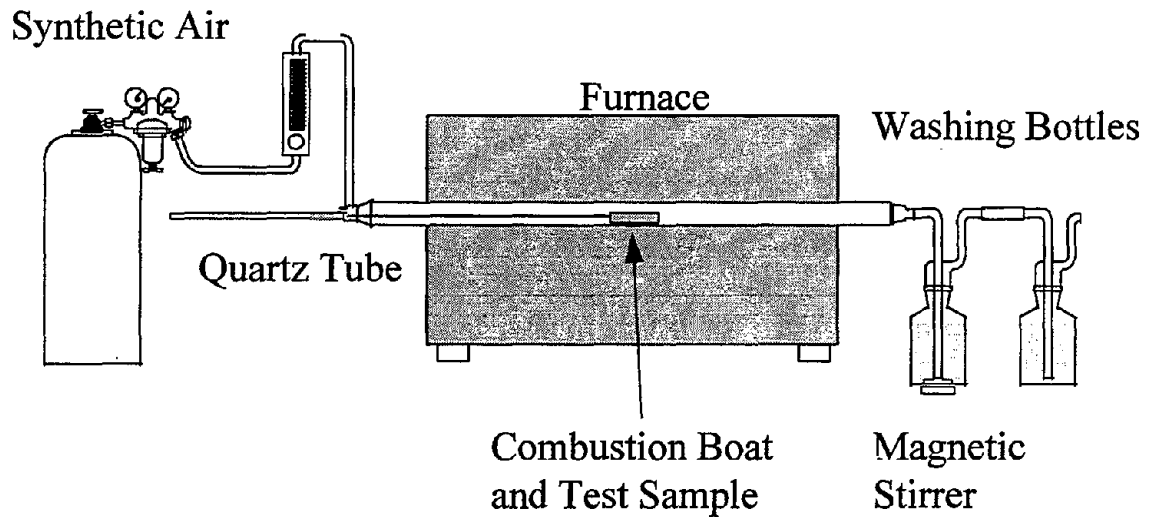


Figure 1 - Typical arrangement of acid gas, pH and conductivity based methods (IEC 754-2)

From Table 1 it may be observed that these methods are material tests. Thus it does not have the ability to determine the influence of finished product construction. IEC 754-2, however, does test the individual materials separately and then provide a weighted average of pH and conductivity of the constituent material of the finished cable. Further, the corrosion potential is inferred from the amount of acid gases (halogen gases), change in pH or electrical conductivity and do not provide a direct measurement the three modes of corrosion.

⁴ MIL-C-24643, section 4.7.25, Acid gas generation, Naval Sea Command, SEA 55Z3, Department of the Navy, Washington DC, 20362.

Direct Measurement Methods

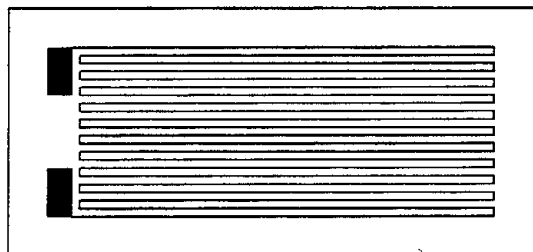
In the US and internationally, some effort has been focused on developing a method that provides a direct measurement of corrosion. In the US, ASTM E-5, and ASTM D-9 considered corrosion methods using metal loss targets. In consideration of the method, several objectives for the test were developed as follows:

- Measure performance
- Ability to test finished product
- Reasonable combustion module
- Possibility of varying combustion conditions
- Reasonable exposure module
- Possibility of varying targets
- Reasonably fast experiments

The last objective may have been identified based on the prolonged post-exposure time to measure loss of metal from coupons exposed to combustion products from shipboard fires⁵. Thus, the need for fast experiments was related to the sensitivity of the measurement technique used.

National Telecommunications laboratory of France (CNET) developed a corrosion test that measured the change in electrical resistance of a printed wiring board. Since the corrosion would reduce the metal loss thickness, the resistance of the target is expected to increase. The test method consists of burning a mixture of 600 mg of test sample, and 100 mg of polyethylene in a 20 liter closed chamber which is initially kept at 50°C. The ignition is accomplished by using an electrically heated coil at a temperature of 800 °C. The combustion products deposit on a water cooled printed wiring board. The temperature of the target is maintained at 40°C during the test. The change in resistance is measured at the end of 1 hour. The test, with some modifications, have now been standardized as ISO 11907-2⁶.

A schematic of the target is shown in Figure 2.



⁵ Powell, E.A., Zinn, B. T., "Corrosion of metals exposed to combustion products during shipboard fires, Georgia Institute of Technology, Prepared for Naval Research Laboratory, 1987.

⁶ ISO 11907-2 Plastics - Smoke Generation - Determination of the Corrosivity of fire effluents - Part 2: Static Method, International Standards Organization, Case Postale 56, CH-1211, Geneva, Switzerland.

Figure 2 - Schematic of the CNET Electrical Resistance Target

In the US a standard was developed (ASTM D5485⁷) using the Cone Calorimeter radiant heater and exhaust system with the addition of a gas sampling and target exposure system. A schematic of the test apparatus is shown in Figure 3.

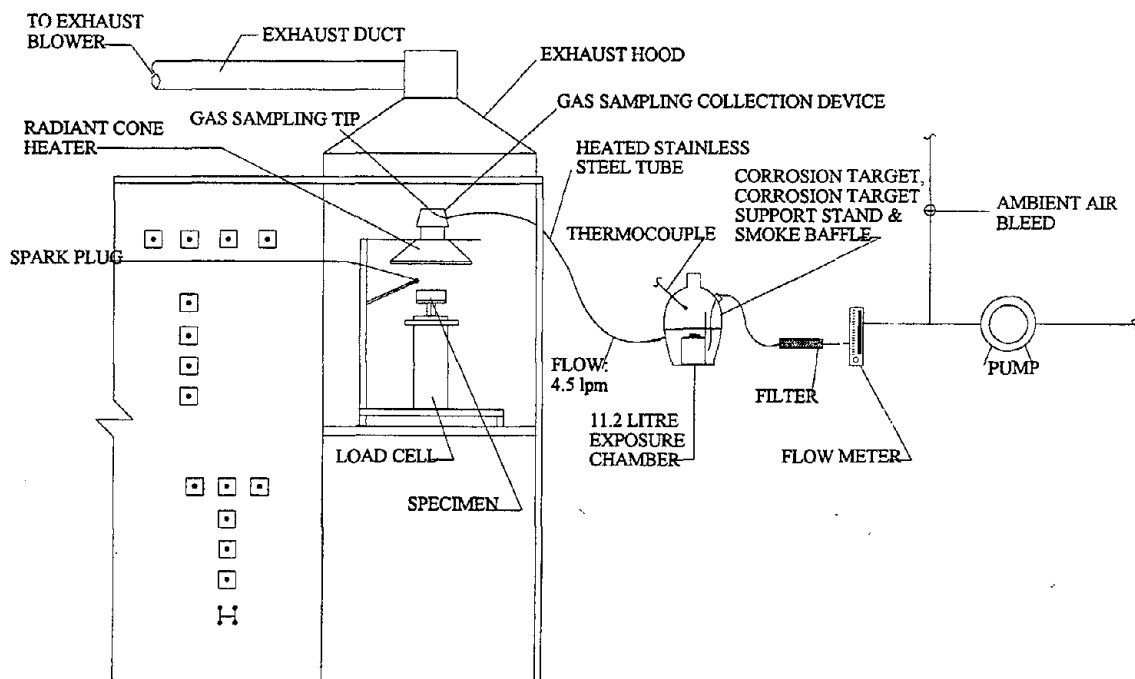


Figure 3 - Schematic of the ASTM D5485 Test Apparatus

This test uses an electrical resistance target as shown in Figure 4.

⁷ ASTM D5485 - Standard Test Method for Determining the Corrosive Effect of Combustion Products Using a Cone Corrosimeter, American Society for Testing and Materials, 100 Barr Harbor Drive, West Conshohocken, PA, 19428-2959.

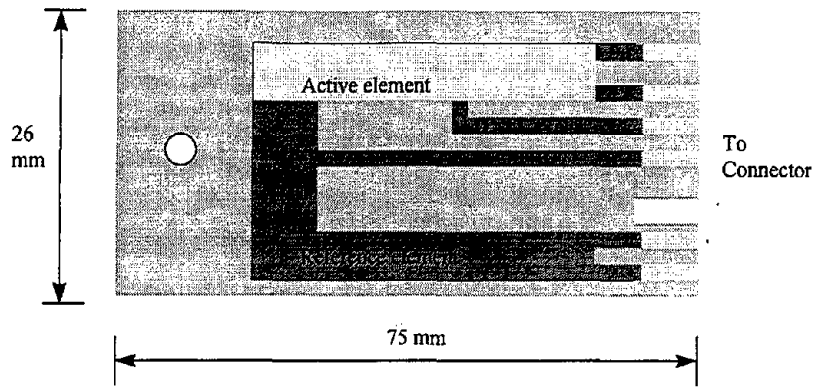


Figure 4 - Schematic of the Electrical Resistance Target for ASTM D5485

This test is conducted in two steps. In the first step, the weight loss characteristics of the sample is determined by conducting two tests at the desired radiant flux level. The corrosion tests are then conducted with the gas sampling until 70% of sample weight loss determined in the first step is attained. The exposure chamber is then sealed, and the target is exposed to the combustion products for a total of 60 minutes. There is an additional 24 hr. post-test exposure at 75% RH, and 75 °F.

Several studies have been conducted to compare the corrosion results obtained from the ISO 11907-2, and the ASTM D5485 test protocols. The data from one of the studies are presented in Figure 5, and Figure 6 respectively^{8,9}.

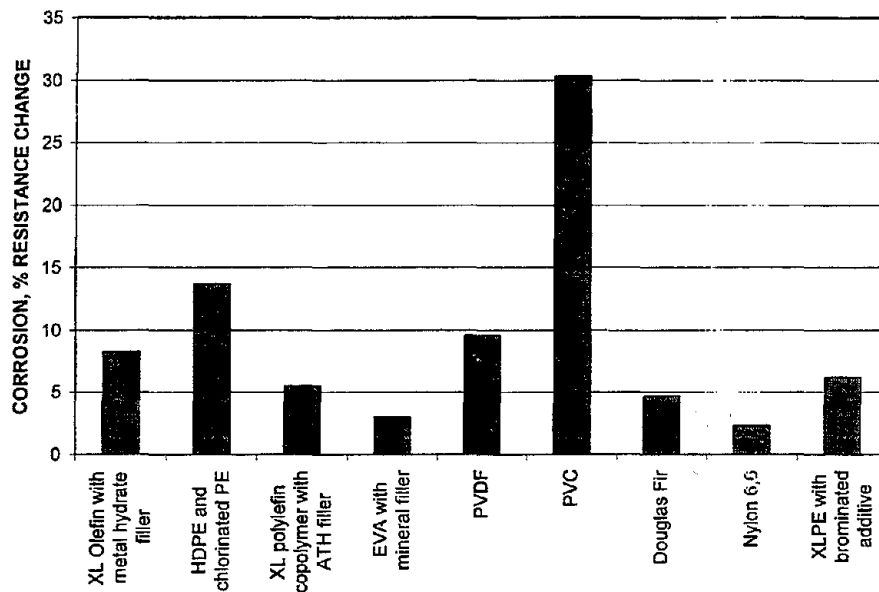


Figure 5 - Results from ISO 11907-2 Test Method (CNET Apparatus)

⁸ Rogers C. E., Bennett J. G. Jr., Kessel, S. L., "Corrosivity Test Methods for Polymeric Materials - Part 2 - CNET Test Method," Journal of Fire Sciences, Vol. 12, No. 2, (1994), pp. 134-154.

⁹ Bennett, J. G. Jr., Kessel, S. L., Rogers, C. E., "Corrosivity Test Methods for Polymeric Materials Part 4 - Cone Corrosimeter Method," Journal of Fire Sciences, Vol. 12, No. 2, (1994), pp. 175-195.

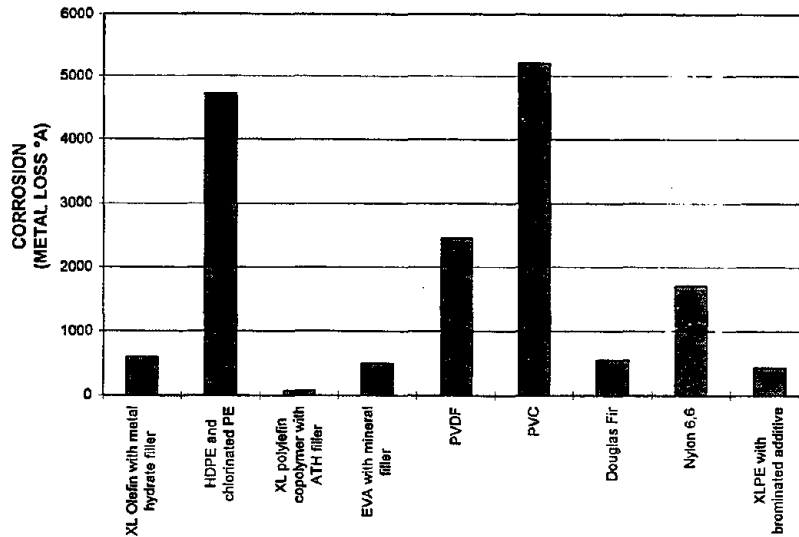


Figure 6 - Results from ASTM D5485 Test Method at 50 kW/m²

It may be observed that a trend is apparent between the data obtained in the CNET and the ASTM D5485 test apparatuses. The CNET test apparatus is a static chamber test. However, the mass of the test sample is small enough that there is more than sufficient oxygen for combustion of the sample¹⁰. On the other hand, in the ASTM D5485 test, the sample burns under well-ventilated conditions. Figure 7 shows a comparison of the data presented in Figure 5, and Figure 6.

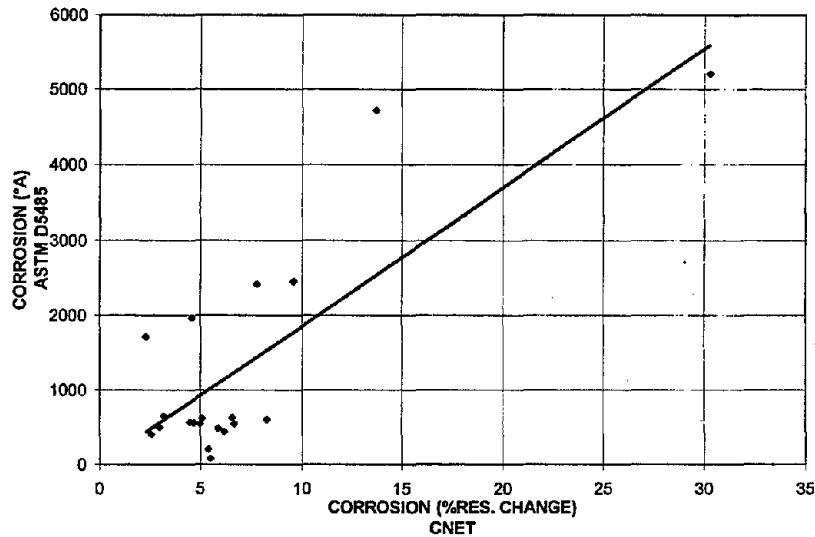


Figure 7 - Comparison of Data from CNET and ASTM D5485 Test Methods

¹⁰ Gandhi P. D., "Modeling Gas Collection Systems for Corrosion Testing," Fire Safety Journal, Vol. 21, (1993), pp. 47-68.

One of the advantages of the ASTM D5485 method is that it permits testing portions end products such as cable samples. This is important since test items may be manufactured with more than one material and co-combustion of materials constituents can influence the corrosion results. Further, product testing also allows determining the influence of construction. Figure 8 depicts some corrosion data obtained from cable samples using ASTM D5485.

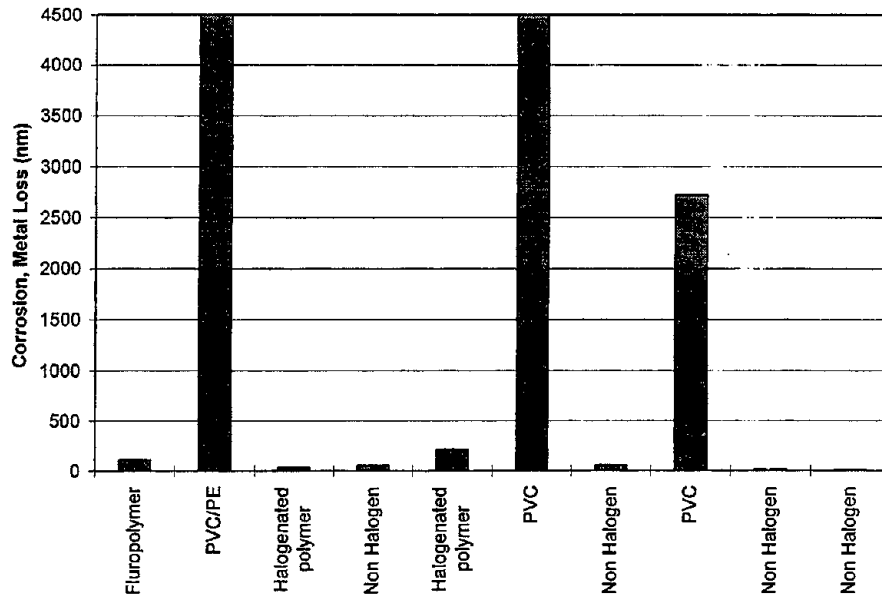


Figure 8 - Results of Corrosion from 4 Pair Communication Cables at 50 kW/m²

Current Leakage

The direct measurement tests that have been developed use metal loss target. This measurement however does not provide information on the impact of deposited combustion products on electronics. In Central Equipment Offices, it has been observed¹¹ that deposition of dust over a period of time can lead to malfunction of circuit boards under appropriate conditions of humidity and temperature. The dust has many ionic substances that cause an increased electrical surface conductance¹². Further, investigation of this phenomenon has shown that the surface conductance, or leakage current increases with % Relative Humidity. In fact, it has been observed that below a critical humidity level, the leakage current is relatively insignificant. Increase in humidity beyond the critical level results in marked increase in leakage current. Figure 9, adapted from

¹¹ Comizzoli, R. B., Frankenthal, P. C., Milner, P. C., Sinclair, J. D., "Corrosion of Electronic Materials and Devices, American Association for the Advancement of Science, Vol. 234, (1986), pp. 340-345.

¹² Sinclair, J. D., Posta-Kelly, L. A., Weschler, C. A., and Shields H. C., "Deposition of Airborne Sulfate, and Chloride Salts as It Relates to Corrosion of Electronics", Journal of Electrochemical Society, Vol. 137, No. 4, (1990), pp. 1200-1206.

Comizzoli et. al¹³, shows the influence of relative humidity on the leakage current from a number of dust samples. It may be noted that below relative humidity of less than 40% the leakage current is negligible, except for dust from the Kuwaiti oil well fires (labeled K10). The high leakage current at low humidity levels for the Kuwaiti samples is suspected to be due to the presence of graphitic carbon resulting from the hydrocarbon fires at the end of the Gulf War.

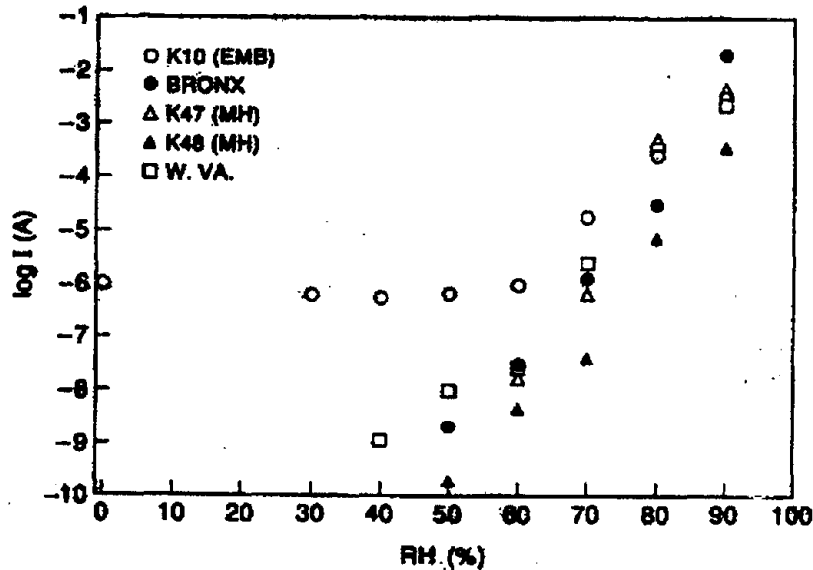


Figure 9 - Influence of Relative Humidity on Leakage Current

Plastics contain fire retardants, fillers, and other additives that may release ionic particles when they are involved in a fire. The thermal plume of a fire then can carry these particles to remote areas where they can deposit on electronic circuitry in an analogous manner to dust particles.

In order to study the influence of combustion products on the leakage current on electronic circuitry, a series of tests were conducted using a tube furnace apparatus similar to that described in IEC 754-2².

Leakage Current Experiments

The combustion tube furnace consisted of furnace, silica tube, combustion boat, air supply system, and a mixing chamber for the combustion products. The tube furnace had an inside diameter of 60.3 mm and a heating zone of 300 mm. The test temperature was controlled by an electronic temperature controller. The silica tube was 1600 mm long,

¹³ Comizzoli, R. B., Franey, J. P., Kammlot, G. W., Miller, A. E., Muller, A. J., Peins, G. A., Psota-Kelly, L. A., and Wetzel, R. C., "The Kuwait Environment and its Effects on Electronic Materials and Components," *Journal of Electrochemical Society*, Vol. 139, No. 7, (1992), pp. 2058-2066.

47.5 mm inside diameter and had a wall thickness of 2.75 mm. The silica tube was placed in the tube furnace such that it extended 400 mm from the rear end of the furnace. The rear end of the tube was ground and was fitted with a glass adapter connected to an air supply from a dry compressed air cylinder. A porcelain combustion boat, 97 mm in length, was used to hold the test sample during the test.

The mixing chamber was made from polymethyl methacrylate (PMMA), with dimensions of 310 x 310 x 340 mm. A stainless steel plate was attached to the inner side of part of the chamber connected to the silica tube. The purpose of the plate was to protect the PMMA surface from flames emanating from the silica tube. The top of the mixing chamber was a blowout panel to release excessive pressure. The chamber had a 6.3 mm opening at the bottom of one of the sides to permit exhaust of combustion products to a smoke abatement system. The mixing chamber was placed 385 mm away from the end of the tube furnace, such that 55 mm of the silica tube protruded inside the chamber.

Test Samples

Test samples were obtained commercially. Six materials were used in this investigation. In the combustion tube furnace experiments the IEC 754-2 test specifies a sample weight of $1,000 \pm 5$ mg. The samples are described in Table 2.

Table 2 - Test Samples

Sample Identification	General Composition
A	Halogenated, flame retardant polyolefin
B	Commercial PVC formulation
C	Non halogenated, flame retardant polyolefin
D	Non flame retardant polyolefin
E	Halogenated, highly flame retarded polyolefin
F	Commercial fluorinated polymer

The samples were conditioned for at least 16 h at a temperature of 23 ± 2 °C, and relative humidity of 50 ± 5 %.

Corrosion Target

The corrosion target consisted of an interdigitated circuit with a spacing between the digits of 12.5 μm . A schematic of the circuit is shown in Figure 10. Prior to testing, the target was cleaned in an ultrasonic bath with 75% isopropyl alcohol, followed by rinsing in de-ionized water for 30 seconds, and drying with compressed nitrogen.

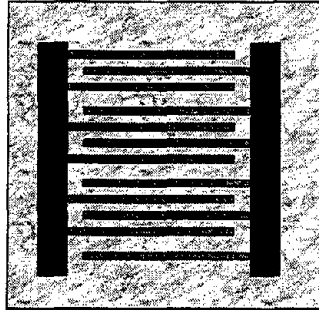


Figure 10 - Schematic of a Interdigitated Corrosion Target

Test Procedure

For each test, the following test procedure was used. The furnace was set at 900 °C. One corrosion target was placed at the bottom and at one of the ends of the mixing chamber as shown in Figure 11. The test samples were weighed to an accuracy of 1 mg and evenly distributed on the bottom of the combustion boat. The test samples with the combustion boat were also weighed. The combustion boat with the test sample were placed inside the rear end of the tube prior to test initiation. The end was closed with the adapter, and an air flow rate of 0.45 liters per minute was established through the silica tube. The combustion products were allowed to react with the corrosion target for 1 hour. At the end of one hour, the target was removed and leakage current characteristics were determined. The combustion boat with residue was weighed and the sample weight loss was determined.

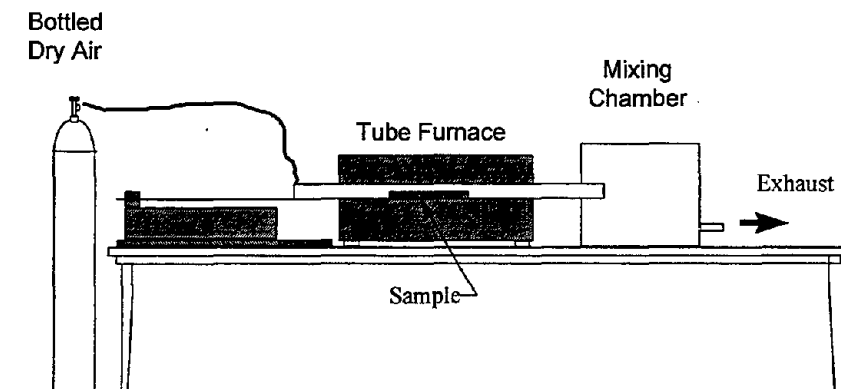


Figure 11 - Leakage Current Test Apparatus

The targets were placed in the controlled RH chamber. A voltage of 5, 50 or 200V was applied. For each voltage, the RH was increased from 30 to 90% and currents were recorded at RH intervals of 5%. Four targets were run as a group.

Results and discussion of Leakage Current Data

The leakage current data for the tube furnace at 5, 50 and 200 volts are presented in Figure 12, Figure 13, and Figure 14.

The leakage current measured on a test pattern is expected to depend not only on the type and quantity of deposited species, but also on the relative humidity (RH), temperature, applied voltage, and the history of the sample including the duration of the RH exposure and voltage application. In light of these factors, the present experiment is a first step demonstration of RH-dependent surface currents after deposition of combusted polymer formulations. Until the effects of RH, time, and voltage are more clearly resolved by the data, a detailed comparison of the polymer formulations may be premature. However, some general observations can be made.

Below about 50% RH, the currents in Figure 12 to Figure 14 are measurable but small, except for Samples B and C. Sample B has significant leakage current, even at 30% RH. At 55% RH Sample B shorted out. Inspection revealed little corrosion, no "growths" of corrosion product, and an apparent smoke "dendrite" bridging two lines. Sample C exhibited unusually large currents at low RH. The current decreased as the RH increased, which is most likely a time effect rather than an RH effect. The current is decaying with time, rather than decreasing because the RH is higher. The current decay is probably related to polarization effects or to formation of corrosion product.

A comparison of current levels at high RH for the three voltages shows that only polymer F has a consistently low current, indicating it is the most benign, at least for these test conditions. Polymer B has a consistently large current, suggesting it may have the most serious smoke effects.

Some of the data shows an approximate exponential dependence of current on RH above about 50% RH. This behavior is typical for surface currents on a wide variety of insulators¹¹. This is attributed to the formation of conducting regions between the metal lines. These regions are conducting independent of RH. In some cases microscopic examination revealed bridging structures of presumably conducting smoke. In other cases, charred regions of circuit board material or conducting corrosion product bridges were observed.

Conducting bridges of corrosion product or of smoke particles can usually be disrupted by the passage of sufficient current. Following the disruption, the resistance of the sample increases and lower currents are measured even at higher voltages. The testing

sequence at different voltages is clearly an important variable. For example, sample A had a larger current at 5V than at 50V for the tube furnace exposure.

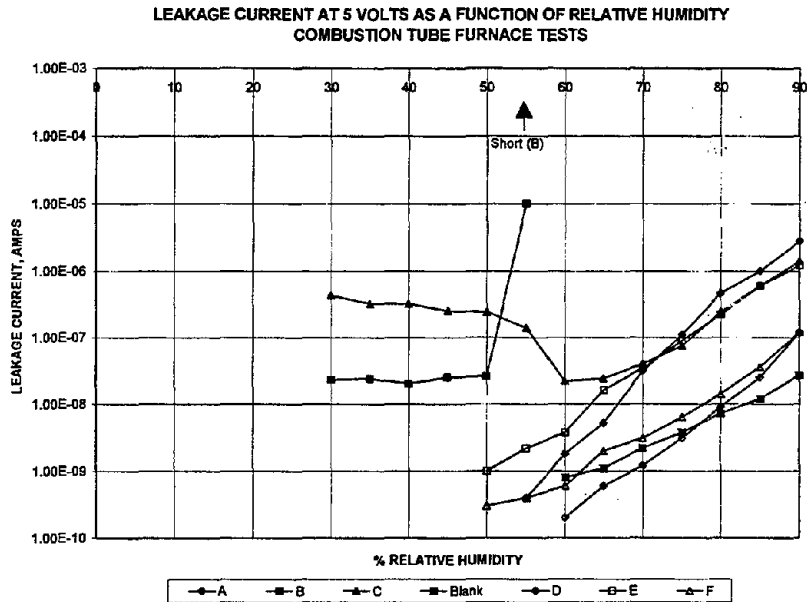


Figure 12 - Leakage Current at 5 Volts

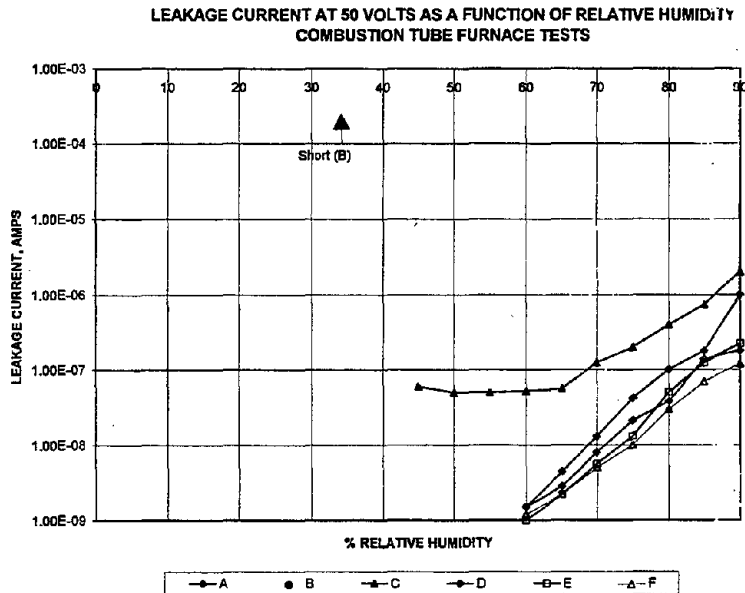


Figure 13 - Leakage Current at 50 Volts

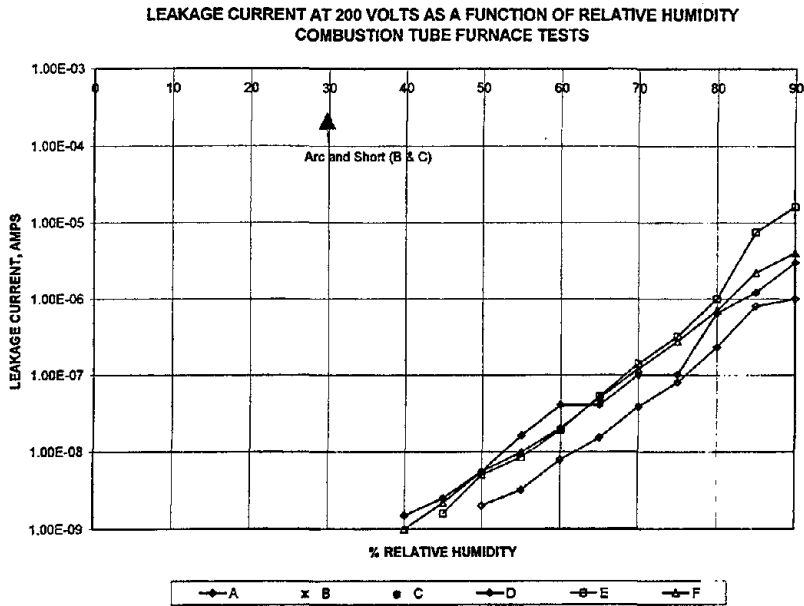


Figure 14 - Leakage Current at 200 Volts

Future Work

This study provides information for understanding the smoke corrosivity behavior of cable jacket and insulation materials. We are anticipating continuing this investigation to refine the test protocol and correlate to large scale testing. Some areas of future work include: 1) comparison of data to metal loss behavior, 2) comparison of data to pH and conductivity data, 3) expanded materials list for testing, 4) conduct SEM/EDAX analysis of test patterns, 5) analysis of smoke particulate, 6) small and large scale product testing.

Discussion

Patrick Pagni: Which of the two do you think is the more serious problem: condensate on particles or gas phase material as a corrosive agent?

Pravinray Gandhi: In my opinion, the particle condensation is the most problem. This is not based upon any measurements I have made, but is made based upon all the observations I've had in studying the targets after exposition to corrosion particles.

ZUKOSKI SYMPOSIUM

Opening Remarks

Zukoski Symposium

Jack E. Snell

It is both an honor and a pleasure for me to comment at this Symposium honoring the work and influence of Professor Edward Zukoski, of Cal Tech. I first met the good professor in Tokyo at my first UJNR meeting in May of 1982.

I have experienced the influence of Professor Zukoski in a number of modes - as a keen researcher and superb experimentalist; as a source of technical inspiration; as a backer and supporter of the cause of fire research in the nation; as warm, caring person and good humored friend; and even as a prod when in his judgment, I, as a relative newcomer to fire research management, have needed his "guidance".

Let me expand on just a few of these influences with specific examples. Ed is a survivor - he is one of the longest standing grantees of the NIST Fire Research Program, with a nearly unbroken string of projects dating from 1978. In this time, his contributions - in addition to mentoring grant monitors such as Rockett, Quintiere, Jones and Cooper - have covered a range of topics, e.g.,

- Two room fire model that formed the basis for the widely used ASET model,
- Entrainment in the upper and lower layers that we heard referenced earlier in the week by Jay Gore,
- Vertical flows in tall shafts that produced the basis for the algorithms for solving smoke flows in shafts in our current fire models,
- Flow visualization of horizontal flows providing a dataset to verify our CFD models,
- Seminal baseline data on the production of CO in fires burning in two layer environments

Paraphrased in Len Cooper's inimical style, "Ed displayed a unique ability for identifying, and successfully solving experimentally, with a unique elegance and clarity, the fundamental research problems of compartment fire phenomena."

Later in the day, Pat Pagni will tell of Ed's influence in his daughter. Well, Ed swayed mine as well. As luck would have it, my daughter came of age for "the science fair project" about the same time Ed's 1985 Howard Emmons award lecture was being presented for him, in absentia, by Professor Kubota. A lifelong aficionado of flow visualization techniques, myself, I "suggested" to my daughter she use this approach to demonstrate the importance of smoke detectors and their proper placement in the home. We developed a two dimensional model of a two story house which nicely illustrated the principles involved. My daughter and I had a great time working together on the project. I was sure it would be a winner. (The judges unfortunately thought they saw too many of my fingerprints on it and passed it off with an honorable mention.) Nonetheless, this was her first venture into the scientific realm and it stuck. She is now working hard but

joyfully to become a pediatrician. Thanks, Ed.

When fire research was dropped from the Reagan budgets, Ed was quick to pitch in to help rectify the situation. The good news is that this effort, small as it is does continue. Without such support, it probably would have gone the route of the recently -deceased Bureau of Mines.

For all of this, Ed, and on behalf of the U.S. Panel and the entire staff of the Fire Research Program at NIST, we thank and applaud you.

A Universal Orifice Flow Formula
 Howard W. Emmons - Professor Emeritus
 Harvard University
 317 Pierce Hall - Cambridge Ma 02138 - USA

Flow metering nozzles and orifices have been studied for a century and with adequate care in installation can measure flow rates to better than one percent. The growing demands of fire science has introduced new flow problems presented by doors and windows, burn through and other holes in the ceiling and fireman opened holes in the roof, horizontal or inclined. This paper presents a unified formula for all these cases. As usual, a practical ideal formula is theoretically derived and then empirical constants are added to correct for omitted phenomena. High precision is neither needed nor attainable since the nature of the vent (size, shape, edge geometry) is poorly known or not known at all. In addition the gas velocities and temperatures on the two sides of the vents are poorly or completely unknown. Finally experimental data for validation of flow coefficients are very limited or are as yet unavailable.

Introduction

It has become conventional to define an ideal flow through a nozzle or orifice by the equation 1 derived by use of Bernoulli's equation.

$$m = A(2\rho_f\Delta p)^{1/2} \tag{1}$$

This equation ignores various inlet and other flow effects and viscous boundary layers. For metering purposes, the Reynolds number is usually 10^4 or higher so equation 1 is corrected as in equation 2 by a flow coefficient

$$m = C_D A(2\rho_f\Delta p)^{1/2} \tag{2}$$

where $C_D \approx .98$ for a nozzle $C_D \approx .6$ for an orifice. Figure 1. shows more detailed accuracy in the region $Re > 10^4$ (1). The low orifice coefficient .6 is caused by the contraction of the exit stream to a vena contracta area of $A_{vc} \approx .6A$.

When this same ideal flow equation 1 is used to compute the fire flow through an orifice in a horizontal surface (2,3,6), the flow coefficients are in the range .1 to .2. Without any apparent concern for how the coefficients got so low, the experimental results, including a region near $\Delta p = 0$ where simultaneous in-out flow occurs, are presented assuming the buoyancy caused by density difference requires a Froude Number for data presentation. Cooper (6) in particular has made an extensive empirical analysis assuming that

$$C_D = \bar{C}_D (\overline{Fr}, \overline{Gr}, \Delta\rho/\rho, \Pi) \tag{3}$$

(Note: $\Pi \neq \pi$ see notation)

Analysis

Consider the horizontal vent fire case of hot gas below and cold gas above. I will set it up with all my initial misconceptions to be corrected later. The positive direction is up. The pressure drop is defined as $\Delta p = p_i - p_o$ (negative if flow is down)

The density change is $\Delta\rho = \rho_o - \rho_i$ (negative if cold gas is below)

h = the distance up to the vena contracta (negative if down)

g' = the component of gravity inward perpendicular to the vent surface.

The flow controlling velocity is at the vena contracta and is given by Bernoulli as

$$v = (2\{\Delta p + \Delta\rho g'h\}/\rho_f)^{1/2} \tag{4}$$

the volume flow and mass flow follow as

$$Q = vA_{vc} \text{ and } m = \rho_f Q = \rho_f v A_{vc} \tag{5}$$

To make these relations correct for all flow directions, pressures, and temperatures we need to insert all the correct signs and add flow coefficients for the omitted effects.

$$v = \text{sign}(\Delta p + \Delta\rho g'h) C_\mu (\text{sign}(h) 2\{\Delta p + \Delta\rho g'h\}/\rho_f)^{1/2} \tag{6}$$

$$Q = \text{sign}(\Delta p + \Delta\rho g'h) C_\mu C_{vc} A (\text{sign}(h) 2\{\Delta p + \Delta\rho g'h\}/\rho_f)^{1/2} \tag{7}$$

$$m = \text{sign}(\Delta p + \Delta\rho g'h) C_\mu C_{vc} A (\text{sign}(h) 2\rho_f\{\Delta p + \Delta\rho g'h\})^{1/2} \tag{8}$$

where C_μ - corrects for viscous and other neglected flow effects

$C_{vc} = A_w/A$ corrects for the flow area change to the vena contracta.

h - corrects for buoyancy effects from orifice to vena contracta

the flow coefficient $C_D = C_\mu C_{vc}$

For high Reynolds numbers (above 10^4) the buoyancy effects are unimportant but by crude observation $h \approx D$.

Consider the metering nozzle and orifice. The nozzle coefficient, C_D , Figure 1, $Re > 10^4$, is required to correct for viscous boundary layers and turbulence. Thus for the metering nozzle $C_D \equiv C_\mu$ ($C_{vc} = 1$). There is no nozzle vena contracta. The orifice coefficient has a viscous effect similar to the nozzle but also has a large dynamic contraction to the vena contracta controlling the flow area. thus for the orifice its flow coefficient $C_D = C_\mu C_{vc}$. Since C_D (orifice) $\approx .6$ and $C_\mu \approx .98$, $C_{vc} \approx .612$. 9

Note that below $Re \approx 10^4$ the nozzle flow coefficient falls while the orifice flow coefficient rises. Clearly viscous effects are increasing in importance relative to the dynamics as Re falls while for an orifice the falling dynamics also prevents the approach fluid from jumping off the orifice lip so vigorously and hence the vena contracta area becomes larger. As the Reynolds number falls C_{vc} is expected to continue to rise toward 1. The dashed line of figure 1 shows the computed C_{vc} by equation 9 for $Re > 10^4$ while the C_{vc} for $Re < 10^4$ is the expected effect (no data available). (much new test data is needed for $Re < 10^4$).

The Horizontal Orifice

The flow is given by equation 8. Figure 2 shows the predicted flows for various cases. For $m > 0$ the flow is up while for $m < 0$ the flow is down. If $\Delta\rho > 0$ (the fire case) and the flow is up $h > 0$, the flow varies with Δp as in figure 2a. Note that at $\Delta p = 0$ there is still upward flow by buoyancy.

$$m_u = C_\mu C_{vc} (2\rho_d \Delta\rho g^* h)^{1/2} \text{ and } m = 0 \text{ at } \Delta p = -\Delta\rho g^* h > 0 \text{ (no up flow. therefor flooding down flow)} \quad 10$$

If $\Delta\rho > 0$ and $h < 0$ the flow is down and at $\Delta p = 0$ there is still down flow by buoyancy

$$m_d = -C_\mu C_{vc} (-2\rho_d \Delta\rho g^* h)^{1/2} \text{ and } m = 0 \text{ at } \Delta p = -\Delta\rho g^* h > 0 \text{ (no down flow. Therefor flooding up flow)} \quad 11$$

If $\Delta\rho < 0$ (high density below) the upward flow ($h > 0$) is zero at $\Delta p = -\Delta\rho g^* h > 0$ 12

and downward flow ($h < 0$) is zero at $\Delta p = -\Delta\rho g^* h < 0$ 13

This last case is shown in figure 2c where a stable region with no flow is predicted as is too be expected.

Finally if $\Delta\rho = 0$ i.e. no density difference, figure 2b shows the result.

Experimental data (3, 4) presents flow coefficients, \bar{C}_D defined by equation 2. For this new theory $C_D = C_\mu C_{vc}$ is defined by equation 8. Thus C_D and \bar{C}_D are related by

$$\bar{C}_D = C_D \{1 + \Delta\rho g^* h / \Delta p\}^{1/2} \quad 14$$

To make the conversion requires values of h . At the lazy flooding flow, the distance "h" to the vena contracta is nearly zero as seen in the shadowgraphs of reference 3. However at flooding $\Delta p = \Delta\rho g^* h$ while experiments give

$$h/D = \Delta p / \Delta\rho g^* D / \Delta p / \Delta\rho g^* h = \Delta p / \Delta\rho g^* D \quad 16$$

This has the experimental value of about 2. (Present data has considerable scatter and no apparent correlation.). Clearly h is not the distance to the vena contracta as first assumed, It is the distance over which buoyancy has an influence on the flow. Some experimental values as high as 6 are not believable. New experimental work is essential to find and correct current mistakes in experiment and theory.

Another important change is to use the conventional dimensional variables for a viscous, buoyant flow. Thus

$$C_D = C_D(Re, Fr) \quad Re = VD/\nu, \quad Fr = V/(g^* d)^{1/2} \quad 17$$

The available data is inadequate to use this relation correctly. Experiments should be made holding one independent variable constant while the other is varied. Such data has never been taken.

The best that can be done with available data is to plot the experimental C_D vs Re as in figure 1. The lower curve shows the data which falls at $5 \times 10^2 < Re < 4 \times 10^3$. The curve between $Re = 4 \times 10^3$ and 10^4 is drawn by eye but the data fits together remarkably well. Using equation 9 and C_μ and C_D from figure 1 permits the calculation of C_{vc} over the whole Reynolds number range. In figure 1 C_μ for Re between 4×10^3 and 10^4 derived as above fits remarkably well. New data in this range is needed.

Since C_D and C_μ curves were drawn (with good fit) by a logarithmic french curve, they plot as straight lines on cartesian coordinate paper and hence are defined by linear equations as shown on figure 1. The C_{vc} curve has a more complex formula, quadratic in $\log Re$.

It is now clear why the flow coefficients are so low for the normal range of horizontal orifice flow. The Reynolds number is so low that the flow is dominated by viscous forces.

The flood point would be expected to be controlled by the Froude Number. Figure 3 shows how the Froude number at flood varies with the density change $\Delta\rho/\rho$. (the data of Tan and Jaluria (3) is puzzling. Their experimental work appears very good. Either their flood data is bad or the other $Fr(\Delta\rho/\rho)$ data (2.5) is some how inadequate). If $\Delta\rho = 0$, the boundary between up and down flow is at $\Delta p = 0$ and hence $Fr = 0$ as plotted. The solid curved line is the best fit while the dashed straight line is accurate enough for fire purposes.

It remains to compute the up and down flow between the flood limits. At flood conditions, measurements (4) at $\Delta p = 0$ gave

$$Q_d / (gD^5 \Delta\rho/\rho)^{1/2} = -.055 \quad 18$$

from which follows the $\Delta p = 0$ downward mass flow

$$m_d / \Delta\rho A [gD]^1/2 = -.202 \quad 19$$

The up and down region is shown in figure 4. The two flood points are shown e which terminates the one way flow regions. There is too little data for the flow in this region, so a linear assumption is used. For up flow, for example, the flow is assumed to vary as the straight line from the upward flood point A to zero at the pressure drop (negative) of the downward flood point.

To find the flow (up or down) at any Δp in the two flow region, we note that at flood

$$Fr_f = V_f / (g'D)^{1/2} = m_f / \rho_f A (g'D)^{1/2} = .591 \Delta\rho/\rho_f \quad 20$$

so that

$$m_f / \text{sign}(h) \Delta\rho A (g'D)^{1/2} = .591 \quad 21$$

The corresponding pressure drop is

$$\Delta p_f = \text{sign}(h) .0873 \Delta\rho^2 g'D / C_D^2 \rho_f \quad 22$$

Note that unlike figure 2 (where it was assumed that $h_u = D$) the magnitude of the pressure drop for up and down flow flood are different because of $C_D^2 \rho$ and therefore h by equation 16 is different for up and down flow. However the linear assumption for the conditions of the experiment of equation 18 (4) at $\Delta p = 0$ gives

$$m_d / \Delta\rho A (g'D)^{1/2} = -.275 \text{ compared to equation 19, } -.202 \quad 23$$

While this agreement is not perfect, it is better than our general knowledge of the size and shape of a burn through hole in a ceiling. Much more experimental work is required to measure the actual up and down flows.

To compute the flow through a horizontal vent given the pressures and densities one must.

1. From the densities compute $\Delta\rho/\rho_f$
2. Compute the Froude number $Fr = .591 \Delta\rho/\rho_f$
3. Compute the Reynolds number $Re = Fr(g'D^3)^{1/2}/\nu$
4. Look up C_D from figure 1 (or compute it from equations given there)
5. Compute m from equation 8
6. Compute m_f from equation 21. Two values + and -
7. If $|m| > |m_f|$ then m is the one way flow through the vent
8. If $|m| < |m_f|$ then there is two way flow through the vent
9. Compute Δp_f from equation 22 for both up and down flow. $\Delta p_f = \Delta p_u > 0$ up, $\Delta p_f = \Delta p_d < 0$ down
10. Compute $m_u = |m_f| (\Delta p - \Delta p_d) / (\Delta p_u - \Delta p_d)$ and $m_d = |m_f| (\Delta p - \Delta p_u) / (\Delta p_u - \Delta p_d)$

These are the up and down flows in the two flow region.

This theory like many others for flow through a horizontal vent contains many assumptions which can only be removed by careful experimentation.

The Vertical Vent

In this case the gravity component perpendicular to the vent surface is zero; $g' = 0$. Gravity acts parallel to the vent surface so that both inside and outside pressures decrease with height which must be found by integration.

$$\Delta p = \Delta p_o + \int_o^y \Delta\rho g dy \quad 24$$

which for constant densities ρ_o and ρ_i becomes

$$\Delta p = \Delta p_o + \Delta \rho g y = \Delta p_s - \Delta \rho g(H - y) \quad 25$$

If $\Delta \rho = 0$, the pressure drop Δp is the same at all levels. Since the pressure difference varies with height y , the equations 6,7,8 must be applied to an area element $dA = w dy$. Thus

$$v = \text{sign}(\Delta p) C_\mu (\text{sign}(h) 2\Delta p / \rho)^{1/2} \quad 26$$

$$dQ = \text{sign}(\Delta p) C_\mu C_{vc} w dy (\text{sign}(h) 2\Delta p / \rho_f)^{1/2} \quad 27$$

$$dm = \text{sign}(\Delta p) C_\mu C_{vc} w dy (\text{sign}(h) 2\rho_f \Delta p)^{1/2} \quad 28$$

These equations have included the customary assumption that the flow velocity at any level y depends upon the difference in pressure at the same level y far from the vent. This ignores the fact that buoyancy causes the in-out flow boundary in the vent to be somewhat higher (7). This omission must also be corrected by the flow coefficients. If the density is everywhere the same, the total mass flow is

$$m = \text{sign}(\Delta p) C_\mu C_{vc} A (\text{sign}(h) 2\rho_f \Delta p)^{1/2} \quad 29$$

Only in this case is zero flow possible (with $\Delta p = 0$)

If both ρ_o and ρ_f are constant at all levels but $\Delta \rho \neq 0$, integration then gives the one way flow as

$$m = \text{sign}(\Delta) 8^{1/2} / 3 C_\mu C_{vc} A \rho_f^{1/2} (|\Delta p_o| + (\Delta p_o \Delta p_o)^{1/2} + |\Delta p_f|) / (|\Delta p_o|^{1/2} + |\Delta p_f|^{1/2}) \quad 30$$

If either or both densities vary with height, then the pressure difference varies with height and equations 26,27,28 must be integrated. However if the densities are constant in layers, equation 30 can be applied to each layer.

Again for constant densities, $\Delta \rho \neq 0$, the flooding flows occur for outflow at $\Delta p_o = 0$ and $\Delta \rho > 0$ or $\Delta p_s = 0$ and $\Delta \rho < 0$ while for inflow $\Delta p_o = 0$ and $\Delta \rho < 0$ or $\Delta p_s = 0$ and $\Delta \rho > 0$. As the pressure drop at the bottom of the vent goes from large positive to large negative, the out flow decreases from a large value to the flood value at $\Delta p_o = 0$. Then the boundary between the in and out flow moves from the bottom to the top of the vent. The inflow flooding flow occurs at $\Delta p_s = 0$ at which time $\Delta p_o = -\Delta \rho g H$. For all $\Delta p < -\Delta \rho g H$ there is inflow only.

Unlike the horizontal vent, there is no zero flow region in Δp and the in-out flow boundary is fixed at one (or more) heights depending on the specific case. For the horizontal case the in-out boundary wanders randomly over the vent area.

An extensive study has not yet been made of the available data. For most fire purposes a flow coefficient of .68 is sufficiently accurate over the whole Reynolds number range. However available data (7) (with considerable scatter) shows that for $Re < 2000$ that the outflow coefficient roughly follows C_μ and the inflow coefficients follow C_D . Also (by eye) (7) $h \approx D$.

The Inclined Vent

Figure 5 shows such a vent. If the pressure drop across the vent at the bottom is Δp_o , the pressure drop at any other height must be found by integration.

$$\Delta p = \Delta p_o + \int_0^y \Delta \rho g \sin \theta dy \quad 31$$

which for constant densities gives

$$\Delta p = \Delta p_o + \Delta \rho g y \sin \theta = \Delta p_s - \Delta \rho g(H - y) \sin \theta \quad 32$$

The equations 6,7,8 must again be applied at each y

$$v = \text{sign}(\Delta p + \Delta \rho g h \cos^2 \theta) C_\mu (\text{sign}(h) 2\{\Delta p + \Delta \rho g h \cos^2 \theta / \rho_f\})^{1/2} \quad 33$$

$$dQ = \text{sign}(\Delta p + \Delta \rho g h \cos^2 \theta) C_\mu C_{vc} w dy (\text{sign}(h) 2\{\Delta p + \Delta \rho g h \cos^2 \theta\} / \rho_f)^{1/2} \quad 34$$

$$dm = \text{sign}(\Delta p + \Delta \rho g h \cos^2 \theta) C_\mu C_{vc} w dy (\text{sign}(h) 2\rho_f \{\Delta p + \Delta \rho g h \cos^2 \theta\})^{1/2} \quad 35$$

Again the flow can only be determined by integration of each specific case. There is no zero flow case since again $\Delta p_o = 0$ and Δp_f are the two flooding limits for ρ_o and ρ constant ($\Delta \rho \neq 0$). The transition from in to out flow occurs by the zero flow location in the vent moving from $y = 0$ to $y = H$. Finally the flow with uniform but different densities is given by equation 30 where the pressure variables are replaced by

$$\Delta p \rightarrow \Delta p + \Delta \rho g h \cos^2 \theta : \Delta p_o \rightarrow \Delta p_o + \Delta \rho g h \cos^2 \theta : \Delta p_s \rightarrow \Delta p_s + \Delta \rho g h \cos^2 \theta \quad 36$$

As the inclination θ approaches zero, the zero flow location which has started at the bottom and moved to the top loses its significance since Δp_f flood is forced by buoyancy before $\Delta p_o = 0$ at the bottom. Therefore as $\theta \Rightarrow 0$ the in-out flow locations wander randomly over the vent area, tripped by vent edge irregularities and inlet flow disturbances. If θ becomes so small that either or both Δp_o or Δp_s fall between the two flood values Δp_f , the flow will become that of a horizontal vent.

Conclusion

The flow through fire vents (often ill defined) can be computed for all vent shapes and orientations. The accuracy is the highest attainable with the present meager data from which to compute the effective flow coefficients C_D and buoyancy effective lengths h . Many more experimental studies are necessary to get the desired accuracy. In fact the accuracy of flow through burn through holes in walls or ceilings may be forever impossible because of the probable impossibility of ever predicting the size and shape of the vent.

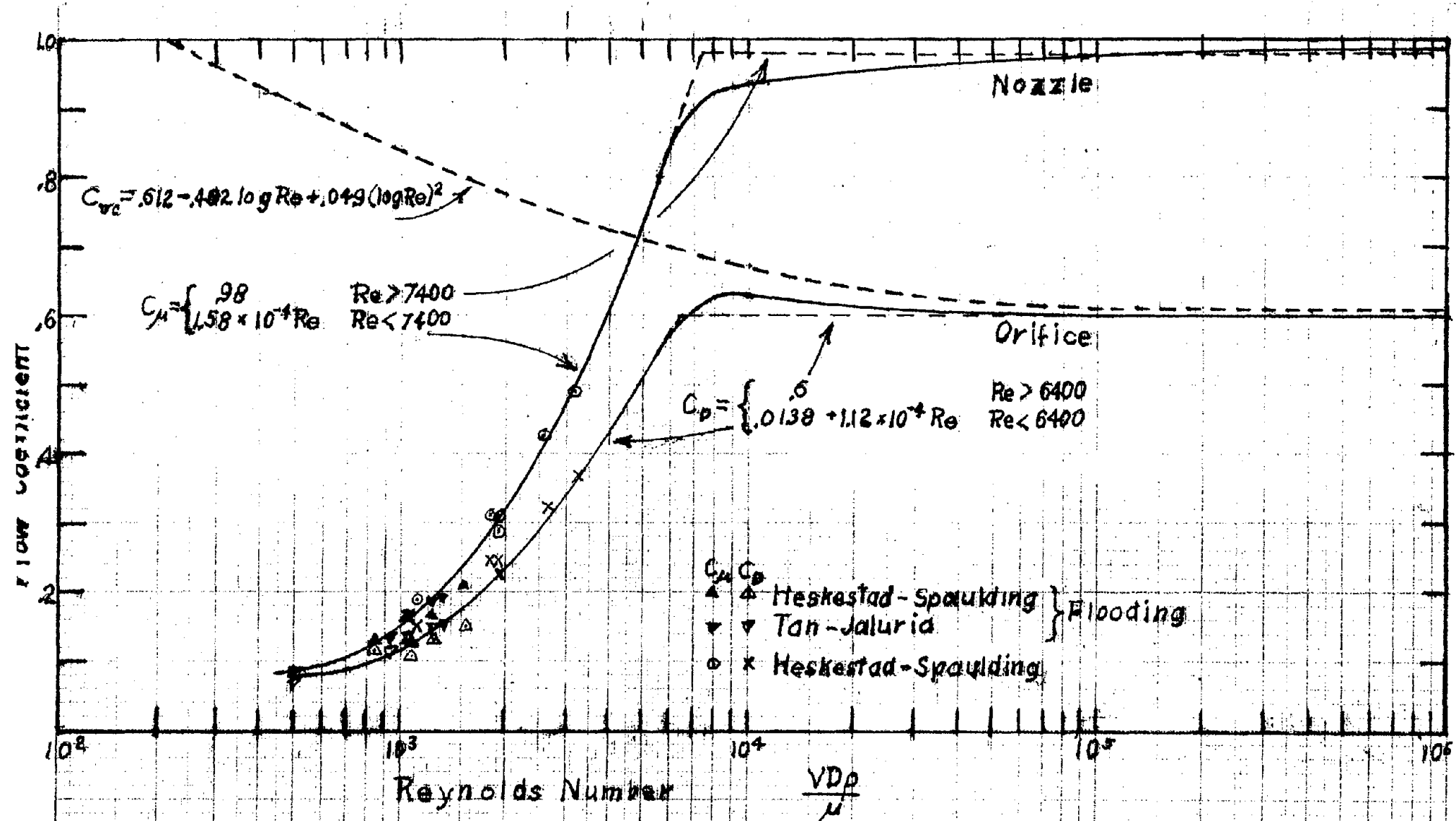
There are obviously enough challenging fire problems to occupy a generation of Ed Zukoskis

Nomenclature

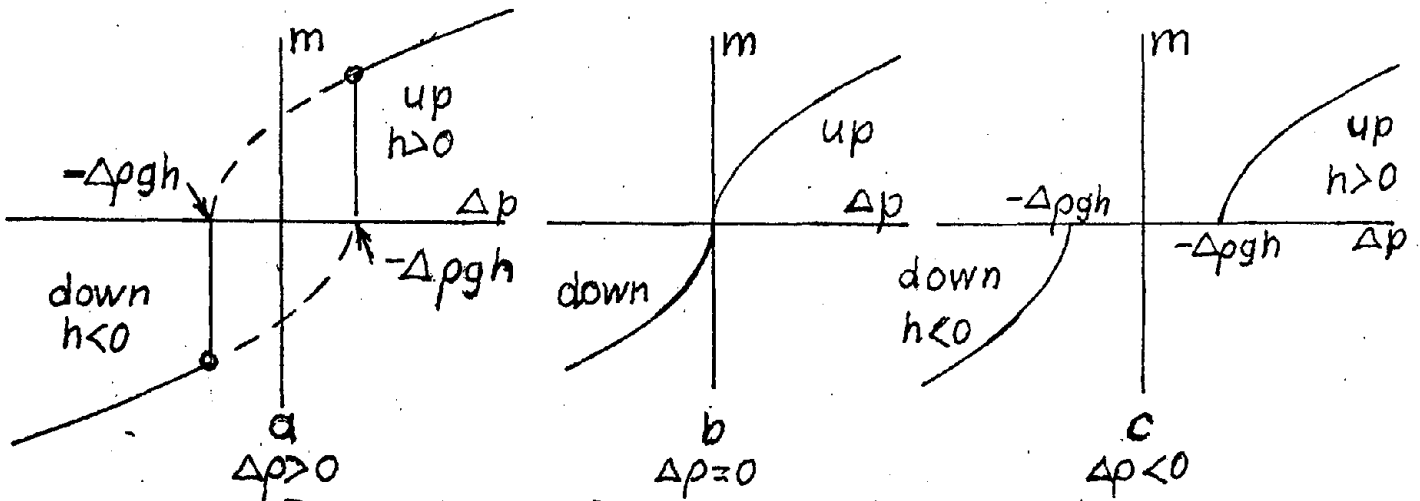
A	vent area	$V = m/\rho_f A$	Velocity in the vent
A_{cv}	vena contracta area	w	width of rectangular vent
C_D	new theory flow coefficient	y	coordinate across vent
C_D	old theory flow coefficient	Greek Letters and Subscripts	
$C_{vc} = A_{vc}/A$	contraction factor	$\Pi = \Delta p/4g\Delta\rho D$	
C_μ	viscous correction factor	θ	roof inclination
D	vent diameter	ρ	density
$Fr = V/(g'D)^{1/2}$	Froude Number	ρ	mean density
$Fr = v/(g'D\Delta\rho/\rho)^{1/2}$		d	lower variable
Gr	Grashoff number	f	density of flowing fluid or flood
g'	component of g normal to vent	i	inside variable
g	gravity constant	o	outside or bottom variable
h	effective buoyancy length	s	soffit variable
H	height of rectangular vent	vc	vena contracta variable
m	Mass flow	u	upper variable
p	Pressure		
$Re = VD\rho/\mu$	Reynolds number		
v	vena contracta velocity		

References

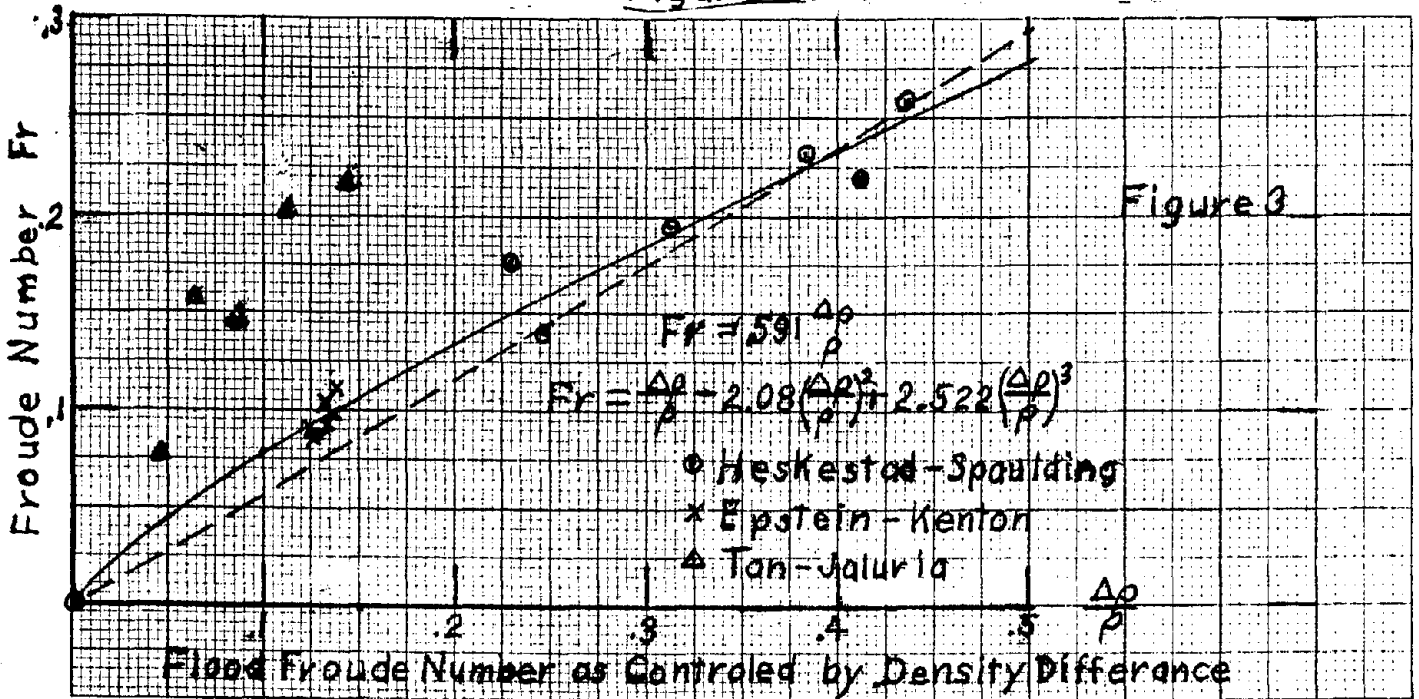
1. Marks L.S. Mechanical Engineers Handbook 5th edition 1951
2. Heskestad G. and Spaulding R.D. Inflow of Air Required at Wall and Ceiling Apertures to Prevent Escape of Fire Smoke Proc. 3rd Simp. Fire Safety Sci. p 919-928, 1991
3. Tan Q. and Jaluria J. Flow Through Horizontal Vents as Related to Compartment Fire Environments. NIST-GCR-92-604 p 1-89, 1992
4. Epstein M. Buoyancy-Driven Exchange Flow Through Small Openings in Horizontal Partitions. J. Heat Transfer 110 p885-893 1988
5. Epstein M. and Kenton M. Combined Natural Convection and Forced Flow Through Small Openings in a Horizontal Partition, with Special Reference to Flows in Multicomponent Enclosures. J Heat Transfer 1989 p980-987 1989
6. Cooper L. Combined Buoyancy and Pressure- Driven Flow Through a Horizontal Vent NISTIR 5384 p1-43 1994
7. Prah J. and Emmons H, Fire Induced Flow Through an Opening Comb. and Flame 25 p369-385 1975.



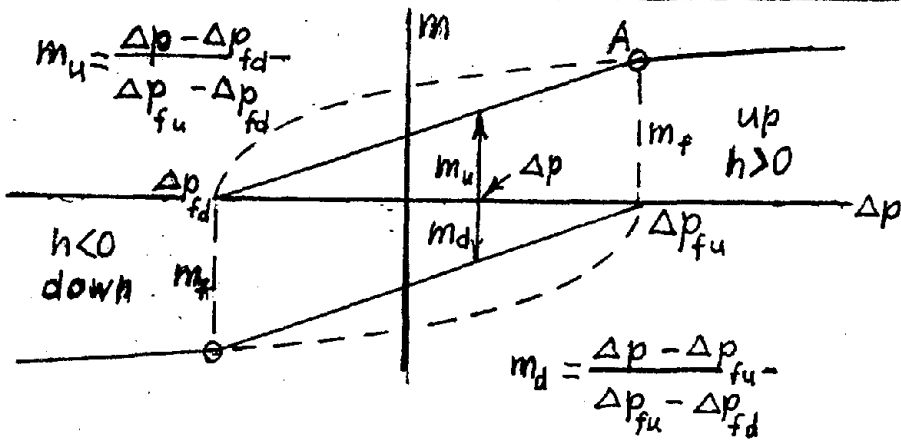
Flow Coefficients for Nozzles and Orificies
Figure 1



Effect of $\Delta\rho$ on Flow Through Horizontal Vent
Figure 2



Flood Froude Number as Controlled by Density Difference



Two Flow Region Figure 4

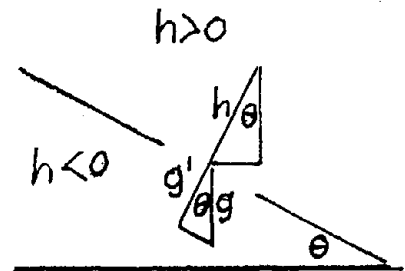


Figure 5
Inclined Vent

Discussion

Henri Mitler: Does this work of yours include the possibility of the periodic motion like when we fill up a bottle with water and then turn it upside down, it goes glug, glug, glug?

Howard Emmons: I have no data to answer that question. I suspect that the corrections are not very significant, but I don't really know. On the other hand, this has not been considered directly and does involve additional effects. In order to have oscillator flow, you have to have a capacity for absorbing extra mass and not oil. So there has to be an influence by the oscillating flow on the fire or something or other to permit that oscillation, that has not been included here at all.

Edward Zukoski: We have tried to do some of these experiments near the flooding point and found that it was the other effects that you talked about, that is how you contain the upper volume and so forth, that were very important in fixing the frequencies and so forth of the glug, glug, glug.

Gunnar Heskestad: Howard, when you presented your data, you presented it as a function of Reynolds number, but the data involved Froude numbers as well. I wanted to know how you decided to just present it as a function of Reynolds number.

Howard Emmons: The decision was fairly simple and elementary. The primary reason was because I tried it with Reynolds number alone and it worked beautifully, which said to me that my correction for buoyancy worked. The flow coefficients that I used in that correlation had to be recomputed based upon my formula. I could not use the one that you and others could correctly use.

Leonard Cooper: We've looked at the fire situation as unstable, heavy fluid or light fluid and you have a general solution which is a different approach. The solutions that we looked at are good and correlate well with data there for high Grashof number data. This idea is also confused with the fact that Heskestad data contains some Grashof number data which also does not correlate. In this sense, Grashof number does play a role and one has to be careful, it would appear.

Howard Emmons:

It is entirely possible that the Grashof number is the number that has to be added, as I mentioned earlier, in order to get a better correlation.

Modeling of Heating Mechanism and Thermal Response of Structural Components Exposed to Localized Fires: A new application of diffusion flame modeling to fire safety engineering

Yuji Hasemi

Building Research Institute, Ministry of Construction, Japan

Yutaka Yokobayashi

Graduate School of Science and Engineering, Science University of Tokyo, Japan

Takashi Wakamatsu

Institute of Construction Technology, Kumagai-gumi Co., Japan

Alexander V. Ptchelintsev

All-Russian Research Institute for Fire Protection, Russia

ABSTRACT

A framework for investigation of the feasibility of unprotected structure from the firesafety point of view is discussed. Experimental heat transfer and temperature correlations for flat ceiling and a beam beneath a flat ceiling exposed to localized fire source are shown. The experimental results suggest feasible range of unprotected structures from the fire safety point of view and basic information for the fire safety design of unprotected structures.

Key Words: localized fire, unprotected structure, heat flux, flame length.

SCOPE AND RESEARCH FRAMEWORK

There is considerable potential need for the development of unprotected or weakly-protected fire-safe structures, although current fire regulation in most of industrialized countries requires that load bearing structures be protected against fire with thermal insulation^{1,2}. However, on-site installation of thermal insulation to structural members is a typical time- and labor-consuming process in construction and its maintenance is often difficult for traffic, seismic or other vibration or for due generation especially in humid climate.

The primary parameter determining the performance of thermal insulation is the severity of the design fire. In many countries, fire resistance tests assume exposure of structural components to a fully developed fire^{1,2}. However, a building fire may remain localized if either the compartment or its opening is enough large. Atrium can be a typical built environment large enough to be exempt from a full involvement by fire. For external structural members, fire of adjacent buildings and flame projection should be the only heating source, and heating by such sources is believed to be weaker than fully developed room fires^{3,4}. Also, parking buildings and such traffic facilities as railway stations are typical occupancies in which the nature and amount of fire load can be easily limited within a predictable range^{2,5,6}. Metal structure has a relative advantage in the simplicity of on-site construction, the lightness and the easiness in future renovation in comparison with masonry or reinforced concrete structures; it is the main reason why metal structures are preferred for traffic facilities and offshore buildings. It is also important that recent efforts for evaluating heat release from burning furnishings are making it possible to predict and control heat release from building contents in fire^{5,7}. If a load bearing member is heated only locally in fire, it is believed not only that the heating condition of the member become less significant than in a fully-developed fire but also that conduction loss through the member itself contribute to keep the exposed part cooler. The second benefit of the localized fire is especially pronounced for metal structures since the thermal conductivity of metal is far larger than that of other major structural materials. However, although estimation of the heating condition in fire is a key for the fire safety design of unprotected structures, only few works have been conducted on the modeling of the heating condition by a

localized fire and on the analysis of thermal and mechanical response of load bearing components to such fires. Quantification of heating condition of load bearing components by fire is also believed to be useful for fire safety design of bare wooden structures using char layer due to fire exposure as the protection layer.

Prediction of the heating condition due to a localized fire, on the other hand, has been a major problem in the field of active fire protection systems and fire growth modeling. Heating of a ceiling by a localized fire is the dominant problem in evaluating the activation of fire detectors and automatic sprinklers⁹⁻¹⁴, and incident heat flux to the interior or exterior lining finish is the key condition for the evaluation of ignitability and flame spread in fire¹⁴⁻¹⁸. There are numbers of measurement and modeling of the heating mechanism by a localized fire with these subjects as the primary interest, which however deal generally with relatively low heat flux range. Once the heating condition of a load bearing component is modeled in engineering manner, its temperature and mechanical behavior could be calculated numerically with the heat flux distribution as the input. Conventional fire safety design guides for steel structures^{1,2,4} do not seem to incorporate such advancement in fire modeling and measurement. Figure 1 is a summary of the diagram necessary for the development of the whole procedure to assess fire safety of structure exposed to localized fires. Detail of this study is reported elsewhere¹⁹⁻²².

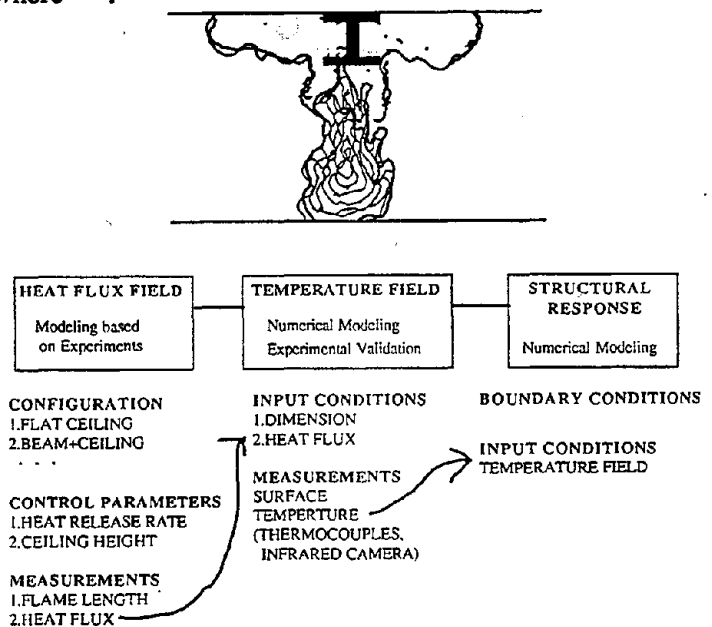


Figure 1 Research Framework

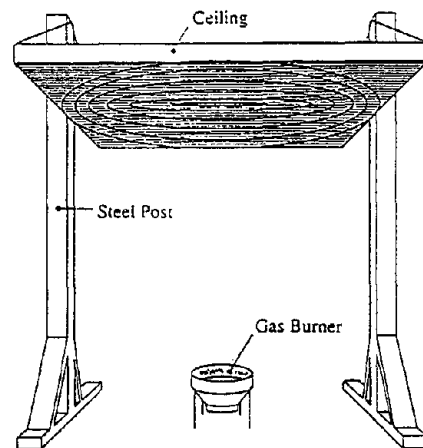


Figure 2 Experimental Setup (Flat Ceiling)

FLAT CEILING EXPOSED TO A LOCALIZED FIRE SOURCE

Heat flux measurement was conducted on an unconfined flat ceiling above an isolated fire source as one of the most basic configurations. Figure 2 is the experimental set up for the flat ceiling above a porous burner. The 1.82 m square ceiling consists of two layers of 12mm mineral-fiber reinforced cement(Perlite) boards and is hung from two steel posts. Height of the ceiling was adjusted by lifting the ceiling along the post. 0.30m and 0.50m diameter round and a 1.0m square porous propane burners were used as the fire source. Intensity of the fire source and the height between the burner surface and the ceiling were changeable. Complete combustion was assumed for the reported values of heat output. Heat flux to the ceiling surface was monitored with 12.5mm diameter Schmidt-Boelter heat flux gages. Temperature of surface and backsurface of the ceiling was measured with 0.2mm K-type thermocouples at various radial distances from the stagnation point to validate numerical models to predict temperature field from heat flux data. Any correction does not have been made on the heat flux data for the difference of the temperature between the sensor and the surface of the specimen. Previous experiments²³ suggest that the heat flux to the specimen surface could be estimated practically within relatively small error by taking $h(T_s - T_g)$ from the heat flux output within the range of heat flux reported in this paper.

Heat Flux at the Stagnation Point

Figure 3 summarizes the dependence of heat flux at the stagnation point on the heat release rate and the ceiling height measured from the burner surface. L_f is the height of unconfined flametips calculated from heat output using

$$L_f = 3.5 Q^{*n} \cdot D \quad (1)$$

where $n=2/5$ for $Q^* > 1.0$ and $n=2/3$ for $Q^* < 1.0$ ^{24,25}. There is significant increase of heat flux at the stagnation point between $L_f/H=1.0$ and $L_f/H=2.5$ until q_s'' approaches the plateau at $q_s'' \cong 80 \sim 120$ kW/m². This significant change in the stagnation point heat flux is believed to reflect the vertical oscillation of the flame beneath the ceiling, since the height of solid flame, the main part of the flame as radiation source, is approximately half the L_f ²⁶.

In the transient domain, $1 < L_f/H < 2.5$, there is clear tendency that, for a given L_f/H , q_s'' become larger as the fire source become smaller. This scattering reminds us of the typical systematic scattering of the axial temperature for a buoyant plume around the theoretical $\theta_m \propto z^{-5/3}$ line, which can be practically corrected to the point source theory using the concept of virtual source. Result of the coordination using the virtual source is summarized in Figure 4, in which the $q_s'' - L_f/(H+z')$ curve for each combination of D and H is almost parallel with large H/D s in the bottom and small H/D s in the top. This order probably represents the order of irradiance from the column of the flame beneath the ceiling, whose proportion is believed to be dependent on H/D . The plateau heat flux for approximately $L_f/H > 2.5$ is apparently an increasing function of heat release rate as summarized in Figure 5. Interestingly, the Q -dependence of q_s'' at the plateau is very close to that for the wall heat flux from solid flame from a pool fire against the wall²⁴.

Horizontal Flame Length Beneath Ceiling and Radial Heat Flux Distribution

For many configurations, relative location of the surface to flame is considered the primary condition controlling the surface flame heat transfer. In order to derive flame length correlations, average of the horizontal distance of the flametips from the stagnation point, LH , was obtained from videotape. LH was correlated against the dimensionless heat release rate, Q_{DH}^* , defined as

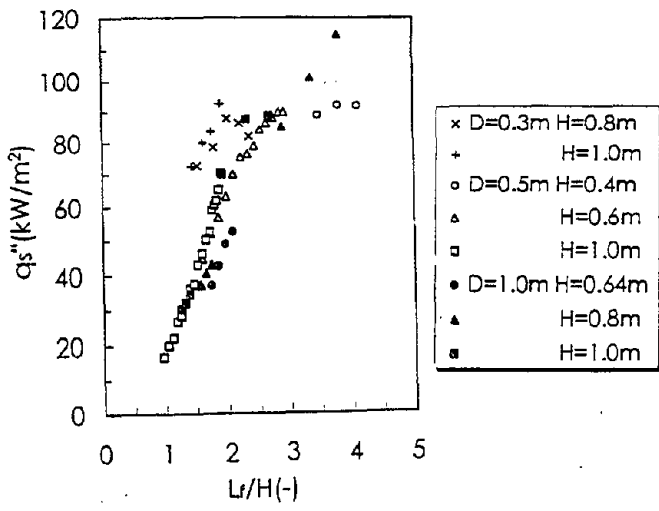


Figure 3 Stagnation Point Heat Flux vs. L_f/H

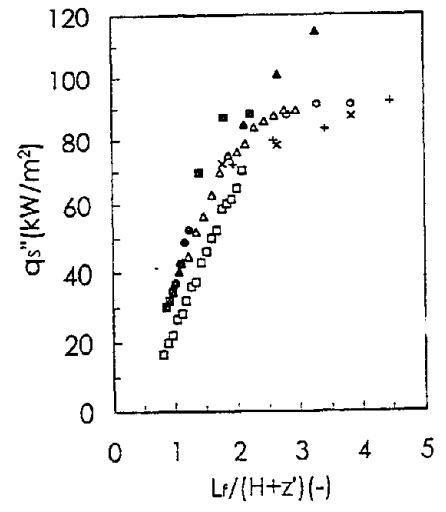


Figure 4 Stagnation Point Heat Flux Relation Corrected with Virtual Heat Source

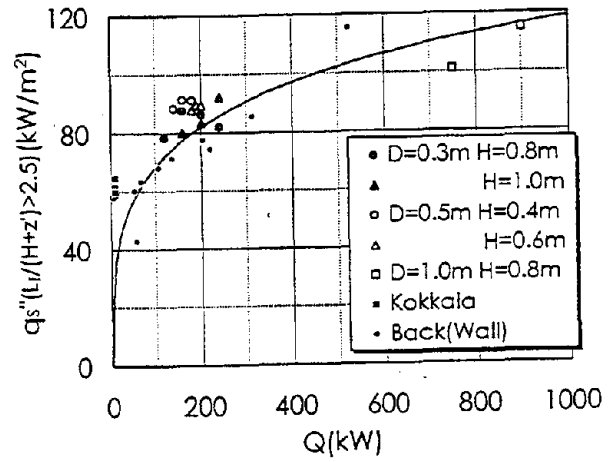


Figure 5 Plateau Heat Flux and Source Heat Output

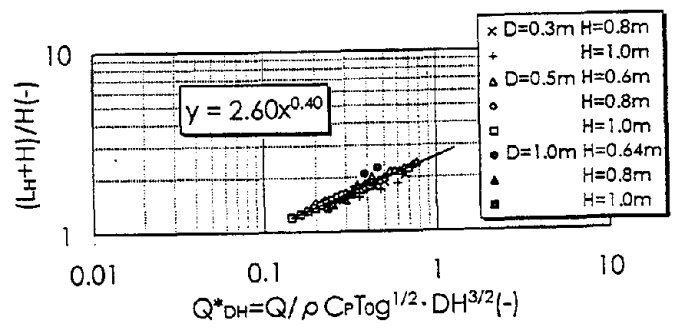


Figure 6 Flame Length Beneath Ceiling vs. Normalized Heat Release Rate

$$Q_{DH}^* = \frac{Q}{\rho C_p T_{0g}^{1/2} D H^{3/2}} \quad (2)$$

as shown in Figure 6. Other dimensionless heat release rate, $Q_H^* = \rho C_p T_{0g}^{1/2} H^{5/2}$, was first examined to explain the flame length data as it had been reported that flame length data in room-corner configuration be correlated against Q_H^{*27} ; however, correlation of LH against Q_H^* from the present test resulted in systematic difference between the 1.0m burner and others. Originally D^2 out of $D^{5/2}$ in the denominator of the dimensionless heat release rate, Q^* , indicates the jet-injection area,

and full replacement of scale length in Q^* by ceiling height is believed to miss the relevance of the dimensionless heat with Froude number. Figure 7 demonstrates relation between the heat flux to the ceiling and the radial distance from the stagnation point normalized by the flame length. The radial distance is corrected again with the virtual source concept. Almost all data are found to concentrate along one curve within relatively small range of scattering.

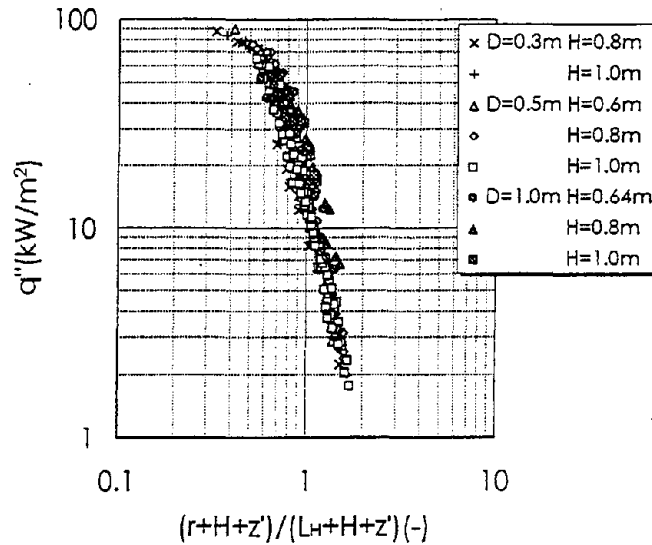


Figure 7 Radial Heat Flux Relation Corrected with Virtual Heat Source

BEAM AND CEILING EXPOSED TO A LOCALIZED FIRE SOURCE

Heating condition of steel beam installed beneath a ceiling slab exposed to a localized fire source has been measured using a 6 mm thick 75mm x 150mm x 3,600mm H-steel beam and a 1.82m x 3.64m rectangular flat ceiling (Figure 8). The cross-sectional size of the specimen could be interpreted as one fourth to half the typical load bearing steel beams in common buildings. The ceiling is composed of two layers of 12mm thick perlite boards. A 0.5m round and a 1.0m square porous propane burners were used as the fire source. Measurements were made on heat flux and temperature at the beam surfaces; heat flux gages were installed on the lower and upper flanges and the web through holes in the beam. Experimental conditions were chosen to cover the transient domain for the stagnation point heat flux, e.g. $1 < L/H < 2.5$, established for the flat ceiling configuration.

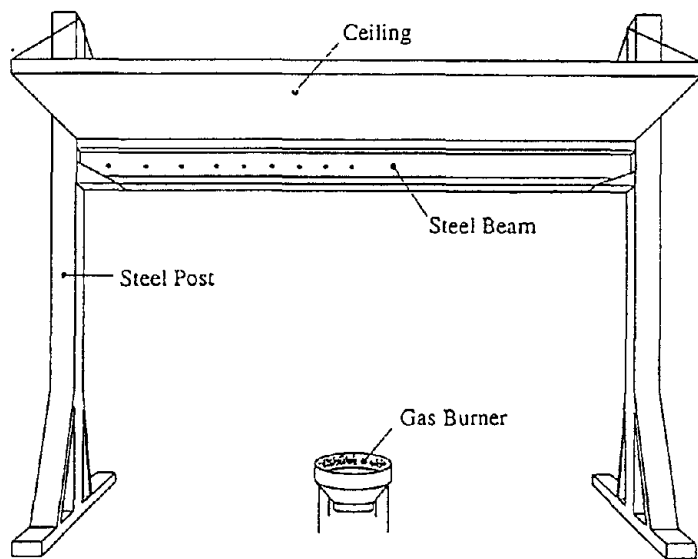


Figure 8 Experimental Setup (Ceiling+Beam)

General Test Result

Figure 9 shows an example of heat flux and surface temperature distributions along the beam at different cross-sectional locations. In the near field of the stagnation point, there is notable difference of heat flux in the vertical cross-section. This difference is more pronounced than its axial profile. Heat flux was generally weaker than the heat flux obtained at the flat-ceiling tests with the identical L_f/H condition. It is probably because of the flame flooding over the lower flange and separation of the flame to the both sides of the beam. Temperature field at each cross-section is more uniform than the heat flux field; it is probably a result of the high conductivity of the steel. Perhaps as result of this effect, temperature of the downward surface of the beam at the stagnation point was considerably lower than estimate from the heat flux at the same location based on the uniform heating, $(q_s''/\epsilon\sigma)^{1/4}$.

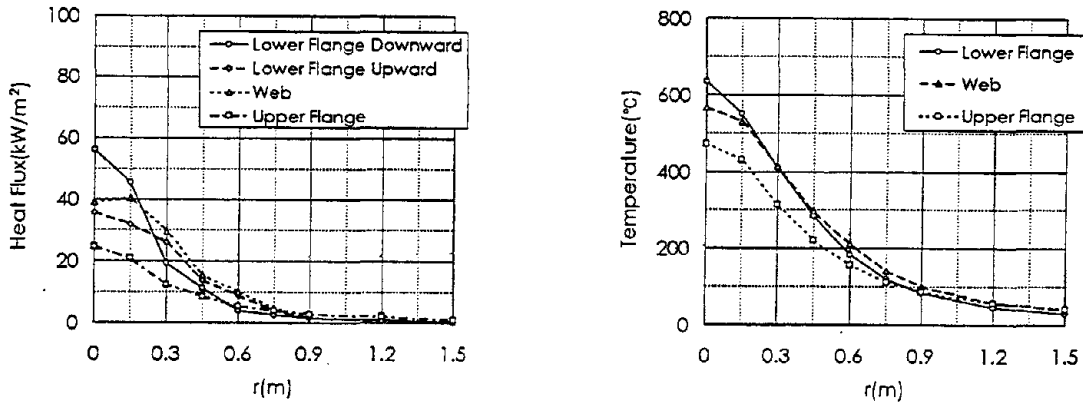


Figure 9 Heat Flux and Surface Temperature on H- Beam($H_B=0.60\text{m}$ and $Q=160\text{kW}$)

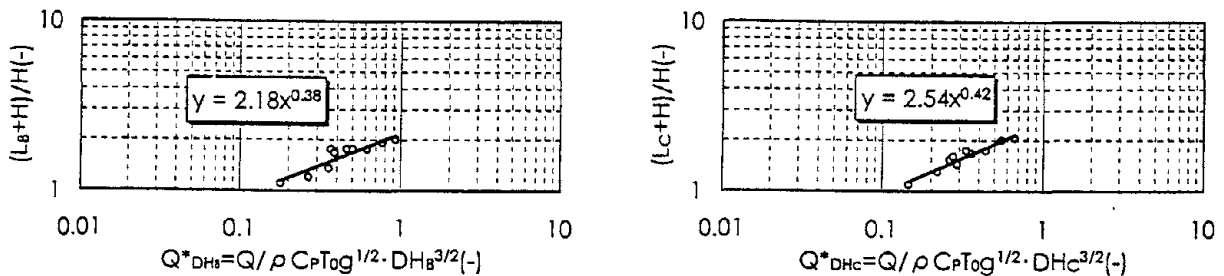
Flame Length

Local horizontal flame development was observed both beneath the ceiling and beneath the lower flange of the beam at each test; it seems that there is systematic difference between the two flame lengths. The flame lengths along the ceiling and along the lower flange of the beam are correlated against dimensionless heat release rates with ceiling height and with height to the lower flange respectively as Figure 10 where Q_{DHB}^* and Q_{DHC}^* are defined respectively as

$$Q_{DHB}^* = Q / \rho C_p T_{og}^{1/2} D_{HB}^{3/2} \quad (3)$$

$$Q_{DHC}^* = Q / \rho C_p T_{og}^{1/2} D_{HC}^{3/2}$$

The normalized flame lengths are nearly proportional to the $2/5$ power of the dimensionless heat release rates for Q_{DHB}^* and Q_{DHC}^* .



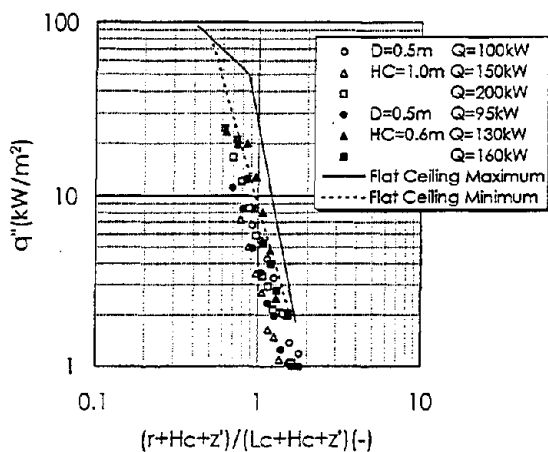
(a) below beam

(b) below ceiling

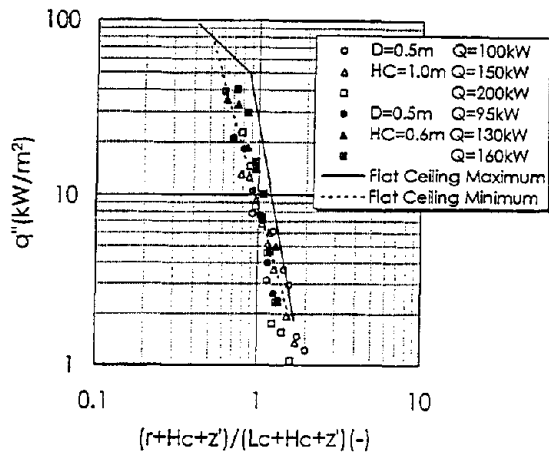
Figure 10 Flame Lengths below Beam and below Ceiling Supported by the Beam

Heat Flux Distribution

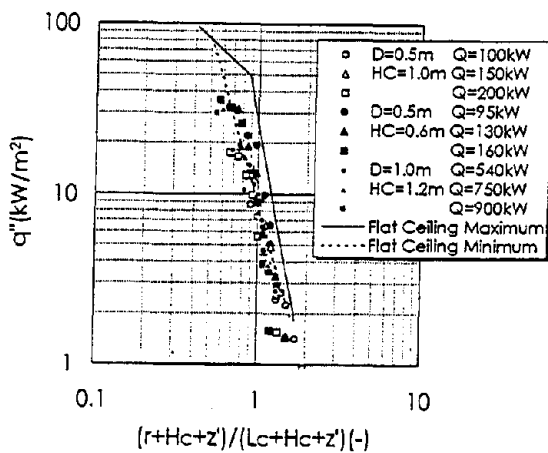
Heat flux data have been correlated against the heat source condition and geometry in a similar way with the flat ceiling tests. Figure 11 is a summary of the horizontal distribution of heat flux at the downward and upper surfaces of the lower flange, the web and the downward surface of the upper flange. The data for the downward lower flange surface were correlated against the flame length beneath the lower flange of the beam. Other data were correlated against the flame lengths beneath the ceiling. The decay of heat flux with horizontal distance for each crosssectional location seems to be faster than the data for the flat ceiling.



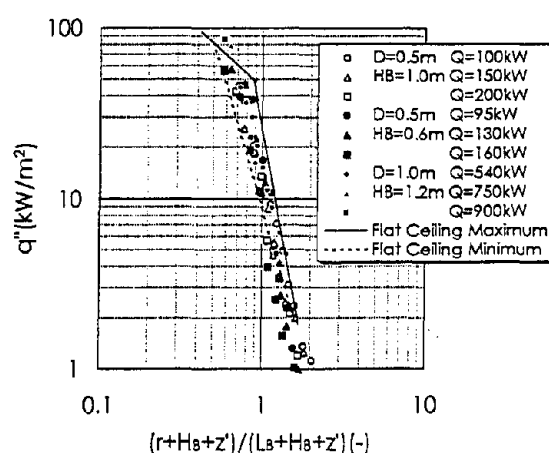
(a) upper flange downward



(b) web



(c) lower flange upward



(d) lower flange downward

Figure 11 Axial Distribution of Beam Surface Heat Flux

COMPARISON OF TEMPERATURE FIELD WITH NUMERICAL CALCULATION

Finite element calculation of the three dimensional temperature field within the beam has been conducted with the heat flux data as input. A general purpose finite element code ANSYS was used for the calculation. Considering the difference between the heat flux gage output and the net heat flux, convective surface heat transfer coefficient was estimated by comparing the temperature field of the flat ceiling between the test and calculation; $hc = 0.01 \text{ kW/m}^2\text{K}$ resulted in the best fit of the calculated ceiling temperature to the measurement. Figure 12 is an example of comparison between the present test and calculation on the upper-flange and lower flange temperatures.

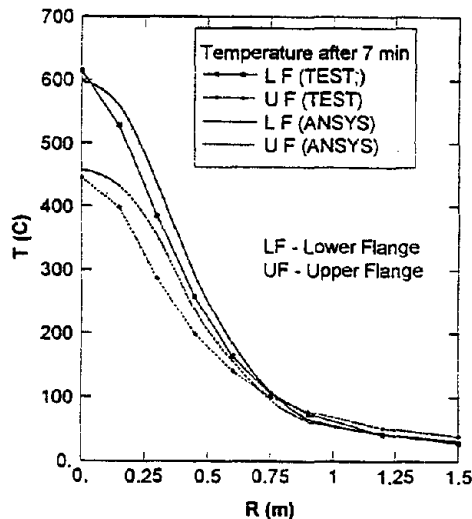


Figure 12 Comparison of Measured and Calculated Beam Flange Temperature ($Q=160\text{kW}$, $H_c=0.6\text{m}$)

CONCLUSIONS

Measurements of flame heat transfer to a flat ceiling and to a beam supporting a flat ceiling by a localized fire have been made. The following conclusions can be drawn from the experiments.

- (1) Horizontal heat flux distribution on a flat ceiling above a localized fire source can be represented as a function of the height of the ceiling and the horizontal length of the flame beneath the ceiling with correction based on the virtual source.
- (2) Horizontal flame length beneath a flat ceiling becomes a function of heat release rate normalized with the ceiling height and fire-source diameter as the characteristic scale-length.
- (3) Heat flux at the stagnation point of the ceiling surface shows significant transiency until $L_f/H=2.5$. The heat flux for greater L_f/H is almost constant within approximately the range of $80 - 120 \text{ kW/m}^2$ and seems to be an increasing function of heat release rate.
- (4) Heat flux to a beam beneath a flat ceiling at the stagnation point is considerably smaller than the heat flux to a flat ceiling.
- (5) Horizontal heat flux distribution along a H- beam supporting a ceiling above a localized fire source can be represented as a function of the heights of the lower flange of the beam and ceiling and the horizontal length of the flame beneath the ceiling with correction based on the virtual source.
- (6) Temperature field within a beam exposed to a localized fire can be reproduced by finite element method with the heat flux correlation obtained from this study.

The horizontal flame length correlations with new characteristic lengths derived in this work should perhaps be considered still temporary, and it is doubtful if the correlations be as universal as the unconfined flame length relation as equation(1). However, it should be emphasized that the present tests cover the range of L/H for which consideration of the localized fire source scenario seems to have the most benefit for the structural fire safety design.

ACKNOWLEDGMENTS

The authors wish to thank Messrs.T.Nakazato and S.Nakagawa of the Kozai(Steel) Club for the arrangement of the specimen. The authors are also indebted to Messrs.T.Namba, E.Onoda, A.Inoue and T.Wakabayashi, students of the Science University of Tokyo, for the assistance in the experiments and for the preparation of drawings. A.V.Pchelintsev was an STA Fellow(1994-1995) at Building Research Institute and a guest scientist at the Science University of Tokyo(1995).

TERMINOLOGY

C_p : specific heat of air, D : characteristic fuel size(e.g. diameter), H : height from fire source, H_B : height of lower flange beam from fire source, H_C : height of ceiling from fire source, L_f : unconfined flame height(flametips), L_H : radial length of flametips from the stagnation point of ceiling, Q : heat release rate, Q^* : dimensionless heat release rate($Q/rC_pT_{og}^{1/2}D^{5/2}$), Q_{DH}^* : $Q/rC_pT_{og}^{1/2}DH^{3/2}$, Q_H^* : $Q/rC_pT_{og}^{1/2}H^{5/2}$, T_g : temperature of the sensitive part of a heat flux gage, T_o :ambient temperature, T_s : surface temperature of specimen, g : gravitational acceleration, h : total surface heat transfer coefficient, q'' : heat flux, q_s'' :heat flux at the stagnation point, z : height from heat source, z' : location of virtual source, ϵ : emmissivity, θ_m : maximum excess temperature, ρ : density of ambient air, σ : Stefan-Boltzman Constant.

REFERENCES

- 1 ECCS Technical Committee 3, European Recommendations of the Safety of Steel Structures Design Manual, 1985.
- 2 Annon., International Fire Engineering Design for Steel Structures: State of the Art, International Iron and Steel Institute, 1993.
- 3 Oleszkiewicz, L, Heat Transfer from a Window Fire Plume to a Building Facade, ASME Winter Annual Meeting, San Francisco, 1989.
- 4 American Iron and Steel Institute, FIRE-SAFE STRUCTURAL STEEL —A Design Guide, 1979.
- 5 Loikkanen, P., and Mangs, J., Fire Tests on Passenger Cars, VTT Fire Technology, Report No.TS-PAL 00455/90, 1991.
- 6 Annon., Report on the Structural Fire Safety Design for Buildings above Railways, Japan Association for Disaster Prevention, 1992(in Japanese).
- 7 Fowell, A.J., Editor, Fire and Flammability of Furnishings and Contents of Buildings, ASTM STP 1233, 1994.
- 8 Sakumoto, Y., Yamaguchi, T., Ohashi, M., and Saito, H., High-Temperature Properties of Fire-Resistant Steel for Buildings, ASCE Journal of Structural Engineering, Vol.118, No.2, 1992.
- 9 Alpert, R.L., Calculation of Response Time of Ceiling-Mounted Fire Detectors, Fire Technology, 8, pp.181-195, 1972.
- 10 Heskestad, G., and Delichatsios, M.A., The Initial Convective Flow in Fire, Seventeenth Symposium(International) on Combustion, pp1113- 1123, 1978.
- 11 You, H.Z., and Faeth, G.M., An Investigation of Fire Impingement on a Horizontal Ceiling, Report for NBS, 1979.
- 12 Cooper, L.Y., and Stroup, D.W., Thermal Response of Unconfined Ceilings above Growing

- Fires and the Importance of Convective Heat Transfer, *Journal of Heat Transfer, Transactions of ASME*, Vol.109, 1987.
- 13 Sako, S., and Hasemi, Y., Response Time of Automatic Sprinklers below a Confined Ceiling, *Proceedings of the Second International Symposium on Fire Safety Science*, Tokyo, 1988.
 - 14 Kokkala, M., Experimental Study of Heat Transfer to Ceiling from an Impinging Diffusion Flame, *Proceedings of the Third International Symposium on Fire Safety Science*, Edinburgh, 1991.
 - 15 Ahmad, T., and Faeth, G.M., Fire Induced Plumes along a Vertical Wall: Part III, the Turbulent Combusting Plume, Report for NBS, Grant No.5-9020, 1978.
 - 16 Hasemi, Y., Experimental Wall Flame Heat Transfer Correlations for the Analysis of Upward Wall Flame Spread, *Fire Science and Technology*, Vol.4, No.2, 1984.
 - 17 Quintiere, J.G., Harkleroad, M., and Hasemi, Y., Wall Flames and Implications for Upward Flame Spread, *Combustion Science and Technology*, Vol.48, pp191-222, 1986.
 - 18 Kokkala, M., Characteristics of a Flame in an Open Corner of Walls, *INTERFLAM '93*, 1993.
 - 19 Hasemi, Y., Yokobayashi, Y., Wakamatsu, T., and Pchelintsev, A.V., Firesafety of Building Components Exposed to a Localized Fire —Scope and Experiments on Ceiling/Beam System Exposed to a Localized Fire—, *ASIAFLAM '95*, Hong Kong, 1995.
 - 20 Wakamatsu, T., Hasemi, Y., Yokobayashi, Y., and Pchelintsev, A.V., Experimental Study on the Heating Mechanism of a Steel Beam under Ceiling Exposed to a Localized Fire, *INTERFLAM '96*, Cambridge, 1996.
 - 21 Pchelintsev, A.V., Hasemi, Y., Nikolaenko, M., Skibin, A., and Wakamatsu, T., Three Dimensional Thermal Analysis of Steel Beams Exposed to a Localized Fire, *INTERFLAM '96*, Cambridge, 1996.
 - 22 Wakamatsu, T., Hasemi, Y., and Pchelintsev, A.V., submitted to Annual Meeting, Japan Association of Fire Science and Engineering, 1996(in Japanese).
 - 23 Hasemi, Y., Yoshida, M. and Nakabayashi, T., Effectiveness of Noncombustible Ceiling for the Improvement of Fire Safety in a Compartment Finished with Wood, *Journal of Structural and Construction Engineering, Transactions of AIJ*, No.446, 1993(in Japanese).
 - 24 Back, G., Beyler, C., Dinneno, P., and Tatem, P., Wall Incident Heat Flux Distribution Resulting from an Adjacent Fire, *Proceedings of the Fourth International Symposium on Fire Safety Science*, Ottawa, 1994.
 - 25 Cetegen, B.M., Zukoski, E.E., and Kubota, T., Entrainment and Flame Geometry of Fire Plumes, *NBS-GCR-82-402*, 1982.
 - 26 Hasemi, Y., and Tokunaga, T., Flame Geometry Effects on the Buoyant Plumes from Turbulent Diffusion Flames, *Fire Science and Technology*, Vol.4, No.1, 1984.
 - 27 Thomas, P.H., Fire, Flames and Dimensional Analysis, *Proceedings of the Third International Symposium on Fire Safety Science*, Edinburgh, 1991.

Discussion

Gunnar Heskestad: I was very intrigued by the picture you showed of the flames underneath the I-beam and with the flame pattern under the bed, and the flame pattern under the ceiling. I wouldn't have guessed that and I've never seen it. Could you just describe that a little bit more?

Yuji Hasemi: Yes, that is based on the picture. But this is a very short time, I don't know how short it was. But if you have a long shut off speed, there's not any such cavity. So it is only because the drawing is based on the very short picture. From a scientific point of view, I am very curious.

Craig Beyler: I wonder if you could put up the first slide you were just talking to a moment ago. There was some work that was done at the Fire Research Station. He was doing a corridor experiment and was measuring heat fluxes to the ceiling. His went up in much the same way your data did. My recollection is that it went up 100 kW/m² and instead of having a simple plateau, it eventually came back down on the right part of the plot. Do you think that phenomenon might occur in your kind of experiment?

Yuji Hasemi: Yes, I tried to compare our results with other previous work. I think it may not be correct to say that it is a plateau because there may be some decay.

Craig Beyler: I wonder if I could ask a practical question. A rule of thumb that we often use in practice in terms of exposure of unprotected steel is based on the flame tip being about 500 °C and the critical temperature for steel failure being about 500 to 600 °C. The rule of thumb is that if you have flame contact, you will probably have a failure. Do your experiments have anything specific to say about that rule of thumb?

Yuji Hasemi: I considered that. We also measure the temperature over the beam. According to our measurement, the temperature was much lower always than the estimation. That is probably because of the high conductivity of the materials.

John Rockett: In a number of experiment of flames under ceilings that I have looked at, where the flame turns to extend out onto the ceiling, it already has entrained enough oxygen to burn all of the fuel present. This was true of Gross's data recently, and way back, Hinkley stated where they nearly had enough fuel so that the flame length under the ceiling would be determined by the ability to contain air in the horizontal ceiling jet. For analysis of fires, for example, some vehicle fires in tunnels, we desperately need data for fuel rich ceiling jets. Have you plans for experiments to those cases?

Yuji Hasemi: I should say yes. I am doing another project, and I think we can get some information from those experiments.

Large Eddy Simulations of Smoke Movement in Three Dimensions

Howard R. Baum, Kevin B. McGrattan, and Ronald G. Rehm

National Institute of Standards and Technology

Gaithersburg, Md. 20899, U.S.A.

Abstract

A methodology for the prediction of smoke movement in enclosures is presented. The method is based on high resolution solutions of the Navier-Stokes equations specialized to the smoke movement problem. Forced ventilation, complex geometry, and water spray effects are incorporated in the model. Sample calculations illustrating the capabilities of this approach are presented, and a comparison of model predictions with room doorway experiments performed by Steckler are shown. The results indicate that the convective transport of smoke and hot gases can be simulated without recourse to empirical models of turbulence.

1 Introduction

This paper describes a methodology for simulating the transport of smoke and hot gases in enclosures. The approach is based on the use of efficient CFD techniques and high performance computers to solve a form of the Navier Stokes equations specialized to the smoke movement problem. The fire is prescribed in a manner consistent with a mixture fraction based approach to combustion, but the combustion phenomena themselves are not simulated. The mixing and transport of smoke and hot gases is calculated directly from an approximate form of the Navier Stokes equations. The computations are carried out as a three dimensional time dependent process, limited only by the spatial resolution of the underlying grid. No turbulence models are employed; the large scale eddies are simulated directly and sub-grid scale motions are suppressed. Present capabilities permit a typical residential room or hotel unit to be simulated at a 3-5 cm. resolution limit. The enclosure can have any shape made up of rectangular blocks, and can be multiply connected. The smoke is simulated by tracking a large number of Lagrangian elements, which originate in the fire. These same elements carry the heat released by the fire, providing a self consistent description of the smoke transport at all resolvable length and time scales. Large temperature and pressure variations are permitted, subject to the limitation that the Mach Number is much less than one. A simulation of the effects of a water sprinkler spray on the smoke movement can also be studied. The following section gives a brief description of the mathematical and computational aspects of the model, while the final section illustrates its capability with sample results and a comparison with experiment. The influence of Prof. Zukoski on the field of smoke movement in general and our work in particular has been profound. It is a pleasure to dedicate this paper to him.

2 Mathematical Model

The Navier Stokes equations are cast in terms of a velocity \vec{u} , a modified temperature \tilde{T} , density $\tilde{\rho}$, and perturbation pressure \tilde{p} . The modified quantities are defined so that the corresponding time dependent spatially averaged thermodynamic quantities $T_0(t)$, $\rho_0(t)$ and $p_0(t)$ are factored out of the equations actually solved on the computer. The spatially averaged quantities play the same role that ambient conditions do in the Boussinesq approximation. The modified variables are related to the physical temperature T , density ρ , and pressure p as follows:

$$\begin{aligned} T &= T_0(t)(1 + \tilde{T}(\vec{r}, t)) \\ \rho &= \rho_0(t)(1 + \tilde{\rho}(\vec{r}, t)) \\ p &= p_0(t) - \rho_0(t)gz + \tilde{p}(\vec{r}, t) \end{aligned} \quad (1)$$

The spatially averaged quantities are obtained by combining global mass and energy balances with the equation of state and a definition of T_0 in terms of p_0 through an adiabatic process.

$$\frac{T_0(t)}{T_0(0)} = \left(\frac{p_0(t)}{p_0(0)} \right)^{\frac{\gamma-1}{\gamma}} \quad (2)$$

$$p_0 \oint \vec{u} \cdot \vec{n} dS + \frac{V}{\gamma} \frac{dp_0}{dt} = \frac{\gamma-1}{\gamma} (\dot{Q} - \oint q_w dS) \quad (3)$$

$$p_0 = \rho_0 R T_0 \quad (4)$$

Here, \vec{n} is a unit normal pointing out of the enclosure, γ is the specific heat ratio, \dot{Q} is the total heat released into the gas, and q_w the local heat flux from the gas to the wall. The integrals are carried out over all the boundaries of the enclosure. In meteorology, the concept of an effective temperature defined in terms of a background pressure is called a "potential temperature".

The local mass and energy conservation equations can now be combined to yield:

$$\nabla \cdot \vec{u} + \frac{1}{\gamma p_0} \frac{dp_0}{dt} = \alpha_0(t) \nabla \cdot (\tilde{k} \nabla \tilde{T}) + \frac{\gamma-1}{\gamma} \frac{\dot{q}}{p_0} \quad (5)$$

$$(1 + \tilde{\rho}) \left(\frac{\partial \tilde{T}}{\partial t} + \vec{u} \cdot \vec{\nabla} \tilde{T} \right) = \alpha_0(t) \nabla \cdot (\tilde{k} \nabla \tilde{T}) + \frac{\gamma-1}{\gamma} \frac{\dot{q}}{p_0} \quad (6)$$

The average thermal diffusivity $\alpha_0(t) = k_0(T_0)/\rho_0 c_p$ where the thermal conductivity $k(T)$ is written in the form $k = k_0(T_0) \tilde{k}$. The momentum equation is written in vector invariant form as follows:

$$\frac{\partial \vec{u}}{\partial t} - \vec{u} \times \vec{\omega} + \nabla \mathcal{H} + \tilde{T} \vec{g} - \vec{F} = (1 + \tilde{T}) \nu_0(t) \nabla \cdot \vec{\tau} \quad (7)$$

$$\mathcal{H} = \frac{\tilde{p}}{\rho_0} + \frac{u^2}{2} \quad (8)$$

$$\begin{aligned} \nabla \cdot \vec{\tau} &= \frac{4}{3} \nabla (\tilde{\mu} \nabla \cdot \vec{u}) + \nabla (\vec{u} \cdot \nabla \tilde{\mu}) - (\nabla^2 \tilde{\mu} \vec{u}) + \\ &\quad \nabla \tilde{\mu} \times \vec{\omega} - (\nabla \cdot \vec{u}) \nabla \tilde{\mu} - \nabla \times \nabla \times (\tilde{\mu} \vec{u}) \end{aligned} \quad (9)$$

The average kinematic viscosity $\nu_0(t) = \mu_0(T_0)/\rho_0$ where the viscosity $\mu(T)$ is written as $\mu = \mu_0(T_0) \tilde{\mu}$. The quantity $\vec{\omega} = \nabla \times \vec{u}$ is the vorticity. The quantity \vec{F} is the droplet drag density transferred to the gas by the water spray.

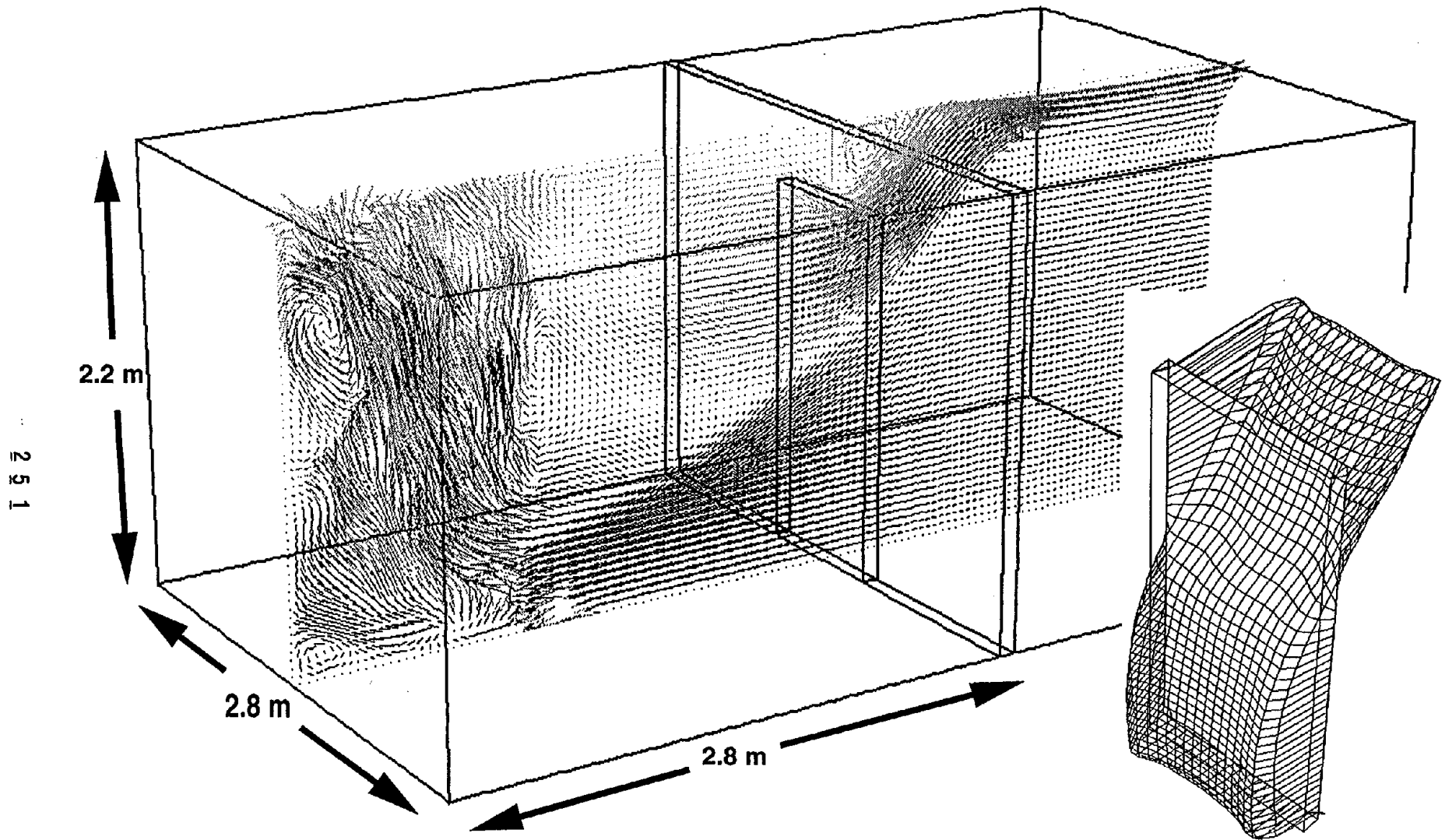


Figure 1. Velocity vectors in vertical center plane of the simulation of Steckler *et al.* experiments. Inset at right shows wire frame display of doorway velocity profiles. Note that velocity maximum at each height occurs at edge in agreement with Figure 5 of Reference [4].

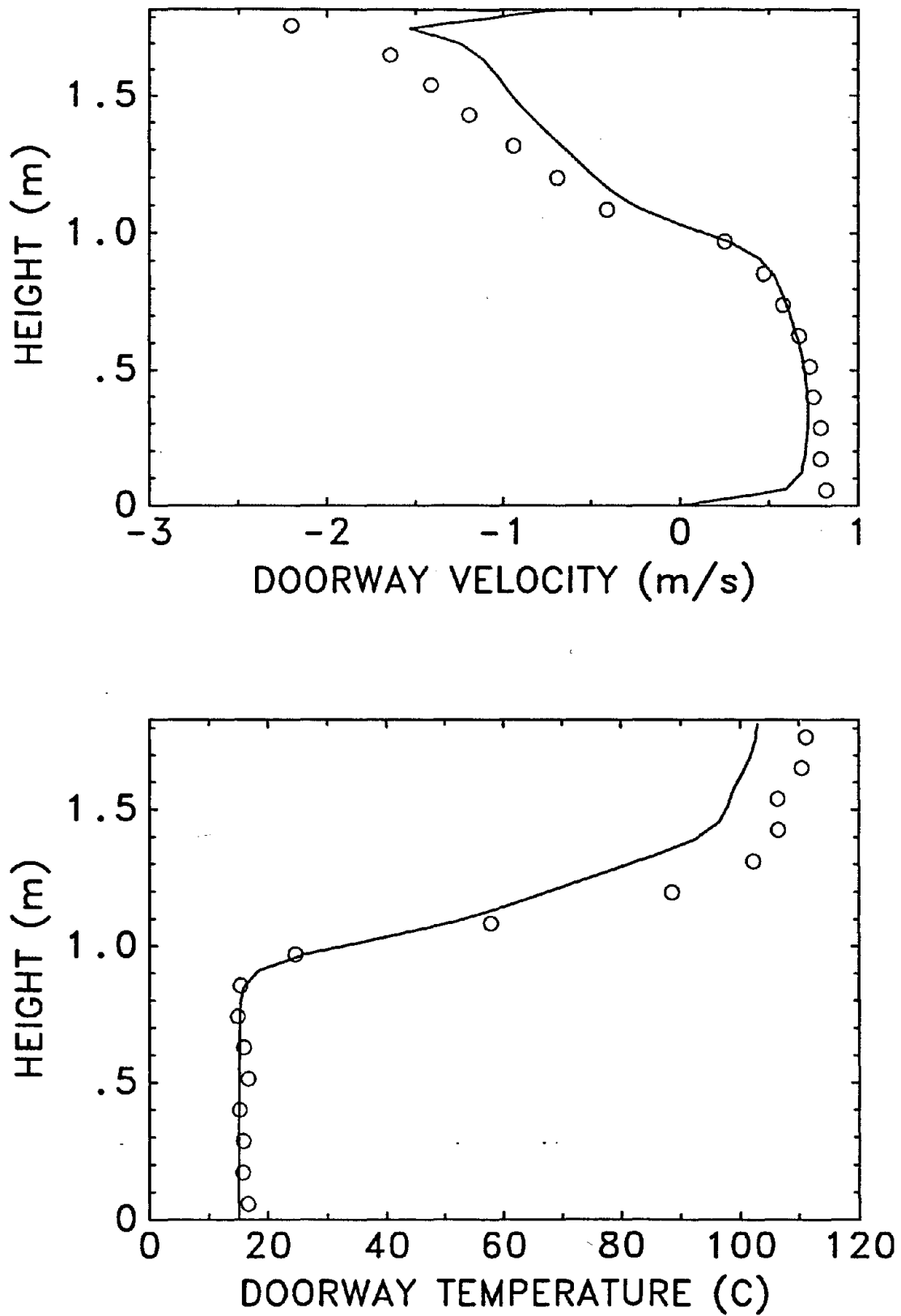


Figure 2. Velocity and temperature profiles in the center of the doorway in the Steckler *et al.* experiments. The circles represent experimental data and the solid lines represent results of the simulation performed at 3 centimeter resolution.

The above form of the conservation equations emphasize the importance of the divergence and vorticity fields, as well as the close relationship between the thermally expandable fluid equations [1] and the Boussinesq equations for which the authors have developed highly efficient solution procedures [2], [3]. These are applied directly to the equations presented here with minor modifications and no loss in performance. The only changes from earlier methodology are a return to a uniform rectangular grid with blocks of cells masked to simulate internal boundaries; and the use of a second order Runge-Kutta scheme to advance the velocity and temperature fields in time.

The fire is represented by introducing a large number of Lagrangian elements which release heat as they are convected about by the thermally induced motion. Since the fluid motion determines where the heat is actually released, and the heat release determines the motion, the large scale features of the coupling between the fire and the smoke transport are retained. It should be noted, however, that the heat release rate is *not* predicted, but is an input parameter in the computer programs implementing this model. The smoke is followed by continuing to track the convected elements after the fuel burnout is completed. A specified percentage of the fuel consumed is assumed to be converted to smoke particulate. Thus, a knowledge of the spatial distribution of the Lagrangian elements is equivalent to a specification of the smoke particulate density at any instant of time. The spray droplet drag density is determined by computing a large number of Lagrangian water droplet trajectories in a quiescent fluid. This technique permits the future substitution of a more realistic spray model and/or experimental spray data without changing the basic approach to smoke movement.

3 Results

Three examples illustrating the present capabilities of the approach outlined are presented. The first, a simulation of enclosure fire experiments conducted by Steckler et. al. [4], [5], shows that reasonably good agreement with experimental results can be obtained at the levels of spatial resolution achievable with current CFD techniques and computer facilities. The second, a study of smoke movement induced by a fire in a hypothetical hotel unit, demonstrates the level of geometrical complexity that can be simulated at present. These simulations are performed at 3 and 4 cm. spatial resolution respectively. The third example is a ceiling jet advancing down a long corridor. It is inspired by a series of experiments performed by Prof. Zukoski.

The overall geometry of the Steckler et. al. experiments is shown in Figure 1. The velocity vectors displayed in the vertical center plane after the flow has reached an apparent steady state are also shown. In addition to giving some idea of the overall flow pattern they give an indication of the spatial resolution achieved in the computation. The wireframe doorway velocity plot shows the characteristic orifice profile, with the maximum speed near the jet edge. This plot is remarkably similar to that given in Figure 5 of Reference [4], where the experimental profiles are displayed. A quantitative comparison between theory and experiment is shown in Figure 2, where time averaged doorway centerline velocity and temperature profiles are displayed. There are no adjustable parameters in the model, so the relatively good agreement between the measured and calculated results is a reasonable indicator of the *predictive* capability of the present approach.

A simulation of a fire on top of a bed in an idealized hotel room unit is shown in Figure 3. The unit also contains a sofa to the right of the bed, as well as a chest of drawers and a desk on the opposite wall. A closet blocked off from the rest of the unit and a bathroom with open doorway are to the left. Air heated 10°C above ambient enters the room at 25 cm./sec. through a duct on

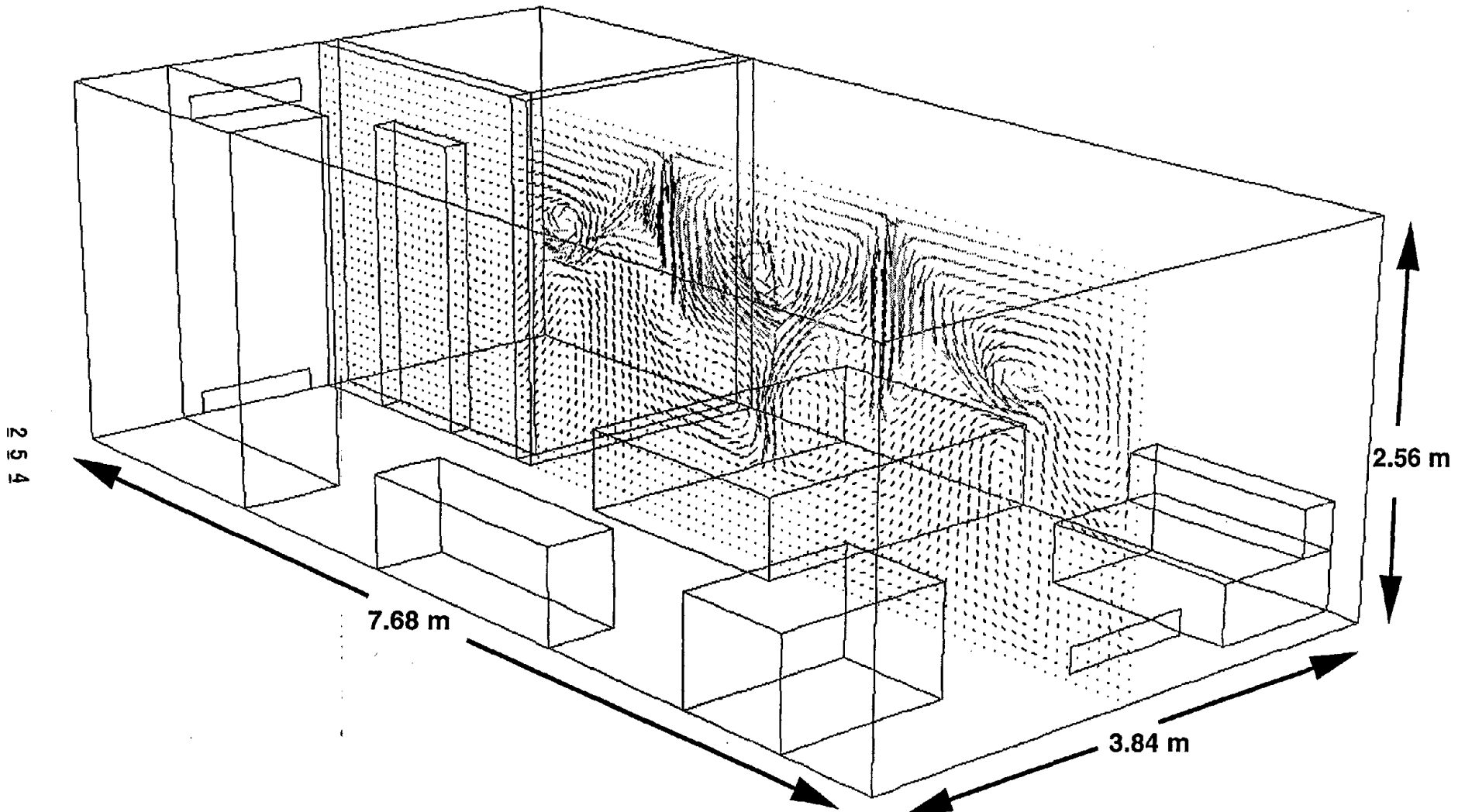


Figure 3. Velocity vectors in the vertical center plane of room 20 seconds after fire initiation. Two sprinklers sited immediately above the bed have just begun to inject water spray at 2 liters/second each. Every other vector in each coordinate direction is shown for clarity. The overall grid size is 192x96x64 cells corresponding to 4 centimeter spatial resolution.

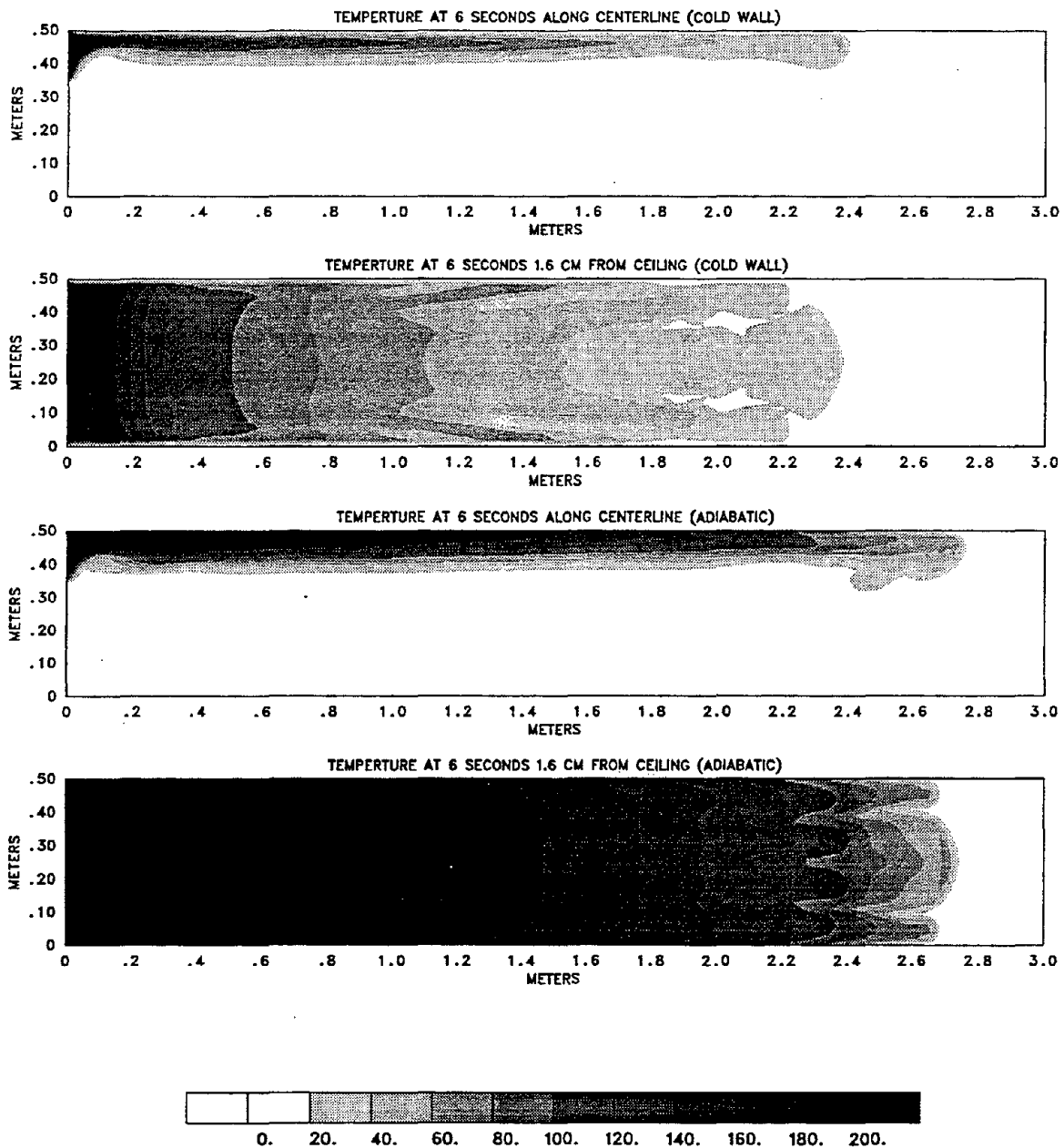


Figure 4. A comparison of two gravity currents, one run under cold wall conditions (top 2 figures) and one run under adiabatic conditions (bottom 2 figures). The grid size for each run was 324x54x64 cells, with the size of the grid cells varying in the vertical direction so that the cells near the top of the enclosure were about half a centimeter thick. The temperature of the gas exiting the vent is 212 C. The shades of the contours represent temperatures in excess of ambient (15 C).

Reproduced from  best available copy

the lower right wall and is extracted on the upper left wall above a closed door with a 2 cm. gap at the floor. The vents operate at fixed outside pressures, so the inflow is reduced and outflow increased as the room pressure rises due to the fire. Figure 3 shows the velocity vectors in the vertical center plane down the length of the room 20 seconds after the fire begins. Only 1/4 of the vectors are shown in the interests of clarity. The overall grid is composed of 64x96x192 4 cm. cubes. Two sprinklers located on the ceiling near on either side of the bed have been triggered. The force fields generated by the sprays are calculated in advance and activated either at a prescribed local ceiling gas temperature or a set time. The calculation simulates about one minute of real time. These computations required approximately 20 microseconds per cell per time step on an IBM RS 6000/58H server, and used 280 MBytes of memory.

Figure 4 shows temperature contours from two simulations of gravity currents generated by injecting air heated to 212°C at 25 cm/s into a 6x1x1 0.5 meter high corridor containing stagnant air at 15°C. The upper plots show top and side views with the walls held at 15°C while the lower two correspond to adiabatic boundary conditions. The cold wall boundary conditions generate intense axial vortices which greatly enhance the ceiling heat transfer and rapidly reduce the temperature in the ceiling jet. Since the force driving the gravity current is the buoyancy induced by the temperature rise, this leads to a rapid slowing of the ceiling jet. These 'convection rolls' were noted explicitly in [6]. The computations were performed using a 324x64x54 grid with a variable grid in the vertical direction.

These examples are intended to demonstrate that smoke movement caused by enclosure fires can be calculated with reasonable accuracy directly from the underlying Navier Stokes equations in scenarios of practical interest. While many other physical mechanisms need to be included before a full predictive capability is achieved, it is clear to us that the methodology outlined above is the only currently available way of *guaranteeing* increasingly accurate predictions of smoke movement in the future.

References

- [1] Rehm, R.G. and Baum, H.R., "The Equations of Motion for Thermally Driven, Buoyant Flows", *Journal of Research of the NBS*, Vol. 83, pp. 297-308, 1978.
- [2] McGrattan, K.B., Rehm, R.G., and Baum, H.R., "Fire Driven Flows in Enclosures", *Journal of Computational Physics*, Vol. 110, pp. 285-291, 1994.
- [3] Baum, H.R., Ezekoye, O.A., McGrattan, K.B., and Rehm, R.G., "Mathematical Modeling and Computer Simulation of Fire Phenomena", *Theoretical and Computational Fluid Dynamics*, Vol. 6, pp. 125-139, 1994.
- [4] Steckler, K.D., Quintiere, J.Q., and Rinkinen, W.J., "Flow Induced by a Fire in a Compartment", *Nineteenth Symposium (International) on Combustion*, The Combustion Institute, Pittsburgh, pp. 913-920, 1982.
- [5] Steckler, K.D., Baum, H.R., and Quintiere, J.Q., "Fire Induced Flows Through Room Openings - Flow Coefficients", *Twentieth Symposium (International) on Combustion*, The Combustion Institute, Pittsburgh, pp. 1591-1600, 1984.
- [6] Chobotov, M.V., Zukoski, E.E., and Kubota, T., "Gravity Currents With Heat Transfer Effects", National Bureau of Standards Report NBS-GCR-522, (1986).

Discussion

Patrick Pagni: I just wanted to start with a comment before the question that it's really appropriate to have the best of modern computational fluid mechanics presented at a symposium honoring Ed Zukoski. Howard, looking to the future, could we have your vision on the right way to add radiation to this problem to the same level of accuracy that you have the fluid mechanics modeled?

Howard Baum: I'd like to answer in two parts. First, I'd like to say something about your first comment. The thing which actually has sustained us over the last few years and gotten us to plunge this far into it after wandering in the desert for a while is Ed Zukoski's salt water experiments. And, in fact, if it wasn't for the both the beautiful simplicity and clarity of those experiments, simple enough so that even I could understand them, then we would not have been able to get some kind of experimental confirmation that this work was on the right track three or four years ago. As to the radiation calculations, we are embarking on them now and the thing which I will say is the crucial part is to not to try to believe that we can predict the radiation from the temperature fields that we calculate. Just as we have these elements moving with the fluid that is releasing chemical energy, we can say that some fraction of that chemical energy is emitted as thermal radiation into the bulk of the gas. And we are then arguing that subsequently, it is either absorbed or not, depending upon the amount of smoke in the gas in the room or in the outdoor plume or whatever. We are just beginning these calculations now and are still developing methodology. So at this point, the only thing that I can say is that this is the approach that we are following and I hope in several months to have something tangible to show for it.

Ronald Alpert: Do you think the trend is going to be in the near future for soaking up the added computational capacity of new machines as they get faster and faster? Is the trend going to be to add more and more physics to the problem, such as thermal radiation, such as putting in the complete two way interaction between sprinkler water droplets and the flow and other such things? Or will the trend be to get better resolution as you have implied?

Howard Baum: For the immediate future for us, I see basically two aspects to the research; one is to hold the spatial resolution fixed and consider more complicated geometries just for smoke movement. I've shown you simulations for a motel room or what you might think of as a bedroom. We believe that the computing capacity exists right now to do that for the equivalent of an office suite or a small house. The second leg of this, which we have already embarked on, is to assume, whether rightly or wrongly, that we have gone far enough with the spacial resolution that we currently have and try to add radiation, which we are actively doing. And we have some simple trajectory models for a sprinkler spray that has to be modified, for example, to make it obey Newton's laws of motion and to gradually increase the amount of physics in the calculation. One last thing as part of that, we want to, rather than postulate what happens on these little small scaled elements moving through the fluid, we want to actually study them as a combustion problem in their own right. Dr. Ruddy Mell, who is working with me as an NRC post-doc, is, in fact, embarked on an investigation of that problem.

Discussion cont.

Richard Gann: Having heard the answers to the last two questions, I feel compelled to put in a bid for one more facet. I'd like to get your views on the capability of adding the spacial and temporal extensiveness of the heat release and chemical species changes as opposed to making them essentially a source term and instantaneous.

Howard Baum: The problem that you are addressing is basically as complicated an issue as everything that I have talked about here. But I think it is important to say what the origin of the complication is. That is, if the chairs that we are all sitting on catch fire, we do not have a clue as to what those fuels really are. If that whole problem of condensed fuel degradation could be understood at a level that would yield predictions on a species-by-species level, then I think the ability probably exists. Not in my head and not in our collaborators. But there are other people in the combustion community who will calculate fairly elaborate chemistry, at least in laminar flames and simple situations. So if that problem could be solved, I could imagine a future, not next year, but at some point when these little elements were actually carrying along real chemical composition calculations and drawing on the local environment that they were seeing to provide the oxidizer visited or not. But my colleague Takashi Kashiwagi informs me that you could write a book just on the reactions that go on in paper and therefore, I believe that some rationalization of the way in which we approach the burning of solid materials is really required before one can even contemplate the next step in gas phase combustion.

EXPERIMENTAL STUDY ON SMOKE MOVEMENT WITH SCALE-MODEL

Makoto Tsujimoto, Dr.Eng.
Nagoya University
Nagoya, Japan

SUMMARY

The laws of scaling for unsteady-state smoke movement were derived by dimensional analysis of the governing equations (continuity, conservation of momentum and conservation of energy) and the boundary condition at the flames and the wall. Experiments were conducted in three stages, two different sizes (1:2.5), real fire test and its reduced model (1/40), and two different sizes (1:1.5) in wind tunnel considering wind effect. And the similarity in each stage was almost confirmed.

1. INTRODUCTION

One of the most important things for fire safety engineering is to predict smoke movement as a fire developing. Otherwise evacuation and extinguishing systems would not be planned adequately.

There are two methods to predict the smoke movement. The one is the method with reduced-scale experiments and the other is the numerical calculation method.

Both methods, however, have defects for analysis in unsteady states respectively. The weak point of the former is that it is impossible to fit all variables to the laws of scaling in experiments. In the latter there is uncertainty from giving exact boundary conditions, such as figure of fire flame and heat transfer from that, and the instability of calculation process.

This paper intends to show the way to predict the unsteady state smoke movement by a reduced scale experiment as similar as possible. The method is derived as follows.

- 1) The phenomenon that the temperature of the flame surface almost constant regardless of the size of heat source is adopted as the boundary condition for deriving the scaling law of heat convection.
- 2) Under the heat release rate which satisfies the scaling law derived in 1), the configuration of the flame becomes similar.
- 3) Simplifying the mechanism of surface heat transfer between smoke layer and (ceiling) wall, the scaling law for selecting wall material is derived. Adequacy of this law is tested by the results of experiments.

2. SCALING LAW

(1) Similarity of heat convection

The scaling law is derived from the π -parameters which are deduced by dimensional analysis of governing equations (continuity, conservation of momentum and conservation of energy). [1]

$$\left. \begin{aligned}
 \pi_1 &= \frac{L_0}{t_0 u_0} \\
 \pi_2 &= \frac{\Delta p_0}{\rho u_0^2} \\
 \pi_3 &= g\beta \frac{\Delta\theta_0 L_0}{u_0^2} \\
 \pi_4 &= \frac{Q_0}{\rho c_p u_0 \Delta\theta_0 L_0^2}
 \end{aligned} \right\} (1)$$

L_0 : characteristic length
 u_0 : characteristic velocity
 t_0 : characteristic time
 Q_0 : characteristic heat release rate
 $\Delta\theta_0$: characteristic temperature difference
 Δp_0 : characteristic pressure difference
 β : coefficient of thermal expansion
 c_p : specific heat under constant pressure
 ρ : density

Since there are four equations for six normalizing parameters, four of them ($u_0, Q_0, t_0, \Delta p_0$) can be represented by the remaining two ($L_0, \Delta\theta_0$). Further, in the case that the same kind of heat source is used in different scale-models, that is, in the case that the temperature difference between flame and its ambient is equal, ($\Delta\theta_M / \Delta\theta_R$) becomes unit on the boundary. Consequently the scaling law is as follows;

$$\left. \begin{aligned}
 n(t) &= \left[\frac{Q_M}{Q_R} \right] = n(L)^{1/2} \\
 n(Q) &= \left[\frac{t_M}{t_R} \right] = n(L)^{5/2} \\
 n(u) &= \left[\frac{u_M}{u_R} \right] = n(L)^{1/2}
 \end{aligned} \right\} (2)$$

subscripts R and M stand for real scale and model, respectively

(2) Similarity of flame

Configuration of fire flame is represented as Eq. (3) [2]

$$\left. \begin{aligned}
 \frac{L_f}{D} &= f(Q_f^*) \\
 Q_f^* &= \frac{Q}{D^{5/2}}
 \end{aligned} \right\} (3)$$

L_f, D : height and diameter of flame
 Q : heat release rate

If $n(Q) = n(L)^{5/2}$ in Eq.(2) is satisfied, then

$$n(Q_f^*) = \frac{n(Q)}{n(D)^{5/2}} = \frac{n(L)^{5/2}}{n(D)^{5/2}} \quad (4)$$

Therefore if $n(D)$ is equal to $n(L)$, $n(Q_f^*)$ becomes unit. In other words, if the heat release rate Q is controlled as $n(Q) = n(L)^{5/2}$ and that the diameter of flame D is similar to L , the configuration of flame becomes similar.

(3) Selection of material of wall

Heat flux from a smoke layer to the (ceiling) wall is governed by the heat transfer from the smoke layer to the surface of the wall and the heat conduction in the wall. Eq.(5) is derived under the assumption that

- 1) the surface temperature of the wall is equal to the temperature of the smoke layer,
- 2) the temperature gradient of smoke layer downstream mainly depends on the heat absorption into the (ceiling) wall, and
- 3) heat absorption into the wall is described approximately as that into semi-finite wall.

$$\dot{q} = \Delta\theta \sqrt{\frac{\lambda_w \rho_w c_w}{\pi t}}$$

$$n(\lambda_w \rho_w c_w) = n(L)^{3/2} \quad (5)$$

λ_w, ρ_w, c_w ; heat conductivity, density, specific heat of the wall, respectively

The vertical temperature profile of the smoke layer along the corridor becomes similar to the real scale experiment by replacing the material of wall of reduced scale model to that which satisfies the Eq.(5).[3]

3. COMPARISON OF SMOKE MOVEMENT BETWEEN SCALES

Experiments were conducted under the scaling laws described in 2. in three stages as follows;

- 1) the experiments using two types of reduced model (1/10 and 1/25) simulated smoke movement in atrium,
- 2) the 1/40 scale experiments simulated the real scale fire test in former KOKUGIKAN SUMO HALL (1984), and
- 3) the experiments in different size (1:1.5) in wind tunnel simulated the effect of wind to the smoke exhaust from the openings.

The similarity of temperature profile and smoke movement in each experiment is almost confirmed. Examples of the results are shown in Fig.1 and 2. Furthermore these results are

are visualized by video recording system and I prepared the picture to be able to compare the phenomena in two different scales by adjusting the time scale. This method is very powerful to understand the mechanism of smoke movement. Please request the video tape to the author.

REFERENCE

- [1] Quintere, J.G., "Scaling Application in Fire Research", Proc. of the International Symposium on Scale Modeling, 1988
- [2] Zukoski, E.E., Kubota, T., Cetegen, B., "Entrainment in fire plumes", Fire Safety Journal, 3(1980/81)
- [3] Wakamatsu, T., et al., "Smoke Control of Underground Shopping Mall (in Japanese)", Transactions of Kantou District of AIJ, 1991

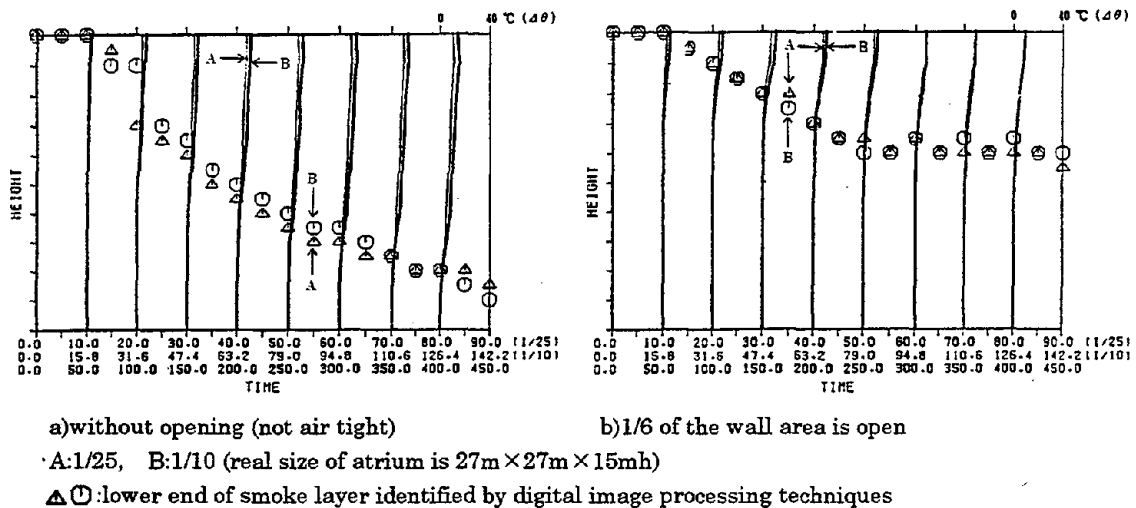


Fig.1. Comparison of the vertical temperature profile and the smoke movement in reduced scale models

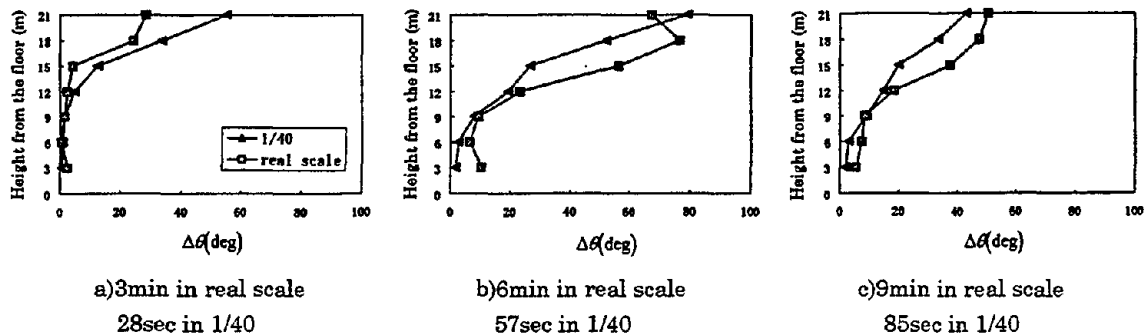


Fig.2. Comparison of the vertical temperature profile with time proceeding in Sumo Hall (82m × 70m × 24mh)

Discussion

Gerard Faeth: I'd be interested if you could tell me the way or the mechanism of making this smoke is these full-scale fires. I can imagine that if you tried that in the United States, you probably would be destroyed by the builder. What do you use for those simulations?

Makoto Tsujimoto: It's a railroad flare, used by the train conductor so that when the train runs into an accident or something, people will know that there's an accident.

Gunnar Heskestad: It seemed like most of the comparisons between full-scale and model were very good. And this is what we like to see. The frequencies and fluctuations seem to be right. Smoke descended about the correct rate. Was there anything during all of these experiments that suggested that the small-scale and large-scale fire might have some difference?

Makoto Tsujimoto: Yes. I think there is a difference in the radiation. For the first experiment, the scaled difference is 2.5. And the temperature is slightly higher in the larger scale. That's the only difference we know at this time.

Patrick Pagni: We are very interested in these excellent experiments. Japan has a long tradition of good computational models for smoke movement. Have you any plans to compare the computational results with your experimental results?

Makoto Tsujimoto: Well, actually, for the first experiment, we made computation using the Tanaka model and we obtained very good agreement.

James Quintiere: As many know, scale modeling is used in fields such as aircraft quite predominantly. To what extent is this kind of scale modeling used in Japan for building fire safety design?

Makoto Tsujimoto: This is used in very few cases.

James Quintiere: Too bad.

RADIATION TRANSFER AND TEMPERATURE DISTRIBUTION IN A FEW SMALL POOL FLAMES

HIROSHI HAYASAKA
Faculty of Engineering
Hokkaido University
Sapporo, 060, JAPAN

ABSTRACT

A new way of using thermography for radiative objects like pool flames is introduced and applied to small pool flames. Radiative characteristics and flame structure of small pool flames are considered by *examining* flame temperature distribution from a radiation point of view. In addition, it is shown that pool flame structure for various fuels becomes more clear when the standard deviation and the coefficient of variation obtained from thermographic data are used.

INTRODUCTION

In fire fighting and fire safety science, the estimation of thermal radiation from tank fires to the surroundings is important. Many experimental and theoretical studies have been performed on this. Recently a new technique has been developed and used in fire experiments: Brötz et al. [1] have developed the equidensitometry technique based on the sensitometric wedge method. By processing a photographic negative using electronic equidensitometry, they determine lifetimes and migration velocities of eddies, etc. in pool flames. This technique is very effective in obtaining both instantaneous and mean characteristics of flames but there are difficulties with extracting statistical data such as standard deviation and coefficient of variation of radiance which would help establish the flame structure of pool flames.

Little is known of the effect of the combined radiation and combustion phenomena in pool flames. In a pool flame, radiation may control the burning rate and affect the combustion conditions in the flame. More information on radiation in pool flames may lead to the development of better ways to control this kind of fire. From this point of view, conversion from temperature to irradiance may be useful and meaningful. To address this, an alternative use of thermography has been developed by the authors [2,3]. Here, commercial thermography is used to obtain the irradiance distribution rather than the temperature distribution in pool flames of various fuels.

Experiments were conducted to determine the radiation characteristics of pool fires. The apparent temperature data obtained by thermography were converted to irradiance and radiance by simple calculations. Finally, statistical analysis related to radiance data was made to obtain the mean radiance and flame structure of the pool fire flames of three different fuels.

EXPERIMENT

Pool fire tests were carried out in a quiescent atmosphere. The experimental setup is shown in Fig. 1. A small stainless steel tank of diameter 48.5 mm and depth 14.5 mm was used for the pool fire tests. The burning rate was measured by an electric balance. Heptane, kerosene, and methanol were used as test fuels. Each fuel was fed into the tank by gravitational force and freeboard was kept almost zero (about 1 mm) by using a valve in the fuel line. The flame temperature distributions were measured by conventional chromel-alumel thermocouples of 0.3 mm diameter.

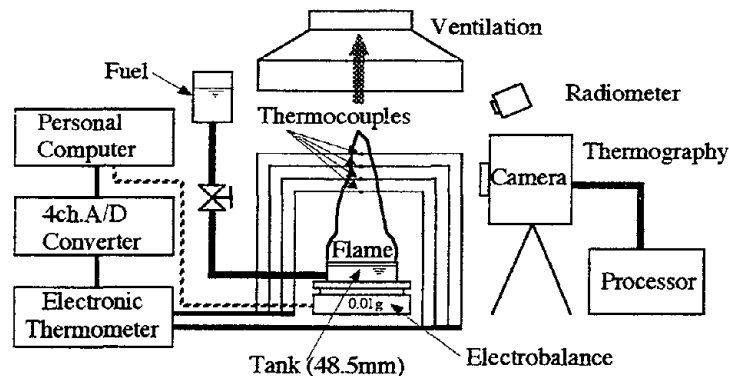


Figure 1. Schematic experimental arrangement for small pool flames.

The apparent temperature distribution of the pool flame was obtained with color television thermography which stored whole images of the pool flame on a floppy disk at a maximum speed of 20 frames/sec.. The thermographic equipment was installed at $25.4D$ (D is the tank diameter, 0.0485 m in this paper). The thermography stored one thermal image as a TV color image with 25,600 data points. The apparent temperature distributions were converted to radiance distributions and irradiance using simple calculations. A series of 40 images were recorded continuously at 10 second intervals and were analyzed statistically to obtain not only the distribution of mean radiance but also standard deviation and coefficient of variation.

The irradiance of the pool flames was also measured with a conventional thermopile type radiometer having wide view angle and flat spectral range installed at $7D$. The radiometer and thermography data were compared to verify the validity of the thermographic data.

THERMOGRAPHY

The thermography used in the experiment has the spectral range from 3 to 5.4 microns. The display levels can be set to 256 colors. The high response InSb detector is cooled by argon gas, and provides whole pool flame images instantaneously. The data of the images can be stored at 0.05 second intervals or slower (0.5, 1 or several seconds). The digital data is recorded in a way that allows it to be reused and converted to physical quantities like temperature, irradiance, etc..

A thermograph is a radiation thermometer. The detector is a radiometer, and the output is interpreted in terms of temperature, considering the distance to the object, emissivity, and the area of the object, defined by the field of view or the thermographic device. This conversion is simple and reliable when the object is a solid with known emissivity and area. The distance to the object, emissivity, and area of object cannot easily be defined when the object is gaseous as with pool flames. As a result, direct thermographic images cannot be used as they indicate incorrect or apparent temperature distributions.

In this paper, an imaginary black body wall is introduced in front of pool flame and conversion of the apparent temperature distribution into radiance distribution is made to determine the thermal structure of the large scale pool flames. It is assumed that the imaginary wall is at the edge of the tank [2,3]. A data point, s , does not always represent the radiance of a pool flame just behind the imaginary wall. However, when the distance L is relatively large, as in this experiment, we may assume that the measured, apparent temperature distribution at the center of a thermographic image will not contain large locational errors.

The apparent temperature distribution can be converted to a radiance distribution by the calculations below. Thermography converts radiation heat to apparent temperature, T_a (K), with Equation (1):

$$T_a = (q_s(i,j) / (\epsilon_s \sigma a_i))^{0.25} - T_\infty^{0.25} \quad (1)$$

where $q_s(i,j)$ is the radiance of data point s on the imaginary wall (kW/m^2), i,j are indices of the horizontal (x -axis) and vertical (z -axis) location and take values of 1 to 100 and 1 to 256 respectively, ϵ_s is the emissivity of data point s ($=1$), σ is the Stefan-Boltzmann constant ($5.67 \times 10^{-8} \text{ W/m}^2/\text{K}^4$); a_i is the area of a data point (m^2) obtained by the equation: $a_i = (2.17375 \times L + 0.3456) \times 10^{-6}$ for the TVS-2000 used. Here L is the measured distance between thermography and imaginary wall (m), T_∞ is the background temperature. The constants in this equation are coefficients in a simple equation related to the view angle of the thermography.

Thus the radiance at s can be determined with $q_s(i,j) = \sigma a_i (T_a^4 - T_\infty^4)$ derived from Equation (1). The total radiant heat from an imaginary wall can be obtained with Equation (2).

$$Q_s = \sum_{i=1}^m \sum_{j=1}^n q_s(i,j) \quad (2)$$

where $m=100$ and $n=256$. Finally, Q_s , which is the irradiance observed at the distance L , is re-scaled to the dimensionless distance $L/D=5$ to compare it with the data of the wide angle radiometer. It has units kW/m^2 ; $q_s(i,j)$ is simply divided by a solid angle (π) for a hemisphere on one side of the imaginary wall to convert it to radiance. This is the radiative heat emitted from the flame surface within a unit area to the surroundings per unit solid angle. Finally, $q_s(i,j)$ has the units $\text{kW/m}^2/\text{sr}$.

Forty continuous thermographic images were stored and processed by a personal computer to obtain the distribution of mean radiance, standard deviation and coefficient of variation. In this process, a 2×2 matrix of sixteen contiguous data points were integrated into one new data point. Thus, 25,600 ($=100 \times 256$) data points were reduced to 6,400 ($=50 \times 128$) to provide a smoother contour. $q_{s,k}(i',j')$ was introduced to represent the radiance of each new data point. The suffix k is the thermographic image number 1 to 40, i',j' indicate the location of a thermographic image and take values of 1 to 50 and 1 to 128 respectively.

RESULTS AND DISCUSSION

Previous Study of Flame Structure of a Pool Flame

Thomas [4] and McCaffrey [5], who studied the flame structure of buoyant diffusion flames similar to pool flames, plotted temperature rise from room temperature on the center line of the flame and defined three regions in the flame, namely the continuous flame region, the intermittent flame region and the plume region. The abscissa of their figure is $z/Q_c^{2/5}$ where z is the vertical height from the tank top, Q_c is the nominal rate of heat release by combustion (kW). According to McCaffrey [5], who measured natural gas diffusion flames, the boundary between the regions are at abscissa values of 0.08 and 0.2. These values may be correct only for a flame from a low sooting, gaseous fuel. Boundary values for liquid fuels depend on the fuel properties because they need evaporation and decomposition regions in the bottom of flames or near the fuel surface. In addition, many hydrocarbon liquid fuels tend to produce soot. These characteristics may make a difference especially when the size of the pool flame is small! Thus fuel properties and flame dimensions may effect the measured temperature profiles. In any event, the region boundary values are a little bit different from the McCaffrey's values.

Irradiance of Three Different Fuels

The irradiances of the three fuels are shown in Fig. 2. The abscissa is the picture number; the 40 pictures are taken at 10 second intervals under steady state conditions. Measured mean burning rates of heptane, kerosene and methanol are 2.22, 1.47 and 2.0 ($\times 10^{-2} \text{ kg/s/m}^2$)

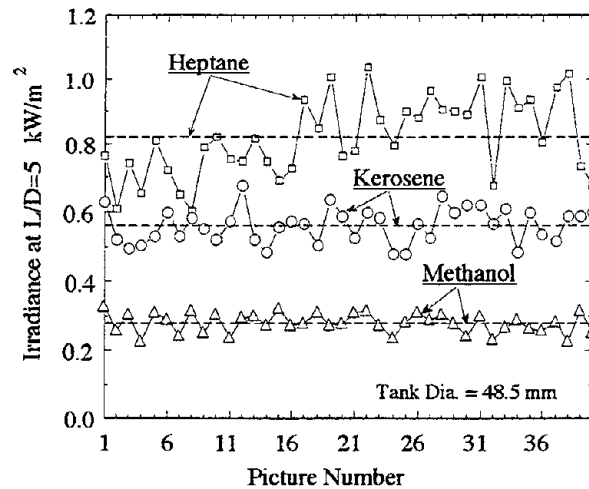


Figure 2. Irradiance of three fuels.

respectively. The ordinate of Fig. 2 is the irradiance at the dimensionless distance $L/D=5$. The irradiances of heptane, kerosene and methanol are shown by squares, circles and triangles respectively. Three dashed horizontal lines show the mean values of the forty data sets for the three fuels. The irradiance values for each fuel are almost the same as those obtained by the conventional wide angle radiometer. Fig. 2 shows that the mean irradiance of heptane is the highest and that of methanol is the lowest. Each symbol in Fig. 2 is the result of a thermographic image containing 25,600 data points.

Radiative Characteristics and Flame Structure

Contours of temperature, mean radiance, standard deviation and coefficient of variation for heptane, kerosene and methanol flames are shown in Figs. 3, 4, 5 and 6 respectively. Horizontal and straight dotted lines of each Fig. show the boundary of the continuous flame region, intermittent flame region and plume region. These boundary lines are drawn using experimental results. The z axis is defined as a vertical line perpendicular to the tank. The left side ordinate of each Fig. is the dimensionless height from the tank top, z/D . A theoretical expression to characterize buoyant diffusion flames proposed by Thomas and McCaffrey, $z/Q_c^{2/5}$, is used in the right side ordinate of each Fig..

Contours of temperature. The contours of temperature in Fig. 3 show that the heptane flame has the highest flame temperature of the three fuels, 1224 K. It also has the largest area of high temperature, indicated on the figure by dot-shading where the temperature exceeds 1000 K. By comparison, the highest flame temperature of kerosene is only 1085 K and the high temperature area, near the bottom of flame, is the smallest. The methanol flame's highest temperature is 1152 K. Its high temperature area is bigger than that of the kerosene flame.

The trace of local maximum temperature versus height is indicated by lines of heavy dots. These lines intersect on the flame axis near $z/Q_c^{2/5} = 0.8$. Inside these lines is relatively cool fuel, outside is air approaching the reaction zone. Along the line is a band of strong mixing where the combustion occurs. According to Bouhafid et al. [6], these bands coincide approximately with the location of the luminous flame envelope, particularly at the flame base.

Only for the methanol flame dose the line approximately coincide with the location of the top of the continuous flame region. Perhaps this is because methanol is sootless, yielding a blue flame. The sooty flames of heptane and kerosene are apparently different except near the base of the flame. Heptane and kerosene flames change their shape from a cone to a mushroom cap periodically. According to the recent report by Ito, et al. [7], this flame shape change cycles at

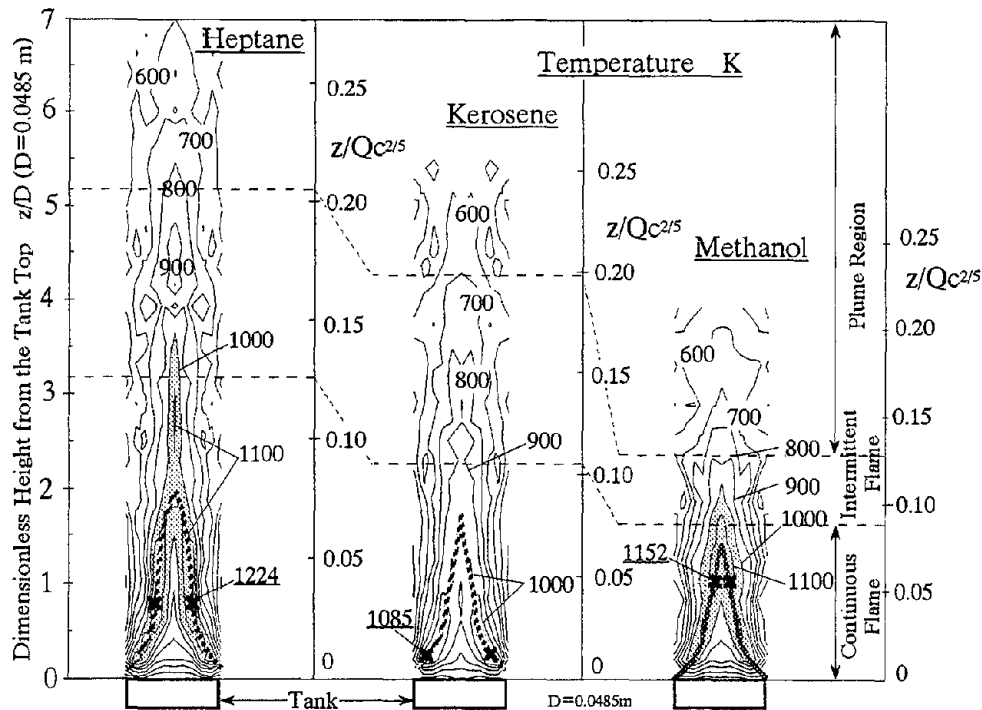


Figure 3. Temperature contours of three flames.

about 10 Hz for the size pool used here. Ito, et al. measured heptane pool flames using a high speed video camera. As a result of measurement, they showed the transition from a conical to a mushroom cap flame. Due to this flame shape change, the boundary of the flame in the middle part of flame could not be defined well using only temperature data measured by thermocouples.

We could not explain the irradiance differences among the three fuels in Fig. 2 using only the contours of temperature in Fig. 3. One should be carefully in interpreting the various contours obtained by thermography data analysis.

Contour of mean radiance. The contours of mean radiance of three fuels are shown in Fig. 4. The two dashed lines drawn in these figures are maximum radiance band. In each flame, a band of high radiance is located just inside the lines of the maximum local temperature shown in Fig. 3. In addition, for kerosene and heptane, there is a second band of high radiance above and detached from the lower one. The kerosene flame has the highest radiance value among the three fuels, $4.54 \text{ kW/m}^2/\text{sr}$. Nevertheless its flame temperature is the lowest. This discrepancy between radiance and temperature may be due to the difference of local soot, CO_2 , and H_2O concentration of the three flames.

The non-luminous flame of methanol has its highest radiance region just above the tank or the fuel surface. This means the concentration of CO_2 , H_2O and the temperature are relatively high compared with other regions. The less luminous upper part of this buoyant flame is diluted considerably by the surrounding air.

On the contrary, the luminous pool flames of kerosene and heptane have two high radiance zones: in the bottom of flame and in the upper part of continuous flame region. One is located at the bottom to middle of the continuous flame region and the other is located at the boundary of the continuous and intermittent flame region.

We may conclude that the high radiance zone in the flame bottom exists in common. This high radiance zone in the flame bottom supplies enough heat both to the fuel surface and to the upper part of flame to sustain pool burning. Thus, a so-called persistent or anchored flame is

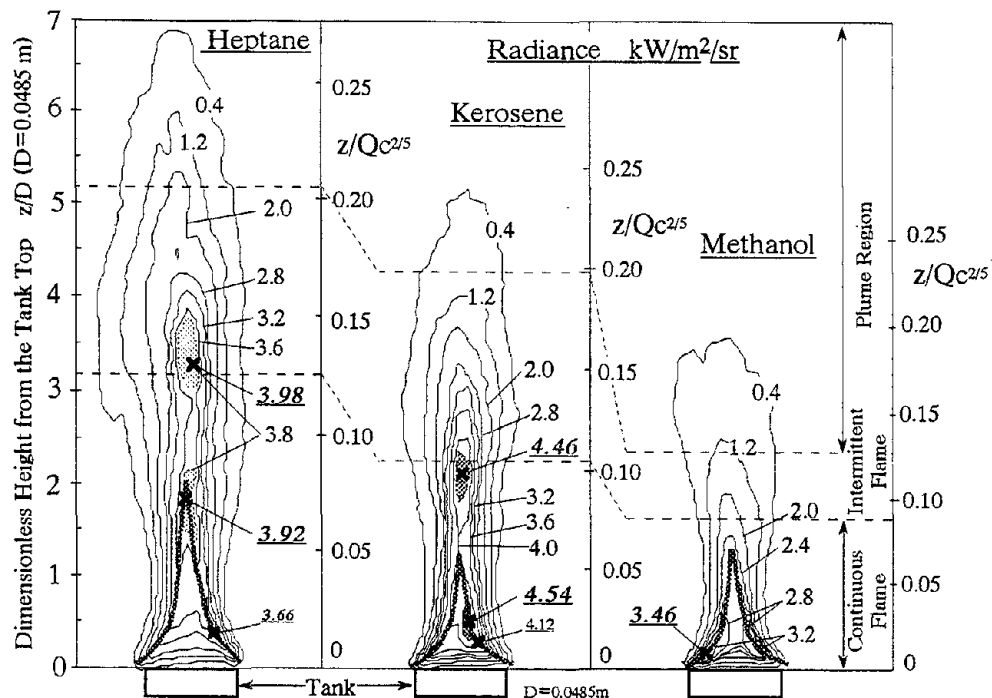


Figure 4. Radiance contours of three flames.

formed in the continuous flame region. The other high radiance zones in the middle of flame do not exist in the methanol flame. We may guess that this high radiance zone is related to soot. Pool flames seem to change their shape from a simple cone to a mushroom with cap periodically [7]. The top of the cone and the bottom of the mushroom cap are always formed near the upper part of continuous flame region or lower part of intermittent flame region. In other words, considerable unburned soot and gaseous fuel reaches the middle of flame and burns there. This area coincides to the above mentioned high radiance zones of kerosene and heptane.

Thus, the thermography technique has allowed us to identify one distinct radiative characteristics of the flame structure of small pool flames. This region was not detected well by the thermocouples because the flame moves upward with rapid radial expansion. This radial movement produces various size mushroom caps periodically. Temperature measurement by the thermocouples is less revealing in this region.

Contour of standard deviation. The contours of standard deviation in Fig. 5 indicate that all the flames have bigger values at the edge than in the center. Where the standard deviation is large, both the mean value and fluctuation are relatively large. This fluctuating flame region is where, alternately, relatively strong and weak combustion reaction occur.

The highest values of the standard deviation are connected by a dashed line in Fig. 5. In relatively large pool flames, the dashed lines are considered to represent the average vortex paths where vortices were formed, grow, and dissipate. In small pool flames, as the vortex is not so large or the flame is laminar, the dashed lines almost coincide with the flame edge of each fuel within the continuous flame region. The high standard deviation region (exceeding 0.8) is observed in the intermittent flame region for each fuel. Especially, the high standard deviation region of heptane and kerosene is located just outside of the upper high radiance zones. The shape of the high standard deviation region may be considered like a ring or annulus. This means the mixing of air and fuel in this region is stronger than in other regions and a relatively large eddy forms here. As a result, the mushroom cap is produced near here; experimental

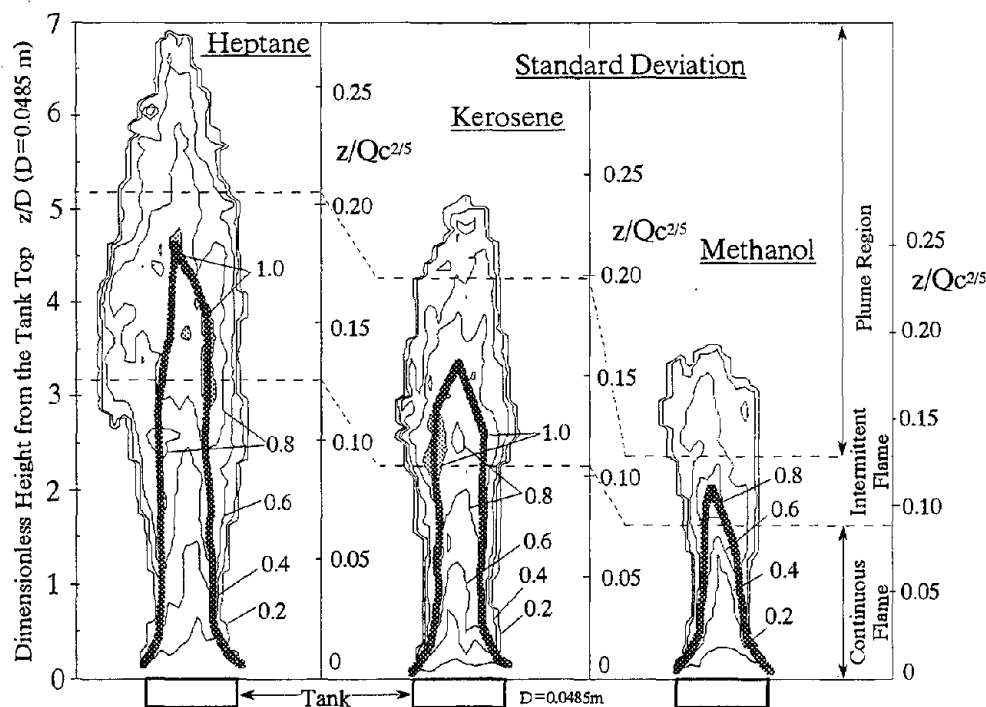


Figure 5. Standard deviation contours of three flames.

results support this idea [7].

Contour of coefficient of variation. Contours of coefficient of variation are shown in Fig. 6. The coefficient of variation expresses the magnitude of relative fluctuations irrespective of the magnitude of the mean radiance value because the coefficient of variation is obtained by dividing the standard deviation by the mean value. The coefficient of variation allows us to identify the stable region of the flame and the vortex formation and dissipation region.

Every flame has a region where the coefficient of variation is below 20%. This is at the base of the flame. Nevertheless there is great locational change of radiance due to active reaction between fuel and air. These stable regions play an important thermal role in pool flames, as described above.

The values of the coefficient of variation, on the flame center line, between the continuous and intermittent flame regions are about 50 % for heptane and kerosene, 70 % for methanol. The boundary values at the flame center between the intermittent and plume region are at 80 % for heptane, 120% for kerosene and 100 % for methanol. These differences may be because the methanol flame is sootless and the mushrooms cap flames are not made in the intermittent region.

Unfortunately, the large vortex formation and dissipation region is not observed in Fig. 6 because small pool flames are laminar. Only small size vortex regions are found at the bottom flame edge.

CONCLUSIONS

A new way of using thermography for radiative objects like pool flames is introduced and applied to small pool flames of three different fuels. Radiative characteristics and flame structure of small pool flames are considered by examining flame temperature distribution from a radiation point of view. In addition, it was shown that pool flame structure of various fuels became more clear when the standard deviation and the coefficient of variation obtained from

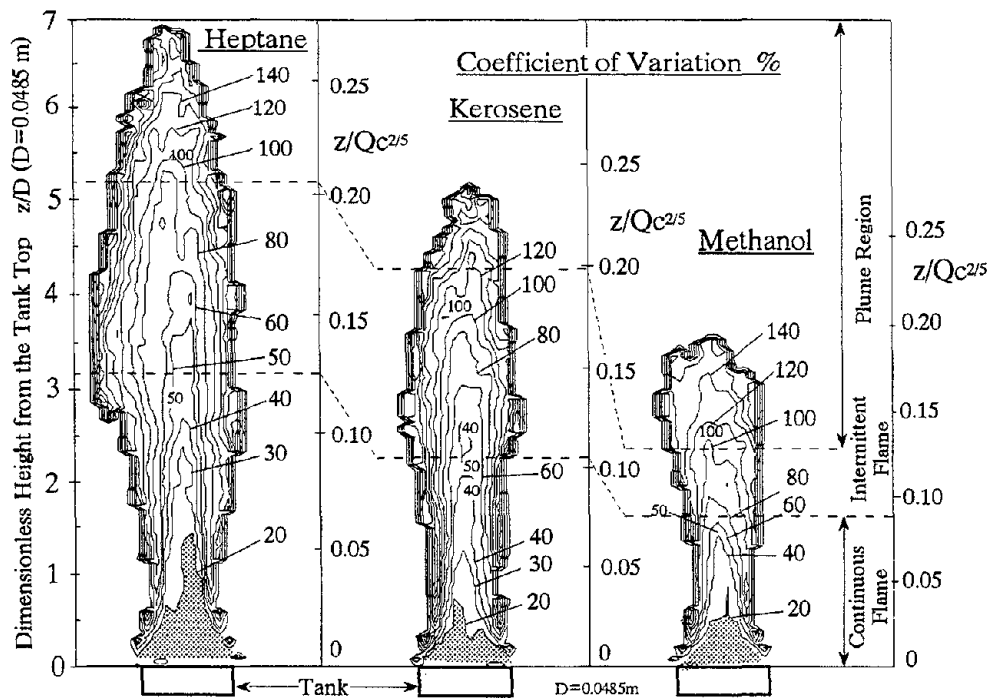


Figure 6. Contours of coefficient of variation of three flames.

thermographic data were used. The discussion allows the following conclusions:

- (1) Small pool flames tend to have a high radiance zone in the continuous flame region. This high radiance zone is important to sustain pool flames thermally.
- (2) In addition to the high radiance zone of the continuous flame region, luminous flames of heptane and kerosene have an upper high radiance zone near the boundary of the continuous and intermittent flame regions. When a mushroom flame cap is observed, it forms here.
- (3) The non luminous flame of methanol does not have the upper high radiance zone because combustion of soot will not occur near the boundary of the continuous and intermittent flame regions.
- (4) The contours of standard deviation give us information about the flame edge and the vortex regions where mushroom flame cap is formed.
- (5) The contours of the coefficient of variation identify the limits of the stable flame region.

ACKNOWLEDGMENTS The authors wish to thank Nippon Avionics Co., LTD. for their help with the instrumentation and Dr. Jonh A. Rockett for editorial assistance.

REFERENCES

1. Brörz, W., Schonbucher, A., Scheller, V. and Kettler A, *Combustion and Flame*, Vol.37, pp.1-24, 1980.
2. Hayasaka, H., Koseki, H., and Tashiro, Y., *Fire Technology*, Vol.28(2), pp.110-122, 1992.
3. Hayasaka, H., Koseki, H., and Tashiro, Y., *HTD-Vol. 203, ASME*, pp.71-77, 1992.
4. Thomas, P.H., *Combustion and Flame*, Vol.5, pp.359-367, 1961.
5. McCaffrey, B. J., *Fire Technology*, Vol.24(1), pp.33-47, 1979.
6. Bouhafid, A., Vantelon, J.P., Joulain, P. and Fernandez-Pello, A.C., *Twenty-Second Symp. (Inter.) on Combustion*, The combustion Institute, Pittsburgh, pp.1291-1298, 1988.
7. Ito, A. and Ohata, K., *Thirty-second National (Japanese) Symp. on Combustion*, The combustion Institute of Japan, pp.603-605, 1994.

Discussion

John Rockett: The nominal heat that you used in defining the boundaries between the regions, was that a total nominal heat based on the heat of combustion or did you correct for the radiated fraction so that the heat that you used was the convective heat? The quantity $q(C)$, you said that was a nominal heat of combustion but have you subtracted the radiated fraction so that's the conductive heat or is that the total heat of combustion? Would the boundaries shift to be more similar to the methanol if you corrected for just using the convective heat to normalize the heights?

Hiroshi Hayasaka: That's the total.

Takashi Kashiwagi: In doing the temperature calculation, do you assume asymmetric or symmetric because your temperature distribution showing is not necessary asymmetric although you are looking at only one slice.

Hiroshi Hayasaka: All the figures I showed you, they are not symmetric.

Takashi Kashiwagi: Then how do you get the temperature?

Hiroshi Hayasaka: The temperature distribution was measured using a thermocouple. And as for radiance distribution, a calculation was made based upon thermographic data.

SELF-PRESERVING BUOYANT TURBULENT PLUMES

G.M. Faeth
Department of Aerospace Engineering
The University of Michigan
Ann Arbor, Michigan, 48109-2118, U.S.A.

Submitted to: Fluid Mechanics of Fires — A Symposium in Honor of Prof. Edward Edom
Zukoski

Date Submitted: August 1995

Address Correspondence: G.M Faeth
3000 FXB Building
1320 Beal Avenue
The University of Michigan
Ann Arbor, MI 48109-2118, U.S.A.
TEL: (313) 764-7202
FAX: (313) 936-0106
E-MAIL: gmfaeth@umich.edu

SELF-PRESERVING BUOYANT TURBULENT PLUMES

G.M. Faeth
Department of Aerospace Engineering
The University of Michigan
Ann Arbor, Michigan, 48109-2118, U.S.A.

Abstract. An experimental study of round buoyant turbulent plumes is described, emphasizing conditions where the flow has lost source momentum and other source disturbances, and has become self preserving. Plume conditions were simulated using dense gas sources in a still and unstratified air environment. Mean and fluctuating mixture fractions and velocities were measured using laser-induced fluorescence and laser velocimetry, respectively. The present measurements extended farther from the source than most earlier work (up to 151 source diameters and 43 Morton length scales) and show that self-preserving plumes are narrower and have larger mean properties near the axis than previously thought. Although contemporary turbulence models yield reasonably good predictions of mean properties in the self-preserving region, there are difficulties with many of the approximations concerning turbulence properties; this raises questions about the potential effectiveness of these models for predicting the properties of the complex buoyant turbulent flows that are encountered in practical fire environments.

Introduction. The structure of round buoyant turbulent plumes in still and unstratified environments is a classical problem that has been widely studied in order to gain a better understanding of buoyancy/turbulence interactions. Conditions far from the source are of particular interest, even though such conditions are rarely encountered in practice, because effects of source momentum and other source disturbances have been lost and the flow becomes self preserving. For such conditions, both theoretical considerations and the interpretation of measurements are simplified and flow properties provide a straightforward evaluation of turbulence modeling concepts. Motivated by these observations, the present investigation undertook new measurements of mean and fluctuating mixture fractions and velocities within self-preserving round buoyant turbulent plumes. The following discussion of the study is brief, additional details can be found elsewhere [1-5].

Present considerations of self-preserving round buoyant turbulent plumes are confined to the buoyant jet sources used in most past studies of this flow, see Refs. 1-20 and references cited therein. Then, in the self-preserving region far from the source, all scalar properties are simple linear functions of the mixture fraction (which corresponds to the mass fraction of source material in a sample) called state relationships. Thus, the state relationship for density in the self-preserving region is as follows [1-4]:

$$\rho = \rho_{\infty} + f\rho_{\infty}(1 - \rho_{\infty}/\rho_0), f \ll 1 \quad (1)$$

Then, noting that the buoyancy flux of self-preserving round buoyant turbulent plumes is conserved, mean properties can be scaled as follows [1-4,19,20]:

$$\bar{u}((x-x_0)/B_0)^{1/3} = U(\eta) \quad (2)$$

$$\bar{f} g B_0^{-2/3} (x-x_0)^{5/3} \text{ld}(\ln \rho)/\text{d}f|_{f \rightarrow 0} = F(\eta) \quad (3)$$

where from Eq. 1, $|\mathrm{d}(\ln \rho)/\mathrm{d}f|_{f \rightarrow 0} = |\rho_0 - \rho_\infty|/\rho_0$ while the universal functions $U(\eta)$ and $F(\eta)$ generally are approximated by Gaussian fits [1-6,12,13,15,16]. Thus, conditions required to reach self-preserving behavior, and the character of $U(\eta)$, $F(\eta)$ and other mean and turbulent properties within the self-preserving region, become central issues for these buoyant turbulent flows.

Numerous studies of self-preserving round buoyant turbulent plumes have been reported [6-20]. Unfortunately, there are considerable differences among the various measurements, which have been attributed to problems of reaching self-preserving conditions [1-3]. In particular, although past measurements generally satisfy Morton's [18] criterion for flows dominated by buoyancy, self-preserving behavior was generally claimed for $(x-x_0)/d$ in the range 6-62. This range of streamwise distances is small compared to nonbuoyant jets where recent measurements only indicate self-preserving behavior for $(x-x_0)/d \geq 70$ [21]. Thus, the objectives of the present investigation were to study mean and fluctuating mixture fraction and velocity properties at greater distances from the source, up to $(x-x_0)/d = 151$, in order to gain a better understanding of the structure of self-preserving round buoyant turbulent plumes and the requirements for the onset of this flow regime.

Experimental Methods. The experiments involved source flows of carbon dioxide and sulfur hexafluoride in still air at normal temperature and pressure, which provided downward-flowing negatively-buoyant round turbulent plumes. The plumes were observed in a $3000 \times 3000 \times 3400$ mm high plastic enclosure within a high-bay test area. The enclosure had a screen across the top for air inflow, to compensate for the removal of air entrained by the plume. The plume flow was removed by 300 mm diameter ducts mounted on the floor at the four corners of the enclosure. The exhaust flow was controlled by a bypass/damper system to match plume entrainment rates, although recent work shows that roughly doubling and halving exhaust rates did not have a significant effect on flow properties [5]. The plume sources consisted of plastic tubes (6.4 and 9.7 mm inside diameter for the SF_6 and CO_2 sources, respectively) that could be traversed vertically and horizontally to accommodate rigidly-mounted instrumentation.

Instrumentation involved combined laser-induced iodine fluorescence (LIF) for measurements of mixture fractions and frequency-shifted laser velocimetry (LV) for measurements of velocities, as described in Ref. 22. The source flows were seeded with iodine vapor for the LIF measurements; the ambient air was seeded with oil drops (roughly 1 μm nominal diameter) for the LV measurements, using several multiple jet seeders that discharged near the top of the enclosure (maximum mixture fractions in the self-preserving region were less than 6%; therefore, effects of concentration bias of velocity measurements, because only the ambient air was seeded, were negligible).

Results and Discussion. Figures 1 and 2 are plots of the evolution of radial profiles of mean and fluctuating mixture fractions with streamwise distance. The variables used in these and subsequent figures are scaled according to the requirements of self-preserving round buoyant turbulent plumes. The results show progressive narrowing of the flow and increasing values near the axis with increasing distance until self-preserving behavior is reached for $(x-x_0)/d \geq 87$. This region is more than 12 Morton length scales from the source so that effects of buoyancy are dominant [18,19], with plume Reynolds numbers of 2500-4200 which are reasonably high for unconfined flows [1-4]. In agreement with the measurements of Papantoniou and List [20], which were made at similar distances from the source, the present self preserving plumes are narrower, with larger scaled values at the axis, than other past results [6-19] which appear to be in the transitional portion of the flow.

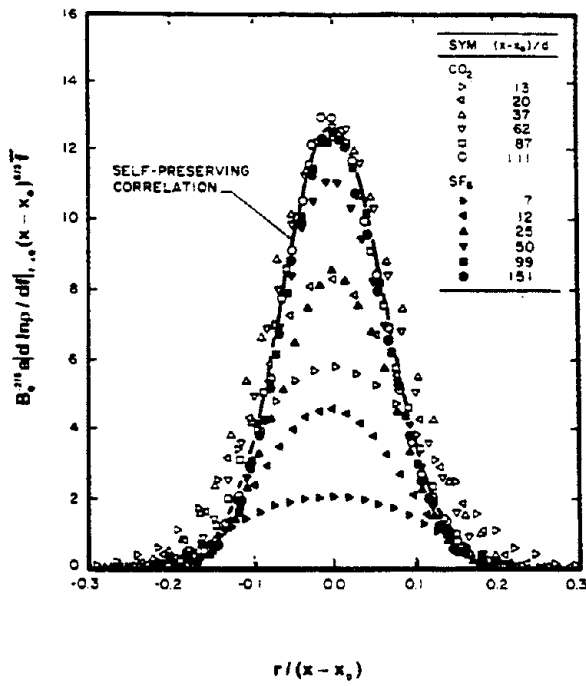


Figure 1. Development of radial profiles of mean mixture fractions. From [1].

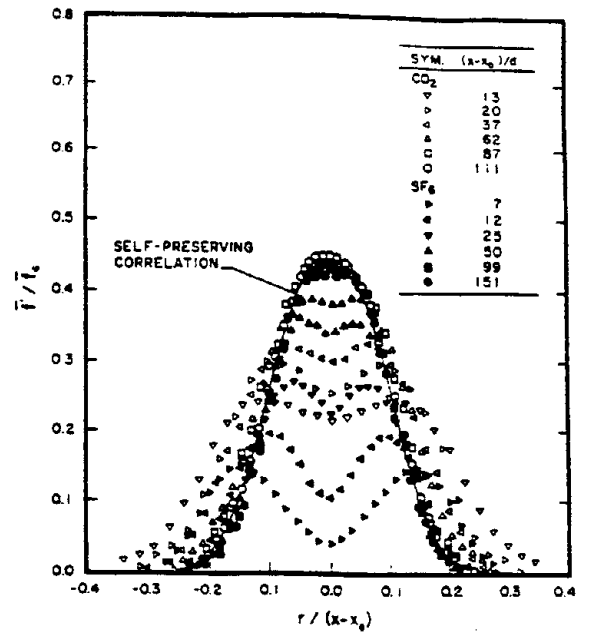


Figure 2. Development of radial profiles of rms mixture fraction fluctuations. From [1].

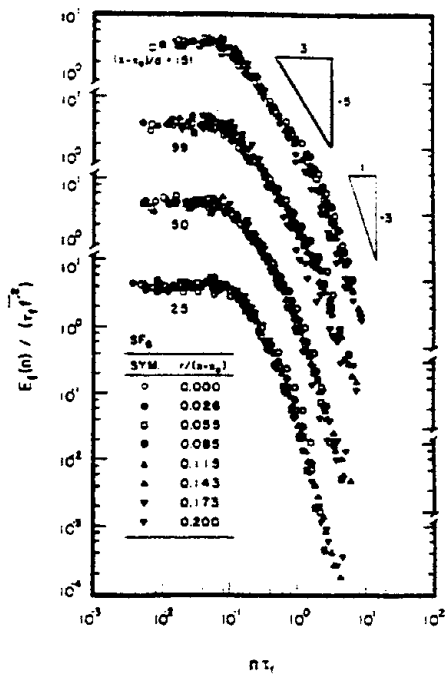


Figure 3. Temporal power spectral densities of mixture fraction fluctuations. From [1].

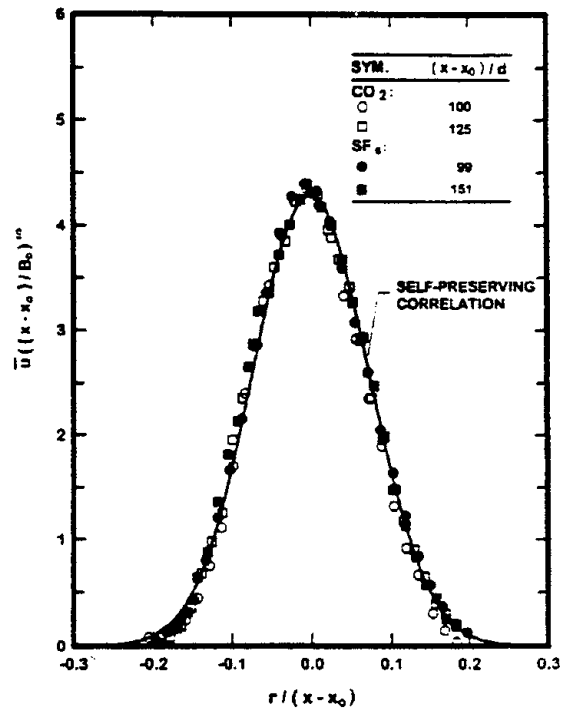


Figure 4. Radial profiles of mean streamwise velocities at self-preserving conditions. From [2].

Effects of buoyancy on the properties of turbulent plumes can be seen from the plots of mixture fraction fluctuations in Fig. 2. In particular, profiles of \bar{f} near the source exhibit a dip near the axis, similar to nonbuoyant jets [21], however, the dip disappears in the self-preserving region yielding values of \bar{f}'_c roughly twice those observed in nonbuoyant jets. This behavior can be attributed to turbulence production near the axis of the plumes due to buoyant instability in the streamwise direction [1-4].

Temporal power spectra of mixture fraction fluctuations, illustrated in Fig. 3, exhibit another interesting effect of buoyancy/turbulence interactions in buoyant plumes. In particular, the conventional $-5/3$ power decay of the temporal power spectra that is associated with the inertial subrange of turbulence, is followed by a prominent -3 power subrange that is not seen in nonbuoyant turbulence. This latter region is called the inertial-diffusive subrange where the local dissipation of turbulence kinetic energy is caused by buoyancy-generated inertial forces rather than viscous forces [15].

Figures 4 and 5 are illustrations of mean streamwise velocities and the three components of velocity fluctuations, respectively. The variables in these figures are scaled according to the requirements of self-preserving round buoyant turbulent plumes [1-4]. These measurements are all confined to $(x-x_0)/d \geq 87$, and properly exhibit self-preserving behavior. Similar to the findings for mixture fractions, the present measurements yield narrower profiles with larger scaled values near the axis than earlier results in the literature [6-19].

Effects of buoyancy are less evident for velocity fluctuations, Fig. 5, than for mixture fraction fluctuations, Fig. 2; in fact, velocity fluctuations exhibit a dip near the axis similar to the behavior of nonbuoyant jets, while turbulence intensities of streamwise velocity fluctuations near the axis are only slightly lower for self-preserving plumes, 0.22, than for nonbuoyant jets, 0.25, see [21]. Thus, buoyancy/turbulence interactions simultaneously act to increase mixture fraction fluctuation intensities and to reduce velocity fluctuation intensities near the axis of self-preserving round buoyant turbulent plumes in comparison to round nonbuoyant turbulent jets. Another effect of buoyancy/turbulence interactions is that a prominent inertial-diffusive subrange with a -3 power decay with increasing frequency, is seen in the temporal power spectra of streamwise velocity fluctuations in self-preserving round buoyant turbulent plumes but is not seen in nonbuoyant turbulent plumes — analogous to behavior discussed earlier for mixture fraction fluctuations [2]. Other properties of velocity fluctuations in the self-preserving region of buoyant turbulent plumes are qualitatively similar to nonbuoyant turbulent jets [19,21]; for example, $\bar{u}' > \bar{v}' = \bar{w}'$ near the axis while isotropic behavior is approached near the edge of the flow.

Present measurements of the three turbulence mass fluxes are illustrated in Fig. 6. The tangential turbulence mass flux is properly zero for the present axisymmetric flow. The streamwise turbulence mass flux is unusually large, exhibiting a correlation coefficient of roughly 0.7 near the axis, contributing roughly 15% to the total buoyancy flux of the plume, and helping to account for the enhanced production of mixture fraction fluctuations near the axis [3]. This behavior is caused by the intrinsic instability of plumes, where large values of f provide a corresponding potential to generate large values of u through effects of buoyancy [9]. Finally, the radial turbulence mass flux is reasonably consistent with other measured properties, based on evaluation using the governing equation for conservation of mean mixture fractions.

Present measurements of Reynolds stress for the self-preserving region of the plumes are illustrated in Fig. 7. The consistency of these measurements was checked using the mean

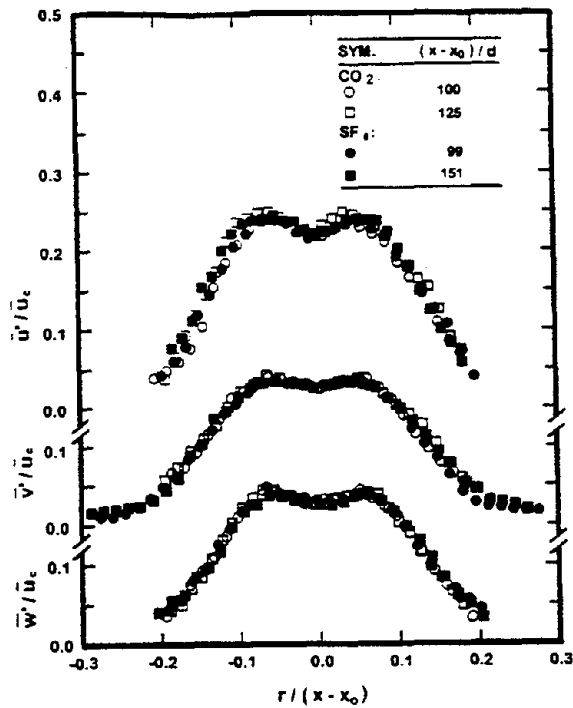


Figure 5. Radial profiles of rms velocity fluctuations at self-preserving conditions. From [2].

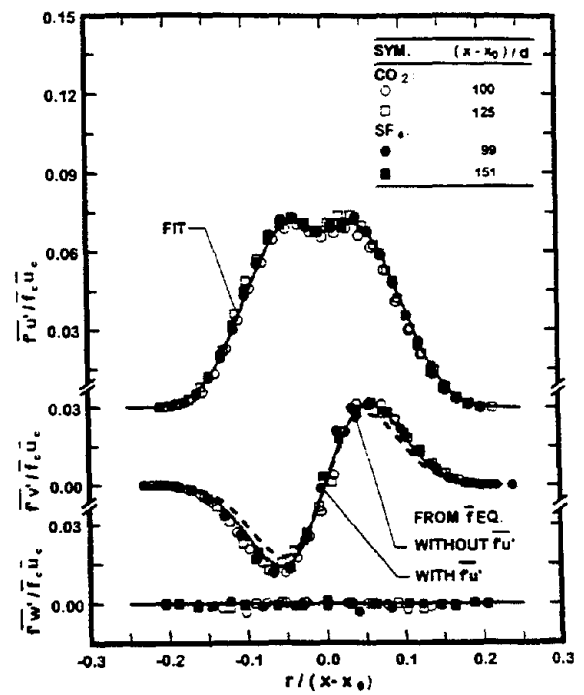


Figure 6. Radial profiles of turbulence mass fluxes at self-preserving conditions. From [3].

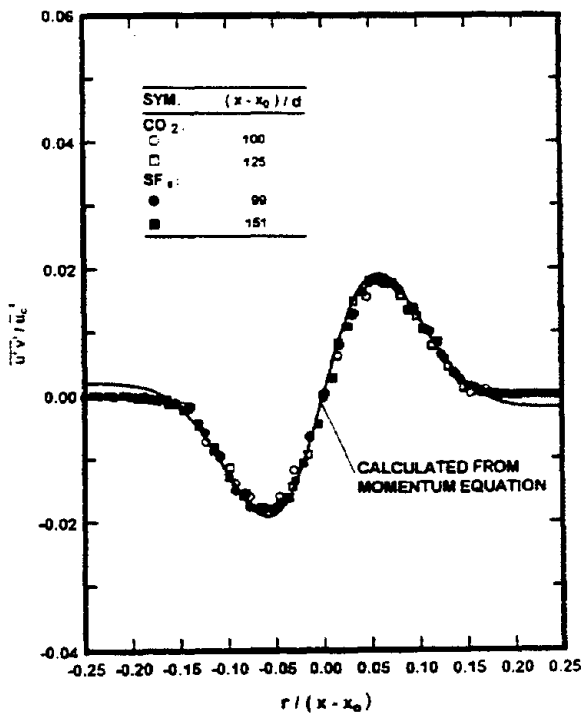


Figure 7. Radial profiles of Reynolds stress at self-preserving conditions. From [2].

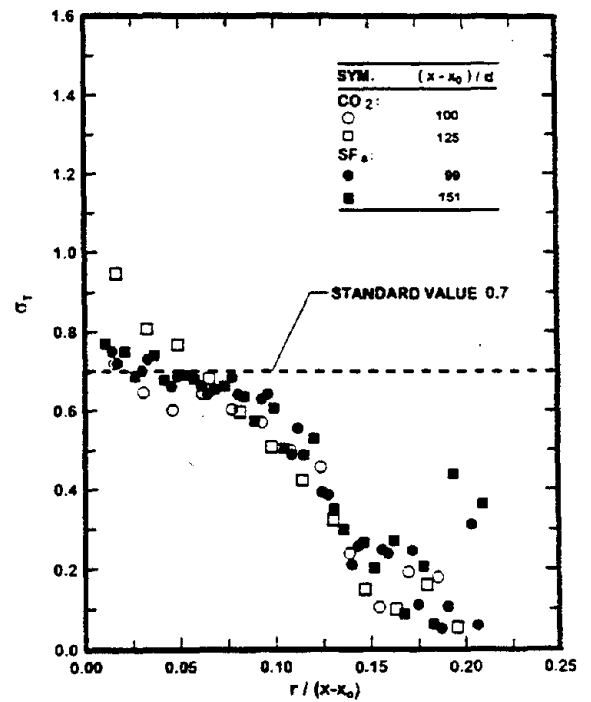


Figure 8. Radial profiles of turbulent Prandtl/Schmidt numbers at self-preserving conditions. From [3].

momentum equation, analogous to earlier considerations of turbulent mass fluxes. These results are in reasonably good agreement in view of experimental uncertainties [2]. In general agreement with other velocity moments, the present results for plumes are rather similar to findings for nonbuoyant turbulent jets [21] in spite of the significant effects of buoyancy/turbulence interactions seen in mixture fraction properties.

Modeling Implications. Present measurements of the properties of self-preserving round buoyant turbulent plumes provide a direct means of evaluating both the performance and approximations of simplified turbulence models. In particular, Pivovarov et al. [23] tested a variety of contemporary turbulence models based on predictions of mean properties assuming self-preserving flow in round buoyant turbulent plumes and compared their predictions with the measurements of Refs. 9, 10, 12, 13 and 16 — all of which involve transitional plumes in view of present findings. Based on these results, Pivovarov et al. [23] recommended substantial changes of turbulence model constants established during extensive past studies of nonbuoyant turbulent flows. In contrast, these same predictions are in excellent agreement with present measurements of mean mixture fractions and streamwise velocities in self-preserving round buoyant turbulent plumes [4]. This apparent success, however, is somewhat misleading because predictions based on even simpler models — e.g., mixing length models — are generally effective for simple free turbulent boundary-layer flows at large Reynolds numbers such as round buoyant turbulent plumes. In fact, upon closer examination, present results highlight a number of serious difficulties of contemporary turbulence models of buoyant turbulent flows that will be discussed next.

A worrisome deficiency of simplified turbulence models involves their use of the gradient-diffusion approximation. Typical of simple turbulent boundary-layer flows, there is no immediate difficulty with the gradient-diffusion approximation in the radial direction for the critical radial turbulence mass fluxes and Reynolds stresses, illustrated in Figs. 6 and 7. On the other hand, the present flows yield unphysical effects of countergradient diffusion for streamwise turbulence mass fluxes in Fig. 6 for $r/(x-x_0) \geq 0.082$ and for streamwise turbulence stresses in Fig. 5 for $r/(x-x_0) \geq 0.042$ [3]. Naturally, these countergradient diffusion effects in the streamwise direction are not very important for boundary-layer flows, such as the present plumes, where streamwise turbulent transport is ignored in any event; nevertheless, these deficiencies raise concerns about the use of gradient-diffusion hypotheses for the more complex buoyant turbulent flows of practical interest.

Use of the simple gradient-diffusion hypothesis, with constant turbulent Prandtl/Schmidt numbers, is even problematical for transport in the radial direction within self-preserving buoyant turbulent plumes [3]. Direct measurements of this property for self-preserving round buoyant turbulent plumes are illustrated in Fig. 8. In view of experimental uncertainties, which are relatively large because σ_T involves several measurements including two gradients, σ_T exhibits self-preserving behavior reasonably well. Nevertheless, σ_T varies from a value near 0.8 at $r=0$ to a value near 0.1 at the edge of the flow, which departs significantly from assumptions of $\sigma_T = 0.7$ or 0.9 across the flow width that are made in simple turbulence models, see Refs. 4, 23, 24 and references cited therein.

Analogous to σ_T , other turbulence modeling constants also exhibit excessive variations across the flow width [3]. One parameter of interest is the ratio of the characteristic velocity to mixture fraction time scales, often denoted C_{g2} [24]. Near the axis C_{g2} is in the range 1.96-2.56, which is comparable to $C_{g2} = 1.87-1.92$ that is often used in simple turbulence models [24]. However, C_{g2} progressively increases with radial distance rather than remaining constant as assumed in the simple models, reaching values of 4.17-4.55 near the edge of the flow. Another parameter having similar importance is the constant, C_μ , in the gradient-

diffusion approximation for the Reynolds stress. In particular, present values of C_μ near the axis are in the range 0.10-0.11, which is comparable to the widely used value, $C_\mu = 0.09$ of simple turbulence models [24]. Nevertheless, present measurements indicate a progressive reduction of C_μ with increasing radial distance, reaching values of 0.031-0.040 near the edge of the flow. Taken together, these difficulties also raise questions about the potential effectiveness of simple turbulence models for treating complex practical buoyant turbulent flows. This observation prompted measurements of a variety of properties used in higher-order closures, see Ref. 3 for a discussion of these results.

Conclusions. Measurements of mixture fraction and velocity statistics in round buoyant turbulent plumes in still and unstratified air has yielded the following major conclusions [1-5]:

1. Present measurements, supported by the earlier findings of Papantoniou and List [21] for similar conditions, indicated that self-preserving round buoyant turbulent plumes were narrower with larger mean values near the axis than previous results in the literature; the reason for these differences is that earlier measurements were limited to $(x-x_0)/d \leq 62$ which was not sufficiently far from the source to reach self-preserving behavior
2. Buoyancy/turbulence interactions in self-preserving round buoyant turbulent plumes are manifested in several ways: radial profiles of mixture fraction fluctuations do not exhibit reduced values near the axis that are seen in nonbuoyant jets; streamwise turbulent mass fluxes are large near the axis, they yield correlation coefficients of roughly 0.7 and they contribute roughly 15% to the plume buoyancy flux due to buoyant instability in the streamwise direction; and the temporal spectra of mixture fraction and streamwise velocity fluctuations exhibit prominent -3 power inertial-diffusive subranges, beyond the inertial subranges, that are not seen in nonbuoyant turbulent flows.
3. Evaluation of simplified turbulence models using the present measurements of mean properties in self-preserving round buoyant turbulent plumes was reasonably satisfactory but this is not definitive because plumes are a simple boundary-layer flow. In addition, several hypotheses concerning turbulence properties made for simple turbulence models were not satisfied very well; for example, streamwise turbulent transport exhibited countergradient diffusion, and several turbulence modeling constants (σ_T , C_{g2} and C_μ) exhibited significant variation over the flow cross section. Taken together, these difficulties suggest that higher-order turbulence models, or more advanced methods, will be needed to reliably treat the complex buoyant turbulent flows encountered in practical fire environments.

Nomenclature. B_0 = source buoyancy flux, C_{g2} and C_μ = turbulence modeling constants, d = source diameter, $E_f(n)$ = temporal power spectral density of f , f = mixture fraction, $F(\eta)$ = scaled radial distribution function of \bar{f} , g = acceleration of gravity, n = frequency, r = radial distance, u = streamwise velocity, $U(\eta)$ = scaled radial distribution of \bar{u} , v = radial velocity, w = tangential velocity, x = streamwise distance, η = dimensionless radial distance = $r/(x-x_0)$, ρ = density, σ_T = effective turbulence Prandtl/Schmidt number, τ_f = temporal integral scale of mixture fraction fluctuations. The subscripts c , o and ∞ refer to conditions at the centerline, the source or virtual origin, and the ambient environment. The symbols $(\bar{\quad})$ and $(\overline{\quad})'$ denote time-averaged mean and rms fluctuating values.

Acknowledgments. This research was supported by the United States Department of Commerce, National Institute of Standards and Technology, Grant Nos. 60NANB1D1175 and

60NANB4D1696, with H.R. Baum and K.C. Smyth of the Building and Fire Research Laboratories serving as Scientific Officers. Z. Dai and L.-K. Tseng contributed to the research.

References

1. Z. Dai, L.-K. Tseng and G.M. Faeth, J. Heat Trans. 116:409-417 (1994).
2. Z. Dai, L.-K. Tseng and G.M. Faeth, J. Heat Trans. 117:138-145 (1995).
3. Z. Dai, L.-K. Tseng and G.M. Faeth, J. Heat Trans., in press.
4. Z. Dai, L.-K. Tseng and G.M. Faeth, *Heat and Mass Transfer 94* (A.R. Balakrishnan and S.S. Murthy, eds.), Tata McGraw-Hill, New Delhi, 1994, pp. 57-66.
5. Z. Dai and G.M. Faeth, J. Heat Trans., submitted.
6. H. Rouse, C.S. Yih and H.W. Humphreys, Tellus 4:201-210 (1952).
7. G. Abraham, ASCE J. Hyd. Div. 86:1-131 (1960).
8. R.A. Seban and M.M. Behnia, Int. J. Heat Mass Trans. 19:1197-1204 (1976).
9. W.K. George, Jr., R.L. Alpert and F. Tamanini, Int. J. Heat Mass Trans. 20:1145-1154 (1977).
10. H. Nakagome and M. Hirata, *Heat Transfer and Turbulent Convection* (D.B. Spalding and N. Afgan, eds.), McGraw-Hill, New York, 1977, pp. 367-372.
11. V.D. Zimin and P.G. Frik, Izv. Akad. Nauk. SSSR. Mekhanika Zhidkosti Gaza 2:199-203 (1977)
12. T. Mizushima, F. Ogino, H. Veda and S. Komori, Proc. Roy. Soc. London A366:63-79 (1979).
13. F. Ogino, H. Takeuchi, I. Kudo and T. Mizushima, Int. J. Heat Mass Trans. 23:1581-1588 (1980).
14. N. E. Kotsovinos, Int. J. Heat Mass Trans. 28:771-777 (1985).
15. P.N. Papanicolaou and E.J. List., Int. J. Heat Mass Trans. 30:2059-2071 (1987); *Ibid.*, J. Fluid Mech. 195:341-391 (1988).
16. A. Shabbir and W.K. George, NASA Tech. Memorandum 105955, 1992.
17. T. Peterson and Y. Bayazitoglu, J. Heat Trans. 114:135-142 (1992).
18. B.R. Morton, J. Fluid Mech. 5:151-163 (1959).
19. E.J. List, Ann. Rev. Fluid Mech. 14:189-212 (1982).
20. D. Papantoniou and E. J. List, J. Fluid Mech. 209:151-190 (1989).
21. N.R. Panchapakesan and J.L. Lumley, J. Fluid Mech. 246: 197-247 (1993).
22. M.-C. Lai and G.M. Faeth, J. Heat Trans. 109:254-256 (1987).
23. M.A. Pivovarov, H. Zhang, D.E. Ramaker, P.A. Tatum and F.W. Williams, Combust. Flame 92:308-319 (1992).
24. F.C. Lockwood and A.S. Naguib, Combust. Flame 24: 109-124 (1975).

Discussion

Craig Beyler: Your observation that you have to go very far downstream to get self-preserving flies in the face of the classical sort of thing where these self-preserving things work from the flame tip on in “real fires.” I wonder what you think that means or what the relationship is between your experiments and those kinds of classic observations.

Gerard Faeth: I think probably the short answer to your question is that fires themselves are extremely complicated phenomena where the standards of what constitutes similarity are generally somewhat relaxed from the kinds of standards that we are trying to apply here. You simply aren't looking that closely and you have many other complicating features that are somewhat involved in the process. That's what I can say. One other brief thing here. For example, if you are willing to relax your standards, say you want to talk about something within 20 to 30%, now you are beginning to talk about distances that are only 25 diameters away.

Howard Baum: Did you record the amount of computational work required to do one of the Reynold's stress computations to simulate this as opposed to the κ - ϵ . I'm trying to get a feeling of the ratio of what the work actually is.

Gerard Faeth: The calculations for our conditions in both instances are sort of trivial and I haven't really tracked the answer to your question. I'll get the information.

Characteristics of Oscillating Buoyant Plumes

Baki M. Cetegen and Kent D. Kasper

Mechanical Engineering Department

University of Connecticut, Storrs, CT 06269-3139

Abstract

Experiments on the oscillatory behavior of axisymmetric buoyant plumes of helium and helium-air mixtures are reported for a range of nozzle diameters ($3.6 \text{ cm.} < d < 20 \text{ cm.}$), source velocities and plume densities. Measurements include pulsation frequencies as determined by velocity fluctuations along plume centerline and phase resolved laser Doppler velocity measurements. These non-reacting buoyant plumes are found to exhibit periodic oscillations of plume boundaries as well as formation of toroidal vortices within one-half diameter above nozzle exit. These oscillations and vortices are similar to those observed in pool fires, although their frequency scaling is somewhat different. The frequency relationship is well represented by the expression $S = 0.83 \text{ Ri}_1^{0.38}$ where $S = fd/V$ and $\text{Ri}_1 = [(\rho_\infty - \rho_p) g d] / \rho_\infty V^2$. Here, f , V , ρ are frequency, source velocity and density and subscripts f and ∞ refer to plume fluid and ambient respectively. Around $\text{Ri}_1 = 100 - 500$, there is a transition in the frequency scaling as evidenced by more turbulent and vigorously mixing plumes beyond the transition. Above this transition, S scales with $\text{Ri}_1^{0.28}$. Phase resolved velocity field of a pulsating buoyant plume reveals a strong buoyant acceleration along the plume centerline followed by a deceleration in the region of toroidal vortex formation. The strong upward acceleration is also accompanied by a radial inflow which determines the entrainment characteristics of these pulsating buoyant plumes.

INTRODUCTION

Periodic pulsations have been observed in pool fires by many investigators including the research group of Prof. Zukoski at Caltech. Oscillations of plume boundaries near the origin of a pool fire result in the formation of toroidal vortical structures which rise through the visible flame region and influence its characteristics such as entrainment, flame height and radiation. Although effects of these pulsations on flame properties have been contemplated by some researchers, it has been put into quantitative use for the first time by Zukoski et al [1] in explaining fluctuations observed in visible flame heights. It is generally believed that inclusion of the effects of these oscillations (frequency and strength of generated vorticity) will result in better description of entrainment process in pool fires and enable better scaling relationships. The first author had the privilege to be part of the fire research group of Prof. Zukoski in the early eighties. Motivation for this work has originated from fire research at Caltech during this time. It is therefore fitting to present some of our recent results on buoyancy induced instabilities in non-reacting buoyant plumes.

Strongly buoyant non-reacting plumes, although somewhat different than pool fires, have been observed to exhibit oscillatory behavior similar in appearance to pool fires. In fact, our earlier experiments with Helium plumes and simulated pool fires [2] have suggested that oscillations are initiated solely as a result of high buoyancy near the source of a plume. In our study, we have examined only a limited number of helium plumes and compared their behavior to pool fires and concluded that oscillation frequency scaling was similar to pool fires. However, Hamins et al [3] reported that non-reacting buoyant plumes of helium had a somewhat different frequency scaling than that for pool fires. In contrast to well accepted scaling of pool fire pulsations with the inverse square root of source diameter, $D^{-0.5}$, non-

reacting buoyant plumes appear to exhibit different scaling as $D^{-0.62}$. Recently, Delichatsios [4] conducted a dimensional analysis of pulsation frequency and showed that buoyant plume frequency should scale as $D^{-2/3}$. In order to further investigate the mechanism responsible for these pulsations, we embarked on an experimental investigation with two main objectives. First objective was to determine the pulsation frequency scaling for non-reacting buoyant plumes for a wide range of source parameters (source diameter, velocity and fluid density), conveniently grouped as a Froude or Richardson number. Second objective was to characterize the flow field in the region of vortex formation to examine its key features during the formation and advection stages of toroidal vortices to help understand the mechanism of this instability.

EXPERIMENTAL

The experimental set-up was designed to conduct detailed velocity measurements by conditional laser Doppler velocimetry as well as to determine the pulsation frequencies of buoyant plumes originating from circular nozzles of 3.6, 5.2, 7.3, 10.0, 15.2 and 20 cm. diameter. Nozzles were constructed from either PVC or metal pipe with tapered outside surfaces at 10° with a lip thickness of 1 mm at the exit. The length to diameter ratio ranged from 3 to 10 for all nozzles with the large values for smaller diameter nozzles. A 64 mesh, flat stainless steel screen was placed across the nozzle exit. The main purpose of this screen was to provide a uniform flow condition at the nozzle exit which was otherwise impossible due to rapid buoyant acceleration of helium with respect to the surrounding air medium. Presence of screen prevented backflow of air upstream of nozzle exit and also insured a plug flow exit condition. In large nozzles, with $L/d \approx 3 - 4$, a honeycomb flow straightener was also placed for flow uniformity upstream of nozzle exit. These nozzles were placed vertically in draft free surroundings as shown in Figure 1. Twenty mesh window screens were formed into a circular cylinder far from the nozzles ($D = 2$ m) to ensure little or no influence of turbulent eddies that might be present in room air. Studied plumes were free of any forced draft above so that no artificial downstream influence was imposed.

Characterization of plume oscillation frequencies was facilitated by a total pressure probe placed along the plume centerline at a height of 0.5 d. Selection of this location was such that large velocity oscillations in vortex formation and convection phases can be easily detected by the pressure probe. The pressure port was connected by a short Tygon tubing to the high pressure side of a differential pressure transducer of capacitance type (Setra Model 264 +/- 0.05 inch of H_2O column) while the low pressure side was exposed to ambient pressure. Considering the total pressure $P(t) = P_0 + \rho U^2(t)/2$, where P_0 is the static pressure, ρ is density and $U(t)$ is the time varying velocity at the probe tip, the differential pressure transducer responds to variations in the square of velocity. The pressure transducer output was first amplified (Tektronix AM502) and filtered by a low pass filter before being processed by a frequency spectrum analyzer (Analogic Data 6000). An example of the pressure trace and its fast fourier transform (FFT) is shown in Figure 2 for a helium plume originating from the 10 cm. diameter nozzle. The frequency peak at 4.5 Hz is unambiguously associated with the pulsation frequency of this helium plume. The frequency peaks below and above this fundamental frequency represent subharmonics and superharmonics of 4.5 Hz. Figure 3 shows a sequence of photographs of this plume as obtained by laser Mie scattering from small water droplets. These photographs, obtained at 15 fps, also suggest that a complete pulsation cycle (for example, frames 1 to 7) occurs at around 5.0 Hz. The probe acoustic response to pressure oscillations was determined based on an analysis by Greitzer and Nikkanen [5] with an estimate of 13 milliseconds for the probe/sensor configuration in our experiments. This value is considerably smaller than the typical period of studied plume oscillations in the range 0.07 to 0.5 seconds.

The velocity field of an oscillating buoyant plume of helium-air mixture was mapped using conditional Laser Doppler Velocimetry using the 10 cm. diameter nozzle. The nozzle was

surrounded by a co-flow chamber, as shown in Figure 1, which provided the external particle seeding in the rapidly contracting region of the plume near the nozzle exit. The plume was seeded with water droplets from two different seeders. Seeding of the core helium air flow was accomplished by a six jet droplet generator (TSI Model No. 9306) while the co-flow seeding was affected by a domestic ultrasonic humidifier. Droplets from both seeders were measured to be less than 2 μm by a phase Doppler particle sizer. The LDV system was a conventional single component velocimeter operating in the backward scatter mode.

Data collection from the pressure transducer and the LDV system was handled by an IBM PC/XT computer, interfaced with two Data Translation DT2801 A/D acquisition boards, running a FORTRAN controlling program. Two methods can be employed to carry out conditional data acquisition. One method is continuous acquisition of the "control" and the measured signals and post processing those data to obtain conditionally averaged quantities. Another method is to trigger the data acquisition only when the condition on the control signal is satisfied. The first method requires high data rates in order to reconstruct conditionally averaged velocities at all phases. However, the second method becomes desirable in situations where the data rate is dependent on uncontrollable factors such as local particle seeding density in the flow. Data were collected by this second method by triggering velocity data acquisition at four phases along the sinusoidal pressure signal: the maximum point (phase A), the negative slope zero crossing (B), the minimum point (C) and the positive slope zero crossing (D). At each spatial location, data acquisition continued until 100 data points were collected at each phase. Experimental uncertainty in the velocity measurement was less than 3 % in the central part of the plume and up to 13 % near the plume edges. Further details of data acquisition procedures can be found in reference [6].

RESULTS AND DISCUSSION

Frequency Measurements

As described in the previous section, a number of experiments were conducted to determine the relationship of plume oscillation frequency to plume parameters. The first set of experiments dealt with pure helium plumes emanating from nozzles of diameters: 3.6, 5.2, 7.3, 10.0, 15.2, and 20.0 cm. In a second set of experiments, mixtures of helium and air were injected through the same nozzles to determine effects of plume density on oscillatory behavior. Parameters in this problem are nozzle exit velocity, V , nozzle diameter, d , gravitational acceleration, g , plume density, ρ_p , and the atmospheric density, ρ_∞ . In the case of pool fires and turbulent reacting jets, variable density effects arise due to the chemical composition and temperature changes which result from exothermic combustion reactions. In the absence of combustion, variable densities arise from compositional variations due to mixing of different density fluids. The aforementioned quantities can be formed into a number of non-dimensional groups given by:

Strouhal number	$S = fD / V$ where $V = V_0$ or \sqrt{gd} or $\sqrt{\Delta\rho gd/\rho}$
Density parameter	$\Pi_1 = (\rho_\infty - \rho_p)/\rho_\infty$ or $\Pi_2 = (\rho_\infty - \rho_p)/\rho_p$
Richardson number	$Ri_0 = g \cdot d / V_0^2$ or $Ri_1 = \Pi_1 Ri_0$ or $Ri_2 = \Pi_2 Ri_0$
Froude number	$Fr_j = Ri_j^{-1}$

Strouhal number describes a non-dimensional oscillation frequency. Density ratio can be constructed with either the ambient fluid or the plume density in the denominator as indicated by Π_1 or Π_2 . Richardson (or inverse Froude) number is a measure of the ratio of buoyancy force to jet momentum. Combinations of these parameters, also being dimensionless, may also be constructed. While the primary dimensionless parameters have been listed in terms of nozzle exit velocity, it can be envisioned that a more relevant velocity scale in buoyant flows can be taken as \sqrt{gd} , or more appropriately as $\sqrt{\Pi_1 gd}$ or $\sqrt{\Pi_2 gd}$.

Experiments were conducted with variations in source diameter, nozzle exit velocity and plume density at the source such that a universal correlation of the form $S = f(Ri_j, \Pi_j)$ can be established. The plume gas density at the source was varied by mixing helium with air at different proportions. When plotted in the form of $S = f(Ri_0)$, data for helium-air mixture plumes exhibited significant deviations from pure helium data. These non-dimensional parameters, also used by Hamins et al [3] to correlate flame and non-reacting plume pulsation frequencies, do not account for the density difference between the plume fluid and its surroundings which, in buoyant flows, provides the driving force for the buoyant fluid motion. While these non-dimensional parameters produce reasonably good correlations of flame and helium plume data because of their similar densities, they do not take account of differing plume fluid densities in general. The density effect was then introduced in Richardson number as $Ri_1 = \Pi_1 Ri_0$ or $Ri_2 = \Pi_2 Ri_0$. Initially, data were plotted using both parameters. It was found however that Ri_2 yielded a much poorer correlation of data than Ri_1 even though Ri_2 is the more appropriate form of Richardson number. Figure 4 shows the correlation of data in the form of $S = f(Ri_1)$. These parameters correlate data for all plumes well, leading to the expression $S = 0.83 Ri_1^{0.38}$ for $Ri_1 < 100$. This correlation also agrees well with that developed by Hamins et al [3]. While this correlation is satisfactory for the majority of the data, helium plume data for 15 and 20 cm. nozzle diameters do not follow this correlation beyond $Ri_1 = 100$. In the region $Ri_1 > 100$, frequency data appear more scattered and exhibit a different scaling as $S \propto Ri_1^{0.28}$. A closer examination of the experimental data for $d = 15$ and 20 cm. diameter nozzles indicate that changes occur in plume structure between $Ri_1 = 100$ and 500 . This transitional behavior had not been observed in other studies as far as we know.

In order to determine the origin of this transition, visual observations and frequency spectra of two pure helium plumes originating from 10 cm. and 20 cm. diameter sources lying below and above the transition were compared. In figure 6a, a photograph and pressure-time trace for a helium plume originating from the 10 cm. diameter source are shown for $Ri_1 = 220$, $Re_d = 50$. The plume starts with a laminar flow field as it rapidly contracts due to buoyancy. There appears to reside an air bubble in the center of the plume penetrating all the way close to the nozzle surface. The upper portions of the plume exhibit transition from laminar to turbulent in the region where a toroidal vortex is formed. For this plume, pressure (or velocity) oscillations are periodic with an apparent long period modulation of its amplitude as seen in Figure 2a. The resulting frequency spectrum shows a single distinct peak associated with the visual pulsations as shown in Figure 7a. In contrast, a helium plume emanating from the 20 cm. diameter nozzle with $Ri_1 = 470$ and $Re_d = 96$ exhibits a significantly more turbulent appearance as shown in Figure 6b. This plume, typical of all plumes above the transition, is more turbulent at its source with considerable amount of air penetrating to its base. The velocity fluctuations are of a less periodic and more chaotic nature compared with the previous case, representative of plumes below transition. In fact, the frequency spectrum, in Figure 7b, contains a number of dispersed peaks around the highest peak associated with puffing. This difference is believed to be the major reason for the change in the frequency scaling.

Pulsation frequencies were non-dimensionalized using the nozzle exit velocity in the correlations presented above and by Hamins et al [3]. Although the source velocity plays a role very close to the nozzle exit, it is expected that the buoyant acceleration rapidly takes over and a buoyant velocity scale may be more appropriate. In figure 5, Strouhal numbers based on two different velocity scales are shown as a function of Ri_1 . Figure 8a shows the Strouhal number based on the buoyant velocity scale of \sqrt{gd} . It appears that this scaling results in poorer correlation of data for individual data sets as well as the large amount of scatter for some data. It, however, is not the proper velocity scale since it does not contain a density difference which drives the buoyant motion. Thus, a modified velocity scale of $\sqrt{(\rho_\infty - \rho_f)gd/\rho_\infty}$ was introduced in Figure 5b. This velocity scale produces a significantly better correlation of data similar to that

of Figure 4. The resulting correlation can be expressed as $S_2 = 0.83 Ri_1^{-0.12}$ for $Ri_1 < 500$. This correlation can be shown to be identical to that obtained from Figure 4.

Scaling differences between pool fires and non-reacting buoyant plumes arise due to change in buoyancy flux with downstream distance. In pool fires, the total buoyancy flux increases with downstream distance due to local heat release yielding $f \propto d^{-1/2}$. In non-reacting buoyant plumes, total buoyancy flux is constant and buoyancy is reduced locally by mixing above the plume source resulting in $f \propto d^{-0.62}$. An explanation of this scaling has been recently given by Delichatsios [4]. It should be noted however that there exists an overlap region where pool fire and non-reacting buoyant plume oscillations exhibit similar values of Strouhal numbers. Our earlier data [1] from a 10 cm. diameter source were obtained in this overlap region. It was then conjectured that flames and helium plumes exhibited similar pulsation frequency characteristics.

Plume Velocity Field:

Phase-resolved velocity measurements were performed on a helium-air mixture plume originating from a 10 cm. diameter nozzle using laser Doppler velocimetry. Plume parameters were $Ri_1 = 50$, $Ri_2 = 195$, plume density ratio, $\rho_p/\rho_\infty = 0.26$. The co-flow velocity was set at 2.4 cm/s, providing minimal interference to plume development. Measurements were concentrated in a region spanning one nozzle diameter height from the nozzle centerline to the nozzle edge. Radial extent of these measurements was limited by available seeding. Although a co-flow chamber provided external seeding at low velocity outside the plume boundary, this stream was quickly ingested into the plume near the vortex formation region. Figure 8 shows the velocity measurements at four instants during one pulsation period. Phase A corresponds to the maximum in the pressure signal, followed by Phase B at the negative slope zero crossing, Phase C at the minimum and Phase D at the positive slope zero crossing. At all phases of plume motion, a strong buoyant acceleration along the plume centerline is evident. Centerline velocity increases from few tens of centimeters per second to over one meter per second in a distance of several centimeters.

At phase A, representing the instant at which plume centerline velocity at $z = d/2$ is maximum, strong axial acceleration occurs over the central 10 - 15 mm. radial region. This is where a toroidal vortex ring is formed. In fact, the toroidal vortex is formed at a height around $z \approx d/2$ as it can be seen in Figure 3. The axial acceleration is also accompanied by a strong radial inflow towards the plume axis near the base. At phase B, toroidal vortex has convected downstream and continues its influence by its induced higher flow velocities behind it. The radial velocity components are somewhat lower than those at phase A, where vortex is closer to the nozzle. At phase C, the toroidal vortex has completely moved out of the measurement region. However, a strong centerline acceleration is still maintained at this instant with lower velocity magnitudes for $z \leq d/2$. Finally, at phase D, the velocity field becomes more uniform and vertically oriented as the strong flow acceleration is re-established between phases D and A.

In addition to the vector plots delineating the general features of the velocity field, the vertical velocity components are plotted in Figure 9. Velocity profiles near the nozzle exit are approximately of "top-hat" shape with rapid acceleration ensuing a short distance above. In particular, velocity profiles deviate considerably from the conventional Gaussian profiles in the region of the toroidal vortex. The maximum velocities occur off-axis and the profiles exhibit inflection points at 50, 60 and 70 mm. locations at phase A. In this vortex formation region, superposition of viscous vortex velocity profile on its convection speed yields these off-center peak velocity distributions. Downstream convection of the vortex can be followed in this figure as indicated by the arrows shown.

In understanding plume oscillation mechanism and the underlying flow dynamics, characteristics of buoyant acceleration along the plume centerline can supply valuable

information. Figure 10 shows plume centerline velocity distributions at four instants during the pulsation cycle. The most striking feature is the rapid acceleration at phase A, followed by a deceleration with the peak velocities occurring around $z \approx 60$ mm. It is precisely in this region where the toroidal vortex formation is initiated by transfer of axial momentum to radial motion. At later phases (B & C), flow velocities are lower below this location due to stagnation behind the vortex and higher above because of the induced suction behind the convecting toroidal vortex. These results imply, as suggested earlier [2], that toroidal vortex formation is a result of rapid buoyant acceleration of light plume fluid in heavier, more or less quiescent surroundings. Once this toroidal vortex forms, it affects the surrounding flow field as it convects upward. Then, its influence decays near the plume source, setting up a strong acceleration in the lower region of a buoyant, non-reacting plume for the next cycle.

CONCLUSIONS

It has been found experimentally that non-reacting buoyant plumes undergo quasi periodic oscillations of the type observed in pool fires. Although the characteristics of the plume instability appear to be similar in both cases, the frequency scaling with source diameter is somewhat different yielding $f \propto d^{-0.62}$ for non-reacting plumes versus $f \propto d^{-1/2}$ for pool fires. In earlier correlations of pulsation frequency of the form $fd/V = f(gd/V^2)$, the density difference between the plume fluid and the surrounding medium was omitted. Our experimental data for plumes of helium-air mixtures correlate significantly better with respect to Richardson number defined as $[(\rho_\infty - \rho_p)gd]/\rho_\infty V^2$. In fact, the velocity scale used in forming the Strouhal number can also be taken as a buoyant velocity scale $\sqrt{(\rho_\infty - \rho_p)gd/\rho_\infty}$. There exists a transition in the scaling of pulsation frequency around $Ri_1 = 100 - 500$. This transition is associated with the rapid turbulent mixing of the plume fluid with its surroundings close to the nozzle exit. To our best knowledge, this transition has not been reported before.

Phase resolved velocity measurements in a periodic helium plume clearly show the various stages during one oscillation cycle. A rapid buoyant acceleration of plume fluid near the centerline is followed by the formation of a toroidal vortex ring around a height of one-half of the source diameter. As this vortex ring convects downstream, it retains its influence on the upstream flow field. Finally, buoyant acceleration reestablishes the formation of the next toroidal vortex. Velocity profiles within the plume are influenced by the presence of the toroidal vortex. Velocity profiles exhibit peak velocities that are displaced from the plume centerline in the region of the toroidal vortex.

REFERENCES

1. Zukoski, E. E., Cetegen, B. M. and Kubota, T., Twentieth Symposium (International) on Combustion, The Combustion Institute, Pittsburgh, p.361. 1984
2. Cetegen, B. M. and Ahmed, T. A., Experiments on the Periodic Instability of Buoyant Plumes and Pool Fires, *Combustion and Flame*, 93:157-184. 1993
3. Hamins, A., Yang, J. C., and Kashiwagi, T., Twenty-Fourth Symposium (International) on Combustion, The Combustion Institute, Pittsburgh, p.1695. 1992
4. Delichatsios, M. A., "Gravitational Fluctuations in Pool Fires and Pool Buoyant Flows", to appear as a technical note in *Combustion Science and Technology*
5. Greitzer, E. M. and Nikkanen, J. P., Pratt & Whitney Aircraft Inter-Office Correspondence, December 17, 1971.
6. Kasper, K. D., An Experimental Investigation of Naturally Oscillating Buoyant Plumes of Helium/Air Mixtures, M.Sc. Thesis, University of Connecticut, (1995)

Acknowledgments

The research reported herein had been supported by National Science Foundation Grant (CTS-8909176). Additional support from UConn. Research Foundation is acknowledged.

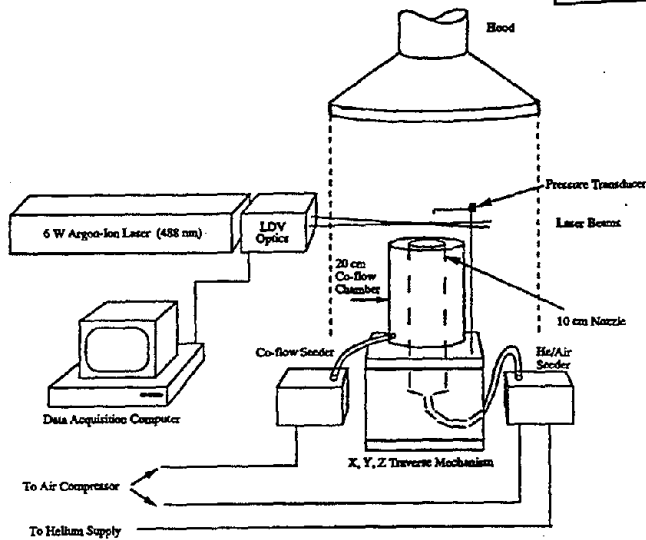


Figure 1. Schematics of the experimental set-up

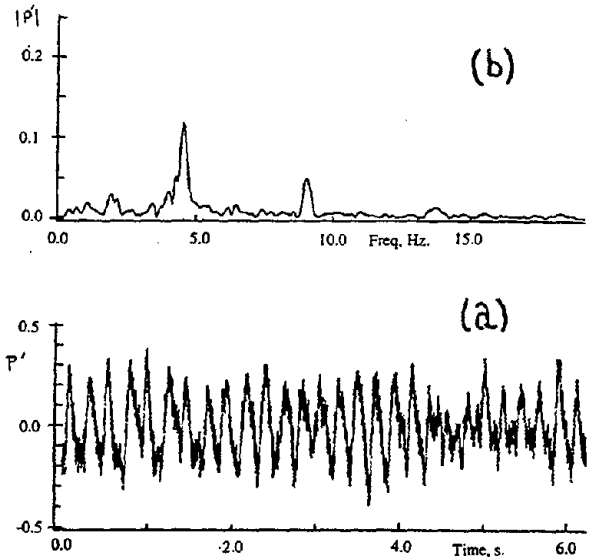


Figure 2. Plume centerline pressure fluctuations (a) and its frequency spectrum (b) for a helium plume originating from a 10 cm. diameter nozzle at $Ri_1 = 316$.



Figure 3. Sequence of images of a helium plume originating from a 10 cm. diameter source with $Ri_1 = 316$. Framing rate is 15 fps.

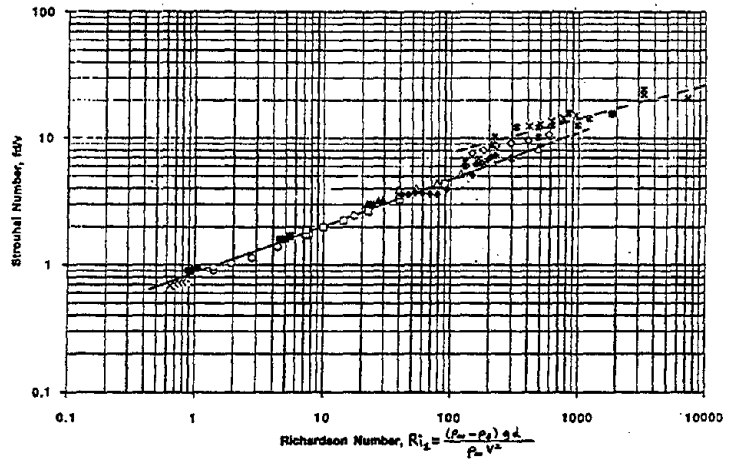


Figure 4. Correlation of pulsation frequency in terms of Strouhal number and Richardson number, Ri_2 . Helium plumes: + $d = 3.6$ cm., \circ $d = 5.2$ cm., \square $d = 7.3$ cm., Δ $d = 10.2$ cm., \diamond $d = 15.2$ cm., \bullet $d = 20.3$ cm. Helium-air mixtures: \times $d = 3.6$ cm., \bullet $d = 5.2$ cm., \blacksquare $d = 7.3$ cm., \blacktriangle $d = 10.2$ cm., \blacklozenge $d = 15.2$ cm., \blacktimes $d = 20.3$ cm.

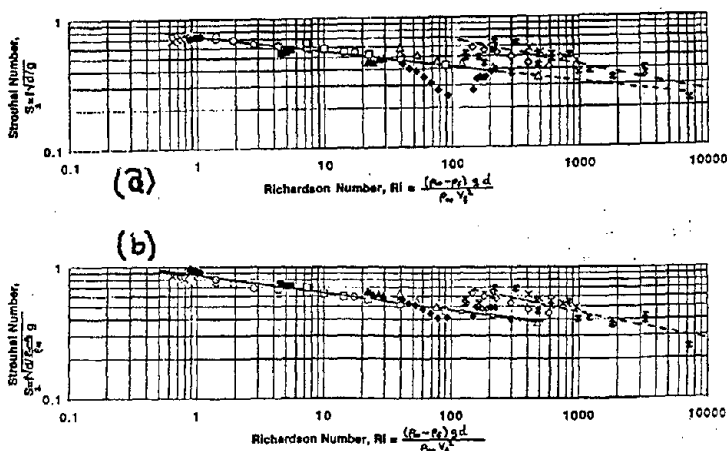


Figure 5. Correlation of pulsation frequency in terms of different definitions of Strouhal numbers (a) $S = f d / g$, (b) $S = f d / ((1 - pf / \rho_0) g)$ as a function of Ri_1

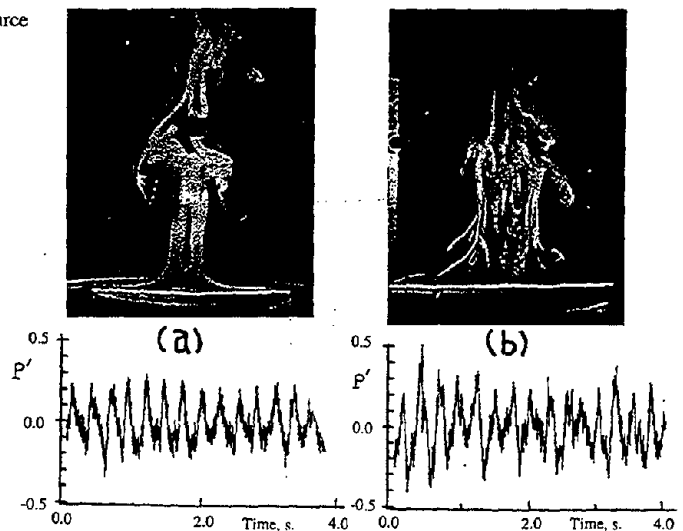


Figure 6. Plume images, pressure-time trace for helium plumes originating from (a) $d = 10$ cm. at $Ri_1 = 220$, $Red = 50$ (b) $d = 20$ cm. at $Ri_1 = 470$, $Red = 96$.

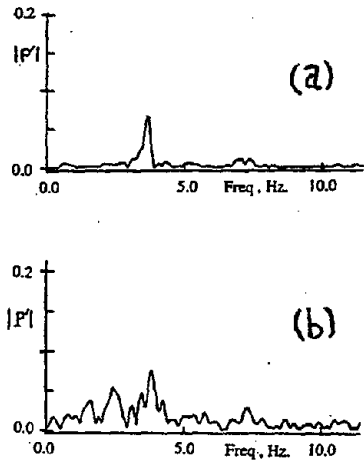


Figure 7 (top) Pulsation frequency spectra for the plumes of figure 6 (a) $d = 10$ cm. (b) $d = 20$ cm.

Figure 8 (right). Velocity distributions at four different phases during pulsation cycle for $d = 10$ cm. nozzle $Ri_1 = 50$.

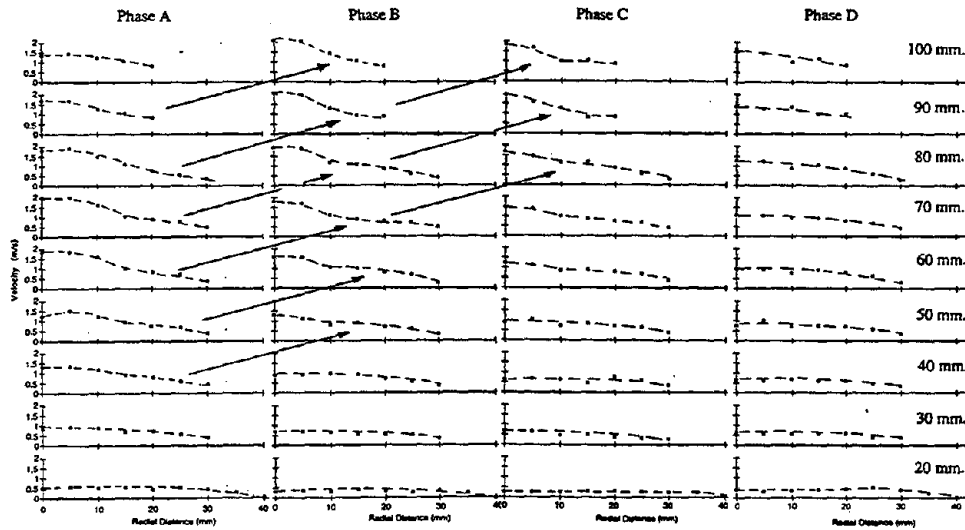
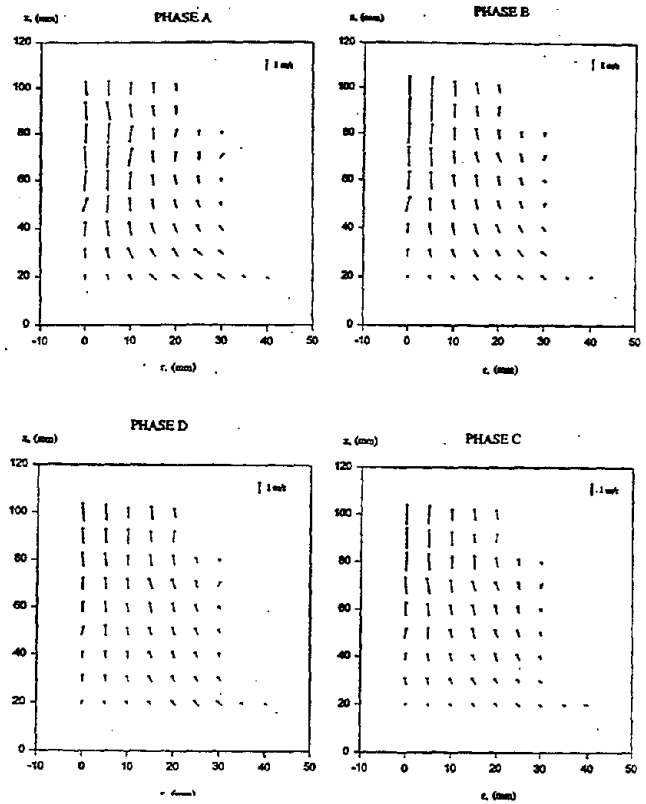


Figure 9.(top) Vertical component of velocity vector throughout the lower part of the plume in Figure 8.

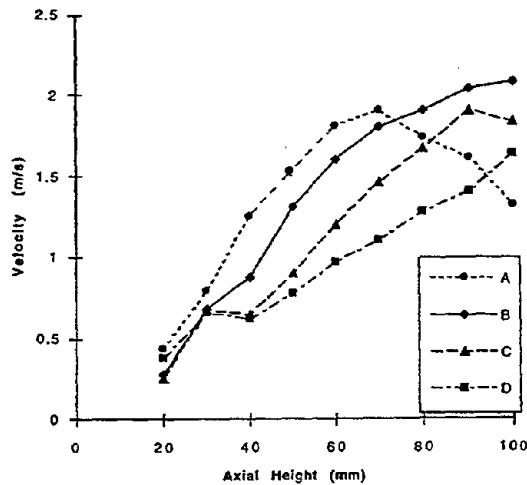


Figure 10.(left) Plume centerline velocity profiles of the same plume depicted in Figures 8 and 9.

Discussion

Gunnar Heskestad: This is a very interesting field. Lot's of research still to do. For instance, in your helium experiments, it seems to me that it should be possible to correlate them without any scatter if we include viscosity and perhaps, density differences of the fluid being discharged.

Baki Cetegen: I agree with you. Those effects should be characterized by further experimentation. What we showed here is the first bit of it, if you will, to look at and include the difference which should be there in the correlation of frequency scaling. The viscosity effects should be looked at. They could introduce secondary effects, but this scaling seems, so far at least, to do well for the data we have.

Gunnar Heskestad: The second part of my question is when we correlating and scaling frequencies and diffusion flames, it seems to me that the flame height ought to be of some consequence for a given diameter.

Baki Cetegen: Yes, in fact, the paper done by Ed Zukoski and me had looked at the effects on the flame height fluctuations. If I understand your question correctly, yes, it has a consequence on the flame height fluctuations and that has been quantified to my knowledge by Ed's Symposium paper.

Edward Zukoski: I think what Gunnar was asking was if you increase the size of the fire, would the frequency change. And what we found was with the accuracy we were measuring, it did not. What did happen was the flapping with the low fuel flow was all the way down to the burner at the bottom. In contrast, when you had a high fuel flow, the flapping was up here. But the remarkable fact is, the frequency was within 10%.

Baki Cetegen: I would like to add that if you use our technique and if you increase the velocity at the source of the plume, you see a small change in the frequency and Anthony Hamins also pointed that out. However, the first-order effect which is the square root of the diameter, that's not affected as Ed said, within 10%. That appears to be constant. But if you look carefully, there is an effect on source velocity and that changes the frequency a little bit.

Henri Mitler: I think it's a pity that people can't leave well enough alone. There was a nice result of a square root and people continue to pick at this. Can you add some clarifying words, for example, between the square root result and the 0.4 result? Both of them are theoretically sensible, but it would be nice to try to get them harmonized.

Baki Cetegen: I think the issue is not leaving the problem alone, it's a different type of situation. In one case, you have local heat release in the flame. In this case, it's just a source buoyancy, so the problem is different. Now, with regard to resolving the 0.4 to 0.5, I'm assuming you are talking about flames. I don't have a good answer for that.

GUNNAR HESKESTAD
Factory Mutual Research Corporation
1151 Boston-Providence Turnpike
Norwood, MA 02062

ABSTRACT

A dimensionless scaling parameter originally derived by Zukoski from analysis of nonreacting turbulent plumes, Q^* , has been applied extensively and successfully in the literature to correlate heights of turbulent diffusion flames. However, from new flame height measurements at laboratory temperature and substantially above and below laboratory temperature it appears that this parameter lacks some generality in the flaming region. An alternative scaling parameter derived some time ago specifically for the flaming region seems to account correctly for the observed variations in flame height with ambient temperature.

1. INTRODUCTION

Analysis of turbulent convective flows resulting from fire leads to a combination of variables with the heat release rate from which a dimensionless heat release rate can be defined, typically represented by the symbol Q^* . Zukoski¹ first introduced a form of this parameter about twenty years ago in describing the centerline values of temperature rise and velocity in nonreacting turbulent plumes. However, the parameter has also been applied to correlate features of the combustion region, such as flame heights. Here we report experiments to test the capability of the parameter to account for effects on flame height of variations in the environment, specifically the ambient temperature, compared to another dimensionless parameter, N , introduced a number of years ago².

2. THE PARAMETER Q^*

Zukoski¹ represented the centerline values of temperature rise, ΔT_o , and velocity, u_o , in turbulent nonreacting plumes as follows:

$$\Delta T_o/T_\infty = C_T(Q^*)^{2/3} \quad (1)$$

$$u_o/(gz)^{1/2} = C_u(Q^*)^{1/3} \quad (2)$$

Here C_T and C_u are dimensionless coefficients, T_∞ is the ambient temperature, g is the acceleration of gravity, and z is the height above the heat source. The dimensionless parameter Q^* is defined:

$$Q^* = Q/[\rho_\infty c_p T_\infty (gz)^{1/2} z^2] \quad (3)$$

where Q is the heat release rate and c_p is the specific heat at constant pressure.

An alternative Q^* was subsequently introduced by Zukoski et al³ to correlate a large body of flame height data, substituting the fire diameter, D , for the height above the fire source, z , in Eq. (3), i.e.:

$$Q_D^* = Q/[\rho_\infty c_p T_\infty (gD)^{1/2} D^2] \quad (4)$$

Dimensionless flame heights, measured under normal laboratory conditions, were shown to correlate very well against this parameter. Other authors subsequently adopted the parameter to correlate flame heights, including Cox and Chitty⁴, Hasemi⁵, and McCaffrey⁶ in his comprehensive review of flame height data and correlations. Still, the rationale for its use in these applications must be said to be unclear, illustrated by Zukoski's recent statement⁷ that the "appropriate scaling parameters for most of the features of fire plumes have not been established with confidence." However, "some consensus has been reached that a dimensionless heat addition parameter, $[Q_D^*]$, or a dimensional parameter that is proportional to $[Q_D^*]$ such as $Q/D^{5/2}$ can be used as the scaling parameter."

3. THE PARAMETER N

The parameter N evolved from a capability of predicting maximum gas velocities associated with buoyancy-controlled turbulent diffusion flames, which led to a global model for correlating flame-height data². Infinite reaction kinetics was assumed. Further, it was assumed 1) that the flame would extend to a height where the total flux of air entrained at lower levels is just sufficient to complete the combustion reactions (recognizing that much of the air entrained below the flame tip never takes part in the combustion reactions), 2) that the air demand from the surroundings is proportional to the stoichiometric requirements of the pyrolysis gases, and 3) that the total air entrainment rate obeys the relationship established by Ricou and Spalding⁸ for the local entrainment rate in jets of different density than the surroundings. Limiting attention to flames where effects of Froude and Reynolds numbers are not important, the following functional relationship for the dimensionless flame height was derived^{2,9}:

$$L/D = \text{fn}(N) \quad (5)$$

where:

$$N = [c_p T_\infty / (g \rho_\infty^2 (H_c/r)^3)] Q^2 / D^5 \quad (6)$$

In Eq. (6), H_c is the heat of combustion per unit mass and r is the stoichiometric mass ratio, air (or other oxidizing atmosphere) to combustible.

Eq. (5) has been found to correlate experimental data on flame height very well over a wide range of fire sizes and combustibles.^{2,9,10} The following correlation equation⁹ represents the entire range of fires from values N near 10^{-6} to 10^5 :

$$L/D = -1.02 + 15.6N^{1/5} \quad (7)$$

The high limit on N corresponds to the beginning of effects of high discharge momentum at the source. The low limit ($N = 1.20 \times 10^{-6}$) corresponds to $L/D = 0$, near which experiments indicate that the flame cover will break up into flaming and nonflaming areas¹⁰.

It is readily shown that N and Q_D^* are related as follows:

$$N = [c_p T_\infty / (H_c/r)^3] (Q_D^*)^2 \quad (8)$$

The ratio H_f/r represents the heat liberated per unit mass of air, or other oxidizing atmosphere, entering the combustion reactions; for the standard atmosphere it does not vary appreciably among various combustibles (most fall within the range 2900 to 3200 kJ/kg). Furthermore, the ambient temperature T_∞ normally does not vary appreciably. Hence, N and $(Q_D^*)^2$ can often be considered proportional to each other, leading McCaffrey⁶ to recast Eq. (7) into the following form:

$$L/D = -1.02 + 3.7 (Q_D^*)^{2/5} \quad (9)$$

Clearly, this conversion applies only to normal atmospheric conditions of temperature, pressure and composition.

To test whether Q_D^* or N is a more suitable parameter, we had the opportunity to conduct a few experiments using a simple methane flame, varying the temperature of the environment substantially above and below normal laboratory temperature. In these experiments, Q_D^* remained practically constant because $\rho_\infty T_\infty$ did not vary much (see Eq. (4)), and inconsequential effects on the flame height are expected if Q_D^* is considered a governing parameter. However, N increased and decreased significantly because of the variations in the ratio T_∞/ρ_∞^2 in the expression for N in Eq. (6), and significant effects on flame height are expected if N is considered a governing parameter.

4. EXPERIMENTS

4.1 Approach

A relatively small turbulent methane flame from a 52.5-mm diameter burner, near 2 kW in heat release rate, was burned at laboratory temperature, approximately 45K above laboratory temperature, and approximately 45K below laboratory temperature. Reference experiments were also run for the elevated and reduced temperature cases at laboratory temperature, matching the parameter N of those cases by, respectively, increasing and decreasing the heat release rate.

4.2 Setup

An environmental chamber was available for conducting the experiments, capable of both elevated and reduced temperatures, Figure 1. Interior dimensions were 3.05 m x 1.88 m x 2.39 m high. The chamber was brought to temperature and then all equipment shut down to provide a quiescent space for each experiment. After an experiment, the door to the chamber was opened and the contents washed out with the discharge of a fan blowing from the outside into the bottom of the doorway.

The exit of the methane burner was at an elevation of 1.27 m below the ceiling at location A or location B. Location A in Figure 1 was used for all experiments except those at reduced temperature (and their reference experiments at laboratory temperature), for which a cold draft was found to descend on the burner from the overhead (deactivated) cooling unit, mounted in close proximity to this location. Location B was selected for the reduced temperature cases and their reference experiments at laboratory temperature.

The chamber was equipped with humidity and temperature sensors. For these experiments, thermocouples were specially installed at three levels on a vertical traverse approximately in the center of the room: level with the top of the burner, 1.12 m above the floor; 1.75 m above the floor; and 2.36 m above the floor (0.025 m beneath the ceiling).

The burner, Figure 2, was made from a 265-mm long section of 2-inch steel pipe, with an internal diameter of 52.5 mm. Methane entered through a tube fitting at the bottom of the burner; the available length-to-diameter ratio was sufficient to meet the requirements¹¹ for a relatively uniform exit flow from the burner. The square-mesh screen above the gas entry was originally installed to support a bed of glass beads for producing a well behaved flame. The beads were not needed but the screen was left in place. After gas flow was stabilized at the beginning of an experiment, the gas was ignited with the aid of a small loop of nichrome wire extending up from the perimeter of the burner opening, energized electrically to bright-yellow color until ignition. Each burn was limited to a duration of 90 seconds to preclude effects of recirculating combustion products.

Flame heights were determined from video records. The camera viewed the flames through a window in the access door to the chamber. Burner location A was directly in view behind the window. To afford a view of the burner at location B, an angled mirror was positioned at location A. A vertical scale was mounted alongside the burner, approximately 0.20 m to one side and in view of the camera.

In addition to chamber temperatures, barometric pressures (p_{∞}) and relative humidities in the chamber (RH) were recorded.

Table 1 Test Summary

Test	Burner Location	p_{∞} (mm Hg)	T_{∞}		RH(%)	Q(kW)	L(mm)	L/D	$10^3 N$	Q_D^*
			°C	°K						
1	A	768	29.2	302	39	2.14	315	6.00	10.5	3.06
2	A	768	29.2	302	39	2.14	305	5.81	10.5	3.06
3	A	768	28.4	301	40	2.14	315	6.00	10.4	3.06
4	A	768	28.6	302	39	2.14	325	6.19	10.5	3.06
5	A	764	69.3	342	13	2.13	334	6.36	15.7	3.10
6	A	764	74.0	347	11	2.13	325	6.19	16.6	3.10
7	A	764	72.7	346	11	2.13	338	6.44	16.3	3.09
8	A	760	27.5	301	42	2.66	353	6.72	16.4	3.85
9	A	760	27.5	301	42	2.66	338	6.43	16.4	3.85
10	A	760	27.7	301	42	2.66	330	6.29	16.4	3.85
11	B	760	27.0	301	43	1.65	250	4.76	6.33	2.39
12	B	760	27.2	301	43	1.65	251	4.78	6.33	2.39
13	B	760	27.6	301	43	1.65	257	4.90	6.33	2.39
14	B	763	-17.4	256	52	2.13	254	4.84	6.40	3.05
15	B	763	-17.7	255	70	2.13	257	4.90	6.26	3.05
16	B	763	-17.8	255	72	2.13	257	4.90	6.26	3.05

4.3 Results

Table 1 is a list of experimental results. Flame heights, L, were determined from 75 seconds of each video record, after the first 15 seconds of each burn, as the height above which the flame spent 50 percent of the time. This definition of flame height was first introduced by Zukoski et al.¹² Values of the parameter N were calculated using Eq. (6). Values of Q_D^* were calculated using Eq. (4). Heat release rates were calculated from the mass flow rate of methane gas, assuming complete combustion.

Figure 3 shows L/D as a function of N . The circles represent cases at laboratory temperature and the squares cases at elevated and reduced temperatures. The results at the elevated and reduced temperatures agree very well with their laboratory temperature counterparts at approximately the same values of N , confirming the efficacy of the parameter N . The flame height data are positioned slightly higher than the dashed curve, which is the correlation in Eq. (7).

For comparison, L/D is shown as a function of $(Q_D^*)^2$ in Figure 4. Cases at laboratory, elevated, and reduced temperatures at $(Q_D^*)^2$ near 9.5 clearly lack consistency. The dashed curve represents Eq. (9).

5. CONCLUSION

Flame height measurements at laboratory temperature and approximately 45K higher and lower temperatures have supported the use of the parameter N (Eq. (6)) as a scaling parameter. The parameter Q_D^* (Eq. (4)) does not appear to be a suitable scaling parameter for the flaming region. In practice, the distinction is important mainly when atmospheric conditions differ significantly from standard.

REFERENCES

1. Zukoski, E.E., "Convective Flows Associated with Room Fires," Semiannual Progress Report to National Science Foundation, California Institute of Technology, June 1975.
2. Heskestad, G., "Peak Gas Velocities and Flame Heights of Buoyancy-Controlled Turbulent Diffusion Flames," Eighteenth Symposium (International) on Combustion, The Combustion Institute, Pittsburgh, PA, 1981, 951-960.
3. Zukoski, E.E., Kubota, T. and Cetegen, B., "Entrainment in Fire Plumes," Fire Safety J., Vol 3 (1980/81), 107-121.
4. Cox, G. and Chitty, R., "Some Source-Dependent Effects of Unbounded Fires," Combustion and Flame, Vol 60 (1985), 219-232.
5. Hasemi, Y. and Nishihata, M., "Deterministic Properties of Turbulent Diffusion Flames from Low Q^* Fires," Fire Science and Technology, Vol 7 (1987), 27-34.
6. McCaffrey, B., "Flame Height," in SFPE Handbook of Fire Protection Engineering (ed. P.J. DiNenno), Second Edition, NFPA and SFPE, 1995, 2-1 - 2-8.
7. Zukoski, E.E., "Mass Flux in Fire Plumes," Fire Safety Science - Proceedings of the Fourth International Symposium, 1994, 137-147.
8. Ricou, F.P. and Spalding, D.B., "Measurements of Entrainment by Axisymmetrical Turbulent Jets," J. Fluid Mechanics, Vol 11 (1961), 21-32.
9. Heskestad, G., "Luminous Heights of Turbulent Diffusion Flames," Fire Safety J., Vol 5 (1983), 103-108.
10. Heskestad, G., "A Reduced-Scale Mass Fire Experiment," Combustion and Flame, Vol 83 (1991), 293-301.

11. Ackeret, J., "Aspects of Internal Flow," in Fluid Mechanics of Internal Flow (ed. G. Sovran), Elsevier Publishing Company, New York, 1967.

12. Zukoski, E.E., Kubota, T. and Cetegen, B., "Entrainment in the Near Field of Fire Plumes," California Institute of Technology, August 1981.

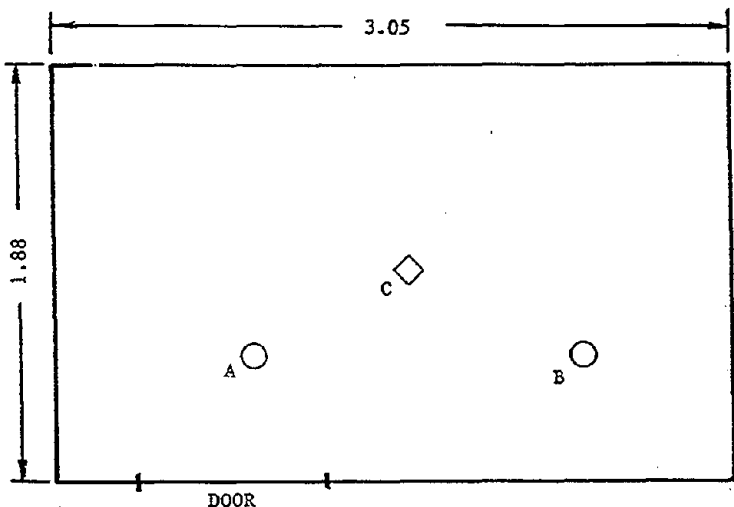


Figure 1 Environmental chamber with locations of burner (A and B) and vertical thermocouple traverse (C) drawn to scale. Interior dimensions in m (chamber height was 2.39 m).

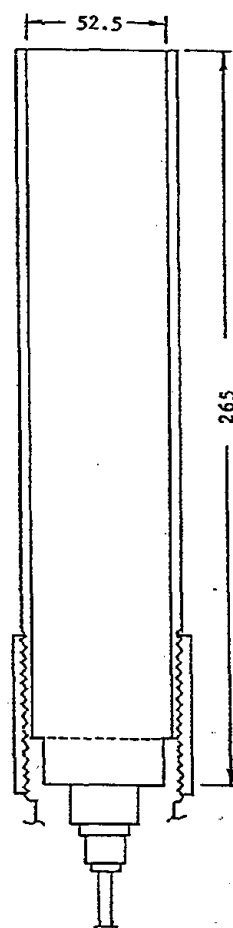


Figure 2 Burner. Methane gas entered at bottom. Dashed horizontal line represents a wire-mesh screen. Dimensions in mm.

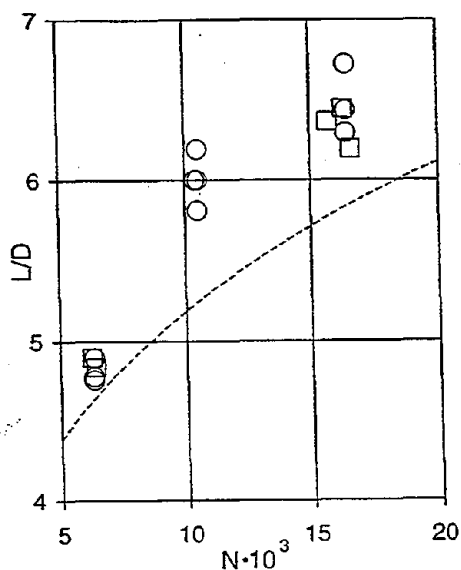


Figure 3 Dimensionless flame height as a function of N . Circular symbols correspond to laboratory temperatures; squares correspond to elevated and reduced temperatures. Dashed curve represents Eq. (7).

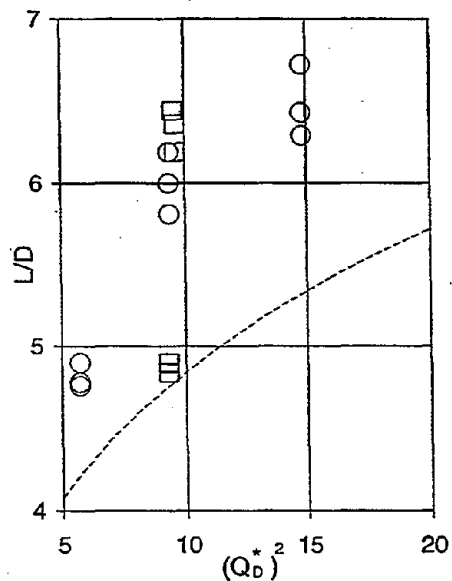


Figure 4 Data in Figure 3 plotted as a function of Q_D^* . Dashed curve represents Eq. (9).

Discussion

Henri Mitler: This morning, Yuji Hasemi pointed out that certain correlations could be improved by taking a mixed set of distances instead of having just D or flame height or whatever. He chose a mixture and tightened up his correlations. I wonder if in the light of what you just described, it might not be worthwhile to revisit the entire thing. Possibly one could reduce the scatter of data still more by very judicious selection of parameters like that.

Gunnar Heskestad: In certain cases in fire dynamics like this one which are very well-defined, we often forget that there are still variations from one case to another. In fluid mechanics, we speak of dynamic similarities. It's required that you have geometric similarity. That's something we have to keep in mind. The second part of my answer is that we should bear that in mind when we look at scatter. It could be departures from geometric similarity.

Edward Zukoski: Is H over R the heating value per kilogram of air?

Gunnar Heskestad: Correct.

Edward Zukoski: Because we've changed the heating value of the fuel by a factor of about 10 by adding nitrogen to it. If I have a constant methane flow and I add 4 moles of nitrogen to the fuel, do you change N ?

Gunnar Heskestad: No. You change these the same way.

Edward Zukoski: Okay. So we have done that and it didn't change Q^* either.

Gunnar Heskestad: Correct.

Edward Zukoski: We also burned 60 kW fires inside a hood, the flame was up in the hood, and the temperatures went from 30 degrees to 150 degrees as the oxygen mass fraction went down and we saw only about a 5% variation in the flame height.

Gunnar Heskestad: That is a more complicated case and I should say that our experiment is probably a little better controlled so, for now, I will stay with that but it is an interesting test case.

Howard Baum: I am intrigued by your fuel parameter there. If I had something like an oxygenated fuel or anything that was sort of carrying along its own oxidizer supply to a certain extent, would that change that parameter?

Gunnar Heskestad: No.

James Quintiere: It would seem to me that the term with the temperature and the heat of combustion comes from the fact that you're burning the air that is entrained. And so realizing that H_C over R is constant, the temperature variation seems to confirm that mechanism. Would you see it the same way?

Discussion cont.

Gunnar Heskestad: I think mainly it's the effect of the entrainment rate.

Howard Baum: One other possible test of this, would it be to look at Archie Tewarson's data where he like to change the oxygen concentration.

Gunnar Heskestad: That type of experiment can be done and I have done it. I submitted a paper to the Combustion Symposium which may or may not be accepted but it includes that.

Richard Gann: Isn't H_c/R nominally the oxygen consumption constant that appears in oxygen consumption calculations?

Gunnar Heskestad: Correct.

Richard Gann: Certainly, there is a temperature effect on H_c .

Gunnar Heskestad: In principal.

Richard Gann: It's real because you start with all the species at a higher temperature and therefore, you don't have to warm them quite as much.

Gunnar Heskestad: We have ignored that.

Richard Gann: Anthony Hamins ran some experiments with various fire suppressants in which he varied the temperature of the system and the effectiveness of the suppressants not only changed but the rate of change curves crossed, indicating that there is certainly some change in the suppression chemistry, but entirely possible that there is also some changes in the relative rates of the combustion chemistry as well.

Gunnar Heskestad: It is an interesting comment and I will consider that.

Takashi Kashiwagi: How about changing the amount of gas, not nitrogen/oxygen but helium/oxygen or halogen/oxygen? Might there be a difference between Q^* and N ?

Gunnar Heskestad: In the paper I mentioned that we changed the oxygen in the environment by introducing nitrogen and we found that would change N , and the flame height should have increased. There was less increase in flame height than we had predicted and there is a discussion in the paper of why that was.

Anthony Hamins: Could you kindly comment on combustion efficiency effects on N ?

Gunnar Heskestad: In these experiments the combustion efficiency probably did not vary a great deal because the flame temperatures were very similar in all cases.

Discussion cont.

Anthony Hamins: We've made measurements with propane, acetylene, and a number of other gaseous fuels. Looking at flame height and looking at the correlations, we had problems fitting the correlations to our data for the very sooty fuels. Can you comment on those findings?

Gunnar Heskestad: The combustion efficiency may effect this ratio. That isn't too well-understood, but I think from Huggett's study, probably that was not a factor. In the paper I referred to, we explained the absence of a significant effect of the ambient oxygen concentration in terms of a parameter. We had to leave it for simplicity. The parameter is question is the convective fraction of the total heat release rate. The originally derived parameter was N divided by that fraction.

Takeyoshi Tanaka: I think that the temperature effect on H_c is very small. I am not an expert in this area, but the value M has to do with entrainment. However, I think the mass of the oxygen in the air would not change, so if the temperature of the air goes down, then oxygen increases and I think that probably effects the flame and that is my thinking. Looking at the data you showed us, the difference is not all that great.

Gunnar Heskestad: In answer to that question, I just wish to say that parameter N was derived through a set of assumptions which have been discussed quite thoroughly in the original paper in 1980.

Zukoski's Intellectual Progeny

Patrick J. Pagni
Mechanical Engineering Department
University of California
Berkeley, CA 94720-1740

Abstract

Professor Zukoski's technical influence, generosity and inspiration to a series of fire safety engineering science doctoral candidates from the University of California at Berkeley are chronicled. Two of his areas of expertise are emphasized: gravity currents and pool fire plumes. It is concluded that he has had an unusually significant impact as a nurturing scientist.

Introduction

In the normal course, scientists transmit their expertise to students and faculty at their home institution with outside communications occurring largely in the archival literature. But some few scientists are nurturers, who extend their sphere of influence to an entire field, informally offering encouragement, insight and accrued wisdom to a wide variety of colleagues.

Fire research has been fortunate to have several of the latter: Kunio Kawagoe, Philip Thomas, Howard Emmons, Howard Baum, and especially for those of us in California, Edward E. Zukoski. Others at this symposium will note Professor Zukoski's contributions at Cal Tech. I would like to highlight his influence on fire research at Berkeley, as the example with which I am most familiar, of his broader impact. There is room here to describe only two of his areas of expertise: gravity currents¹ and pool fire plumes².

Gravity Currents

In his definitive article³ on gravity currents, T. B. Benjamin credits "An excellent set of experimental results...by Zukoski¹" for his theoretical interest in the topic. My daughter, Christina Pagni, visited Professor Zukoski when she attended the 1989 California State Science Fair in Los Angeles. As a result of that encounter, she developed a report, "Gravity Current Velocities," which won the Grand Prize at the 1990 California State Fair for the best Earth and Space Science Project, Junior Division. Ed has the technical generosity, ability, honesty and enthusiasm to inspire us all.

When Dr. Charles Fleischmann began his seminal set of experiments on backdrafts^{4,5,6}, one of the first things we did was visit Cal Tech. In response to our complaint that an hydrocarbon meter in the appropriate range wasn't available, Zukoski suggested a small vertical pipe in the chamber ceiling with a spark at the top. If a flame existed there, the compartment hydrocarbon concentration exceeded the lean flammability limit. We called it the "Zukoski Meter." In addition he guided our efforts at salt water modeling⁷ of the gravity currents which play such a crucial role in backdraft phenomena⁸. These salt water experiments, Fig. 1 shows an example along with an example of the corresponding gas phase backdraft experiment, allow calculation, from Table I, of the speed and size of the gravity currents that always precede backdrafts. We continue to encounter practical examples of gravity currents in real fires².

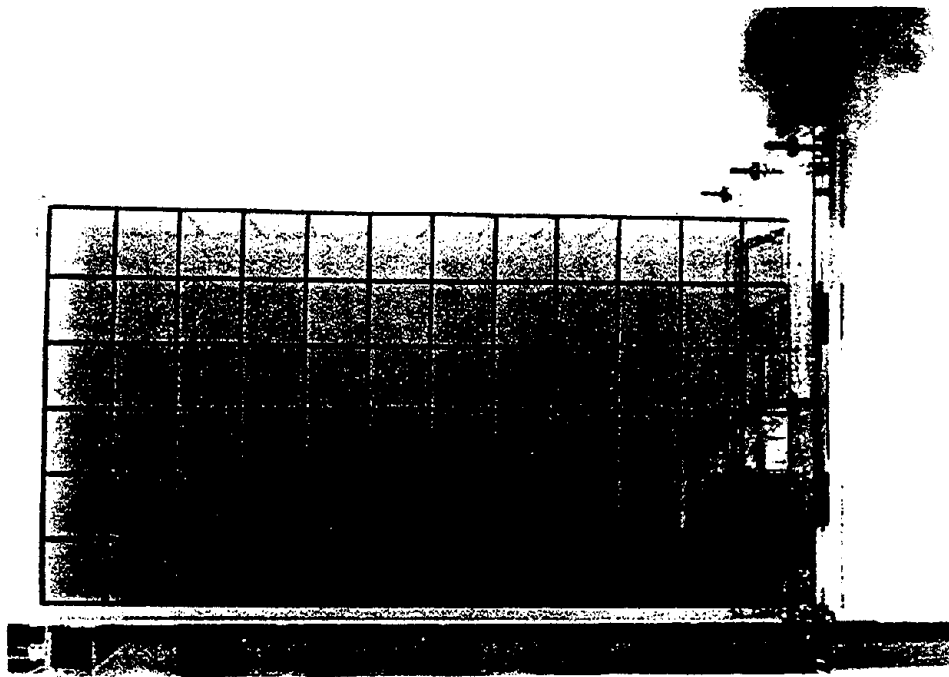


Figure 1a - Photograph of the salt water model showing the entering gravity current. $\beta=0.080$ opening was the $h_1/3$ horizontal slot - 2.4 s after opening.

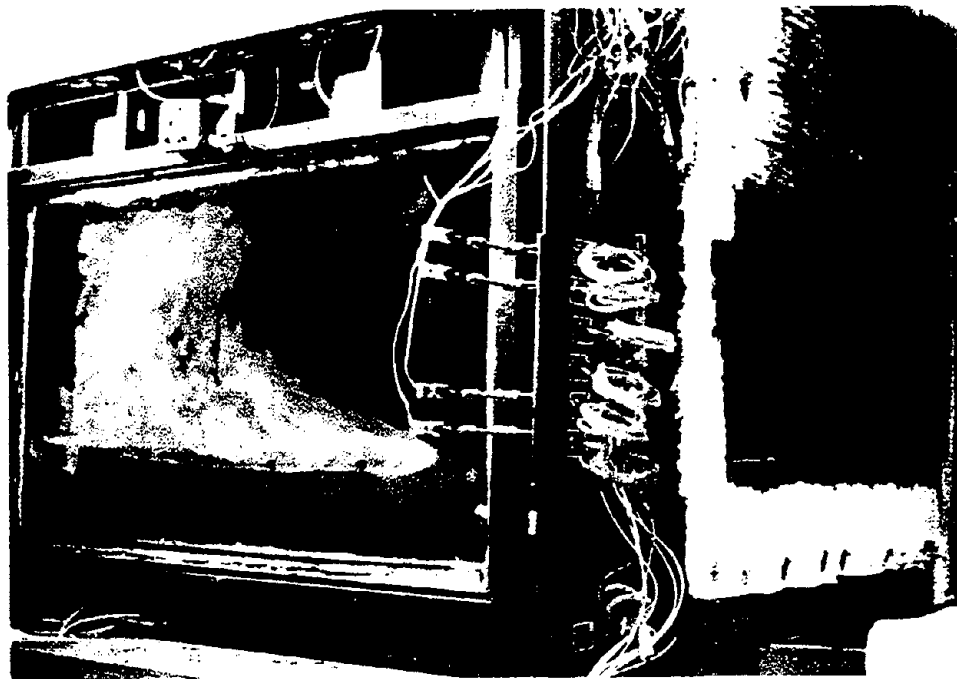


Figure 1b - Photograph of the flame propagation along the top of the entering gravity current. The ignition spark is turned when the compartment is opened. Compartment is 1.2 m wide by 2.4 m long by 1.2 m high and the opening is 1.1 m wide by 0.4 m high.

Table I. Gravity current velocities and heights in fire compartments with $\beta = (\rho_0 - \rho_1)/\rho_1$, where 0 is ambient and 1 is the uniformly hot compartment.

	Fully Open Wall	1/3 Height Horizontal Slot	1/3 Height Centered Window	1/3 Width 4/5 Height Door
Velocity $v^* \equiv v/(\beta gh_1)^{1/2}$	0.44	0.32	0.35	0.22
Height $h^* \equiv h/h_1$	0.50	0.38	0.33	0.29

Pool Fire Plumes

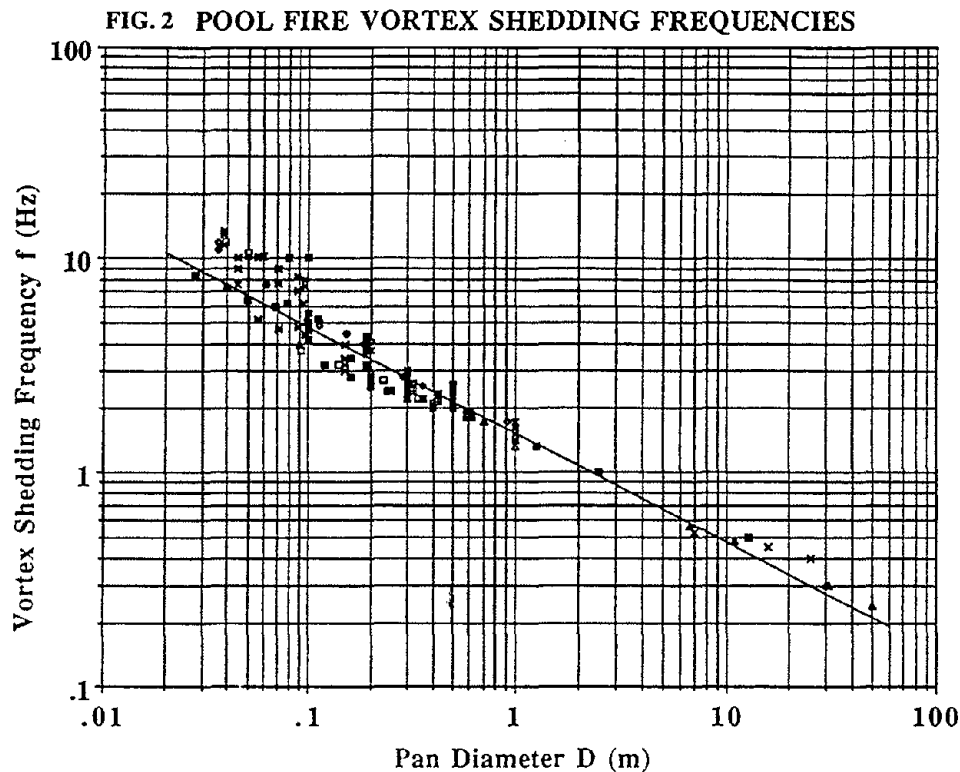
At Berkeley I have a reputation as being a fanatic about nondimensionalization, but when in 1990 I first published⁹ the fit

$$f = 1.5 D^{-0.5} \quad (1)$$

with f in Hz and D in m to the pool fire toroidal vortex shedding frequency shown in Fig. 2, it was Zukoski who told me I had it wrong. It should be dimensionless, as $f(D/g)^{1/2} = 0.48$. He was right of course. As far as I have been able to determine this buoyant Strouhal number does not have a name of its own. May I formally propose that we call $f(D/g)^{1/2}$ the "Zukoski Number."

$$Zu \equiv f(D/g)^{1/2} \approx 0.5 \quad (2)$$

then gives the pool fire vortex shedding frequency. The solid rectangles at $D = 0.1, 0.19$ and 0.5 m in Fig. 2 are data from Zukoski et al.'s¹⁰ elegant paper on buoyant diffusion flame structure. $2C_2$ should replace C_2 in Eq. (3) of Ref. 10¹¹.



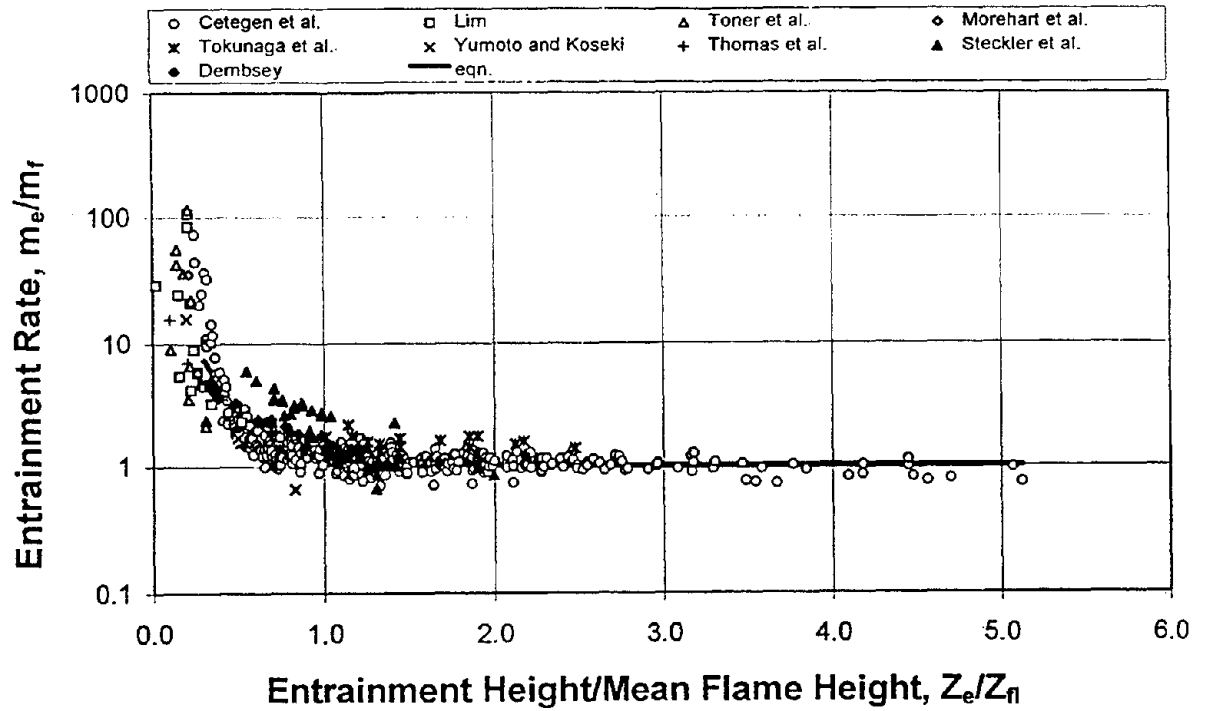


Fig. 3a Compiled entrainment mass flow rate data and curve fit. Entrainment rate normalized by far field model and entrainment height normalized by mean flame height.

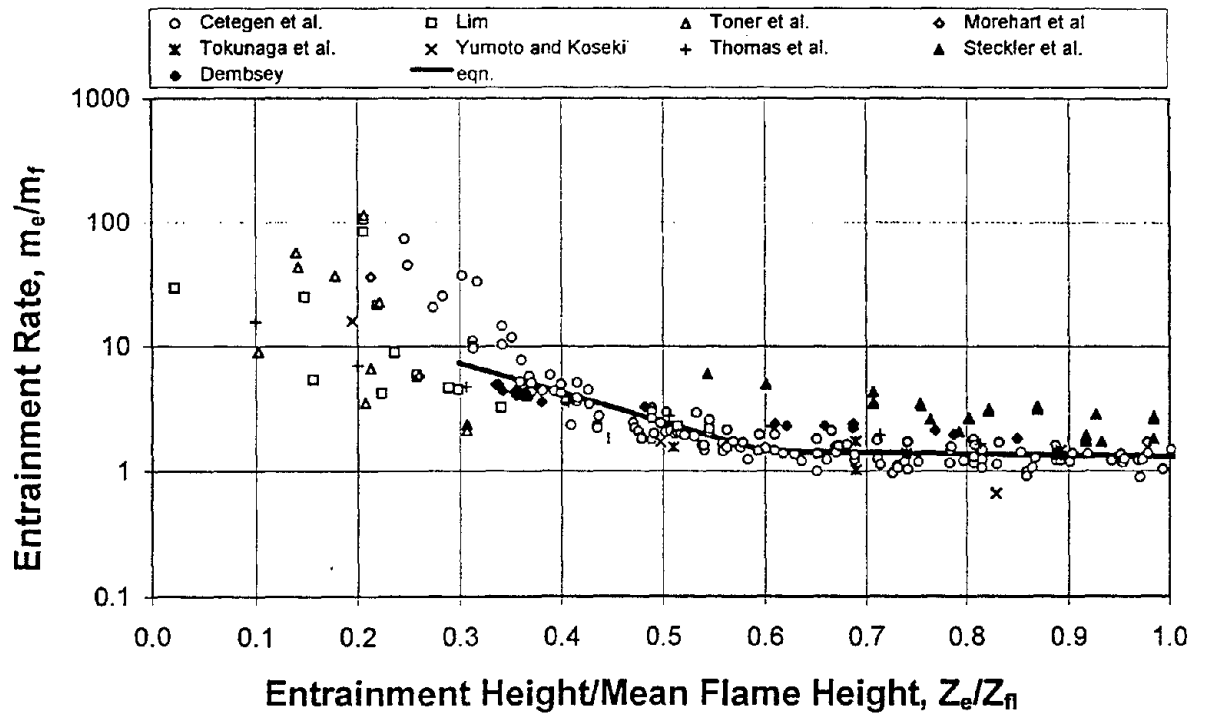


Fig. 3b Compiled entrainment mass flow rate data and curve fit, abscissa 0.0-1.0. Entrainment rate normalized by far field model and entrainment height normalized by mean flame height.

Professor Zukoski has long been recognized as the leader in measurements of the mass entrainment rate in pool fires with application to compartment fires¹²⁻¹⁶. This rate is important to compartment fire modeling since it is the entrainment by the fire plume that acts as a pump carrying fresh oxygen into the flame and products into the hot upper layer. He has repeatedly called for entrainment data from large fires in small compartments. Partly in response to his urging, Professor Nicholas Dembsey began such experiments in an especially constructed compartment near the Berkeley campus¹⁷. Mass entrainment data were obtained for fire heat release rates up to 1 MW in a 2.5 m × 3.7 m × 2.5 m high compartment. The data were normalized on the Zukoski mass entrainment expression¹² for an offset point source plume as shown in Figs. 3a and 3b.

$$m_f = 0.21 \rho_\infty g^{1/2} z_v^{5/2} Q_z^{*1/3} \quad (3)$$

where m_f is the offset far field mass entrainment rate, $z_v = z_e + z_0$, $z_0 = 0.8D - 0.33 z_{fl}$, $Q^* = Q/(\rho c T g^{1/2} z^{5/2})$ with z_e the entrainment height above the burner surface which was here at 0.6 m above the floor, z_0 is the offset Zukoski introduced to apply the far field plume to pool fires¹⁸, D is the pool diameter and z_{fl} is the mean (50% intermittancy) flame height. $z_{fl}/D = 3.3 Q_D^{*2/5}$. Dembsey's data suggest that the Zukoski offset plume can be applied, with slight modification, to even large fires in small compartments where the entrainment (layer interface) height is less than the flame height. The modification is to increase m_f , given by Eq. (3), by a factor of β , i.e., $m = \beta m_f$ where β is the following function of the ratio z_e/z_{fl} :

z_e/z_{fl}	β
≥ 2	1
0.6-2	$\exp(0.26(2 - z_e/z_{fl}))$
0.3-0.6	$1.4 \exp(5.4(0.6 - z_e/z_{fl}))$

As seen in Fig. 3, for the entrainment height in the bottom third of the flame height, the data are too scattered to fit. Zukoski is currently developing improved models^{2,16,17} based on Thomas et al.¹⁹ and Morton et al.²⁰ for entrainment in the combustion zone at the base of the flame.

Finally, as we continue to increase the scale of the fires to which Zukoski's models are applicable, we come to the 20 October 1991 Oakland Hills Fire²¹. Dr. Javier Trelles, has used the Baum and McCaffrey²² mass fire model to calculate the fire induced winds²³ in this fire. We estimate that the steady portion of the heat release rate curve from a single family U.S. dwelling would be approximately 50 MW. Applying the Zukoski offset far field model to a burning structure follows the pioneering work of Yokoi²⁴. The centerline plume profiles are shown in Fig. 4²³. Comparisons with the Baum and McCaffrey plume show good agreement above the flame tip. The centerline velocity is

$$U_{cl}(z) = 3.9(gz)^{1/2} Q_z^{*1/3} ; \quad (4)$$

while the centerline temperature is

$$(T_{cl}(z) - T_\infty)/T_\infty = 9.1 Q_z^{*2/3} \quad (5)$$

The plume radius is $r(z) = 0.13z$ where z in these equations is the altitude above ground level plus an offset Δz given by

$$\Delta z/D = 1.02 - 1.36 Q_D^{*0.4} \quad (6)$$

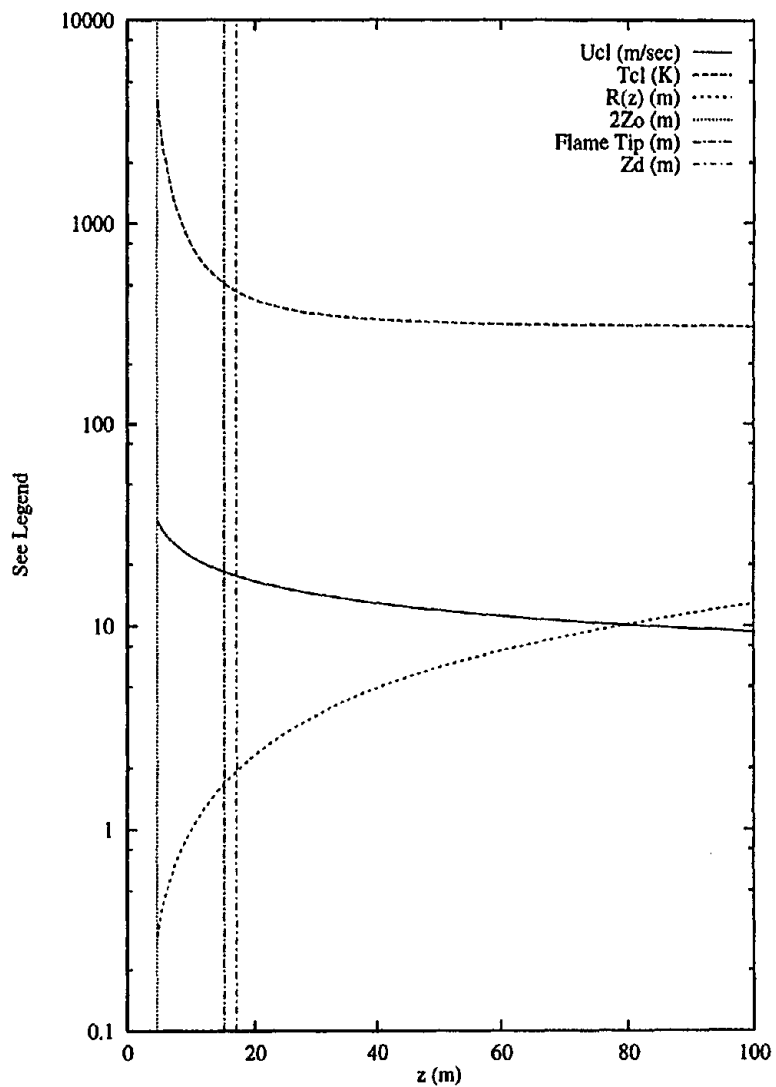


Fig. 4 Profiles for the Zukoski plume applied to a 50 MW house fire are plotted versus z using log-linear scaling. The solid line is for the center-line vertical velocity, U_{cl} , the long-dashed line is for the center-line temperature, T_{cl} , and the short dashed line is for the plume radius, $R(z)$. The virtual origin is located $Z_0 \approx |\Delta z| = 2.3$ m above ground level. Profiles are started at $2|\Delta z|$ above ground level in order to avoid unphysically high values near the origin.

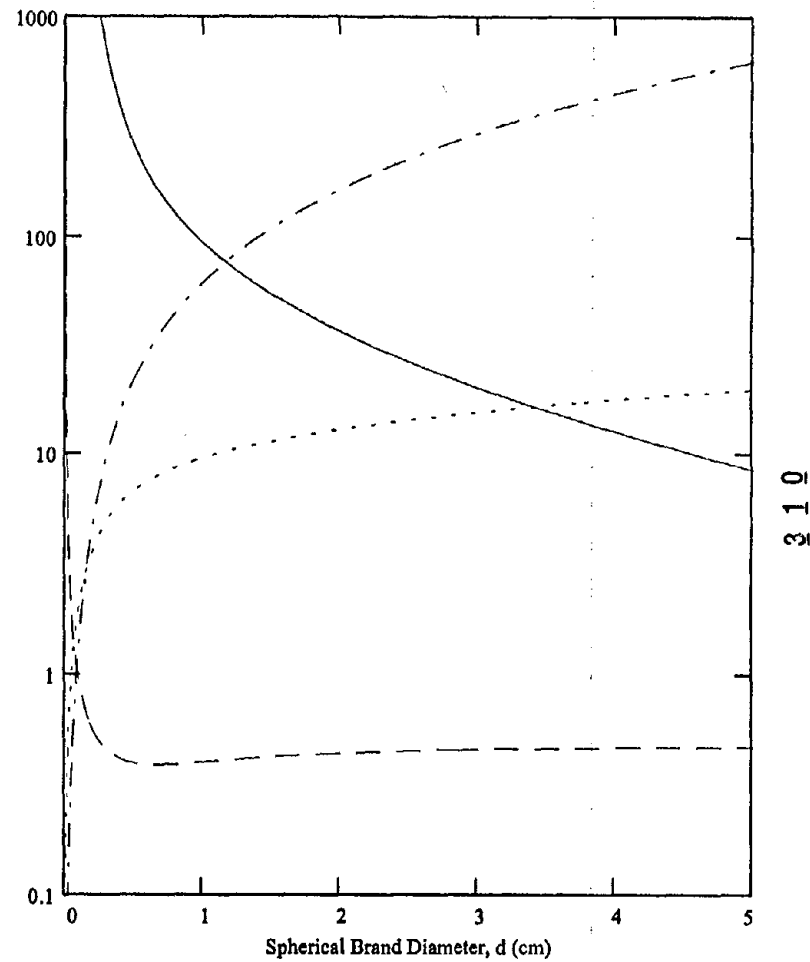


Fig. 5 Lofting of spherical brands on the centerline of a Zukoski plume — Maximum brand altitude, m; ··· Brand terminal velocity, m/s; - · - · Reynolds number, $Re/100$; - - - Drag coefficient, C_D .

For the offset we've used a dimensionless form of Heskestad's mean fit²⁵ to the offset data of Zukoski, Hasemi, McCaffrey and Kung. $\Delta z > 0$ implies a plume origin below ground level while $\Delta z < 0$ ($Q_D^* \geq 0.5$) gives a plume origin in the flame. Here, $Q = 50$ MW with $D \approx 4$ m to agree with Baum and McCaffrey, gives $Q_D^* = 1.5$ and the offset is $\Delta z = -2.3$ m.

As a final application of Zukoski's ideas by students at Berkeley, consider Fig. 5. Here my current NIST supported student, John Woycheese, has improved Tarifa's²⁶ work on brand lofting by replacing the constant vertical velocity Tarifa used with the Zukoski plume centerline velocity. The question addressed in Fig. 5 is how high spherical wooden brands will be lofted by the velocity field shown in Fig. 4. Using standard definitions, e.g., $C_D \equiv F_D/0.5 \rho U^2 A$, a C_D (Re) from Haider and Levenspiel²⁷, and allowing the brand to rise until the local plume centerline velocity equals its terminal velocity, produces the maximum altitude plot shown in Fig. 5. The properties of Tarifa's lightest wood, pine, are used here. The next step is to calculate the time each brand requires to reach the altitude shown. Comparing that time to the brand's burn-up time will eliminate the smallest brand diameters. The result will be a most probable lofted brand diameter, which we expect to be on the order of a few centimeters.

Conclusions

On one of my pilgrimages to Cal Tech, we were discussing fires after earthquakes and I asked Professor Zukoski what would happen if the Santa Ana winds were blowing when the big one struck California. He said, "That's no problem — we'd all die." There is wisdom in knowing the limits to technology.

When Professor Cetegen first suggested this symposium, I began thinking about Professor Zukoski's contributions to Berkeley's efforts in fire research and realized that no student of mine in the last twenty years has escaped his beneficial influence. I suspect most of us here could come to the same conclusion.

Acknowledgments

All of the work described in this paper was partially supported by USDOC-NIST-BFRL grants. The current grant no. is 60NANB3D1438.

References

1. E. E. Zukoski, "Influence of viscosity, surface tension and inclination angle on motion of long bubbles in closed tubes," *J. Fluid Mech.*, 25:4, 821-837, 1966.
2. E. E. Zukoski, "Properties of Fire Plumes," in *Combustion Fundamentals of Fire*, G. Cox ed., Academic Press, London, 1995, pp. 101-220.
3. T. B. Benjamin, "Gravity currents and related phenomena," *J. Fluid Mech.*, 31:2, 209-248, 1968.
4. C. M. Fleischmann, P. J. Pagni and R. B. Williamson, "Exploratory Backdraft Experiments," *Fire Technology*, 29:4, 298-316, 1993.
5. C. M. Fleischmann, P. J. Pagni and R. B. Williamson, "Quantitative Backdraft Experiments," in *Fire Safety Science — Proc. of the Fourth Intl. Symp.*, pp. 337-348, IAFSS, Boston (1994).
6. C. M. Fleischmann, P. J. Pagni and R. B. Williamson, "Backdraft Experiments Using a Simulated Window Opening," submitted to *Fire Safety J.*
7. M. V. Chobotov, E. E. Zukoski and T. Kubota, "Gravity Currents with Heat Transfer," NBS-GCR-87-522, N.I.S.T., Gaithersburg, MD, 1987.
8. C. M. Fleischmann, P. J. Pagni and R. B. Williamson, "Salt Water Modeling of Compartment Gravity Currents," *Fire Safety Science — Proc. of the Fourth Intl. Symp.*, pp. 253-264, IAFSS, Boston (1994).

9. P. J. Pagni, "Pool Fire Vortex Shedding Frequencies" in *Some Unanswered Questions in Fluid Mechanics*, L. M. Trefethan and R. L. Panton, eds., *Applied Mechanics Reviews*, 43:8, 166-167, 1990.
10. E. E. Zukoski, B. M. Cetegen and T. Kubota, "Visible Structure of Buoyant Diffusion Flames," *20th Int'l. Symp. on Comb.*, 361-366, The Combustion Institute, Pitts., PA (1984).
11. E. E. Zukoski, private communication.
12. B. M. Cetegen, E. E. Zukoski and T. Kubota, "Entrainment in the Near and Far Field of Plumes," *Combust. Sci. and Tech.*, 39, 305-331, 1984.
13. S. J. Toner, E. E. Zukoski and T. Kubota, "Entrainment, Chemistry and Structure of Fire Plumes," California Institute of Technology, Pasadena, CA, NIST Grant No. 60NANB6D0638, 1986.
14. J. H. Morehart, E. E. Zukoski and T. Kubota, "Species Produced in Fires Burning in Two-Layered and Homogeneous Vitiated Environments," California Institute of Technology, Pasadena, CA, NIST Grant No. 60NANB6D0638, 1990.
15. C. S. Lim, "I. Mixing in Doorway Flows, II. Entrainment in Fire Plumes," Engineer's Degree Thesis, California Institute of Technology, Pasadena, CA, 1984.
16. E. E. Zukoski, "Mass Flux in Fire Plumes," *Fire Safety Science — Proc. of the Fourth Intl. Symp.*, pp. 137-147, IAFSS, Boston (1994).
17. N. A. Dembsey, P. J. Pagni and R. B. Williamson, "Compartment Fire Near-Field Entrainment Measurements," *Fire Safety J.* 24:4, 383-419, 1995.
18. E. E. Zukoski, "Fluid Dynamic Aspects of Room Fires," in *Fire Safety Science — Proc. of the First Intl. Symp.*, pp. 1-30, Hemisphere, NY (1986).
19. P. Thomas, P. Hinkley, L. Theobald and D. Simms, "Investigation into the flow of gases in roof venting," BRE-FRS Tech. Papers 7 and 10, HMSO, London, 1963.
20. B. R. Morton, G. I. Taylor and J. S. Turner, "Turbulent gravitation convection from maintained and instantaneous sources," *Proc. Royal Soc.*, A234, 1-23, 1956.
21. P. J. Pagni, "Causes of the 20 October 1991 Oakland Hills Conflagration," *Fire Safety J.*, 21:4, 331-340, 1993.
22. H. R. Baum and B. J. McCaffrey, "Fire Induced Flow Field — Theory and Experiment," in *Fire Safety Science — Proc. of the Second Intl. Symp.*, pp. 129-148, Hemisphere, NY (1989).
23. J. Trelles, "Mass Fire Modeling of the 20 October 1991 Oakland Hills Fire," doctoral dissertation, Mech. Engr. Dept., Univ. of Calif., Berkeley, CA, 1995.
24. S. Yokoi, "Upward Convection Current from a Burning Wooden House," *Fire Research Abs. and Rev.* 2:1, 22-27, 1960.
25. G. Heskestad, "Fire Plumes" in *The SFPE Handbook of Fire Protection Engineering*, 2nd ed., P. J. DiNenno et al. eds., NFPA, Quincy, MA, 1995, pp. 2-9 to 2-19, Eq. (25).
26. C. S. Tarifa, P. P. Del Notario and F. G. Moreno, "On the flight paths and lifetimes of burning particles of wood," *Tenth Intl. Symp. on Comb.*, pp. 1020-1037, The Combustion Institute, Pitts., PA (1965).
27. A. Haider and O. Levenspiel, "Drag Coefficient and Terminal Velocity of Spherical and Nonspherical Particles," *Powder Tech.*, 58, 63-70, 1989.

Discussion

Walter Jones: You did some fairly extensive work on the Oakland Hills fire. The question is have the people there learned anything about how to build houses that are more fire safe now and have they followed the advise?

Patrick Pagni: I think the answer here is that the fire departments in our area have learned a lot. One of the problems in the early stages of the Oakland fire was that the military nature of the fire departments prohibited their interaction in an effective way. Now, all three fire departments that were in the area involved that day, Oakland, Berkeley, and the East Bay, hold regular training sessions together. What has happened is there is now a new fire station here on land that was donated by the East Bay region, built with Berkeley money, and staffed by the Oakland fire department. The people, I think, also have learned something. Most of the houses that are rebuilt have the style of roofs that we enjoy seeing so much in Japan, which I think are called fire safety roofing.

Takeyoshi Tanaka: I tried to do an experiment with brands, but so far, it has not been successful. With respect to the drag coefficient, sometimes the moving object is the moving fluid. However, in the case of brands, the object is actually flying and tumbling and that's probably the reason the drag coefficient is different.

Patrick Pagni: That's exactly right. That's why we started with spheres where that effect is not important. However, there are some excellent articles that talk about that function of Reynold's number in different regimes. A very low Reynolds number would come down in a position of maximum drag. As the Reynolds number increases, it tends to sort of feather on the way down. As the Reynolds number increases even further, it tumbles. And we hope to do some more of these experiments.

Takeyoshi Tanaka: Actually, we suspended various different objects from a load cell and tried to measure how much such an object would be lifted by flames. However, this experiment did not succeed because the noise was too high. Next, we flowed air in the tube, dropped objects in it, and then looked at whether it drops or it comes out and then determine the threshold. However, this did not provide us with good data because the of the effect from the tube wall. From the data we got from this experiment, it looked to me that the drag coefficient was smaller that the one shown in the literature.

Patrick Pagni: I think we have just found our first joint project for the next meeting.

Edward Zukoski: I'd like to make one comment. If you look at the way that rivers carry dirt and move it around, once the particles get off the bottom, you can handle it easily. The main problem is how they get off the bottom. How do you get the brand up in the air to start with? And that may come about when the house falls in on itself or the roof collapses or something like that where there is some violent action going on and that may be harder to model.

Gunnar Heskestad: We will use the same approach that Baum initiated in particles when they just zapped them into a plume or something.

KAWAGOE MEMORIAM

Opening Address—Kawagoe Memorial Symposium

Yoshio Mimura

Director General, Building Research Institute, Ministry of Construction, Japan

Ladies and Gentlemen :

At the beginning of Kawagoe Memorial Symposium, I would like to make a few remarks. It is especially meaningful to hold a session commemorating the late Dr. Kawagoe, who passed away in 1994, at the occasion of this 13th meeting of the UJNR Panel on Fire Research and Safety under the collaboration of US and Japanese fire research experts.

As you know, Dr. Kawagoe devoted his life to research and international cooperation in fire and building technology. On behalf of the Japanese delegates to this UJNR meeting, it is my pleasure to introduce briefly Dr. Kawagoe's achievements in building research especially in fire research and his energetic international cooperative work.

Dr. Kawagoe started his research career at Building Research Institute, Ministry of Construction, in 1946 at the time of its establishment. He served BRI's Director General from 1969 to 1973, and accepted professorship at the Science University of Tokyo in 1973. Throughout his life, Dr. Kawagoe promoted various activities for research, education and administration in building technology, but the fire research can be said as one of his most representative and outstanding achievements.

As time is limited, it is not possible to introduce all his accomplishment. However, his work can not be satisfactorily introduced without talking about his research on post-flashover fires in fire resistive buildings. This research was started during the early days of his research life and BRI itself. Through this research, he pioneered the development of scientific prediction methods for fire phenomena, and clarified that such buildings can have some unique fire problems different from those common for wooden buildings with which Japanese fire experts already had been familiar before the world war.

He also promoted research on smoke movement, modeling of preflashover compartment fires and risk analysis even since most of researchers or administrators were not yet aware of the importance of these subjects for fire safety. In all areas his research was successful. Some fields of fire research in which Japanese fire experts are now working actively are highly evaluated in the world, but it is not too much to say that most of these were pioneered by Dr. Kawagoe's early works.

Dr. Kawagoe especially insisted on the necessity of establishing an engineering system for fire safety design and he himself led the Ministry of Construction's project to develop comprehensive fire safety design methods for buildings in 1980's. This is now considered as the basis for the performance-based fire safety design of buildings in Japan. Result of this project is now widely applied for ensuring safety of building designs for cases when special certification is required due to the Article 38 of the Building Standards Law (and has also been introduced to the foreign countries as well.)

Besides these research activities, Dr. Kawagoe was also involved actively in international cooperative projects such as CIB, ISO and UJNR from their early stages. He was active and offered Japanese leadership in the establishment of International Association for Fire Safety Society (IAFSS) and served as its Vice President for 6 years from its establishment in 1985. At the Second

International Symposium on Fire Safety Science held in Tokyo in 1988, the first international symposium on fire safety science after the establishment of IAFSS, he was awarded the Emmons Lectureship, the highest honor of the IAFSS, and in 1994, the Kawagoe Prize was established by IAFSS to honor life-time contribution of international fire experts to fire safety science and practice. These certainly tell us about his highly admired personality as well as his excellent achievements.

He always gave kind advice to his young colleague and students, and encouraged them to enrich themselves through research and enjoy their research. He was very pleased to back up them. I myself was given his precious advice in many ways. He often sent me valuable foreign documents, and I learnt much about research in my own field from such documents. Dr. Kawagoe was really a challenging researcher. As a former Director-General of BRI, a governmental institute, he often pointed out and was anxious about conflict between the demands of governmental policy and pure research. He himself often offered positive and stimulating suggestions for the future of BRI.

We have followed his trail in fire research based on his achievement in research as well as with help of international cooperation. We wish all involved in fire research to understand his work and his wish to enhance fire safety with hand in hand. Thank you very much.

Memory of Professor Kawagoe

Jack E. Snell

Professor Kawagoe was a very special man in the field of fire safety. He was a gentle giant, a pioneer, and a wonderful inspiration and friend to many around the world. On a personal note, I miss him. I sense we all do. He would have had fun with us at the reception in my home, and Friday celebrating and honoring the work of Ed Zukoski, and Saturday on the bus tour. He had a delightful sense of humor and brightened any group with his presence.

I had the privilege and pleasure to be with this remarkable man on a number of occasions, in particular the meetings of the UJNR Panel on Fire Research and Safety, from 1982 to the last Japan meeting of this panel in 1992 at the mini-symposium in Nasu where this photo was taken. I also was with him in Avila, Spain, at the first international meeting of fire research and test centres; and at 1st and 3rd IAFSS meetings - here and in Edinburgh - and at Interflam.

When I came to fire research in 1982, Kawagoe had already completed his tours as Director General of BRI and as a member of the Board of CIB. (He remained active in CIB W14 for some 40 years.)

Over the years, there have been close parallels between Kawagoe's work and our research here at NIST - response of steel structures to fire, smoke strata in room fires, burning behavior of mattresses and upholstered furniture, and, of course, mathematical fire modeling. In FRIS, the NIST Fire Research Information Service, we have some 37 English language papers authored by Kawagoe, 16 of which he is lead or sole author.

In the early 1980's, inhalation toxicity of the products of combustion was a matter of wide concern in a number of countries. Work was underway to develop a small scale test method to address this issue. NIST and Japan used similar furnaces for smoke generation. NIST used rats and Japan mice for the smoke exposures. In Europe, work centered around the DIN method, based on a tube furnace and analytical testing of combustion products. Kawagoe approached us with his concerns about this DIN method, which was not based on an established relationship to real fire exposures, becoming accepted as the basis for international standardization. As a result, Fumiharu Saito came to the U.S. and we formed a tripartite - Japan-USA-Canada - research program on smoke toxicity to provide definitive data and hopefully an alternative to the DIN method. That strategy paid off. Just now, about a dozen years later, a method based on that research is moving towards ISO acceptance.

This illustrates the point Kawagoe made in his 1988 Howard Emmons lecture at the Second IAFSS symposium in Tokyo. Many of you will remember that paper, it was entitled, "Real Fires and Fire Modeling". In it, Kawagoe emphasized the importance of full-scale fire experiments as a part of any research project. The tripartite research program led to the only definitive full-scale

smoke toxicity data collected to date and consequently to the only experimentally-verified toxicity test method.


In Nasu, Kawagoe and I got going on the subject of the potential for application of fire models in fire safety design. In the mini-symposium, we had just heard a number of papers describing the use of such models in Japanese Fire Safety Design Method and by leading Japanese construction engineering firms. Kawagoe insisted NIST “stay the course” and continue to press for further development and use of these tools.

When I read the obituary on Kawagoe by Phillip Thomas that appeared in the Fire Safety Journal (volume 23, 1994), I was startled to read what Thomas said that Kawagoe had told him some thirty years earlier was the aim of fire research. It is he said, “to abolish the fire resistance test”. This sounded just like what he was telling me in Nasu.

How many of us are pursuing that same vision, to get beyond the old traditions of “unscientific” rating and ranking methods. Kawagoe did indeed have a wonderfully direct way of making his point. He had a clear vision for the future of fire safety engineering. I think he must be delighted to see us remembering him today by continuing the important work of fulfilling that dream.



Figure 7. The fire at approximately 8:50 a. m.

Reproduced from
best available copy. 

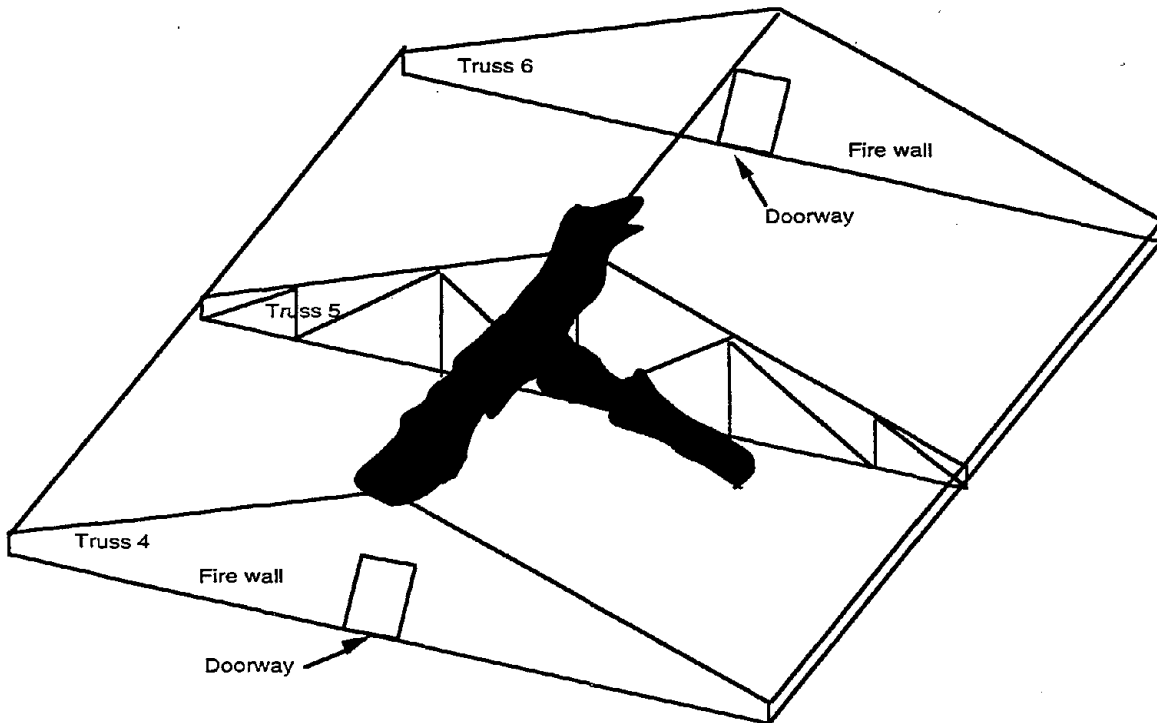


Figure 8. Fire growth in the loft at approximately 8:35 a. m.

rate in this confined space (Figure 6). The associated pressure increase forced flames through available void spaces. As the hole to the loft became larger, the increased air flow rate would also promote a larger flaming fire in the rafter spaces. The flow of the flaming combustion products would follow the rafter channel to the end points at trusses 4 and 5. Hence, the first flames are seen at an opening near truss 4. As the hole to the loft became even larger, flames would lap upward under the sloping wood ceiling of the loft. The person in the loft before this time would not have been aware of the fire since smoke would not permeate into the loft until the hole became large. In fact, he only saw flames when he descended to the machine room after being warned of the fire.

Evidence to support this scenario is shown in the photograph of Figure 7. The small white vapor plume rising from the roof indicates a hole in the roof. This hole is unlike the larger holes on the fire-wall protected side of truss 4 where grey smoke is emanating. Flames are seen to have emerged from the roof on the other side of truss 4 and above the first hole of the most confined rafter space as shown in Figure 3. This is the area that smoldering would have been sustained. The hole indicated by the white vapor plume is in the area of the larger void space where fire was likely initiated, but smoldering was not sustained.

Fire Growth in the Cock Loft

Flame spread would rapidly move from the hole, up and under the loft wood ceiling. It is estimated that flames would move from the hole region up and along the peak of the loft to truss 4 and through truss 5 in 2-3 minutes. This time was estimated from a flame spread model (Quintiere, 1994) using an ignition time of 30 s, and an energy release rate per unit area of 150 kW/m². This rapid spread (Figure 8) seemed incredulous; and, with the low confidence in flame spread calculations, an experiment was performed in a similar, but smaller loft. Flashover occurred in the experiment in approximately 1 minute. In the store loft, flashover was estimated to occur when the wood contribution is 6 to 12 MW in the section of the loft between trusses 4 and 6. The flame spread calculation indicated that this would occur in approximately 2 1/2 minutes. Full involvement was estimated to take up to 5 minutes more. Hence, from the onset of flaming at the hole, full involvement of the loft

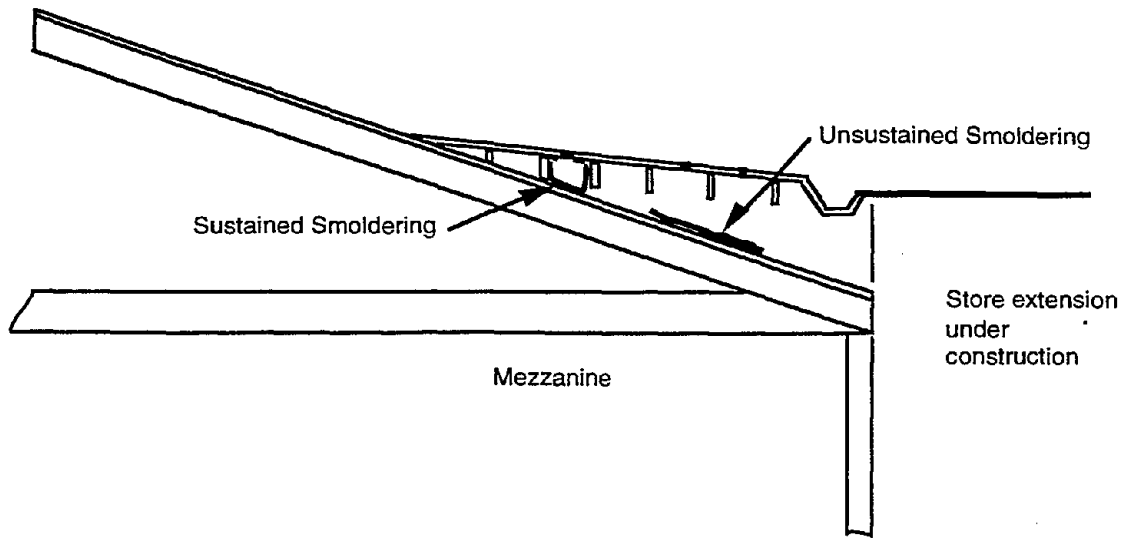


Figure 5. Smoldering combustion at approximately, 6:05 a. m.

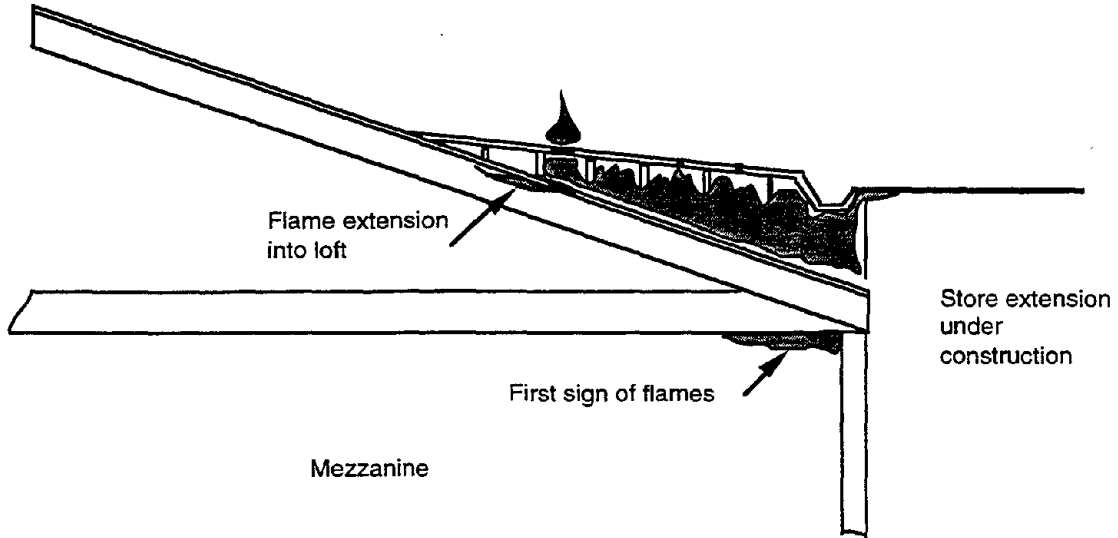


Figure 6. Flaming erupts in the roof cavity space shortly before 8:30 a.m.

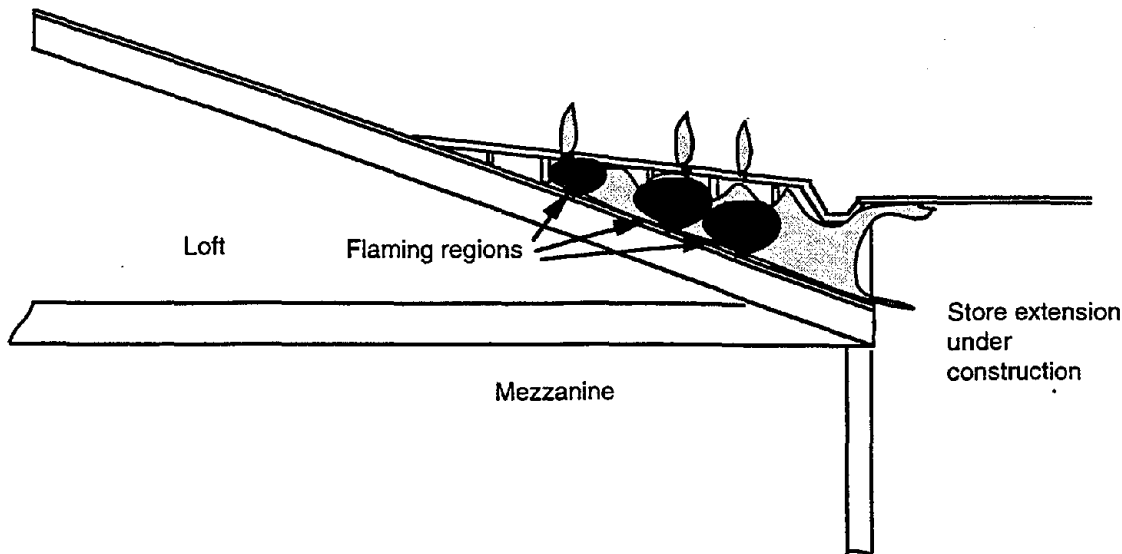


Figure 4. Ignition at approximately 6 a. m.

Smoldering Stage

Oxygen depletion would cause flaming to cease in about 1-2 minutes following wood ignition. However, sustained smoldering would be possible, especially in the smaller rafter spaces where radiant heat transfer would be high. Ohlemiller (1991) reports that sufficient radiant heat transfer is necessary to sustain smoldering in wood cavities. He also reports smoldering propagation rates of 1 to 6 cm/hr. Using the smaller value, smoldering can propagate through the old 3/4 inch plank roof in roughly 2 hours. Hence, a short time before 8:30, a hole would form between the loft and the roof cavity. With air velocity increased to 25 cm/s Ohlemiller (1991) found the smoldering wood would change to flaming combustion. Such velocities would be realized at the hole as air was naturally induced to flow from the loft into the hole. Hence flames would erupt in the false roof cavity space.

Onset of Flaming: Shortly before 8:30 a.m.

At approximately 8:30 am flames are observed in the mezzanine area at the wall and ceiling near truss 4. It is believed that this is due to the expansion of the flames as flashover caused a rapid rise in energy release

analysis will not be presented, but the results will be described.

Early dawn: Ignition (approximately 6 a.m.)

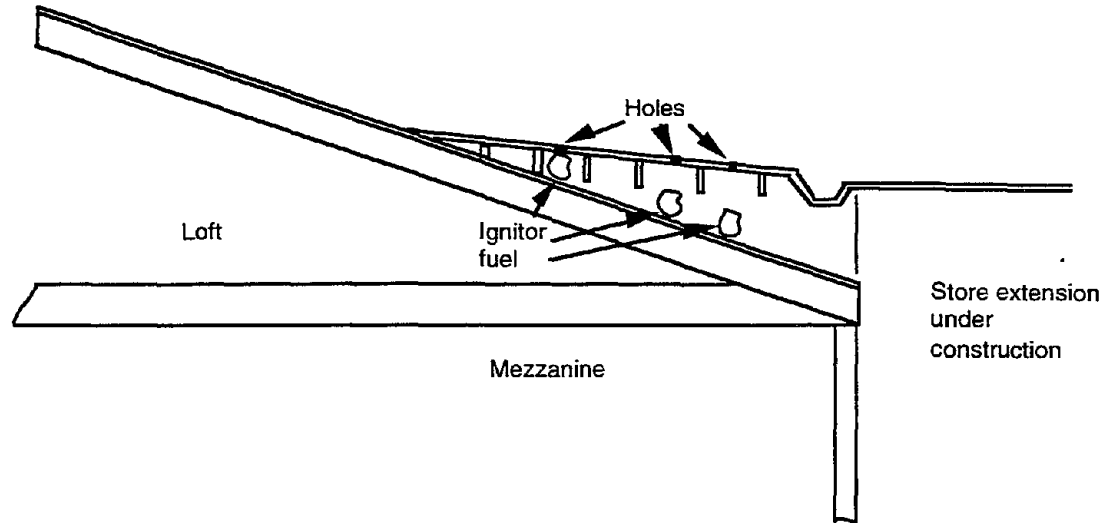


Figure 3. Flammable liquids soaked newspapers inserted into roof holes.

At approximately 6 a. m., an intentional fire is considered to have been set in the roof area adjacent to the construction of the building extension (Fig. 3). The fire is set by stuffing paper through holes in the new roof extension along with a liquid accelerant. The splayed roof extension has been built over the existing roof and forms a void space between the two roofs. The new roof is supported by rafters. The fire is set in channels of the wood rafters which extend between the primary wood trusses 4 and 5. Gaps under the rafters allow air to flow into the fire, but the space is mainly enclosed with temporary partitions at the wall adjacent to the new building extension. The accelerant soaked paper probably caused a fire of 100 to 500 kW in one or more rafter channels, involving no more than 1 m² (Fig. 4).

Under expected heat fluxes of 40 - 50 kW/m², the wood members would ignite in 30 seconds to one minute, and begin to contribute roughly 500 kW. The accelerant fire would probably burn-out in one to 2 minutes. The wood fire could progress to roughly 1000 kW, but then it would become limited in further growth due to combustion products filling this confined space.

and structural support trusses. The trusses were made of 3 x 12 in. Members were interlaced together in bundles of 4 or 5. Trusses 2, 4, and 6 were covered on one side with plaster to form fire walls in the loft. However, for passage, these trusses had doorway openings. The roof had been modified with an added rain roof at the peak. This formed a double layer roof at the peak. Also the new construction called for a splayed roof section to meet the new roof of the extension. This formed another double roof triangular section along the north wall as shown in Figure 2. Due to the construction and the addition of new columns along the wall to the extension, construction voids existed along this wall.

The store opened for business at 8 a. m. and the construction work had been underway since 7 a. m. Flames were first seen at 8:30 a. m. along the interface between the ceiling and extension wall of the mezzanine Men's room and the machine room. The fire eventually spread into the loft between truss sections 4 and 6, and collapsed truss 5 at approximately 9:15 a. m. This caused 6 firefighters to fall into the flames to their death.

A man was tried and convicted in 1978 of setting this fire. His confession stated that he and two others set the fire near dawn (approximately 6 a. m.) by making holes in the roof and using newspaper and lighter fluid to initiate the fire below. This confession was later questioned and discounted in a retrial that was held in 1994. The fire scenario was never explained. The original fire investigators could not agree on a cause, and later suggested that it may have been of electrical origin. However, there was no electrical power in the ceiling area where flames were first seen, and a man in the loft at the onset of the flames saw no evidence of fire. The prosecutors sought advice on how to explain an alleged fire start at 6 a. m., but not seen until 8:30 a. m.

I was asked to assist William J. Petretis, Special Agent, of the Bureau of Alcohol, Tobacco and Firearms in the investigation of this fire 16 years after it occurred. Agent Petretis discovered the splayed roof extension shown in Figure 2, and reasoned the fire had to begin in that space. We then examined the hypothesis of the fire beginning there at approximately 6 a. m. to see if it could be consistent with later known events. A fire scenario was developed and calculations were examined to support the plausibility of the events and their duration. All of this

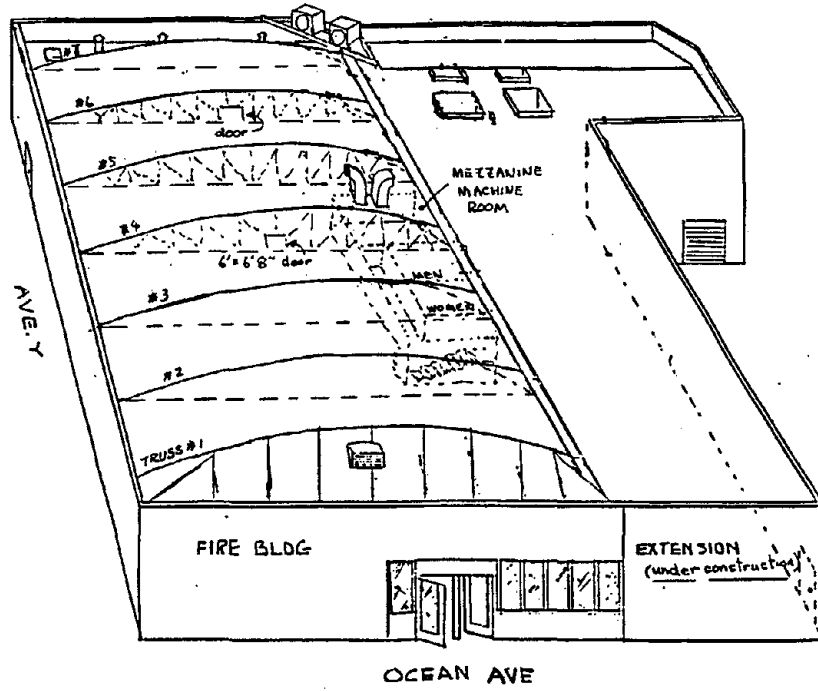


Figure 1. Overview of store with the extension under construction.

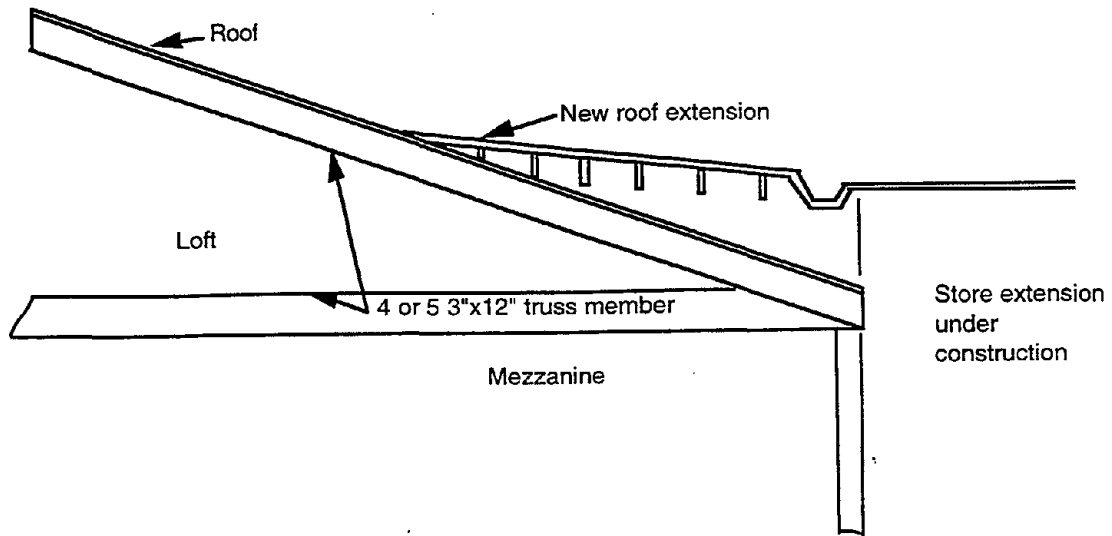


Figure 2. Splayed roof extension.

FIRE INVESTIGATION
An Analysis of the Waldbaum Fire, Brooklyn, NY
August 3, 1978

J.G. Quintiere
University of Maryland
College Park, MD 20742

Dedication: Prof. Kunio Kawagoe provided inspiration as an administrator, researcher, and teacher in the field of fire safety. I have benefitted greatly from his scientific contributions, and have memories of many friendly moments. I think he sought to have fire science confront the real world, and therefore I submit this paper to the Kawagoe Memoriam in his honor.

ABSTRACT

An analysis of the Waldbaum supermarket fire, Brooklyn, NY, August 3, 1978 is presented. It is argued that the fire went from flaming to smoldering and back to flaming over a period of several hours. This mostly hidden fire broke into the loft and led to the collapse of the roof. As a result, 12 firefighters fell into the flames and six perished. The fire was never satisfactorily explained, and a retrial of a man convicted of arson prompted this analysis.

Introduction

Fire investigation has not generally used the tools of fire science to explain the scenario of the fire. It has relied on chemical evidence to identify ignition causes, but has not necessarily relied on the characteristics of the fire to explain its cause. The application of fire science to investigation has a dual benefit since it not only can assist the fire investigator, but it also reveals fire behavior that should be recognized by fire scientists. We shall consider one such application.

On August 3, 1978 a fire occurred at the Waldbaum supermarket in Brooklyn, NY. A sketch of the store is shown in Figure 1. At the time of the fire, an extension was under construction as indicated. The store was a typical supermarket with a mezzanine along a portion of the north wall. The loft was completely of wood construction comprising the floor, roof,

Discussion

Robert Levine: Do I understand correctly that the long building that was shown in the first slide was actually designed as a fire break? Has that been done frequently in Japan? How many times?

Takashi Sekine: That is the only case.

Charles Scawthorn: Thank you very much for the talk. I should just mention that long building has many fire defense features, water curtains, and doors that come down and other features like that. The one question I have is that while that provides an excellent fire break and a barrier for high temperatures and so on, what about defects of branding? I think in the conflagration of 1923, brands were found many miles away. I was just curious about the potential or the effects of burning flaming fire debris being carried over that wall, perhaps two or three kilometers downwind or something like that.

Takashi Sekine: That fire break was built next to a very densely inhabited area. It is my personal opinion, not the opinion of a scientist, there is still some risk that the fire brands would fly over the building. But behind the building there is only open space, so unless people bring many things to the place, there is not a very big risk that any big fire would take place in that open space.

Charles Scawthorn: So the real purpose of it is not so much as a fire stop as a protective area?

Takashi Sekine: Yes.

Ai Sekizawa: This idea of creating a fire break is wonderful. However, it is very costly. This type of thing was built in 1970; since then, nothing similar has been built because it costs too much. So these days, they are establishing fire breaks along the main roads by using fire resistive materials. If I may make one comment, I have been involved in research on the flow field around buildings, and if there are many tall buildings, then air flow around those buildings would change because of those buildings. Depending on the air flow, the flight of the brand would also vary. So research on branding, I think, is a very important research subject to be addressed in the future.

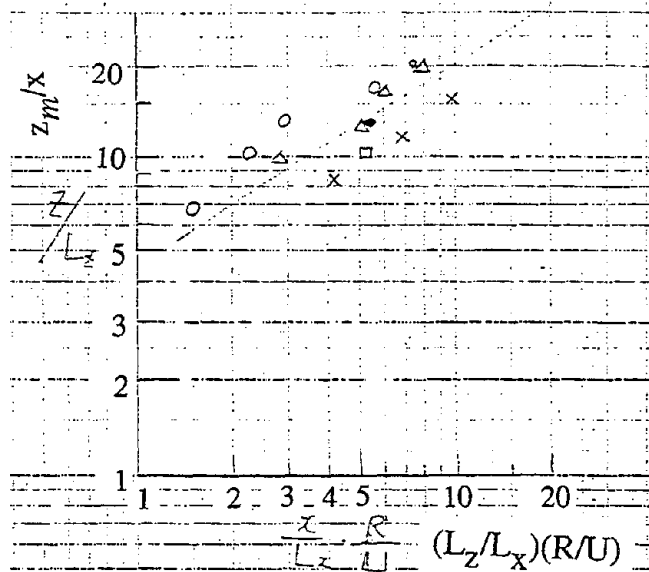


Figure 6 z_m/L_z vs. $(x/L_x)(R/U)$

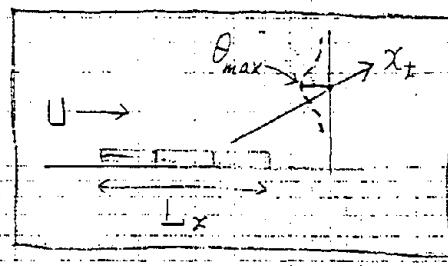
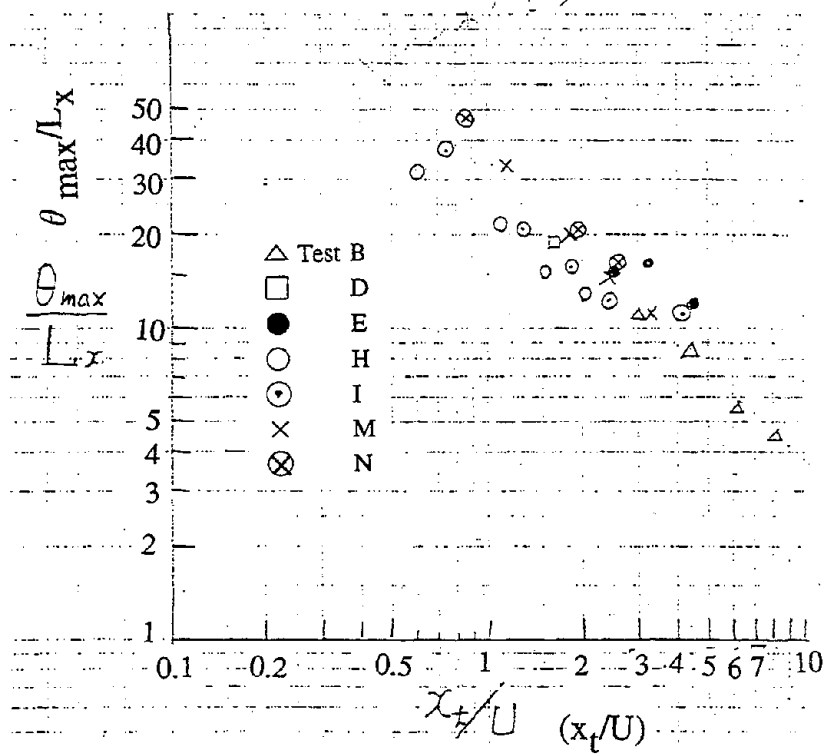


Figure 7 Relation between Temperature on the Trajectory and Distance along the Trajectory

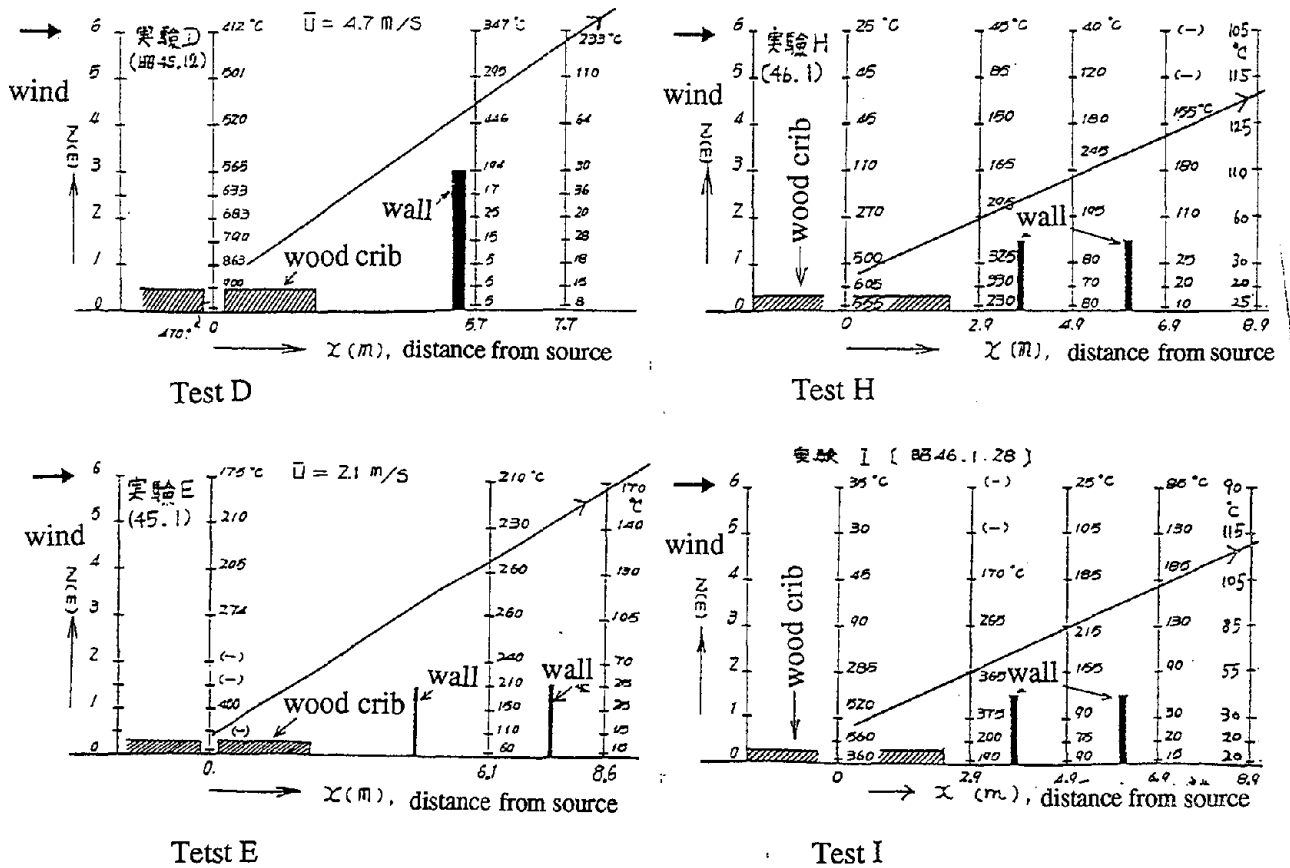


Figure 4 Temperature Field in AIJ Tests, average for 3~5 minutes after ignition

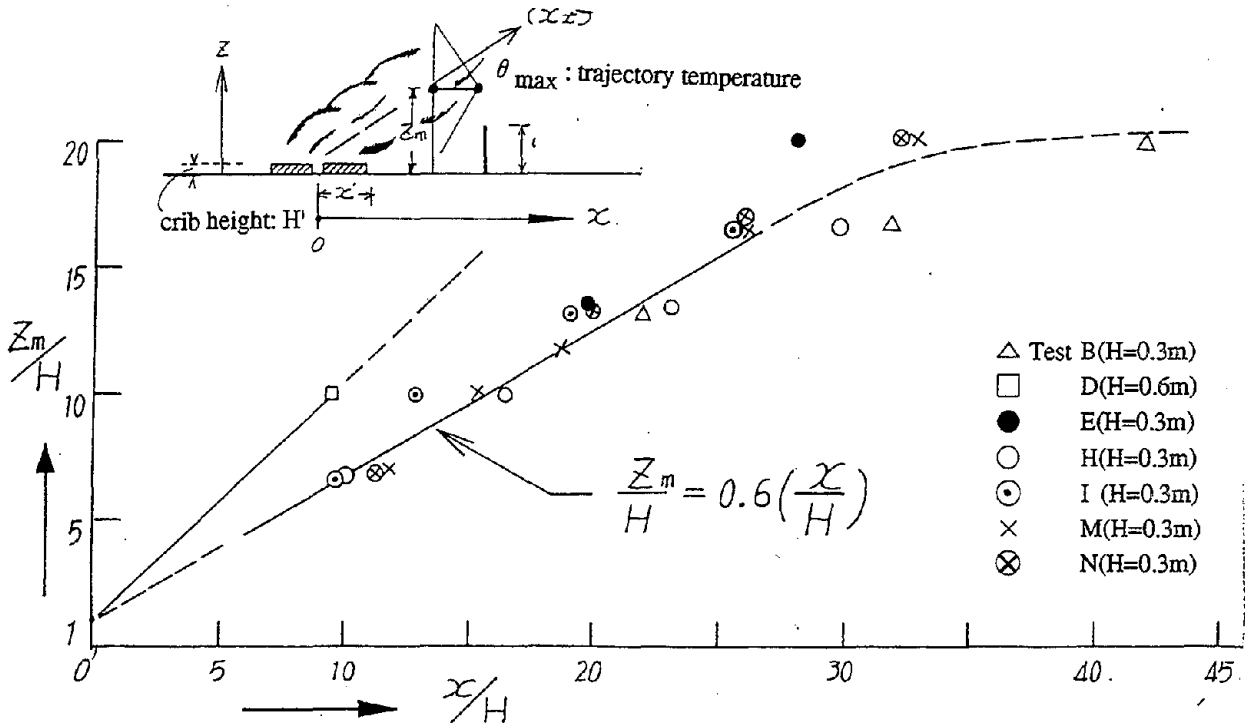


Figure 5 Trajectory Axis, AIJ Tests

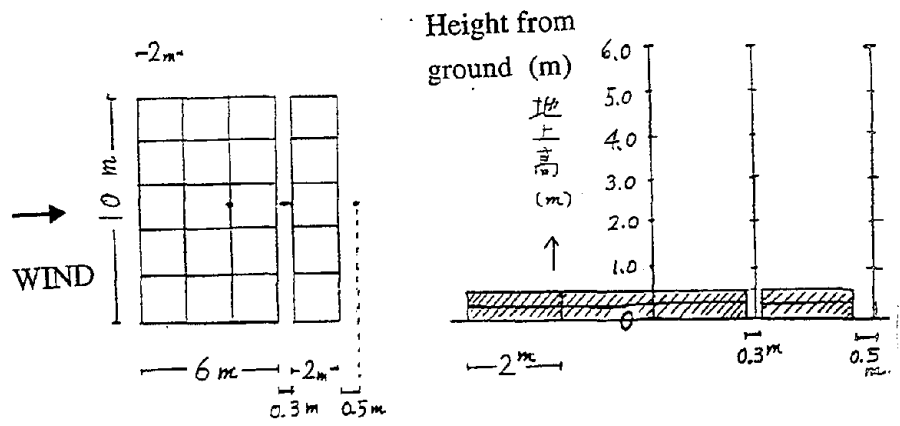


Figure 2 (a) Layout of Wood Cribs and Instrumentation, BRI FY 1970 Test A

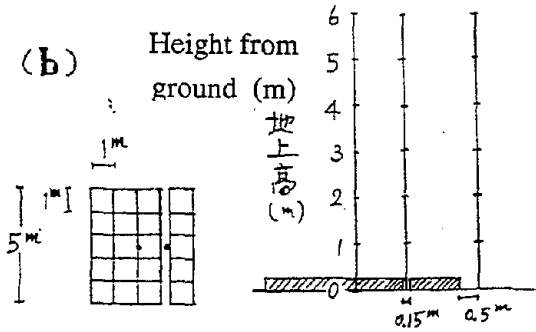


Figure 2 (b) Layout of Wood Cribs and Instrumentation, BRI FY 1970 Test B

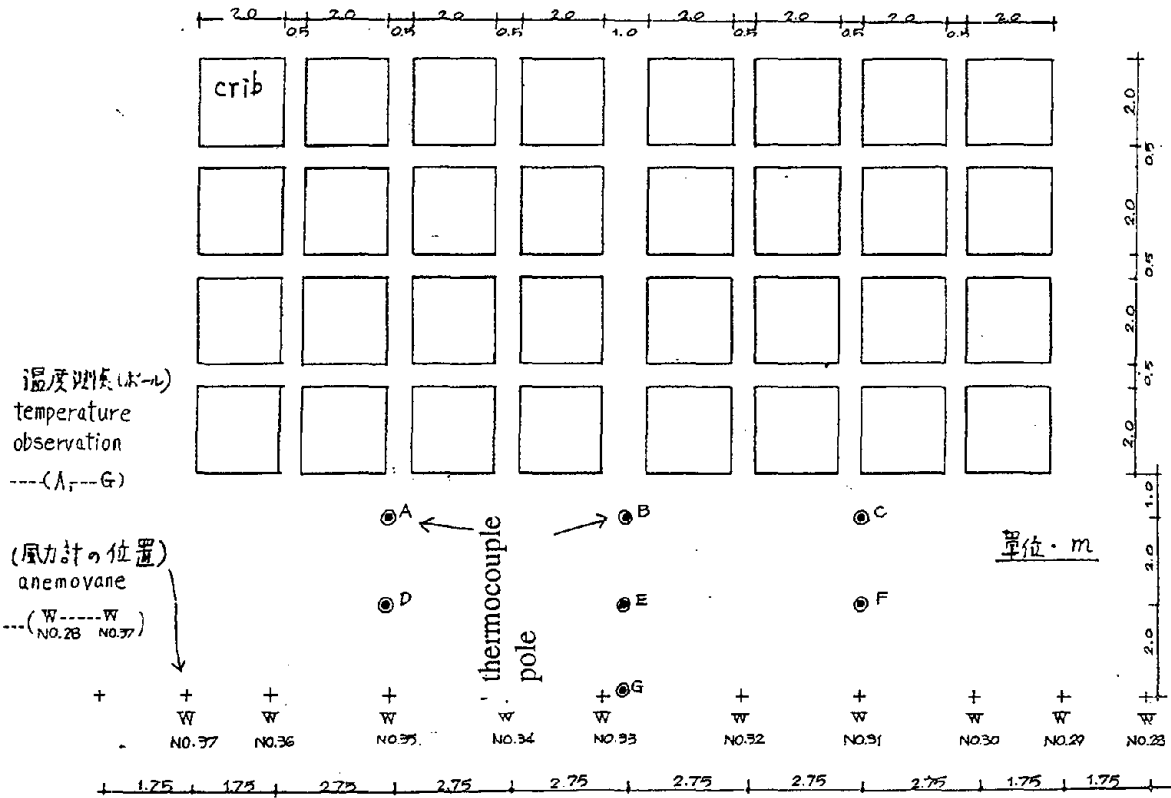


Figure 3 Layout of Wood Cribs and Instrumentation, BRI FY 1971 Test

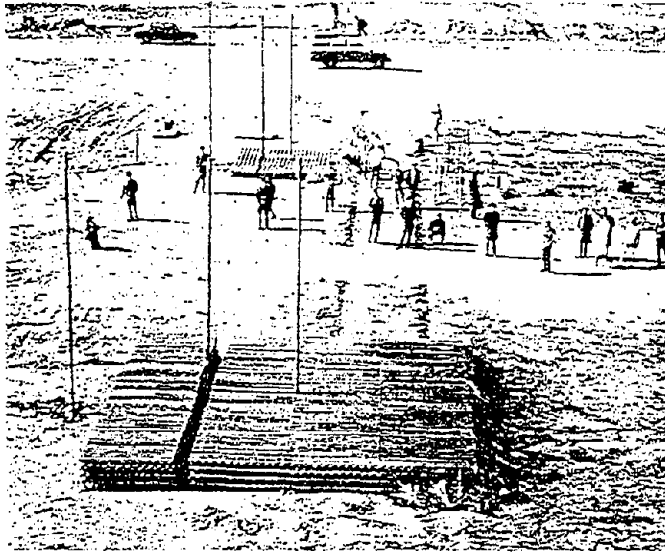


Photo 1 BRI FY 1970 Test-A Arrangement(before ignition)
The small cribs behind the Test-A cribs are for Test-B.

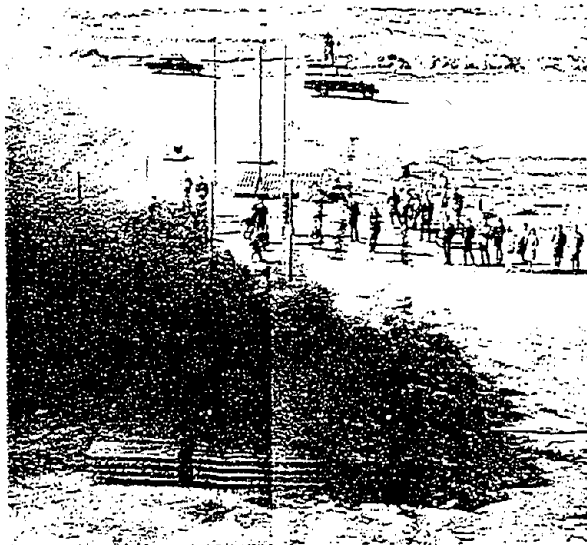


Photo 2 BRI FY 1970 Test-A (just after ignition)

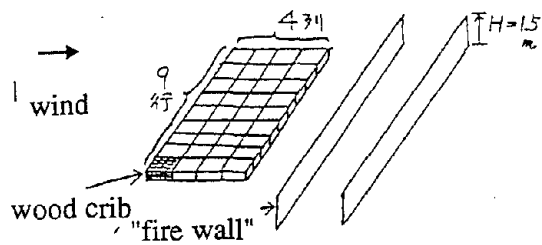


Figure 1 Layout of Wood Cribs and "Fire Walls", AIJ Tests

~0.7 independent of the size and wind velocity. This tendency has also been confirmed by the BRI tests. However, the plume stops to rise or even starts to decline in the far field, say for $x/H \geq 30$ in the AIJ tests where H is the height of the fuel. At the BRI tests, the plume started to decline even earlier, at around $x/H=20$. Further analysis has been made using another parameter, $(x/L_x)(R/U)$, where L_x is the horizontal length of fuel in the wind direction and R is the mass consumption rate of fuel per unit area. z_m/L_z where L_z is the fuel height has been correlated against $(x/L_x)(R/U)$ as seen in Figure 6. R was estimated from the weight of the cribs measured before each test and the time from ignition to the autonomous extinction. z_m/L_z is nearly proportional to $(x/L_x)(R/U)$, which suggests the following relation for the trajectory axis angle.

$$z_m/x \propto (L_z/L_x)(R/U) \quad (1)$$

Temperature along the trajectory axis, θ_{\max} , was found to be nearly inversely proportional to the distance measured along the trajectory, x_t , divided by wind velocity as summarized in Figure 7, and can be approximated by

$$\theta_{\max}/L_x \propto (x_t/U)^{-1} \quad (2)$$

ACKNOWLEDGMENT BY THE EDITORS OF THIS REPORT

This report in English is summarized by Y.Hasemi and Y.Hayashi for the Kawagoe Memorial Symposium held at the 13th Joint Panel Meeting of UJNR, 1996, from previous publications and unpublished notes of Prof.Sekine. The experimental description and its analysis is essentially a contribution by Prof.Sekine, and the report does not include any personal opinions nor analysis by the editors. The drawings in this report were taken from his publication and his unpublished notes. Prof.Sekine worked at Building Research Institute from 1946 to 1979, and was one of the closest colleague to the late Prof.Kawagoe. Prof.Sekine is known also as the author of the first paper deriving the ventilation factor, $AH^{1/2}$ as the dominant parameter for postflashover fires in 1959.

The results of the research projects introduced in this report were applied to the design of the Shirahige Disaster Mitigation Position in the Koto district of Tokyo in 1970's, which consists of a large refuge on Sumida River and wall-like high rise apartment buildings between the refuge and urban blocks.

REFERENCES

Sekine,T.: Hot gas movement in reduced scale city fire experiments, Annual Meeting of Architectural Institute of Japan, p.95 ~ 96, 1971(in Japanese).

H.Takahara, and Sekine,T.: Experimental research on the spread of the fire, Comprehensive report on disaster prevention science, No.31, 1973(in Japanese).

Sekine,T.: Fire Tests in Open Field, unpublished note prepared for seminars, 1983 - 1984(in Japanese).

Sekine,T.: Room Temperature in Fire Resistive Room, Building Research Institute Report No.29, 1959

tests in 1969 - 70 and 1970 - 71 were analyzed by Sekine(1971). A material prepared by Sekine at a seminar in 1983 and 1984 compares results from the 1971-72 winter tests with those from the former tests. A city block of wooden buildings were simulated with cribs of 7 layers of twelve 2 m long 4 cm x 4 cm wood sticks. Table 1 summarizes the test conditions, and Figure 1 demonstrates a typical layout of the fuel and the fire wall. Temperature field was monitored with thermocouples mounted on 6 m tall poles, and wind velocity was monitored basically windward to the fuel. All cribs were ignited simultaneously.

Table 1 AIJ Tests Conditions, Summary

Identification	Date	Number of cribs	Height of wall	Wind velocity(direction)
Test B	Dec 1969	36(9 x 4)	1.5 m(single)	U= 1.2 m/s(N)
D	Dec 1969	72(9 x 8)*	3.0 m(single)	4.7 m/s(N)
E	Jan 1970	54(9 x 6)	1.5 m(double)	2.1 m/s(N)
H	Jan 1971	36(9 x 4)	1.5 m(double)	5.0 m/s(N)
I	Jan 1971	36(9 x 4)	none	4.0 m/s(N)
M	Feb 1972	15(5 x 3)	1.5 m(double)	3.5 m/s(N)
N	Feb 1972	15(5 x 3)	1.5 m(single)	3.5 m/s(N)

* 14 layers of sticks were used while 7 layers were used in other tests.

BRI Tests

The test project started with smaller models in FY 1970 and then was extended to a larger test in FY 1971.

At the FY1970 tests, two different scale models for city fire experiments were built with wood cribs, and temperature field in the wind direction was monitored with thermocouples mounted on 6 m tall poles (Figure 2 (a) and (b)). The larger model(model-A) consisted of 20 cribs of 14 layers of twelve 2 m long 4 cm x 4 cm wood sticks. The most leeward row of the cribs was located 0.30 m away from the other cribs to study the fire spread across a vacant space such as a street. The smaller model(model-B) consisted of 20 cribs of 7 layers of six 1 m long 4 cm x 4 cm wood sticks. The most leeward row of the cribs was located 0.15 m away from the other cribs. Wind direction and velocity were measured windward to the fuel. At the two tests, ignition was made on the most windward row of the cribs.

At the FY1971 tests, 32 cribs of 7 layers of 2 m long 4 cm x 4 cm wood sticks were arranged with interval of 0.50 m to make a 20 m x 10m total burning area(Figure 3). Measurements were made on temperature with thermocouples mounted on 6 m tall steel poles and wind direction and velocity windward and leeward to the fuel. Although it had been planned that only the most windward row of the cribs, the two windward rows were ignited by accident. Also weather was somewhat unstable because of the low pressure passing near the Tokyo Bay on that day.

SUMMARY OF TEST RESULTS AND DISCUSSIONS

Figure 4 summarizes temperature field measured at several of the AIJ tests. The inclined straight line in each drawing demonstrates the trajectory axis of the plume estimated from the maximum temperature at each distance. Interestingly, the trajectory axis is practically straight, and is found not to be very dependent on test conditions including wind velocity. The height for the maximum temperature rise at each distance x , z_m , has been summarized as a function of x as shown in Figure 5. The angle of the trajectory axis, ϕ , was between 30° and 35° and $\tan \phi$ was approximately 0.6

BEHAVIOR OF WIND BLOWN CRIB FIRES

Takashi Sekine

formerly Professor, Labor Training College, Ministry of Labor

formerly Head, Fire Safety Section, Building Research Institute

INTRODUCTION

City fire has been one of the most significant disasters that Japan had to fought against throughout its industrialization. The two big earthquakes which attacked the greater Tokyo area during the Japanese modernization, Ansei Earthquake(1855) and Kanto Earthquake(1923) caused over 10,000 and 100,000 victims only by postearthquake fires. Even after the World War II, big city fires were rather frequent, say at least one time a year, until 1960's, most of which occurred by strong wind. Since late 1960's, big city fires became rare partly as the fire defense had been modernized. However, recent two big earthquakes in Japan, Hokkaido Southwest-off Earthquake in 1993 and Hyogo-Nambu Earthquake in 1995, revealed risk of city fires especially at the occasion of big earthquake.

Since establishment of BRI in 1946, considerable efforts have been made on the analysis of city fires and fire spread in urban district. Early works on city fires by BRI staff include characterization of fires of wooden structures from fire-spread point of view in 1940's(Fujita), probabilistic formulation of fire spread in urban fires in early 1950's(Yokoi), and modeling of meteorological aspect and fire plumes in city fires in 1950's(Yokoi and Sekine). Also a research project on the prevention and mitigation of city fires through city planning was organized at BRI in 1969~1972 while the late Prof.Kawagoe served BRI's Director General. This research project was combined with another governmental investigation project for the redevelopment of the Koto district, east of Sumida River, where city fires were the most significant at the occasion of Kanto Earthquake and the postwar reconstruction was done with weak wooden structures. A series of model fire tests were carried out at the Tokyo Bay landfill area in fiscal 1969~1972 as a part of these projects under the cooperation of BRI, Tokyo Fire Department, Tokyo Metropolitan Material Inspection Office, and Architectural Institute of Japan(AIJ). This report tries to summarize this experiment project and its outcome.

THE EXPERIMENTS

Two different series of fire tests with wood cribs were carried out. One series were run in 1969~1971 with AIJ as the secretariat and the other were done in 1970 and 1971 with BRI as the secretariat. Although numbers of research organizations and individual experts joined the tests, the two test series will be referred to as the AIJ tests and BRI tests respectively only for simplicity. The two test series were coordinated with each other and some of the AIJ tests were even carried out at the same time with the BRI tests for efficiency, but the AIJ tests featured analysis of the effectiveness of a "fire wall" against the spread of fire in urban district, while the BRI tests dealt with more general aspects of fire behavior in urban area. Summary of the AIJ tests were reported by Sekine(1971) and the BRI tests were reported by Takahara and Sekine(1973) both in the Japanese language.

AIJ Tests

Numbers of tests were made in the winter of 1969 - 70, 1970 - 71, and 1971 - 72. Five out of the

1960. Kawagoe, at that time, had spent part of a year as a guest worker at the Fire Research Station (FRS) Borehamwood. He contributed two papers at the meeting, the first on fire behavior in a compartment with a large window. The second involved a fire resistance test of a prestressed concrete beam.

The first part of the CIB/CTF meeting involved planning further experiments on the international study of behavior of fires in compartments. Five national laboratories had contributed data. I believe Kawagoe's paper involved a report on a proposed extension of this work with much larger compartments. He reported on his experience at FRS with one of these large enclosures.

Kawagoe's second paper described a fire resistant test on a prestressed concrete beam. I believe it was related to a cooperative study we had undertaken at NBS at the request of Dr. Lea, the Director of the UK Building Research Station. It involved the conduct of fire endurance tests of several pre-stressed concrete beams of greater size than would be possible at the Fire Research Station at that time. It developed that the beam had not performed as well as expected because of failure of the concrete cover of the reinforcing steel strands. I believe Kawagoe's experiment had shown that by using steel mesh at the lower edges of the concrete beam, spalling of concrete was greatly reduced and much better fire performance could be achieved.

My second meeting with Kawagoe was at the end of his year at FRS. He stopped on his trip home for brief visits in Washington. He visited the Fire Section at NBS on 24 April, 1961. Surely he was interested in the experimental unconfined crib fires as well as compartment fires being developed by Gross and many part time college students. These experiments were an outgrowth of, but not a part of, the CIB/CTF work that had been discussed in the UK. Surely too he must have been interested in the NBS large scale fire endurance furnaces, as well as other work we were doing. From this time on, Kawagoe or his associates attended and contributed much to the later meetings of CIB/CTF (or WG14).

Thus, in conclusion, I suggest that the award to me of the "Kawagoe Medal" may have resulted from three factors:

1. our early and continuing exchange of fire research information with Japan;
2. an appreciation of CIB related fire burn research being pursued by Gross and others in our group; and
3. the capability and competence we at NBS had for a wide range of fire studies.

I appreciate the personal honor of this award, but prefer to think of it as recognition of the work of the fire research staff that Kawagoe met and their later findings. I therefore suggest that we all take a moment of silence in memory of Kawagoe san and the contributions that he made to fire safety.

RECOLLECTION OF MEETINGS WITH KUNIO KAWAGOE

Alexander F. Robertson

I would like to contribute comments in recognition of Kawagoe san. I was very surprised, but pleased, to learn of an impersonation of me which took place last year at the Ottawa meeting at the Fourth International Symposium of Fire Safety Science, at which I was presented the "Kawagoe Medal." I have tried to understand why I was singled out for this honor. I plan in this brief talk to present you with a partial explanation for this.

I was employed at the National Bureau of Standards (NBS) in May 1950 by Douglas Parsons, Chief of the newly established Building Technology Division. The NBS fire activities were then being reorganized in this Division following the retirement of Simon Ingberg. Parsons had made it clear that he expected me to try to upgrade fire safety through engineering science, rather than through ad hoc routine tests. He further expected me to see that work I and associates might accomplish would be incorporated in written documents. He had apparently been visited by Dr. Fujita of the Building Research Institute in Japan, who had furnished him with reports of pioneer work done there on building fire problems. These, as I recall, were primarily related to ventilation characteristics of openings in compartment walls. It was clear to me that we were expected to reciprocate whenever we could contribute.

At that time, and even today, any formal NBS publication had to survive a rather lengthy approval process. However, documentation of our findings might be in the form of NBS Technical Reports (*gray backs*). These were considered semi-classified documents for limited distribution. With Parsons agreement, we developed a mailing list through which we circulated copies of these to laboratories, on an exchange basis, doing work related to ours. Of course, we were careful to avoid releasing reports containing classified or proprietary information.

In October 1957, Professor Toshiro Kimbara of the University of Tokyo visited Washington to contribute to an early meeting of the Committee on Fire Research (CFR) of the National Academy of Sciences, National Research Council (NAS/NRC). I met him there and invited him to visit us at NBS. He arrived on 4 November and we showed him work we had in progress. At the CFR meeting we had been told of works underway both at his University and by others at the Building Research Institute in Japan. Kimbara visited us again with Siguro Yokoi two years later on 11 November, 1959 (see photograph).

From this time on, we sent information on our work on the fire problem in the form of *gray backs* and received numerous copies of their work in Japan. Through these documents, we first learned of Kawagoe's and others work in Japan.

I feel confident that Kawagoe, then at the Building Research Institute of Japan, received information on our work from the reports we forwarded to the University. Thus, I was pleased to meet Kawagoe at the fourth meeting of "Le Council International du Batiment pour Recherche et Documentation" (CIB/CTF). This was organized as a sub-group of the United Nations. We were participating at that time on an informal basis. The meeting was held in London in May

section would take approximately 5 to 10 minutes. Because of the false roof sections and the truss fire-wall sections, the firefighters on the roof were unaware of the raging fire in the loft section below them.

Collapse of the Roof due to Truss Member Failure

If one assumes that the roof collapse is due to the failure of a truss member as a result of fire degradation, the burn through time of a member can be estimated. The fire exposure assumed is a fully involved loft with a 3 inch thick truss member within the flame. Using a mass burning rate per unit area of 11 g/m²s, typical for wood under these conditions, leads to a burn through time estimate of approximately 35 minutes. This results in a truss member failure at 9:10 a. m. compared to the recorded roof collapse 5 minutes later.

Concluding remarks

This fire scenario was a complex series of phenomena that are not usually appreciated in the study of fire. Experienced fire investigators were not able to deduce this process. Yet relatively simple scientific analysis could produce a plausible and consistent series of events within the period of the recorded observations of this fire. Some may question the details, but the scenario fits the time-line of what is known and alleged.

Studies like this are very useful because they provide a test of science against the real world. The process can provide valuable answers to the investigator and valuable questions for the scientist.

References

Hughes, B. J. , Private Communications of Statements and Records, Office of the District Attorney, Kings County, Brooklyn, NY, 1994.

Ohlemiller, T. J., Smoldering Combustion Propagation on Solid Wood, Fire Safety Science -- Proc. Of the Third Internat. Symp., pp. 565-574, 1991.

Quintiere, J. G., Estimating the Fire Growth on Compartment Interior Finish Materials, SFPE Seminar, San Francisco, CA, May 16-18, 1994.

Discussion

Charles Scawthorn: I'm just asking what was the supposed motive for the defendant?

James Quintiere: It was allegedly paid arson because of business competition in that area.

SIMPLE FORMULA FOR VENTILATION CONTROLLED FIRE TEMPERATURES

Takeyoshi TANAKA

Building Research Institute, Ministry of Construction
1 Tatehara, Tsukuba-shi, Ibaraki-ken, 305 JAPAN

Masafumi SATO

Tokyu Construction Corporation
1-16-14 Shibuya, Shibuya-ku, Tokyo, 150 JAPAN

Takao WAKAMATSU

Faculty of Science and Engineering, Science University of Tokyo
2641 Yamasaki, Noda-shi, Chiba-ken, 278 JAPAN

ABSTRACT

Simple equations for predicting the fire temperatures of the room of origin and the connected corridor are proposed. These are obtained by applying the existing equation for predicting pre-flashover compartment fire temperature by Quintiere et al. to ventilation controlled fire. The results of the predictions using the simple equations are compared with the predictions by a more detailed computer fire model. The accuracy of the equations is as good as the computer model and deemed to be acceptable for many of such practical applications as structural fire safety designs of buildings.

1. INTRODUCTION

Fire resistance of structural elements and fire walls are being assessed under the heating conditions defined by a prescribed temperature-time curve in virtually every country. Sometimes, this curve is expressed in an analytical formula, such as the famous ISO 834 curve given $T - T_0 = \log_{10}(8t - 1)$. Any of such temperature-time curves, however, cannot take into account the conditions of compartment boundary and openings, which definitely affect the fire temperature.

As a result, computer fire models, which often assumes ventilation controlled fire, are invoked when more rational assessment is desired for the compartment fire temperatures. However, it will be undoubtedly convenient for many practical applications if a simple analytical equation is available for fire room temperature. Also, it might be convenient if a simple formula is provided for the temperature of the spaces connected to the fire room in such a case as assessing the endurance of the fire doors installed at places somewhat remote from the fire room.

In this paper, the existing equation for pre-flashover room fire temperature developed by Quintiere et al. is extended to obtain simple equations for ventilation controlled fire temperatures of the room of origin and the corridor connected to the room.

2. COMPUTER FIRE MODEL

It is practically impossible to experimentally investigate compartment fire behavior under a variety of conditions. Hence, only possible way to validate the simple equations to be developed is to compare with the predictions by a more detailed computer model. A multi-room computer fire model in which all the physical properties are assumed as homogeneous is developed for this purpose. The schematic of the model is shown in Figure 1, and the outline of the mathematical formulation is as follows:

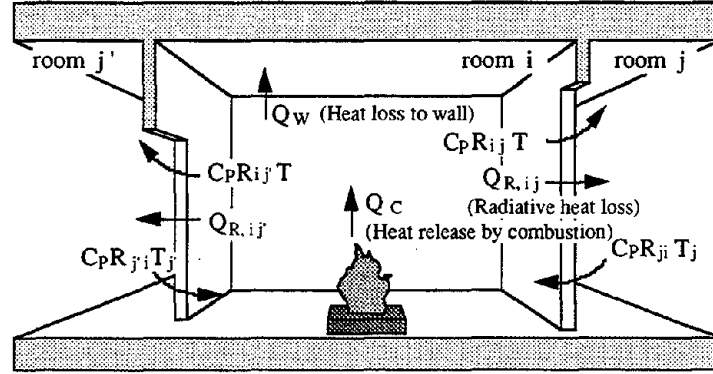


Figure 1 Schematic of the computer model

2.1 The Zone Equations

Considering the conservation of mass, oxygen and energy, and the state of ideal gas for each of the spaces involved in a fire, the following equations for the temperature, oxygen mass concentration and the room static pressures, which hold for any of the indoor spaces considered, are derived.

(a) Room temperature

$$\frac{dT}{dt} = \frac{T}{C_p V \rho_\infty T_\infty} \left(Q_c - Q_w - \sum_{j=0}^n Q_{R,ij} \right) - \frac{T}{V \rho_\infty T_\infty} \left\{ \sum_{j=0}^n m_{ji} (T - T_j) + m_b (T - T_p) \right\} \quad (1)$$

(b) Oxygen mass concentration

$$\frac{dY_{O_2}}{dt} = - \frac{T}{V \rho_\infty T_\infty} \left\{ \sum_{j=0}^n m_{ji} (Y_{O_2} - Y_{O_2,j}) + m_b Y_{O_2} + \frac{Q_c}{\Delta H_{O_2}} \right\} \quad (2)$$

(c) Room static pressure

$$\frac{1}{C_p T} \left(Q_c - Q_w - \sum_{j=0}^n Q_{R,ij} \right) + \frac{1}{T} \sum_{j=0}^n m_{ji} T_j - \sum_{j=0}^n m_{ij} + \frac{T_p}{T} m_b = 0 \quad (3)$$

Note that subscript i , which denotes an arbitrary room, is omitted from every variable in the above equations for simplicity. Subscript j stands for a space connected with room i , and $j=0$ specifically stands for the outdoor space. The summations in Eqns.(1) through (3) are taken for all the spaces connected with room i .

The ordinary differential equations (1) and (2) are numerically integrated using Runge-Kutta method. Each flow term of Eqn.(3) is formulated as a function of the room pressures and Eqn.(3) is solved for the pressures using Newton-Raphson method.

2.2 Transfer Terms

The terms for transfer of mass and energy included in Eqns.(1) through (3) are formulated as follows:

(1) Heat transfer to compartment boundary

Assuming the homogeneous temperature of the compartment boundary, the rate of heat transfer from the room gases to the boundary is calculated as

$$Q_w = \left\{ \varepsilon_w \sigma (T^4 - T_w^4) + \alpha_w (T - T_w) \right\} A_T \quad (4)$$

where the convective heat transfer coefficient is assessed by

$$\alpha_w = \begin{cases} 5 \times 10^{-3} & (T_\alpha \leq 300K) \\ (0.02T_\alpha - 1) \times 10^{-3} & (300K < T_\alpha \leq 800K) \\ 15 \times 10^{-3} & (800K < T_\alpha) \end{cases}$$

with T_α defined as

$$T_\alpha = (T + T_w) / 2$$

The temperature of the boundary surface T_w , which is indispensable for the calculation of heat transfer to the boundary, is calculated by numerically solving the one-dimensional heat conduction equation using finite difference method.

(2) Radiative heat exchange through openings

In this model, radiative heat transfer from a room to its adjacent rooms connected by opening of area $A_{D,ij}$ is taken into account by:

$$Q_{R,ij} = \sigma (T^4 - T_j^4) A_{D,ij} \quad (5)$$

(3) Mass flow rate through openings

The equations for the mass flow rates through the opening m_{ij} between room i and room j are provided as a function of the room static pressure P , room gas density ρ , and opening width B , soffit height H_u and sill height H_l as shown in Table 1. The equations in Table 1 cover all the flow patterns conceivable in the multi-room fire model under the assumption of uniform temperature in every space.

(4) Mass burning rate

The mass burning rate in ventilation controlled compartment fire experimentally established by Kawagoe-Sekine is used in this model.

$$m_b = 0.1 A_w \sqrt{H_w} \quad (6)$$






where A_w and H_w are the area and the height of the opening, respectively. For the stability of the numerical computation, the burning rate is increased linearly up to this value in one minute.

(5) Heat release rate in the compartment

The theoretically maximum rate of the heat that can be released within a compartment under ventilation controlled fire is governed by the rate of oxygen supplied along with air entering into the compartment through the openings, i.e:

$$Q_C = \Delta H_{O_2} \sum_{j=0}^n m_{ji} Y_{O_2,j} \quad (7)$$

Table 1 Opening flow rate under various conditions

condition		pressure difference	flow rate eqns.
$\rho_j = \rho_i$	$p_j \leq p_i$		$m_{ij} = \alpha B_w (H_u - H_i) \sqrt{2 \rho_i \Delta p}$ $m_{ji} = 0$
	$p_j > p_i$		$m_{ij} = 0$ $m_{ji} = \alpha B_w (H_u - H_i) \sqrt{2 \rho_i \Delta p}$
$\rho_i > \rho_j$	$Z_n \leq H_i$		$m_{ij} = 2/3 \alpha B_w \sqrt{2g \rho_i \Delta p} \times \{(H_u - Z_n)^{3/2} - (H_i - Z_n)^{3/2}\}$ $m_{ji} = 0$
	$H_i < Z_n < H_u$		$m_{ij} = 2/3 \alpha B_w \sqrt{2g \rho_i \Delta p} (H_u - Z_n)^{3/2}$ $m_{ji} = 2/3 \alpha B_w \sqrt{2g \rho_j \Delta p} (Z_n - H_i)^{3/2}$
	$H_u \leq Z_n$		$m_{ij} = 0$ $m_{ji} = 2/3 \alpha B_w \sqrt{2g \rho_j \Delta p} \times \{(Z_n - H_i)^{3/2} - (Z_n - H_u)^{3/2}\}$

where $\Delta P = |P_i - P_j|$ $\Delta \rho = |\rho_i - \rho_j|$ $Z_n = (P_i - P_j) / (\rho_i - \rho_j) g$

Although the concentration of oxygen may not become to be completely zero even in fully developed stage, the heat release rate in this model is assumed as Q_C given by Eqn.(7).

The burning rate given by Eqn.(6) causes ventilation controlled fire, but for a short period of starting up fire there is a fuel controlled stage as shown in Figure 2. The heat release rate in this stage is calculated by

$$Q_C = \Delta H_{wood} m_b \tag{8}$$

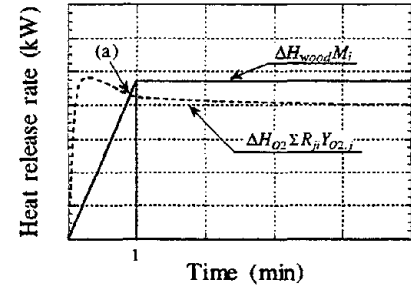


Figure 2 Transition of heat release rate

2.3 Prediction of Temperature by the Computer Fire Model

Sample calculations are made to investigate how the temperatures of the room of origin and the adjacent corridor are affected by the conditions of the spaces.

(1) Calculation conditions

a) Space geometries

The room of origin and the connected corridor as shown by Figure 3 are employed as the object of the sample calculations. The dimensions of the spaces and the openings which are given a specific number in the figure are fixed at the value in all the calculations, and those whose dimensions are not specified in the figure are varied depending on the calculation condition.

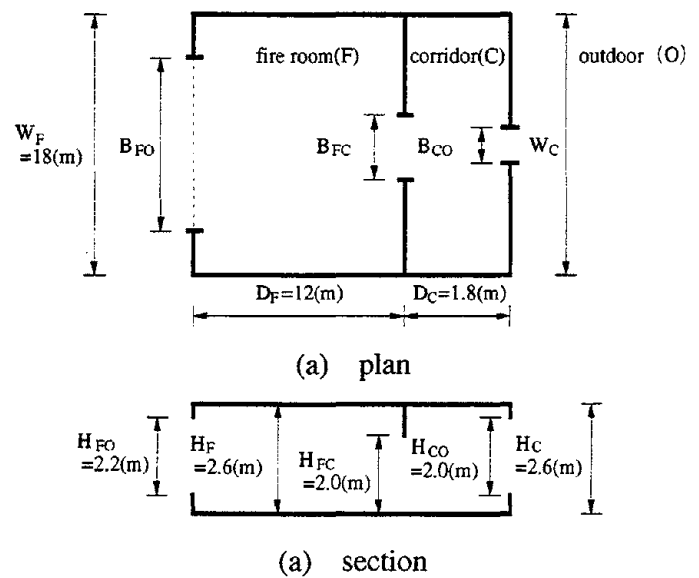


Figure 3 Configuration of the object space

b) Thermal properties of space boundaries

Normal concrete, light weight concrete and ALC are assumed as the boundary walls of the room of origin and the corridor. The thermal properties of each of the walls used in the calculations are shown in Table 2.

Table 2 Wall thermal properties

	conductivity k (kW/m/K)	density ρ (kg/m ³)	specific heat c (kJ/kg/K)	τ (=t/k ρ c)
normal concrete	0.00163	2,250	0.895	0.3t
light weight concrete	0.000523	1,350	1.39	1.02t
ALC	0.000151	600	1.09	10.13t


c) Fire load

The fire load density in the room of origin is fixed at 30 kg/m² for all the cases, and the total fire load is determined by multiplying this value by the floor area.

d) Combination of the conditions

The calculations are made for the combination of the conditions of the space dimensions and the thermal properties of the boundary shown in Table 3. The effect of the condition of a specific factor is investigated by changing the value of the factor while fixing the other factors to the reference values, which are shaded in Table 3.

Table 3 Calculation conditions

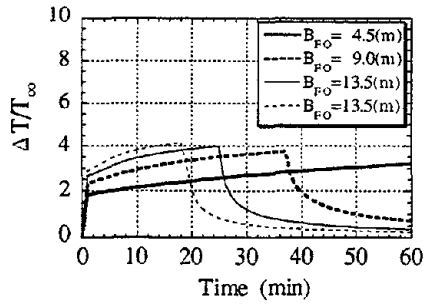
 denote reference value

fire room	dimensions W×D×H (m)	18.0×12.0×2.6			
	fire load density (kg/m ²)	30.0			
	window H _w ×B _w (m)	2.2×4.5	2.2×9.0	2.2×13.5	2.2×18.0
	doorway H _w ×B _w (m)	2.0×1.0	2.0×2.0	2.0×3.0	2.0×4.0
corridor	dimensions W×D×H (m)	9.0×1.8×2.6	18.0×1.8×2.6	27.0×1.8×2.6	36.0×1.8×2.6
	window H _w ×B _w (m)	2.0×0	2.0×1.5	2.0×4.5	2.0×13.5
wall	wall type	normal concrete	light weight concrete	ALC	
	thickness (cm)	10.0			
outdoor (°C)		20.0			

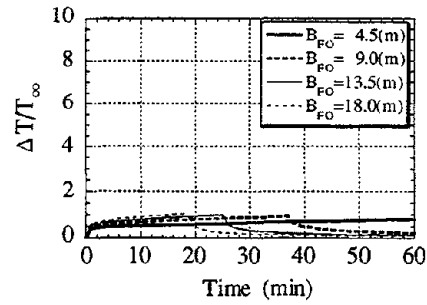
(2) Results of the calculations

The predicted results in Figure 4 illustrates the effect of each factor on the temperatures of the room of origin and the corridor.

It is shown that the conditions of the external opening of the room of origin have a significant effect on the temperatures of the corridor as well as the room of origin. Also, the effect of thermal properties is significant on the temperatures both of the two spaces. The conditions of the openings of the corridor, external and internal, seem to primarily affect the corridor temperature.

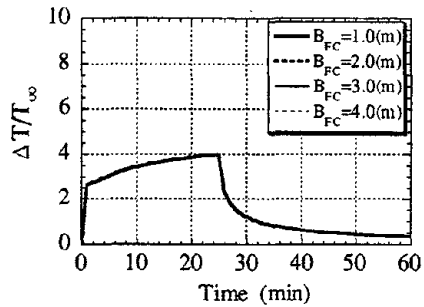


(a) fire room temperature

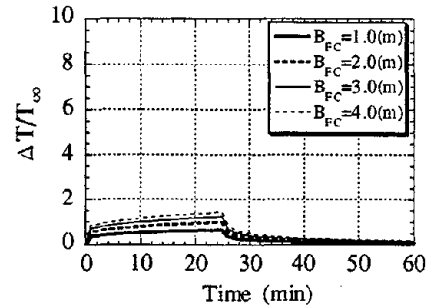


(b) corridor temperature

(1) Effects of fire room window size

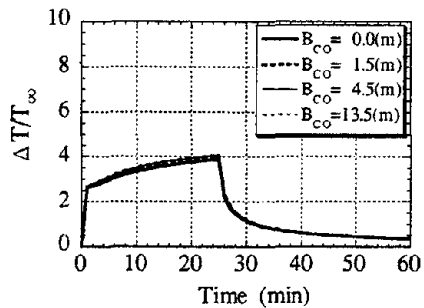


(a) fire room temperature

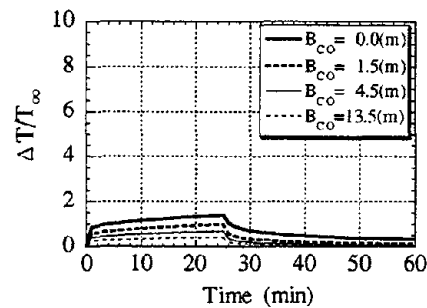


(b) corridor temperature

(2) Effects of doorway size

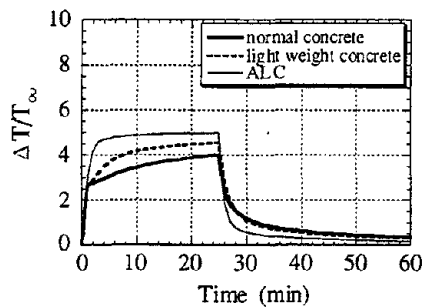


(a) fire room temperature

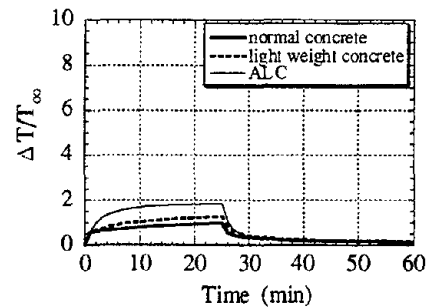


(b) corridor temperature

(3) Effects of corridor window size



(a) fire room temperature



(b) corridor temperature

(4) Effects of wall thermal properties

Figure 4 Effects of factors on fire temperature

3. SIMPLE EQUATIONS FOR FIRE TEMPERATURE

Simple equation for predicting pre-flashover room fire temperature was proposed by Quintiere et al. Here, the equation is extended to the room of origin under ventilation controlled fire and a connected corridor configuration.

3.1 Simple Equations

According to Quintiere et al., the temperature of fire compartment with the heat release rate Q can be reasonably predicted by

$$\frac{\Delta T}{T_{\infty}} \left(= \frac{T - T_{\infty}}{T_{\infty}} \right) = 1.6 \left(\frac{Q}{\sqrt{g C_p \rho_{\infty} T_{\infty} A_w \sqrt{H_w}}} \right)^{2/3} \left(\frac{h_k A_T}{\sqrt{g C_p \rho_{\infty} A_w \sqrt{H_w}}} \right)^{-1/3} \quad (9)$$

with the effective heat transfer coefficient defined as

$$h_k = \left(\frac{k \rho c}{t} \right)^{1/2} \quad (10)$$

Substituting Eqn.(10) into Eqn.(9) and the concrete values of g , C_p , ρ_{∞} and T_{∞} yields

$$\frac{\Delta T}{T_{\infty}} = 0.023 \left(\frac{Q}{A_w \sqrt{H_w}} \right)^{2/3} \left(\frac{A_w \sqrt{H_w}}{A_T} \right)^{1/3} \left(\frac{t}{k \rho c} \right)^{1/6} \quad (11)$$

(1) Temperature of the room of origin

In ventilation controlled fire, the rate of heat released within the compartment Q is controlled by the rate of air supply through the opening. The air inflow rate through an opening in a fully developed fire m_a can be estimated as

$$m_a = 0.5 A_w \sqrt{H_w} \quad (12)$$

On the other hand, the heat release per unit mass of air consumed in combustion is 3,000 kJ/kg-air regardless the kind of fuel, hence, Q becomes as

$$Q = 1,500 A_w \sqrt{H_w} \quad (13)$$

Most of the air available for the combustion in fire compartment is undoubtedly supplied through the opening directly open to the outdoor, but some the air can be supplied through the doorway open to the connected corridor. Figure 5 shows the oxygen concentrations predicted by the computer model described in the above. According to the results, the oxygen concentration quickly becomes zero when the corridor has no opening to the outdoor, but the concentration stays at considerably high level even when the width is considerably small. Hence, we employ the following approximations as

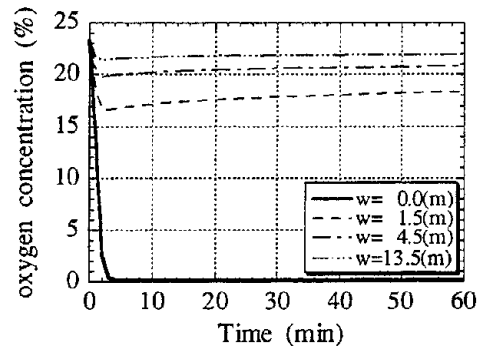


Figure 5 Oxygen concentration in the air through doorway (B_{CO} : doorway width)

a) When there is no opening between the corridor and the outdoor

$$Q = 1,500 A_{FO} \sqrt{H_{FO}} \quad (14-1)$$

b) When there is an opening between the corridor and the outdoor

$$Q = 1,500 (A_{FO} \sqrt{H_{FO}} + A_{FC} \sqrt{H_{FC}}) \quad (14-2)$$

Substituting Eqns.(14-1) and (14-2) into Eqn.(11) yields the equations for the fire room temperatures for the cases:

a) When there is no opening between the corridor and the outdoor

$$\frac{\Delta T_F}{T_\infty} = 3.0 \left(\frac{A_{FO} \sqrt{H_{FO}}}{A_{FO} \sqrt{H_{FO}} + A_{FC} \sqrt{H_{FC}}} \right)^{2/3} \left(\frac{A_{FO} \sqrt{H_{FO}} + A_{FC} \sqrt{H_{FC}}}{A_{T,F}} \right)^{1/3} \left(\frac{t}{k\rho c} \right)^{1/6} \quad (15-1)$$

b) When there is an opening between the corridor and the outdoor

$$\frac{\Delta T_F}{T_\infty} = 3.0 \left(\frac{A_{FO} \sqrt{H_{FO}} + A_{FC} \sqrt{H_{FC}}}{A_{T,F}} \right)^{1/3} \left(\frac{t}{k\rho c} \right)^{1/6} \quad (15-2)$$

respectively, where $A_{T,F}$ is the total surface area of the fire room boundary.

Incidentally, both Eqn.(15-1) and (15-2) become as

$$\frac{\Delta T_F}{T_\infty} = 3.0 \left(\frac{A_{FO} \sqrt{H_{FO}}}{A_{T,F}} \right)^{1/3} \left(\frac{t}{k\rho c} \right)^{1/6} \quad (16)$$

when there is no opening between the room of origin and the connected corridor. This can be used for predicting the temperature of single fire room.

(2) Temperature of the corridor

It is assumed that Eqn.(12) holds for the flow rate through the doorway between the fire room and the corridor, then the rate of heat convected to the corridor is given by

$$Q_C = C_P m_{FC} (T_F - T_\infty) = 150 A_{FC} \sqrt{H_{FC}} \left(\frac{\Delta T_F}{T_\infty} \right) \quad (17)$$

where $T_\infty = 300\text{K}$ is employed.

This Q_C can be considered as the rate of heat given to the corridor. Substituting Q_C into Q in Eqn.(11) and using Eqns.(15-1) and (15-2) yields:

a) When there is no opening between the corridor and the outdoor

$$\frac{\Delta T_C}{T_\infty} = 1.35 \left(\frac{A_{FC} \sqrt{H_{FC}}}{A_{T,C}} \right)^{1/3} \left(\frac{A_{FO} \sqrt{H_{FO}}}{A_{FO} \sqrt{H_{FO}} + A_{FC} \sqrt{H_{FC}}} \right)^{4/9} \left(\frac{A_{FO} \sqrt{H_{FO}} + A_{FC} \sqrt{H_{FC}}}{A_{T,F}} \right)^{2/9} \left(\frac{t}{k\rho c} \right)^{5/18} \quad (18-1)$$

b) When there is an opening between the corridor and the outdoor

$$\frac{\Delta T_C}{T_\infty} = 1.35 \left(\frac{A_{FC} \sqrt{H_{FC}} + A_{CO} \sqrt{H_{CO}}}{A_{T,C}} \right)^{1/3} \left(\frac{A_{FC} \sqrt{H_{FC}}}{A_{FC} \sqrt{H_{FC}} + A_{CO} \sqrt{H_{CO}}} \right)^{2/3} \left(\frac{A_{FO} \sqrt{H_{FO}} + A_{FC} \sqrt{H_{FC}}}{A_{T,F}} \right)^{2/9} \left(\frac{t}{k\rho c} \right)^{5/18} \quad (18-2)$$

respectively, where $A_{T,C}$ is the total surface area of the corridor boundary.

(3) The parameters determining temperature

According to Eqns.(15-1), (15-2), (18-1) and (18-2), the temperatures of the room of origin and the corridor are determined by the following 5 parameters defined as:

$$\tau = \frac{t}{k\rho c}$$

$$K_F = \frac{A_{FO}\sqrt{H_{FO}}}{A_{FO}\sqrt{H_{FO}} + A_{FC}\sqrt{H_{FC}}} \quad F_{O,F} = \frac{A_{FO}\sqrt{H_{FO}} + A_{FC}\sqrt{H_{FC}}}{A_{T,F}} \quad (19)$$

$$K_C = \frac{A_{FC}\sqrt{H_{FC}}}{A_{FC}\sqrt{H_{FC}} + A_{CO}\sqrt{H_{CO}}} \quad F_{O,C} = \frac{A_{FC}\sqrt{H_{FC}} + A_{CO}\sqrt{H_{CO}}}{A_{T,C}}$$

In fact, as can be seen in Figure 6, which demonstrates some examples of the predictions using the above computer model for the different conditions having the same values of the parameters, the temperatures become the same except for the difference due to the duration of fire.

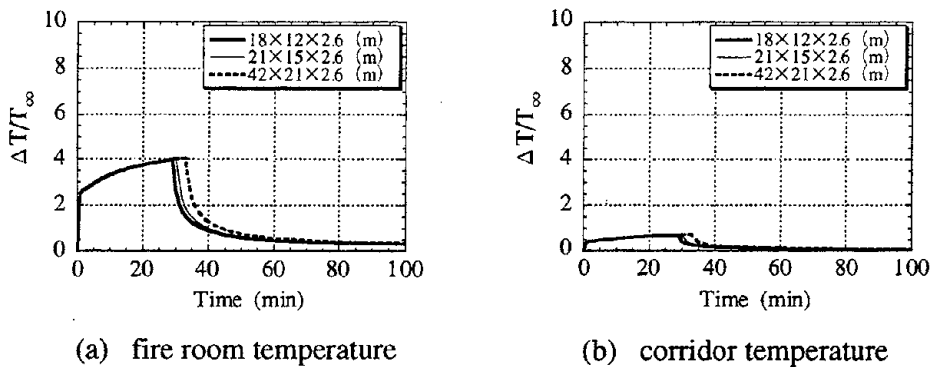


Figure 6 Temperatures for the same parameter

3.2 Comparison between the Predictions by the Computer Model and the Simple Model

The applicability of the simple model is studied by comparing the predictions by the simple model and the computer model for the cases already shown in Table 3. Some examples of the predictions of the temperatures of the fire room and the corridor are shown in Figure 7.

For the cases of concrete boundary, the predictions by the simple model show a fair agreement with the predictions by computer model, and for the cases of light weight concrete boundary, somewhat worse but still acceptable for the period of less than an hour. On the other hand, the discrepancies are huge from very early stage for the case of ALC, whose thermal inertia is remarkably smaller than the others.

4. REFINED SIMPLE EQUATIONS

4.1 Wall Thermal Properties and Transient Change of Fire Temperature

According to the results shown in Figure 7, in which the temperature predicted by the simple equations and the computer model are compared for real time t , the accuracy of the simple equation seem

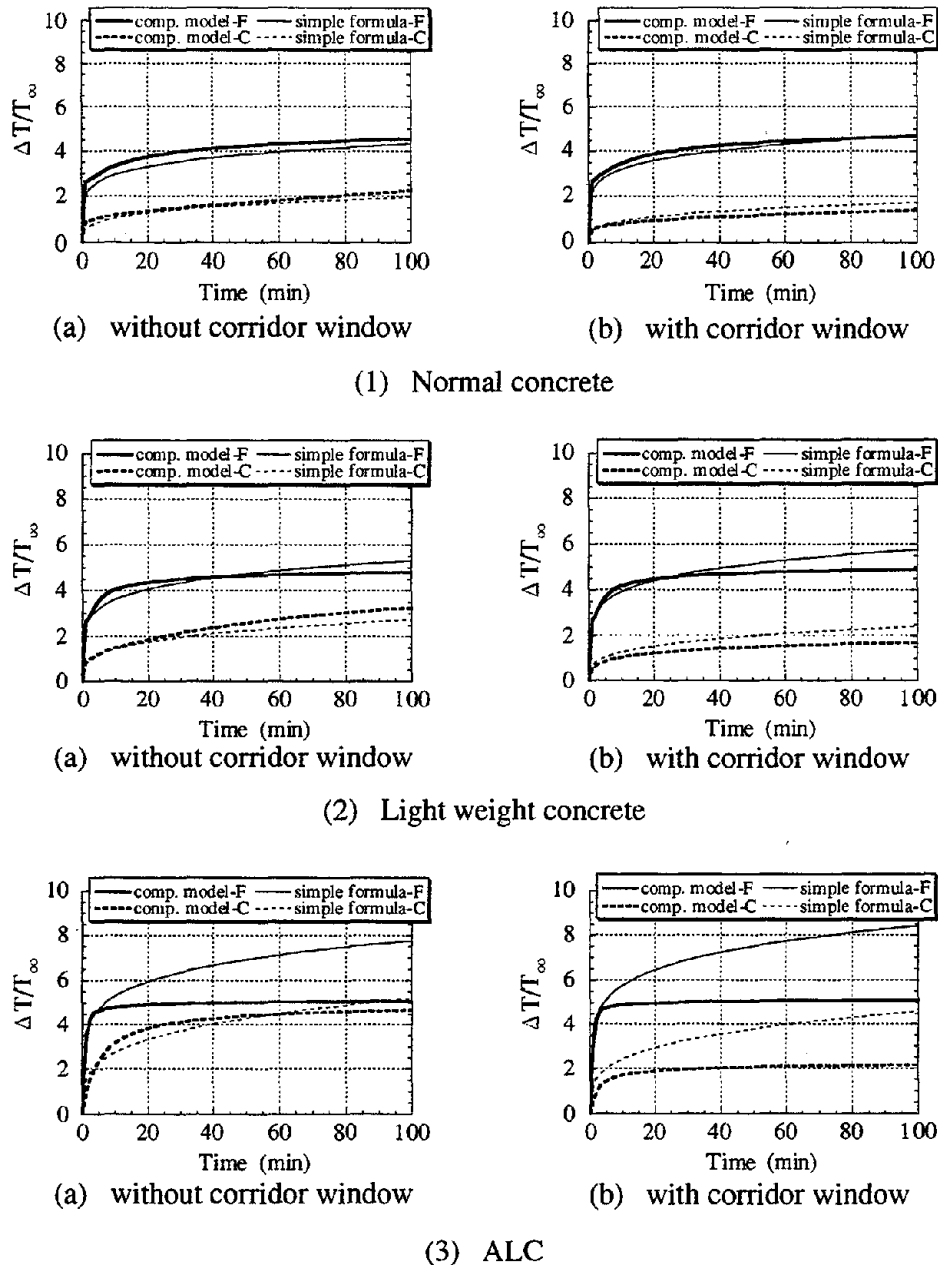


Figure 7 Comparison between the simple formulas and computer model

to become lower as the space boundary wall becomes more thermally insulative. However, the difference between the simple equation and the computer model becomes the same regardless the difference of the boundary wall if we compare the predictions for the parameter t shown in Eqn.(19). In fact, as is demonstrated by the sample calculations shown in Figure 8, the temperatures change along the same curve for any of the three kinds of wall materials as long as the dimensions of the spaces and the openings are the same.

The reason why the gap develops between the predictions by the simple equations and the computer model as t becomes large is considered to be partly because the radiative heat loss from the external opening is not taken into account and partly because the heat transfer model is somewhat crude in the simple equations.

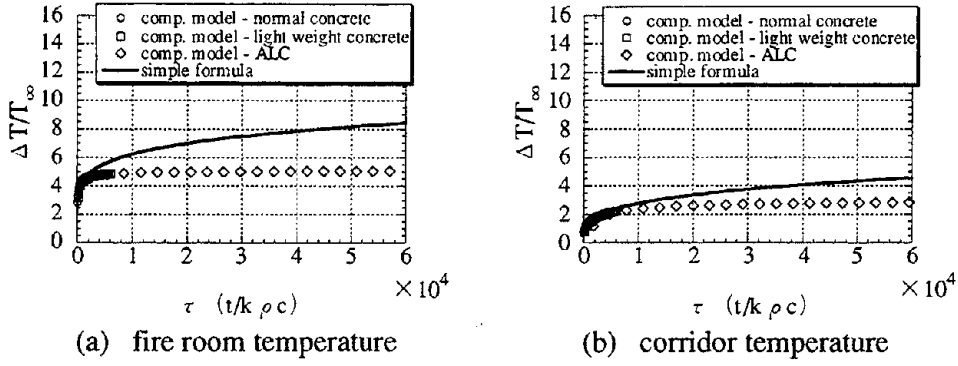


Figure 8 Predicted temperature v.s. τ

4.2 Refinement of The Simple Equations

(1) Fire room temperature

Firstly, the parameter $\beta_{F,1}$ and $\beta_{F,2}$ are defined as

$$\beta_{F,1} = K_F^{2/3} \cdot F_{O,F}^{1/3} \cdot \tau^{1/6} \quad \text{and} \quad \beta_{F,2} = F_{O,F}^{1/3} \cdot \tau^{1/6} \quad (20)$$

respectively. Note that Eqn.(15); the simple equation for the fire room temperature; may be expressed using these parameters as

$$\frac{\Delta T_F}{T_{\infty}} = \begin{cases} 3.0\beta_{F,1} & \text{(without external opening in corridor)} \\ 3.0\beta_{F,2} & \text{(with external opening in corridor)} \end{cases} \quad (21)$$

Next, let's consider the ratio of the fire room temperature predicted by the computer model to the parameters defined by Eqn.(20) as follows:

$$\gamma_{F,1} = \left(\frac{\Delta T_F}{T_{\infty}} \right) / \beta_{F,1} \quad \text{and} \quad \gamma_{F,2} = \left(\frac{\Delta T_F}{T_{\infty}} \right) / \beta_{F,2} \quad (22)$$

Figure 9 shows the ratios $\gamma_{F,1}$ and $\gamma_{F,2}$ plotted for $\beta_{F,1}$ and $\beta_{F,2}$, respectively. The relationship in Figure 9 may be expressed by the following regression formulas which hold regardless the wall thermal properties as

a) When there is no opening between the corridor and the outdoor

$$\gamma_{F,1} = \begin{cases} 3.50 + (\beta_{F,1} - 1.00) & (\beta_{F,1} \leq 1.00) \\ 3.50 - (\beta_{F,1} - 1.00) & (\beta_{F,1} > 1.00) \end{cases} \quad (23-1)$$

b) When there is an opening between the corridor and the outdoor

$$\gamma_{F,2} = \begin{cases} 3.25 + (\beta_{F,2} - 1.25) & (\beta_{F,2} \leq 1.25) \\ 3.25 - (\beta_{F,2} - 1.25) & (\beta_{F,2} > 1.25) \end{cases} \quad (23-2)$$

Substituting Eqns.(23-1) and (23-2) into Eqn.(22) yields the refined formulas for fire room temperature which better agree with the predictions by computer model as follows:

a) When there is no opening between the corridor and the outdoor

$$\frac{\Delta T_F}{T_\infty} = \begin{cases} \beta_{F,1}(2.50 + \beta_{F,1}) & (\beta_{F,1} \leq 1.00) \\ \beta_{F,1}(4.50 - \beta_{F,1}) & (\beta_{F,1} > 1.00) \end{cases} \quad (24-1)$$

b) When there is an opening between the corridor and the outdoor

$$\frac{\Delta T_F}{T_\infty} = \begin{cases} \beta_{F,2}(2.00 + \beta_{F,2}) & (\beta_{F,2} \leq 1.25) \\ \beta_{F,2}(4.50 - \beta_{F,2}) & (\beta_{F,2} > 1.25) \end{cases} \quad (24-2)$$

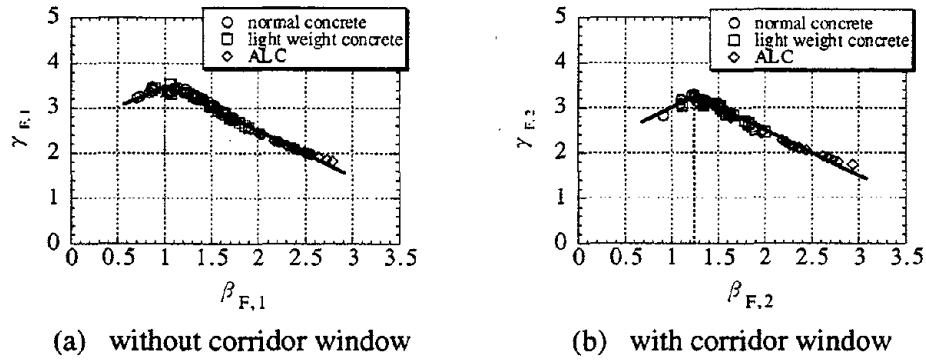


Figure 9 Ration of computed fire room temperatures to β_F

(2) Corridor temperature

Similarly with fire room temperature, the parameters for corridor temperature $\beta_{C,1}$ and $\beta_{C,2}$ are defined as follows:

$$\beta_{C,1} = K_F^{4/9} \cdot F_{O,C}^{1/3} \cdot F_{O,F}^{2/9} \cdot \tau^{5/18} \quad \text{and} \quad \beta_{C,2} = K_C^{2/3} \cdot F_{O,C}^{1/3} \cdot F_{O,F}^{2/9} \cdot \tau^{5/18} \quad (25)$$

respectively. Note that Eqn.(18); the simple equation for corridor temperature; may be expressed using these parameters as

$$\frac{\Delta T_C}{T_\infty} = \begin{cases} 1.35\beta_{C,1} & (\text{without external opening in corridor}) \\ 1.35\beta_{C,2} & (\text{with external opening in corridor}) \end{cases} \quad (26)$$

Next, let's consider the ratio of the corridor temperature predicted by the computer model to the parameters defined by Eqn.(25) as follows:

$$\gamma_{C,1} = \left(\frac{\Delta T_C}{T_\infty} \right) / \beta_{C,1} \quad \text{and} \quad \gamma_{C,2} = \left(\frac{\Delta T_C}{T_\infty} \right) / \beta_{C,2} \quad (27)$$

Figure 10 shows the ratios $\gamma_{C,1}$ and $\gamma_{C,2}$ plotted for $\beta_{C,1}$ and $\beta_{C,2}$ respectively.

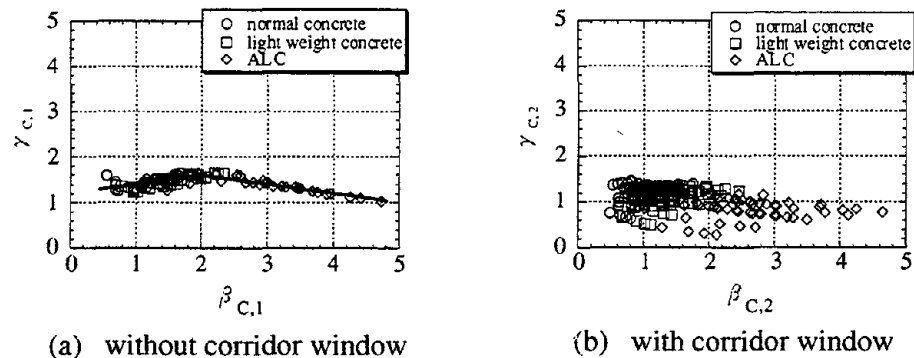


Figure 10 Ration of computed corridor temperatures to β_C

a) When there is no opening between the corridor and the outdoor

As can be seen in Figure 10 (a), when there is no opening between the corridor and the outdoor the ratio $\gamma_{C,1}$ converge reasonably well with the use of parameter $\beta_{C,1}$ regardless the wall type. The regression line may be expressed as

$$\gamma_{C,1} = \begin{cases} 1.60 + 0.20(\beta_{C,1} - 2.00) & (\beta_{C,1} \leq 2.00) \\ 1.60 - 0.20(\beta_{C,1} - 2.00) & (\beta_{C,1} > 2.00) \end{cases} \quad (28)$$

Substituting Eqn.(28) into Eqn.(27) yields the equation which agree better with the computer prediction than Eqn.(18-1) as follows:

$$\frac{\Delta T_C}{T_\infty} = \begin{cases} \beta_{C,1}(1.20 + 0.20\beta_{C,1}) & (\beta_{C,1} \leq 2.00) \\ \beta_{C,1}(2.00 - 0.20\beta_{C,1}) & (\beta_{C,1} > 2.00) \end{cases} \quad (29)$$

b)When there is an opening between the corridor and the outdoor

On the other hand, when there is an opening between the corridor and the outdoor, the conversion of the data is poor. In Figure 11 (a) and (b), the temperatures predicted by the computer model are plotted versus $\beta_{C,1}$, for the cases without opening, and $\beta_{C,2}$, for the cases with an opening, respectively. As can be seen, while the temperatures for the cases without opening contract to the same line, those for the cases with an opening spread to asymptotically reach at different values as $\beta_{C,2}$ increases. We have not succeeded to find the parameter which brings nice conversion, however, Eqn.(18-2) may be used for many practical cases where the boundary wall is not extremely insulative.

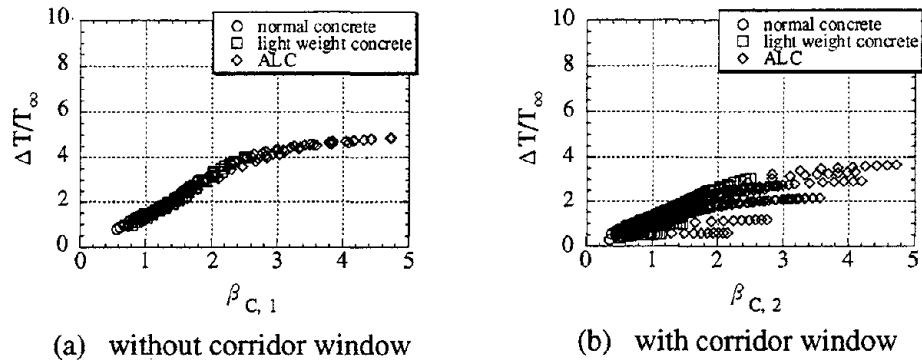


Figure 11 Computed corridor temperatures v.s. β_c

4.3 Comparison of the Predictions by the Computer Model and the Simple Formulas

Figure 12 compares the predictions by the computer model and the refined simple equations for fire room temperature, i.e. Eqns.(24-1) and (24-2), and for corridor temperature for the cases without opening, i.e. (29). The conditions of the calculations are the same as those in Figure 6. It may be said that an excellent agreement has been attained by the refinement.

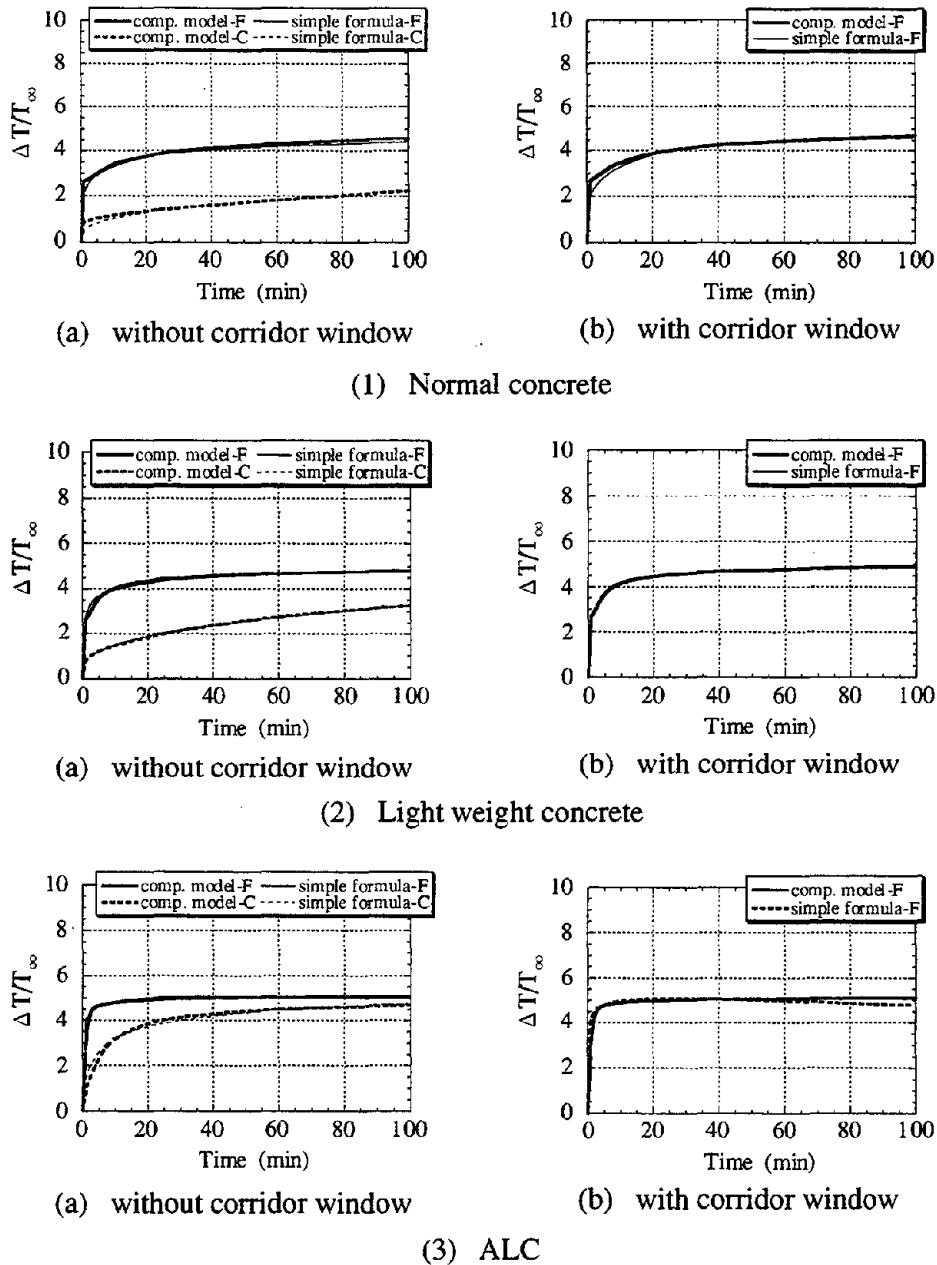


Figure 12 Comparison of the predictions by the computer model and the refined simple formulas

5. CONCLUSION

Simple formulas for predicting the temperatures of ventilation controlled fire room and the connecting corridor were developed. By the use of the formulas, the fire room temperature can be predicted as accurately as by the use of the computer model regardless the wall type. The temperature of the corridor connected to the fire room can be predicted as well when there is no opening between the corridor and the outdoor. The formulas are more advantageous than the computer model in that the parameters affecting the temperature are explicitly known by the user in addition to the accessibility.

NOMENCLATURE

A	: Area (m ²)
B	: Opening width (m)
c	: Specific heat of wall (kJ/kgK)
C_P	: Specific heat of gas at constant pressure (kJ/kgK)
D	: Depth of room (m)
g	: Acceleration due to gravity (m/s ²)
H	: Height (m)
ΔH_{O_2}	: Heat of combustion per unit mass of oxygen consumed (kJ/kg)
ΔH_{wood}	: Heat of combustion of wood (kJ/kg)
h_k	: Effective heat transfer coefficient (kW/m ² K)
k	: Thermal conductivity of wall (kW/mK)
M	: Mass burning rate (kg/s)
m	: Mass opening flow rate (kg/s)
n	: Number of rooms
P	: Relative pressure (Pa)
Q	: Heat release rate (kW)
Q_C	: Combustion heat release rate (kW)
Q_R	: Radiative heat loss through opening (kW)
Q_W	: Heat loss to wall (kW)
T	: Temperature (K)
ΔT	: Temperature difference (K)
t	: time (s)
V	: Room volume (m ³)
W	: Room width (m)
Y_{O_2}	: Mass fraction of oxygen
Z_n	: Height of neutral plane (m)
α	: Opening flow coefficient
ε	: Emissivity
ρ	: Density (kg/m ³)
σ	: Stefan-Boltzmann constant (kW/m ² K ⁴)

Subscript

C	: Corridor
D	: Door
F	: Fire room
O	: Outdoor
T	: Total
i	: Arbitrary room
j	: Room connected to room i
ij	: From room i to room j , Between room i and j

REFERENCES

1. K. Matsuyama, T. Fujita, H. Kaneko, Y. Ohmiya, T. Tanaka, T. Wakamatsu: A Simple Predictive Method for Room Fire Behavior, J. Struct. Construct. Eng., AIJ, No.469 (1995.3)
2. T. Tanaka and K. Nakamura: A Model for Predicting Smoke Transport in Buildings -Based on Two Layer Zone Concept-, Report of The Building Research Institute, No.123, (1989.10)
3. B. J. McCaffery, J. G. Quintiere, and M. F. Harkleroad: Estimating Room Temperatures and the Likelihood of Flashover Using Test Data Correlation, Fire Technology, Vol. 17, No.2, 98-119 (1981)

Discussion

Patrick Pagni: I have two questions. First, the formula for the heat transfer coefficient is only good for a semi-infinite medium. The time that the heat transfer coefficient is good for is the length squared of the thickness divided by 16α , where α is the thermal conductivity. You might compare that time for the three different materials and see if that would explain the difficulty with the ALC.

Takeyoshi Tanaka: Actually, Prof. Quintiere gave us an effective heat transfer for two stages. One is the transitional stage and then a steady stage. We checked the two cases, but we got funny results, so we decided to use only the transitional stage.

Patrick Pagni: Second, in the calculation of the temperature in the room of origin in the case with the corridor window, you don't have an expression that takes into account the size of the corridor window. As I read the paper, it's only the size of the window between the room and the corridor. Is that a possible explanation for why the agreement could not be found with the simple expression?

Takeyoshi Tanaka: With respect to the size of the corridor, we used the total surface area of the wall.

Patrick Pagni: No. I mean the temperature within the room, not within the corridor.

Takeyoshi Tanaka: With respect to temperature of the room, the hypothesis here is very simple. We thought that air coming from the corridor would have some effect on ignition of the fire, so we did not take into consideration the size of the corridor in this calculation. The purpose of this calculation is not to get a very precise agreement on temperatures. Rather, we wanted to develop the calculation method which would enable us to get the approximate number. For that reason, we did not consider a complicated factor here.

Zone Model Plume Algorithm Performance

Dr. John A. Rockett
Fire Modeling & Analysis

Abstract

Four plume algorithms used by three zone type building fire simulators are evaluated against experiential data of Steckler and Nakaya. Significant differences in the room flow predictions are found with even the best performing plume algorithms predicting flows well below the measured values. Differences in plume behavior is attributed to (1) the background noise (turbulence) present when the data used in formulating the algorithms was collected, and (2) the inability of the plume algorithms to easily simulate the effect of plume blowing.

The behavior of the McCaffrey plume in situations where the over-fire region dominates the plume flow is discussed.

Key words

Room fires, plumes, zone fire models

Introduction

It is appropriate, in a seminar honoring Prof. Kawagoe, to take up the subject of room fire modeling, a field in which he made pioneering and major contributions.

Some years ago the author coded into Harvard V/NIST FIRST six of the then published plume algorithms.[1,10] Their performance was compared with data from Steckler [2] and used to assess the probable behavior of a proposed Fire Fighter Training Facility for the U.S. Navy.[3] This and additional experience in using some of these plume algorithms suggested at least three problems: (1) their behavior in tall buildings where the over-fire part of the plume was dominant,[4] (2) their ability to predict behavior of plumes from large fires,[3] and (3) their capability to express the behavior of plumes subject to a cross wind - for example, a door jet.[5] An additional problem associated with door jets - the behavior of the plume when the fire straddled the edge of the door jet - was encountered.[6] This situation can result in considerable swirl in the plume as studied by Emmons and Ying.[7] Recently the effect of background turbulence on plume entrainment, noted by Zukoski,[8] has appeared.

A major ISO program to assess and calibrate fire models has recently started.[9] The first test description has been circulated to participants who must now return simulations for comparison with undisclosed test data. This first test is a single room, not unlike that used by Steckler.[2] The ISO program again raises questions about the capability of the available plume algorithms. It has stimulated a revisit to the Steckler room data, this time with several zone-type fire simulators. The simulators used were FIRST [10], CFAST20 [11], and BRI2 version VR, a modification of the BRI release version V [12,13,14]. The VR version of BRI2 is not documented at this writing although an English language user's guide is in preparation.

Plume algorithms

The current FIRST includes the same six plume algorithms used earlier, but two of these - the Delichatsios and Hasemi/Tokunaga plumes - did not operate reliably in the current version of FIRST with the Steckler room as input and are not included in this study. The algorithms used are (1) the Thomas/Hinkley modification (M-T-H) of the Morton, Turner and Taylor plume (M-T-T) - their modification displaces downward the point source [15]; (2) an un-displaced M-T-T point source plume (Pt), (3) the McCaffrey plume (McC)[16], and (4) the Cetegen-Kubota-Zukoski plume (C-K-Z)[17]. BRI2VR includes both the Zukoski plume, standard in recent Building Research Institute release versions, and also the McCaffrey plume, transcribed from BRI1. CFAST uses a modified version of the McCaffrey plume. The modification is not so much to the plume algorithm as to the way in which it is imbedded in the overall simulation.[11]

Zukoski's recent re-correlation of the Cal Tech data [18] has not been included in this study because the author was unsure of some details of the procedure.

Effect of ambient turbulence

FIRST allows, as a user input option, adjustment of the plume entrainment coefficient used in the M-T-H and Pt plume algorithms.[10] The default value, $\alpha = 0.1$, is the result of studies early in the development of the Harvard single room simulator in which the M-T-H plume was used and α was varied. The present default value was the one found to give the best overall agreement with the three FM bed-room tests and a number of allied tests in which urethane foam mats (simulated mattresses) were burned in a room. Thus the default α represents the plume entrainment expected in a "normally noisy" room environment.

McCaffrey conducted his tests with a square gas burner "... 0.75 m above the floor and under a passive hood in a large laboratory." [19] There were no screens around the burner. Thus his plume measurements were made, again, in a "normally noisy" room environment.

The McCaffrey and Thomas/Hinkley plumes give similar results where the over-fire region is not important.

Cetegen's data was collected using a steel box placed inside a larger forced flow hood. "Two layers of 16x18 mesh screens made of 0.05 cm diameter wire were hung from the bottom rims of the hood and allowed to fall around the floor, the floor-screen arrangement was used to reduce the strength of the disturbances present in the laboratory ...". [17] Thus the C-K-Z plume data was collected in a relatively noise free environment.

It will be seen that the C-K-Z plume entrains noticeably less than the M-T-H and McC plumes under similar conditions.

The Delichatsios plume model entered in FIRST is based on FM measurements made in an enclosing tank.[20] Air was fed from a settling chamber below the gas burner, up through screens and a pebble bed. Exhaust was sucked from the top of a conical, converging section of the tank well above the measuring station. Thus the FM data probably represents entrainment from a very low noise level environment. Although the Delichatsios plume model has not been used here, it has been found to entrain somewhat less than the others.[1]

Plume blowing

Quintiere, using the Steckler room, measured the angle of tilt of plumes in a cross wind and estimated the increased entrainment resulting.[21] Their data is for small fires relative to the room size.

If the fire is large enough, relative to the room in which it is found, the plume will penetrate the hot-cool interface while still within its "initial" or "continuous flame" region. In this case, if the C-K-Z plume flow correlation [17] is used, a correction for blowing can be made. Entrainment for the C-K-Z correlation applicable to the flame base depends directly on fire diameter; the correction is to artificially increase the fire diameter by the estimated amount of plume entrainment argumentation.[5] This "fix" will not work for situations where the hot-cool interface is higher because the correlation depends differently on fire diameter for the "intermittent" and "over-fire" regions.

The Thomas/Hinkley plume can be "adjusted" to simulate blown plumes by artificially increasing the fire diameter. The relation between the fire diameter increase and entrainment increase is not linear as is the case with the C-K-Z plume. As mentioned, the Harvard single room simulator includes as, an input item, the plume entrainment coefficient. To correct the M-T-H plume for blowing, rather than adjusting the fire diameter, it appears preferable to increase the default entrainment coefficient.

Vent mixing

All three fire simulators used here include mixing at the vents. Very little data is available against which to test their mixing algorithms. As far as the author knows, the only direct, quantitative measurement of vent mixing is from experiments of Lim, Zukoski and Kubota [22] and from Quintiere et. al.[23] who provide experimental evidence of mixing for fires in a small room. Data from fire experiments can be used to infer mixing based on layer temperatures.[21] However, conclusions about mixing algorithms based on layer temperatures are clouded by the wall/floor heating algorithms used, gas emissivity estimates, modeling of radiation exchange, and convective heat transfer assumptions.

Simulation Procedure

Three room configurations were modeled: Steckler's 2.8 x 2.8 x 2.18 m high room [2], Figure 1; a two room version of much the same experiment [24], Figure 2, and the CIB W14 Scenario A [9], Figure 3. The Steckler report lists 55 room/fire configurations that were tested. Comparisons presented here are for (1) a set of seven tests with four fire sizes with the gas burner fire flush with (0.02 m above actually) and centered on the room floor (A location) and the "6/6" door (0.74 wide by 1.83 m high). (2) A set of four tests with the raised burner in four locations (AR, FR, GR and HR), with a 62.9 kW fire and the 6/6 door. (3) A set of 11 tests with the flush, centered burner operating at fixed output but with varying width doors. (4) Comparisons with the 28 tests of [24]. (5) A brief look at the variation among predictions that might be made for the ISO-W14 fire [9].

It is not possible to strictly model the identical fire with the three simulators chosen for this study. Each models the fire somewhat differently. In addition, although the McCaffrey plume algorithm is available and nominally the same for all three models, its use differs in detail. FIRST and BRI2VR include several user selectable plume algorithms. Four from FIRST and the two of BRI2VR were used. CFAST20 [11] uses only a modified version of the McCaffrey plume. In all cases, input for the simulations was made as much alike as

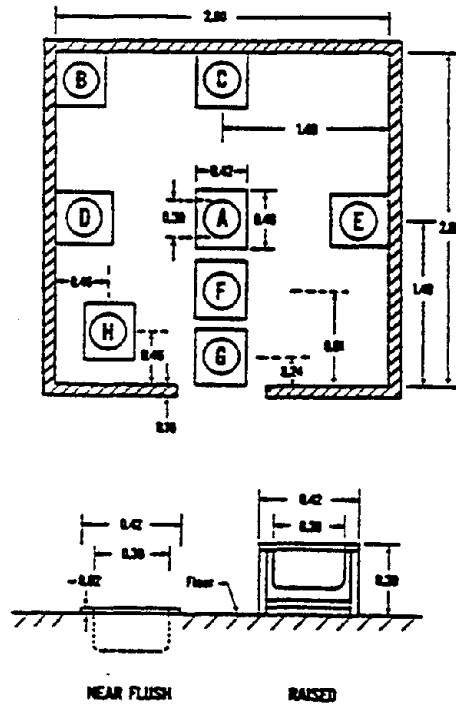


Figure 1: Steckler room: plan, burner locations, and burner arrangement.

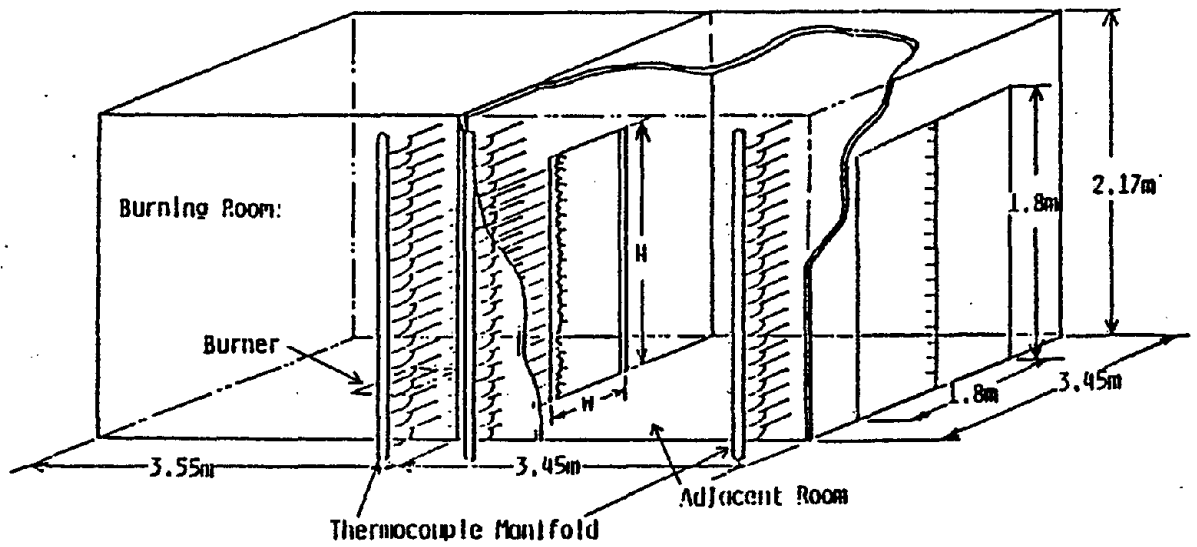


Figure 2: Nakaya et. Al. 2 room facility and instrument placement.

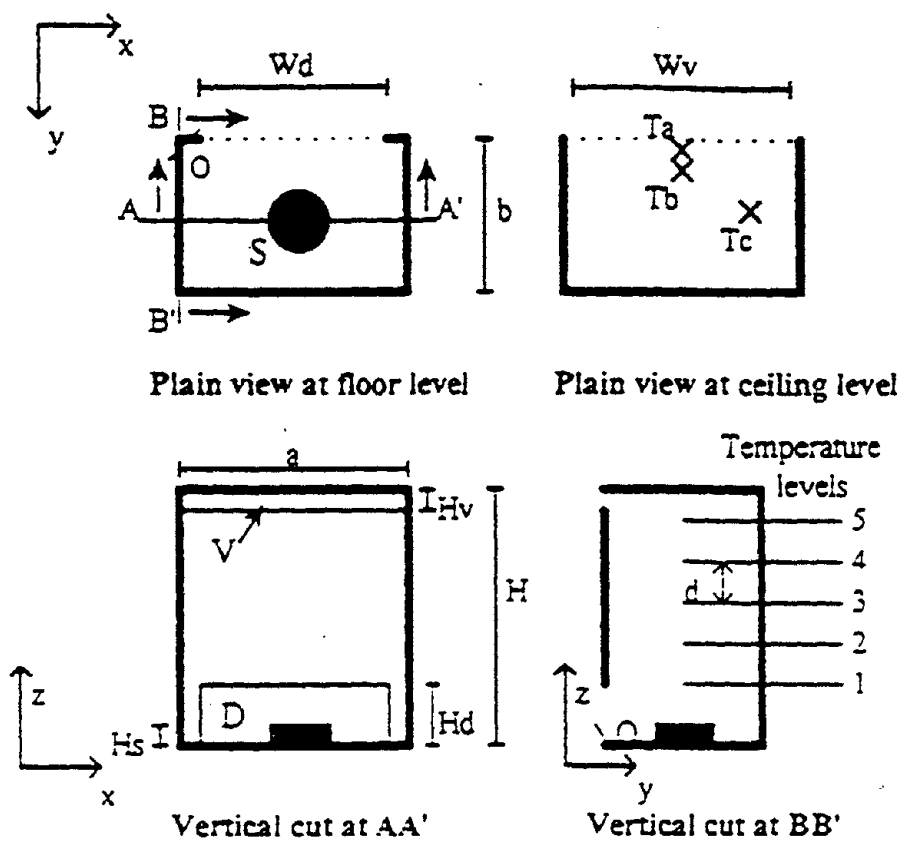


Figure 1. Basic scenario A.

Table 2. Properties of the different wall types in scenario A.

Wall name	Thickness (mm)	Conductivity (W/m.K)	Specific heat (J/kg.K)	Density (kg/m ³)	Surface emissivity
Wall1	10	0.16	900	790	0.9
Wall2	220	0.8	1000	1600	0.94
Wall3	560	0.8	1000	1600	0.94
Wall4	10	0.036	795	105	0.9

Figure 3: ISO W14 scenario A test room.

possible. It is believed that the results presented here reflect primarily differences in the plume algorithms and the way in which they are used.

The two-room simulation report, [24], lists fuel flow rates in [l/min]. These were converted to [kg/s] using a propane density, from [25], of 2.014 [g/l] at 0 C. Thus a flow of 100 [l/min] at 20 C converted to 0.003054 [kg/s]. This flow rate yielded slightly different rates of heat release for BRI2V (129.28 [kW]) and CFAST20 (140.0 [kW])¹, although both used the same heat of combustion 46,450 [kJ/kg] - the value provided for Propane in the BRI2V data base. This value is close to the 46,343 [kJ/kg] in [26] for the higher heat of combustion and 46,600 based on 13.1 [MJ/kg-O₂] used. Lewis and von Elbe [27] list a value which, after units conversion, is 50,374 [kJ/kg] and NFPA [28] a similar number - 49,982 [kJ/kg]. Figure 6 of [24] suggests their estimate of heat release rate for 100 [l/min] to be about 170 [kW] (implied heat of combustion 55,700 [kJ/kg]). Data is presented here based on fuel flow rate, rather than heat release rate. The 46,450 [kJ/kg] value for Propane was used with all three simulators. The results for a given set of room conditions depend weakly on rate of heat release; conclusions drawn here should not change if fires from each simulator released the same heat.

All simulations were run to 3600 simulation seconds although essentially steady state was achieved at about 1800 seconds.

Simulation Comparisons

1) Variation of vent flow as a function of fire rate-of-heat-release for fixed fire location and vent geometry

The fire chosen was at Steckler's location A: centered in the room, its surface 0.02 m above the floor; the "6/6" door was used. Figure 4a compares BRI2VR simulations for (1) the Cetegen-Kubota-Zukoski plume [17], (2) the McCaffrey plume [16] and (3) the Steckler data [2]. Figure 4b is a similar comparison for CFAST20, and Figure 4c for four plume algorithms from FIRST. For these simulations, the C-K-Z plume entrains less than the McCaffrey plume resulting in a thinner, hotter upper layer and lower door flow (layer temperature data not shown here).

All the plume models predict lower entrainment than the data suggests.

Figures 5a and b compare two-room simulations of the tests of [24] with the test data. Only flow through the burn room to foyer door is considered. BRI2VR simulations with the McC plume were very

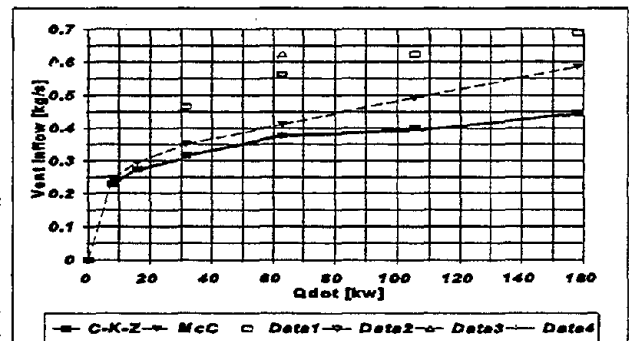


Figure 4a: Steckler room, A location, 6/6 door; data and BRI2VR simulations.

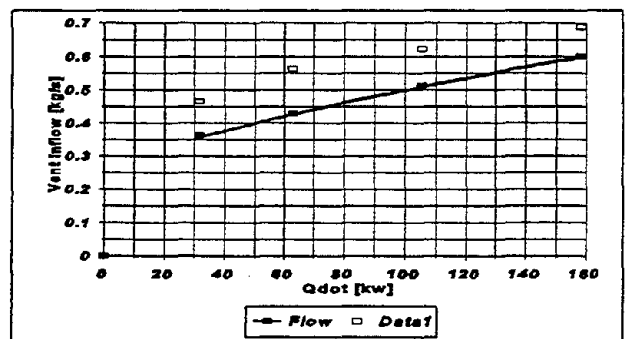


Figure 4b: Steckler room, A location, 6/6 door; data and CFAST20 simulations.

¹ CFAST20 rounds the fuel flow rate from 0.0030524 (entered) to 0.0031. This accounts for only a small part of the difference.

close to the CFAST20 results and are not shown in figure 5a. The predicted flows are generally less than the experimental values over rates of heat release similar to those of Steckler. At higher heat release rates the predicted flows approach and sometimes slightly exceed the measured values. The figure includes simulations and data for all the reported Nakaya runs - the effect of heat release rate and of door width are presented on a single plot. Figure 5b compares the McC and C-K-Z plume (BRI2VR) for two door widths - the narrowest, 0.29 m, and the widest, 0.89 m. The C-K-Z plume gave generally similar flows to the McC plume and the data for the narrowest door, but was well below the data and below the McC results for the widest door.

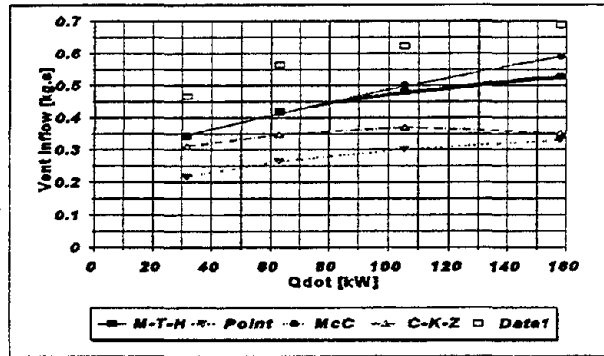


Figure 4c: Steckler room, A location, 6/6 door; data and FIRST simulations.

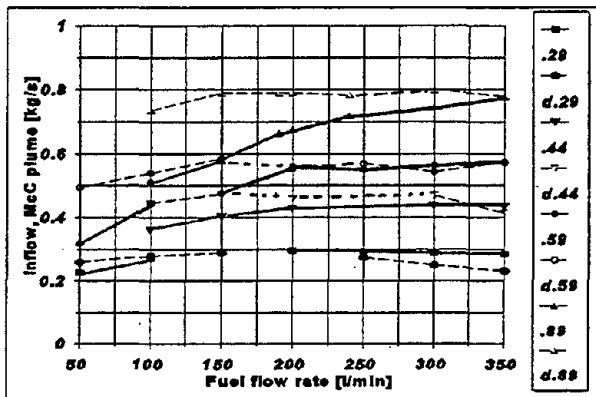


Figure 5a: Nakaya et. al. 2 room test; rm 1 data and CFAST20 simulations.

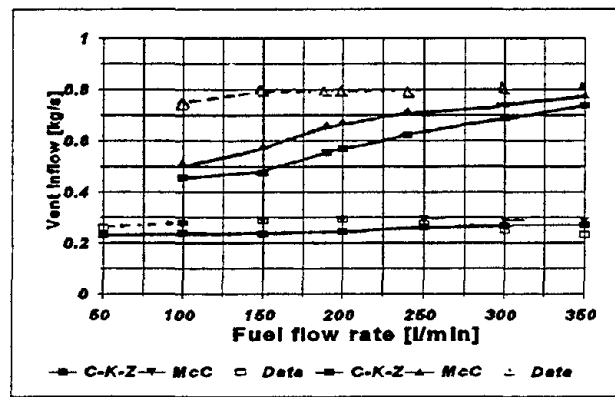


Figure 5b: Nakaya et. al. 2 room test; rm 1 data and BRI2VR simulations.

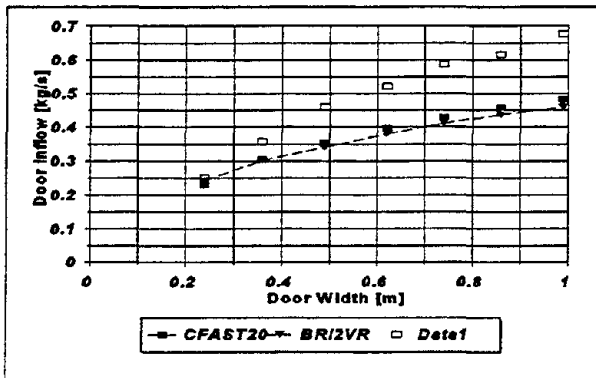


Figure 6: Steckler room, A location, 62.9 kW fire; vent inflow as a function of door width, CFAST 20 and BRI2VR, McC plume.

Figure 6 shows the variation of door inflow as the door width was varied. The fire was centered in the room (Location A) and the fire fixed at 62.9 kW. BRI2V and CFAST results, using the same plume are very similar. A similar comparison may be inferred from the data of figure 5.

Figure 7a compares CFAST lower layer temperatures with the Steckler data. Simulations are presented for Kaowool and concrete. [2] describes the room as: "The lightweight walls and ceiling were covered with a ceramic fiber insulation board..." The floor is not described but was "Marinite" over plywood on wood joists. Marinite is a low density mineral board.[29, p12]; Kaowool is less conductive than Marinite. CFAST was used to compare the effect of the floor material as it allows definition of the ceiling, walls, and floor separately. FIRST uses the same material for all the room surfaces; BRI2 uses one material for the ceiling and upper walls, another for the lower walls and floor. Figure 7b shows lower layer temperature comparisons with

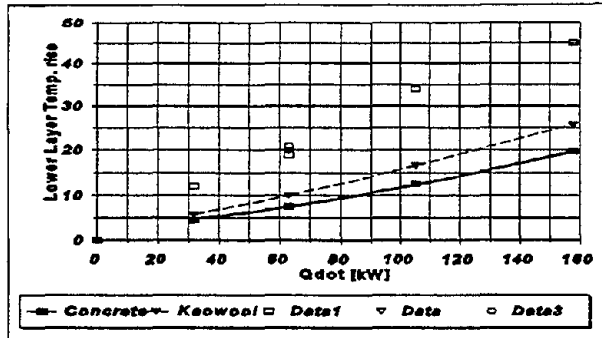


Figure 7a: Steckler room, A location, 6/6 door; lower layer gas temperature for two floor materials, CFAST simulations.

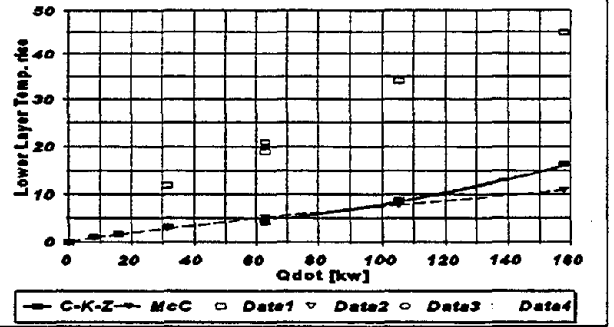


Figure 7b: Steckler room, A location, 6/6 door; lower layer gas temperature for two plume algorithms, BRI2VR simulations.

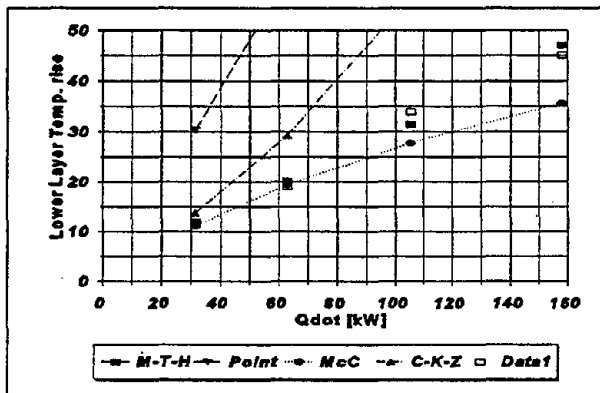


Figure 7c: Steckler room, A location, 6/6 door; lower layer gas temperature for four plume algorithms, FIRST simulations.

BRI2VR and Figure 7c for FIRST. It is seen that the CFAST20 and BRI2VR predictions are all well below the data. FIRST, which uses a data based vent mixing algorithm, does well with the M-T-H and McC plumes but over predicts lower layer temperatures for the other two. Due to a lack of data, similar plots can not be made for the runs of [24].

Not shown are comparisons of upper layer temperature and layer thickness. The lower plume flows resulted in hotter, thinner layers.

A correction for wall flows was made in [1]. This was small and would not change any of the above results.

2) Steckler room: Variation of fire location for fixed fire size and vent

The Steckler tests and these simulations used the "raised fire": burner surface 0.30 m above the floor, and a 62.9 kW fire. Fire locations AR, FR, GR, and HR were examined with the 6/6 door. Figure 8 compares the predictions with data for four fire locations. BRI2VR treats all fire locations alike. FIRST and CFAST20 request fire location as part of the input. However, for these simulations, it was found that FIRST and CFAST gave identical results for the four fire locations considered, hence only one entry is made for each model. It is seen that all the simulated flows are well below the data. Since no correction was made for blowing, this is not surprising for the AR, FR and GR locations. The HR location is close to, but away from the walls in a location

where it should not have been blown by the door jet nor was it close enough to the jet edge to have induced swirl.² Nevertheless, this fire location resulted in a significantly larger door flow than the models predicted.

The ratio of the highest predicted flow (Figure 8, CFAST) to the measured HR flow is 3/4.

The increase of entrained flow as the fire was moved toward the door, AR->FR->GR, suggests the effect of plume blowing. Quintiere et. al. [21], provide a way of estimating the enhanced entrainment due to a cross wind, in this case the door jet. Their paper is based on data obtained using the Steckler room. Substituting numbers in their formula gives an estimated maximum dimensionless cross wind, $V = v/u = 0.309$ for the 62.9 kW fire. This would decrease as the location of interest moved into the room since v , the average gas velocity, would decrease toward 0 at the rear wall. The associated decreased blowing is clear from the GR->FR->AR data. One estimate of the entrainment argumentation is to compare the blown plumes to the sheltered one (HR location). The ratio of the AR to HR flows is 1.08 and for the GR to HR, 1.19

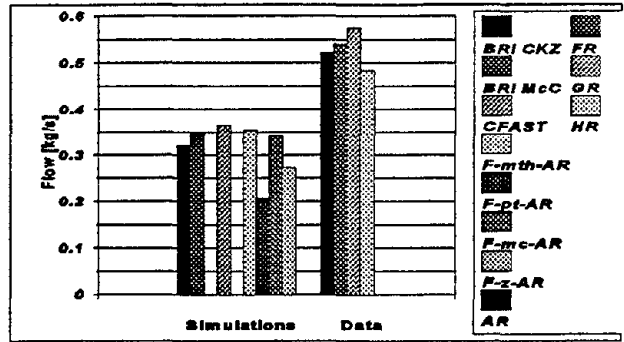


Figure 8: Steckler room, door inflow versus fire location; BR12VR, CFAST, FIRST, data.

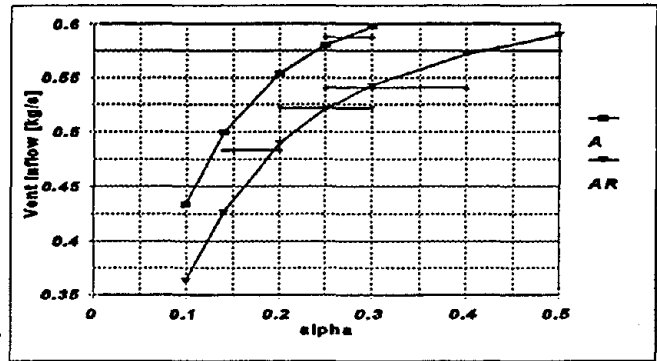


Figure 9: Steckler room, A location, 6/6 door, M-T-H plume; variation of inflow as plume entrainment coefficient, alpha, is varied.

3.) Simulations with FIRST and the M-T-H plume and variable plume entrainment coefficient, alpha

Figure 9 shows the effect on the Steckler room, 62.9 kW fire, 6/6 door inflow as the M-T-H plume entrainment coefficient, alpha, is varied. The two curves are for the fire at the A (flush) and AR (raised) locations. To bring the predicted A location door flow up to the average of four tests, 0.588 [kg/s], alpha had to be increased from 0.1 to 0.275. To obtain agreement between prediction and test data for the AR location required an increase from 0.1 to 0.250. In order to make the prediction agree with test for the GR location, alpha had to be made 0.415, for the FR location, 0.295 and, for the HR location, 0.195. These increases would include only the effect of blowing if it is assumed that the noise level in the absence of blowing has already been subsumed in the Harvard/FM selected default, 0.1. Table 1 lists other calculated values and their experimental measurements for several inputs and alphas.

² The author never witnessed a test with the fire in the HR location. At that time, Rininen had a small, table top model room - ceiling and walls with door opening placed over a fixed burner set into a large "floor". The room box could be moved relative to the burner. When the box was positioned so that the plume was entirely within the door jet it was blown back toward the rear of the room. When the room was moved so that the plume approached the edge of the door jet it began to swirl vigorously. Still further movement toward the side of the room brought the plume into relatively still air. It was quiet but leaned slightly toward the corner of the room without actually touching the corner. It is understood that the AH burner location was found by trial, the burner being moved toward the side wall until it became quiet. A slight movement back toward the door jet would produce intermittent swirl. The AH position avoided this. Nevertheless, the plume must have been in a region with considerable secondary flows.

Table 1

Comparison of predicted and measured values for various alpha

Location	Calculation FIRST M-T-H plume					Steckler data			
	alpha	flow	del Tul	Layer	del Tll	flow	del Tul	Layer	del Tll
A	.1	0.434	128.23	1.196	20.21				
	.25	0.581	93.92	0.833	16.77	.588	100.	.985	20.3
AR	.1	0.363	155.22	1.325	28.91				
	.25	0.521	105.74	1.010	15.82	.522	130.	1.26	15.
FR	.3	0.543	101.09	0.950	15.70	.541	122.	1.14	17.
GR	.4	0.572	95.54	0.861	16.30	.575	110.	1.09	21.
HR	.2	0.490	113.00	1.088	16.69	.483	143.	1.26	12.

ISO, scenario A

The prescribed input for this is 90 [kW] from time 0 to 10 s, 180 [kW] 10-30 s and 90 [kW] 30-300 s. The room has two vents, a low, wide door, 3.4x1 [m] high open throughout and a window just under the ceiling, 3.6x0.2 [m] high open after 120 s. During the first 30 s the flow is dominated by heat addition (gas expansion). Later the effect of the plume algorithm choice is seen. It is clearest during the steady burning period after the window opening transient has been passed, after about 150 s. The dimensionless cross wind, $V = v/u_c = 0.20$, was found from preliminary simulation results which included no correction for plume blowing. If the plume entrainment were increased v and V would increase. Thus similar plume blowing to that for the Steckler room might be anticipated. From the above, one could surmise that the zone models will under-predict the flow through the room, over predict upper layer temperature and under predict the upper layer thickness, unless a plume blowing correction is made.

Discussion

Blown plumes in noisy spaces

Above it was suggested that varying alpha for the M-T-H plume might be used to correct the entrainment for blowing and noise. From figure 9 it is seen that this is both a substantial and very non-linear correction. Changing alpha with the M-T-H plume changes the basic entrainment in direct proportion. Thus a change from $\alpha = 0.1$ to 0.25 should produce 2.5 times the flow. However, in a room, the stronger entrainment causes the layer to move down so that entrainment occurs over a shorter length of plume. Hence the diminishing return as alpha is increased and the shape of the curve in figure 9. It has been argued above that the M-T-H plume with $\alpha = 0.1$ has been corrected for typical noise except possibly for the HR location. For the A location the blowing effect would be the difference between 0.434 [kg/s] (Table 1 and figure 4c) and 0.588 (average of 4 tests). These flows are in the ratio of 1:1.4. From figure 9 it is seen that increasing alpha from .1 to .14 did not yield the desired flow. An increase to about $\alpha = 0.25$ was needed. A factor of 2.5 increased flow due to blowing is within the expected range for a V of about 0.3.[21] Table 1 shows that when the calculated and measured flows have been made to agree, the calculated layer interface is too low and the upper layer temperature too low. Changing the wall thermal properties changes the predicted response of the room. The wall values used and the default heat transfer coefficients of FIRST apparently do not reproduce the test conditions. Apparently,

too much heat was lost to the walls. With less wall heat loss the alpha correction to yield equal vent inflow would be somewhat smaller than those of Table 1. Upper layer temperature and thickness would be improved.

To match the experimental flow at the HR location, an alpha of about 0.2 was needed. Considering that the default 0.1 presumably accounts for normal noise levels for room experiments where the room is in an open laboratory, this seems rather a large correction. The HR plume location would appear from the simulations done here to have been either subjected to an abnormally noisy background or not to have been completely free of swirl.

A weakness of the M-T-H plume is its lack of detail. The McC and C-K-Z algorithms distinguish between the flame and over-fire regions. With the M-T-H plume there is only one region.³ For many applications this may not matter. However, what is needed is usable data correlations that separately distinguish the effect of background noise and of blowing with appropriate input parameters available to the user to allow recognition of these evidently important effects. Presumably the added mixing associated with high noise levels and/or blowing would change the plume region boundaries, thus there appears no simple "correction" that can be used in general. If, as mentioned above, the interface will always be low enough to expose only the lowest plume region, a simple area correction can be used for the C-K-Z plume. It must correct for both noise and blowing, since the correlation is based on a relatively quiet surround. The author's experience with this correction has not been uniformly successful.

In reconstructing actual fires, it is the exception, rather than the rule to find the fire directly in the unobstructed door jet of a room. Furniture may be between the door and the fire, or the location of the fire may place it out of the jet's direct path. In the case of obstructions, the noise level at the fire may be unusually high. In the case of fires away from the door, it may be difficult to estimate the local blowing velocity. To a limited extent Quintiere [21] looked at this problem. The effect of both doors and windows were examined, but only fires flush with the floor were included. They did not measure local velocity near the fire; an upper limit estimate for blowing velocity was provided. Local turbulence levels were not measured nor were fires away from the room center or out of the direct path of the jet included.

The modeler has several options: the fire may be modeled using several plumes (for example, C-K-Z and M-T-H) to bracket the effect of "normal" noise. Similarly, blowing may be bracketed by estimating the maximum and minimum blowing velocities and varying alpha, with the M-T-H plume, to cover this range. If the noise and blowing effects are small, this may be sufficient. However, it has been seen in the case of the Steckler room that blowing may increase plume entrainment by a factor of about three over still air. In the case of the HR fire location, presumably local noise increased room inflow in the ratio of 0.35:0.48 or about 37% (equivalent alpha double the normal noise value).

Data is clearly needed to provide the fire simulators with documented plume algorithms able to represent the various entrainment regimes of the fire plume and, in addition, allow input parameters such that they are capable of expressing the effect of local noise and blowing. Additional tests to document local blowing and turbulence levels in realistic fire situations would be very useful.

³ The theory of [1] extended the Fang variation of Steward's analysis.[30] This analysis included burning over the lower part of the plume. The flame length was close to the experimental values without artificial increasing it as Steward had done. The plume necked in strongly near its base as did the Steward and Fan models. The model depends on entrainment coefficient, alpha, similarly to the M-T-T plume so could be used to estimate blowing.

Plumes in tall spaces

A major problem with the McCaffrey plume is its behavior in the over-fire region. The Morton-Taylor-Turner theory, and much experimental data suggests that the plume entrainment in the over-fire region should depend on height raised to the $5/3$ power. The McCaffrey correlation uses the 1.895 power.[16] This may be related to his plume width assumption. It results in what appears to be a severe over-prediction of plume flows far above the fire. The author found theoretical support for the McCaffrey's correlation in the immediate over-fire region but the flow prediction changed rapidly with height, resulting in a shift to the $5/3$ power.[1]

The original BRI simulator[31] used the McC plume but, with BRI2, a shift was made to the C-K-Z algorithm. Justification for this change may be found in [12], pp 98-100. Here experimental data from three fire tests in a 23.7 m high, domed Sumo Hall are compared with BRI2 calculations. The experimental and calculated values for the descent of the hot layer and of its temperature as functions of time are presented. Satisfactory agreement was found. The calculations used only the C-K-Z plume.

Figure 10 shows FIRST simulations of the main concourse of New York's Grand Central Terminal. This is a 93.6 x 61.3 x 36.6 m high room ventilated by doors at floor level and forced exhaust just below the ceiling. The simulations were for a 5 MW fire on the floor and 140 m³/s forced exhaust. It is seen that the McC plume results in a much lower hot-cool interface than the M-T-H or C-K-Z plumes. To bring the McC predicted interface up to the level of the other two required almost 350 m³/s exhaust. The cost differential between fans of 350 versus 140 m³/s capacity for this building alone would probably cover the cost of an experimental program to settle the issue of which algorithm (if any) is correct.

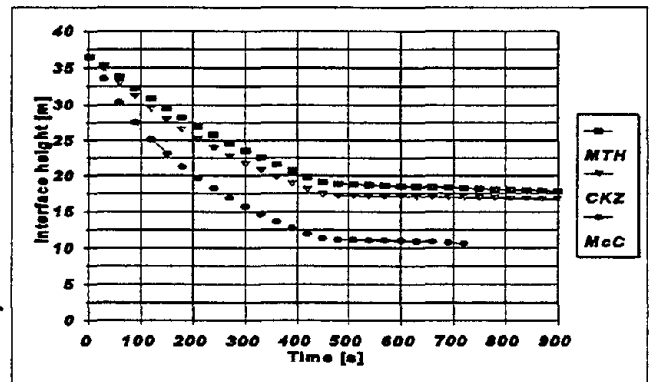


Figure 10: Descent of the hot layer, 36.6 m high room, 140 m³/s exhaust at ceiling; three plumes, FIRST simulations.

Conclusions

The McCaffrey plume and Thomas/Hinkley modification of the Morton, Turner and Taylor plume (M-T-H) give the best agreement with both the Steckler and Nakaya data. The M-T-H plume has two advantages over the McC plume: (1) its behavior in the over-fire region seems to accord better with tests of fires in high rooms, and (2) it can be "adjusted" for plume blowing by using an entrainment coefficient increased over the preferred value for normally noisy, still air. The C-K-Z plume gives lower entrainment for fires of the size and Q^* range of the Steckler room but better results for the larger fires and Q^* ranges of the Nakaya tests. It may be preferable to the McC plume, based on high-bay tests where the over-fire region dominated. All the plumes studied, if uncorrected for blowing, gave generally lower entrainments than the data. This may be because they are based on experimental data obtained under relatively quiet conditions as compared with actual room-fire test conditions. At present there is insufficient data available to make a quantitative assessment of the effect of background turbulence level on plume entrainment.

An experimental program is needed to document the local blowing velocity and turbulence levels in a wider range of room fire situations than has been tested. From these tests, correlations which will assist the modeler in assessing the local environment of his particular fire should be developed.

An experimental and theoretical program is needed leading to well documented plume models which can (1) represent the various entrainment/burning regimes of the fire and (2) capture the effects of blowing and local turbulence levels (3) be documented for a wider range of fire sizes (i.e.: larger) than present models. They should be structured to allow a user to input local turbulence and blowing conditions.

An experimental and theoretical program is needed to document the interlayer gas mixing at vents between rooms of a multi-room building. The present algorithms are plausible, but insufficiently supported by experimental data and appear to be inaccurate. Logically based correlations should be developed from the experimental data and reduced to algorithms usable in present zone building fire models.

References

- 1] Rockett, J.A., "A Comparison of Plume Entrainment Models", unpublished. Some of the material from this paper appears in Section 7 of
Rockett, J.A., "Using the Harvard/NIST Mark VI Fire Simulation", NISTIR 4464, U.S. National Bureau of Standards, Gaithersburg, MD 20899, November 1990
- 2] Steckler, K.D., Quintiere, J.G. and Rinkinen, W.J., "Flow Induced by Fire in a Compartment", NBSIR 82-2520, U.S. National Bureau of Standards, Gaithersburg, MD 20899, September 1982
- 3] McCaffrey, B.J., Rockett, J.A. and Levine, R.S., "Naval Fire Fighting Trainers - Effect of Ventilation on Fire Environment (Model Calculations for 19F3 FFT)", NBSIR 85-3238, U.S. National Bureau of Standards, Gaithersburg, MD 20899, December 1985
- 4] Rockett, J.A., Howe, J.M. and Hanbury, W.D., "Modeling Fire Safety in Multi-use Domed Stadia", J. of Fire Prot. Eng. 6(1), 1994, pp 11-22
- 5] Rockett, J.A., Keski-Rahkonen, O. and Heikkila, Liisa, "HDR reactor containment fire modeling with BRI2", VTT Publications 113, VTT, Technical Research Centre of Finland, Espoo, 1992
- 6] Rockett, J.A., "Park Service Room Fire Test Simulations Using the Harvard Level 5.2 Computer Fire Model", NBSIR 83-2085, U.S. National Bureau of Standards, Gaithersburg, MD 20899, June 1984
- 7] Emmons, H.W. & Ying, S-J, "The Fire Whirl", Eleventh Symposium on Combustion, International, The Combustion Institute, Pittsburgh PA 1967, pp 475-488
- 8] Zukoski, E.E. (personal communication): In early plume entrainment tests the door to the large laboratory room was often open and no screens were placed around the plume apparatus. To reduce scatter in the data, for subsequent tests, the laboratory door was kept closed and turbulence suppressing screens surrounded the apparatus. Data scatter was much reduced, but the flows recorded appeared to be 28-30% less than in the "noisy" room.
- 9] Keski-Rahkonen, O. and Hostikka, S., "CIB W14 Round Robin of Code Assessment; Design Report of Scenario A", VTT Building Technology, VTT, Technical Research Centre of Finland, Espoo, 1995

- 10] Mitler, H.E. and Rockett, J.A., "User's Guide to FIRST, A Comprehensive Single-room Fire Model", NBSIR 87-3595, U.S. National Bureau of Standards, Gaithersburg, MD 20899, September 1987
- 11] Peacock, R.D., Forney, G.P., Reneke, P., Portier, R. and Jones, W.W., "CFAST, the Consolidated Model of Fire Growth and Smoke Transport", NIST Tech. Note 1299, U.S. National Bureau of Standards, Gaithersburg, MD 20899, February 1993
- 12] Tanaka, T. and Nakamura, K., "A Model for Predicting Smoke Transport in Buildings", Report of the Building Research Institute, No 123, Ministry of Construction, Tokyo Japan, October 1989 (in Japanese)
- 13] Tanaka, T and Nakamura, K, "Predicting Capability of a Multiroom Fire Model", Fire Safety Science, Proceedings of the second international symposium, Hemisphere, 1989
- 14] Yamada, S. and Tanaka, T., "A model for predicting concentrations of carbon monoxide in building fires", Fire Safety Science, Proceedings of the fourth international symposium, IAFSS 1995
- 15] Thomas, P.H. and Hinkley, P.L., "Design of roof-venting systems for single-story buildings", Fire Res. Tech. Paper No 10, Her Majesty's Stationary Office, London, 1964
- 16] McCaffrey, B.J., "Momentum Implication for Buoyant Diffusion Flames", NIST, May 1982
- 17] Cetegen, B.M., Zukoski, E.E. and Kubota, T., "Entainment and flame geometry of fire plumes", Cal. Inst. of Tech., Daniel and Florence Guggenheim Jet Propulsion Center, Pasadena, CA, August 1982
- 18] Zukoski, E.E., "Mass Flux in Fire Plumes", Fire Safety Science - Proceedings of the Fourth International Symposium, IAFSS, 1994, pp 13
- 19] McCaffrey, B.J., "Purely buoyant diffusion flames: some experimental results", NBSIR 79-1910, U.S. Nat. Bureau of Stds, Gaithersburg MD 20899, October 1979
- 20] Delichatsios, M.A., "Air entrainment into buoyant jet flames and open pool fires", FMRC, Norwood MA 02062, August 1985
- 21] Quintiere, J.G., Rinkinen, W.J. and Jones, W.W., "The effect of room openings on fire plume entrainment", Comb. Sc. and Tech., 18, pp 1-19
- 22] Lim, C.S., Zukoski, E.E. and Kubota, T., "Mixing in Doorway Flows and Entrainment in Fire Plumes", Cal. Inst. of Tech., Pasadena, CA, June 1984
- 23] Quintiere, J.G., McCaffrey, B.J. and Harkleroad, M., "The Burning of Wood and Plastic Cribs", Products Research Committee, December 1979
- 24] Nakaya, I., Tanaka, T. and Yoshida, M., "Doorway Flow Induced by a Propane Fire", Fire Safety Journal, 10 (1986) 185-195
- 25] Hodgman, C.D., "Handbook of Chemistry and Physics", Chemical Rubber Publishing Co., 1943

- 26] "Fuel Flue Gases, 1941 ed", Am. Gas Assoc.
- 27] Lewis, B. and von Elbe, G., "Combustion, Flames and Explosions of Gases", 2nd ed, Academic Press 24, 1961
- 28] "Fire Protection Handbook, 14th Ed.", Nat. Fire Prot. Assoc., Boston, 1976
- 29] Gross, D., "Data Sources for Parameters Used in Predictive Modeling of Fire Growth and Smoke Spread", NBSIR 85-3223, U.S. National Bureau of Standards, Gaithersburg, MD 20899, September 1985
- 30] Fang, J.B., "Analysis of the behavior of a freely burning fire in a quiescent atmosphere", NBSIR 73-115, Nat. Bur. of Stds, Washington D.C., 20234, February 1973
- 31] Tanaka, T., "A model of multiroom fire spread", NBSIR 83-2718, U.S. Nat. Bur. of Stds., Gaithersburg, MD 20899, August 1983

Table 1

Comparison of predicted and measured values for various alpha

Location	Calculation FIRST M-T-H plume					Steckler data			
	alpha	flow	del Tul	Layer	del Tll	flow	del Tul	Layer	del Tll
A	.1	0.434	128.23	1.196	20.21				
	.25	0.581	93.92	0.833	16.77	0.588	100.	0.985	20.3
AR	.1	0.363	155.22	1.325	28.91				
	.25	0.521	105.74	1.010	15.82	0.522	130.	1.26	15.
FR	.3	0.543	101.09	0.950	15.70	0.541	122.	1.14	17.
GR	.4	0.572	95.54	0.861	16.30	0.575	110.	1.09	21.
HR	.2	0.490	113.00	1.088	16.69	0.483	143.	1.26	12.

Table 2

Upper and lower layer mass balances, Nakaya 2 room test, .89 door, 350 l/min fire.

C-K-Z, Rm 1 door inflow: 0.73904		McC, Rm 1 door inflow: 0.66797	
Room 1, layer: 1.30 m		Room 1, layer 0.57 m	
Lower layer, T: 218.59 C		Lower layer, T: 82.87 C	
Inflow [kg/s]		Inflow [kg/s]	
Door AA	0.73904	Door AA	0.66797
Fuel flow	<u>0.01068</u>	Fuel flow	0.01068
Total	0.74972	Mixing from ul	<u>0.12305</u>
Outflow [kg/s]		Total	
Penetrating interface	0.26158		0.80170
Door AS	0.00003	Outflow [kg/s]	
Door AA	<u>0.48858</u>	Penetrating interface	
Total	0.75019		<u>0.80188</u>
Excess out	0.00047	Excess out	
			0.00018
Upper layer, T: 788.57 C		Upper layer, T: 490.98 C	
Inflow [kg/s]		Inflow [kg/s]	
Penetrating interface	<u>0.26158</u>	Penetrating layer	0.80188
Total	0.26158	Door AS	<u>0.11104</u>
Outflow [kg/s]		Total	
Door SS	0.26170		0.91292
Excess out		Outflow [kg/s]	
	0.00012	Door SS	
		Door SA	
		Mixing to ll	
		Total	
		Excess out	
			0.00014

Table 2 continued

Room 2, layer height 1.30 m		Room 2, layer height: 1.25	
Lower layer, T: 34.41 C		Lower layer, T: 33.38 C	
Inflow [kg/s]		Inflow [kg/s]	
Door AA	0.98335	Door AA	1.00890
Mixing from ul	0.00003	From rm 1 SA	<u>0.39246</u>
From rm 1, AA	<u>0.48858</u>		
Total	1.47196	Total	1.40136
Outflow [kg/s]		Outflow [kg/s]	
To outside AA	0.14889	To outside AA	0.08419
To rm 1 AA	0.73904	To rm 1 AA	0.66797
Mixing to ul	<u>0.58422</u>	To rm 1AS	0.11104
		Mixing to ul	<u>0.53828</u>
Total	1.47215	Total	1.40148
Excess out	0.00019	Excess out	0.00012
Upper layer, T: 323.08 C		Upper layer, T: 350.23 C	
Inflow		Inflow	
From rm1 SS	0.26170	From rm 1 SS	0.39755
Mixing from ll	0.58422	Mixing from ll	<u>0.53828</u>
From rm 1AS	<u>0.00003</u>	Total	0.84595
Total	0.93583		
Outflow		Outflow	
To outside SA	0.84594	To outside SA	<u>0.93595</u>
Mixing to ll	<u>0.00003</u>		
Total	0.84597		
Excess out	0.00002	Excess out	0.00012

Discussion

Edward Zukoski: I have a couple of comments. The first one is that I think we do not distinguish well enough between the flaming region and the far field plume. The data we have are not well digested, but they certainly show that there is a marked difference between the near field where the fire is visible and the far field where the heat addition is virtually zero. We also have to worry about Q^* or something like Q^* . In that Factory Mutual data that John talked about, the flames were very long, skinny flames, almost jet-like flames, whereas most fires are about not much more than times two of the burning area height. The second comment is that we need a lot more data. We have good data for 20 cm and 50 cm burners; and if you're going to use an offset, you can't get there from here. McCaffrey's data is based on a single sized burner and the larger fires that Phil Thomas and Hinkley analyzed many years ago and more recently showed unambiguously that the diameter was an important parameter. Thank you.

Mathematical Modeling for Building Fire

Masahiro Morita

Department of Applied Mathematics,
Faculty of Science,
Science University of Tokyo

1-3 Kagurazaka, Shinjuku-ku,
Tokyo 162, JAPAN

ABSTRACT

Theoretical and experimental numerical analysis have proposed the capable of being executed computational finite difference method for fire induced natural convective heat flow using the viscous heat conductive compressible fluid with $K-\epsilon$ model in the fire compartment. Because two-point upwind difference scheme give the numerical viscosity, the computational results are different from the approximate solutions at the large velocity. The practical stability and the truncation errors for computing finite difference equations approximating fire governing equations have been introduced by theoretical numerical analysis. The sensitivities of numerical solutions have been evaluated by the theoretical and experimental numerical analysis. As the results of numerical experiments we proposed that the reasonable time interval and space mesh size are chosen considering the CPU time. Furthermore we have introduced the Re^* for the equation of motion or Pe^* for the equation of energy. We proposed that the values of Re^* and Pe^* indicate the trust in the approximate solutions in consequence of the numerical experiments.

1. Introduction

The numerical computations of a natural convective flow have been studied mainly in fluid dynamics [1]. In applied mathematics the theoretical and numerical analysis of Navier-Stokes (N-S) type equations have been investigated [2]. Ladyzhenskaya [2] proposed that the unique solution and the existence of analytical solution of N-S equation for the incompressible fluid flow are not guaranteed in high Reynolds number and only guaranteed at small Re number (less than about 100) at the initial and boundary conditions. The mathematical analysis for the compressible fluid flow does not be reported yet. None the less, the computer simulations for the field model applied to the fire phenomena have been reported by Hasemi [3]. However it is necessary to investigate the methods of numerical solution of the non-linear parabolic partial difference equations which are the basic governing fire equations.

Because most workers using numerical methods for the convection terms in the governing equations have adopted two-point upwind difference scheme, the computational results

do not give us the approximate solution because numerical viscosity is left out of consideration. Furthermore there is need to know how the truncation errors are dependence upon the time and space meshes in a fire problem influence the numerical solution.

In this paper, we have conducted calculations with several numerical computational finite difference methods for fire induced heat flow in the fire compartment using viscous heat-conductive compressible fluid (K- ϵ model) and have made a comparison with the computational results. Since numerical experiments are a difficult computational problem requiring considerable computer power, the problem was tackled using a super computer. We have also investigated the sensitivities of the numerical solutions with the time and space meshes by using numerical experiments, and investigated the stabilities of computational scheme.

2. Governing Equation

Fire induced heat flow of the growth and spread fire must be represented the compressible viscous fluid flow because of high temperature. However the heat flow of the smoldering fire is enough to represent the incompressible viscous fluid flow.

Mathematical field modeling for the heat flow represents two methods. Lagrange method is adopted that heat flow is treated by the moving fluid particles. It can be expressive of the appearance of the induced fluid flow. On the other hand, Euler method means that the heat flow is presented each flow pattern in a moment of fire. Euler method is in general used because of easier treatment than Lagrange method. The fire field model is important to model the turbulence for the fire induced heat flow with flow properties such as flame, plume and jet stream which are described maximum Reynolds number, maximum Prandtl number and Grashof number etc. of heat flow by experiments.

There are two kinds of equations which are the dimensional equations and nondimensional equation. Until now the nondimensional equation is used for the fire simulational equation. This is never the best model because the nondimensional mesh size is depend upon the size of fire domain and is not represent the real size. However the nondimensional mesh size and the eddy length for the turbulence should have a close connection with each other.

The classification of numerical methods for turbulence of Navie-Stokes type equations follows:

(1) Direct method

(2) Average method

(2-1) Time average method

(2-1-1) Integral method

(i) Entrainment method

(2-1-2) Differential method

(2-1-2-1) Turbulence viscous model

• 0-equation model

(i) Mixing length model

(ii) Cebeci-Smith model

- 2-equation model
 - (i) $K - \epsilon$ model
- (2-1-2-2) Stress equation model
 - Bradshaw's 1-equation model
 - 3-equation model
- (2-2) Space average method
 - (i) Large Eddy Simulation (LES) model
- (2-3) Ensemble average method

Let us consider a series of the governing equations of the turbulent natural convection by using turbulent viscous transport model which is mathematically obtained by Reynolds decomposition in a fire compartment [3]. The well known field equations governing the thermophysical and thermochemical dynamics, and heat/mass transfer of a turbulent fluid are described, in principle, by the following set using Cartesian coordinate system.

2.1. Equation of continuity

$$\frac{\partial \bar{\rho}}{\partial t} + \frac{\partial \overline{\rho u_j}}{\partial x_j} = 0$$

or

$$\frac{\partial^2 \bar{P}}{\partial x_i^2} = \frac{\partial^2 \bar{\rho}}{\partial t^2} + \frac{\partial^2}{\partial x_i \partial x_j} \left\{ \bar{\tau}_{ij} + K \left(\frac{\partial \overline{\rho u_j}}{\partial x_i} + \frac{\partial \overline{\rho u_i}}{\partial x_j} \right) - \overline{\rho u_i u_j} \right\} - g \frac{\partial \bar{\rho}}{\partial x_2}$$

2.2. Equation of Motion

$$\frac{\partial \overline{\rho u_i}}{\partial t} + \frac{\partial \overline{\rho u_i u_j}}{\partial x_j} = -\frac{\partial \bar{P}}{\partial x_i} + \frac{\partial}{\partial x_j} \left\{ \bar{\tau}_{ij} + K \left(\frac{\partial \overline{\rho u_j}}{\partial x_i} + \frac{\partial \overline{\rho u_i}}{\partial x_j} \right) \right\} - \delta_{i2} \bar{\rho} g$$

2.3. Equation of energy

$$\frac{\partial \bar{\rho} \bar{h}}{\partial t} + \frac{\partial \overline{\bar{h} \rho u_j}}{\partial x_j} = \frac{\partial}{\partial x_j} \left(\lambda \frac{\partial \bar{\theta}}{\partial x_j} + \bar{\rho} K \frac{\partial \bar{h}}{\partial x_j} \right) + \bar{Q}$$

$$\bar{h} = c_p \bar{\theta}$$

2.4. Equation of state

$$\bar{P} = \bar{\rho} R \bar{\theta}$$

2.5. Transport equation of turbulent energy

$$\frac{\partial \bar{\rho} \bar{q}}{\partial t} + \frac{\partial \overline{\bar{q} \rho u_j}}{\partial x_j} = \frac{\partial}{\partial x_j} \left(\bar{\rho} K \frac{\partial \bar{q}}{\partial x_j} \right) + \mu \frac{\partial^2 \bar{q}}{\partial x_j^2} + g K \frac{\partial \bar{\rho}}{\partial x_2} - \bar{\rho} \bar{\epsilon}$$

$$+ K \frac{\partial \bar{u}_i}{\partial x_j} \left(\frac{\partial \overline{\rho u_j}}{\partial x_i} + \frac{\partial \overline{\rho u_i}}{\partial x_j} \right)$$

2.6 Eddy viscosity and energy decay rate

$$\begin{cases} K = c\bar{q}^2/\bar{\epsilon} \\ \bar{\epsilon} = c\bar{q}^3/l \end{cases}$$

Where $\bar{\rho}$ is density of fluid; x and y are spatial coordinate, horizontal and vertical direction; \bar{u} and \bar{v} are velocity, x - and y - direction; t is time; K is eddy viscosity coefficient; δ is Kronecker delta; g is acceleration of gravity; μ is dynamic viscosity; c_p is heat capacity; $\bar{\theta}$ is temperature; \bar{q} is turbulent energy; $\bar{\epsilon}$ is energy decay rate; λ_θ is thermal conductivity; \bar{h} is enthalpy; \bar{P} is pressure; \bar{Q} is generation of energy; l is Prandtl's length; R is gas constant; $\bar{\tau}$ is viscosity stress.

3. Numerical Computaional Method

We have only discussed the equation of energy, which is the non-linear parabolic 2nd order partial differential equation, in the governing equation because the other equations will be able to deal with the same manner. The energy equation is represented by using rectangular coordinate system; x , y and t for reason of simplifying. The velocities, x - and y -direction, are denoted \bar{u} and \bar{v} respectively. The energy equation is transformed by Reynolds stress [3] as follows;

3.1 Partial differential equation

$$\begin{aligned} \frac{\partial \bar{\theta}}{\partial t} + \bar{u} \frac{\partial \bar{\theta}}{\partial x} + \bar{v} \frac{\partial \bar{\theta}}{\partial y} &= \left(\frac{\lambda_\theta}{\bar{\rho} c_p} + K \right) \left\{ \frac{\partial^2 \bar{\theta}}{\partial x^2} + \frac{\partial^2 \bar{\theta}}{\partial y^2} \right\} \\ &+ \left\{ 2 \frac{K}{\bar{\rho}} \frac{\partial \bar{\rho}}{\partial x} + \frac{\partial K}{\partial x} \right\} \frac{\partial \bar{\theta}}{\partial x} + \left\{ 2 \frac{K}{\bar{\rho}} \frac{\partial \bar{\rho}}{\partial y} + \frac{\partial K}{\partial y} \right\} \frac{\partial \bar{\theta}}{\partial y} \end{aligned}$$

where no generation of internal heat in the equation of energy is adapted $\bar{Q} = 0$.

3.2. Finite difference approximation

As the analitical solutions of fire governing equations are not given yet, the above partial differential equation is transformed to discreat equations by Taylor expansion method etc. For the purpose of obtaining the approximate solution of the energy equation, let $\Delta x, \Delta y$ and Δt be small increments of variables x , y and t ; where $\Delta x = L/I$ and $\Delta y = H/J$, I and J being integers, and L and H being length and height of the domain respectively. The set of point in x, y, t -plane given by $x = i\Delta x$, $y = j\Delta y$ and $t = n\Delta t$; where $i = 0, 1, 2, \dots, I$, $j = 0, 1, 2, \dots, J$ and $n = 0, 1, 2, \dots$; is called a grid whose mesh size is determined by Δx , Δy and Δt . The approximation to $\bar{\theta}(i\Delta x, j\Delta y, n\Delta t)$ is denoted by θ_{ij}^n . In the same way, $\bar{u}(i\Delta x, j\Delta y, n\Delta t)$, $\bar{v}(i\Delta x, j\Delta y, n\Delta t)$, and $\bar{\rho}(i\Delta x, j\Delta y, n\Delta t)$, are denoted by u_{ij}^n , v_{ij}^n and ρ_{ij}^n , respectively. The finite difference equation [4] approximating

the energy equation is obtained

$$\begin{aligned} \frac{\theta_{ij}^{n+1} - \theta_{ij}^n}{\Delta t} + u_{ij}^m \left[\frac{\partial \theta}{\partial x} \right]_{ij}^k \\ = \left[\sigma_{ij}^m + K_{ij}^m \right] \left\{ \frac{\theta_{i+1j}^k - 2\theta_{ij}^k + \theta_{i-1j}^k}{\Delta x^2} + \frac{\theta_{ij+1}^k - 2\theta_{ij}^k + \theta_{ij-1}^k}{\Delta y^2} \right\} \\ + \left\{ \frac{K_{ij}^m \rho_{i+1j}^m - \rho_{i-1j}^m}{\rho_{ij}^m \Delta x} + \frac{K_{i+1j}^m - K_{i-1j}^m}{2\Delta x} \right\} \frac{\theta_{i+1j}^k - \theta_{i-1j}^k}{2\Delta x} \\ + \left\{ \frac{K_{ij}^m \rho_{ij+1}^m - \rho_{ij-1}^m}{\rho_{ij}^m \Delta y} + \frac{K_{ij+1}^m - K_{ij-1}^m}{2\Delta y} \right\} \frac{\theta_{ij+1}^k - \theta_{ij-1}^k}{2\Delta y} \end{aligned}$$

where

$$\begin{cases} \sigma_{ij}^m = \frac{\lambda_\theta}{\rho_{ij}^m c_p} \\ k = \begin{cases} n & \text{explicit scheme} \\ n+1 & \text{implicit scheme} \end{cases} \\ m = \begin{cases} n & \text{decoupled method} \\ n+1 & \text{coupled method} \end{cases} \end{cases}$$

The coupled method is exactly presented the original continuous fundamental equations. However as this method is more complicate for computaions and is difficult to have the computaional stability, it is not general used. Furthermore the computational results of coupled method are almost same values of those decoupled method. The decoupled method is used in our system for above reason. The time derivative term is approximated with two-point backward implicit ($k = n + 1$) time difference scheme. The diffusion terms and first order derivative terms are approximated with five-point or three-point central space difference scheme, respectively. The convection terms $u_{ij}^n \left[\frac{\partial \theta}{\partial x} \right]_{ij}^k$ and $v_{ij}^n \left[\frac{\partial \theta}{\partial y} \right]_{ij}^k$, which are represented by $a \left[\frac{\partial f}{\partial h} \right]_i$, are approximated with following scheme:

3.2.1. Central difference scheme

$$a \left[\frac{\partial f}{\partial h} \right]_i = \frac{f_{i+1} - f_{i-1}}{2\Delta h}$$

3.2.2 Two-point upwind difference scheme

$$a \left[\frac{\partial f}{\partial h} \right]_i = \begin{cases} a \frac{f_i - f_{i-1}}{\Delta h} & \text{if } a \geq 0 \\ a \frac{f_{i+1} - f_i}{\Delta h} & \text{if } a < 0 \end{cases}$$

3.2.3 Three-point upwind difference scheme

$$a \left[\frac{\partial f}{\partial h} \right]_i = \begin{cases} a \frac{3f_i - 4f_{i-1} + f_{i-2}}{\Delta h} & \text{if } a \geq 0 \\ a \frac{-f_{i+2} + 4f_{i+1} - 3f_i}{\Delta h} & \text{if } a < 0 \end{cases}$$

3.3. Truncation errors

The truncation errors are worthy of some discussions to estimate the accuracy of numerical solutions. The estimates are obtained by Taylor series analysis. The solutions of each scheme of the difference equation of energy are equivalent to the solutions of the following differential equations.

3.3.1 Tow-point upwind difference scheme

$$\begin{aligned} \frac{\partial \bar{\theta}}{\partial t} + \bar{u} \frac{\partial \bar{\theta}}{\partial x} + \bar{v} \frac{\partial \bar{\theta}}{\partial y} &= \left\{ \left(\frac{\lambda_{\theta}}{\bar{\rho} c_p} + K \right) + \Delta x \frac{|\bar{u}|}{2} \right\} \frac{\partial^2 \bar{\theta}}{\partial x^2} \\ &+ \left\{ \left(\frac{\lambda_{\theta}}{\bar{\rho} c_p} + K \right) + \Delta y \frac{|\bar{v}|}{2} \right\} \frac{\partial^2 \bar{\theta}}{\partial y^2} + \left\{ 2 \frac{K}{\bar{\rho}} \frac{\partial \bar{\rho}}{\partial x} + \frac{\partial K}{\partial x} \right\} \frac{\partial \bar{\theta}}{\partial x} \\ &+ \left\{ 2 \frac{K}{\bar{\rho}} \frac{\partial \bar{\rho}}{\partial y} + \frac{\partial K}{\partial y} \right\} \frac{\partial \bar{\theta}}{\partial y} + O(\Delta t) + O(\Delta x^2) + O(\Delta y^2) \end{aligned}$$

as $\Delta t, \Delta x, \Delta y \rightarrow 0$

3.3.2 Central and Three-point upwind difference scheme

$$\begin{aligned} \frac{\partial \bar{\theta}}{\partial t} + \bar{u} \frac{\partial \bar{\theta}}{\partial x} + \bar{v} \frac{\partial \bar{\theta}}{\partial y} &= \left(\frac{\lambda_{\theta}}{\bar{\rho} c_p} + K \right) \frac{\partial^2 \bar{\theta}}{\partial x^2} + \left(\frac{\lambda_{\theta}}{\bar{\rho} c_p} + K \right) \frac{\partial^2 \bar{\theta}}{\partial y^2} \\ &+ \left\{ 2 \frac{K}{\bar{\rho}} \frac{\partial \bar{\rho}}{\partial x} + \frac{\partial K}{\partial x} \right\} \frac{\partial \bar{\theta}}{\partial x} + \left\{ 2 \frac{K}{\bar{\rho}} \frac{\partial \bar{\rho}}{\partial y} + \frac{\partial K}{\partial y} \right\} \frac{\partial \bar{\theta}}{\partial y} \\ &+ O(\Delta t) + O(\Delta x^2) + O(\Delta y^2) \end{aligned}$$

as $\Delta t, \Delta x, \Delta y \rightarrow 0$

The coefficient of the terms $O(\Delta t)$, $O(\Delta x^2)$ and $O(\Delta y^2)$ involves the derivations of high order than it appears in these equations. The truncation errors are evaluated by $O(\Delta t) + O(\Delta x^2) + O(\Delta y^2)$. As the differencing of the convection terms are applied to two-point upwind difference scheme, the diffusion terms are made additions to $\Delta x \frac{|\bar{u}|}{2}$ and $\Delta y \frac{|\bar{v}|}{2}$ which are called numerical viscosity. Using the other difference scheme, however, the numerical viscosity does not come out. Therefore the accuracy of the numerical solutions depends only upon the time and space mesh sizes under no existence of rounding-off errors by numerical computations.

3.4. Practical stability and spurious oscillation

The integration of the parabolic partial differential energy equation in time and space requires the practical stability for the finite difference method. Practical stability imposed restrictions on the size of time mesh and space meshes for the finite difference scheme, but the sizes of Δt , Δx and Δy are arbitrarily given. We obtained the practical stability conditions [5] impose restrictions for each scheme on the mesh sizes of Δt , Δx and Δy as shown in Table 1.

Table 1. The practical stability condition

Numerical scheme	Explicit method	Implicit method
Central	$\Delta t \leq \left[\max_{ijn} \left\{ 2\sigma_{ij}^n \left(\frac{1}{\Delta x^2} + \frac{1}{\Delta y^2} \right) \right\} \right]^{-1}$ $\Delta x \leq \max_{ijn} \frac{2\sigma_{ij}^n}{\bar{u}_{ij}^n} \quad \text{and} \quad \Delta y \leq \max_{ijn} \frac{2\sigma_{ij}^n}{\bar{v}_{ij}^n}$	stable
2-point upward	$\Delta t \leq \left[\max_{ijn} \left\{ \frac{\bar{u}_{ij}^n}{\Delta x} + \frac{\bar{v}_{ij}^n}{\Delta y} + \frac{2\sigma_{ij}^n}{\Delta x^2} + \frac{2\sigma_{ij}^n}{\Delta y^2} \right\} \right]^{-1}$	stable
3-point upward	unstable	stable

We consider the accuracy of computational results for high Reynolds number because of turbulent fluid flow. The computational results have the spurious error [6] under the condition of the effective maximum cell Reynolds number (Re^*) greater than 2 for the equation of motion and the effective maximum cell Peclet number (Pe^*) greater than 2 for the equation of energy because of discretizing the central difference scheme in FDM (Finite Difference Method). However as the diffusion coefficient for the two-point upwind scheme is added to the numerical viscosity, the spurious oscillation is repressed or decreased by numerical viscosity for large value of velocity. Pe^* is defined as follows;

$$Pe^* = \max \left\{ \max_{ijk} \frac{|u_{ij}^n| \Delta x}{\sigma_{ij}^n + K_{ij}^n}, \max_{ijk} \frac{|u_{ij}^n| \Delta y}{\sigma_{ij}^n + K_{ij}^n} \right\}$$

4. Numerical Experiments

We consider the transient natural convection in a fire compartment of two-dimensional rectangular room (2.4 m height and 2.4 m length). Steady flat plate heat source (800°C) is placed [A] at the center of the floor (10 cm width) in Fig. 1 and [B] at the left hand side wall (2.4 m length) in Fig. 2. The fluid in the fire compartment is initially motionless and at a uniform temperature of 30°C. Initial pressure and density distribution are obtained by computation of the equation of state. The ceiling, floor and left side wall are the solid boundary and the right side is the free space boundary. The solid boundaries are assumed to be thermally adiabatic, Neumann type, except to the heating plate and the velocity on the solid boundary is assumed to be Dirichlet type non-slip condition. The boundary conditions on the free space boundary are assumed to be Neumann type condition for out-flow and Dirichlet type condition for in-flow. The simultaneous equations introduced by the implicit difference scheme are solved numerically by the sparce line successive over-relaxation method (SLSOR) for Poisson type equation and two-point upwind difference scheme, and by the sparce conjugate residual II method (SCR2) for other difference scheme to reduce the computer memories of data area. Several numerical experiments were carried out on super computer with FORTRAN 77 used to double precision as follows:

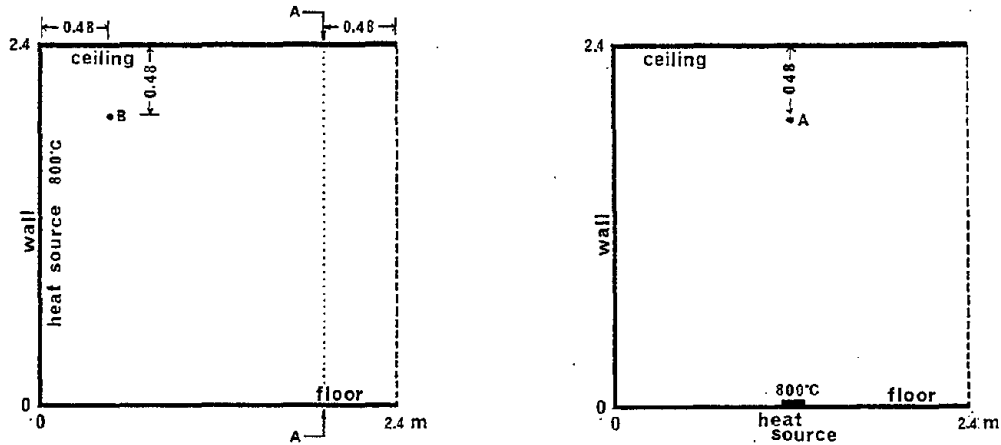


Figure 1. Outline of computational domain Figure 2. Outline of computational domain

4.1. Estimate of the computational results with space mesh

The constant line heat source (800°C and 2.4 m width) is located on the left side solid wall in Fig. 1. The computational domain is subdivided with the total 11×11 , 16×16 , 21×21 , 31×31 , 41×41 and 61×61 meshes corresponding to 24, 16, 12, 8, 6, and 4 cm mesh sizes respectively. The temperature, the velocity \bar{u} and \bar{v} of computational results at the location B (48 cm below ceiling and 48 cm far from heat source) and the cross section A (48 cm far from open area on free boundary) in Fig. 1 were compared each space mesh.

4.2. Estimate of the computational results with different finite difference scheme for convection terms

For save charge computing time, the numerical computations were carried out with space mesh size 12 cm and time interval 10 msec in which the heat source is located on the left side solid wall and on the floor in cases of Fig. 1. The scheme for convection term is proposed numerically.

4.3. Estimate of the computational results with time interval

As the results of the estimate of the space mesh, the computational domain is subdivided into 41×41 grids corresponding to 6 cm mesh size in Fig. 2. The computations were carried out with time intervals which are chosen 2.5, 5, 7.5, 10, 15, 20, 30 and 40 msec considering truncation errors. The temperature, the velocity \bar{u} and \bar{v} of computational results at the location A (center of ceiling and 48 cm below ceiling) and the cross section on the free boundary in Fig. 2 were compared.

5. Results and Discussions

5.1. Estimate of the computational results with space mesh

In order to estimate the accuracy of computational results applied to two-point upwind difference, the space meshes are chosen 24, 16, 12, 8, 6 and 4 cm, and the time interval is fixed constant 10 msec. Fig. 3 shows the computational results of the temperature and the velocity \bar{u} at the location B. The temperature differences and the velocity component \bar{u} differences among the space meshes 4, 6 and 8 cm in Fig. 3-a and 3-b respectively are the much same values (less than 5% errors). In Fig. 3-a, the computational results show the oscillation called "spurious oscillation".

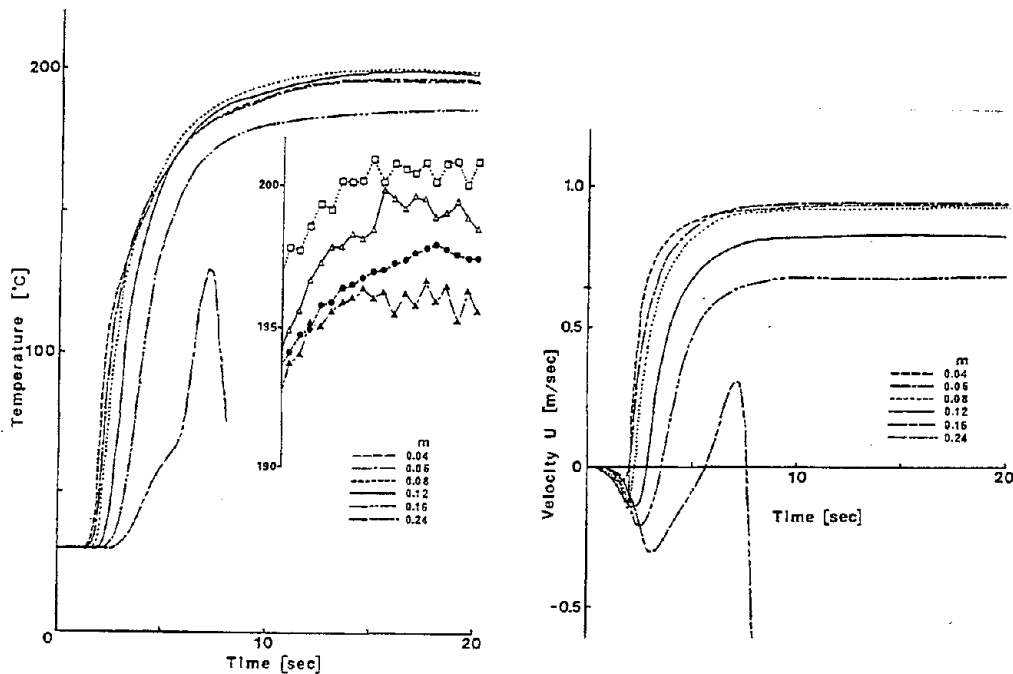


Figure 3. Computational results at the location B in Fig. 1
(a) Temperature and (b) Velocity u

Fig. 4 shows the relationship between Re^* from the computational results and time. This Re^* of 4 cm mesh in Fig. 4 gives the smallest values less than 10 after 10 sec, so the period of spurious oscillation would give the large and the amplitude would give the small. Before 10 sec the flow motion is numerically unstable because of initially putting the constant line heat source temperature 800°C , so the numerical computation with 24 cm mesh and 10 msec time interval was diverged and in the case of 2 cm and 10 msec time interval was also diverged because the simultaneous equations for implicit method were unstable to be solve numerically by the truncation errors and rounding-off errors.

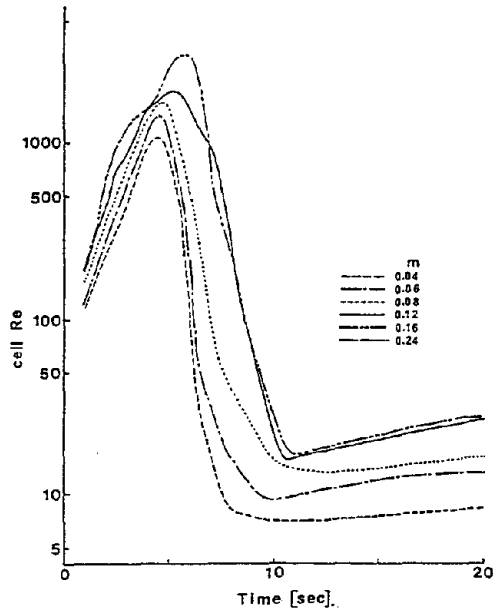


Figure 4. Relationship between Re^* and time

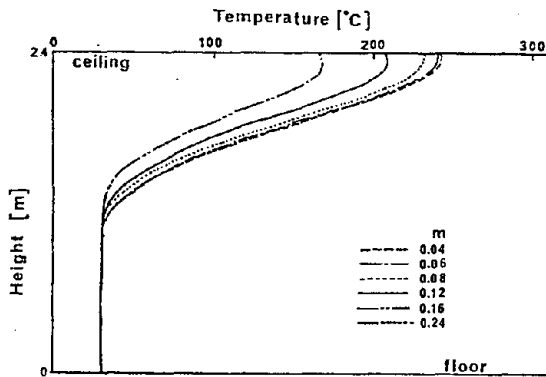


Figure 5. Computational results of temperature at the cross section in Fig. 1.

Fig. 5 shows the computational results of the temperature at the cross section A. The results with space mesh sizes 6 and 4 cm are the much same and the other mesh sizes are quite different from them. On the other hand Fig. 6 shows the temperature distribution at the cross section A with time intervals 10 and 5 msec in the case of space mesh 6 cm, and with time intervals 10 msec, 5 msec and 2.5 msec in the case of 4 cm. These time intervals are given by considering truncation errors. As the results the temperature difference is about 10% errors each other.

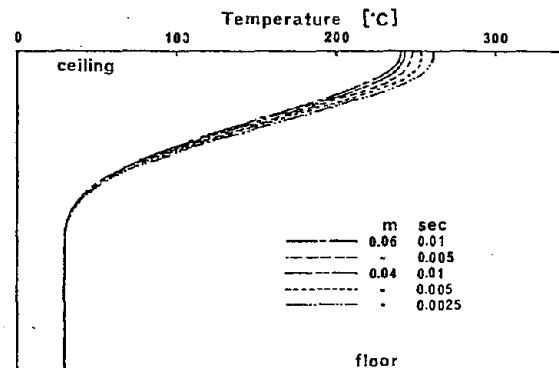


Figure 6. Computational results of temperature at the cross section in Fig. 1.

Table 2 shows the computational run time (CPU time) of 20 simulation seconds.

Table 2. CPU time ratio

Mesh size (cm)	Time interval (msec)		
	10.0	5.0	2.5
16	0.073	—	—
12	0.147	—	—
8	0.418	—	—
6	1.000	1.346	—
4	5.412	7.360	11.419

5.2. Estimate of the computational results with different finite difference scheme for convection terms

Fig. 7 shows the distributions of temperature with the different scheme for convection term in the case of 10 msec time interval and 12 cm mesh at the cross section of free boundary in Fig. 1. As the results the two-point upwind scheme is only quite differences among other scheme, that is, it gives under estimate because of adding the numerical viscosity. Table 3 shows the CPU time until 20 simulation seconds. In above mentions the three-point upwind difference scheme for convection term applied implicit method would be better way.

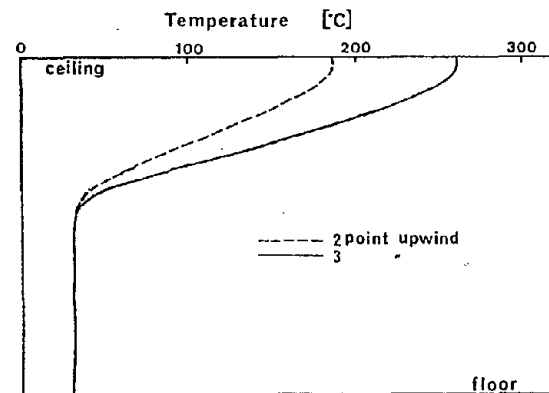


Figure 7. Computational results of temperature at the cross section of free boundary in Fig 1.

5.3. Estimate of the computational results with time interval

The computations were carried out for the accuracy of time interval with 6 cm mesh applied to three-point upwind scheme in the case of Fig. 2. The time intervals are chosen 2.5, 5, 7.5, 10, 15, 20, 30, and 40 msec. In the case of 40 msec time interval the computation miscarried due to numerical errors. It should be noted that the computations were only success the time intervals 7.5, 10, and 15 msec by three-point upwind difference scheme. Fig. 8 shows the temperature and the velocity \bar{u} at the location A.

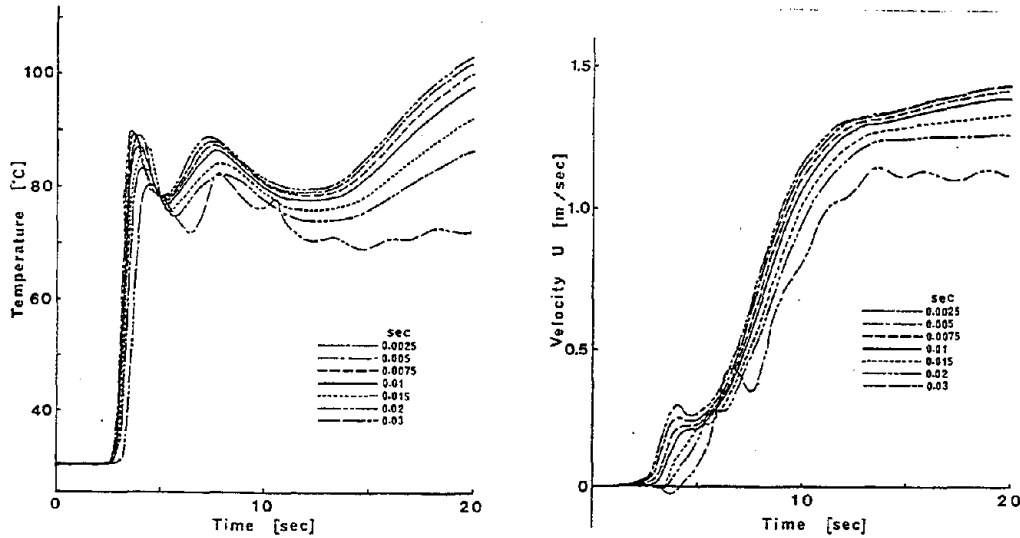


Figure 8. Computational results at the location A in Fig. 2
 (a) Temperature and (b) Velocity u

Fig. 9 shows the temperature distributions at the cross section of free boundary. In these figures the results of temperature with 10 msec to 2.5 msec time intervals give about 5% errors each other. The results of the time interval 10 msec come to a full application of its values from above mentions.

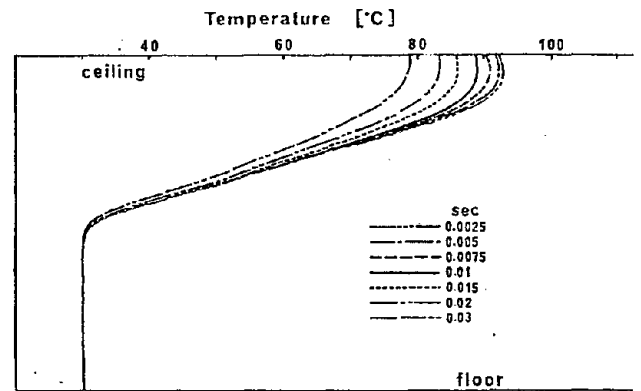


Figure 9. Computational results of temperature at the cross section of free boundary in Fig 2.

6. Conclusion

When the implicit method is used in field model simulations of a compartment fire, our personal point of view from computational experiments is that the time interval and space mesh should be chosen less than 10 msec and 5 cm for high Re and the difference scheme for the convection term should be the three-point upwind difference scheme. The better way is to take $O(\Delta t) \simeq O(\Delta x^2) \simeq O(\Delta y^2)$ and small increment. The mesh sizes, time and space, influence the accuracy from truncation errors under the condition of no rounding-off errors, and the scheme avoids errors due to numerical viscosity. They can be

observed the trust in numerical results by Re^* for the equation of motion and Pe^* for the equation of energy. $Re^* < 20 \sim 30$ or $Pe^* < 20 \sim 30$ could be accepted from numerical experiments.

7. References

- [1] J.E. Fromm & J.J. Smolderen; Numerical Solution of the Navier-Stokes Equation at High Reynolds Number and the Problem of Discretization of Convective Derivatives; Numerical Methods in Fluid Dynamics; AGARD Lecture Series, No. 48 (1972)
- [2] O.A. Ladyzhenskaya; The Mathematical Theory of Viscous Incompressible Flow; Gordon and Beach (1969)
- [3] Y. Hasemi; Numerical Simulation of the Natural Convection in Fire Compartment; 2nd Joint Meeting UJNR (1976)
- [4] Richtmyer & Morton; Difference Methods for Initial Value Problems; John Wiley & Sons (1967)
- [5] M. Morita et.al; Feasibility of Numerical Computational Methods of Heat Flow in Fire Compartment; 2nd International Symposium of IAFSS (1988)
- [6] S. Ono & K. Hane; Advances in Numerical Method for Larger Sparse Set of Linear Equation No. 2 (1986)

PERFORMANCE BASED FIRE SAFETY

H. E. Nelson
Hughes Associates, Inc.
Baltimore, MD 21227-1652

1. INTRODUCTION.

In recent years there has been significant activity in the fire safety field in the areas of performance codes and other forms of performance prediction in fire safety decisions. In many nations there are in existence building codes or regulations that are based on a performance concept. Japan is a leader in this area. There, also, are important others. The United States has held many conferences on the subject and developed several concepts but to date no major jurisdiction or code authority has adopted a total performance concept. The world wide effort has been documented in numerous papers and conferences. Some of the most informative include papers by Wakamatsu¹; Bukowski²; Bukowski and Tanaka³; Bukowski and Babrauskas⁴; Meacham⁵; and Yamada⁶. The purpose of this paper is to categorize the approaches in the author's view of a useful manner and highlight the elements needed for confident application.

CATEGORIES OF CODE APPROACHES

A review of the approaches currently in use or development shows that the term "performance" does not have a single meaning. Each nation or entity that has adopted a performance methodology has used or developed an approach that the proponents feel best meet their needs. It is felt useful to group fire safety code approaches in five overlapping categories. While these groupings are not absolute nor fully mutually exclusive they provide a basis for examining an existing approach or guiding the development of a new one. The suggested categories are:

Specification Code. In a true specification code the allowable design methods are each individually specified in terse on dimension, materials, construction methods and other features. While almost all modern codes are no longer rigid specification codes, many contain detailed specification components such as the common U.S. requirements for stair construction. Many codes also incorporate by reference specification documents such as the standards for sprinkler or fire alarm installation or the electric system installation.

Component Performance Code. In a component performance code the performance requirement of individual building systems or components (e.g. doors, fire resistance of framing, smoke control systems) is stated. In a component performance code there is no

allowance for considering the value of one component as a justification for adjusting the performance requirement of another component. The user may install any item or system that meets the stated performance. In the U. S. the concept of performance and the movement from specification codes to component performance codes (then called performance codes) took place through the late 1940's into the 1950's. The key research document triggering this was the National Bureau of Standards document BMS92⁷. Even so most current U. S. building codes have major component performance elements mixed with elements that are still specified in detail. These codes all have some type of general equivalency clause that allows alternative approaches that produce results as safe as explicit conformance with the code, but there are few established methods to accomplish this.

Environment Performance Code. The term environment as used herein addresses the total fire produced environment in a building (e.g. hot gases, radiation, flashover, non-thermal combustion products.) In a pure environment performance code there are no restrictions on the methods used to provide safety so long as it is demonstrated that the fire produced environment can not exceed specified conditions. A typical environmental specification might limit the maximum temperature in a space to 100°C and CO to 10,000 ppm. While environment performance codes are not in use in the U.S. environment performance is frequently proposed by designers and their fire protection engineering consultants when seeking acceptance of an alternative approach that is not specifically allowed by the ruling code or standard.

Threat Potential Code. In a threat potential code there are no restrictions on the methods used, provided it is demonstrated that a specified harm to life, property, or other value will not occur given design fire conditions. In terms of life safety this approach can consider the impact of occupant mobility. There are strong elements of this approach in the Japanese performance concepts. As with an environment performance code, this approach assumes that a serious fire has occurred. Sound analysis usually involves conducting a series of scenarios representing a spectrum of potential exposures.

Risk Potential Code. A risk potential code attempts to measure the cumulative risk of harm rather than the potential of individual scenarios. The risk approach does not attempt to identify a specific serious or design case scenario. Rather it attempts to identify all significant scenarios their potential impact and their frequency of probable occurrence. The sum of the products of impact and frequency is a measurement of the risk of harm incurred in the use and operation of the facility. Both the Australian⁸ and Canadian⁹ performance approaches are risk based. In these approaches the use of selected fire scenarios and the application of modeling and other modern fire physics are integrated into the determination of impact. Fire incident statistics are used as the underpinning for frequency analysis. Earlier approaches to performance based on risk most notably the

GSA Goal-Oriented Systems Approach to Building Firesafety¹⁰ and the successor adaptations developed by Fitzgerald and his colleagues^{11, 12} are based primarily on judgement approaches derived from fire history and the expertise of the users. Fire physics and fire modeling are not excluded from these methods but are primarily used to assist and justify the impact and probability judgements made.

APPLICATION FACTORS

The successful application of Environment Performance, Threat Potential or Risk Potential code approaches all depend on:

1. Selection of the proper fire scenarios. For the first two approaches it is essential that the fire scenarios represent the realistic severe threat. In most cases a number of scenarios will be required to make an adequate evaluation. For the third case it is necessary to include every scenario that can cause significant harm and those other scenarios that are both frequent in occurrence and capable of measurable harm.

2. Choice of Representative Fires. Given the current state of fire prediction science, it is necessary for each scenario to define the rate of heat release and other characteristics of the potential fire. At some future date (but not at this time) it may be possible to model the exposing fire with sufficient confidence to derive the actual fire source input and response from the properties and arrangement of the building and its contents. As long as the description of the source fire is an arbitrary entry, the choice is critical. In the cases of environment performance or threat potential codes the selector selects a fire that is more the mean than extreme faults the safety of the facility by not considering the impact of serious though rare situations. Conversely, if the very maximum possible fire threat is considered, the resulting requirements can be excessive, massively exceeding that currently widely accepted in practice. A reasonable target may be to base the fire on the most severe expected potential given reasonable and common use of the facility. In the case of a risk potential approach the user must decide which extremely severe fire conditions are sufficiently within the realm of possibility to be included and which are so remote as to be ignored.

3. Selection of Models and other Computation Means. In selecting the computational method the user must either select that are sufficiently comprehensive to fulfill the objectives of the approach being followed or use specific conservative specification requirements or other means to fill the gap. At the end of the analysis the code authority or other impacted person must be able to address the full question being asked, such as is the building satisfactory safeguarded. The models selected need also to be accepted and competent. Frequently, a performance method is assembled using a specific battery of models. In such case there

is a danger of assuming that the models meet the need without sufficient analysis to assure that the full universe of the problem is being addressed.

4. Uncertainties/ Safety Factors. The uncertainties, leading to the need for factors of safety fall into two basic types.

a. Uncertainties in the Science. The state-of-the-art of fire science and the development of models is an emerging rather than an established science. Both the quantification of the physical relationships and the measurement of the material properties and other input data have made significant and worthy advances in recent years. There are still, however, important unknowns and measurement problems leading to uncertainties the can be cumulative.

b. Uncertainties in Life Cycle (of the Facility). As the facility is erected and as it is used there are uncertainties in terms of the workmanship of construction, the details of the actual (as opposed to expected) use of the facility, the maintenance of the facility (including fire safety features), and the specific arrangement of physical features (e.g. doors, windows, fans, fuel configurations, occupants) at the time of a fire.

The resolution of uncertainties can be addressed by:

a. Worst Case Analysis. In this approach it is assumed that all features that may fail are in their failure mode and the worst case fire occurs. All computations are assumed at the poorest performance level indicated by uncertainties in the physics involved. This extreme case is normally reserved for situations where a national or at least area wide tragedy is potential in case of fire. For example nuclear generating stations.

b. Element Safety Factors. In this approach each element of threat (e.g. fire size) is increased and each element of protection (e.g. fire resistance rating, suppression capability is reduced). The development of this type of safety factor is as good as the implementer understands the physics involved in terms of the impact of the change on the development of hazardous conditions or situations.

c. Overall Safety Factors. In this approach no safety factors are applied to individual elements but the value of the required calculated results are adjusted to compensate for uncertainties. For example in a threat potential approach the calculated time available for egress may be reduced and/or the time required for emergency movement increased. Similarly the calculated rate of application of a suppression agent my be increase or the structural fire resistance requirement increased.

d. Redundant Safeguards Approach. All codes currently include a degree of fire safety redundancy. One purpose is to protect against uncertainties in the performance of individual safeguards. One method of analyzing the degree of protection against failures due to uncertainties is to conduct parametric studies. These studies would progressively assume the full or partial failure of safeguards to determine the impact of such failure. In this concept a reasonable degree of safety should remain with the failure of any single safeguard. In most cases several safeguards should be removable without catastrophic consequences.

5. Acceptability of Performance. Each approach involves a difference set of performance criteria.

a. Specification Code. Exact conformance with the specified requirements. At the construction stage of a building all code will be reduced to a set of specification instructions to the workmen.

b. Component Performance Code. The code include the performance requirements of each component where performance is allowed. Acceptability is based on a mixture of submission of materials and arrangements shown to meet he component performance and the exact conformance with specification elements in that code.

c. Environment Performance Code. The code documentation needs to specifically state the acceptable environmental conditions. Acceptability is base on demonstration that the listed conditions are not exceeded.

d. Threat Potential Code. Acceptability is base on demonstration that the threatened persons, property, or operational capability will not be harmed in the design case senecios.

e. Risk Potential Code. Acceptability is based on demonstration the potential of harm will not exceeded a specified level in a given exposure time. The requirement may be in single terms (e.g. the potential of death of any occupant) or distributed terms (e.g. the potential of death versus the number of deaths).

In many cases the level of performance required by a performance code is determined by developing the performance measuring system and then using that to measure the type of facility allowable by the current code. This is assumed to represent the current level of public desire.

CONCLUSIONS

All of the above approaches to performance codes are useful and in current use. In the authors opinion the most viable approach, at this time is a code based on Threat Potential allowing the use of any acceptable analytical method proving performance equal or better than the existent code or regulation. It is also felt that the most workable approach to uncertainty at this time is parametric studies to demonstrate failure safeguarded performance through redundancy.

REFERENCES

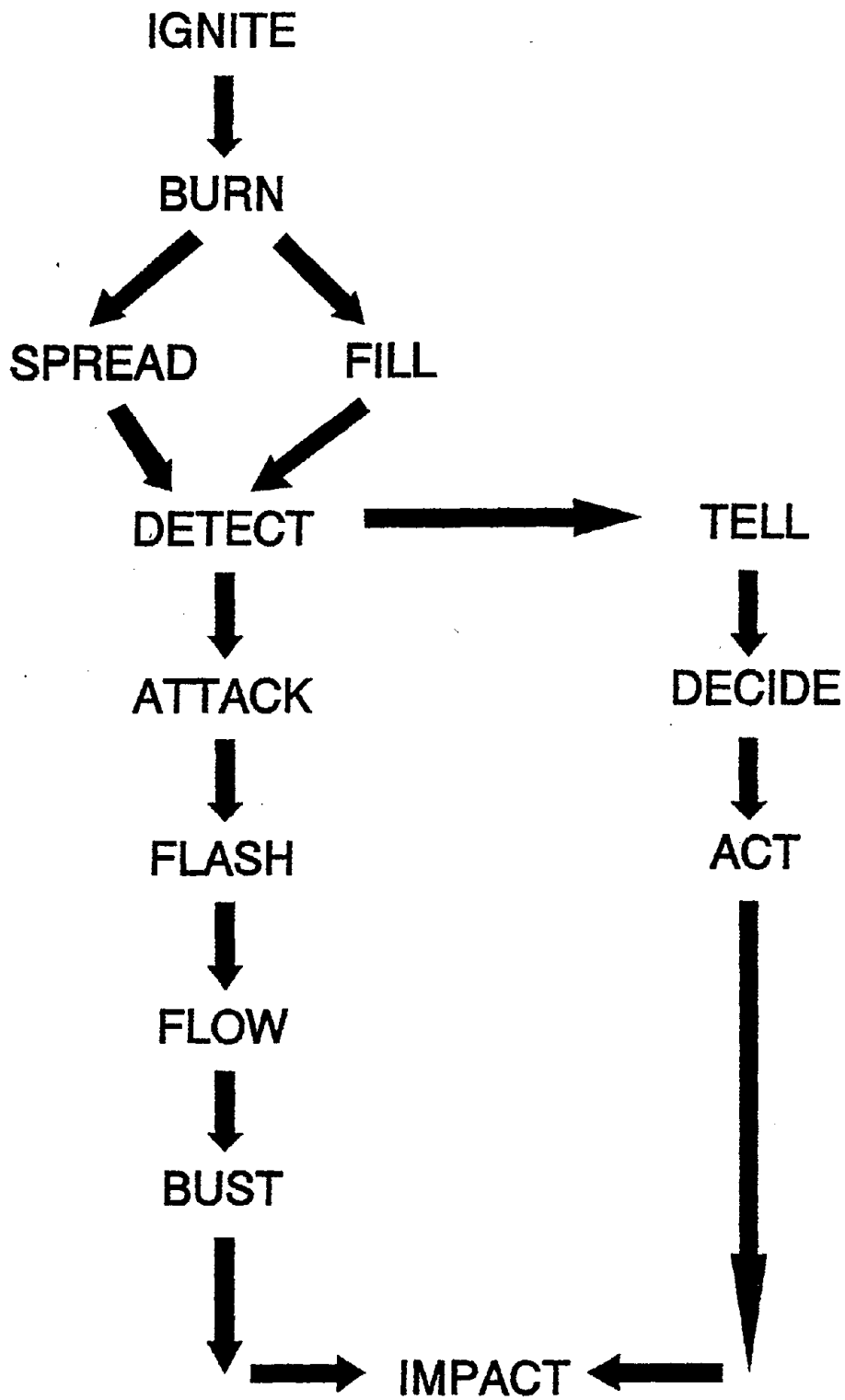
1. Wakamatsu, T.; Development of Design System for Building Fire Safety, Fire Safety Science - Proceedings of the Second International Symposium, pp881-895, 1988
2. Bukowski, R. W., Fire Codes for Global Practice, Progressive Architecture, pp 117-119, June 1995
3. Bukowski, R. W. and Tanaka, T.; Toward the Goal of a Performance Fire Code
4. Bukowski, R. W. and Babrauskas, V.; Developing Rational, Performance-based Fire Safety Requirements in Model Building Codes; Fire and Materials Vol 18, 173-191, 1994
5. Meacham, B. J.; International Development and Use of Performance-Based Building Codes and Fire Safety Design Methods; SFPE Bulletin, March/April 1995
6. Yamada, T.; Evaluation System of Code-equivalency for Alternative Designs of Fire Protection System in Japan - Towards the Intelligent Fire Protection System.
7. Fire Resistance Classification of Building Constructions, Report BMS92, National Bureau of Standards, Washington, D.C., 1992
8. Beck, B. R.; Performance Based Fire Safety Design - Recent Developments in Australia" Proceedings of the Technical Conference "Fire Safety by Design: A Framework for the Future"; Fire Research Station, Borehamwood, UK, 1993
9. Yung, D.; The Research Involved and the Development of the Procedures Related to Performance Based Codes" presentation at the AEBO Section Meeting, 1994 Fall NFPA Meeting, Toronto, Ontario, Canada, November, 1994
10. General Services Administration; Building Firesafety Criteria, Appendix: Interim Guide for Goal-Oriented Systems Approach to Building Firesafety, U.S. General Services Administration Handbook 5920.9, 1972

11. Fitzgerald, R. W.; An Engineering Method for Building Fire Safety Analysis; Fire Safety Journal, Vol. 9, No 2 July 1985, pp 233-243

12. Fitzgerald, R. W., Richards, R.C. and Beyler, C.L.; Firesafety Analysis of the Polar Icebreaker Replacement Design"; SFPE Journal of Fire Protection Engineering, Vol III, No. 4, pp 137-150, 1991

Approach	Level of Safety	Flexibility	Cost/ Effectiveness	Responsiveness to Overall Life Safety and Other Goals	Presentation Form of Results	Responsiveness to Building Technical Advances (and Innovation)	Implementation Effort and Talent Level
Specification Code	Not normally stated. Judgement based.	Limited to detailed alternatives.	No ability to vary from rigid requirements to improve cost benefit.	Undeterminable. Goals not stated.	Conformance - not quality is only measurement.	Resistive	Simple (Cook Book) Application
Component Performance Code	No analytic measurements.	Limited to the a component or a detailed alternative.	Limit range of options allows some cost benefit optimization.			Limited to advances within a component.	Special technicians and information desirable.
Environment Performance Code	Indirectly set in terms of maximum allowed conditions.	Broad but limited to a space by space analysis.	Increases ability to increase cost benefit due to increase in available options.	Depends on accuracy in selection of maximum allowable conditions.	Results are determined by models & other science that predict the potential environment in terms of the specified allowable conditions. To that extent results are fully measurable.	Readily responsive to innovations so long as both the impact of such innovations affects the specified allowable concentrations and the established measurement method can determine that impact.	Requires competent engineering capabilities and either a consensus or sound judgement on selection of scenarios.
Threat Potential Code	Potentially can measure level of safety in terms of the ability to assure a specific limitation of harm for an assigned "design case" scenario of physical and human conditions.	Provides broad capabilities that can be determined on a building wide as well a compartment basis.	High level of ability to measure and provide for safe allowance of cost effective innovations.	Can directly measure the achievement of safety for the selected design case scenarios. Reasonable analysis requires multiple scenarios.	Results as based on both fire development and human behavior modeling. Predication is in terms of harm given the specified scenarios.	Very responsive to innovations that relate to the potential of harm given the occurrence of the specified scenarios. Unresponsive to fire prevention innovations.	Requires competent engineering capabilities and either a consensus or sound judgement on selection of scenarios.
Risk Potential	Measures the probability that any specified type of harm (e.g. life, property of productivity for a specified period of exposure.	As flexible as science and data allows.	Maximum potential for cost effectiveness.	If goals are expressed in risk terms and needed data are available.	Results are in terms of harm potential.	Very responsive to innovations of all types.	Requires competent engineering capabilities.

ELEMENTS OF FIRE HAZARD ANALYSIS



ELEMENTS OF FIRE HAZARD ANALYSIS
H. E. NELSON, Revised 7/26/95

- IGNITION The application of heat to a combustible material in sufficient quantity for a sufficient time to raise the material to its ignition temperature (assumes sufficiency of an oxidizer). Key engineering data include ignition temperature, critical ignition flux, incident flux and thermal inertia.
- BURN The sustained continuation of the combustion process. It may be with or without external flux. The ability to return sufficient energy to the source fuel is critical. Key engineering data include thermal inertia, incident flux, heat of combustion, heat of gassification, and non-thermal products of combustion.
- FILL The collection of products of combustion in a room or other entity as a result of the burning process. Key engineering data include rate of heat release, thermal inertia of the bounding surfaces, natural and powered vents, size and shape of the space.
- SPREAD The increase in the area of fire involvement. This may be by spread over a surface of a fuel item or by transfer of ignition from one item to another across a space. The spread of fire is a form of successive ignitions. Key engineering data include ignition temperature, critical ignition flux, thermal inertia, incident flux from the exposing flame or other hot body, and flame gas dynamics (expressed by the factor ϕ .)
- DETECT The discovery of the fact of fire by whatever means. From an engineering standpoint, the most interesting are those involving automatic detection. Key engineering data include rate of heat release, plume entrainment, heat losses to surfaces, heat transfer to detection devices, rate of detectable non-thermal product production, product reactions, movement of detectable products, and detection device characteristics.
- ATTACK Those actions that are intended to terminate or mitigate the act of burning. The most common are based on water but many other extinguishing media can be involved. In all cases detection is a necessary precursor to attack. Key engineering data include detection method, rate of application, point or area of application, suppression capabilities, delivery system fluid dynamics, and system reliability.
- FLASH This factor is in recognition of the major importance of flashover. The transition from a free burning fire to flashover has major consequences. Key engineering factors are rate of heat release, thermal inertia of the bounding surfaces and convective energy movement through vents.
- FLOW The movement of fire products from the point of fire origin to other spaces near and far from the fire. The driving forces include the fire itself (most impacting near the source), building HVAC systems or other air movement systems, stack effect and wind. At locations

remote from the fire source the relative impact on flow is generally in the reverse order of this listing. Key engineering data include sizes of openings (including cracks in some cases), flow paths such as ducts, other leakages, fan curves, wind speeds, inside and outside temperatures, building height, changes in the flow paths caused by emergency evacuation, fire fighting efforts, or the impact of the fire itself.

BUST The impact of the fire on the structural framing and compartmentation of the building. This recognizes that the fire intensity and the time that intensity is applied can either weaken members to the point where they can not carry their load or transmit unacceptable levels of heat from the exposed to the unexposed side of a partition or other membrane. Key engineering data include the strength-temperature capabilities of the material, the load on it, the heat applied to the element and the thermal inertial of the material and any insulation protection it.

TELL No human action can occur until the person(s) involved are informed of the need. Telling can be by signal, announcement, word of mouth, or fire indicators (smoke, heat, flame, noise, etc.). In recent years there is an increasing awareness of the importance of providing the most accurate information possible. There are many in fire and related officialdom, however, who do not trust occupants to act wisely and still prefer uninformative signals. Inherent in the TELL function is the notification of emergency forces. Key engineering data include sound transmission factors, message composition, and alarm transmission.

DECIDE No person moves or takes any other action until that persons decides to do so. It is assumed that every person will take the action that individual perceives necessary and best for his protection, all things being considered. This may or may not be the best for that individual's or the group's well being. Key engineering data include form of announcements, training, warden or other guidance, preplanning.

ACT Once a decision is made a person will act accordingly. Actions include those related to investigation, rescue, fire fighting, escape, refuge, and other actions. Engineering data include egress path data and number of individuals involved.

Discussion

Howard Emmons: We are a long way from the ideal performance codes that have been proposed by you and many others. In the structural area, the effect of the current code is that the building you design will not collapse if built as designed. Of course, they don't design for the meteor hitting the building and various other extreme situations. I think, we, as fire protection people, should have an ultimate design requirement. There, of course, would still be some extreme cases for which we cannot account. I propose three statements: 1) Everyone can get out or to a region of safety, no matter where or when the fire starts, 2) There will be no collapse for some specified period of time so that firemen can very safely enter the building and make rescue as needed, and 3) a more arguable point, given fire service response in some reasonable time, the structural loss of the building will not exceed some percentage of its initial value, say 25%.

Harold Nelson: Except for the last one, I believe you are right on and will have no problem in finding that acceptable to anybody in design or any code authority. Inherent in your structural analogy is the conception of "used as intended." In the United States, and I'm sure in other nations, there are national consensus standards stating the expected dead and live loads brought together by leading engineers in that profession. In the United States, we need such a thing in fire. One of the committees I chair, which happens to be smoke management, is attempting to write that into those standards, but that's an obscure place. With regard to your last point on loss limitation, that's an underwriter's item, in my opinion, and should be reflected in the insurance premium. In some cases, it can be very small, and some can be a write off. Certainly, if I had a small warehouse storing railroad fuses, I might just say let it go. That happens to be an example from my past.

Flame Length and Width produced by Ejected Propane Gas Fuel from a Pipe

by

Osami Sugawa and Kikuko Sakai
 Center for Fire Science and Technology
 Science University of Tokyo
 2641 Yamasaki, Noda, Chiba 278 Japan

ABSTRACT

Flame tip height, width, and height to base of a lifted flame, formed by a ejected fuel gas through a pipe of 1/8B, 1/4B, 3/8B, 1/2B, 3/4B, and 1B, were observed as a function of dimensionless heat release rate. Fuel gas was supplied at the rate of 100ℓ/min, 200ℓ/min, and 400ℓ/min. Pipe heights from the ground level were set at 200mm, 700mm, and 1700mm. Radiative heat fluxes were also measured at 0.1m, 0.27m, 0.71m, 1.1m, 1.27m, 1.71m, 1.9m, 2.9m from the pipe. Temperatures along the center line of the flame were measured. Dimensionless flame height, H_a/D , and dimensionless flame width, W_f/D were correlated well by 1/3 power of dimensionless heat release rate. Radiative heat fluxes to the dummy vessel were also estimated using the view factor and center-line temperature. Estimated radiative heat fluxes to the targets were compared with the measured ones and good agreement between them was obtained. This implies that the view factor on radiative heat flux to the target from a jet flame is useful to estimate the radiative heat flux to assess the fire safety.

Key Words: jet flame, flame height, flame width, heat release rate, lifted flame, view factor

1. Introduction

Fuel gas is supplied through piping networks in urban area but its suburbs propane gas, as a fuel gas for house use, is supplied by vessels of 20~30kg. In order to get the higher cost performance and lower consumption of labor in the delivery service, in other words to get infrequent delivery service and lessen the numbers of vessels transported to houses, it is planned to set a big volume vessel of 1500kg in house yard (or in basement) and of which refuel will be made directly by connecting with a LPG bulk loll track. However, the setting of a big vessel in house yard may have high potential of fire risk in case of a neighbor fire occurred. Fire in neighbor may give radiative heat to the vessel and which may result high pressure and ejection of fuel jet. Pressure reduction is designed by the ejection of gas through a safety-pipe and bulb system so that jet flame will be generated on/above the nozzle of the pipe and which may feed extra radiative heat to the vessel and surroundings. It is demanded to assess the potential of radiative heat which may be fed from the jet flame to the vessel. In the first series of the experiment, the semi-full scale test had been carried out using a big vessel which was exposed to model fires (wood crib fires). Temperatures of vessel surface and its atmosphere were measured, and also function of a safety bulb for pressure reduction was verified [1]. In the second series of the test, fire safety assessment of the big vessel was carried out. And a part of the second test, basic information on a jet flame formed on a safety pipe is required, and we dealt with the measurements and observations on jet flame height, flame width, height to the base of lifted jet flame from a pipe, and radiative heat flux to the dummy vessel.

2. Experimental Procedure

2-1. Piping and Experimental system

Figure 1 shows the outline of the layout of experiments. Fuel gas was let into the system through pressure reducers and valve system controlling the supply rate of 100ℓ/min, 200ℓ/min, and 400ℓ/min. The final flow rate of the piping system was monitored by a mass flow meter every 10sec. Nozzle height were adjusted at 200mm, 700mm, and 1700mm high from the grand level. Fuel gas supply rates, pipe size with mm Φ , nozzle height and dimensionless heat release rate designed are shown in Table 1.

2-2. Measurements and Observations

Temperatures in the ejected flame were measured along the center at 1m, 2m, 3m, 4m, 5m, 6m, and 7m high from the ground level. Radiation heat flux meters were set at 0.1m, 0.27m, 0.71m, 1.1m, 1.27m, 1.71m, 1.9m, and 2.9m apart from the center of a pipe. Two sets of video system, focusing from North and East, were used for recordings of the flame images.

Table 1 Experimental Conditions

Experiment Number	Fuel Flow Rate (ℓ/min)	Bore Size (mm)	Nozzle Height (mm)	Q* (-)
1	100	1/8B, 6.5mm	700	3.99x10 ⁴
2	200 →180→160	1/8B, 6.5mm	700	6.39 x10 ⁴
3	100	3/8B, 12.7mm	700	7.48 x10 ³
4	200	3/8B, 12.7mm	700	1.50 x10 ⁴
5	300	3/8B, 12.7mm	700	2.25 x10 ⁴
6	400	3/8B, 12.7mm	700	2.99 x10 ⁴
7	100	1B, 27.6mm	700	1.07x10 ³
8	200	1B, 27.6mm	700	2.15 x10 ³
9	400	1B, 27.6mm	700	4.30 x10 ³
10	400	1/4B, 9.2mm	200	6.70 x10 ⁴
11	200	1/4B, 9.2mm	200	3.35 x10 ⁴
12	100	1/4B, 9.2mm	200	1.68 x10 ⁴
13	400	3/8B, 12.7mm	200	2.99 x10 ⁴
14	200	3/8B, 12.7mm	200	1.50 x10 ⁴
15	100	1/2B, 16.1mm	200	4.14 x10 ³
16	200	1/2B, 16.1mm	200	8.27 x10 ³
17	400	1/2B, 16.1mm	200	1.65 x10 ⁴
18	400	1B, 27.6mm	200	4.30 x10 ³
19	400	3/4B, 21.6mm	200	7.93 x10 ³
20	200	3/4B, 21.6mm	200	3.97 x10 ³
21	100	1/8B, 6.5mm	1700	3.99 x10 ⁴
22	400	1/4B, 9.2mm	1700	6.70 x10 ⁴
23	200	1/4B, 9.2mm	1700	3.35 x10 ⁴
24	100	1/4B, 9.2mm	1700	1.68 x10 ⁴
25	400	3/8B, 12.7mm	1700	2.99 x10 ⁴
26	200	3/8B, 12.7mm	1700	1.50 x10 ⁴
27	400	1/2B, 16.1mm	1700	1.65 x10 ⁴

28	200	1/2B, 16.1mm	1700	8.27×10^3
29	400	3/4B, 21.6mm	1700	7.93×10^3
30	200	3/4B, 21.6mm	1700	3.97×10^3
31	400	1B, 27.6mm	1700	4.30×10^3

* In the test #2, gas supply rate was changed 200ℓ/min to 160ℓ/min with the changing rate of 20ℓ/min to observe the blow-off of the flame.

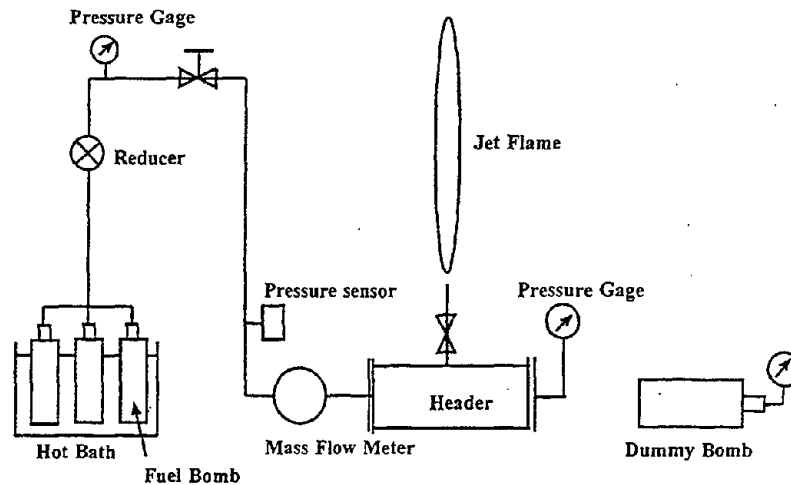


Figure 1 Outline of the experimental sets. Fuel gas vessels are set outside of the facility. Temperatures along a jet flame and on the surface of the dummy vessel were measured by sheathed K-type thermocouples. Radiation meters were set on the same level of the dummy vessel.

3. Results and Discussion

3-1. Flame Height and Width

Flame tip heights, H_a , were estimated from 90 successive images and are shown representatively in Figure 2 by a rigid line. In this case about 600kW (400ℓ/min) flame from 1/4B pipe was used, and the averaged flame tip height estimated was 3.04m with its maximum and minimum heights of 3.43m and 2.75m, respectively. The difference between highest and lowest flame tip height was about 0.6m and of which standard deviation was about 10% of the full flame length. The flame widths, W_f , were estimated from the same images and are superimposed representatively in Figure 2 by a broken line. Standard deviation for W_f is about 20% and the fluctuation in both height and width of the flame is almost coincided with each other as shown in Figure 2. Average flame tip height, H_a , was normalized by pipe size, D , and are obtained in the dimensionless flame height of H_a/D . Figure 3 shows the logarithmic plots of dimensionless flame tip height, H_a/D , as a function of dimensionless heat release rate $Q^* = \dot{Q} / \rho C_p \Delta T \sqrt{g D D^2}$. [4] The figure indicates the relation of $H_a/D = 9.61 \cdot Q^{*1/3}$ for higher flame height, $H_a/D = 6.69 \cdot Q^{*1/3}$ for lower flame height, and $H_a/D = 8.14 \cdot Q^{*1/3}$ for average jet flame height for the range of Q^* of $10^3 \sim 6.7 \times 10^4$ based on the tests. The number of power, 1/3, for the relation is greater than that 0.23 which is reported by McCaffrey [2].

Flame widths, W_f , were also estimated and averaged based on 90 images and which was normalized by D as W_f/D . Figure 4 shows the relation of dimensionless flame width and Q^* in logarithmic scale. This figure shows W_f/D increased with the increase of $Q^{*1/3}$

and is expressed by $W_f/D = 1.92 \cdot Q^{*1/3}$. Figures 3 and 4 indicate that the characteristic flame length, both height and width, grows with $Q^{*1/3}$.

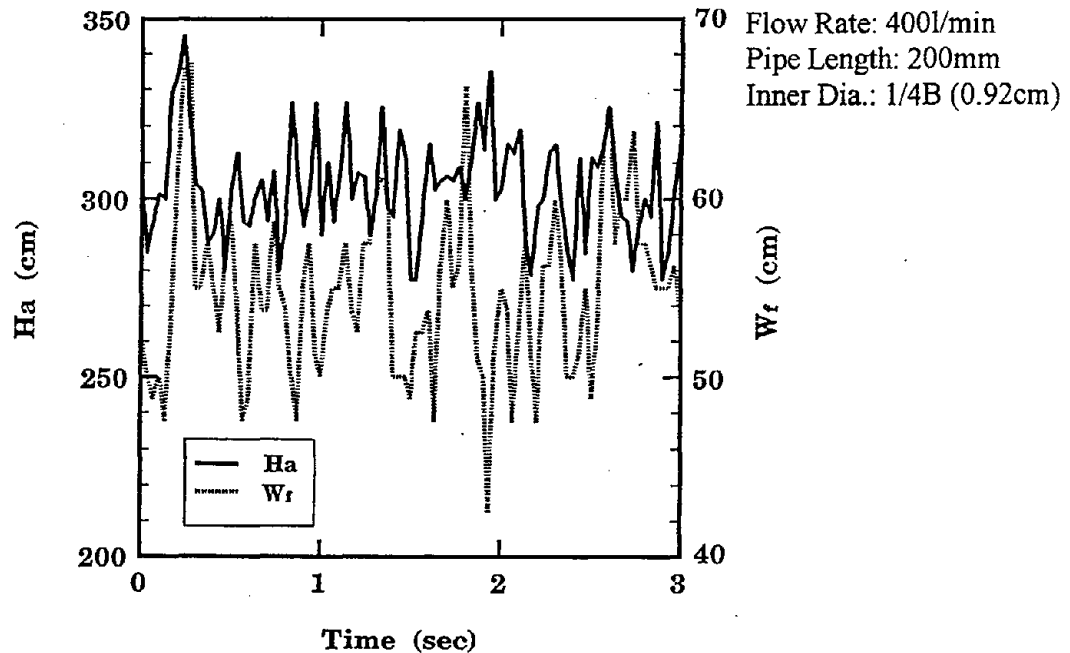


Figure 2 Typical time histories of flame tip height and its width. In this case, propane gas as a fuel was supplied at the rate of 400l/min from a 1/4B (0.92cm Φ) pipe of which length was 200mm from the ground.

3-2. Height to the base of lifted flame, h

Some of the tests showed the lifted flames. When we gave 200l/min and 180l/min to the 1/8B pipe, the lifted flame was observed once but it extinguished soon showing the lifting flame. In the case of ejection velocity exceeded 250m/sec at the bore resulted in the blow off of the flame. Except the test #2, we observed the stable flame with lifting. When lifted flame was observed, the height from the opening of pipe to the base of lifted flame, h, were estimated and averaged based on the 90 frames of successive images on the video system. Averaged one was normalized by pipe diameter, giving a dimensionless lifted height h/D , were plotted against Q^* . Figure 5 shows the h/D as a function of Q^* in log-log scale, and which implies that h/D increased with $3/5$ power to Q^* in the region of $10^3 \sim 10^4$ and is expressed empirically by $h/D = 1.39 \times 10^{-2} \cdot Q^{*3/5}$.

3-3. Excess Temperatures, ΔT , along the center line of a flame

In the lower region of a flame, $(Ha/D)/Q^{*2/5} \leq 2$, excess temperature, ΔT , showed almost constant of 850 - 950 $^{\circ}$ C for the vertical direction. And ΔT decreased with Ha^n ($n = -3/2 \sim -5/3$) for the region of $(Ha/D)/Q^{*2/5} > 2$. These gradients are quite similar to the ones obtained in the flame and plume in a diffusion flame as McCaffrey reported [3]. However, decreasing mode for intermittent, $(Z/Q^{*2/5})^{-1}$, was not observed clearly in our tests as shown in Figure 6. Decreasing modes for vertical direction along the center line were characterized into two regions and are expressed by empirical equations as,

$$\Delta T = \alpha \cdot ((Ha/D)/Q^{*2/5})^{-3/2}, \text{ where } \alpha = 1600^{\circ}\text{C for } (Ha/D)/Q^{*2/5} > 2 \text{ and}$$

$$\Delta T = 850 \sim 950^{\circ}\text{C for lower flame region of "the base of flame" } \leq (Ha/D)/Q^{*2/5} \leq 2.$$

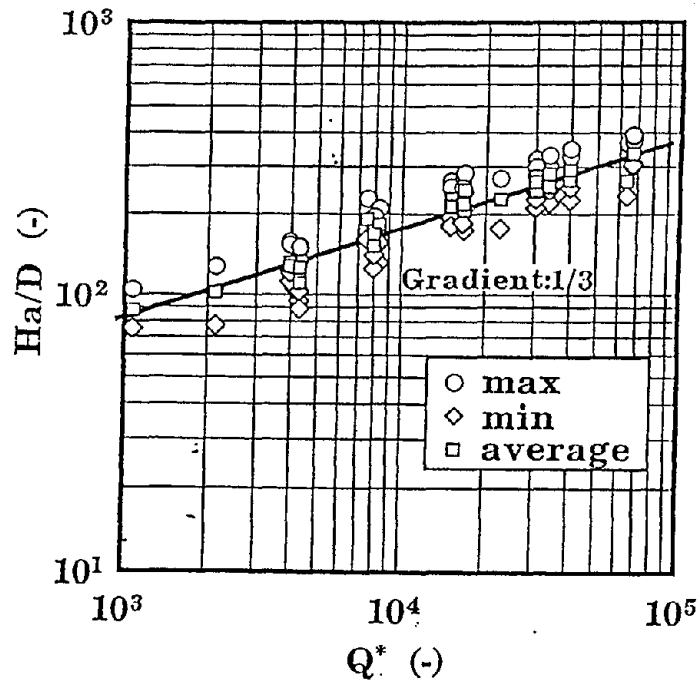


Figure 3 Logarithmic plots of dimensionless flame height, Ha/D , as a function of dimensionless heat release rate Q^* with gradient of 1/3.

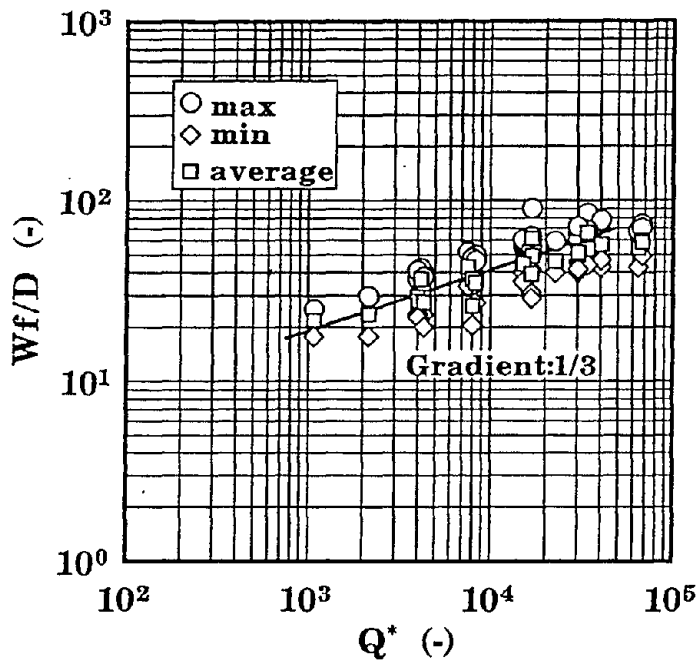


Figure 4 Dimensionless flame width, Wf/D , as a function of dimensionless heat release rate Q^* . Wf/D increased with 1/3 power of Q^* .

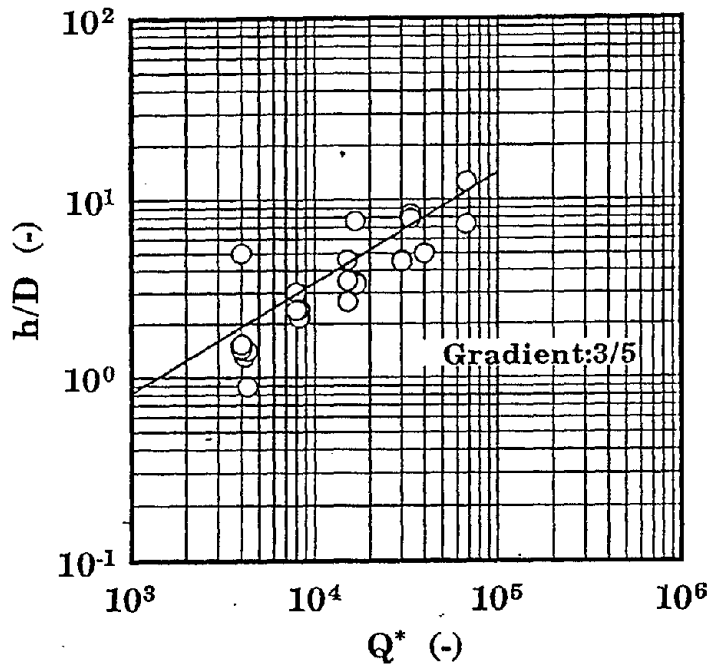


Figure 5 Dimensionless height to the base of lifted flame, h/D , are plotted against Q^* when no blow-off was observed.

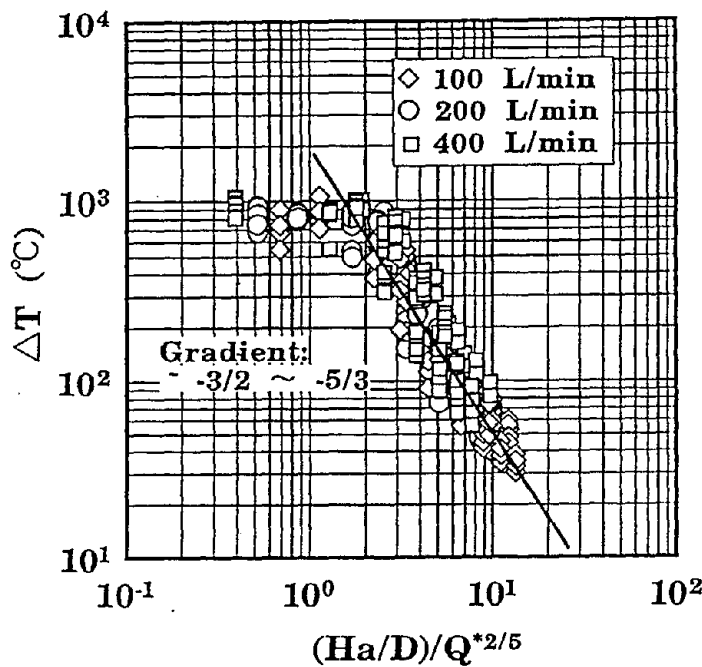


Figure 6 Excess temperatures along the center line of jet flame are plotted against normalized height by $Q^{*2/5}$. Vertical distribution of excess temperatures showed two regions with no decreasing and $-3/2 \sim -5/3$ power to the dimensionless height.

3-4. Radiation Heat Flux

Figure 7 shows the typical distribution profiles of radiation heat flux for horizontal direction with pipe heights of 200mm, 700mm, and 1700mm. It is clearly observed that distribution of radiation heat flux showed flat in the near region from the pipe and then decayed in the far region.

In order to estimate the radiation heat flux to the vessel, we adopted following assumptions and two models for a jet flame to estimate the view factors between a flame and a target.

- Flame figure could be expressed by thin cylinder (including its bottom and of which view factor was presented in a text[5]) or by thin cone (or trapezoid) piled up to the average flame height, H_a , as shown in Figure 8-(a) and (b). Both models forms a conical flame in total shape.
- Maximum diameter of each cylindrical or trapezoidal flame appeared at the height of $0.9H_a$ and was estimated as a function of Q^* and D . Diameter at arbitrary height was estimated based on the angle of flame jet which was determined by D at H_a and the length to the base of the flame.
- Flame is translucent and its representative temperature at arbitrary heights can be estimated by the empirical equation described along the center line.

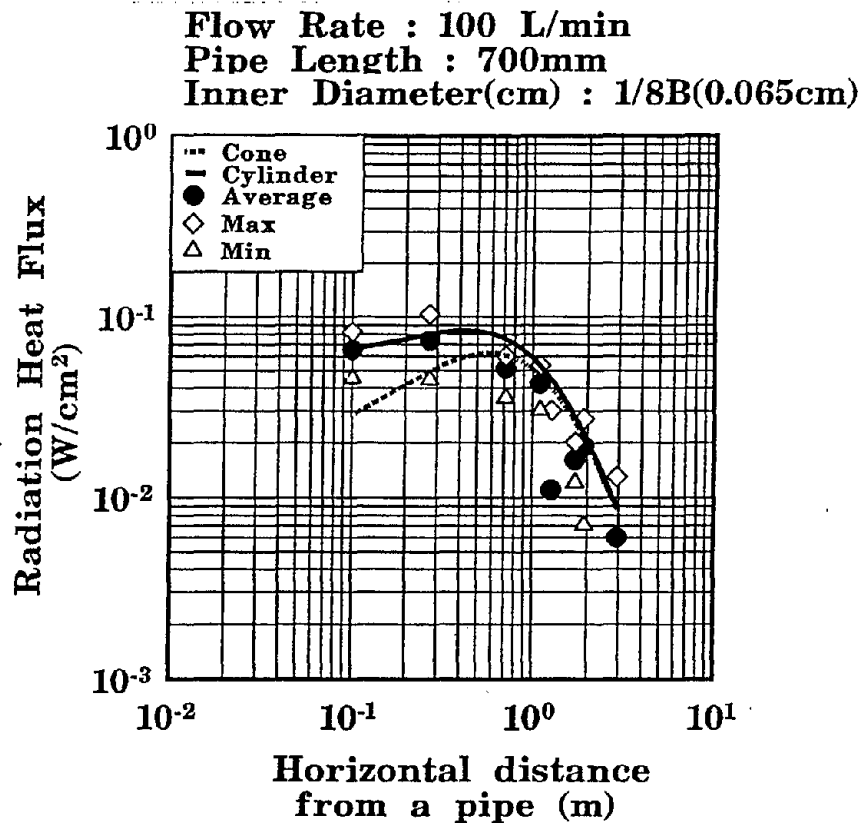


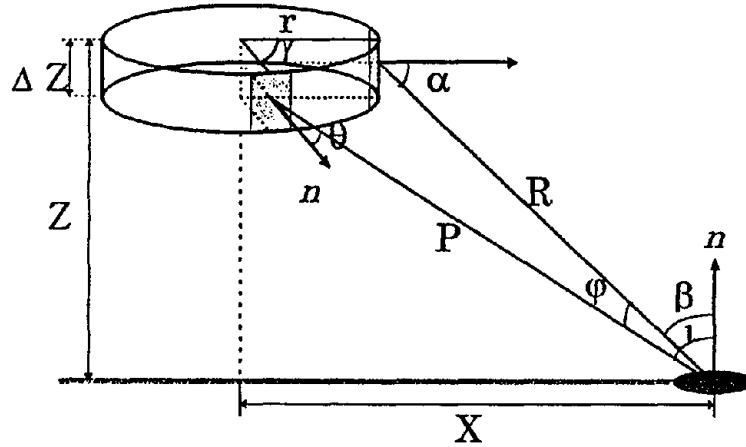
Figure 7 Horizontal distribution of radiation heat flux to the targets measured and calculated ones based on two models on jet flame figures illustrated in Figure 8-(a) and (b)

Figure 7 also shows the representative distribution of radiative heat flux calculated based on the above flame models. This figure shows that the better coincidence was obtained between the estimated values and measured one if we adopt the cylindrical flame model than we adopt the trapezoidal model. The marginal part between flame and atmosphere is turbulent so that flat inclined surface of the trapezoidal flame model gave less radiation heat to the target.

4. Conclusions

This work showed that the jet flame figures of height and width, and height to the base of lifted flame can be predicted by the power function of dimensionless heat release rate.

Excess temperature along the center line of the jet flame can be divided into two regions; lower flame region, and upper flame region. In the lower flame region, ΔT showed



taking the lengths and angles in the above illustration,

$$R = \sqrt{(X - r)^2 + Z^2}$$

$$P = \sqrt{(X - r \cdot \cos \gamma)^2 + (r \cdot \sin \gamma)^2 + Z^2}$$

$$= \sqrt{X^2 + r^2 + Z^2 - 2Xr \cdot \cos \gamma}$$

$$\cos \alpha = \frac{(X - r)}{R}, \quad \cos \beta = \frac{Z}{R}, \quad \cos \phi = \frac{\sqrt{(X - r \cdot \cos \gamma)^2 + Z^2}}{P}$$

the view factor F can be expressed as

$$F = \int_s \frac{\cos \theta \cdot \cos \iota}{\pi \cdot P^2} dS$$

$$= \int_s \frac{\cos \alpha \cdot \cos \gamma \cdot \cos^2 \phi \cdot \cos \beta}{\pi \cdot P^2} dS$$

$$= \frac{2r}{\pi} \int_0^Z \int_0^{\frac{\pi}{2}} \frac{(X - r) \cdot \cos \gamma \cdot ((X - r)^2 + Z^2) \cdot Z}{R^2 \cdot P^4} d\gamma dZ$$

where

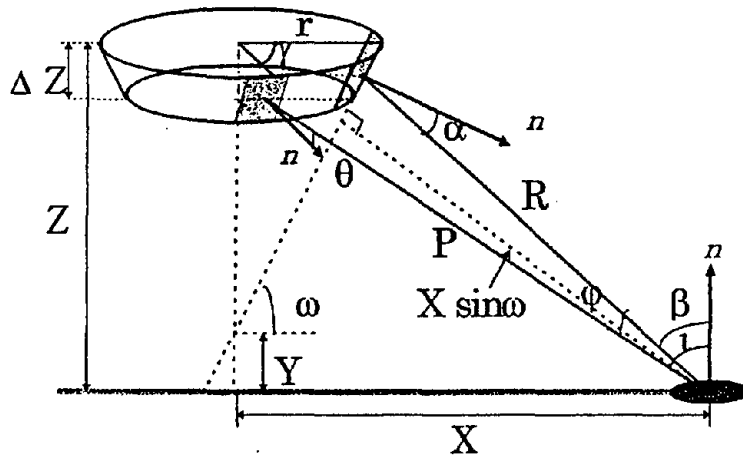
$$\cos \theta = \cos \gamma \cdot \cos \alpha \cdot \cos \phi$$

$$\cos \iota = \cos \phi \cdot \cos \beta$$

$$dS = r \cdot d\gamma \cdot dZ$$

Figure 8-(a) Cylinder model for a jet flame to estimate the view factor.

almost constant of $850 \sim 950^\circ\text{C}$, and upper flame regions, ΔT decreased with $-3/2 \sim -5/3$ power to the height. This decreasing rate is similar to the plume region of a diffusion flame from a pool fire. We observed no clear temperature decreasing mode of -1 power to height for the intermittent region.



taking lengths and angles in the above illustration

$$R = \sqrt{(X-r)^2 + Z^2}$$

$$P = \sqrt{(X-r \cdot \cos \gamma)^2 + (r \cdot \sin \gamma)^2 + Z^2}$$

$$= \sqrt{X^2 + r^2 + Z^2 - 2Xr \cdot \cos \gamma}$$

$$\cos \alpha = \frac{\left(X + \frac{Y}{\tan \omega}\right) \cdot \sin \omega}{R}, \quad \cos \beta = \frac{Z}{R}, \quad \cos \varphi = \frac{\sqrt{(X-r \cdot \cos \gamma)^2 + Z^2}}{P}$$

The view factor, F , between a trapezoidal flame part and a target

$$F = \int_S \frac{\cos \theta \cdot \cos \iota}{\pi \cdot P^2} dS$$

$$= \int_S \frac{\cos \alpha \cdot \cos \gamma \cdot \cos^2 \varphi \cdot \cos \beta}{\pi \cdot P^2} dS$$

$$= \frac{2r}{\pi} \int_0^Z \int_0^{\pi/2} \frac{\left(X + \frac{Y}{\tan \omega}\right) \cdot \cos \gamma \cdot \left((X-r)^2 + Z^2\right) \cdot Z}{R^2 \cdot P^4} d\gamma dZ$$

where

$$\cos \theta = \cos \gamma \cdot \cos \alpha \cdot \cos \varphi$$

$$\cos \iota = \cos \varphi \cdot \cos \beta$$

$$dS = r \cdot d\gamma \cdot \frac{dZ}{\sin \omega}$$

Figure 8-(b) Cone model for a jet flame to estimate the view factor.

It is important to note that the cylindrical flame piled up model, as shown in Figure 8-(a), indicates that the jet flame is translucent and has very turbulent marginal part between flame and atmosphere. The representative flame temperature is well approximated by the center line temperature. And the cylindrical flame model was better than trapezoidal model to estimate the radiation heat flux to the vessel from a jet flame

5. Acknowledgment

This work was supported financially by KHK (Kohatu-Gas Hoan Kyokai), and authors are grateful to Mr. T. Miura (KHK) and Mr. S. Ohsugi (Sci. Univ. of Tokyo) for their assistance in carrying out the experiments and observation on jet flame figures. One of authors (O.S.) wish to sincere acknowledge to Prof. Toshisuke Hirano (Tokyo Univ.) and Prof. Satoshi Ishizuka (Hiroshima Univ.) for their kind and valuable suggestions.

6. Reference

- [1] Technical Report on 'Tank Temperatures exposed to Wood Crib Fires', Kohatsu-Gas Hoan Kyokai (KHK: High Pressure Gas Safety Association) Report (1994) (in Japanese)
- [2] McCaffrey, B.J., 'Flame Height', Section 1/Chapter 18, The SFPE Handbook of Fire Protection Eng., First Edition, SFPE and NFPA (1988)
- [3] McCaffrey, B.J. 'Purely buoyant diffusion flames: some experimental results', NBSIR 79-1910 (1979)
- [4] Zukoski, E. E., Kubota, T., and Cetegen, B. 'Entrainment in Fire Plumes', Fire Safety Journal, vol.3, pp.107-121, (1980/81)
- [5] for example, "Handbook of Chemical Engineering", Section 6.3, 5th Edition (1988) published by Maruzen (in Japanese)

Nomenclature

D: bore size (m)

Ha: flame height from nozzle along the center line of a jet flame (m)

h: height to the base of lifted flame from bore (m)

ΔT : excess temperature from room temperature (°C or K)

W_f : width of jet flame (m)

Discussion

Edward Zukoski: I'd like to make a comment and ask a question also. If the Q^* parameter works anywhere, it works for a buoyant diffusion flame. So if you want to compare some of your data with other peoples, it might be better to look at Froude number scaling in the region where momentum is dominating the flow. My question is: you mentioned that the velocity was 250 m/s at the nozzle exit, which sounds like the flow was super sonic.

Osami Sugawa: It was not a stable flame. Yes. It was supersonic for very short time.

Edward Zukoski: Because there are techniques for handling that. When the flow is supersonic, you get a rapid expansion of the jet, and you get a different effective diameter for the jet flow.

Osami Sugawa: Yes.

Patrick Pagni: The delivery system you showed in your early slides currently exists in rural United States such as Lake Tahoe. The standards there are 3 meters from the residence and 6 meters from the adjacent residence for a roughly one meter cubed propane tank at 80% full. A comment and a question quickly. Your method is very interesting and I would very much like to see a calculation of the radiation from a leak as your data show to the adjacent wall in the conditions that exists in the typical US application. In our situation, the concern is not so much a high pressure leak, but our experience is that the shifting of the tank in the snow creates a leak at low pressure, at low flow, that allows the heavier-than-air propane to go down hill and form a pocket that then explodes. Have you worried about that problem?

Osami Sugawa: Yes. I think that's kind of a problem in Japan.

THE EFFECT OF POOL DIAMETER ON THE PROPERTIES OF SMOKE PRODUCED BY CRUDE OIL FIRES

G.W. Mulholland and W. Liggett
National Institute of Standards and Technology
Gaithersburg, MD 20899

H. Koseki
Fire Research Institute
Mitaka, Tokyo, 181, Japan

ABSTRACT

The smoke production from the burning of crude oil was investigated for a 1 m diameter pan and for a 2.7 m × 2.7 m pan, which is the largest pan size used within a fire test facility for smoke characterization. The smoke yield, as measured by two procedures both based on the carbon balance method, increased by about 50% as the pan size increased. Analysis of the smoke by transmission electron microscopy showed that the volume mean diameter of the primary spheres increased by about 80% as the pan size increased. These results are compared with other studies ranging in scale from a pool diameter as small as 8.5 cm to as large as 12 m crude oil "spill" fires and 100 m pool fires set during the 1991 war in Kuwait.

INTRODUCTION

This study is directed at extending the data base for quantitative smoke yield for the burning of crude oil within an enclosure to include a 1 m pan diameter and a 2.7 m × 2.7 m pan. The experiments were performed at the large scale fire facility at the Fire Research Institute in Japan. A previous study [1] based on a single large pool burn suggested that the smoke yield increased by at least 50% as the pan size was increased from 1 to 2.7 m. To ensure reliable results in the present study triplicate tests were performed at both scales and two measurement approaches were employed. A key feature of the study is the use of the carbon balance method for the quantitative measurement of smoke yield.

A second objective of the present study was to determine the effect of pan size on the primary sphere size of the smoke, which is made up of clusters of primary spheres. Previous measurements of primary sphere diameter for a wide range of hydrocarbon fuels extends from 30 to 50 nm for fires ranging in size from 2 to 20 kW [2]. For large fires, there appears to be no systematic study of the primary sphere size of the smoke.

EXPERIMENTAL APPROACH

A mixture of 80% murbane and 20% arabian crude oil was burned in pans placed at the center of the test facility, which has an open area 24 m × 24 m under a 20-m high ceiling. The crude oil was burned in a 1-m diameter circular pan and in a 2.7 m square pan with an oil layer of 2 cm floating on water. In this study we focussed on the smoke property measurements, while in earlier studies [1,3] the burning rate and radiant output before and during boilover were measured.

The major experimental focus was on the application of the carbon balance method [4] in the measurement of the smoke yield, defined as the mass of smoke particulate produced per mass of fuel consumed. This is accomplished by dividing the smoke mass collected on a filter to the sum of the smoke mass and the mass of carbon contained in the forms of CO and CO₂. The equation for calculating smoke yield, ϵ , as expressed in terms of CO₂ and CO concentrations is given by:

$$\epsilon = \frac{f m_s}{[m_s + 0.012n_s(\Delta X(\text{CO}) + \Delta X(\text{CO}_2))]} \quad (1)$$

The quantity f is the carbon mass fraction of the fuel (0.855 for the crude oil blend used in this study), m_s is the mass of the smoke sample collected on a filter, n_s is the number of moles of air sampled, and the constant 0.012 represents the molar mass of carbon in kilograms. The quantities $\Delta X(\text{CO})$ and $\Delta X(\text{CO}_2)$ are the mole fractions of CO and CO₂ of the gas sample taken during the test minus the ambient background concentrations of these gases.

Two different procedures, both based on the carbon balance method, were used for measuring the smoke yield. In one, a sampling probe was positioned 4 m above the pan for the 1 m fire and in the exhaust duct of the facility for the case of the 2.7 m square pan. The smoke/gas entered a 6.5 mm diameter sampling probe at near isokinetic velocity of about 5 m/s for the smaller pan and about 10 m/s for the larger pan. The smoke particulate was collected on a ceramic filter while the gases flowed to a CO/CO₂ nondispersive infrared analyzer.

The second method utilized an airborne smoke sampling package (ASSP) originally designed to be flown suspended below a tethered helium-filled balloon or helicopter [5]. The basic components of the device are a filter, a diaphragm pump, and a gas sampling bag. In this case, a fraction of the gas sampled by the pump is directed into the sampling bag throughout the sampling period. After the test is completed, the CO and CO₂ content of the gas is determined by gas chromatography. Transmission electron micrograph (TEM) grids were attached to the aluminum surface of the ASSP using double stick tape for subsequent analysis of the size and structure of the smoke agglomerates. The agglomerates are deposited by thermophoresis as a result of the metal surface being cooler than the air. Sedimentation and diffusion also contribute to the deposition of the smoke.

RESULTS

Smoke Yield

The results of all the tests are summarized in Table 1. The average smoke yields obtained by the two methods for the 2.7 m square pan agree well, 0.148 vs 0.149. The coefficients of variation, standard deviation/average, equal 0.081 for the ASSP and 0.101 for the continuous sampling. The average yield for the 1 m pan is 0.100 for the ASSP and 0.061 based on continuous sampling. One reason for the lower value for the continuous sampling is that the smoke is collected throughout the burn including the boilover period during which the yield is reduced [6]. The smoke is not collected during boilover by the ASSP to avoid damage to the plastic components (collection bag, plumbing, and pump housing). A difference in yield for the two approaches is not expected for the larger pan

because the boilover effect is minimal. The key observation is that the smoke yield increases by about 50% as the pan size is increased from 1 m to 2.7 m. The corresponding burning rates for the two pan sizes are approximately 0.022 and 0.26 kg/s.

Primary Sphere Size

In Fig. 1 we show representative micrographs of the smoke collected from the 1 m and 2.7 m pans. The most striking feature is the apparent bimodal size distribution of large (100 - 150 nm) and smaller (30 -70 nm) primary spheres for the larger pan. Furthermore, the larger spheres are grouped together and the smaller ones are also grouped together.

The particle size analysis for each fire size is based on the analysis of a single TEM grid. For each grid on the order of 20 locations were selected at random and photographs were taken. The size distribution is based on 10-30 primary spheres from each photograph for a total of 404 spheres for the 1 m diameter pan and 483 for the 2.7 × 2.7 m pan. The spheres selected for sizing for each photograph are determined from a transparent template with 100 randomly selected points. From the size distribution, the volume mean diameter, D_v , is found to be 58 nm for the 1 m diameter pan, 106 nm for the 2.7 × 2.7 m pan. Limited data sets were also analyzed for an 0.1 m diameter pan with the same crude oil and a 12 meter diameter pan involving the burning of Baton Rouge crude [8]. The values of D_v are 101 nm and 51 nm for the 12 m and 0.1 m pans, respectively.

DISCUSSION

Smoke Yield

In Fig. 2 the smoke yield is plotted versus pool diameter. We define the effective diameter of the 2.7 m square pan as the diameter of a circle (3.05 m) with area equal to the square pan. Fig. 2 includes other crude oil fires with "pan sizes" ranging from 0.085 m to 100 m [1, 7, 8, 9, 10, 11]. The present study with pan sizes of 1 m and 3.05 m matches two of the sizes used in a previous study [1]. The average yields obtained by the ASSP in the present study are 0.148 and 0.100 compared to 0.194 (1 test) and 0.087 (3 tests) obtained in the previous study [1] for the 3.05 m and 1 m pan size, respectively. Our present experiments confirm the trend of increasing smoke yield with increasing pan size though the magnitude of the increase, about 50%, is less than the more limited results of the previous study [1].

The results for 2 m pan size for two different studies involving 2 burns each [1, 5] fall between the current results for the 1 m and 3.05 m pan size. The data at the smaller pan sizes of 0.085 m and 0.6 m indicate a further reduction of yield with decreasing pan size [1, 8] down to a value of about 0.055 for the 0.085 m pan diameter.

The data from 2 m to 15 m based on 5 studies [1, 7, 8, 9 and the present study) with 5 types of crude oils (murban, Arabian light, Louisiana crude, murban-Arabian light mixture, and Newfoundland crude) appear to be independent of size; with one exception the data fall in the range 0.13 to 0.16. For the pan sizes larger than 3 m, the burns were performed outside where the ambient wind may affect the smoke yield.

The results from two series of tests at 17.2 m are significantly lower than the results from 2 m to 15 m. The results from one series [9] range from 0.101 to 0.111 with a mean of 0.107 while the other was a single test with a value of 0.127 [8]. The cause for an apparent decrease is not known.

Fig. 2 also contains the results obtained from sampling smoke produced by individual oil well fires in Kuwait [10, 11]. The University of Washington's Convair C-131A research aircraft was used for sampling in the plume for one study [10] and a Royal Saudi Air Force UH1N helicopter fitted with a NASA smoke sampling package was used in the other [11].

We believe their values significantly underestimate the true value for two reasons. First, the total particle yield is about twice the smoke yield. We surmise that the total particle yield is a better estimate of the smoke yield than the actual smoke measurements in part because no other major component was found in the particulate besides the smoke.

Secondly, the sampling methods could affect the results. In an oil burn test in Canada [12], both the ASSP and aircraft sampling were used on the same test with the ASSP giving an average yield of 0.151 compared to the aircraft value of 0.073 for the carbonaceous component of the particulate (including "elemental" carbon and organic carbon) and 0.087 for the total particulate yield. These results suggest that sampling is an issue, though the exact collection method used in Canada was not identical to the one used in Kuwait.

Primary Sphere Size

Our observation that the volume mean diameter of the primary sphere increases by more than 80% (58 nm vs. 106 nm) as the pan diameter increases from 1 to 3.05 m appears to be new. This change is expected to affect both the optical and aerodynamic properties, since for a 106 nm sphere the optical size parameter, $\pi D/\lambda=0.7$ for wavelength $\lambda = 0.5 \mu\text{m}$, and Knudsen number, 1.2, are both approaching the value 1, which marks a change from Rayleigh to Mie scattering and free molecular to continuum dynamics.

How do these sizes compare with other fuels studied? The geometric mean sphere diameter and geometric standard deviation were measured for the smoke produced by burning seven fuels as buoyant turbulent diffusion flames with a burner diameter of 5 to 25 cm [2]. The volume mean diameter derived from these measurements extends from 33 nm to 56 nm for fuels ranging from the least sooting, isopropanol, to the most sooting, toluene. This result suggests that a large fire size is needed to obtain a large volume mean diameter for a buoyant diffusion flame at ambient conditions.

There are very limited data for large scale fires. Surprisingly there are no published data on the primary sphere size distribution for the smoke from the Kuwait fires. Our result for the volume mean diameter for a 12 m pool fire, 101 nm [8], is similar to the result for the 2.7 m \times 2.7 m pan fire, 106 nm. Radke *et al.* [13] also observed large primary spheres for smoke collected from the burning of a 30 m diameter pool of aviation fuel. They comment that "most of the particles in the smokes consisted of two types of chain aggregates: one comprised of fairly uniform spheres with approximately 30 nm diameter and the others of spheres with approximately 150 nm."

Conclusions

1. Smoke yield increases as the pan diameter increases up to a value of 0.14 - 0.15 at a pan diameter of 2 m - 3 m and stays relatively constant up to a pan diameter of about 15 m. The reported yields from the Kuwait oil well fires, 0.02 - 0.03, are underestimates because of difficulties in particle sampling and analysis.
2. The volume mean diameter of the primary spheres of smoke produced from the burning of crude oil increases by about 80% from 58 nm to 106 nm as the pan size increases from 1 to 3.05 m. The limited results available for larger pool fires are similar to the results for the 3.05 m pan. The large and small primary spheres are segregated on separate agglomerates or subsections of agglomerates.

Acknowledgment

The electron microscopy was performed by Dr. Hashimoto from Tokyo Science University.

REFERENCES

1. Koseki, H., and Mulholland, G.W., *Fire Technology* 27:54-65 (1991).
2. Koylu, U.O., and Faeth, G.M., *Comb. Flame*, 89:140-156 (1992).
3. Koseki, H., Kokkala, M., and Mulholland, G.W., in *Proceedings of the Second Fire Safety Science International Symposium* (G. Cox and B. Langford, Eds), Elsevier, London, 1991, pp. 865-874.
4. Mulholland, G.W., Henzel, V., and Babrauskas, V., *Proceeding of the Second International Conference on Fire Safety Science*, T. Wakamatsu, Y. Hasemi, A. Sekizawa, P.J. Pagni, and C.E. Grant, Eds), Hemisphere pub., N.Y., 1989, pp. 347-357.12. Ward, D.E., Nelson, R.M., and Adams, D.F., in *Proceedings of the Seventy-Seventh Annual Meeting of the Air pollution Control Association*, Air And Waste Management Assoc., Pittsburg,PA., 1979, Pap. 079-6.3.
5. Lawson, J.R., Mulholland, G.W., and Koseki, H., *Fire Technology*, 30: 155-173 (1994).
6. Benner, B.A., Bryner, N.P., Wise, S.A., Mulholland, G.W., Lao, R.C., and Fingas, M.F., *Envir. Sci. and Tech.*, 24: 1418-1427 (1990).
7. Walton, W., Twilley, W., McElroy, J., and Evans, D., in *Proceedings of the Seventeenth Arctic and Marine Oil Spill Program Technical Seminar*, Ministry of Supply and Services Canada, 1994, Vol.2, pp. 1083-1098.
8. Evans, D., Walton, W., Baum, H., Notarianni, K., Lawson, J., Tang, H., Keydel, K., Rehm, R., Madrzykowski, D., Zile, R., Koseki, H., and Tennyson, E., in *Proceedings of the Fifteenth Arctic and Marine Oil Spill Program Technical Seminar*, Ministry of Supply and Services Canada, Cat. # En 40-11/5-1992), 1992, pp. 593-657.
9. Walton, W., Evans, D., McGratten, K., Baum, H., Twilley, W., Madrzykowski, D., Putorti, A., Rehm, R., Koseki, H., and Tennyson, E., in *Proceedings of the Sixteenth Arctic and Marine Oil Spill Program Technical Seminar*, Ministry of Supply and Services Canada, 1993, pp. 679-734.
10. Laursen, K.K., Ferek, R.J., Hobbs, P.V., and Rasmussen, R.A., *J. Geophys. Res.*, 97: 14,491-14,497 (1992).

11. Cofer, W.R. III, Steven, R.K., Winstead, E.L., Pinto, J.P., Sebacher, D.I., Abdulraheem, M.Y., Al-Sahafi, M., Mazurek, M.A., Rasmussen, R.A., Cahoon, D.R., and Levine, J.S., *J. Geophys. Res.*, 97: 14,521-14,525 (1992).
12. Ferek, R.J., Ross, J.L., and Hobbs, P.V., Final Report from University of Washington to Environment Canada entitled "Airborne Sampling of Smoke Emissions from the Controlled Burn of 20,000 Gallons of Crude Oil During Open Ocean Conditions Off Newfoundland," 1995.
13. Radke, L.F., Lyons, J.H., Hobbs, P.V., and Weiss, R.E., *J. Geophys. Res.*, 95: 14,071-14,076 (1990).

Table 1. Results for Smoke Yield and Primary Sphere Size

PAN SIZE	ϵ (ASSP)	ϵ (continuous sampling)	Volume Avg. Primary Sphere Diameter
1 meter diameter	0.090		
"	0.109	0.065	58 nm
"	0.097	0.057	
"	0.103		
Avg \pm sigma	0.100 \pm 0.008	0.061	
2.7 meter square	0.148	0.133	
"	0.160	0.153	106 nm
"	0.137	0.162	
Avg \pm sigma	0.148 \pm 0.012	0.149 \pm 0.015	

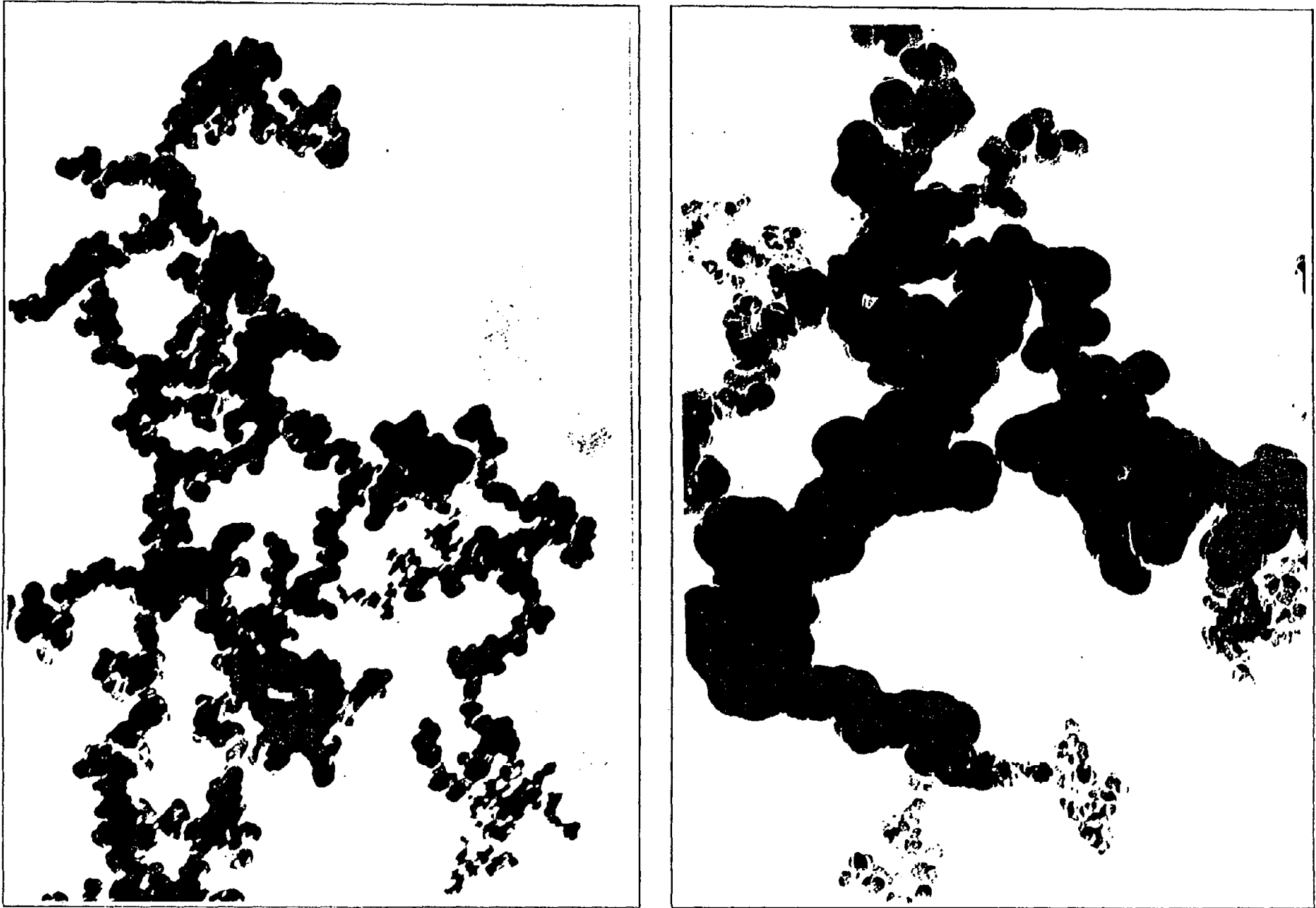


Fig. 1 TEM photographs of smoke collected from crude oil fires for 1 m diameter pan (left) and 2.7 x 2.7 m (right) pan.

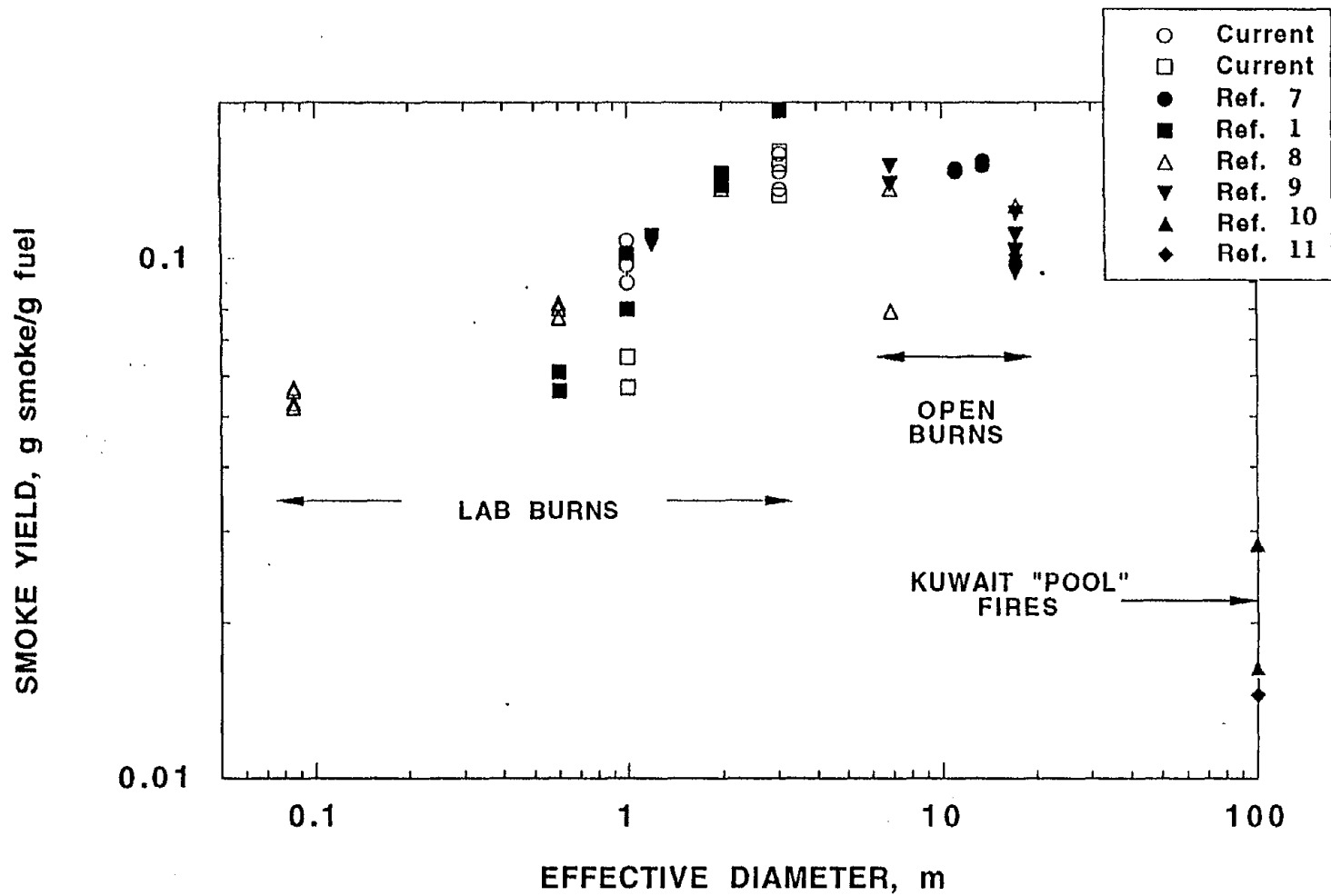


Fig. 2 The effect of pan diameter on the smoke yield of burning crude oil

Discussion

Edward Zukoski: If you go back in the literature on small diffusion flames, there seems to be a time history of the particles. They are big and wet to start with, and they get dried out and they get smaller as they go up. Have you tried to take that sort of time scaling into account in what you've done here?

George Mulholland: My chemist's view of the controlling factors of the particle growth consists of basically two things; one is the time and the other is the temperature. When you look in the carbon black industry, you find that they are very clever in controlling the size. If they want their particles bigger, they lower the temperature, and if they want them smaller, they increase the temperature. So I thought that might be an important parameter along with the time. The problem is that the data do not seem to indicate that the bigger flames have a lower temperature. But when I use a correlation similar to yours, the time scale goes from something like 0.7 s for the total residence time in the flame to something like 1.1 s as you go from the 1 to 3 pool.

Edward Zukoski: It goes in the wrong direction.

George Mulholland: No that's going in the right direction, but I'm skeptical that the time by itself would account for it.

John Rockett: It seems to me that I've seen data for smoky fires: the larger the fire, the higher the core temperature because of the radiation blanketing. The outer surface of the flame can radiate, but the interior radiation is trapped inside. Would that have a bearing on the particle size seeming to go in the wrong direction?

George Mulholland: I agree with that assessment. It's an expected effect that the bigger fire with the radiation trapped would have a higher temperature, at least high up. I think much of the formation of the primary size soot occurs very close to the surface, so I thought that maybe the temperature is lower there, but Hiroshi's data suggests that there's really not much difference if you scale your heights. So, we've looked but it's not obvious.

Howard Baum: I think that there are two factors that are possibly different as you go up in this size. The first, which you've already mentioned, is the residence time of these particles. I suspect that the ratio is much larger than simply even a ratio of D or of D^* . The larger fires with a larger dynamic range of active scale are probably going to have a much more meandering path for the soot particles. So I would expect the age to be much higher for the larger fires than a simple relationship might indicate. The second, a kind of fractal surface volume effect would not be on the particles but on the apparent surface of the smoke exposure to the oxygen. In other words, it might be much harder to see oxygen or spend a smaller fraction of it's time in regions that did have oxygen with the larger fire.

George Mulholland: Howard makes good points. The correlation that I used was actually from Gerry Faeth's paper. But when I look at the non-dimensional expression, it is very similar to the kind of scaling used by Ed Zukoski, as well as Howard Baum and Bernie McCaffrey, in terms of

Discussion cont.

a velocity and height vs. velocity to integrate to get a time. I basically used the expression Faeth developed, but it is based on a scaling approach and may not be realistic for an actual trajectory in any one place within the flame. I think from Howard's comment about the oxygen, one might suspect two populations of particles, if one can envision some reason why the flame structure would be two different, distinct regions that lead to different populations of particles. If something occurs in the vortex on the outside and something else occurs higher up, it requires a chemist's level of understanding.

Heat and Mass Transfer in the Walls Subjected to Fire

Kazunori HARADA

Toshio TERAI

Building Research Institute,
Ministry of Construction
Tatehara 1, Tsukuba, 305, Japan

Department of Architecture,
Kinki University
Takaya-Umenobe, 1, Higashi-Hiroshima,
729-17, Japan

ABSTRACT

The physical process of heat and mass transfer in concrete walls was described by a model. The model consist of heat conduction in the skeleton, mass (air, water vapor and adsorbed water) transfer in the pore. The desorption of the adsorbed water and the decomposition of the water of crystallization were included explicitly. The model was applied to two practical problems. The first application was to investigate the variation of insulation performance of flat wall by the change in initial water content. The range of variation was quantified and compared with the variation caused by mix design. From the calculated results, a methodology was proposed to carry out the mix design of concrete for arbitrate required insulation performance taking into account of the variation caused by uncertainty in initial water content. The second application was to define the optimum cross sectional shapes of composite floor of profiled steel sheet and concrete. The model was extensively used to analyze the dependence of the insulation performance upon the cross sectional shape. Simple but useful concept of "thermally optimum" was proposed to assure sufficient insulation performance.

1. INTRODUCTION

Concrete is a wet porous material. When concrete members are intensely heated, water in the pore evaporates to vapor. As a consequence, temperature rise is delayed in the temperature range of 100 and 150°C. This phenomenon is called "creeping of temperature". To predict the temperature histories of concrete members, this phenomenon should be modeled appropriately.

In the early 1960's, simple models were proposed by Kawagoe¹⁾, Wakamatsu²⁾, Pettersson *et al*³⁾, Wickstrom⁴⁾, Lie⁵⁾ and others. They assumed that the temperature is sustained at 100°C as long as liquid water remains in the pore. This method gives reasonable results of temperature rise. Thus it is widely used in many applications up to today. However the model is not enough when we needs information other than temperature. More sophisticated models treats the problem as a drying process of wet porous material. Desorption (evaporation) of physically adsorbed water, and corresponding mass transfer in the pore are described. Harmathy⁶⁾ proposed a model for brick walls. Similar approaches were proposed by Huang *et al*⁷⁾, Sahota *et al*⁸⁾ for concrete.

When we focus on concrete, two types of water, physically adsorbed water and the water of crystallization, exist. Physically adsorbed water evaporates in the temperature range of 100 to 150°C, which results in the creeping of temperature and the pore pressure rise. The water of crystallization are decomposed into vapor at higher temperature. This process corresponds with the deterioration of the material. In order to know the behavior of concrete

during fire, it is important to take the both phenomena into account.

A model of heat and mass transfer in concrete was developed by the authors⁹⁾ to take into account of both desorption and decomposition. In this paper, the physical and mathematical basis of the model is briefly described. Then the model is applied to two practical problems. The first application is to analyze the variation of the insulation performance of flat walls heated by ISO fire. The effect of initial water content and mix design is quantified, which enables the rational mix design of concrete walls for insulation performance. The second application is a problem of finding the optimum cross sectional shape of composite floor. So far these applications deals with only the insulation performance (temperature rise of unexposed surface). The correlation with material integrity and deterioration is under investigations. A preliminary idea will be briefly mentioned as a plan of future investigations.

2. PHYSICAL PROCESS OF HEAT AND MASS TRANSFER IN CONCRETE

2.1 Experimental Investigation

The process of heat and mass transfer was investigated by small scale experiments. The specimen was a flat mortar wall of 40 mm thickness. As shown in Figure 1, the wall was heated by an electric furnace. Temperature, water content and pore pressure were measured at the locations shown in the figure. Temperature was measured by type K thermocouples. Water content was measured by hand made probes. Pore pressure was measured indirectly via a oil pressure in a pipe embedded in the mid thickness of the specimen.

An example of the results is shown Figure 2 by symbols. Among the data, the data at the mid thickness point (point 3) is analyzed in the following. Temperature gradually rose until 100°C. Then the creeping of temperature began at 15 minutes. Until temperature reached 140°C at 25 minutes, the temperature rise was very slow. In the early stage, the water content increased because of the re-adsorption of water vapor that came from the zone closer to the exposed surface. During the period of creeping of temperature, water content decreases monotonously. The pore pressure increased during the same period. The peak value appeared at 26 minutes. At almost the same time, the creeping of temperature is finished. As described above, complex transport phenomena take place in the material during the period of creeping of temperature.

2.2. A Model of Heat and Mass Transfer

The above described physical process could be modeled by a system shown in Figure 3. Water is physically adsorbed in the pore. The rest of the pore is occupied by a gaseous mixture of air and water vapor. Water vapor and adsorbed water are in equilibrium. When the temperature and/or the partial pressure of water vapor changes, desorption or adsorption takes place to sustain the equilibrium. Skeleton is made of thermally stable material and water of crystallization. At high temperature, the water of crystallization is removed from skeleton to pore. Heat is conducted in skeleton. Water vapor and air move through pore by diffusion and convection. Adsorbed water diffuses through the pore by capillary actions.

To consider these phenomena, conservation of heat, gaseous mixture (air and water vapor), water vapor, physically adsorbed water and water of crystallization were applied.,

$$\rho c \frac{\partial \theta}{\partial t} = \nabla(\lambda \nabla \theta) - L_s R_{sorp} - L_d R_{dcmp}, \quad (1)$$

$$\frac{\partial(\varepsilon \rho_g)}{\partial t} + \nabla(\rho_g \mathbf{u}) = R_{sorp} + R_{dcmp}, \quad (2)$$

$$\frac{\partial(\varepsilon \rho_v)}{\partial t} + \nabla(\rho_v \mathbf{u}) = \nabla(D_v \nabla \rho_v) + R_{sorp} + R_{dcmp}, \quad (3)$$

$$\rho_0 \frac{\partial w}{\partial t} = \nabla(\rho_0 D_w \nabla w) - R_{sorp}, \quad (4)$$

$$\rho_0 \frac{\partial w_e}{\partial t} = -R_{dcmp}. \quad (5)$$

To close the system, Darcy's law for gas filtration, rates of desorption and decomposition, ideal gas laws were coupled.

Gas Filtration through the Pore : The pore structure of concrete is usually fine so that the flow in the pore is laminar. Therefore the Darcy's law for gas filtration can be applied for gas velocity,

$$\mathbf{u} = -\kappa_D \nabla P_g, \quad (6)$$

Rate of desorption : Normally the condition of water vapor and the adsorbed water is close to equilibrium state. Thus, the rate of desorption was described by the Langmuir's equation,

$$R_{sorp} = \gamma(w - w_{eq}), \quad (7)$$

where $w_{eq}(=f(\theta, P_v))$ is the equilibrium water content.

Rate of Decomposition : The water of crystallization is decomposed gradually as the temperature is increased. There are many kinds of water of crystallization in concrete¹⁰⁾. However, for simplicity, they were classified into three groups: (1) gel water (decomposition temperature 100 - 400°C), (2) calcium hydroxide (450 - 550°C) and (3) calcium silicate hydrated (600°C-). The rates of decomposition of the three groups were described by Arrhenius type rate equations,

$$R_{dcmp} = \rho_0 \sum_{k=1}^3 w_{c,k} A_k \exp(-E_k / RT), \quad (8)$$

where subscript k ($=1,2,3$) corresponds with the above three groups.

Equations of State : The ideal gas law for water vapor and gaseous mixture are

$$\rho_v = M_v P_v / RT, \quad \rho_g = \rho_v + \rho_a = [(M_v - M_a)P_v + M_a P_g] / RT. \quad (9) (10)$$

2.3. Numerical Implementation

The governing equations are non linear and stiff because of the non linear source term, and because of the difference in characteristic time for diffusion (Fourier number) between heat and water. To avoid the numerical difficulty, integral equation method developed by Terai was applied¹¹⁾. After discretization, we get a set of simultaneous ordinary differential equations of temperature, total pressure of gaseous mixture (pore pressure), partial pressure of water vapor, content of physically adsorbed water and water of crystallization,

$$\frac{d\mathbf{x}}{dt} = f(t, \mathbf{x}), \quad (11)$$

where $\mathbf{x} = \{\theta_1, \theta_2, \dots; P_{g,1}, P_{g,2}, \dots; P_{v,1}, P_{v,2}, \dots; w_1, w_2, \dots; w_{c,1}, w_{c,2}, \dots\}^T$ is a vector of nodal variables. The diagonally implicit Runge- Kutta method was applied to integrate equation (11).

2.4. the Computer Code FRECS

The model was implemented in a Fortran 77 program named FRECS (Fire REsistance of Concrete Structures). The source code consists of about 4200 lines. It was developed on a super computer, however now it is available on UNIX workstation. A typical CPU time is about three hours to solve a problem with 40 elements for four hours of simulation time. The code was verified by comparison with several experiments. In most cases, the agreement is good. An example is shown in Figure 2 by solid lines⁹⁾.

3. VARIATION OF THE INSULATION PERFORMANCE OF WALLS BY INITIAL WATER CONTENT AND MIX DESIGN

In this chapter, a methodology for rational mix design of concrete walls for insulation performance is discussed. Insulation performance of concrete walls depends on initial water content. Moist concrete has better insulation performance than dry concrete. However the initial water content depends on the surrounding environment before fire. Thus it is hardly controllable. Due to the uncertainty in initial water content, rational design of concrete is difficult. On the other hand, the hygro-thermal properties (thermal conductivity, specific heat, permeability and so on) depend upon the mix design (type of aggregate and mix fraction). Mix design is controllable to a certain extent.

If the uncertainty by initial water content is smaller than the variation caused by mix design, it is possible to specify an acceptable range of mix design of concrete in order to assure the required insulation performance. To investigate the relative importance of initial water content and mix design, the code FRECS was applied to a flat wall with 70 mm thickness heated by ISO fire. The analysis consists of two stages. In the first step, the hygro- thermal properties were estimated for a variety of mix design and water content. Six kinds of aggregate, lightweight (LW), basalt (BA), sandstone (S1, S2), tuff (TU), and chart (CH), were selected to account for commonly used aggregates. Initial water content was varied in the range of 1 to 4 % by weight. Then, in the second step, the insulation performance was calculated using the estimated hygro- thermal properties.

3.1. Relationship between the Mix Design of Concrete and Hygro- Thermal Properties

A simple relationship between the mix design of concrete and hygro- thermal properties were developed by the authors¹²⁾. Let the volume fraction of coarse and fine aggregate, cement paste be V_{ag} , V_s , V_p , respectively. Simple additive rule can be applied to estimate the density, volumetric heat capacity and void fraction as

$$\rho = \sum_i \rho_i V_i, \quad \rho c = \sum_i \rho_i c_i V_i, \quad \varepsilon_0 = 1 - \sum_i V_i. \quad (12) (13) (14)$$

As to the thermal conductivity, Maxwell's formula for the two phases mixture of dispersed phase and continuous phase

$$\lambda_{i+j} = \lambda_i \frac{\lambda_j + 2\lambda_i - 2v_i(\lambda_i - \lambda_j)}{\lambda_j + 2\lambda_i + v_i(\lambda_i - \lambda_j)}, \quad (15)$$

was applied to the mixing of cement paste and sand, then to the mixing of cement mortar and coarse aggregate, where λ_i and λ_j are the thermal conductivity of continuous and dispersed phase, v is the ratio of volume fraction of dispersed phase. Variation of the thermal conductivity is shown in Figure 4 for the six kinds of aggregate in case of $V_{ag}= 0.362$, $V_s= 0.299$ and $V_p= 0.155$.

3.2. Variation of the Insulation Performance of 70 mm Walls by the Change in Initial Water Content and Mix Design¹³⁾

(1) Initial Water Content :

The effect of initial water content was analyzed in case of sandstone concrete (S1). The initial water content was varied in the range of 1 and 4 % by weight. Using the value S1 in Figure 4, the temperature rise of the 70 mm thick wall was calculated. The results are shown in figure 5. In case of 1% of initial water content, the duration of the creeping of temperature is only 4 minutes. As the initial water content is increased, the duration is increased to 12 minutes. The critical time for insulation performance (as defined by ISO 834) varies in the range of 64 to 74 minutes. The magnitude of variation in critical time is almost the same as in the duration of the creeping of temperature. The sensitivity is 3.3 minutes per 1% change in initial water content.

(2) Mix Design

The effect of mix design was analyzed in a similar way. While the initial water content was kept 3% wt., the type of aggregate was changed to the other five kinds in figure 4. The calculated results are shown in Figure 6. Here, the temperature rise is greatly altered. The lightweight concrete has the best insulation performance, while the worst one is chart concrete. The critical time varies between 54 and 83 minutes.

Similar analysis was carried out changing the mix proportion of coarse aggregate. The critical time was calculated for each case. The results are summarized in Figure 7 as a function of the volume fraction of coarse aggregate V_{ag} and the temperature averaged thermal conductivity of coarse aggregate,

$$\overline{\lambda_{ag}} = \int_{RT}^{800} \lambda_{ag}(\theta) d\theta / (800 - RT) \quad (16)$$

The worst case is again the chart concrete when the volume fraction of coarse aggregate is increased. The best case is the lightweight concrete. The total variation is between 50 and 83 minutes.

Comparing the variation caused by initial water content and mix design, the effect of mix design is dominant. Thus, in the purpose of design, the variation of initial water content is relatively unimportant. Approximately the effect could be added linearly. For example, to assure the 60 minutes of fire resistance time, mix design should be selected in the non hatched region in Figure 7 where the critical time is greater than 67 (=60 +3.3 × 2) minutes.

4. OPTIMUM CROSS SECTIONAL SHAPE OF COMPOSITE FLOOR¹⁴⁾

In this chapter, a methodology to design the optimum cross sectional shape of composite floor is discussed. When we consider the load bearing capacity of the slab, the lib should be as large as possible. However, when the concrete volume is limited, minimum thickness of the slab is decreased as the rib size is increased. This results in poor insulation performance. Therefore, it is expected that there is a certain limit of lib size in order to assure the insulation performance of the composite floor.

To find the limit, code FRECS was applied to various cross sectional shape. The examined cross sectional shapes are shown in figure 8. The average thickness of all these cross sectional shapes are 115 mm. From the calculated results, the critical time for insulation performance was defined by,

$$t_{fr} = \min(t_{ave}, t_{max}) \quad (17)$$

where, t_{ave} is the critical time for average temperature rise (140°C) of unexposed surface, t_{max} is the critical time for maximum temperature rise (180°C) of unexposed surface.

4.1 Examples of Results

As examples, the time- dependent temperature distributions at the unexposed surface of series A, are shown in figure 9(above). In the same figure (below), the isothermal lines at the critical time, t_{fr} , are drawn. In case of type H, the isothermal lines are considerably curved, thus the insulation criterion for the maximum temperature rise was exceeded ($t_{fr} = t_{max}$). On the contrary, in case of type L, the isothermal lines were similar to horizontal lines, therefore the insulation criterion for the average temperature rise was exceeded ($t_{fr} = t_{ave}$). In case of type S, both criteria for average and maximum temperature rise were exceeded at the same time ($t_{fr} = t_{max} = t_{ave}$).

4.2 Concept of Thermally Optimum

The variation of two critical times are shown in figures 10 and 11 as functions of rib width and height. The critical time for average temperature rise, t_{ave} , is not significantly changed by the cross sectional shapes, whereas the critical time for maximum temperature rise,

t_{max} , is strongly influenced. It drastically decreases as the rib width and/or height is increased.

The resulting critical time t_{fr} is shown in Figure 12. It is clear that the critical time is considerably reduced if the rib size is greater than a certain limit. The bold line indicates the cross sectional shapes where the both criteria are exceeded at the same time ($t_{ave} = t_{max}$). In these cross sectional shapes, there is no redundancy of the concrete location. Thus we name this feature as “thermally optimum”. The line of thermally optimum shape is a good indicator of the limit of rib size acceptable to assure the insulation performance.

5. SUMMARY AND FUTURE DEVELOPMENTS

5.1. Summary

A model of heat and mass transfer was applied to analyze the insulation performance of 1) flat walls and 2) composite floor of profiled steel plate and concrete.

Through the investigation of the flat walls, the effect of initial water content and the mix design of concrete was examined. The calculated results show that the variation by initial water content is much smaller than that by mix design of concrete. Thus the mix design for insulation performance is possible including the variation caused by initial water content.

The analysis on composite floor demonstrated that the insulation performance of composite floor depends on its cross sectional shapes. When the available concrete volume is limited, there is a certain limit of rib size in order to assure the insulation performance. From the results of calculations, the limit was derived as thermally optimum shapes, where the two insulation criteria are exceeded at the same time.

From the two applications, it was revealed that the analytical model is an effective tool to derive a design methodology for insulation performance of concrete members.

5.2. Future Developments

The present model assumes no significant change of material structure. However, material integrity is one of the important aspect of fire resistance. Heat and mass transfer process is concerned with this problem. Especially, the pore pressure rise and the temperature gradient are closely related to spalling and/or separation of surface layers, which would drastically decrease the fire resistance of concrete members.

To investigate the correlation between material integrity and heat and mass transfer, small scale experiments are being conducted. Cement mortar slab is intensely heated under sustained load. Interaction between heat and mass transfer and deformation will be analyzed.

NOTATIONS

Alphabets		H_{min}	minimum height of composite floor	[mm]	
A^*	pre-exponential factor	[1/s]	H_r	rib height of composite floor	[mm]
c	specific heat	[J/kg·K]	L_s	latent heat of desorption	[J/kg]
D_v	vapor diffusion coefficient	[m ² /s]	L_d	latent heat of decomposition	[J/kg]
D_w	water diffusion coefficient	[m ² /s]	P	pressure	[Pa]
E^*	apparent activation energy	[J/kmol]	R_{sorp}	rate of desorption	[kg/m ³ ·s]
$f(\dots)$	function of ...		R_{dcmp}	rate of decomposition	[kg/m ³ ·s]
H_{ave}	average height of composite floor	[mm]	t	time	[s]

t_{ave}	critical time for average temperature rise of unexposed surface	[min.]	Greek Letters	
t_{fr}	critical time for insulation performance defined by ISO 834	[min.]	γ	rate constant of desorption [kg/m ³ .s]
t_{max}	critical time for maximum temperature rise of unexposed surface	[min.]	ε	void fraction [m ³ /m ³]
T	absolute temperature	[K]	θ	temperature [°C]
u	apparent velocity of gas	[m/s]	ρ	density [kg/m ³]
V	volume fraction	[m ³ /m ³]	λ	thermal conductivity [W/m·K]
w	content of physically adsorbed water	[kg/kg]	κ_D	permeability [m ² /Pa·s]
w_{eq}	equilibrium water content	[kg/kg]	Subscripts	
w_c	content of water of crystallization	[kg/kg]	a	air
W_r	rib width of composite floor	[mm]	ag	aggregate
			v	water vapor
			g	gaseous mixture
			0	dry concrete

REFERENCES

- 1) Kawagoe, K., Bulletin of Fire Prevention Society of Japan, Vol. 13(2), pp. 29-35, 1964, in Japanese
- 2) Wakamatsu, T., Transactions of Architectural Institute of Japan, No.109, pp. 73-79, No.111, pp. 31-36, 1965
- 3) Pettersson, O., Magnusson, S., E., Fire Engineering of Steel Structures, Lund Institute of Technology, 1976
- 4) Wickstrom, U., TASEF-2 - A Computer Program for Temperature Analysis of Structures Exposed to Fire, Report 79-2, Dept. of Structural Mechanics, Lund University, 1979
- 5) Lie, T., T., "A procedure to calculate fire resistance of structural members", Fire and Materials, Vol. 8(1), pp. 40-48, 1984
- 6) Harmathy, T., Z., "Simultaneous moisture and heat transfer in porous systems with particular reference to drying", Industrial and Engineering Chemistry - Fundamentals, Vol. 8, pp. 92-103, 1969
- 7) Huang, C., L., D., Ahmed, G., N., Fenton, D., L., "Response of concrete walls to fire", Int. J. on Heat and Mass Transfer, Vol. 34, pp. 649-661, 1991
- 8) Sahota, M., S., Pagni, P., J., "Heat and mass transfer in porous media subjected to fires", Int. J. on Heat and Mass Transfer, Vol. 22, pp. 1069-1081, 1979
- 9) Harada, K., Terai, T., "Heat and Mass Transfer in an Intensely Heated Mortar Wall", Fire Safety Science, Vol. 3, pp. 781-790, Elsevier Applied Science, 1991
- 10) Schneider, U., Verhalten von Beton bei hohen Temperaturen, 1982
- 11) Terai, T., Harada, K., "Fire Behaviour of Concrete Members Taking into Account Simultaneous Transfer of Heat and Moisture", Proc. Asian Fire Seminar 93', pp. 49 - 58, Science University of Tokyo, 1993
- 12) Terai, T., Harada, K., "A Model of Heat Conduction of Concrete during Fire", the twelfth Japan Symposium on thermophysical Properties, pp. 181-184, 1991
- 13) Harada, K., Terai, T., "Fire Resistance of Concrete Walls", Proc. 1st. Asian Conference on Fire Science and Technology, pp. 215-219, 1992
- 14) Harada, K., Terai, T., "Dependence of Thermal Responses of Composite Slabs Subjected to Fire on Cross Sectional Shapes", Fire Safety Science, Vol. 4, pp. 1159-1170, 1994

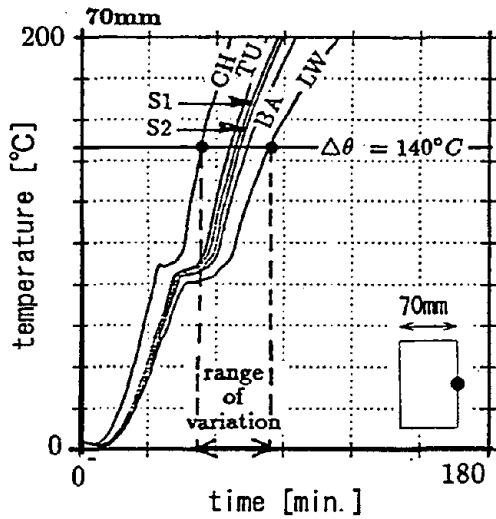


Figure. 6 calculated unexposed surface temperature for different kind of aggregate. ISO 834 standard fire. Volume fraction of coarse aggregate is 0.362. Initial water content is 3 % by weight.

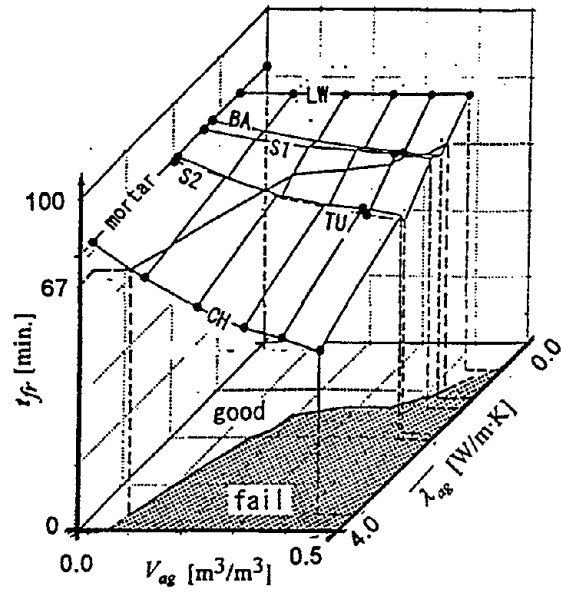
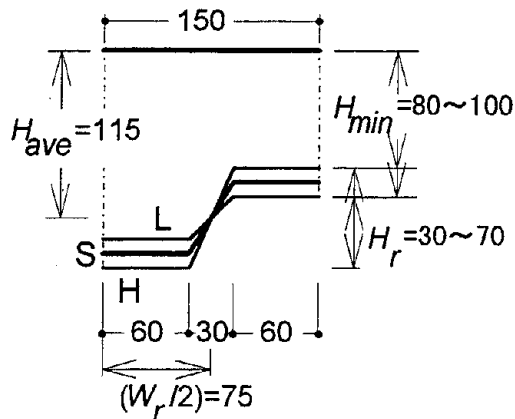
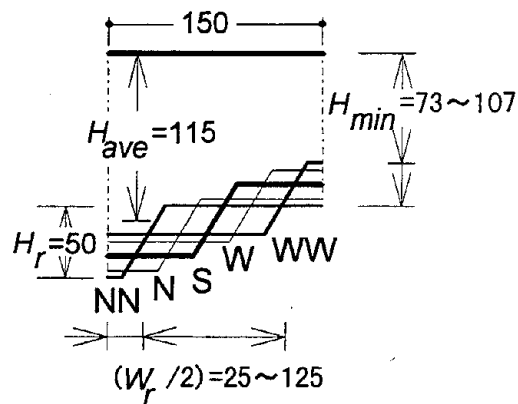


Figure 7 critical time for insulation performance as a function of volume fraction of coarse aggregate V_{ag} and temperature-averaged thermal conductivity of coarse aggregate $\overline{\lambda}_{ag}$. Initial water content is 3%.



series A: variations of rib height H_r



series B: variations of rib width W_r

Figure 8 Variations of the cross sectional shapes (unit in mm)

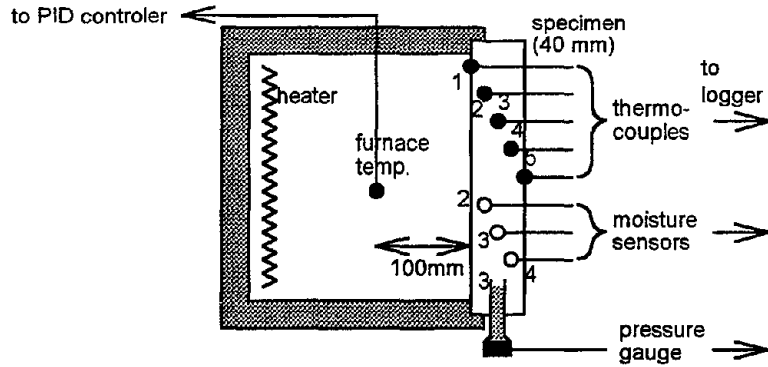


Figure 1 Schematics of experiment. A 40 mm thick specimen is equipped to a electric furnace. Temperature, water content and pore pressure are measured. (Drawing is not to scale.)

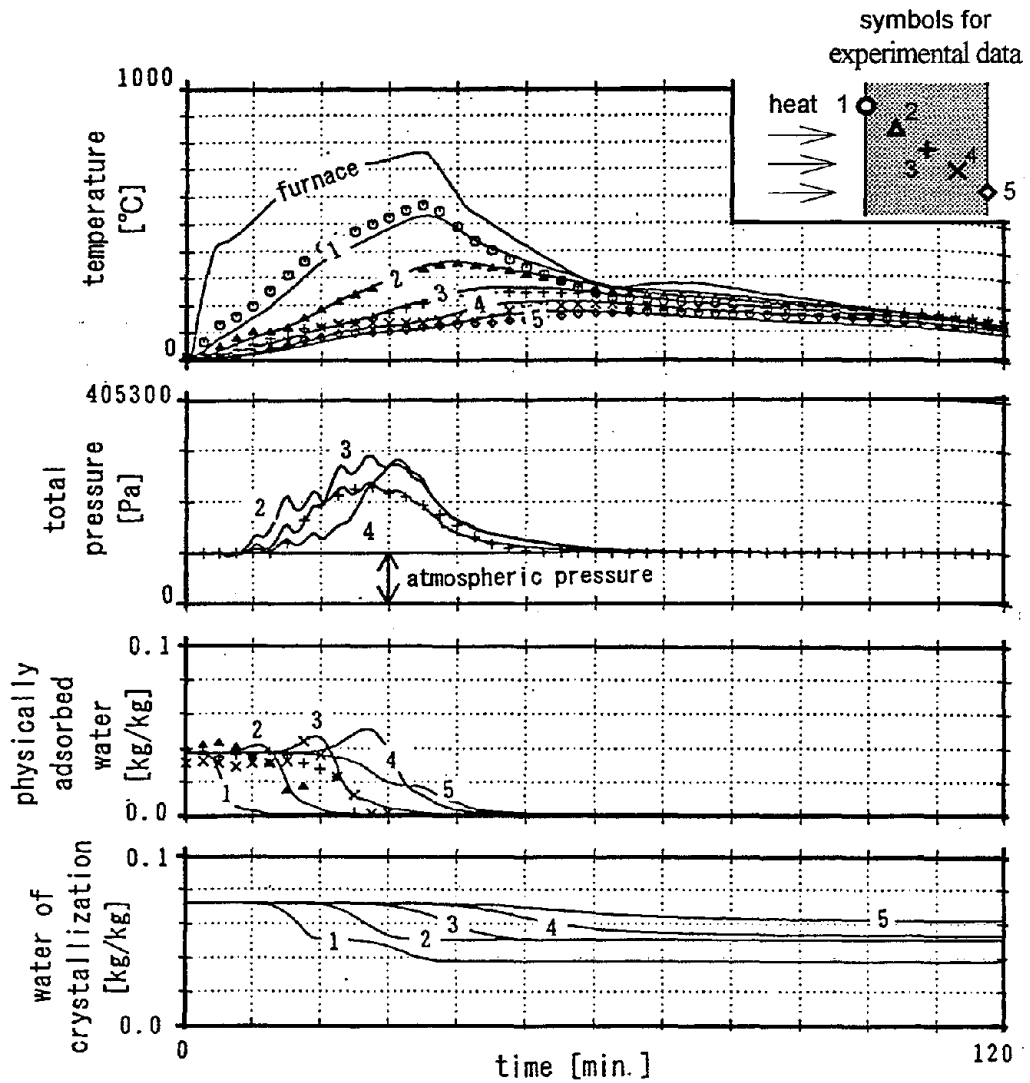


Figure 2 results of an experiment with 40 mm thick mortar wall. (symbols : measured data, solid lines : calculated results)

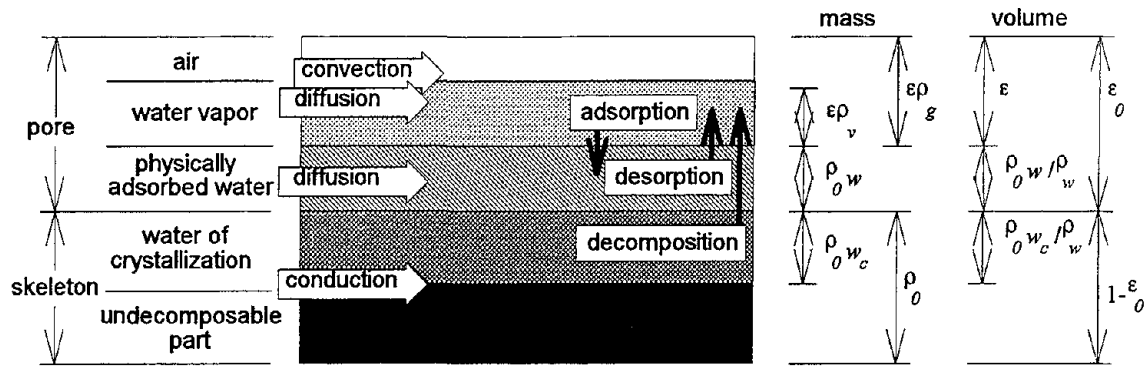


Figure 3 A model of heat and mass transfer in concrete during fire, considering the heat conduction, filtration of gaseous mixture, diffusion of water vapor and physically adsorbed water. These phenomena are coupled by sorption and decomposition

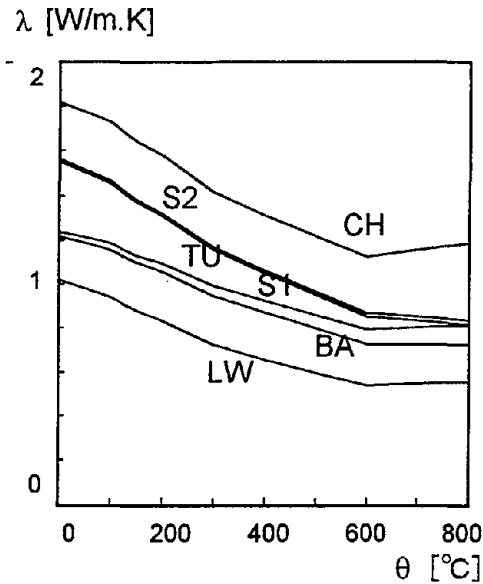


Figure 4 estimated thermal conductivity of six kinds of concrete where $V_{ag}= 0.362$, $V_s= 0.299$ and $V_p= 0.155$ (LW = light-weight aggregate, BA = basalt, S1, S2= sandstone, TU = tuff, CH = chart)

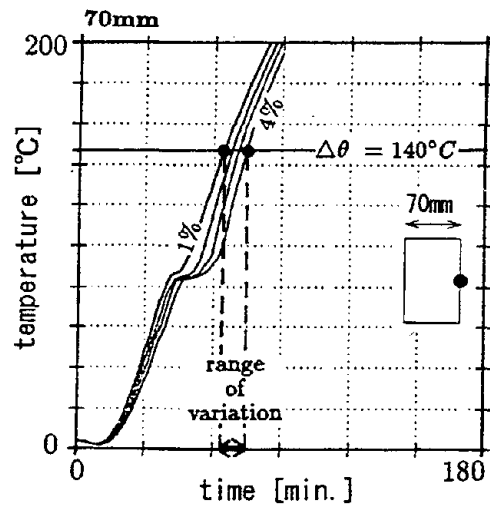


Figure. 5 calculated unexposed surface temperature rise under ISO fire for different initial water content in case of sandstone concrete (S1).

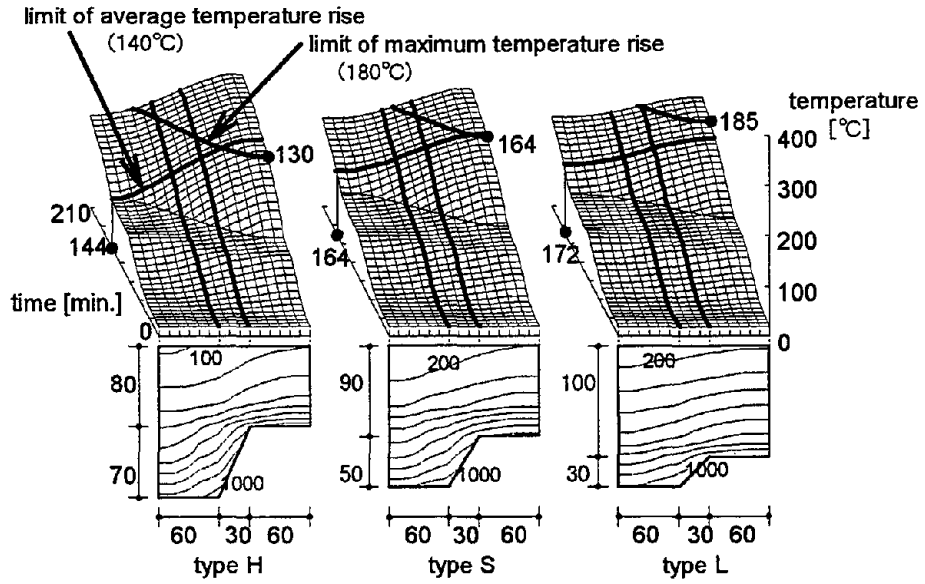


Figure 9 Change of temperature distribution of the unexposed surface with time (above) and isothermal lines at critical time for insulation criteria, t_{fr} (below)

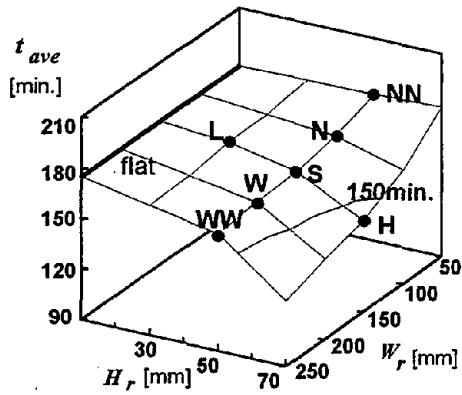


Figure 10 critical time for average temperature rise

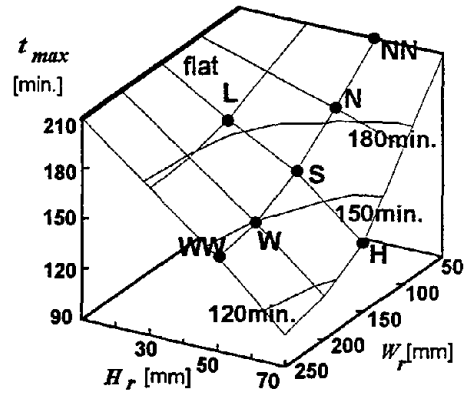


Figure 11 critical time for maximum temperature rise

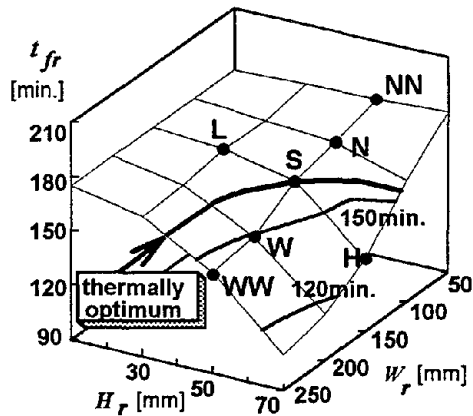


Figure 12 critical time for insulation performance as a function of rib height and width.

Discussion

Takashi Kashiwagi: I have two questions. First, did you include migration of the water in both directions. One is to the heated surface side, the other one is to a cooler side. On the cooler side, condensation is happening.

Kazunori Harada: Yes. This has been taken into consideration. We gradually heat from the left hand side and as we heat, steam will be generated. The steam would then migrate to both sides, and condensation occurs on the cooler side. That is the reason why such a peak is shown in the graph.

Takashi Kashiwagi: My second question is that there are many constants, such as a degradation constant to the absorption, and a dependency of the temperature of conductivity. Are these all measured directly for each sample?

Kazunori Harada: Yes. First of all, with respect to absorption coefficient, it is difficult to measure it, so we didn't. However, if we use a coefficient which is larger, then we found out that we could get good results. The reason is that the local absorption speed is faster than diffusion or migration, that is the reason why we can obtain good results.

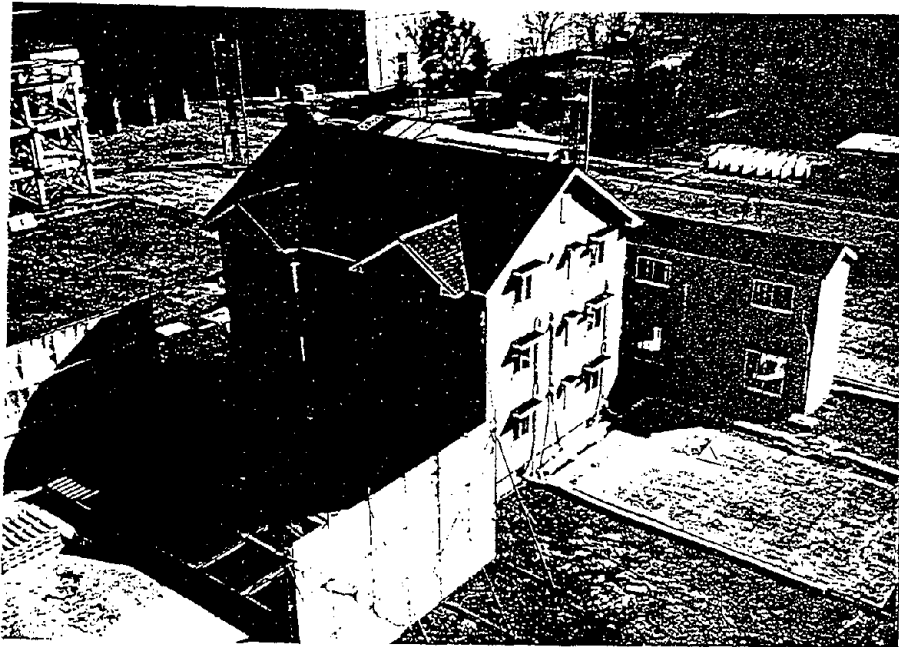
Patrick Pagni: Your fire resistance of concrete structure is a very valuable and useful program. Do you think it would be possible to add the internal stress equations to model microcrack changes in properties and eventually, perhaps even spalling phenomena?

Kazunori Harada: Yes and we are doing experiments using small samples. The purpose of these is to find out the relationship between the heat moisture migration and the spalling of materials.

FULL-SCALE BURN TEST OF WOODEN THREE-STORY APARTMENT BUILDING

Building Research Institute, Ministry of Construction

March 1996



From left to right: Urban Fire Simulator, Wooden Three-story Apartment Building
and A Test Structure for the Assessment of Fire Spread(Post and Beam Construction)

OBJECTIVE

A full-scale fire experiment has been planned using actual wooden three-story collective housing to obtain technical knowledge necessary for the review of the current building standards regarding wooden structures for possible restructuring. In doing so, the test will examine not only fire safety of a single building but its effects to the neighboring area assuming a city fire.

CONCEPT OF THE BURN TEST

The burn test essentially tries to assess fire safety of wooden three-story collective housing in urban area. As revealed by the recent Hanshin Earthquake, urban fire is still a potential disaster especially in densely inhabited urban area, and it is a main reason for the exclusion of large wooden buildings in urban area in the current building regulation. Although the previous wooden three-story apartment building burn test in 1991 dealt with risk of fire spread from a dwelling unit to other units and to adjacent structures, impact that fire of such building may cause in urban fire scenario is not yet clarified in engineering manner. In order to assess fire safety of wooden three-story apartment building in urban fire scenario, the test will simulate an urban fire with liquid-fuel pools and porous burners assuming a city area with dense unprotected or only weakly-protected wooden structures, and expose a wooden three-story apartment building. As repression of fire spread velocity is the important fire safety performance of buildings needed specifically in urban area, the test tries to evaluate risk of fire spread to buildings behind the wooden three-story apartment building through various measurements and observations. For this purpose, two wooden two-story buildings have been built at the minimum distance allowed by relevant regulations from the wooden three-story apartment building. These buildings have been built according to the Building Standard Law and reflect very common design specifications. Also heat flux, radiation and temperature are measured on the external walls and the windows of the buildings for further analysis and generalization of the test data.

Walls of the buildings used for this test have been damaged artificially to simulate leakage due to earthquake. Although there are different construction methods of wooden buildings such as post and beam construction, 2 x 4 construction and prefabricated construction, the 2 x 4 construction has been adopted for the wooden three-story apartment building. In order to assess fire safety performance of the other construction methods, a series of loaded fire resistance tests are planned on external wall panels of the 2 x 4 construction, the post and beam construction and the prefabricated construction. Fire resistance tests on undamaged external wall panels of these three construction methods were conducted at the occasion of the previous wooden three-story apartment building burn test. At this present project, the specimens will be deflected horizontally at two levels before fire resistance tests to reproduce post-earthquake condition of the wall assemblies.

FACILITY

The burn test is carried out using the urban fire simulator, a wooden three-story apartment building test house and two test structures for the assessment of fire spread. These facilities have been built in BRI's Fire Test Field for this particular project.

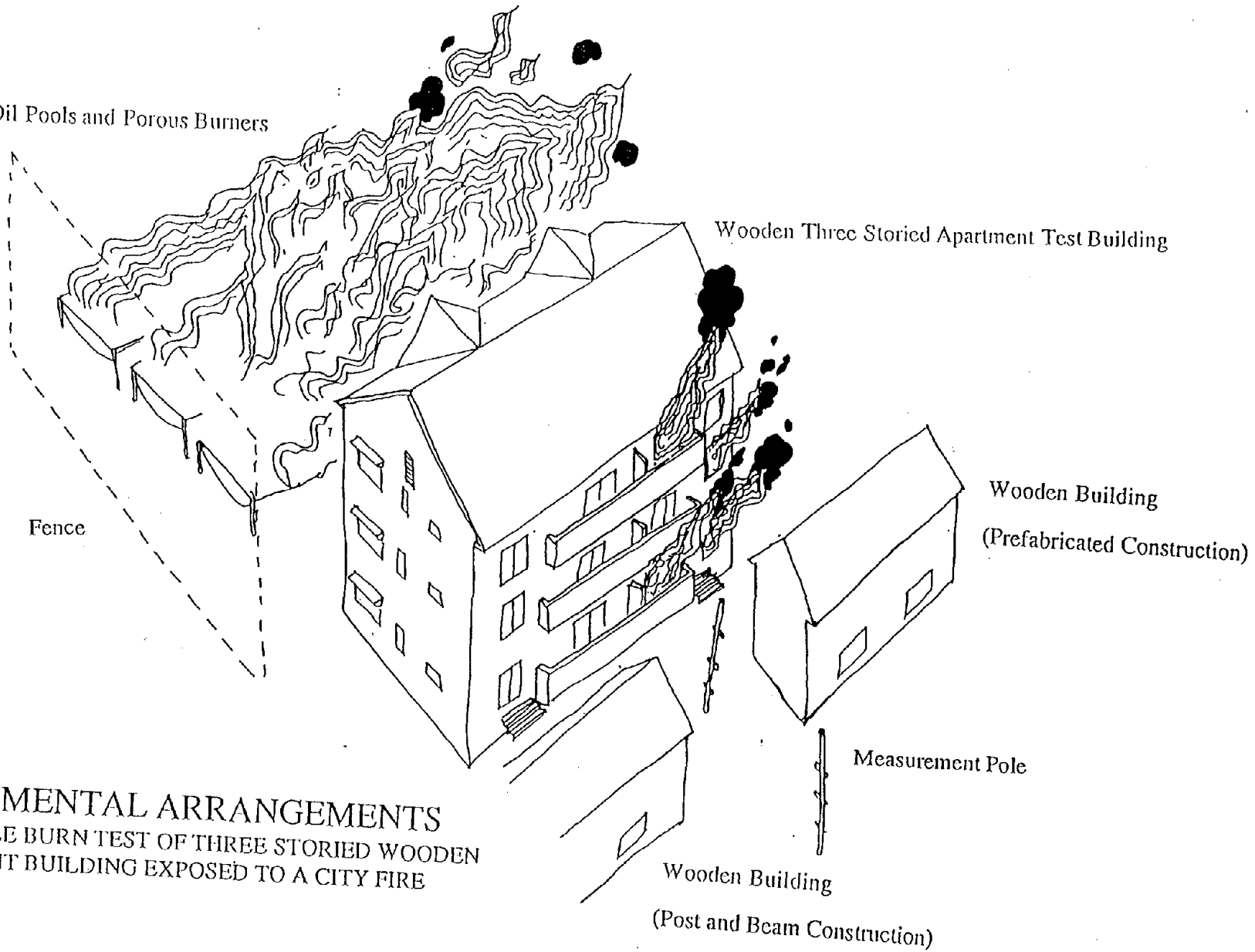
1) Urban Fire Simulator

A facility to reproduce flames at a city fire in densely inhabited urban area with approximately 2.0 square liquid-fuel pools and porous propane burners. The 12 square pools with n-heptane as the fuel are designed to simulate flaming wooden buildings in urban area, and the 6 propane burners are used to adjust heat release rate and to simulate remaining fires of collapsed buildings.

2) Wooden Three-story Apartment Building

A wooden three-story apartment building(2x4 construction, 2 dwelling units per floor, total 6 dwelling units) has been built next to the urban fire simulator. The building's north external wall is 3 m away from the south edge of the urban fire simulator. Each dwelling unit occupies 55.9m², so the total floor area excluding the external staircase and balconies becomes approximately 335m². Fire safety aspects of the building was designed basically to conform the current Japanese Building

Large Oil Pools and Porous Burners



Wooden Three Storied Apartment Test Building

Wooden Building
(Prefabricated Construction)

Measurement Pole

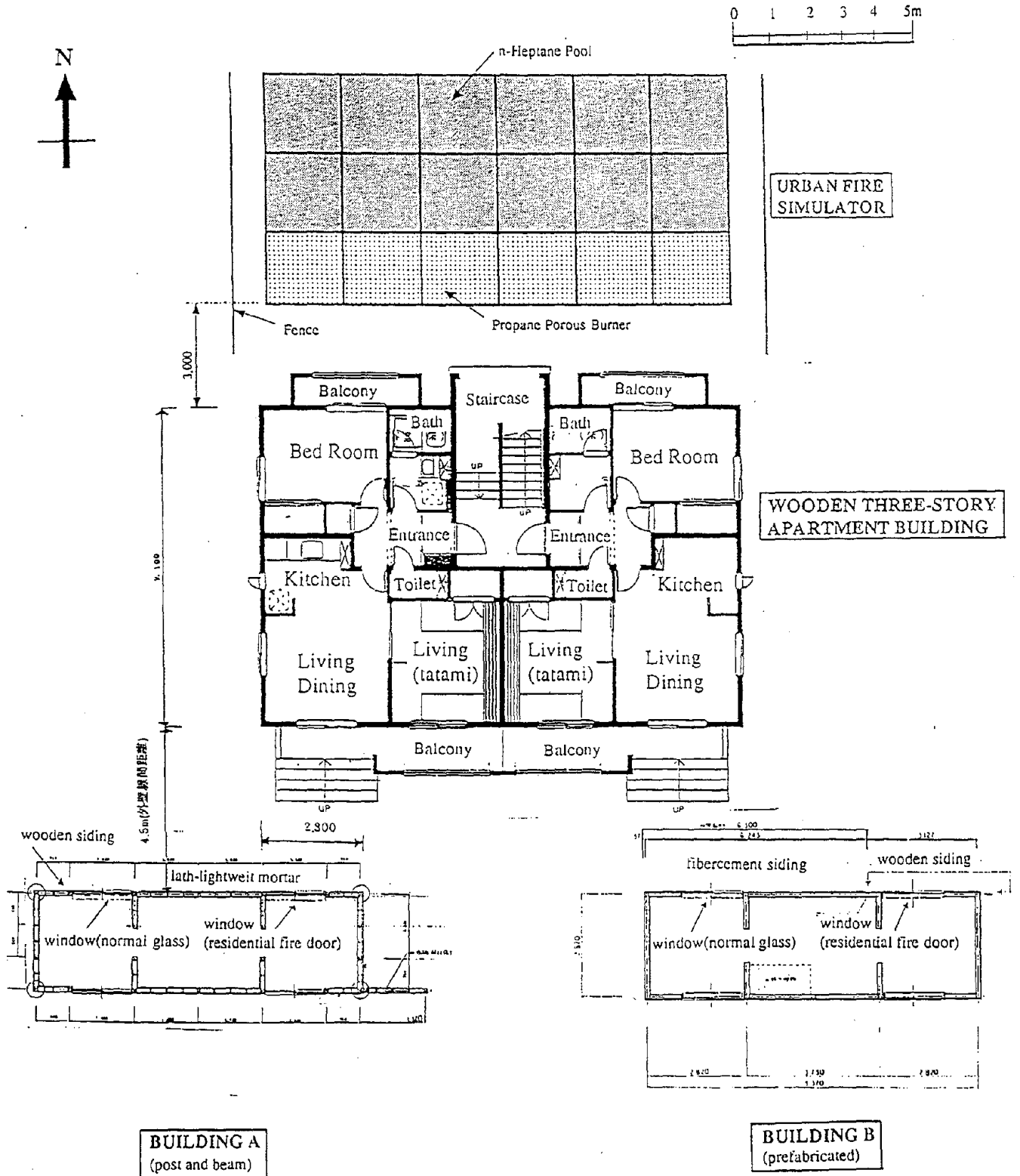
Wooden Building
(Post and Beam Construction)

Fence

4 3 9

EXPERIMENTAL ARRANGEMENTS
FULL-SCALE BURN TEST OF THREE STORIED WOODEN
APARTMENT BUILDING EXPOSED TO A CITY FIRE

FULL-SCALE BURN TEST OF WOODEN THREE-STORY APARTMENT BUILDING FACILITY LAYOUT



Wooden Three-story Apartment Building

General

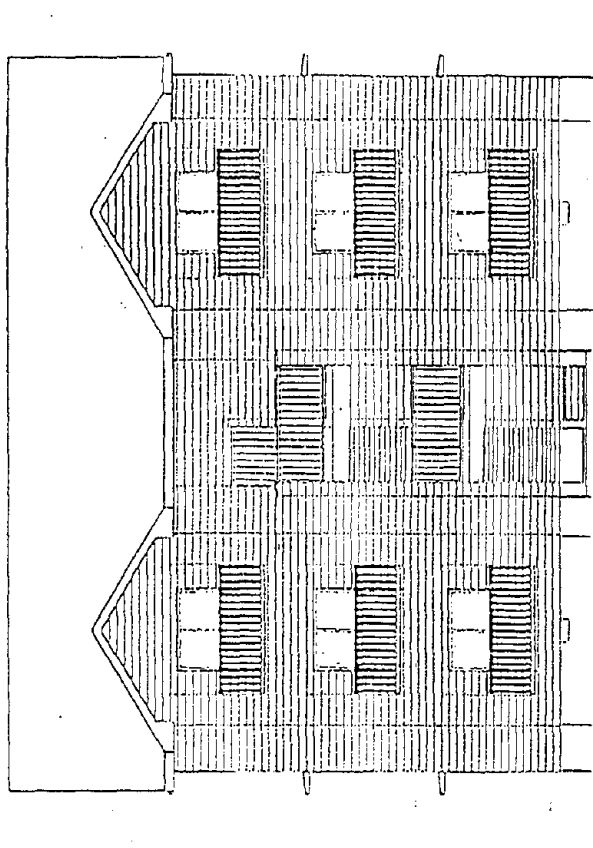
construction	2 x 4 construction
height	11.69 m
total floor area	335.37 m ² (excluding the external staircase and balconies)
floor area of dwelling unit	55.89 m ²

Main specifications

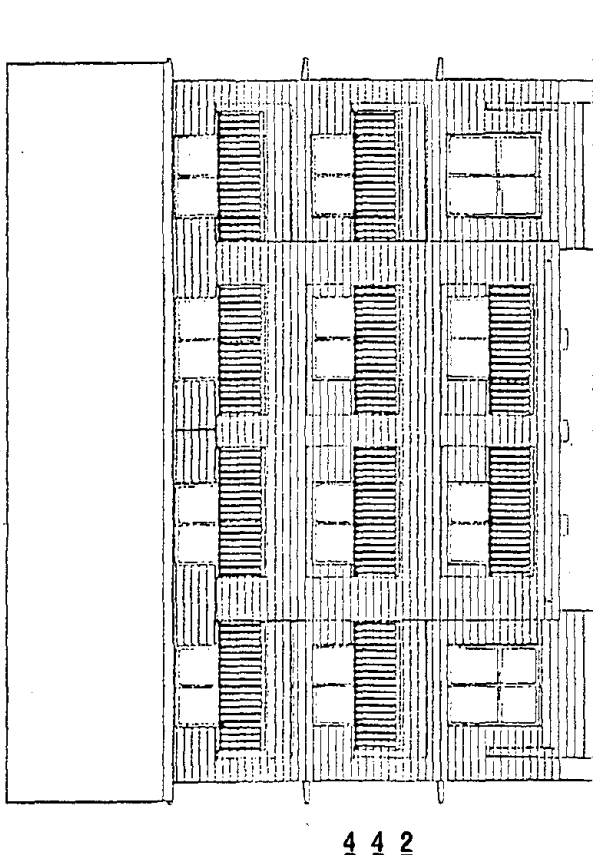
External Surfaces			
roof	residential roofing slate		
eaves	hard tip cement board 12mm		
external wall	fiber cement board siding 15mm		
entrance door	Type-B fire door		
window	residential fire window with wired glass, pilot model(Type-B fire door) (within the possible <i>portion liable to catch fire</i>) ----- normal glass(outside the possible <i>portion liable to catch fire</i>)		
attic ventilator (at eaves)	with fire damper		
Internal Surfaces			
	1st floor	2nd floor	3rd floor
floor	wood 12mm	gypsum board 12.5mm	
internal surface of external walls	gypsum board 12.5 mm + 12.5 mm		
partitions(load bearing walls)	gypsum board 12.5 mm + 12.5 mm		
partitions(other than load bearing walls)	gypsum board 12.5 mm		
ceiling	gypsum board 12.5 mm + 12.5 mm		gypsum board 9.5mm + 9.5mm(west unit)* gypsum board 12.5mm + 12.5mm(east unit)**
interior lining finish	vinyl cloth	none	none
equipments	with building service equipments and lights (west unit) none(east unit)	none	none
fire load	furnitures(30kg/m ³) (west unit) wood crib(30kg/m ³) (east unit)	wood crib(30kg/m ³)	wood crib(30kg/m ³)
staircase(external)	wooden		

* 30 minutes *quasi fire resistance*(according to *wooden three-story collective housing*)

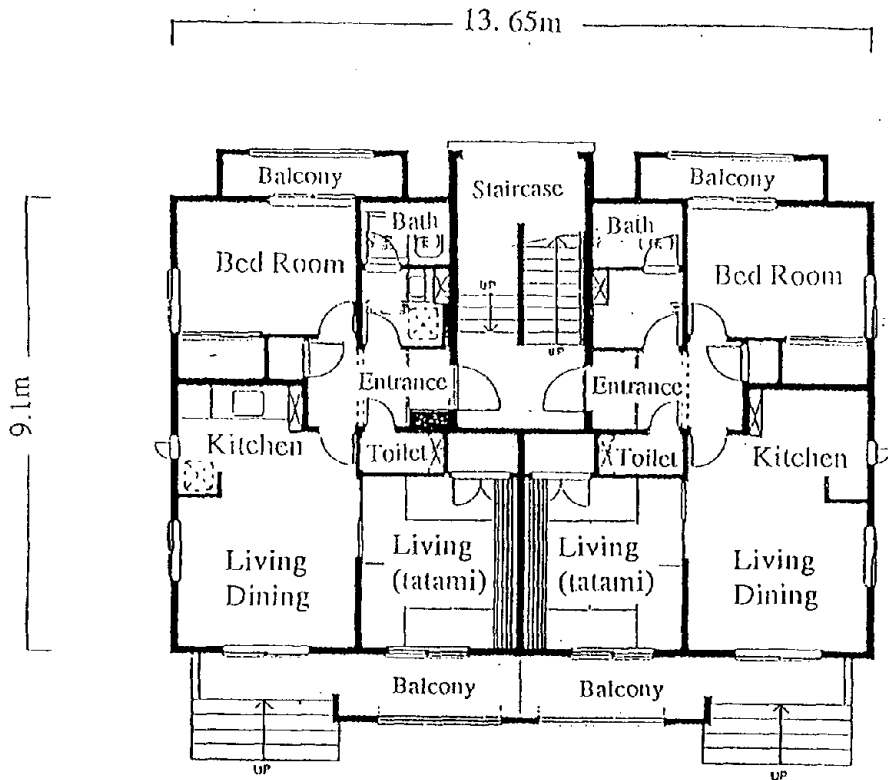
** 45 minutes *quasi fire resistance*(according to *three-story wooden independent house*)



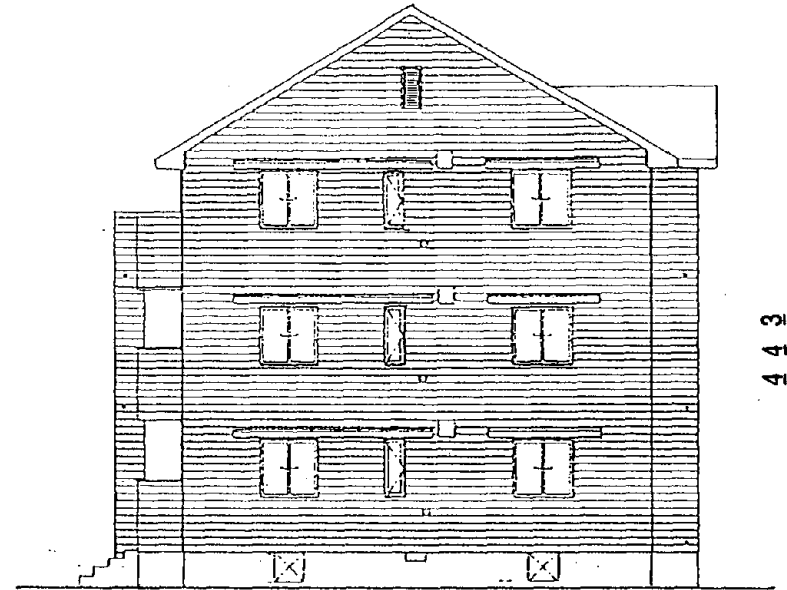
North Elevation



South Elevation



1st Floor Plan



East Elevation

Test Condition of the Wooden Three-story Apartment Building

	west	east	
<u>Attic</u>	Attic ventilation opening installed with fire damper	attic ventilation opening installed with fire damper	
<u>3rd Floor</u> Short pent roof, Normal glass	Fire load: 30kg/m ² (wood crib) Windows: north Type-B closed south Type-B closed Partitions with cracks Mattress hang from balcony	Fire load: 30kg/m ² (wood crib) Windows: north Type-B open south Type-B open Partitions without cracks	<u>3rd Floor</u> Long pent roof, Type-B fire door
<u>2nd Floor</u> Short pent roof, Normal glass	Fire load: 30kg/m ² (wood crib) Windows: north Type-B closed south Type-B open Partitions with cracks	Fire load: 30kg/m ² (wood crib) Windows: north Type-B open south Type-B closed Partitions with cracks Mattress hang from balcony	<u>2nd Floor</u> Long pent roof, Type-B fire door
<u>1st Floor</u> Short pent roof, Normal glass	Fire load: 30kg/m ² (furniture) Windows: north Type-B open south Type-B open Partitions with cracks	Fire load: 30kg/m ² (wood crib) Windows: north Type-B closed south Type-B closed Partitions with cracks	<u>1st Floor</u> Long pent roof, Type-B fire door
	Ventilation opening under floor : open	Ventilation opening under floor : with metal mesh	
	↓	↓	
	Two-story building A(post & beam)	Two-story building B(prefabricated)	

Standard Law for *wooden three-story collective housings** which are allowed to build outside the *fire protection and quasi-fire protection districts* with a few exceptions for research purposes. The ceiling of one dwelling unit at the third floor was designed to have 45 minutes *quasi-fire resistance* performance, a requirement for *three-story wooden independent houses*, whereas the another unit on the third floor has 30 minutes *quasi-fire resistant* ceiling according to the requirement for the *wooden three-story collective housings*.

* Terms in italics in this section represent translation of legal terms appearing in the Building Standard Law.

The external and internal walls of five units out of the six dwelling units have been damaged artificially to reproduce post-earthquake condition of the load bearing walls. The leakage data at the previous wooden three-story apartment building burn test in 1991 has been referred to at the present test. No artificial damage was given to the load bearing walls of the east dwelling on the third floor in order to evaluate influence of the damage on leakage and fire resistance through comparison with results from other dwelling units.

Windows with wired glass conforming the *Type-B fire doors* are applied to the windows located virtually within the *portion liable to catch fire*. Each window at the north and south side of the building has curtains. One window at the north side on each floor is left open and the other on each floor is closed. Layout of the opening condition of the windows on the south side has been arranged to produce all possible combinations of opening conditions of the dwelling units. Fire load of the living room, tatami room, bed room and entrance hall of each dwelling unit is 30kg/m^2 , approximately 50% higher than the average reported by investigations. This fire load is represented by real furnitures in the west dwelling unit on the first floor and by timber cribs in other units.

3) Test Structures for the Assessment of Fire Spread

Two wooden two-story buildings(post-and-beam construction and prefabricated construction) of almost identical plan have been built 4.5m south of the external wall line of the wooden three-story apartment building in order to assess the risk of fire spreading to adjacent buildings from wooden three-story apartment in city fire scenario. Each building has approximately 50m^2 total building floor area, and its fire safety aspects were determined according to the Building Standard Law. Most common materials are selected for the external wall lining of the two buildings. The distance to the wooden three-story apartment building is the minimum according to the regulation on the *wooden three-story collective housings*(at least 4 m between the external wall and property line) and the Civil Law restriction(at least 0.5 m from property line). The external walls and the windows within the *portion liable to catch fire* are of fire preventive construction and *Type-B fire doors*(wired glass) respectively.

MEASUREMENTS

1) Temperature

K-type thermocouples are installed in each room of the dwellings, within major load bearing separation walls, and external-wall surfaces.

2) Heat Flux

Schmidt-Boelter heat flux gages are installed to monitor surface heat flux at the north side walls of the wooden three-story apartment building and the north side of the adjacent two wooden buildings. A heat flux gage is arranged at roughly the center of each north side window on each floor and each south side window on the second and third floor. A pole with heat flux gages and

Test Structures for the Assessment of Fire Spread

<u>General</u>	Building A(west)	Building B(east)
construction	post and beam construction	prefabricated construction
height	7.825m	6.812m
total floor area	49.68m ²	52.84m ²
<u>Main specifications</u>		
<u>External Surfaces</u>		
roof	residential roofing slate	residential roofing slate
eaves	lath-lightweight mortar 17mm (within the <i>portion liable to catch fire</i>)	fiber cement board 12mm
	wood 15mm (outside the <i>portion liable to catch fire</i>)	wood 15mm
external wall	lath-lightweight mortar 17mm (within the <i>portion liable to catch fire</i>)	fiber cement board siding 12mm
	wood siding 15mm (outside the <i>portion liable to catch fire</i>)	wood siding 15mm
window	residential fire window with wired glass, pilot model(<i>Type-B fire door</i>) (within the <i>portion liable to catch fire</i>)	
	normal glass(outside the <i>portion liable to catch fire</i>)	
<u>Internal Surfaces</u>		
floor	structural plywood 12mm	structural plywood 12mm
internal surface of external wall	gypsum board 12.5mm	gypsum board 12.5mm
ceiling	gypsum board 12.5mm	gypsum board 12.5mm
fire load	none	none



Urban Fire Simulator(Preliminary Test)



thermocouples is built between the urban fire simulator and the wooden three-story apartment building. Two similar poles are built on the south side of the wooden three-story apartment building at different distances from the external wall.

3) Gas Analysis

Air in the bed room of each dwelling unit is sampled continuously and analyzed.

4) Smoke Density

Optical smoke density is measured in the living room and the bed room of each dwelling unit.

5) Static Pressure

Static pressure is measured inside a south side opening of each dwelling unit.

6) Infrared Image

Infrared image is recorded from outside the buildings at three different directions.

7) Visual Observation and Video Camera

Several teams watch and record the building and its environment from different angles. Video cameras make visual records of the buildings and fire from at least three different directions. A video camera is installed in the bed room of each dwelling unit to make observation of fire penetration to the room from the urban fire simulator.

TEST SCHEDULE

The burn test will be initiated with the ignition to the urban fire simulator planned at 9:30. In order to make it possible to observe post-fire stability of the wooden three-story apartment buildings, fire suppression of the test buildings will be started at 16:30 unless any risk of fire spread to outside the restricted area or other danger is anticipated.

1) Opening

Introduction of the burn test project and other informations are presented by the BRI Director General and the Director of the Fire, Environment and Design Department. Invited guests are kindly requested to be around the control desk and guest seat by 9:00.

2) Tour in the Restricted Area

Prior to the ignition to the urban fire simulator, invited guests and press crews are invited to a tour to see the building conditions and the instrumentation. The tour members will walk with a guide in the restricted area through the path between the wooden three-story apartment building and the prefabricated test structure. For safety reasons, the tour cannot approach the urban fire simulator.

3) Ignition to the Urban Fire Simulator

Ignition to the urban fire simulator is scheduled at 9: 30. Ignition will be made with torches.

4) Possible Ignition to Dwelling Units

If fire spread from the urban fire simulator to any dwelling unit does not occur, the wooden three-story apartment building will be ignited in the west dwelling unit on the first floor. Even if any dwelling units survive the heating from the urban fire simulator or fires of other dwelling units, all surviving dwelling units will finally be ignited artificially in order to evaluate post-fire structural stability of the wooden three-story apartment building.

5) Briefing in Japanese

It is planned to make brief report in the Japanese language twice at 12:00 and at 17:00 at the Lecture Room of the BRI's International Institute of Seismology and Earthquake Engineering on the first floor of the BRI Main Building.

6) Briefing in English

It is planned to make brief report in English at 17:30 at the Lecture Room of the BRI's International Institute of Seismology and Earthquake Engineering on the first floor of the BRI Main Building.

SAFETY PRECAUTIONS

The burn test is one of the largest scale fire tests in Japan. Generation of a flame large enough and considerable smoke is anticipated from the result of the preliminary test. Also the test deals with large amount of liquid fuel. BRI requires everyone except for the test team not to enter the restricted area. Smoking in the test site not only in the restricted area is prohibited. BRI also requests everyone at the test site to follow advice and directions from the headquarter and from the safety crew especially at emergency.

FOR YOUR CONVENIENCE

? Information

For general questions in English or French, please look for Dr.A.Marchal, a guest scientist at the BRI Fire Safety Division. Dr.I.Nakaya is also available for English speakers.

Rest Rooms

Rest rooms for gentlemen and ladies are available on the first floor of the Full Scale Fire Test Laboratory and in the Main Building.

Lunch and Beverage

BRI cafeteria, first floor of the Main Building, is open to public. There are few restaurant around the BRI campus. There are numbers of restaurants in the Central Tsukuba area. Lunch for invited guests is prepared at the reception rooms for invited guests on the second floor of the Main Building. Beverage is available at the entrance lobby of the Main Building.

Smoking

Smoking is not allowed in the test site for safety reasons. The entrance lobby lounge is available for smoking.

First Aid

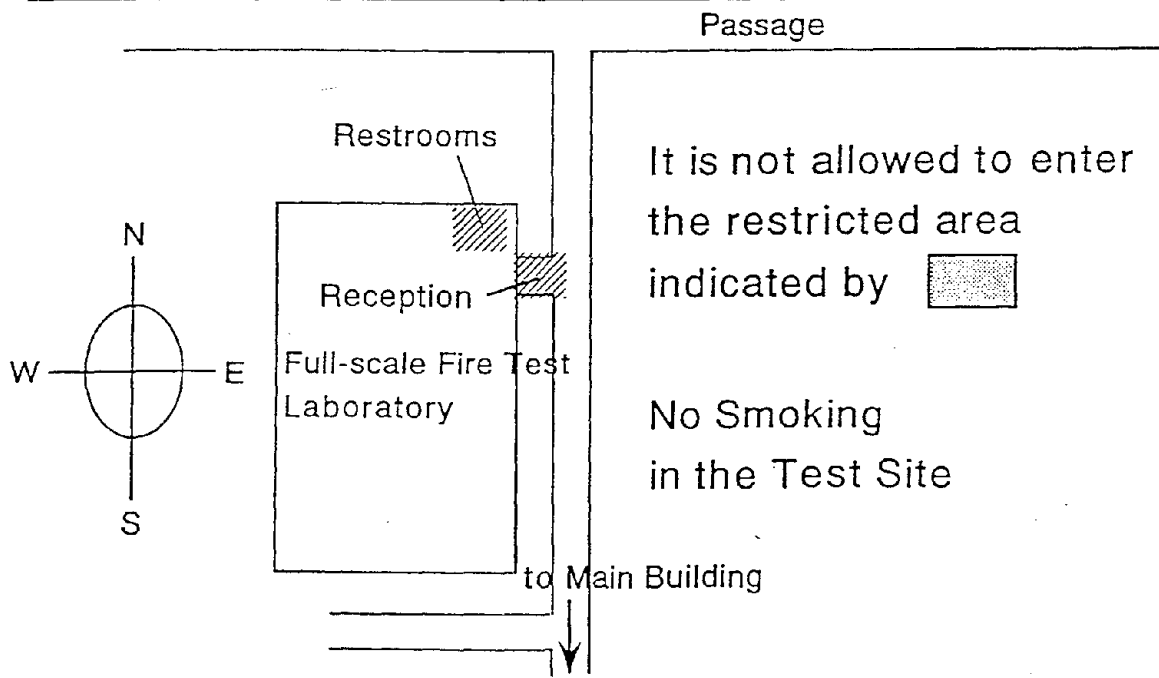
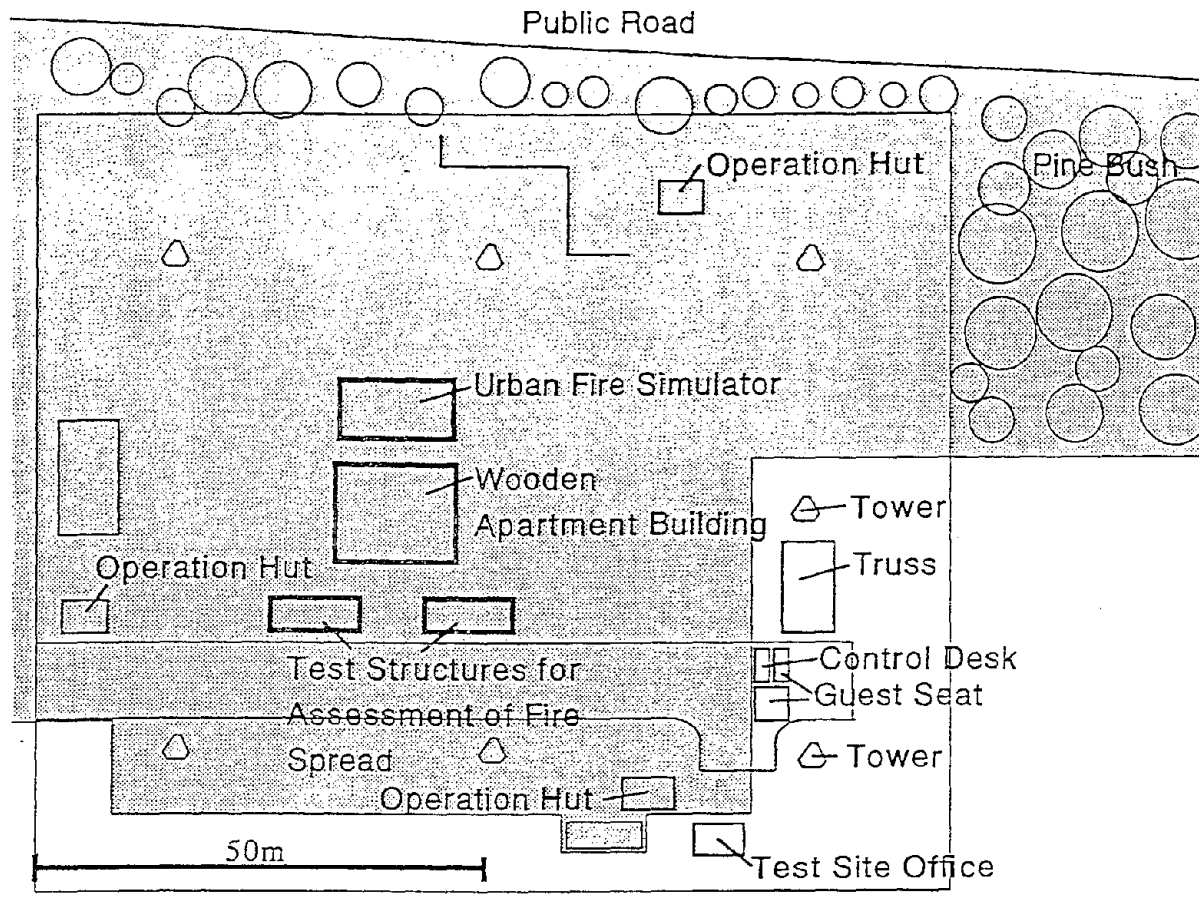
In case of any injury or sudden illness at the test site, please try to contact anyone with an arm band or visit the test site office almost at the south end of the Fire Test Field.

Reception Rooms for Invited Guests

Two meeting rooms on the second floor of the BRI Main Building are reserved for rest and meal of the guests.

Transportation

Free bus to Tsukuba Center Bus Terminal is available near the gate of BRI frequently from 11:00.



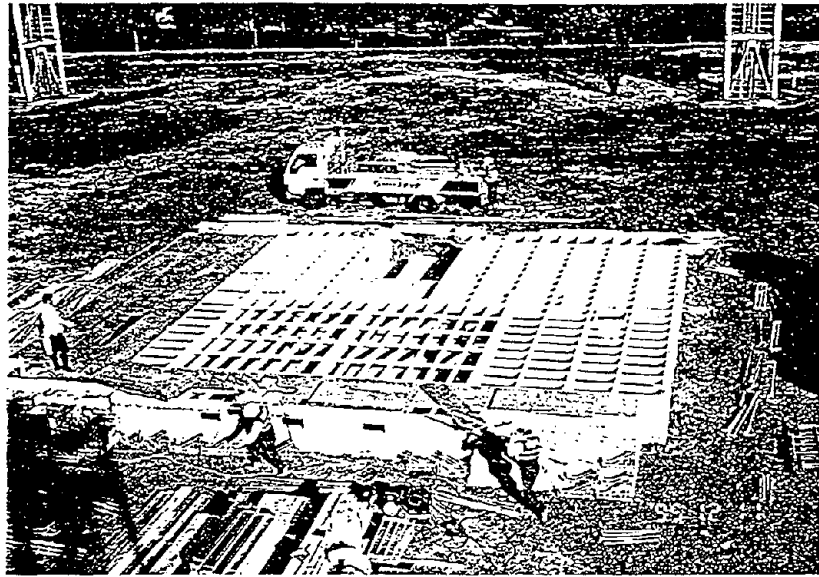
TEST SITE MAP

木造3階建共同住宅実大火災実験棟 工事写真

Construction Works in the Wooden Three-story Apartment Building

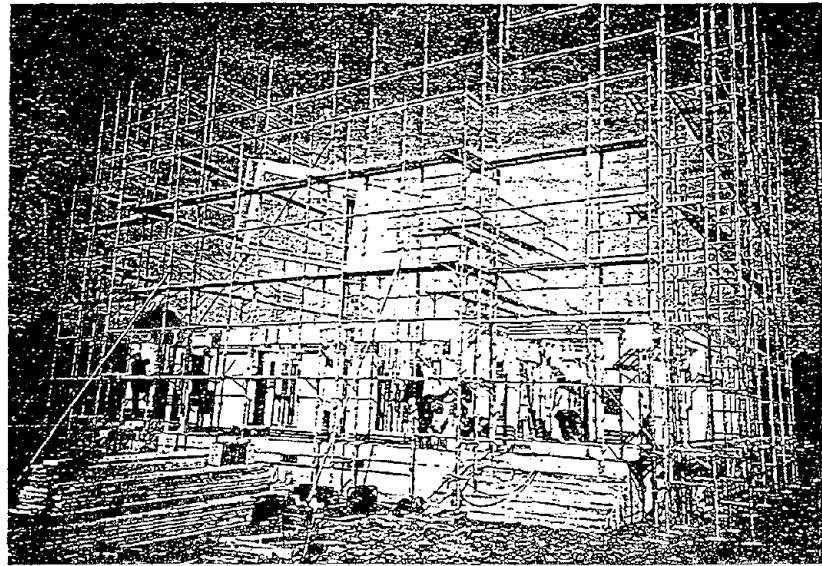
基礎工事終了
1階床組工事中

in process of the first floor
framing work after
completion of the foundation
work



1階壁建起し中

in process of raising the
external walls of the first
floor



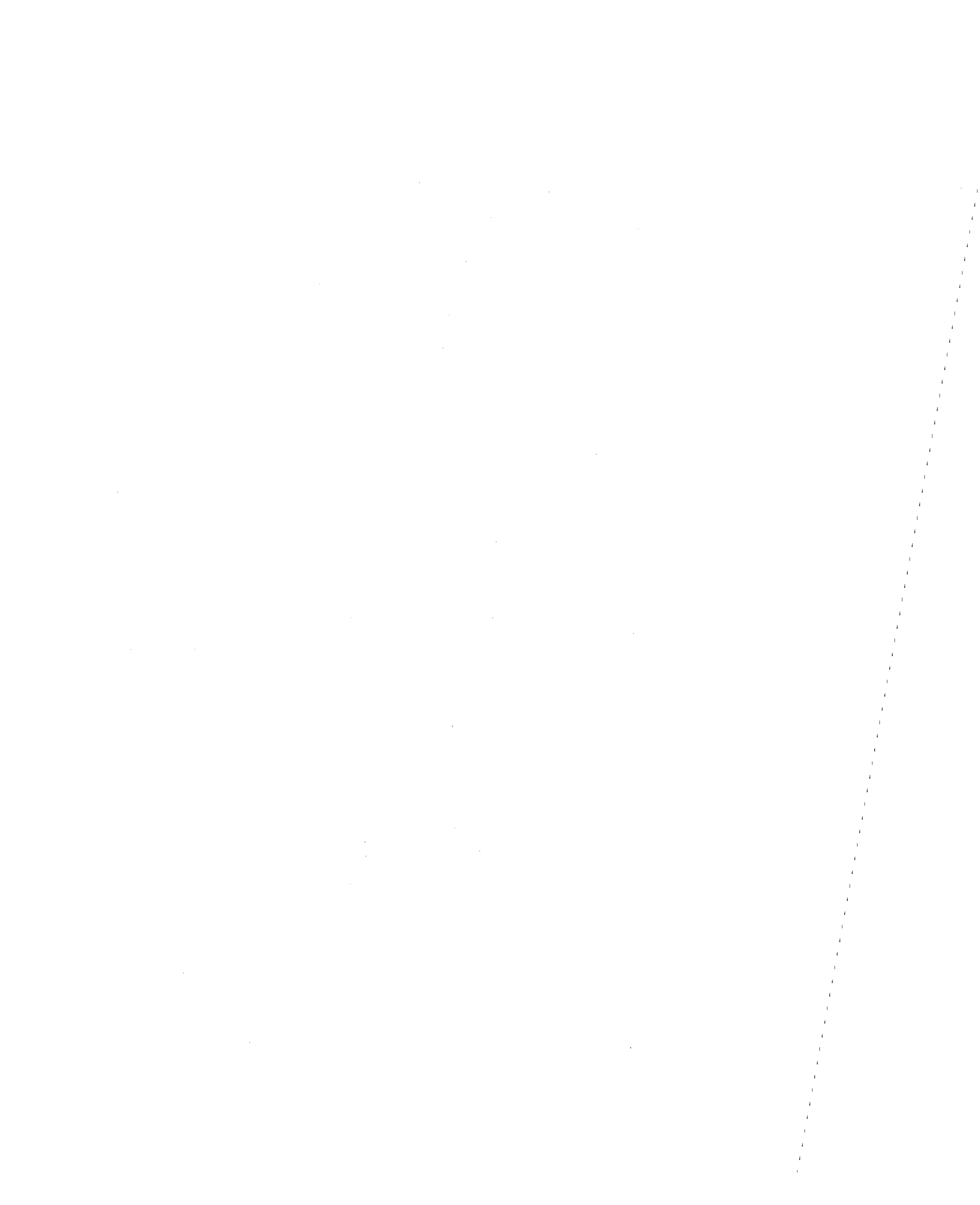
3階壁建起し中

in process of raising the
external walls of the third
floor



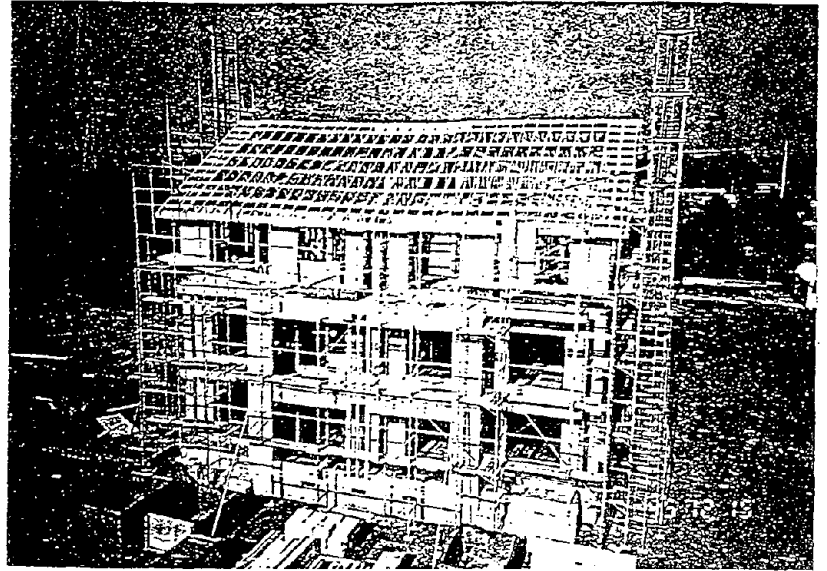
Reproduced from
best available copy.





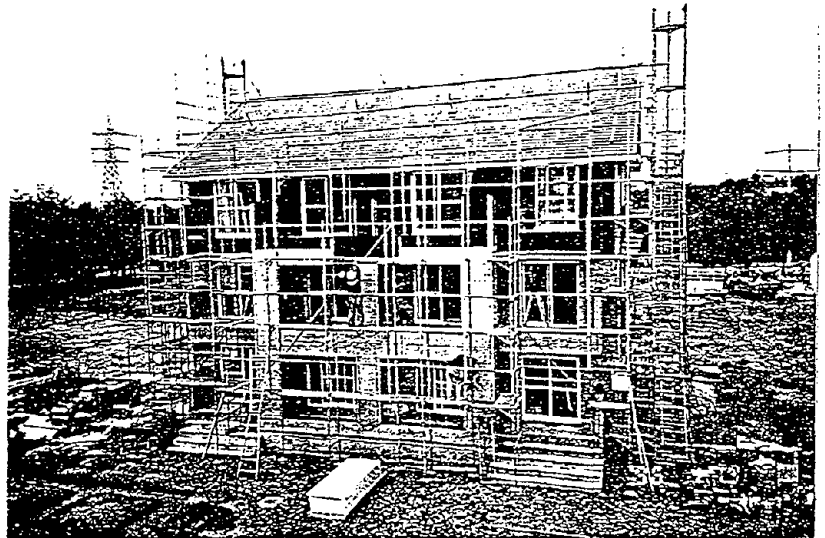
小屋組工事中

in process of the roof truss work



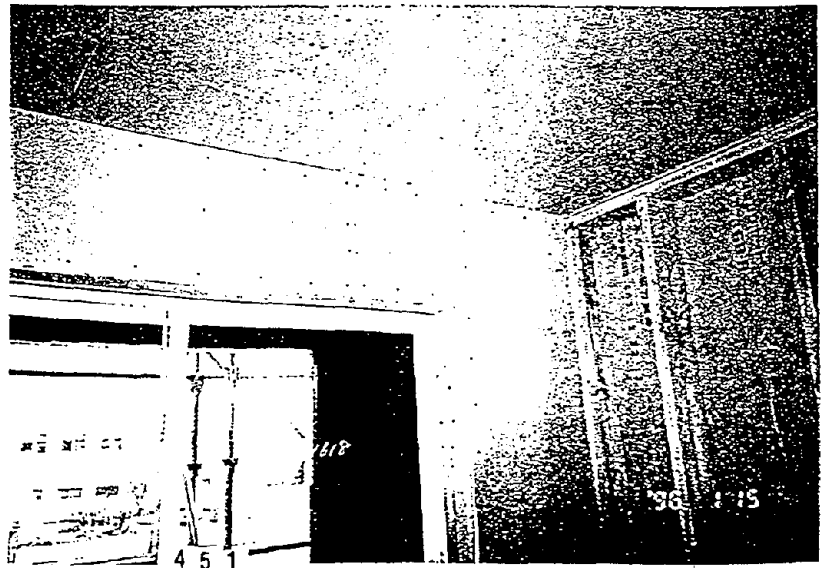
外部仕上工事中

in process of the exterior finishes



室内石膏ボード張り

interior walls: gypsum board



Reproduced from
best available copy.



36 115

4 5 1

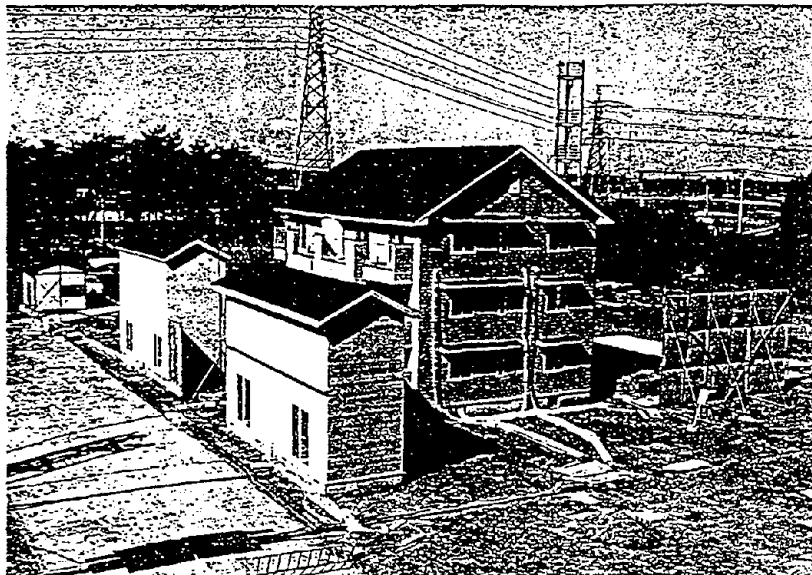


工事完了

left: Post and beam construction building

right: Prefabricated building

behind the two-story buildings: wooden three-story apartment building



居間・食堂


(室内に置かれているポールは
実験用センサー)

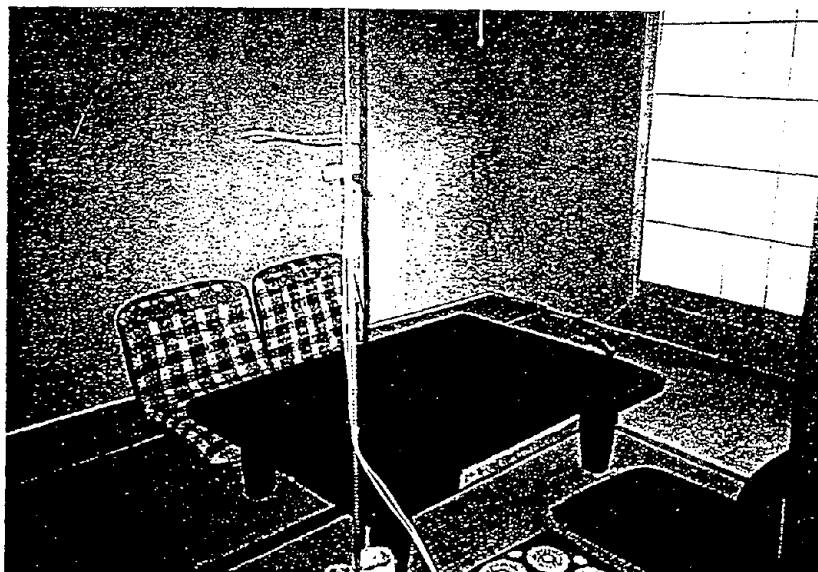
Living+Dining Room
(First floor west dwelling)
Poles inside the room are for
measurement sensors



和室

Tatami Room
(First floor west dwelling)

Reproduced from
best available copy. 





AUTHOR INDEX
VOLUME 1

B

Baum, H., 201, 249
Beyler, C., 121
Bukowski, R., 79

C

Cetegen, B., 285

E

Ebihara, M., 27, 43
Emmons, H., 229

F

Faeth, G., 275
Fahy, R., 35

G

Gandhi, P., 209
Gore, J., 201

H

Hagiwara, I., 53, 65
Hall, J., 7
Harada, K., 423
Hasemi, Y., 129, 165, 237,
437
Hayasaka, H., 265
Heskestad, G., 295
Hunt, S., 121

I

Iqbal, N., 121

K

Kakegawa, S., 27
Kasper, K., 285
Koseki, H., 413

L

Liggett, W., 413
Lippiatt, B., 97

M

McGrattan, K., 249
Meacham, B., 19
Mimura, Y., 3, 53, 65, 317
Mitler, H., 187
Morita, M., 375
Mulholland, G., 413

N

Nelson, H., 389
Notake, H., 43

O

Ohlemiller, T., 107
Orloff, L., 153

P

Pagni, P., 305
Ptchelintsev, A., 237

Q

Quintiere, J., 331

R

Rehm, R., 249
Robertson, A., 321
Rockett, J., 357

S

Sakai, K., 401
Sato, M., 341
Sekine, T., 323
Snell, J., 227, 319
Stroup, D., 89
Sugawa, O., 115, 401

T

Takashima, S., 129
Tanaka, T., 15, 53, 65, 341
Terai, T., 423
Tewarson, A., 153
Tsujimoto, M., 259

W

Wakamatsu, T., 237, 341
Weber, S., 97
Williams, F., 121
Wright, R., 1
Wu, P., 153

Y

Yashiro, Y., 27, 43
Yokobayashi, S., 129, 237
Yoshida, M., 129

Z

Zhou, X., 201



NTIS does not permit return of items for credit or refund. A replacement will be provided if an error is made in filling your order, if the item was received in damaged condition, or if the item is defective.

Reproduced by NTIS

National Technical Information Service
Springfield, VA 22161

*This report was printed specifically for your order
from nearly 3 million titles available in our collection.*

For economy and efficiency, NTIS does not maintain stock of its vast collection of technical reports. Rather, most documents are printed for each order. Documents that are not in electronic format are reproduced from master archival copies and are the best possible reproductions available. If you have any questions concerning this document or any order you have placed with NTIS, please call our Customer Service Department at (703) 487-4660.

About NTIS

NTIS collects scientific, technical, engineering, and business related information — then organizes, maintains, and disseminates that information in a variety of formats — from microfiche to online services. The NTIS collection of nearly 3 million titles includes reports describing research conducted or sponsored by federal agencies and their contractors; statistical and business information; U.S. military publications; audiovisual products; computer software and electronic databases developed by federal agencies; training tools; and technical reports prepared by research organizations worldwide. Approximately 100,000 *new* titles are added and indexed into the NTIS collection annually.

For more information about NTIS products and services, call NTIS at (703) 487-4650 and request the free *NTIS Catalog of Products and Services*, PR-827LPG, or visit the NTIS Web site
<http://www.ntis.gov>.

NTIS

*Your indispensable resource for government-sponsored
information—U.S. and worldwide*



U.S. DEPARTMENT OF COMMERCE
Technology Administration
National Technical Information Service
Springfield, VA 22161 (703) 487-4650
